UNIVERSITY OF OKLAHOMA

GRADUATE COLLEGE

STEREOSELECTIVE SPIROCYCLIZATIONS INITIATED BY METAL CARBENES

A DISSERTATION

SUBMITTED TO THE GRADUATE FACULTY

in partial fulfilment of the requirements for the

Degree of

DOCTOR OF PHILOSOPHY

by

ARIANNE C. HUNTER

Norman, Oklahoma
2019

STEREOSELECTIVE SPIROCYCLIZATIONS INITIATED BY METAL CARBENES

A DISSERTATION APPROVED FOR THE
DEPARTMENT OF CHEMISTRY AND BIOCHEMISTRY

BY

Dr. Indrjaeet Sharma, Chair

Dr. Michael Jablonski

Dr. Ronald Halterman

Dr. Adam Duerfeldt

Dr. Daniel Glatzhofer

DEDICATION

This dissertation is dedicated to every woman that does not let societal norms define her.

Continue to be the change you want to see in the world.

ABSTRACT

Within the field of drug design, there is a great interest in the development of synthetic libraries that mimic the structural complexity of natural product scaffolds. Recent cheminformatic analyses have revealed that 83% of the core ring scaffolds found in natural products are absent among commercially available drug molecules. Spirocycles are one of these cores presumably due to the difficulty found in synthesizing this scaffold. In order to address the limitation in synthetic technology, a novel approach to spiroethers, azaspiro-ring systems, spirocarbocycles, spiroketals, and spiroaminals has been developed using metal carbene initiated cascade reactions.

The identification of two novel catalytic systems were critical to the success of synthesizing these varying spirocycles. The first development was identification of $Rh_2(esp)_2$ as a catalyst for the efficient insertion of carboxylic acids into acceptor/acceptor diazocarbonyls. The second development was the identification of $Rh_2(esp)_2/PPh_3AuOTf$ as a synergistic catalytic combination for an O–H insertion/Conia-ene cascade for the stereoselective synthesis of tetrahydrofurans and γ-butyrolactones.

These systems were applied to the synthesis of spiroethers using an O–H insertion/Conia-cascade and azaspiro-ring systems using an N–H insertion/Conia-ene cascade. Subsequently, the Rh(II)/Au(I) system was applied to the synthesis of 5-, 6-, and 7-membered oxindole hybridized spirocarbocycles. Lastly, direct access to spiroketals and spiroaminals using a metal carbene initiated cascade reaction dependent on the use of α-diazoketones was developed. Within each synthetic effort, valuable mechanistic insights were obtained to justify stereochemistry and applicability to a substrate scope.

ACKNOWLEDGEMENTS

First and foremost, I would like to thank Dr. Siobhan Milde, my first undergraduate chemistry professor at Dartmouth College who continued to be a mentor and friend to me throughout graduate school. You believed in me when no one else did and your unwavering support up until your last breath on this beautiful earth meant more to me than you could have ever imagined. I wish you were here with me to celebrate this accomplishment, but I know you are in heaven enjoying an ice-cold Pepsi and smiling down on me.

Secondly, I would like to thank the University of Oklahoma and the Department of Chemistry and Biochemistry for allowing me to pursue my doctoral studies at such a wonderful university in my beloved home state of Oklahoma.

Very importantly, I would like to thank my Ph.D. advisor, Dr. Indrajeet Sharma. Your guidance over the past five years has been remarkable and having the opportunity to be the first student to obtain their Ph.D. under your guidance is such a high honor. Thank you for being the best mentor, teacher, and leader; your efforts have shaped me into not only a highly skilled synthetic chemist, but also a better human being. I would also like to thank the members of the Sharma Lab for their camaraderie and teamwork, specifically every member that helped me complete the projects within this dissertation (Dr. Kiran Chinthapally, Steven Schlitzer, Joseph Stevens, and Anae Bain).

Lastly, I would like to thank my family. I am eternally grateful for each and every one of you. To my parents, Anthony and Cynthia Woody, words cannot explain how thankful I am for you, every sacrifice you made and lesson you have taught shaped, me into the woman I am today

TABLE OF CONTENTS

LIST OF FIGURES

CHAPTER 1

CHAPTER 2

CHAPTER 3

CHAPTER 4

CHAPTER 5

LIST OF SCHEMES

CHAPTER 1

CHAPTER 2

CHAPTER 3

CHAPTER 4

CHAPTER 5

LIST OF TABLES

CHAPTER 2

CHAPTER 3

CHAPTER 4

CHAPTER 5

LIST OF ABBREVIATIONS

Å	Ångstrom
$[\alpha]_D$	specific rotation at wavelength of sodium D line
Ac	acetyl
app.	apparent
aq	aqueous
Ar	aryl
atm	atmosphere
Bn	benzyl
Boc	tert-butyloxycarbonyl
bp	boiling point
br	broad
Bu	butyl
n-Bu	n-butyl
t-Bu	tert-butyl
Bz	benzoyl
c	concentration for specific rotation measurements
°C	degrees Celsius (centigrade)
calc'd	calculated
cat.	catalytic
CCDC	Cambridge Crystallographic Data Centre
CI	chemical ionization
comp.	complex
Cy	cyclohexyl
d	doublet
dba	dibenzylideneaceton
DCE	dichloroethane
dec.	decomposition
DMAP	4-dimethylaminopyridine
DMF	N,N-dimethylformamide
DMSO	dimethyl sulfoxide
dr	diastereomeric ratio
ee	enantiomeric excess
EI	electron impact
equiv	equivalent
ESI	electrospray ionization
Et	ethyl
FAB	fast atom bombardment
g	gram(s)
GC	gas chromatography
hr	hour(s)
HMDS	1,1,1,3,3,3-hexamethyldisilazane
HPLC	high-performance liquid chromatography

HRMS	high-resolution mass spectroscopy
hv	light
Hz	Hertz
IR	infrared (spectroscopy)
J	coupling constant
λ	wavelength
L	liter
L_n	L-type ligand
m	multiplet or milli
m	meta
m/z	mass to charge ratio
μ	micro
M	metal or molar
Me	methyl
MHz	megahertz
min	minute(s)
mol	mole(s)
mp	melting point
MS	molecular sieves
n	nano
N	normal (normality)
NMR	nuclear magnetic resonance
o	ortho
p	para
Ph	phenyl
pH	hydrogen ion concentration in aqueous solution
PhH	benzene
ppm	parts per million
i-Pr	isopropyl
Py	pyridine
q	quartet
ref	reference
R_f	retention factor
s	singlet or selectivity factor
sat.	saturated
t	triplet
TBAF	tetrabutylammonium fluoride
TBS	tert-butyldimethylsilyl
Tf	trifluoromethanesulfonyl (trifyl)
THF	tetrahydrofuran

TLC	thin-layer chromatography
TMS	trimethylsilyl
Ts	p-toluenesulfonyl (tosyl)
X	anionic ligand or halide

CHAPTER 1

Natural Products as Inspiration for the

Synthesis of Bioactive Spirocycles in Drug Discovery

1.1 INTRODUCTION

If one were to probe today's American population and ask, "What is your greatest issue with healthcare in the United States?" an opinion that would often be expressed is, "Drugs are too costly". To date, the cost of drug development, including the price of failure and the opportunity cost, has more than doubled in the past decade. [1] A study published in the *Journal of Health Economics* showed that the annual price for new drug development costs $2.6 billion, a 145% increase (accounting for inflation) since a widely cited study in 2003.[2] The higher price tag can be attributed to a variety of factors, but the major contributing factor is the higher failure rates of new drug molecules that are entering clinical trials.[2] The business of developing innovative drugs is extremely risky and it is well understood in our society that the development of a new drug requires major investment of capital, human resources, and technological expertise. However, what is not well

understood by the majority is the impact of ineffective research and development efforts at the chemical level on the price of the drugs that are purchased at local pharmacies.

New drug development, from the synthesis of a compound to approval of a New Drug Application, can take on average 10–15 years.[1] With this timeframe and the aforementioned amount of money required to develop a new drug annually, it is easy to understand why the price paid at the pharmacy for drugs is on a steady incline. The drug approval process in the United States can be categorized into three sections (**Figure 1.1**) : 1) Preclinical testing and research and development; 2) Clinical research and development; and 3) New Drug Application review.[3] The stage where more effective research and development efforts can have the greatest impact, devoid of human safety concerns, can be found at the "Preclinical testing and research and development" stage. This is the stage in which drug molecules are initially being discovered and/or synthesized and tested for hit-compound identification by high-throughput screening of chemical libraries

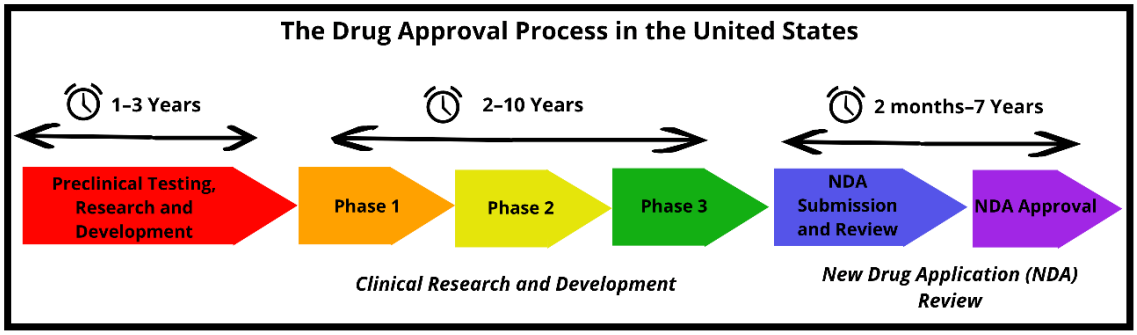

Figure 1.1. *Visual depiction of drug approval process in the United States*

Currently in the field of drug design and delivery, a significant number of scientists believe it is necessary to make drug molecules that more closely mimic the complexity of molecules derived from nature.[4] There is great interest in the development of synthetic libraries that mimic the structural complexity of natural product scaffolds. The reasoning for this interest was inspired by cheminformatic analyses that revealed that many natural product scaffolds remain underexploited in probe and drug discovery.[5] Presently, 83% of the core ring scaffolds found in natural products are absent among commercially available drug molecules and drug candidate screening libraries.[6] Therefore, designing molecules for screening that contain scaffolds found in natural products but are absent from current drug molecules is an ideal starting point when designing chemical libraries or developing the foundation of a synthetic chemistry research program.[7] This is due to the fact that molecules with three-dimensional features such as stereochemistry and bond saturation have increased binding specificity, decreased toxicological liabilities, and favorable pharmacological properties.[5]

The chemo-diversity, structural complexity, and three-dimensionality of natural products provides scientists with molecular scaffolds that the human mind oftentimes cannot fathom piecing together in a laboratory setting. This described uniqueness of natural products is what allows these scaffolds to occupy regions of chemical space that current drug molecules are not accessing. Due to the high structural diversity of molecules obtained from terrestrial and marine organisms, natural products have been the source of many successful drug leads.[8] In the last 25 years, of the 877 novel drug molecules developed 33% were natural products or their derivatives, evidence of the importance of

biogenic structural motifs.[9] However, the major challenge in accessing scaffolds found in complex natural products is the development of efficient synthetic routes to obtain these molecules.[5] Given this rising challenge, synthetic chemists must identify methods to quickly and efficiently synthesize complex molecules and scaffolds that are inspired by natural products. One example of a complex scaffold that is currently underrepresented in chemical space and difficult to access using known literature protocols are ring systems possessing a spirocenter.

Spirocyclic ring systems are found in a variety of bioactive natural products and approved drugs (**Figure 1.2**).[10] Spirocyclic ring systems contain a "spirocenter" which is a tetra-substituted carbon atom that is used to perpendicularly fuse two ring systems to create a highly rigid scaffold.[11] The rigidity of this system allows molecules to possess well-defined conformations in biological systems.[11g] The spirocyclic scaffold increases the metabolic stability of drug compounds and allows them to have higher probabilities of interaction with protein binding sites.[12] Key classes of spirocycles include spiroethers[13], spirolactones[14], spiroamines[15], spirolactams[15c], spirooxindoles[16], spiroketals[17], and spiroaminals. Spiroethers such as the pseurotin family, are secondary microbial metabolites isolated from a culture broth of *Pseuderotium ovalis.*[18] They possess a wide range of biological activities including antibiotic, antifungal, anti-angiogenic, and anti-cancer activities.[19] Also, the spiroether drug griseofulvin is on the World Health Organization's (WHO)'s list of essential medicines.[20] The spirolactone core is found in the hyperolactone natural products, which were isolated from the leaves of the plant *Hypericum Chinese L.*[21] In particular, hyperlactone C and biyouyanagin A are of significant

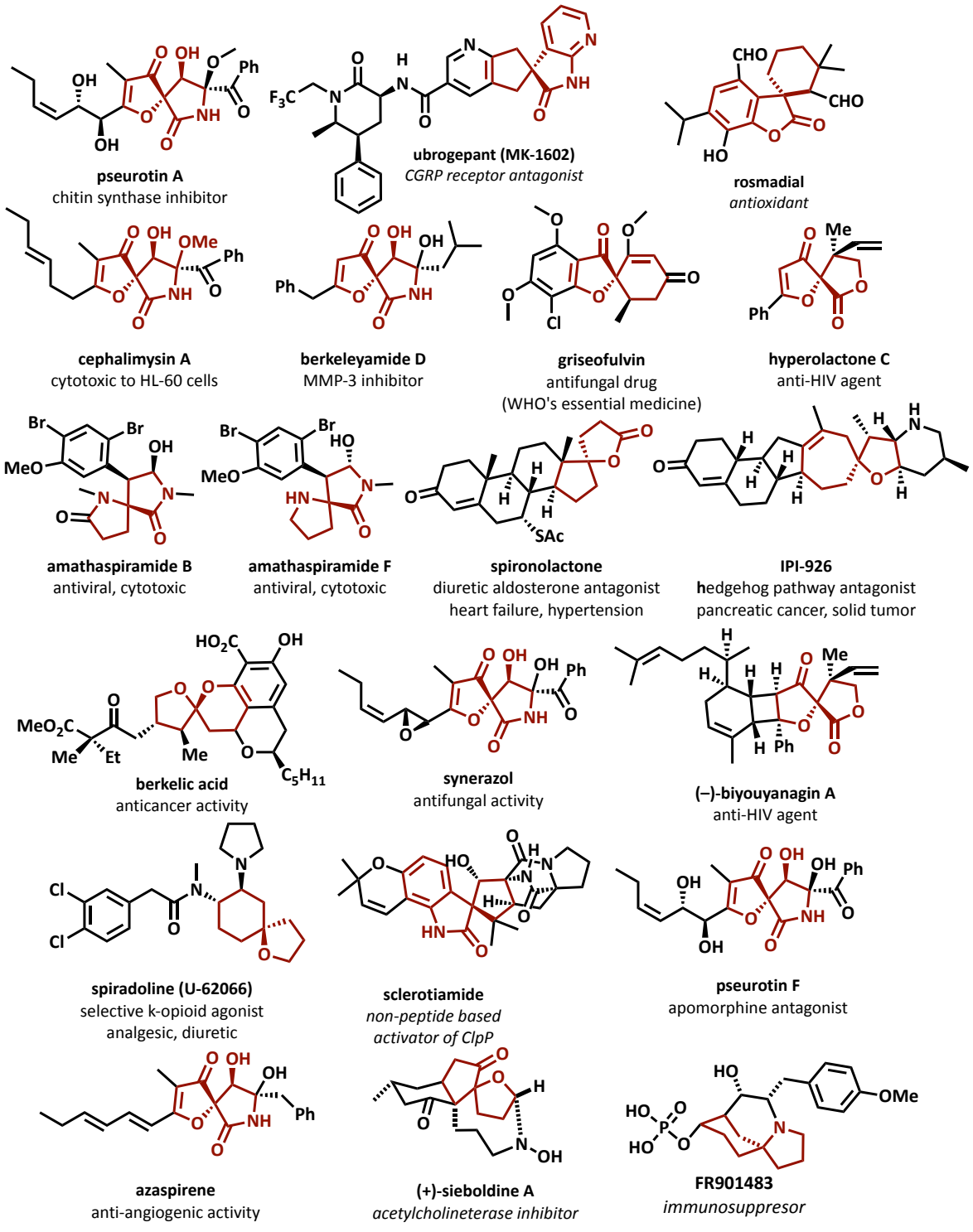

Figure 1.2. *Biologically active natural products containing a spirocenter*

interest because of their anti-HIV activity.[22] In addition, γ-butyrolactones are very common structural motifs found in about 10% of all-natural products.[23]

Despite the impressive biological pedigree of spirocyclic molecules, not many of these scaffolds have advanced to clinical use due to low isolated yields or synthetic challenges associated with the stereoselective installation of the spirocenter. As a result, most of these drugs are either semi-synthetic natural product derivatives or synthetic molecules in which the spirocenter is achiral. Thus, there remains a tremendous opportunity to exploit the biological capabilities of spirocycles in chemical biology and drug discovery, provided that the synthetic challenges associated with the stereoselective synthesis of these molecules can be overcame.

1.2 TOTAL SYNTHESES OF SPIROCYCLIC NATURAL PRODUCTS

In this section, recent representative developments made toward the synthesis of spirocyclic natural products are described. Most of these methods involve the synthesis of a densely functionalized core which needs multiple synthetic steps to obtain prior to setting the spirocenter. With insights from these total syntheses, one can conclude that a general approach to all classes of spirocycles is of great need in the chemical community. This dissertation hopes to establish a method that solves this need.

1.2.1 TOTAL SYNTHESIS OF HYPEROLACTONE C – SPIROETHER

In 2009, Du et al. completed the total synthesis of hyperlactone C through the efficient construction of two vicinal quaternary carbon centers.[25] The authors were able to accomplish this daunting task by using a palladium-catalyzed asymmetric allylic alkylation reaction. This strategy enabled the concise and efficient total synthesis of their desired natural product, hyperolactone C (depicted in **Scheme 1.1**) and also (–)-biyouyanagin A in overall 20% and 8% yields, respectively. Starting from methyl acetoacetate **1** and benzaldehyde, the authors synthesized **2** through the formation of a

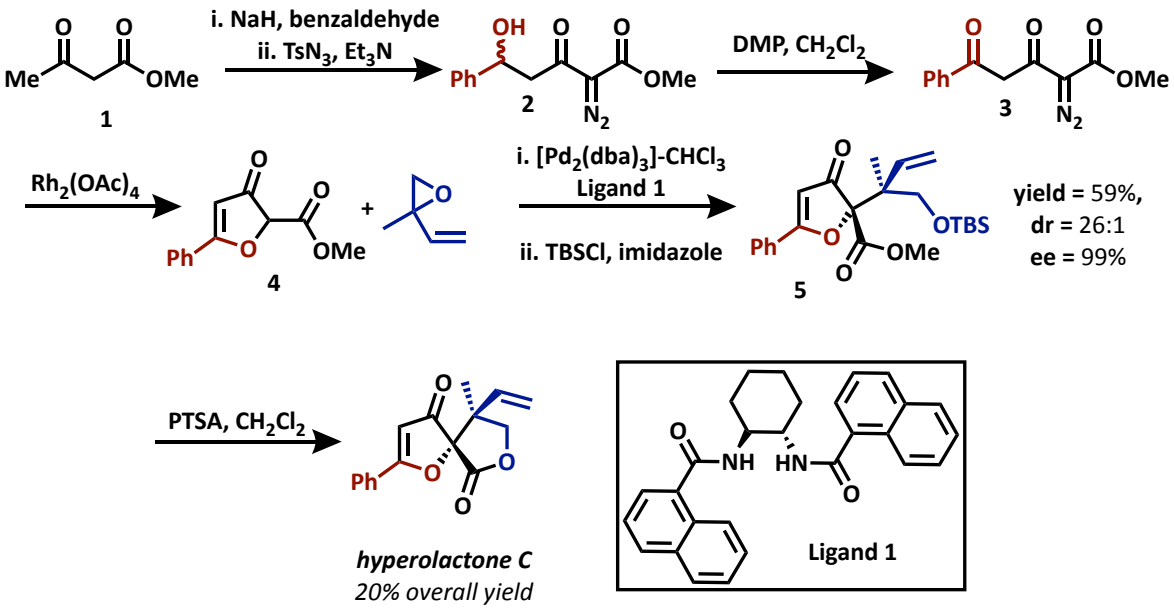

Scheme 1.1. *Total synthesis of hyperlactone C by Du et al.*

dianion followed by quenching with benzaldehyde. After diazotization with TsN_3 and oxidation with Dess-Martin periodinane, the authors obtained their desired α-diazo-β-ketoester **3**. This compound was cyclized through a Rh(II)-catalyzed intramolecular O–H

insertion of the enol-form of **3**. With this key intermediate in hand, a Pd(II) catalyzed allylic alkylation was conducted to set the desired quaternary centers with high stereoselectivity. The desired spirocenter was set through a lactonization reaction of **5** to obtain hyperolactone C.

1.2.2 TOTAL SYNTHESIS OF AMATHASPIRAMIDE F – AZASPIRO-RING SYSTEM

A unique [2,3]-Stevens rearrangement which was prompted by a palladium-catalyzed allylic amination gave way to the diastereoselective total synthesis of amathaspiramide F by Tambar and coworkers (**Scheme 1.2**).[26] The authors were interested in utilizing a diastereoselective [2,3]-Stevens rearrangement to construct the two contiguous stereocenters of the natural product prior to setting the desired spirocenter. An easily obtainable prenylated proline derivative **6** underwent an allylic alkylation using carbonate **7** under Pd(II) conditions. Intermediate **8** underwent an immediate rearrangement to the desired product **9** whose *N*-prenyl group was cleaved under olefin isomerization conditions. The desired intermediate **10** was treated with trifluoroacetic acid to conduct a global deprotection followed by treatment with $TMSCHN_2$ to furnish **11**. This intermediate was known in a previous total synthesis of amathaspiramide F and the spirocenter was set through ozonolysis of **11** followed by spirohemiaminal formation using $MeNH_2$ to obtain **13**. Four subsequent steps were necessary to obtain the desired natural product amathaspiramide F.

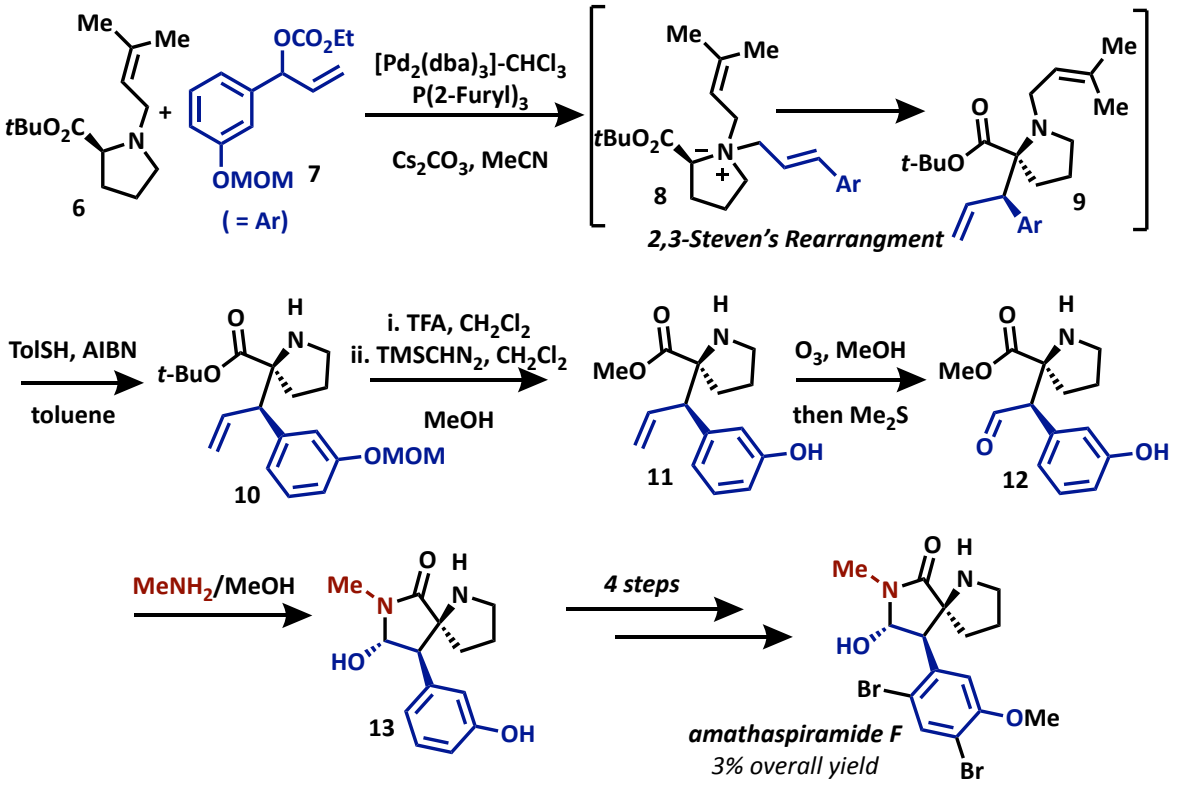

Scheme 1.2. *Total synthesis of amathaspiramide F completed by Tambar et al.*

1.2.2 TOTAL SYNTHESIS OF UBROGEPANT – SPIROCARBOCYCLE

A newly developed and highly economical synthetic route to the potent CGRP receptor agonist, ubrogepant, was developed recently in 2017 (**Scheme 1.3**).[27] Yasuda et al. were able to obtain the desired enantiomer of a key intermediate through chiral resolution using a phase transfer catalyst (PTC). The synthesis consisted of a condensation of **14** onto the azaindole **15**. Once the alkene was obtained from this reaction it was immediately reduced with $NaBH_4$ to provide **16**. Chlorination of this product provided **17** which was the intermediate needed to conduct the key spirocyclization. Under basic conditions in the presence of the phase transfer catalyst, the desired spirocyclization

occurred through an substitution reaction in 99.5% ee. With the optically pure spirocarbocycle **18** in hand, a palladium catalyzed carbonylation was conducted to synthesize carboxylic acid **19** which was then coupled with the pre-synthesized lactam (**20**) portion of the natural product. This synthesis successfully made over 100 kilograms of ubrogepant in an overall 43% yield.

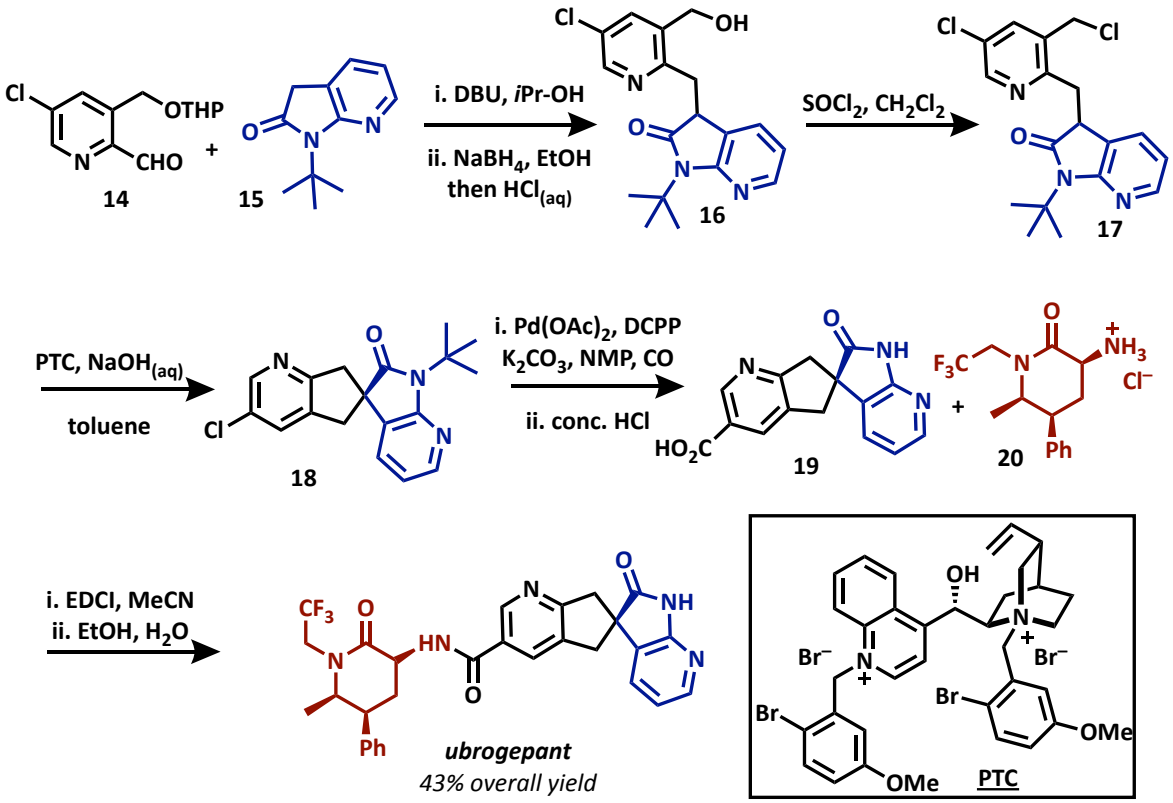

Scheme 1.3. *Total synthesis of ubrogepant by Yasuda et al.*

1.2.4 TOTAL SYNTHESIS OF BERKELIC ACID – SPIROKETAL

A gram scale total synthesis of berkelic acid was reported in 2012 by Fañanàs et al. from Spain (**Scheme 1.4**).[28] The authors had previously developed a palladium(II)-catalyzed one-pot three-component coupling reaction for the diastereoselective

construction of chroman spiroacetals which proceeded through the in situ formation of an *exo*-enol ether and *ortho*-quinonemethide. These two intermediates underwent a [4+2] annulation to form the desired products. This methodology was applied to the total synthesis of berkelic acid by starting with compound **22** and **23**. However, upon optimization it was realized that their desired spiroketalization could be achieved with Ag(I) catalysis instead of Pd(II) catalysis. After spiroketalization, the desired product was immediately reduced to give **24** to avoid decomposition of the unstable intermediate. Once this highly complex molecule underwent iodination only a few more straightforward synthetic steps were needed to make the natural product. Compound **25** underwent an umpolung alkylation in the presence of **26** and LDA. This reaction delivered the berkelic acid methyl ester which was exposed to selective benzylic ester cleavage to achieve the total synthesis of berkelic acid in a 38% overall yield.

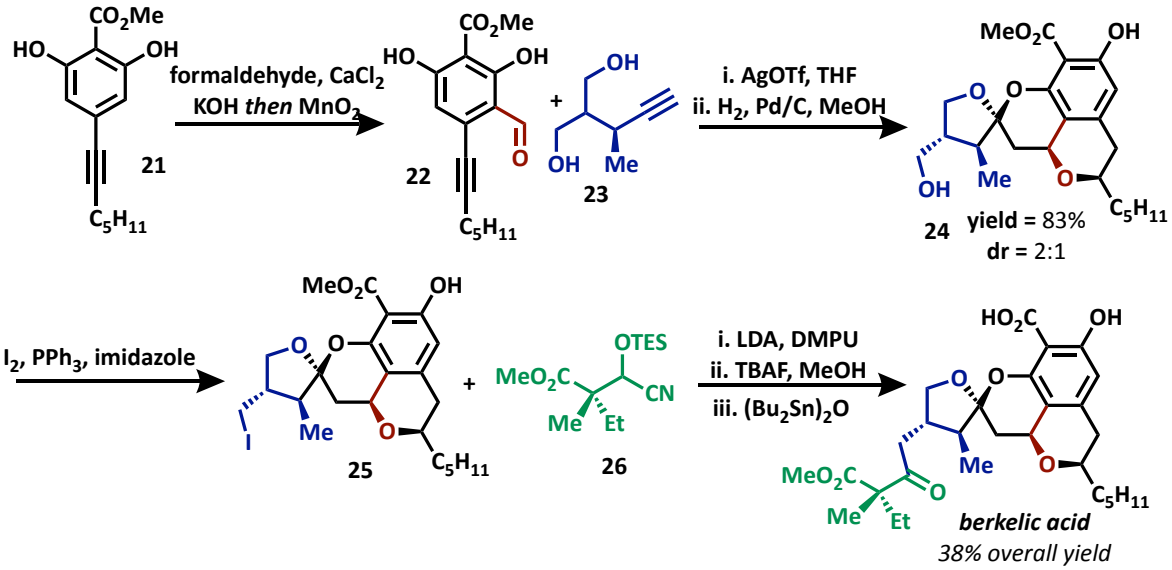

Scheme 1.4. *Total synthesis of berkelic acid by Fañanàs et al.*

1.3 GOALS OF THIS DISSERTATION

The representative synthetic efforts presented in the previous section were successful in achieving their respective molecules in an efficient and concise manner. However, the key spirocyclization step for each scaffold was extremely specific and thereby could not be applied in a general manner to obtain all classes of spirocycles. Envisaging a strategy to construct every class of spirocycle through similar retrosynthetic bond disconnections would aid the evolution of synthetic planning and reaction development for the construction of more complex and diverse chemical libraries for drug screening programs. With the desire to develop methodology in alignment with this strategy in our mind, we dissected spirocycles down the middle to create a simple and straightforward retrosynthetic design (**Figure 1.3**). This disconnection would provide convergent access to all classes of spirocycles if two ambiphilic reacting partners were used to convergently set the desired spirocenter. We hypothesized that through the use of metal carbenes derived from diazo compounds, a cascade reaction with a tethered nucleophile and electrophile could give access to a wide range of spirocycles. Therefore, *the goal of this dissertation is to successfully utilize metal carbene initiated cascade reactions to achieve the efficient synthesis of spirocyclic scaffolds.*

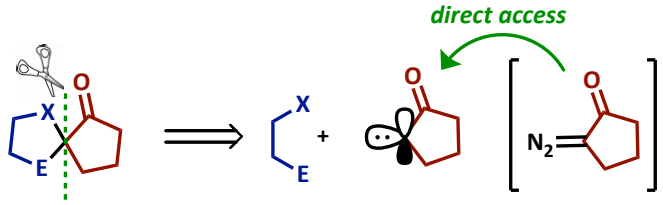

Figure 1.3. *Novel disconnection to spirocycles developed by Sharma Lab*

1.4 REFERENCES FOR CHAPTER 1

[1] M. G. Dickson, J. P., *Nat. Rev. Drug Discov.* **2004**, *3*, 417–429.

[2] a) A. Mullard, *Nat. Rev. Drug Discov.* **2014**, *13*, 877–877; b) J. A. H. DiMasi, R.W.; Grabowski, H.G., *J. Health Econ.* **2003**, *22*, 151–185.

[3] a) D. S. Lagorce, O.; Miteva, M.A.; Villoutreix, B.O., *In Silica Lead Discovery* **2011**, 01–19; b) R. A. W. Bauer, J.M.; Tan, D.S., *Curr. Opin. Chem. Biol.* **2010**, *14*, 308–314.

[4] a) R. A. Bauer, J. M. Wurst, D. S. Tan, *Curr. Opin. Chem. Biol.* **2010**, *14*, 308–314; b) P. A. Bartlett, M. Entzeroth, *Exploiting Chemical Diversity for Drug Discovery*, RSC Publishing, **2006**.

[5] I. Sharma, D. S. Tan, *Nat. Chem.* **2013**, *5*, 157–158.

[6] J. Hert, J. J. Irwin, C. Laggner, M. J. Keiser, B. K. Shoichet, *Nat. Chem. Biol.* **2009**, *5*, 479–483.

[7] R. S. Bohacek, C. McMartin, W. C. Guida, *Med. Res. Rev.* **1996**, *16*, 3–50.

[8] a) A. M. Boldi, *Combinatorial Synthesis of Natural Product-based Libraries*, CRC Press, **2006**; b) K. Grabowski, G. Schneider, *Curr. Chem. Biol.* **2007**, *1*, 115–127; c) J. Y. Ortholand, A. Ganesan, *Curr. Opin. Chem. Biol.* **2004**, *8*, 271–280.

[9] A. Ganesan, *Curr. Opin. Chem. Biol.* **2008**, *12*, 306–317.

[10] a) Y.-J. Zheng, C. M. Tice, *Expert Opin Drug Discov* **2016**, 1–4; b) Y. Zheng, C. M. Tice, S. B. Singh, *Bioorg. Med. Chem. Lett.* **2014**, *24*, 3673–3682.

[11] a) X.-H. Ding, W.-C. Cui, X. Li, X. Ju, D. Liu, S. Wang, Z.-J. Yao, *Tetrahedron Lett.* **2013**, *54*, 1956–1959; b) Z. W. Jiao, S. Y. Zhang, C. He, Y. Q. Tu, S. H. Wang, F. M. Zhang, Y.

Q. Zhang, H. Li, *Angew. Chem. Int. Ed.* **2012**, *51*, 8811–8815; c) S. Kotha, N. R. Panguluri, R. Ali, *Eur. J. Org. Chem.* **2017**, *2017*, 5316–5342; d) F. V. Singh, P. B. Kole, S. R. Mangaonkar, S. E. Shetgaonkar, *Beilstein J. Org. Chem.* **2018**, *14*, 1778–1805; e) H. Waldmann, A. Antonchick, S. Murarka, C. Golz, C. Strohmann, *Synthesis* **2016**, *49*, 87–95; f) X. Xie, W. Huang, C. Peng, B. Han, *Adv. Synth. Catal.* **2018**, *360*, 194–228; g) P.-W. Xu, J.-S. Yu, C. Chen, Z.-Y. Cao, F. Zhou, J. Zhou, *ACS Catal.* **2019**, *9*, 1820–1882.

[12] C. Marti, Erick M. Carreira, *Eur. J. Org. Chem.* **2003**, *2003*, 2209–2219.

[13] S. Rosenberg, R. Leino, *Synthesis* **2009**, 2651–2673.

[14] A. Bartoli, F. Rodier, L. Commeiras, J.-L. Parrain, G. Chouraqui, *Nat. Prod. Rep.* **2011**, *28*, 763–782.

[15] a) M. A. Perry, R. R. Hill, J. J. Leong, S. D. Rychnovsky, *Org. Lett.* **2015**, *17*, 3268–3271; b) G. Dake, *Tetrahedron* **2006**, *62*, 3467–3492; c) B. B. Snider, B. J. Neubert, *J. Org. Chem.* **2004**, *69*, 8952–8955.

[16] a) S. Peddibhotla, *Curr. Bioact. Compd.* **2009**, *5*, 20–38; b) C. V. Galliford, K. A. Scheidt, *Angew. Chem., Int. Ed.* **2007**, *46*, 8748–8758; c) A. K. Franz, N. V. Hanhan, N. R. Ball-Jones, *ACS Catal.* **2013**, *3*, 540–553.

[17] a) Q. Zheng, Z. Tian, W. Liu, *Curr. Opin. Chem. Biol.* **2016**, *31*, 95–102; b) F. M. Zhang, S. Y. Zhang, Y. Q. Tu, *Nat. Prod. Rep.* **2018**, *35*, 75–104.

[18] P. Bloch, C. Tamm, *Helv. Chim. Acta* **1981**, *64*, 304–315.

[19] M. Ishikawa, T. Ninomiya, H. Akabane, N. Kushida, G. Tsujiuchi, M. Ohyama, S. Gomi, K. Shito, T. Murata, *Bioorg. Med. Chem. Lett.* **2009**, *19*, 1457–1460.

[20] J. X. Min, G.; Sun, J., *J. Org. Chem.* **2017**, *82*, 5492–5498.

[21] Y. Aramaki, K. Chiba, M. Tada, *Phytochemistry* **1995**, *38*, 1419–1421.

[22] K. C. Nicolaou, S. Sanchini, D. Sarlah, G. Lu, T. R. Wu, D. K. Nomura, B. F. Cravatt, B. Cubitt, J. C. de la Torre, A. J. Hessell, D. R. Burton, *Proc. Natl. Acad. Sci. U. S. A.* **2011**, *108*, 6715–6720.

[23] M. Seitz, O. Reiser, *Curr. Opin. Chem. Biol.* **2005**, *9*, 285–292.

[24] K. L. White, A. P. Scopton, M.-L. Rives, R. V. Bikbulatov, P. R. Polepally, P. J. Brown, T. Kenakin, J. A. Javitch, J. K. Zjawiony, B. L. Roth, *Mol. Pharmacol.* **2014**, *85*, 83–90.

[25] C. Du, L. Li, Y. Li, Z. Xie, *Angew. Chem. Int. Ed. Engl.* **2009**, *48*, 7853–7856.

[26] A. Soheili, U. K. Tambar, *Org. Lett.* **2013**, *15*, 5138–5141.

[27] N. Yasuda, E. Cleator, B. Kosjek, J. Yin, B. Xiang, F. Chen, S.-C. Kuo, K. Belyk, P. R. Mullens, A. Goodyear, J. S. Edwards, B. Bishop, S. Ceglia, J. Belardi, L. Tan, Z. J. Song, L. DiMichele, R. Reamer, F. L. Cabirol, W. L. Tang, G. Liu, *Org. Process Res. Dev.* **2017**, *21*, 1851–1858.

[28] F. J. Fananas, A. Mendoza, T. Arto, B. Temelli, F. Rodriguez, *Angew. Chem. Int. Ed. Engl.* **2012**, *51*, 4930–4933.

CHAPTER 2

Identification of Rh(II)/Au(I)

Synergistic Cascade Catalysis

2.1 INTRODUCTION

Recently in the field of synthetic chemistry, synergistic cascade catalysis has become an effective method to install molecular complexity in methodology development and the total synthesis of natural products.[1] Synergistic catalysis is a mode of catalysis in which two catalysts and two catalytic cycles cooperatively work to create a new single bond.[2] This mode of catalysis provides opportunities to efficiently and selectively assemble molecules with high levels of molecular complexity when compared to mono-catalytic systems. In mono-catalysis one substrate is catalytically activated, altering the energy of only a single component of the reaction system. However, in synergistic catalysis both the HOMO and LUMO of the reacting system are concurrently activated using distinct catalysis, thereby creating two catalytic cycles that must simultaneously work together (**Figure 2.1**).[2b]

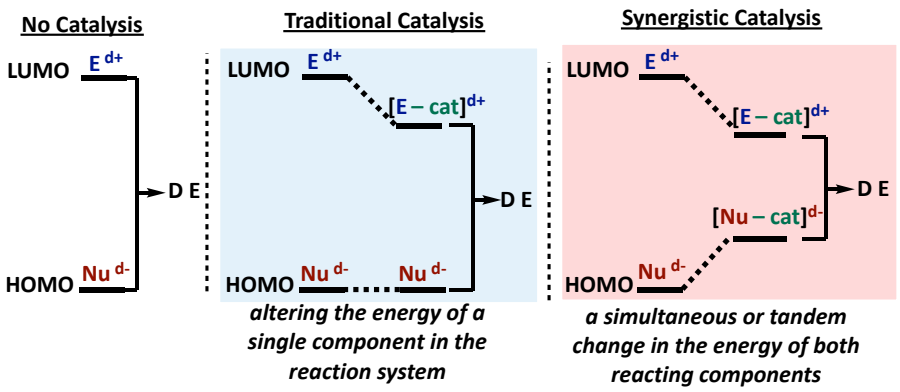

Figure 2.1. *The classification of synergistic catalysis and the difference between traditional catalytic systems.*

Synergistic catalysis enables transformations that are usually *impossible* or *inefficient* using traditional mono-catalytic systems. While there are many benefits to synergistic cascade catalysis, this mode of catalysis has been underexplored due to the difficulty in ensuring that the metal catalysts needed in the transformation are redox compatible in order to avoid catalyst deactivation. The development of synergistic catalytic cascades stands as a challenging feat in synthetic chemistry.[1c, 2a, 2b, 3] When nature implements synergistic catalysis, enzymes typically have the advantage of physical separation between catalytic sites within the enzyme.[3a] Conversely, in laboratory syntheses, the catalysts are free to interact with each other, thereby leading to the possibility of deactivation of both catalysts.[2b] However, it is important to note that the molecular freedom of each individual catalyst in the reaction system allows one to optimize the reaction easily through modification of individual catalysts separately.

Recently the use of diazo derived rhodium carbenes in synergistic catalysis has gained recognition in the chemical community. It has been widely known since the early 1970s that dirhodium(II) catalysts are the most effective catalysts for the formation of rhodium carbenes from diazo compounds due to the control of reactivity and selectivity that is induced by the bridging carboxylate ligands in the paddlewheel metal-ligand complex.[4] Rhodium carbenes are attractive partners for synergistic transformations due to their ease of formation, relative stability, controlled reactivity in typical catalytic reactions, and redox compatibility with a variety of transition metals.[5]

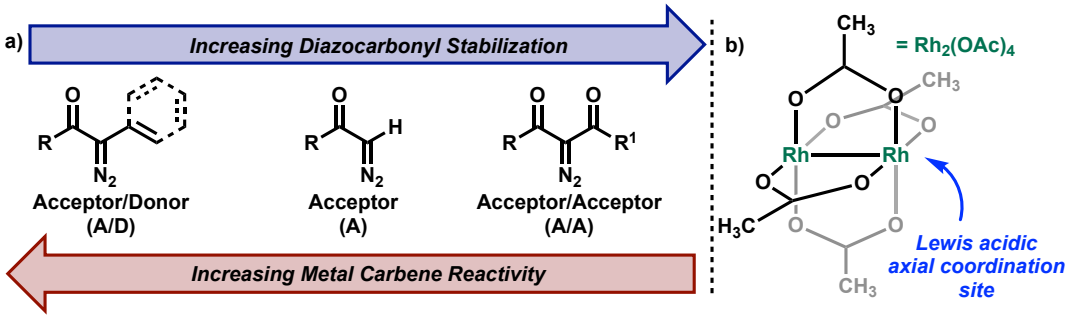

Figure 2.2. *a) Overview of diazocarbonyl stabilization and metal carbene reactivity; b) dirhodium(II) paddlewheel complex.*

Rhodium carbenes are typically formed from diazo compounds which are inherently unstable substrates. However, the stability of diazo compounds can be attenuated through substitution of proper electron withdrawing groups at the diazo functionality. Carbonyl compounds have been used throughout history as electron withdrawing groups to create stable "diazocarbonyl" compounds that are highly useful in synthetic transformations due to their ease of formation, relative stability, and controlled reactivity in catalytic reactions.

Diazocarbonyl compounds can be categorized into three subgroups: 1) acceptor/acceptor [A/A] - possessing two carbonyl groups, 2) acceptor [A] - possessing a single carbonyl group, 3) acceptor/donor [A/D] - possessing a single carbonyl group and a vinyl or aromatic group. The order of stability toward diazo decomposition and subsequent metal-carbene formation has A/D diazocarbonyls as the most reactive while A/A diazocarbonyls are the least reactive. However, in the case of metal carbene reactivity, this trend is reversed (**Figure 2.2a**).

Metal carbene formation from diazocarbonyls using dirhodium(II) catalysts proceeds through a unique mechanism. Dirhodium(II) catalysts have an open axial coordination site on each terminal end of the paddlewheel complex that serves as a Lewis acidic center (**Figure 2.2b**). This characteristic allows the catalyst to undergo electrophilic addition to the diazo compound at the α-carbon (**Scheme 2.1**). Subsequent loss of dinitrogen

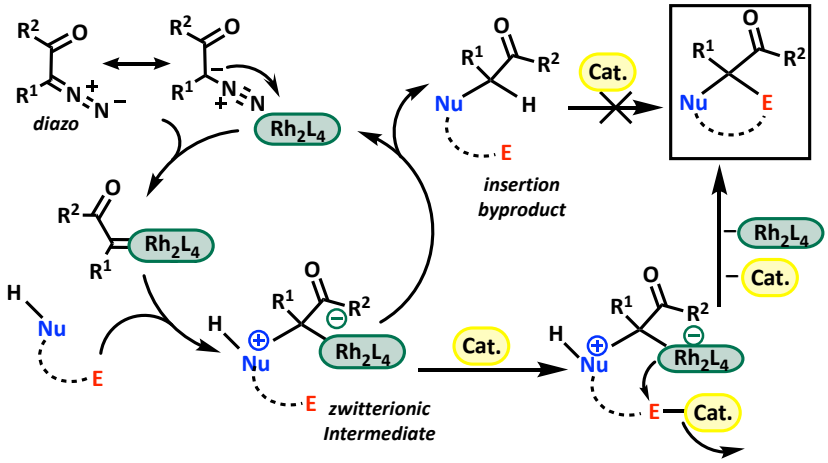

Scheme 2.1. *General mechanism for synergistic catalysis in rhodium carbene chemistry.*

from the rhodium-associated diazocarbonyl prompts formation of an electrophilic rhodium carbene intermediate. The rhodium carbene is transferred to a coupling partner and the catalyst is regenerated. Within this dissertation, the coupling partner is a "X–H" bond (X = O, N, S, sp^2-C). Upon X–H insertion into the rhodium carbene, a highly reactive zwitterionic intermediate is formed prior to catalyst extrusion. This zwitterionic intermediate has the ability to proceed down two different pathways: 1) undergo 1,2-proton transfer/protodemetalation to provide the formal X–H insertion product, or 2) be trapped by an adequately activated electrophilic species in a synergistic catalytic cascade (**Scheme 2.1**). The objective of this research is to understand the reactivity of rhodium carbenes and their application in synergistic cascade reactions where the active zwitterionic intermediate is trapped by an activated electrophilic species.

We hypothesized that in order to have a viable synergistic cascade, the initial step of the catalytic cycle must be proficient. Therefore, when initiating our studies toward the development of a synergistic catalytic cocktail for spirocyclizations, it was important to identify a catalyst that could efficiently decompose diazocarbonyls to produce a stable carbene intermediate that was able to undergo X–H (X = O, N, sp^2 C–H) insertions efficiently.

It was decided that optimization of the initial X–H insertion step would begin with A/A diazocarbonyls as our model substrates. A/A diazocarbonyls are important chemical building blocks in organic synthesis that are capable of novel transformations such as cyclopropanation, cyclopropenation, sp^3 and sp^2 C–H activations, and various cascade rearrangements.[6] Although these substrates have been applied in a wide variety of

transformations, their stability, requires harsh conditions in order to extrude N_2 and generate a metal carbene reactive species. These harsh conditions are not suitable for the development of synergistic catalytic cascades. Due to this limitation, the implementation of A/A diazocarbonyls in many cascade transformations is scarce.

When surveying the literature, it was observed that O–H insertion reactions of alcohols into A/A diazocarbonyls were thoroughly investigated. However, only a few examples of O–H insertion reactions of carboxylic acids had been reported in the literature (**Scheme 2.2**).[7] In 2005 Jørgensen et al. identified $Rh_2(OAc)_4$ as a catalyst for the O–H insertion of carboxylic acids into α-diazo-β-ketoesters (**Scheme 2.2a**).[7a] To enable the desired transformation, the reaction needed to be heated at 40 ºC for 16 hours to provide compound **1a** in a 75% yield. These conditions are not adequately efficient for use in a synergistic catalytic cascade. Later in 2011, Kitamura et al. identified $Pd(OAc)_2$ as an efficient catalyst for carboxylic acid O–H insertion into A/A diazocarbonyls (**Scheme 2.2b**).[7b] However, the reaction conditions necessitated the use of the carboxylic acid as solvent and a heightened temperature of 70 ºC. These conditions are extremely harsh when considering including an additional highly reactive organometallic intermediate for the development of a synergistic cascade. Most recently in 2014, Dong et al. identified a catalytic cocktail of $Cu(OAc)_2$ and isocyanide for the carboxylic acid O–H insertion into A/A diazocarbonyls (**Scheme 2.2c**).[7c] Although the identification of an earth abundant Cu(II) catalyst was appreciated by the chemical community, the need of the carboxylic acid as a solvent and the use of a reactive isocyanide made these conditions unsuitable for the

development of a synergistic cascade. Additionally, the reaction was conducted at 100 ºC, a temperature that initiates thermal decomposition for many organometallic complexes.

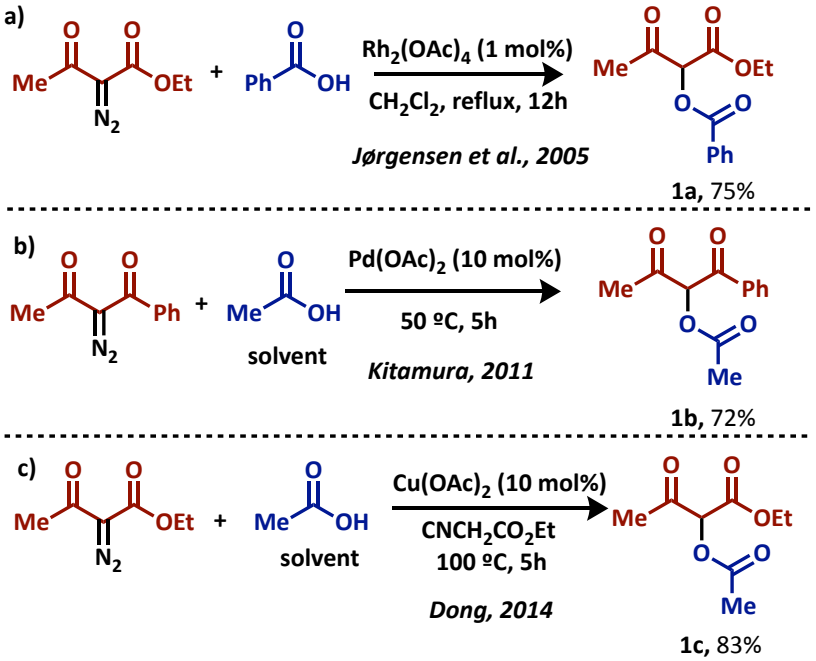

Scheme 2.2. *Previous methods for the carboxylic acid O–H insertion into metal carbenes.*

2.2 IDENTIFICATION OF "$Rh_2(esp)_2$" AS AN EFFICIENT CARBOXYLIC ACID O–H INSERTION CATALYST

2.2.1 INITIAL SCREENING OF CATALYTIC CONDITIONS

Confronted by the aforementioned limitations in reaction conditions we decided to develop reaction conditions that would enable the efficient O–H insertion of highly functionalized carboxylic acids into A/A diazocarbonyls. For the initial optimization diethyl diazomalonate **2a** and Boc-protected phenylalanine **3a** were selected as model substrates and exposed to the most efficient catalyst known in literature, $Rh_2(OAc)$ (**Table 2.1,** entry

1)$_4$.[7a] To our delight the desired insertion compound **4a** was obtained in 64% yield after stirring at room temperature for 12 hours. The Pd(II) conditions[7b] were also screened and after refluxing in dichloromethane for 8 hours, the desired compound was obtained in a

Table 2.1: *Optimization of Carboxylic O–H Insertion into A/A Diazocarbonyls*

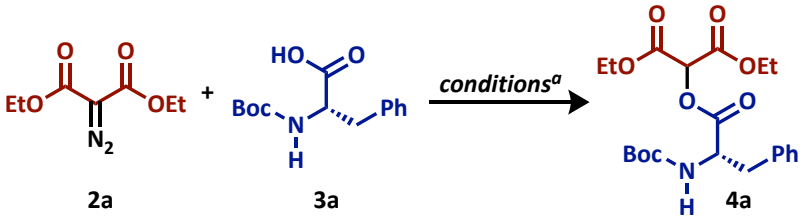

2a **3a** **4a**

entry	catalyst system	solvent, T (ºC), t	**4a** (yield%)[b]
1	$Rh_2(OAc)_4$	CH_2Cl_2, rt, 12h	64
2	$Pd(OAc)_2$	CH_2Cl_2, reflux, 8h	58
3	$Cu(OAc)_2$/ $CNCH_2CO_2Et$	DCE, reflux, 12h	55
4	$Rh_2(TFA^c)_4$	CH_2Cl_2, rt, 6h	46
5	$Rh_2(HFB^d)_4$	CH_2Cl_2, rt, 6h	67
6	**$Rh_2(esp)_2$**	**CH_2Cl_2, rt, 10 min**	**94**
7	-	TFE[e], reflux, 12h	NR
8	Hoveyda Grubbs2nd	CH_2Cl_2, reflux, 10h	40
9	$Cu(acac)_2$	DCE, reflux, 5h	62
10	$Cu(OAc)_2$	DCE, reflux, 5h	43

[a]All optimization reactions were performed with **2a** (1.5 equiv), **3a** (1 equiv) and catalyst (1 mol%). [b]Isolated yields after column chromatography. NR = no reaction; [c]TFA = trifluoroacetate; [d]HFB = heptafluorobutyrate; [e]TFE = trifluoroethanol.

mediocre 58% yield (**Table 1**, entry 2). Next the Cu(II) conditions[7c] were screened and after refluxing in dichloroethane for 12 hours, the desired compound was obtained in 55% yield (**Table 1,** entry 3).

Inspired by the preliminary efficiency and ambient reaction temperature of $Rh_2(OAc)_4$, we decided to screen more electrophilic Rh(II) catalysts (**Table 2.1,** entries 4–5). We hypothesized that through increasing the electrophilicity of the Rh(II) paddlewheel ligand-metal complex, an increased rate of diazo decomposition would occur[8], thereby enabling a more efficient transformation. The electrophilic catalysts $Rh_2(TFA)_4$ and $Rh_2(HFB)_4$, primed with trifluoroacetate (TFA) and heptafluorobutyrate (HFB) ligands respectively, decreased the time of the desired transformation to 6 hours with no significant change in yield from $Rh_2(OAc)_4$. However, to our surprise, $Rh_2(esp)_2$, which was developed by the Du Bois group for C–H amination[9], provided the desired compound at room temperature within minutes in an excellent 94% yield (**Table 2.1,** entry 6). Various other conditions were also screened such as trifluoroethanol as a solvent, the Hoveyda–Grubbs catalyst, and different Cu(II) catalysts, but these conditions were met with limited success or no reaction.

2.2.2 APPLICATION TO SUBSTRATE SCOPE

Encouraged by the identification of optimized conditions we undertook a thorough study of the substrate scope of the reaction. We began by examining diethyl diazomalonate and its applicability to a range of amino acids (**Scheme 2.3**). Sterically hindered Boc-protected proline inserted in a good 83% yield (**4b**). Next, the reaction showed high levels of chemoselectivity when Boc-protected serine, which possesses a free hydroxyl side chain,

† The work within Section 2.2 was published in 2016 as a featured cover article for *European Journal of Organic Chemistry,* see reference: **Hunter, A. C.**; Chinthapally, K.; Sharma, I., $Rh_2(esp)_2$: An Efficient Catalyst for O-H Insertion Reactions of Carboxylic Acids into Acceptor/Acceptor Diazo Compounds. *Eur. J. Org. Chem.* **2016,** *2016* (13), 2260–2263.

gave the desired compound **4c** in 74% yield. The undesired double insertion into the free hydroxyl sidechain (highlighted in orange) of **4c** was only observed in a minimal 18% yield. After that, we screened Boc-protected tryptophan that has highly electron rich and reactive C–sp^2 and N–H indole centers. The varying electron rich reactive sites of the indole moiety had little effect on the efficiency of the transformation, producing the desired compound **4d** in 62%.

After screening different amino acids, a wide variety of carboxylic acids with differing functionality were also studied. Aliphatic carboxylic acids underwent the desired transformation efficiently (**4e–4f**). Next we screened alkynyl- and alkenyl-carboxylic acids that are primed with functionality known to undergo cyclopropenation and cyclopropanation[60] in the presence of Rh(II) carbenes. These carboxylic acids underwent the desired transformation efficiently to give the alkynyl substrate **4g** in 94% yield and the alkenyl substrates **4h** and **4i** in 90% and 93% yields, respectively. Lastly, we screened the electronic effects of aryl substituents on the reactivity of various benzoic acids. Benzoic acid produced the desired compound **4j** in 87% yield. However, the decreased nucleophilicty of 4-nitrobenzoic acid had a resounding effect on the efficiency of the reaction. The desired product **4k** was produced in a lessened 69% yield and a slow addition of diethyl diazomalonate via syringe pump was needed in order to avoid unproductive decomposition of the diazocarbonyl. Conversely, the electron-rich 4-methoxybenzoic acid was highly reactive and provided the desired insertion product **4l** in an excellent 94% yield. Finally, as another probe for chemoselectivity, we screened salicylic acid which has a free phenolic O–H. The desired carboxylic acid O–H insertion product **4m** was obtained in an

excellent yield with no production of the double insertion product into the free phenolic O–H in **4m**.

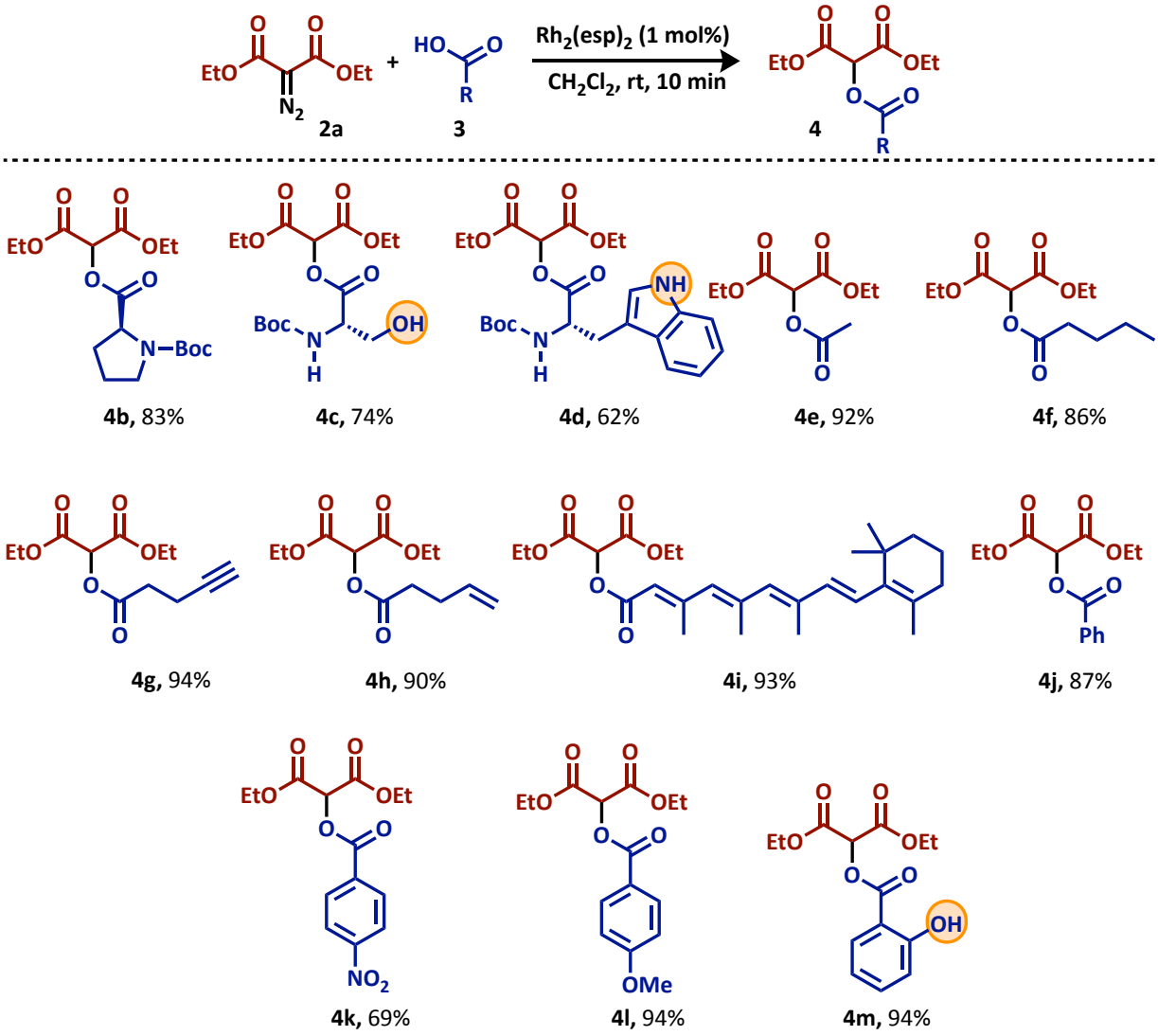

Scheme 2.3. *Scope of $Rh_2(esp)_2$-catalyzed room temperature O–H insertion reactions of carboxylic acid in diethyldiazomalonates.*

Once we completed screening of various carboxylic acids, we examined the applicability of numerous diazocarbonyls (**Scheme 2.4**). The bulky dibenzyl diazomalonate,

primed with benzylic C–H bonds susceptible to intramolecular sp^3–C activation, underwent the desired transformation to provide **4n** in 83% yield. The highly stable α-diazo-β-amidoesters provided the desired insertion compounds **4o** and **4p** in 73% and 96% yields respectively. The α-diazo-β-ketoester and α-diazo-1,3-diketone substrates efficiently provided compounds **4q** in 86% yield and **4r** in 85% yield. Next, the cyclic A/A diazocarbonyl, 1,3-indanone diazo, provided **4s** in 73% yield, however, a longer reaction time of 3 hours was needed due to this diazocarbonyls increased stability.

As a final effort in expanding the substrate scope, we investigated whether these conditions could apply to A/D and A-diazocarbonyls (**Scheme 2.4**). *N*-methyl isatin diazo and free N–H isatin diazo both underwent the desired transformation to provide oxindole scaffolds **4t** and **4u** in 82% and 78% yields. Lastly, commercially available ethyldiazoacetate gave the desired compound **4v** in 78% yield.

The identification of $Rh_2(esp)_2$ as an efficient catalyst for the O–H insertion of carboxylic acids into a wide variety of diazocarbonyls provided us with reaction conditions that are mild, efficient and highly chemoselective in the presence of alkenes, alkynes, hydroxyl and phenolic O–H's, and electron rich arenes. The characteristics of this catalytic system were ideal for application in a synergistic catalytic cascade, which was the next feat in our research efforts.

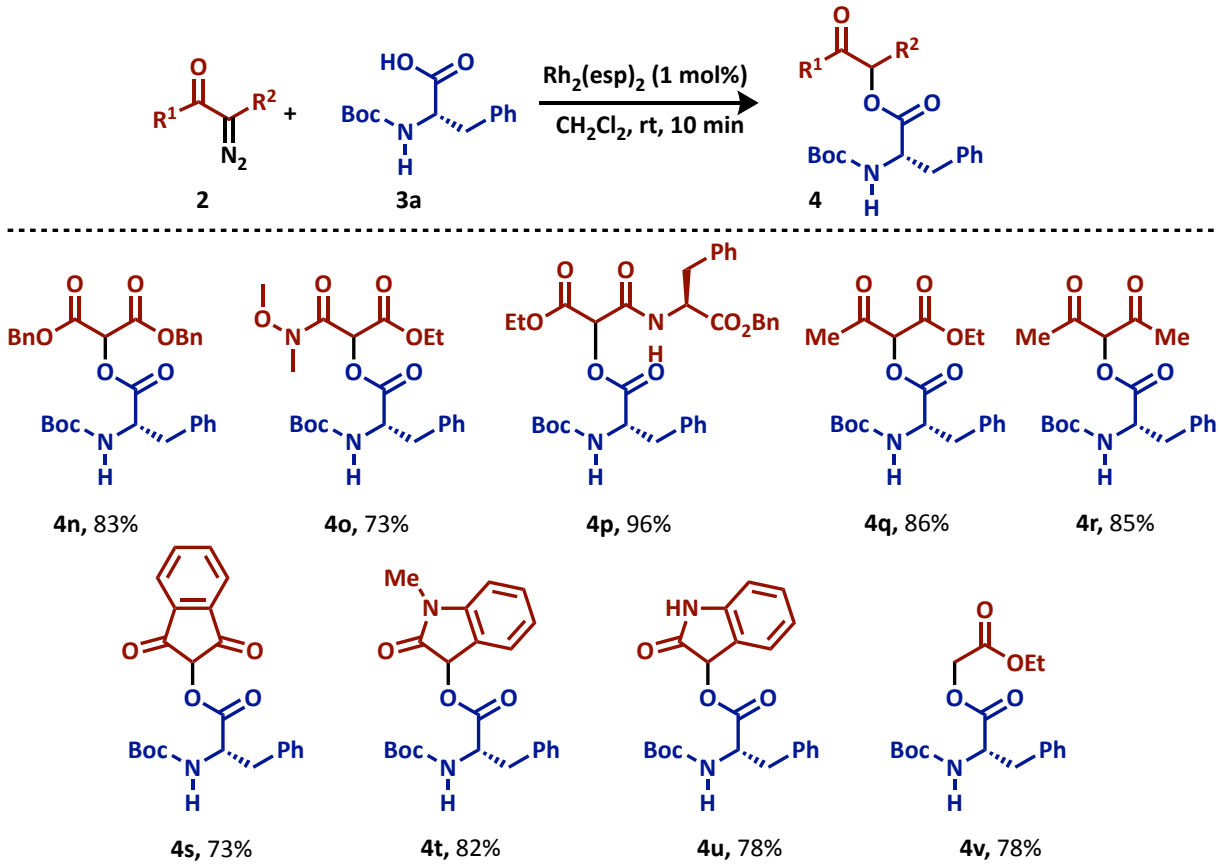

Scheme 2.4. *Scope of $Rh_2(esp)_2$-catalyzed room temperature O–H insertion reactions of Boc-proctected phenylalanine into various diazocarbonyls*

2.3 INDENTIFICATION OF "$Rh_2(esp)_2$" AND "PPh_3AuOTf" FOR O–H INSERTION/CONIA-ENE SYNERGISTIC CASCADES†

During the identification of $Rh_2(esp)_2$ as a highly efficient catalyst for the O–H insertion of carboxylic acids into diazocarbonyls[10], we observed an unexpected side product **5a** during the insertion of 3-butynoic acid into methylbenzoylacetate diazo. This γ-butyrolactone, produced in < 5% yield, formed presumably from the Rh(II) catalyzed Conia-

ene cyclization of the zwitterionic intermediate that formed during the O–H insertion reaction (**Scheme 2.5**).

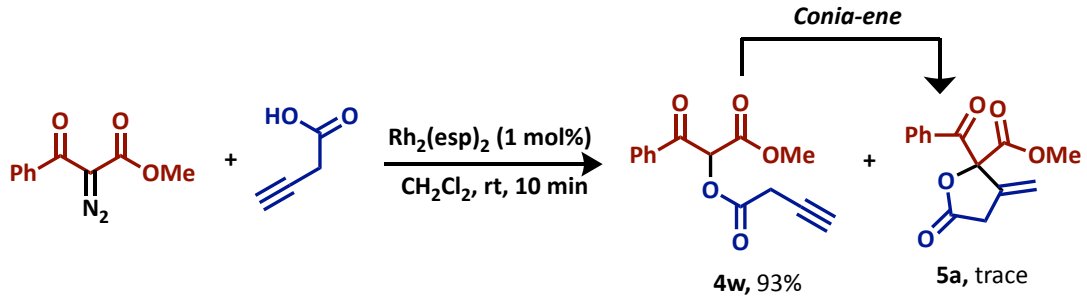

Scheme 2.5. *Preliminary observation of Rh(II)-catalyzed Conia-ene cyclization to form* ***5a*** *in trace amounts.*

This observation allowed us to hypothesize a direct method for the formation of γ-butyrolactones from readily available homo-propargylic acids and diazocarbonyl compounds.[11] If we were able to stabilize the zwitterionic intermediate while simultaneously activating the alkyne moiety through addition of an appropriate Lewis acid, we could promote a one-pot O–H insertion/Conia-ene cascade through synergistic catalysis. The design of cascade reactions, such as this, can provide novelty and efficiency in a synthetic strategy that would typically require multiple individual reaction steps to achieve.[2b] Although the carboxylic acid O–H insertion into diazocarbonyls and the Conia-ene cyclization are known individually, their existence in concerted synergism was previously unreported, thereby providing us with the opportunity to make a novel advancement in the field of synthetic chemistry.

2.3.1 SCREENING OF LEWIS ACIDS FOR STEPWISE CONIA-ENE CYCLIZATION

To begin our work, we decided to optimize the individual Conia-ene cyclization of α-acyloxy diazocarbonyl compound **4w** to form γ-butyrolactone **5a** (**Table 2.2**). Similar to the hypothesis that led to the identification of $Rh_2(esp)_2$ as an efficient catalyst for O–H insertion of carboxylic acids into diazocarbonyls, we believed it was necessary to also identify a highly efficient catalyst for the stepwise Conia-ene cyclization if we hoped to create an efficient synergistic catalytic cascade.

For the initial optimization, **4w** was exposed to a variety of conditions known in literature to promote Conia-ene cyclizations (**Table 2.2**).[12] When exposed to Zn(II) salts, $ZnCl_2$ and $Zn(OTf)_2$, the reaction was extremely sluggish and after 20 hours at room temperature the conversion of these reactions did not reach above 15% (**Table 2.2,** entries 1–2). Next, we screened copper salts $Cu(OTf)_2$ and $(CuOTf)_2$-toluene (**Table 2.2,** entries 3–4). While Cu(II) triflate provided a negligible 14% conversion after 20 hours at room temperature, the more active Cu(I) triflate gave 100% conversion after 20 hours at room temperature. Other metal salts such as $Pd(OAc)_2$, $Yb(OTf)_3$, $In(OTf)_3$, and PPh_3AuCl were screened, but none of them provided 100% conversion. Lastly, taking inspiration from Toste's seminal identification of cationic Au(I) for the Conia-ene cyclization of β-ketoesters with alkynes[13], we exposed **4w** to a mixture of $AgOTf/PPh_3AuCl$ at room temperature (**Table 2.2**, entry 10). In under 2 hours, these conditions provided complete conversion of **4w** into **5a**.

---

† The work within Section 2.3 was published in 2016 in *Chemistry a European Journal,* see reference: **Hunter, A.C.;** Schlitzer, S.C.; Sharma, I., Synergistic Diazo-OH Insertion/Conia-Ene Cascade Catalysis for the Stereoselective Syntheis of γ-Butyrolactones and Tetrahydrofurans. *Chem. Eur. J.* **2016,** *22*(45), 16062–16065.

***Table 2.2**: Optimization of Step-wise Conia-ene Cyclization*

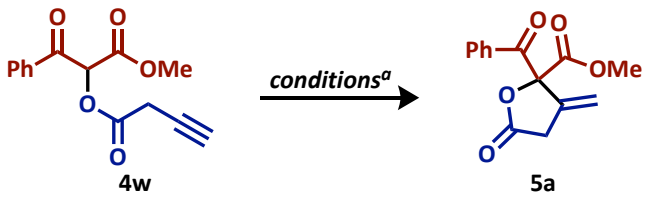

4w **5a**

entry	Lewis acid	solvent, T (ºC), t	**4a** (%conversion)[b]
1	$ZnCl_2$	CH_2Cl_2, rt, 20 h	12
2	$Zn(OTf)_2$	CH_2Cl_2, rt, 20 h	9
3	$Cu(OTf)_2$	CH_2Cl_2, rt, 20 h	14
4	$(CuOTf)_2$.tol	CH_2Cl_2, rt, 20 h	100
5	$Pd(OAc)_2$	CH_2Cl_2, rt, 20 h	77
6	$Yb(OTf)_3$	CH_2Cl_2, rt, 20 h	10
7	$In(OTf)_3$	CH_2Cl_2, rt, 20 h	41
8	AgOTf	CH_2Cl_2, rt, 20 h	27
9	PPh_3AuCl	CH_2Cl_2, rt, 20 h	18
10	**AgOTf/PPh_3AuCl**	**CH_2Cl_2, rt, 2 h**	**100**

[a]All optimization reactions were performed with 0.2M solution of **3a**, Lewis acid (10 mol%) and 4 Å molecular sieves; [b]Conversion (%) was determined from the crude ^{1}H NMR spectrum.

After establishing the optimized conditions for the Conia-ene cyclization, we decided to study the possibility of a tandem synergistic Rh(II)/Au(I) catalyzed O–H insertion/Conia-ene cascade (**Table 2.3**). For the initial optimization, 3-butynoic acid and 1 mol% of $Rh_2(esp)_2$ were mixed with 10 mol% of PPh_3AuOTf in dichloromethane and allowed to stir for 5 minutes at room temperature. Next, a solution of the diazo was added to the reaction dropwise over 1 minute and immediate emittance of N_2 was observed. The desired product **5a** formed instantly (under 1 minute) without any trace of the insertion product **4w** observed. This reaction was repeated with a decreased loading of 1 mol% of PPh_3AuOTf,

and the reaction was found to be equally efficient. However, a 10 mol% catalytic loading of PPh_3AuOTf was used for future reactions due to ease of experiment set up.

Table 2.3: *Optimization of Synergistic O–H Insertion/Conia-ene Cascade*

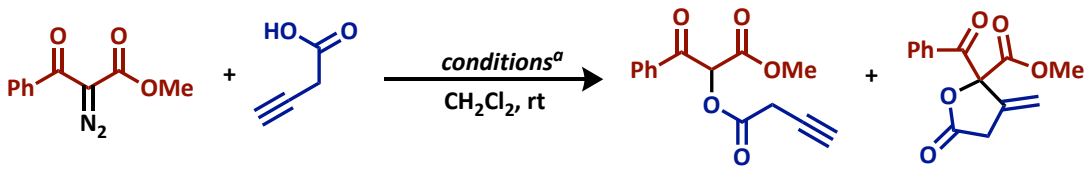

entry	Rh(II)/Lewis acid	time[b]	3a:4a[c]
1	**$Rh_2(esp)_2$/AgOTf/PPh_3AuCl**	**Instant**	**0:100**
2	**$Rh_2(esp)_2$/AgOTf/PPh_3AuCl[d]**	**Instant**	**0:100**
3	$Rh_2(OAc)_4$/AgOTf/PPh_3AuCl	5 h	44:56[e]
4	$Rh_2(TFA)_4$/AgOTf/PPh_3AuCl	2.5 h	38:62
5	$Rh_2(HFB^f)_4$/AgOTf/PPh_3AuCl	2.5 h	41:59
6	$Rh_2(esp)_2$/$(CuOTf)_2$.tol	10 min	93:7
7	$Rh_2(esp)_2$/AgOTf	10 min	93:7
8	$Rh_2(esp)_2$/PPh_3AuCl	10 min	96:4
9	AgOTf/PPh_3AuCl	10 min	0:0[g]

[a]All optimization reactions were performed in 0.1 M CH_2Cl_2 with **1a** (1.20 equiv.), **2a** (1 equiv.), Rh_2L_4 (1 mol%), and Lewis acids (10 mol%) along with 4 Å molecular sieves; [b]time required for the complete consumption of **1a**; [c]Conversion (%) was determined from the crude ^1H NMR spectrum; [d]AgOTf/PPh_3AuCl (1 mol%) was used; [e]6-*endo*-dig product was also observed; [f]HFB = heptafluorobutyrate; [g]5-*endo*-dig lactonization to form furan-2(3H)-one.

To follow, we screened other Rh(II) catalysts known for OH insertion into diazocarbonyls in the presence of PPh_3AuOTf (**Table 2.3**, entries 35). It was observed that none of these catalysts had a synergistic effect with PPh_3AuOTf as observed with $Rh_2(esp)_2$. Each catalyst ($Rh_2(OAc)_4$, $Rh_2(TFA)_4$, and $Rh_2(HFB)_4$) provided ratios of **4w** to **5a** after

multiple hours of reaction time. This study highlighted the importance and necessity of $Rh_2(esp)_2$ in the synergistic catalytic cascade. Next, we screened $Rh_2(esp)_2$ with various Group 11 metals (Cu(I), Au(I) alone, Ag(I) alone) and these combinations provided negligible amounts of conversion to the cyclized product **5a** (**Table 2.3,** entries 68). Lastly, we decided to negate $Rh_2(esp)_2$ from the reaction mixture to determine if PPh_3AuOTf was active enough to catalyze the entire transformation on its own (**Table 2.3**, entry 9). However, to our surprise, premixing of 3-butynoic acid with PPh_3AuOTf resulted in the formation of furan-2(3H)-one presumably via a 5-*endo*-dig-lactonization prior to the addition of the diazocarbonyl. The culmination of these studies suggest that this catalyst system is extremely specific, novel, and effective in the O–H insertion/Conia-ene cascade.

2.3.2 APPLICATION TO SUBSTRATE SCOPE

Once the optimized conditions were identified and thoroughly studied, we began to explore the generality of this transformation with differing A/A diazocarbonyls to provide a variety of γ-butyrolactones (**Scheme 2.6**). Increasing the bulk of the ester group to *tert*-butyl slightly decreased the yield of **5b** to 73%. The diazo derived from ethylacetoacetate, which possesses a methylene group active toward intramolecular C–H activation[14], provided **5c** in 76% yield. Lastly, the highly reactive diazo derived from pentane-2,4-dione gave **5d** in a 76% yield also. Next, we screened the same diazocarbonyls with the corresponding 3-butynol for a hydroxyl-OH insertion/Conia-ene cascade, and the reaction was observed to be equally efficient to provide a range of tetrahydrofurans (**5e**–**5h**).

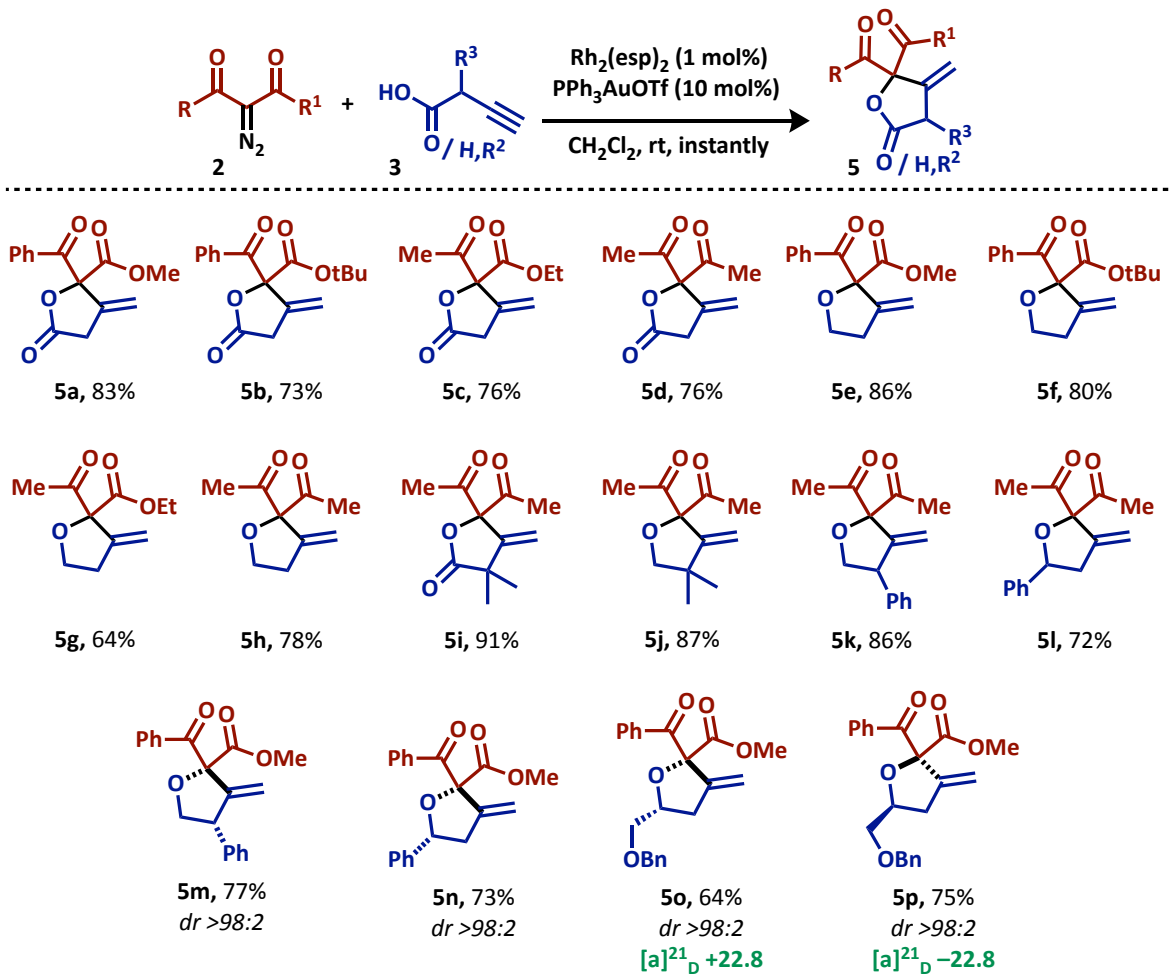

Scheme 2.6. *Scope of $Rh_2(esp)_2$/PPh_3AuOTf catalyzed O–H insertion/Conia-ene cyclization for the synthesis of γ-butyrolactones and tetrahydrofurans.*

Subsequently, we began to investigate substituents on the alkynoic acids and alkynols. Sterically hindered carboxylic acids and the corresponding neo-pentyl alcohol afforded the corresponding γ-butyrolactone **5i** in 91% yield and tetrahydrofuran **5j** in 87% yield. Mono-substituted alcohols with phenyl groups also participated in the reaction efficiently (**5k**–**5l**) and when exposed to unsymmetrical diazocarbonyls the corresponding products were obtained as single diastereomers (**5m**–**5n**). Lastly, when the enantiopure *R*-

and *S*- isomers of an alcohol were used in two separate transformations with the same diazo, **5o** and **5p** were produced as single diastereomers. When their optical rotations were taken, they were observed to be equal and opposite, proving that the pair were enantiomers. This study shows that we are able to induce asymmetry in this transformation using a chiral pool for our nucleophiles.

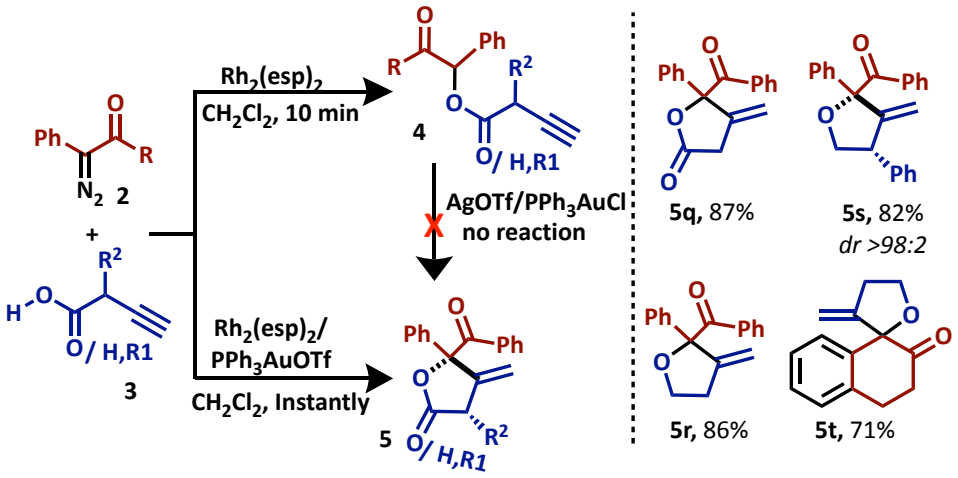

Scheme 2.7. *Scope of $Rh_2(esp)_2$/PPh_3AuOTf catalyzed O–H insertion/Conia-ene cascade using A/D diazos. The corresponding insertion compounds (**4**) are unable to undergo stepwise cyclization to form the cyclic scaffolds.*

To further probe the generality of this transformation we exposed alkynoic acids and alkynols to A/D diazos in the presence of our Rh(II)/Au(I) catalyst system (**Scheme 2.7**). When 3-alkynoic acid was exposed to 2-diazo-1,2-diphenylethan-1-one in the presence of our optimized conditions, the desired γ-butyrolactone **5q** was isolated in 87% yield. The same diazo was then exposed to 3-butynol and provided the desired tetrahydrofuran **5r** in 86% yield. When a substituted alkynol was used in the same transformation, the reaction

was observed to be diastereoselective (**5s**). Lastly, 2-tetralone diazo, which is a cyclic A/D diazocarbonyl, provided the desired spiroether **5t** in 71% yield.

2.3.3 MECHANISTIC INSIGHTS

For mechanistic insights into the reactivity of A/D diazocarbonyls in this system, we decided to synthesize the insertion compounds from each of the aforementioned A/D diazocarbonyls. When these substrates were exposed to PPh_3AuOTf in a stepwise fashion there was no observed Conia-ene cyclization even after reacting for 12 hours. This observation proved that the synergism of Rh(II)/Au(I) was necessary to invoke the desired transformation with A/D diazocarbonyls.

Next, to gain a deeper level of understanding for this transformation, non-terminal homopropargylic acid **3w** was subjected to the stepwise and synergistic catalysis conditions (**Scheme 2.8**). However, under the synergistic Rh(II)/Au(I) condition we did not observed any insertion or Conia-ene product. Instead we observed a completely unexpected [3.1.0]-fused ring system **7** as the exclusive product and single diastereomer (**Scheme 2.9**). The product forms presumably through the stereoselective cyclopropanation of the resulting unsaturated furanone that is produced when 3-pentynoic acid was premixed with the catalyst solution via a 5-*endo*-dig lactonization. It is important to note that non-terminal homopropargylic acids self-lactonize at a rate 5x faster than the terminal 3-butynoic acid.[15]

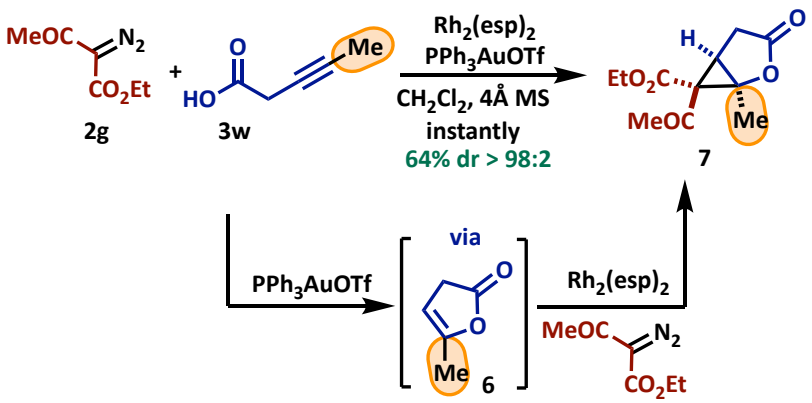

Scheme 2.8. *Limitation of synergistic transformation when applied to non-terminal alkynes.*

Lastly, to further substantiate our observations, we conducted ^{1}H and ^{13}C NMR experiments for mechanistic insights. When 3-butynoic acid was exposed to $Rh_2(esp)_2$ alone, there was an observed loss of the carboxylic acid proton H_A (**Figure 2.3**). When 3-butynoic acid was mixed with a stoichiometric amount of $Rh_2(esp)_2$/AgOTf/PPh_3AuCl in CD_2Cl_2 at room temperature, alongside disappearance of H_A, we also observed a complete loss of the alkyne proton H_C within minutes and formation of a new proton in the alkene region (5.82 ppm) having coupling with the H_B protons. This suggests the formation of a gold acetylide/gold vinylidene as the reactive intermediate.[16] When the acid was exposed to either Rh/Ag or Rh/Au alone there was no distinct proton losses observed that differed from what was seen with $Rh_2(esp)_2$ alone. Lastly, when the acid was exposed to AgOTf/PPh_3AuCl without $Rh_2(esp)_2$ present, furan-2(*3H*)-one was observed via 5-endo-dig lactonization.

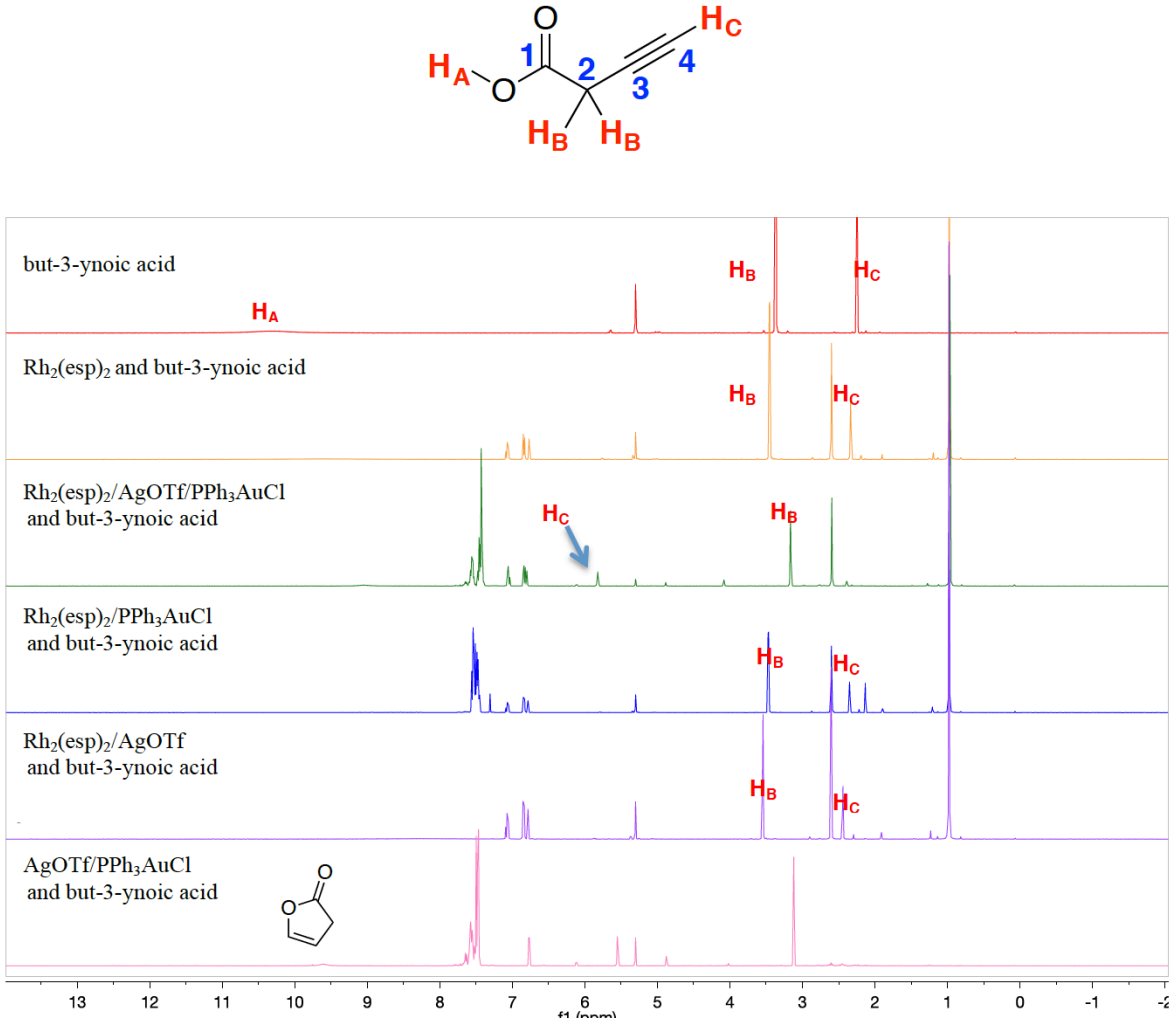

Figure 2.3. *NMR experiments for mechanistic insights*

These findings, alongside the other mechanistic insights, allowed us to propose a reaction mechanism wherein upon formation of a dually activated zwitterionic intermediate a Conia-ene cyclization occurs. However, when added in a stepwise fashion Rh(II) and Au(I) work independently of each other without exerting any synergistic effect (**Scheme 2.9**).

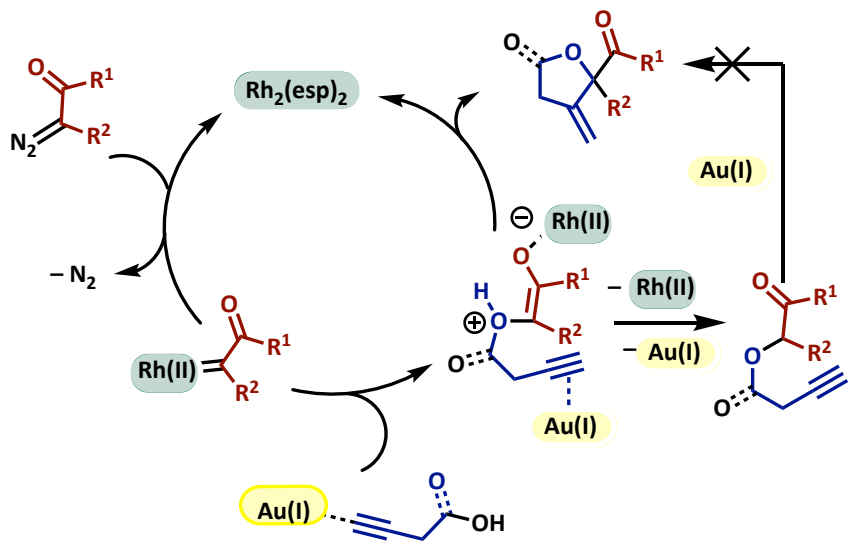

Scheme 2.9. *Proposed mechanism for the synergistic transformation*

2.4 SUMMARY

After completion of this work we have developed strategies to prepare *a*-acyloxy carbonyl scaffolds, *y*-butyrolactones, and tetrahydrofurans from readily available starting materials. We have also identified two novel catalytic systems that were critical to our success: 1) $Rh_2(esp)_2$ as a single catalyst for the efficient insertion of carboxylic acids into A/A diazocarbonyls[10] and 2) $Rh_2(esp)_2$/PPh_3AuOTf as a synergistic catalytic combination for the O–H insertion/Conia-ene cascade.[17] The reactivity and stereoselectivity of the O–H insertion/Conia-ene cascade was proven to be quite general and even expanded to substrates that were unable to undergo the corresponding stepwise transformation, thereby proving the synergism of the Rh(II)/Au(I) catalyst system.

2.5 REFERENCES FOR CHAPTER 2

[1] **For insights into cascade catalysis in organic synthesis:** a) K. C. Nicolaou, D. J. Edmonds, P. G. Bulger, *Angew. Chem. Int. Ed. Engl.* **2006**, *45*, 7134–7186; b) T. Newhouse, P. S. Baran, R. W. Hoffman, *Chem. Soc. Rev.* **2009**, *38*, 3010–3021; c) K. C. Nicolaou, J. S. Chen, *Chem. Soc. Rev.* **2009**, *38*, 2993–3009.

[2] **For reviews on synergistic catalysis:** a) J. J. Hirner, Y. Shi, S. A. Blum, *Acc. Chem. Res.* **2011**, *44*, 603–613; b) A. E. Allen, D. W. Macmillan, *Chem. Sci.* **2012**, *2012*, 633–658; c) Y. B. Huang, J. Liang, X. S. Wang, R. Cao, *Chem. Soc. Rev.* **2017**, *46*, 126–157; d) D. R. Pye, N. P. Mankad, *Chem. Sci.* **2017**, *8*, 1705–1718.

[3] **For recent applications of synergistic catalysis in methodology development:** a) S. Yang, K. H. Rui, X. Y. Tang, Q. Xu, M. Shi, *J. Am. Chem. Soc.* **2017**, *139*, 5957–5964; b) P. Basnet, S. Kc, R. K. Dhungana, B. Shrestha, T. J. Boyle, R. Giri, *J. Am. Chem. Soc.* **2018**, *140*, 15586–15590; c) M. Meazza, V. Polo, P. Merino, R. Rios, *Org. Chem. Front.* **2018**, *5*, 806–812; d) W. Xu, J. Ma, X. A. Yuan, J. Dai, J. Xie, C. Zhu, *Angew. Chem. Int. Ed. Engl.* **2018**, *57*, 10357–10361; e) L. Wei, S. M. Xu, Q. Zhu, C. Che, C. J. Wang, *Angew. Chem. Int. Ed. Engl.* **2017**, *56*, 12312–12316.

[4] M. P. Doyle, M. A. McKervey, T. Ye, *Modern Catalytic Methods for Organic Synthesis with Diazo Compounds*, John Wiley & Sons, **1998**.

[5] **For reviews of metal carbenes:** a) M. P. Doyle, in *Metal Carbenes in Organic Synthesis*, **2004**, pp. 203–222; b) H. M. Davies, J. R. Denton, *Chem. Soc. Rev.* **2009**,

38, 3061–3071; c) A. Padwa, *Chem. Soc. Rev.* **2009**, *38*, 3072–3081; d) D. Xing, W. Hu, *Tetrahedron Lett.* **2014**, *55*, 777–783.

[6] **For insights into different transformations involving diazocarbonyls:** a) J. F. Briones, H. M. L. Davies, *Org. Lett.* **2011**, *13*, 3984–3987; b) Z.-Y. Cao, Y.-H. Wang, X.-P. Zeng, J. Zhou, *Tetrahedron Lett.* **2014**, *55*, 2571–2584; c) H. M. L. Davies, J. R. Denton, *Chem. Soc. Rev.* **2009**, *38*, 3061-3071; d) H. M. L. Davies, D. Morton, *Chem. Soc. Rev.* **2011**, *40*, 1857–1869; e) H. M. L. Davies, J. Nikolai, *Org. Biomol. Chem.* **2005**, *3*, 4176–4187; f) H. M. L. Davies, S. A. Panaro, *Tetrahedron* **2000**, *56*, 4871–4880; g) A. Ford, H. Miel, A. Ring, C. N. Slattery, A. R. Maguire, M. A. McKervey, *Chem. Rev. (Washington, DC, U. S.)* **2015**, *115*, 9981–10080; h) X. Guo, W. Hu, *Acc. Chem. Res.* **2013**, *46*, 2427–2440; i) M. Hu, C. Ni, J. Hu, *J. Am. Chem. Soc.* **2012**, *134*, 15257–15260; j) Y. Jie, P. Livant, H. Li, M. Yang, W. Zhu, V. Cammarata, P. Almond, T. Sullens, Y. Qin, E. Bakker, *J. Org. Chem.* **2010**, *75*, 4472–4479; k) X. Li, D. P. Curran, *J. Am. Chem. Soc.* **2013**, *135*, 12076–12081; l) Y. Liu, X. Shao, P. Zhang, L. Lu, Q. Shen, *Org. Lett.* **2015**, *17*, 2752–2755; m) J. J. Medvedev, V. A. Nikolaev, *Russ. Chem. Rev.* **2015**, *84*, 737–757; n) C. J. Moody, R. J. Taylor, *Tetrahedron Lett.* **1987**, *28*, 5351–5352; o) R. R. Nani, S. E. Reisman, *J. Am. Chem. Soc.* **2013**, *135*, 7304–7311; p) A. Padwa, M. D. Weingarten, *Chem. Rev.* **1996**, *96*, 223–269; q) C. S. Shanahan, P. Truong, S. M. Mason, J. S. Leszczynski, M. P. Doyle, *Org. Lett.* **2013**, *15*, 3642–3645; r) M. Uehara, H. Suematsu, Y. Yasutomi, T. Katsuki, *J. Am. Chem. Soc.* **2011**, *133*, 170–171; s) Z. Zhang, J. Wang, *Tetrahedron* **2008**, *64*, 6577–6605; t) S. Zhu, X. Xu, J. A. Perman, X. P. Zhang, *J. Am. Chem. Soc.* **2010**, *132*, 12796–12799.

[7] **Previous methods for insertion of carboxylic acids into A/A diazocarbonyls:** a) S. Bertelsen, M. Nielsen, S. Bachmann, K. A. Jorgensen, *Synthesis* **2005**, 2234–2238; b) M. Kitamura, M. Kisanuki, R. Sakata, T. Okauchi, *Chem. Lett.* **2011**, *40*, 1129–1131; c) Z. Wang, X. Bi, Y. Liang, P. Liao, D. Dong, *Chem. Commun.* **2014**, *50*, 3976–3978.

[8] M. P. Doyle, M. A. McKervey, T. Ye, *Modern Catalytic Methods for Organic Synthesis with Diazo Compounds: From Cyclopropanes to Ylides*, Wiley, **1998**.

[9] C. G. Espino, K. W. Fiori, M. Kim, J. Du Bois, *J. Am. Chem. Soc.* **2004**, *126*, 15378–15379.

[10] A. C. Hunter, K. Chinthapally, I. Sharma, *Eur. J. Org. Chem.* **2016**, *2016*, 2260–2263.

[11] F. Urabe, S. Miyamoto, K. Takahashi, J. Ishihara, S. Hatakeyama, *Org. Lett.* **2014**, *16*, 1004–1007.

[12] D. Hack, M. Bluemel, P. Chauhan, A. R. Philipps, D. Enders, *Chem. Soc. Rev.* **2015**, *44*, 6059–6093.

[13] J. J. Kennedy-Smith, S. T. Staben, F. D. Toste, *J. Am. Chem. Soc.* **2004**, *126*, 4526–4527.

[14] H. M. Davies, L. M. Hodges, J. J. Matasi, T. Hansen, D. G. Stafford, *Tetrahedron Lett.* **1998**, *39*, 4417–4420.

[15] V. Belting, N. Krause, *Org. Lett.* **2006**, *8*, 4489–4492.

[16] **For insights into Au(I)-acetylide/vinylidene complexes:** a) J. Bucher, T. Wurm, K. S. Nalivela, M. Rudolph, F. Rominger, A. S. K. Hashmi, *Angew. Chem., Int. Ed.* **2014**, *53*, 3854–3858; b) M. M. Hansmann, F. Rominger, A. S. K. Hashmi, *Chem. Sci.* **2013**, *4*, 1552–1559.

[17] A. C. Hunter, S. C. Schlitzer, I. Sharma, *Chem. Eur. J.* **2016**, *22*, 16062–16065.

2.6 EXPERIMENTAL SECTION

2.6.1 GENERAL PROCEDURES FOR CARBOXYLIC ACID INSERTION

General Procedure I: Carboxylic acid (1 equiv.) and $Rh_2(esp)_2$ (1 mol%) were added to a round bottom flask, dissolved in anhydrous dichloromethane (0.5 M), and sonicated to ensure solubility. The acceptor-acceptor (1.5 equiv.) diazo was then added drop-wise via syringe over a span of 5 minutes. Once the release of N_2 gas ceased, reaction was observed to be complete by TLC (10 min–2 h). After completion rotary evaporation provided the crude compound. Purification by flash chromatography (4:1 – 2:3 Hex/EtOAc) afforded the pure compound.

General Procedure II: Carboxylic acid (1 equiv.) and $Rh_2(esp)_2$ (1 mol%) were added to a round bottom flask and half of the anhydrous dichloromethane (0.2 M) was added. The flask was sonicated to ensure solubility of the reagents. The acceptor-acceptor diazo (1.5 equiv.) was dissolved in the other half of the anhydrous dichloromethane and added to the reaction flask via syringe pump (2–4 h addition time). Once addition was complete rotary evaporation provided the crude product. Purification by flash chromatography (4:1–1:1 Hex/EtOAc) provided the pure product.

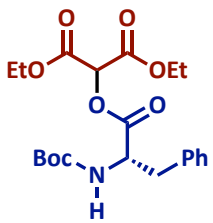

Diethyl 2-(((tert-butoxycarbonyl)-L-phenylalanyl)oxy)malonate (4a). Prepared from diethyl 2-diazomalonate and Boc-*L*-phenylalanine using general procedure **EI**. Colorless

liquid (42 mg, 94%). **TLC**: R_f 0.37 (4:1 hexanes/EtOAc). **IR** (NaCl): 3390, 2933, 1752, 1716, 1502, 1452, 1369, 1249, 1165, 1087, 1028, 858, 702. **^{1}H NMR** (400 MHz) δ 7.33 – 7.19 (m, 5H), 5.56 (s, 1H), 4.90 (d, *J* = 8.0 Hz, 1H), 4.75 (d, *J* = 8.0 Hz, 1H), 4.30 (ddq, *J* = 10.2, 6.6, 3.2 Hz, 4H), 3.29 (dd, *J* = 14.0, 5.1 Hz, 1H), 3.08 (dd, *J* = 4.0, 12.0 Hz, 1H), 1.39 (s, 9H), 1.31 (t, *J* = 7.1 Hz, 6H). **^{13}C NMR** (101 MHz) δ 170.63, 164.06, 163.92, 154.95, 135.64, 129.38, 128.52, 127.01, 80.01, 71.96, 62.62, 54.07, 37.77, 30.87, 28.20, 13.93, 13.91. **HRMS** (ESI) *m/z* calcd for $C_{21}H_{29}NO_8Na$ ([M+Na]$^+$) 446.1790; found 446.1777.

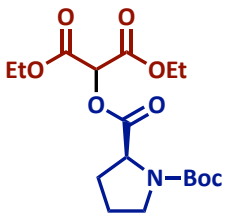

1-(Tert-butyl) 2-(1,3-diethoxy-1,3-dioxopropan-2-yl) (S)-pyrrolidine-1,2-dicarboxylate (4b). Prepared from diethyl 2-diazomalonate and Boc-*L*-proline using general procedure **EI** and obtained as a mixture of rotamers (1:1). Colorless liquid (28 mg, 83%). **TLC**: R_f 0.24 (4:1 hexanes/EtOAc). **IR** (NaCl): 3511, 2981, 2939, 2884, 1763, 1701, 1368, 1245, 1162, 1123, 1091. **^{1}H NMR** (400 MHz) δ 5.52 (s, 1H), 5.48 (s, 1H), 4.43 (dd, *J* = 4.0, 8.0 Hz, 1H), 4.34 (dd, *J* = 8.6, 3.8 Hz, 1H), 4.29 – 4.17 (m, 8H), 3.51 (ddq, *J* = 16.8, 8.3, 4.6 Hz, 2H), 3.42 – 3.38 (m, 1H), 3.36 – 3.29 (m, 1H), 2.28 – 2.10 (m, 4H), 1.99 – 1.80 (m, 4H), 1.40 (s, 7H), 1.35 (s, 9H), 1.24 (tq, *J* = 7.1, 3.9 Hz, 12H). **^{13}C NMR** (101 MHz) δ 171.73, 171.42, 165.71, 164.37, 164.20, 164.16, 164.12, 153.60, 80.13, 79.88, 71.82, 71.67, 62.52, 62.40, 62.23, 58.68, 58.43, 46.56, 46.28, 30.69, 29.73, 28.37, 28.19, 24.13, 23.43, 13.95, 13.92. **HRMS** (ESI) *m/z* calcd for $C_{17}H_{27}NO_8Na$ ([M+Na]$^+$) 396.1634; found 396.1634.

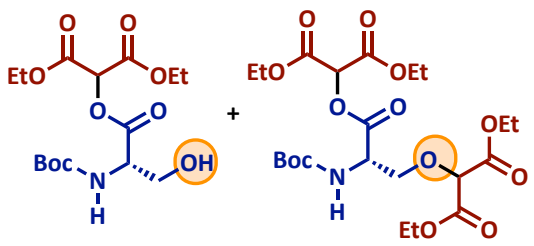

Diethyl 2-(((*tert*-butoxycarbonyl)-*L*-seryl)oxy)malonate (4c). Prepared from diethyl 2-diazomalonate and Boc-*L*-serine using general procedure **EII**. clear oil (161 mg, 74%). **TLC**: R_f 0.52 (1:1 hexanes/EtOAc). **IR** (NaCl): 3505, 2927, 1754, 1719. **^{1}H-NMR** (400 MHz): δ 4.39 – 4.22 (m, 4H), 3.89 – 3.80 (m, 1H), 2.82 (s, 1H), 1.45 (s, 9H), 1.36 – 1.28 (m, 6H). **^{13}C-NMR** (101 MHz, Chloroform-d) δ 169.89, 72.08, 63.22, 62.95, 28.25, 13.92, 13.90. **HRMS** (ESI) *m/z* calcd for $C_{15}H_{25}NO_9$ ($[M+Na]^+$) 386.1427; found 386.1418. **Diethyl 2-((*N*-(*tert*-butoxycarbonyl)-*O*-(1,3-diethoxy-1,3-dioxopropan-2-yl)-*L*- seryl)oxy)malonate (4c-bis).** Prepared from diethyl 2-diazomalonate and Boc-*L*-serine using general procedure **EII**. Clear oil (48 mg, 16%). **TLC**: R_f 0.6 (1:1 hexanes/EtOAc). **IR** (NaCl): 2981, 1749, 1718, 1508, 1369, 1296, 1244, 1159, 1095, 1028. **^{1}H-NMR** (400 MHz): δ 5.78 – 5.62 (m, 1H), 5.59 (s, 1H), 4.68 – 4.60 (m, 1H), 4.57 (s, 1H), 4.26 (dddd, *J* = 12.7, 11.2, 6.5, 3.8 Hz, 8H), 4.14 (dd, *J* = 10.0, 3.6 Hz, 1H), 4.05 (d, *J* = 2.9 Hz, 1H), 1.45 (s, 9H), 1.34 – 1.25 (m, 12H). **^{13}C-NMR** (101 MHz): 168.78, 165.79, 163.92, 163.90, 155.35, 155.27, 80.13, 79.19, 72.14, 70.70, 70.67, 62.60, 62.53, 62.10, 62.05, 53.78, 28.26, 13.99, 13.94, 13.92, 13.89. **HRMS** (ESI) *m/z* calcd for $C_{22}H_{35}NO_{13}$ ($[M+Na]^+$) 544.2006; found 544.2015.

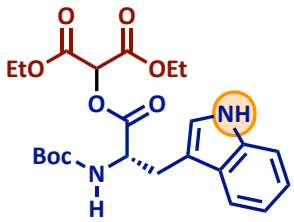

Diethyl 2-(((*tert*-butoxycarbonyl)-*L*-tryptophyl)oxy)malonate (4d). Prepared from diethyl 2- diazomalonate and Boc-*L*-tryptophan from general procedure **EII**. clear oil (171 mg, 62%). **TLC**: R_f 0.47 (1:1 hexanes/EtOAc). **IR** (NaCl): 3061, 2980, 2927, 1750, 1503, 1460. **^{1}H-NMR** (400 MHz): δ 8.13 (s, 1H), 7.59 (d, *J* = 7.9 Hz, 1H), 7.35 (d, *J* = 8.0 Hz, 1H), 7.21 – 7.05 (m, 3H), 5.53 (s, 1H), 5.02 (d, *J* = 8.5 Hz, 1H), 4.82 (d, *J* = 7.5 Hz, 1H), 4.38 – 4.20 (m, 6H), 3.57 – 3.23 (m, 2H), 1.40 (s, 9H), 1.31 (td, *J* = 7.1, 2.6 Hz, 10H). **^{13}C-NMR** (101 MHz) δ 170.95, 123.31, 123.28, 122.12, 122.11, 119.63, 118.67, 118.66, 111.14, 111.12, 111.10, 109.99, 109.74, 72.01, 62.61, 54.14, 28.26, 27.50, 13.96, 13.93. **HRMS** (ESI) *m/z* calcd for $C_{23}H_{30}N_2O_8$ ($[M+Na]^+$) 485.1900; found 485.1899.

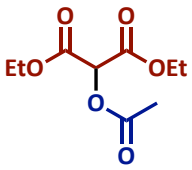

Diethyl 2-acetoxymalonate (4e). Prepared from diethyl 2-diazomalonate and acetic acid using general procedure **EI**. clear oil (21.5 mg, 92%). **TLC**: R_f 0.31 (4:1 hexanes/EtOAc) **IR** (NaCl): 2925, 1751. **^{1}H-NMR** (400 MHz): δ 5.51 (s, 1H), 4.29 (qq, *J* = 7.4, 3.6 Hz, 4H), 2.22 (s,

3H), 1.30 (t, *J* = 7.1 Hz, 6H). **^{13}C-NMR** (101 MHz) δ 169.44, 164.44, 71.81, 62.51, 29.67, 20.37, 13.94. **HRMS** (ESI) *m/z* calcd for $C_9H_{14}O_6$ ([M+Na]$^+$) 241.0688; found 241.0905.

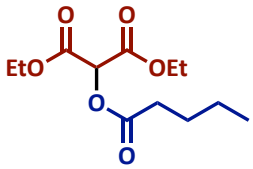

Diethyl 2-(pentanoyloxy)malonate (4f). Prepared from diethyl 2-diazomalonate and pentanoic acid using general procedure **EI**. Colorless liquid (22 mg, 86%) .**TLC**: R_f 0.54 (4:1 hexanes/EtOAc). **IR** (NaCl): 2963, 2875, 1754, 1467, 1373, 1181, 1160, 1113, 1031, 858. **^{1}H NMR** (400 MHz) δ 5.51 (s, 1H), 4.28 (tdt, *J* = 10.8, 8.0, 3.6 Hz, 4H), 2.48 (t, *J* = 7.5 Hz, 2H), 1.70 – 1.63 (m, 2H), 1.42 – 1.34 (m, 2H), 1.29 (t, *J* = 7.1 Hz, 6H), 0.91 (t, *J* = 7.3 Hz, 3H). **^{13}C NMR** (101 MHz) δ 172.31, 164.55, 71.61, 62.45, 33.33, 26.71, 22.07, 13.93, 13.62. **HRMS** (ESI) *m/z* calcd for $C_{12}H_{20}O_6Na$ ([M+Na]$^+$) 283.1157; found 283.1155.

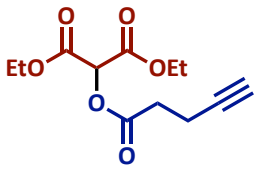

Diethyl 2-(pent-4-ynoyloxy)malonate (4g). Prepared from diethyl 2-diazomalonate and 4-pentynoic acid using general procedure **EII**. clear oil (182 mg, 94%). **TLC**: *Rf* 0.5 (4:1 hexanes/EtOAc). **IR** (NaCl): 3284, 2983, 2924, 2357, 1747, 1373, 1153, 1093, 1028. **^{1}H-NMR** (300 MHz): δ 5.53 (s, 1H), 4.32 – 4.23 (m, 4H), 2.76 – 2.71 (m, 2H), 2.57 – 2.51 (m, 2H), 2.02 – 2.01 (m, 1H), 1.29 (t, *J* = 7.1 Hz, 6H). **^{13}C-NMR** (75 MHz): δ 170.26, 164.15, 81.79, 71.73,

69.20, 62.48, 32.64, 14.03, 13.84. **HRMS** (ESI) *m/z* calcd for $C_{12}H_{16}O_6$ ($[M+Na]^+$) 279.0845; found 279.0847.

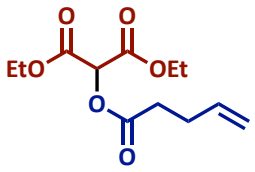

Diethyl 2-(pent-4-enoyloxy)malonate (4h). Prepared from diethyl 2-diazomalonate and pent-4- enoic acid using general procedure **EI**. clear oil (25 mg, 90%). **TLC**: R_f 0.87 (7:3 hexanes/EtOAc). **IR** (NaCl): 3152, 2927, 2855, 1751, 1676, 1465. **^{1}H-NMR** (400 MHz) δ 5.84 (ddt, J = 16.7, 10.2, 6.4 Hz, 1H), 5.53 (s, 1H), 5.19– 4.96 (m, 2H), 4.28 (dt, J = 7.2, 3.6 Hz, 4H), 2.69 – 2.56 (m, 2H), 1.30 (t, J = 7.1 Hz, 6H). **^{13}C-NMR** (101 MHz) δ 171.56, 164.45, 136.08, 115.80, 71.69, 62.50, 32.87, 28.50, 13.95. **HRMS** (ESI) *m/z* calcd for $C_{12}H_{18}O_6$ ($[M+Na]^+$) 281.1001; 281.1000 found.

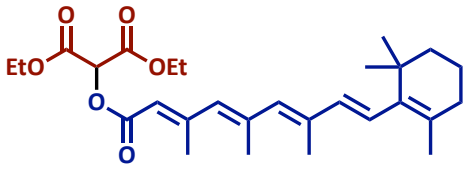

Diethyl 2-(((2E,4E,6E,8E)-3,7-dimethyl-9-(2,6,6-trimethylcyclohex-1-en-1-yl)nona-2,4,6,8- tetraenoyl)oxy)malonate (4i). Prepared from diethyl 2-diazomalonate and retinoic acid using general procedure **EI**. Pale yellow oil (21 mg, 93%). **TLC**: R_f 0.14 (9:1 hexanes/EtOAc). **IR** (NaCl): 2658, 2927, 1749, 1722, 1583, 1371, 1230, 1182, 1136, 1095, 1029. **^{1}H NMR** (400 MHz) δ 7.05 (dd, J = 15.0, 11.5 Hz, 1H), 6.30 (d, J = 15.3 Hz, 2H), 6.16 (s, 1H), 6.13 (d, J = 8.0 Hz, 1H), 5.94 (s, 1H), 5.57 (s, 1H), 4.29 (dd, J = 7.0, 5.4 Hz, 4H), 2.36 (s, 3H), 2.00 (s, 3H), 1.71 (s, 3H), 1.64 – 1.57 (m, 3H), 1.51 – 1.42 (m, 2H), 1.31 (t, J = 7.1 Hz, 6H), 1.02 (s, 6H). **^{13}C NMR** (101 MHz) δ 165.13, 164.89, 155.90, 140.47,

137.61, 137.12, 134.54, 132.16, 130.19, 129.33, 129.12, 116.02, 71.39, 62.38, 39.58, 34.23, 33.09, 28.93, 21.72, 19.18, 14.15, 13.96, 12.91. **HRMS** (ESI) *m/z* calcd for $C_{27}H_{38}O_6Na$ ($[M+Na]^+$) 481.2566; found 481.2568.

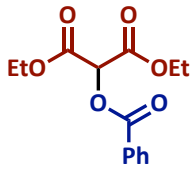

Diethyl 2-(benzoyloxy)malonate (4j). Prepared from diethyl 2-diazomalonate and benzoic acid using general procedure **EI**. clear oil (26.1 mg, 87%). **TLC**: R_f 0.43 (4:1 hexanes/EtOAc). **IR** (NaCl): 2927, 2855, 1752, 1684. **^{1}H-NMR** (400 MHz): δ 8.21 – 8.08 (m, 2H), 7.61 (t, *J* = 7.4 Hz, 1H), 7.47 (t, *J* = 7.8 Hz, 2H), 5.75 (s, 1H), 4.33 (qq, *J* = 7.4, 3.6 Hz, 4H), 1.33 (t, *J* = 7.1 Hz, 6H). **^{13}C-NMR (101 MHz)** δ 165.10, 164.50, 133.77, 130.16, 128.49, 72.11, 62.54, 29.69, 13.99 **HRMS** (ESI) *m/z* calcd for $C_{14}H_{16}O_6$ ($[M+Na]^+$) 303.0845; found 303.0847.

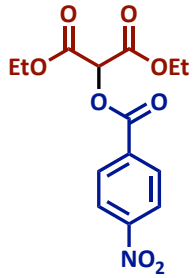

Diethyl 2-((4-nitrobenzoyl)oxy)malonate (4k). Prepared from diethyl 2-diazomalonate and 4- nitro benzoic acid from general procedure **EII**. clear oil (81 mg, 69%). **TLC**: R_f 0.55 (7:3 hexanes/EtOAc). **IR** (NaCl): **^{1}H-NMR** (400 M Hz): δ 8.31 (s, 4H), 5.76 (s, 2H), 4.34 (qd, *J* = 7.1, 4.3 Hz, 4H), 1.33 (t, *J* = 7.1 Hz, 6H). **^{13}C-NMR** (101 MHz): δ 163.93, 163.28, 151.00, 133.83, 131.31, 123.65, 77.39, 77.20, 77.06, 72.49, 62.82, 14.03, 13.98. **HRMS** not mass active.

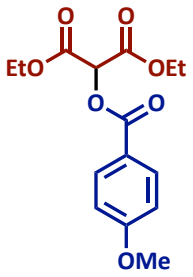

Diethyl 2-((4-methoxybenzoyl)oxy)malonate (4l). Prepared from diethyl 2-diazomalonate and 4-methoxy benzoic acid using general procedure **EI**. Colorless liquid (29.7 mg, 94%). **TLC**: R_f 0.29 (9:1 hexanes/EtOAc). **IR** (NaCl): 3528, 2982, 2939, 2845, 1751, 1719, 1607, 1513. **^{1}H NMR** (400 MHz) δ 8.08 (d, *J* = 8.8 Hz, 2H), 6.93 (d, *J* = 8.8 Hz, 2H), 5.72 (s, 1H), 4.31 (qq, *J* = 7.5, 3.6 Hz, 4H), 3.86 (s, 3H), 1.31 (t, *J* = 7.1 Hz, 6H). **^{13}C NMR** (101 MHz) δ 164.74, 164.67, 164.02, 132.28, 120.73, 113.75, 71.93, 62.44, 55.44, 13.96. **HRMS** (ESI) *m/z* calcd for $C_{15}H_{18}O_7Na$ ($[M+Na]^+$) 333.0950; found 333.0949

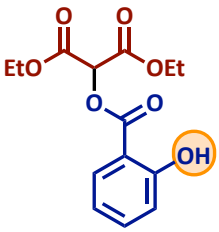

Diethyl 2-((2-hydroxybenzoyl)oxy)malonate (4m). Prepared from diethyl 2-diazomalonate and salicylic acid from general procedure **EII**. clear oil (127 mg, 94%). **TLC**: R_f 0.55 (7:3 hexanes/EtOAc). **IR** (NaCl): **^{1}H-NMR** (400 MHz): δ 10.57 – 10.44 (m, 1H), 10.13 (s, 1H), 8.02 (dd, *J* = 8.0, 1.6 Hz, 1H), 7.64 – 7.46 (m, 1H), 7.00 (d, *J* = 7.9 Hz, 1H), 6.96 – 6.90 (m, 1H), 5.74 (s, 1H), 4.34 (tq, *J* = 7.1, 3.9 Hz, 4H), 1.34 (t, *J* = 7.1 Hz, 6H). **^{13}C-NMR** (101 MHz): δ 168.30, 164.01, 161.76, 136.72, 136.66, 136.64, 130.77, 130.60, 119.56, 119.43, 117.75,

117.66, 111.15, 72.02, 62.79, 13.98. **HRMS** (ESI) *m/z* calcd for $C_{15}H_{25}NO_9$ ($[M+Na]^+$) 386.1427; found 386.1418.

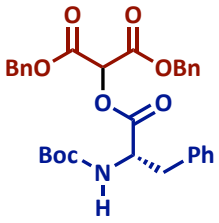

Dibenzyl 2-(((tert-butoxycarbonyl)-L-phenylalanyl)oxy)malonate (4n). Prepared from dibenzyl 2-diazomalonate and Boc-*L*-phenylalanine using general procedure **EI**. Colorless liquid (34 mg, 83%). **TLC**: R_f 0.31 (4:1 hexanes/EtOAc). **IR** (NaCl): 3396, 2974, 2927, 1753, 1716, 1498, 1456, 1367, 1251, 1215, 1163, 1083, 1028, 748. **^{1}H NMR** (400 MHz) δ 7.33 – 7.27 (m, 7H), 7.25 – 7.19 (m, 6H), 7.17 (d, *J* = 6.6 Hz, 2H), 5.68 (s, 1H), 5.23 (s, 4H), 4.90 (d, *J* = 8.0 Hz, 1H), 4.75 (d, *J* = 6.3 Hz, 1H), 3.25 (dd, *J* = 14.1, 5.3 Hz, 1H), 3.03 (dd, *J* = 14.0, 7.0 Hz, 1H), 1.39 (s, 9H). **^{13}C NMR** (101 MHz) δ 170.58, 163.78, 163.63, 135.58, 134.42, 129.36, 128.62, 128.60, 128.51, 128.28, 126.99, 80.03, 71.90, 68.15, 54.07, 37.75, 28.21. **HRMS** (ESI) *m/z* calcd for $C_{31}H_{33}NO_8Na$ ($[M+Na]^+$) 570.2103; found 570.2108.

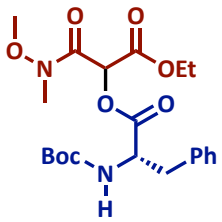

Ethyl 2-(((*tert*-butoxycarbonyl)-*L*-phenylalanyl)oxy)-3-(methoxy(methyl)amino)-3-oxopropanoate (4o) . Prepared from ethyl 2-diazo-3-(methoxy(methyl)amino)-3-oxopropanoate and Boc-*L*-phenylalanine using general procedure **EI** and obtained as a mixture of diasteromers (1:1). Light yellow oil (106 mg, 73%). **TLC**: R_f 0.66 (1:1

hexanes/EtOAc). **IR** (NaCl) 2980. 2936, 1751, 1717, 1507, 1392. **^{1}H-NMR** (400 MHz) δ 7.34 – 7.27 (m, 4H), 7.24 – 7.18 (m, 6H), 6.01 (s, 1H), 5.95 (s, 1H), 4.92 (d, *J* = 6.6 Hz, 2H), 4.72 (d, *J* = 6.9 Hz, 2H), 4.28 (p, *J* = 7.2 Hz, 4H), 3.75 (s, 3H), 3.73 (s, 3H), 3.30 (dd, *J* = 13.8, 6.1 Hz, 2H), 3.24 (s, 6H), 3.08 (dt, *J* = 14.5, 7.7 Hz, 2H), 1.38 (s, 18H), 1.30 (td, *J* = 7.1, 3.9 Hz, 6H). **^{13}C-NMR** (101 MHz) δ 170.83, 164.48, 154.97, 135.88, 135.78, 129.50, 129.46,128.57, 128.51, 128.49, 126.98, 126.91, 79.95, 77.21, 70.55, 70.17, 62.39, 61.64, 38.04, 37.78, 32.49, 28.22, 28.13, 14.02, 13.99. **HRMS** (ESI) *m/z* calcd for $C_{21}H_{30}O_8$ ([M+Na]$^+$) 461.1900; found 461.1903.

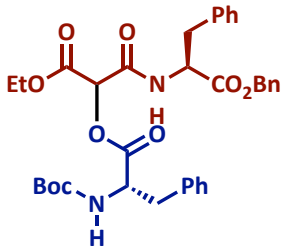

Ethyl 3-(((*S*)-1-(benzyloxy)-1-oxo-3-phenylpropan-2-yl)amino)-2-(((*tert*-butoxycarbonyl)-*L*- phenylalanyl)oxy)-3-oxopropanoate (4p). Prepared from ethyl (*S*)-3-((1-(benzyloxy)-1-oxo-3- phenylpropan-2-yl)amino)-2-diazo-3-oxopropanoate and Boc-*L*-phenylalanine using general procedure **EI** and obtained as a mixture of diastereomers (1:1). Light yellow oil (204 mg, 96%). **TLC**: R_f 0.46 (1:1 hexanes/EtOAc). **IR** (NaCl): 2981, 2935, 1750, 1700, 1584, 1168. **^{1}H-NMR** (400 MHz): δ 7.41 – 7.26 (m, 8H), 7.26 – 7.12 (m, 9H), 7.06 – 6.88 (m, 3H), 5.50 (s, 1H), 5.44 (s, 1H), 5.24 – 5.09 (m, 2H), 4.96 – 4.84 (m, 2H), 4.23 (ddt, *J* = 14.2, 7.1, 3.5 Hz, 2H), 3.18 (dddt, *J* = 26.4, 20.8, 13.8, 6.7 Hz, 3H), 3.02 (dd, *J* = 13.9, 7.2 Hz, 1H), 1.42 (s, 18H), 1.27 (t, *J* = 7.1 Hz, 3H). **^{13}C-NMR** (101 MHz): δ 170.42, 170.37, 129.41, 129.33, 129.29, 128.65, 128.64, 128.61, 128.54, 127.21, 127.13, 72.92, 72.80, 67.46, 67.38, 62.77, 62.71,

54.36, 53.48, 53.33, 37.52, 28.25, 13.93, 13.91. **HRMS** (ESI) *m/z* calcd for $C_{35}H_{40}N_2O_9$ ([M–H]$^-$) 631.2656; found 631.2677.

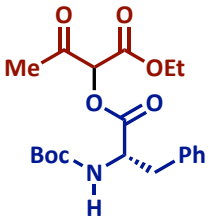

Ethyl 2-(((tert-butoxycarbonyl)-L-phenylalanyl)oxy)-3-oxobutanoate (4q). Prepared from ethyl 2-diazo-3-oxobutanoate and Boc-*L*-phenylalanine using general procedure **EI** and obtained as a mixture of diastereomers (1:1). Colorless powder (25 mg, 86%). **TLC**: R_f 0.31 (4:1 hexanes/EtOAc). **IR** (NaCl): 3371, 2950, 2853, 1755, 1733, 1505, 1538, 1524. **^{1}H NMR** (400 MHz) δ 7.30 (t, *J* = 7.0 Hz, 4H), 7.25 – 7.18 (m, 5H), 5.49 (s, 1H), 5.47 (s, 1H), 4.93 (s, 1H), 4.72 (d, *J* = 6.5 Hz, 2H), 4.28 (p, *J* = 6.7 Hz, 4H), 3.25 (td, *J* = 15.7, 15.2, 5.8 Hz, 2H), 3.10 (dt, *J* = 14.0, 6.8 Hz, 2H), 2.28 (s, 3H), 2.24 (s, 3H), 1.39 (s, 18H), 1.30 (td, *J* = 7.1, 3.1 Hz, 6H). **^{13}C NMR** (101 MHz) δ 170.78, 164.16, 163.98, 155.05, 135.66, 129.35, 129.29, 128.63, 128.58, 127.12, 127.08, 80.17, 80.16, 78.06, 78.02, 62.59, 54.32, 54.20, 38.03, 37.75, 28.21, 27.08, 13.97, 13.94. **HRMS** (ESI) *m/z* calcd for $C_{20}H_{27}NO_7Na$ ([M+Na]$^+$) 416.1685; found 416.1685.

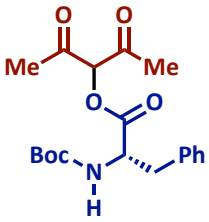

2,4-Dioxopentan-3-yl (tert-butoxycarbonyl)-L-phenylalaninate (4r). Prepared from 3-diazopentane-2,4-dione and Boc-*L*-phenylalanine using general procedure **EI** and obtained

as a mixture of keto-enol form. Colorless powder (32 mg, 85%). **TLC**: R_f 0.36 (4:1 hexanes/EtOAc). **IR** (NaCl): 3367, 2978, 2929, 1757, 1716, 1504, 1452, 1363, 1278, 1251, 1165, 1078, 748. **^{1}H NMR** (400 MHz) δ 7.30 (q, *J* = 5.7, 5.2 Hz, 2H), 7.27 – 7.21 (m, 3H), 5.45 (s, 1H), 4.96 (d, *J* = 7.7 Hz, 1H), 4.75 – 4.66 (m, 1H), 3.22 (dd, *J* = 14.0, 6.4 Hz, 1H), 3.09 (ddd, *J* = 29.6, 13.9, 7.5 Hz, 1H), 2.22 (s, 3H), 2.19 (s, 3H), 1.40 (s, 9H). **^{13}C NMR** (101 MHz) δ 198.70, 198.27, 171.43, 170.74, 155.09, 135.72, 135.38, 129.26, 129.19, 128.84, 128.67, 127.39, 127.17, 85.16, 80.45, 80.27, 54.50, 54.40, 38.06, 37.62, 28.21, 28.17, 27.24, 27.16, 20.67. **HRMS** (ESI) *m/z* calcd for $C_{19}H_{25}NO_6Na$ ($[M+Na]^+$) 386.1579; found 386.1577.

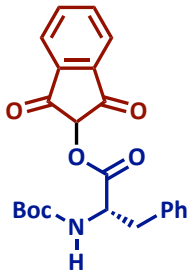

1,3-Dioxo-2,3-dihydro-1*H*-inden-2-yl (*tert*-butoxycarbonyl)-*L*-phenylalaninate (4s). Prepared from 2-diazo-1*H*-indene-1,3(2*H*)-dione and Boc-*L*-phenylalanine using general procedure **EI**. Orange oil (110 mg, 70%). **TLC**: R_f 0.44 (7:3 hexanes/EtOAc). **IR** (NaCl): 2978, 2926, 2855, 1808, 1768, 1725, 1507. **^{1}H-NMR** (400 MHz) δ 8.07 – 7.96 (m, 2H), 7.91 (dd, *J* = 5.7, 3.1 Hz, 2H), 7.38 – 7.27 (m, 4H), 5.37 (s, 1H), 4.86 (dd, *J* = 13.6, 7.1 Hz, 2H), 3.26 (dd, *J* = 13.8, 5.4 Hz, 1H), 3.14 (dd, *J* = 13.8, 5.4 Hz, 1H), 1.40 (s, 9H). **^{13}C-NMR** (101 MHz) δ 192.06, 192.02, 139.74, 136.46, 135.38, 135.37, 129.77, 129.76, 129.72, 129.68, 128.76, 128.58, 128.51, 127.06, 123.89, 123.84, 123.83, 80.05, 80.03, 53.69, 53.67, 38.20, 28.24. **HRMS** (ESI) *m/z* calcd for $C_{23}H_{23}NO_6$ ($[M+Na]^+$) 432.1423; found 432.1425.

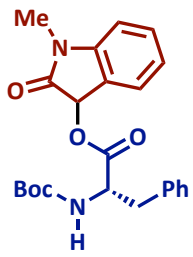

1-Methyl-2-oxoindolin-3-yl (tert-butoxycarbonyl)-L-phenylalaninate (4t). Prepared from 3- diazo-1-methylindolin-2-one and Boc-*L*-phenylalanine using general procedure **EI** and obtained as a mixture of diastereomers (1:1). Red liquid (25 mg, 82%). **TLC**: R_f 0.33 (7:3 hexanes/EtOAc). **IR** (NaCl): 3438, 2980, 2931, 1751, 1719, 1617, 1496, 1164. **^{1}H NMR** (400 MHz) δ 7.36 (t, *J* = 7.7 Hz, 2H), 7.27 – 7.21 (m, 5H), 7.12 (d, *J* = 7.0 Hz, 2H), 7.05 (t, *J* = 7.5 Hz, 2H), 6.83 (d, *J* = 7.7 Hz, 2H), 6.08 (s, 1H), 5.97 (s, 1H), 4.98 (s, 1H), 4.77 – 4.66 (m, 1H), 3.22 (s, 6H), 3.16 – 3.05 (m, 2H), 1.42 (s, 7H), 1.38 (s, 9H). **^{13}C NMR** (101 MHz) δ 171.34, 144.50, 135.57, 130.49, 129.57, 129.51, 128.54, 128.48, 127.01, 126.07, 125.86, 123.63, 123.59, 123.12, 122.99, 108.46, 79.98, 70.42, 70.11, 54.41, 54.29, 38.02, 38.00, 37.88, 37.87, 28.23, 26.34. **HRMS** (ESI) *m/z* calcd for $C_{23}H_{26}N_2O_5Na$ ($[M+Na]^+$) 433.1739; found 433.1730.

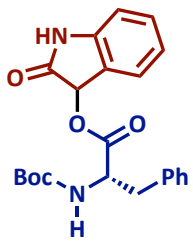

2-Oxoindolin-3-yl (tert-butoxycarbonyl)-L-phenylalaninate (4u). TLC: R_f 0.50 (1:1 hexanes/EtOAc). Prepared from 3-diazoindolin-2-one and Boc-*L*-phenylalanine using general procedure **EI** and obtained as a mixture of diastereomers (1:1). Red liquid (25 mg,

78%). **IR** (NaCl): 3273, 2978, 2927, 1732, 1622, 1500, 1471, 1367, 1165, 1055, 1026, 910, 752. **^{1}H NMR** (400 MHz) δ 8.26 (d, *J* = 22.8 Hz, 2H), 7.32 – 7.21 (m, 9H), 7.16 – 7.14 (m, 2H), 7.06 – 7.01 (m, 3H), 6.87 (d, *J* = 7.8 Hz, 2H), 4.99 (d, *J* = 8.1 Hz, 2H), 4.77 – 4.70 (m, 2H), 3.27 – 3.10 (m, 4H), 1.42 (s, 10H), 1.38 (s, 9H). **^{13}C NMR** (101 MHz) δ 173.54, 171.40, 171.37, 155.03, 141.57, 135.59, 135.56, 130.51, 129.59, 129.56, 128.59, 128.53, 127.07, 126.34, 126.18, 124.15, 124.10, 123.16, 123.03, 110.29, 80.09, 70.73, 70.40, 54.41, 54.33, 38.05, 37.89, 28.26. **HRMS** (ESI) *m/z* calcd for $C_{22}H_{24}N_2O_5Na$ ([M+Na]$^+$) 419.1582; found 419.1570.

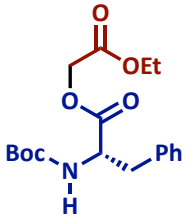

2-Ethoxy-2-oxoethyl (*tert*-butoxycarbonyl)-*L*-phenylalaninate (4v), Prepared from ethyl 2-diazoacetate and Boc-*L*-phenylalanine using general procedure **EI**. White powder (160 mg, 78%). **TLC**: R_f 0.44 (4:1 hexanes/EtOAc). **IR** (NaCl): 3375, 2855, 1763, 1719, 1684. **^{1}H-NMR** (400 MHz): δ 7.30 (dd, *J* = 7.8, 6.4 Hz, 2H), 7.25 – 7.13 (m, 3H), 4.93 (d, *J* = 7.7 Hz, 2H), 4.79 – 4.48 (m, 5H), 4.24 (q, *J* = 7.1 Hz, 2H), 3.25 (dd, *J* = 14.1, 5.3 Hz, 3H), 3.06 (dd, *J* = 14.0, 7.0 Hz, 3H), 1.39 (s, 9H), 1.29 (t, *J* = 7.1 Hz, 3H). **^{13}C-NMR** (101 MHz) δ 171.47, 167.28, 155.05, 135.90, 129.38, 129.00, 128.52, 128.19, 126.99, 79.97, 61.54, 61.13, 54.16, 37.99, 28.24, 14.09. **HRMS** (ESI) *m/z* calcd for $C_{18}H_{25}NO_6$ ([M+Na]$^+$) 374.1580; found 374.1583.

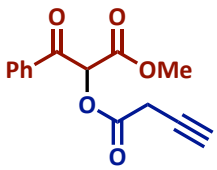

1-Methoxy-1,3-dioxo-3-phenylpropan-2-yl but-3-ynoate (4w). Prepared from methyl 2-diazo-3-oxo-3-phenylpropanoate and but-3-ynoic acid using general procedure **F1**. Yellow oil (26 mg, 93%). **TLC**: R_f 0.42 (7:3 hexanes/EtOAc). **^{1}H NMR** (400 MHz) δ 7.72–7.37 (m, 5H), 6.37 (s, 1H), 3.79 (s, 3H), 3.49 (t, J = 2.9 Hz, 2H), 2.21 (t, J = 2.7 Hz, 1H). **^{13}C NMR** (101 MHz) δ 188.8, 166.7, 165.1, 134.4, 133.9, 129.3, 128.9, 75.0, 74.3, 72.5, 53.3, 25.4. **ESI-MS** *m/z* calcd for $C_{14}H_{12}O_5$ ($[M+Na]^+$) 283.5; found 283.1.

2.6.2 GENERAL PROCEDURE FOR THE SYNTHESIS OF γ-BUTYROLACTONES AND TETRAHYDROFURANS

Alkynoic acid/alkynol (1 equiv.), $Rh_2(esp)_2$ (1 mol%), AgOTf (10 mol%), PPh_3AuCl (10 mol%), and activated 4Å molecular sieves (36 mg per mL of solvent) were added to a round bottom flask, dissolved in anhydrous dichloromethane (0.2 M), and allowed to pre-mix for 5 minutes. The diazo (1.2 equiv.) was dissolved in anhydrous dichloromethane (0.2 M making a total 0.1 M solution for the reaction) was then added drop-wise via syringe manually over a span of 2 minutes. Once the release of N_2 gas ceased, reaction was observed to be complete by TLC and TLC-MS. After completion, molecular sieves were removed by filtration over a pad of celite and rotary evaporation provided the crude compound. Purification by flash chromatography (9:1–7:3 Hex/EtOAc) afforded the pure compound.

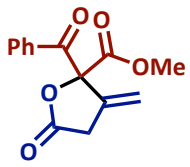

Methyl 2-benzoyl-3-methylene-5-oxotetrahydrofuran-2-carboxylate (5a). Prepared from methyl 2-diazo-3-oxo-3-phenylpropanoate and 3-butynoic acid using general procedure **EI**. Yellow liquid (28 mg, 83%). **TLC**: R_f 0.54 (7:3 hexanes/EtOAc). **IR** (NaCl): 2957, 2920, 2850, 1808, 1744, 1698, 1597. **^{1}H NMR** (400 MHz) δ 8.01–7.95 (m, 2H), 7.59 (ddt, J = 7.9, 6.9, 1.3 Hz, 1H), 7.52 – 7.42 (m, 2H), 5.68 (td, J = 2.8, 1.0 Hz, 1H), 5.62 (td, J = 2.5, 1.0 Hz, 1H), 3.81 (s, 3H), 3.39 (td, J = 2.6, 1.7 Hz, 2H). **^{13}C NMR** (101 MHz) δ 188.4, 172.3, 167.4, 134.4, 130.0, 129.1, 116.7, 90.1, 54.1, 33.7. **HRMS** (ESI) *m/z* calcd for $C_{14}H_{12}O_5$ ([M+Na]$^+$) 283.0583; found 283.0584.

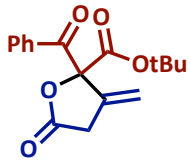

***tert*-Butyl 2-benzoyl-3-methylene-5-oxotetrahydrofuran-2-carboxylate (5b).** Prepared from *tert*-butyl 2-diazo-3-oxo-3-phenylpropanoate and 3-butynoic acid using general procedure **EI**. Yellow liquid (68 mg, 73%) .**TLC**: R_f 0.67 (7:3 hexanes/EtOAc). **IR** (NaCl): 2980, 2926, 2852, 1811, 1748, 1700, 1598, 1581. **^{1}H NMR** (400 MHz) δ 8.07–7.89 (m, 2H), 7.46 (t, J = 7.6 Hz, 3H), 5.65 (d, J = 2.4 Hz, 1H), 5.60 (t, J = 2.5 Hz, 1H), 3.38 (q, J = 2.0, 1.6 Hz, 2H), 1.36 (s, 9H). **^{13}C NMR** (101 MHz) δ 191.2, 170.0, 143.8, 134.3, 133.3, 129.7, 128.4, 112.6, 90.2, 68.9, 53.0, 32.9. **HRMS** (ESI) *m/z* calcd for $C_{17}H_{18}O_4$ ([M+Na]$^+$) 325.1052; found 325.1034.

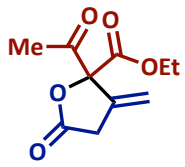

Ethyl 2-acetyl-3-methylene-5-oxotetrahydrofuran-2-carboxylate (5c). Prepared from ethyl 2-diazo-3-oxobutanoate and 3-butynoic acid using general procedure **EI**. Yellow oil (47.3 mg, 76%). **TLC**: R_f 0.37 (7:3 hexanes/EtOAc). **IR** (NaCl): 2965, 2925, 2880, 2683, 1734, 1712, 1659. **^{1}H-NMR** (400 MHz) δ 5.66 (td, J = 2.4, 1.3 Hz, 1H), 5.45 (dt, J = 2.5, 1.5 Hz, 1H), 4.28 (qdd, J = 7.2, 3.4, 0.7 Hz, 2H), 3.47 – 3.21 (m, 2H), 2.32 (d, J = 0.6 Hz, 3H), 1.29 (td, J = 7.1, 0.6 Hz, 3H). **^{13}C-NMR** (101 MHz) δ 197.7, 172.1, 165.3, 133.9, 118.5, 115.4, 91.0, 63.2, 33.4, 25.9, 13.9. **HRMS** (ESI) *m/z* calcd for $C_{10}H_{12}O_5$ ([M+Na]$^+$) 235.0583; found 235.0579.

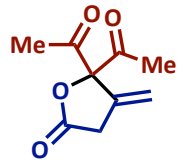

1,1'-(3-Methylene-5-oxotetrahydrofuran-2,2-diyl)bis(ethan-1-one) (5d). Prepared from 3-diazopentane-2,4-dione and 3-butynoic acid using general procedure **EI**. Yellow oil (55 mg, 76%). **TLC**: R_f 0.57 (7:3 hexanes/EtOAc). **IR** (NaCl): 2923, 2851, 1806, 1737, 1718, 1665, 1638. **^{1}H-NMR** (400 MHz): δ 5.60 (tt, J = 2.8, 1.1 Hz, 1H), 5.43 (dt, J = 2.5, 1.2 Hz, 1H), 3.31 – 3.26 (m, 2H), 2.31 (s, 6H). **^{13}C-NMR** (101 MHz) δ 198.9, 172.5, 164.5, 133.9, 115.2, 33.6, 26.3. **HRMS** (ESI) *m/z* calcd for $C_9H_{10}O_4$ ([M+Na]$^+$) 205.0477; found 205.0476.

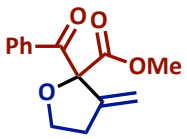

Methyl 2-benzoyl-3-methylenetetrahydrofuran-2-carboxylate (5e). Prepared from methyl 2-diazo-3-oxo-3-phenylpropanoate and 3-butynoic acid using general procedure **EI**. Yellow liquid (52 mg, 86%). **^{1}H NMR** (400 MHz) δ 8.05–7.99 (m, 2H), 7.57–7.51 (m, 1H), 7.46–7.39 (m, 2H), 5.50 (t, *J* = 2.1 Hz, 1H), 5.41 (t, *J* = 2.3 Hz, 1H), 4.21 (q, *J* = 7.8 Hz, 1H), 4.08 (dt, *J* = 8.3, 6.4 Hz, 1H), 3.74 (s, 3H), 2.73 (ddt, *J* = 7.5, 4.4, 1.4 Hz, 2H).**^{13}C NMR** (101 MHz) δ 191.2, 170.0, 143.8, 134.3, 133.2, 129.7, 128.4, 112.6, 90.2, 68.9, 53.0, 32.9. ***Compound matched literature known values***

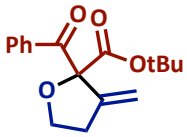

***tert*-Butyl 2-benzoyl-3-methylenetetrahydrofuran-2-carboxylate (5f).** Prepared from *tert*-butyl 2-diazo-3-oxo-3-phenylpropanoate and 3-butynol using general procedure **EI**. Yellow oil (47 mg, 80%). **TLC**: R_f 0.5 (4:1 hexanes/EtOAc). **IR** (NaCl): 2958, 2924, 2854, 2127, 1722, 1598, 1583. **^{1}H NMR** (400 MHz) δ 8.07–8.03 (m, 2H), 7.57–7.50 (m, 1H), 7.47–7.39 (m, 2H), 5.50 (t, *J* = 2.1 Hz, 1H), 5.41 (t, *J* = 2.2 Hz, 1H), 4.23 (q, *J* = 7.8 Hz, 1H), 4.07 (dt, *J* = 8.2, 6.3 Hz, 1H), 2.73 (ddt, *J* = 8.3, 4.4, 1.7 Hz, 2H), 1.32 (s, 9H). **^{13}C NMR** (101 MHz) δ 191.3, 168.5, 144.3, 134.8, 132.9, 129.6, 128.3, 111.9, 90.1, 83.1, 68.8, 33.2, 29.7, 27.6. **ESI-MS** *m/z* calcd for $C_{17}H_{20}O_4$ ([M+Na]$^+$) 311.1; found 311.1.

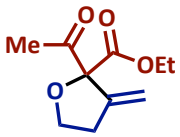

Ethyl 2-acetyl-3-methylenetetrahydrofuran-2-carboxylate (5g). Prepared from ethyl 2-diazo-3-oxobutanoate and 3-butynol using general procedure **EI**. Yellow oil (45 mg, 64%). **TLC**: R_f 0.60 (7:3 hexanes/EtOAc). **IR** (NaCl): 2963, 2925, 1745, 1662. **^{1}H NMR** (400 MHz) δ 5.32 (t, J = 2.4 Hz, 1H), 5.30 (t, J = 2.2 Hz, 1H), 4.17 (qd, J = 7.1, 2.9 Hz, 2H), 4.09–3.97 (m, 2H), 2.70–2.59 (m, 2H), 2.17 (s, 3H), 1.21 (t, J = 7.1 Hz, 3H). **^{13}C-NMR** (101 MHz) δ 201.6, 168.1, 143.3, 112.0, 90.2, 68.4, 61.9, 32.7, 30.8, 25.4, 13.9. **HRMS** (ESI) *m/z* calcd for $C_{10}H_{14}O_4$ ([M+Na]$^+$) 221.0790; found 221.0784.

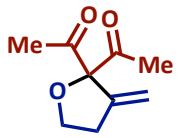

1,1'-(3-Methylenetetrahydrofuran-2,2-diyl)bis(ethan-1-one) (5h). Prepared from 3-diazopentane-2,4-dione and 3-butynol using general procedure **EI**. Orange oil (52 mg, 78%). **^{1}H NMR** (400 MHz) δ 5.34 (t, J = 2.2 Hz, 1H), 5.30 (t, J = 2.4 Hz, 1H), 4.08 (t, J = 7.1 Hz, 2H), 2.67 (ddd, J = 7.1, 4.9, 2.3 Hz, 2H), 2.23 (s, 6H).**^{13}C-NMR** (101 MHz) δ 198.8, 178.9, 144.7, 112.9, 95.5, 42.3, 25.9. ***Compound matched literature known values.***

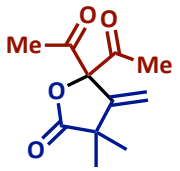

1,1'-(4,4-Dimethyl-3-methylene-5-oxotetrahydrofuran-2,2-diyl)bis(ethan-1-one) (5i). Prepared from 3-diazopentane-2,4-dione and 2,2-dimethylbut-3-ynoic acid using general

procedure **EI**. Yellow oil (45 mg, 91%). **TLC**: R_f 0.71 (7:3 hexanes/EtOAc). **IR** (NaCl): 2977, 2932, 2874, 2853, 1798, 1740, 1720, 1644, 1582. **^{1}H NMR** (400 MHz) δ 5.53 (d, J = 1.5 Hz, 1H), 5.34 (d, J = 1.5 Hz, 1H), 2.28 (s, 6H), 1.29 (s, 6H). **^{13}C-NMR** (101 MHz) δ 198.8, 178.9, 144.7, 112.9, 95.5, 42.3, 25.9. **HRMS** (ESI) *m/z* calcd for $C_{11}H_{14}O_4$ ([M+Na]$^+$) 233.0790; 233.0787 found.

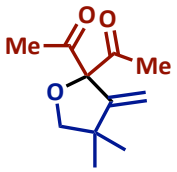

1,1'-(4,4-Dimethyl-3-methylenetetrahydrofuran-2,2-diyl)bis(ethan-1-one) (5j). Prepared from 3-diazopentane-2,4-dione and 2,2-dimethylbut-3-yn-1-ol using general procedure **EI**. Pale yellow oil (51 mg, 87%). **TLC**: R_f 0.57 (4:1 hexanes/EtOAc). **IR** (NaCl): 2966, 2931, 2871, 1736, 1714, 1660, 1583. **^{1}H NMR** (400 MHz) δ 5.28 (t, J = 0.8 Hz, 1H), 5.18 (t, J = 0.8 Hz, 1H), 3.78 (s, 2H), 2.25 (s, 6H), 1.12 (s, 6H). **^{13}C NMR** (101 MHz) δ 203.0, 152.0, 109.3, 98.5, 80.5, 26.4, 25.7. **HRMS** (ESI) *m/z* calcd for $C_{11}H_{16}O_3$ ([M+Na]$^+$) 219.0997; found 219.0997.

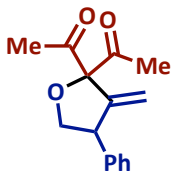

1,1'-(3-Methylene-4-phenyltetrahydrofuran-2,2-diyl)bis(ethan-1-one) (5k). Prepared from ethyl 2-diazo-3-oxobutanoate and 2-phenylbut-3-yn-1-ol using general procedure **EI**. Yellow oil (81 mg, 86%). **TLC**: R_f 0.60 (4:1 hexanes/EtOAc). **^{1}H NMR** (400 MHz) δ 7.36–7.27 (m, 3H), 7.18 (dd, J = 6.9, 1.6 Hz, 2H), 5.46–5.39 (m, 1H), 5.07–5.00 (m, 1H), 4.55–4.44 (m, 1H), 3.96–3.91 (m, 2H), 2.30 (d, J = 4.9 Hz, 6H). **^{13}C NMR** (101 MHz) δ 203.1, 202.6, 147.0,

138.7, 128.8, 128.5, 127.4, 113.7, 75.3, 50.4, 26.2, 25.8. **HRMS** (ESI) *m/z* calcd for $C_{15}H_{16}O_3$ ($[M+Na]^+$) 267.0997; found 267.0995.

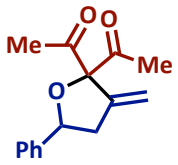

1,1'-(3-Methylene-5-phenyltetrahydrofuran-2,2-diyl)bis(ethan-1-one) (5l). Prepared from 3-diazopentane-2,4-dione and 1-phenylbut-3-yn-1-ol using general procedure **EI**. Yellow oil (72mg, 72%). **TLC**: R_f 0.63 (7:3 hexanes/EtOAc). **^{1}H NMR** (400 MHz) δ 7.46–7.30 (m, 5H), 5.37 (dd, *J* = 2.8, 1.6 Hz, 1H), 5.34 (dd, *J* = 3.0, 1.6 Hz, 1H), 5.07 (dd, *J* = 10.3, 6.1 Hz, 1H), 3.03 (ddt, *J* = 15.7, 6.1, 1.6 Hz, 1H), 2.65 (ddt, *J* = 15.8, 10.3, 2.9 Hz, 1H), 2.31 (d, *J* = 5.4 Hz, 6H). **^{13}C NMR** (101 MHz) δ 203.3, 202.6, 142.6, 139.9, 128.7, 128.3, 126.1, 111.9, 81.4, 41.2, 26.3, 26.0. **HRMS** (ESI) *m/z* calcd for $C_{15}H_{16}O_3$ ($[M+Na]^+$) 267.0997; found 267.0993.

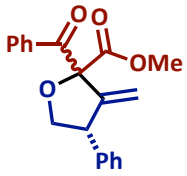

Methyl-2-benzoyl-3-methylene-4-phenyltetrahydrofuran-2-carboxylate (5m). Prepared from methyl 2-diazo-3-oxo-3-phenylpropanoate and 2-phenylbut-3-yn-1-ol using general procedure **EI**. Clear oil (47 mg, 77%). **TLC**: R_f 0.65 (4:1 hexanes/EtOAc). **^{1}H NMR** (400 MHz) δ 8.14–8.02 (m, 2H), 7.63–7.53 (m, 1H), 7.52–7.37 (m, 2H), 7.40–7.15 (m, 5H), 5.55 (d, *J* = 3.0 Hz, 1H), 5.13 (d, *J* = 2.7 Hz, 1H), 4.47 (t, *J* = 8.2 Hz, 1H), 4.27 (dd, *J* = 10.1, 8.3 Hz, 1H), 3.97 (ddt, *J* = 10.7, 8.1, 2.8 Hz, 1H), 3.80 (s, 3H). **^{13}C NMR** (101 MHz) δ 190.6, 170.2, 148.7,

138.5, 134.2, 133.4, 129.8, 128.9, 128.7, 128.5, 127.3, 114.4, 91.4, 76.1, 53.1, 50.6.

Compound matched literature known values

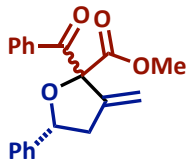

Methyl-2-benzoyl-3-methylene-5-phenyltetrahydrofuran-2-carboxylate (5n). Prepared from methyl 2-diazo-3-oxo-3-phenylpropanoate and 1-phenylbut-3-yn-1-ol using general procedure **EI**. Clear oil (52 mg, 77%). **TLC**: R_f 0.64 (7:3 hexanes/EtOAc). **^{1}H NMR** (400 MHz) δ 8.16–8.03 (m, 4H), 7.60–7.50 (m, 1H), 7.48–7.39 (m, 1H), 7.37–7.19 (m, 4H), 5.53 (dd, *J* = 2.8, 1.3 Hz, 1H), 5.46 (dd, *J* = 3.1, 1.2 Hz, 1H), 5.42 (dd, *J* = 10.8, 5.6 Hz, 1H), 3.77 (s, 3H), 3.04 (ddt, *J* = 15.2, 5.7, 1.3 Hz, 1H), 2.67 (ddt, *J* = 15.1, 10.8, 2.9 Hz, 1H). **^{13}C NMR** (101 MHz) δ 190.8, 170.3, 144.2, 140.0, 134.4, 133.2, 129.9, 128.4, 128.4, 128.3, 127.9, 125.9, 112.6, 82.2, 52.9, 41.9. **HRMS** (ESI) *m/z* calcd for $C_{20}H_{18}O_4$ ([M+Na]$^+$) 345.1095; found 345.1102.

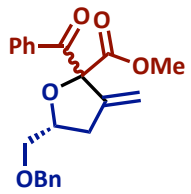

Methyl (5*R*)-2-benzoyl-5-((benzyloxy)methyl)-3-methylenetetrahydrofuran-2-carboxylate (4o). Prepared from methyl 2-diazo-3-oxo-3-phenylpropanoate and (*R*)-1-(benzyloxy)pent-4-yn-2-ol using general procedure **EI**. Clear oil (62 mg, 64%): $[\alpha]_D^{21}$+22.8 (c = 1, $CHCl_3$). **TLC**: R_f 0.52 (7:3 hexanes/EtOAc). **^{1}H NMR** (400 MHz) δ 8.13–8.00 (m, 2H), 7.40 (t, *J* = 7.8 Hz, 3H), 7.23 (dd, *J* = 5.2, 1.7 Hz, 3H), 7.16 (dd, *J* = 6.9, 2.8 Hz, 2H), 5.48 (dd, *J* = 2.7, 1.6 Hz, 1H), 5.40 (dd, *J* = 2.9, 1.6 Hz, 1H), 4.43 (s, 2H), 3.75 (s, 3H), 3.66 (ddd, *J* =

14.6, 4.8, 2.4 Hz, 1H), 3.53 (t, *J* = 4.3 Hz, 2H), 2.84 – 2.72 (m, 1H), 2.68 (ddt, *J* = 8.9, 5.9, 2.7 Hz, 1H). **^{13}C NMR** (101 MHz) *δ* 191.3, 170.2, 143.8, 138.0, 134.4, 133.1, 129.9, 129.3, 128.6, 128.3, 128.3, 128.2, 127.5, 127.4, 112.8, 90.9, 79.9, 77.3, 73.2, 71.1, 53.0, 35.2. **HRMS** (ESI) *m/z* calcd for $C_{22}H_{22}O_5$ ([M+Na]$^+$) 389.1357; found 389.1365.

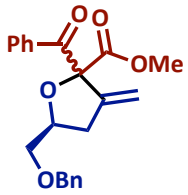

Methyl (5*S*)-2-benzoyl-5-((benzyloxy)methyl)-3-methylenetetrahydrofuran-2-carboxylate (4p). Prepared from methyl 2-diazo-3-oxo-3-phenylpropanoate and (*S*)-1-(benzyloxy)pent-4-yn-2-ol using general procedure **EI**. Clear oil (47 mg, 75%): $[\alpha]_D^{21}$ –22.8 (c = 1, $CHCl_3$). **TLC**: R_f 0.52 (7:3 hexanes/EtOAc). **^{1}H NMR** (400 MHz) *δ* 8.13–8.00 (m, 2H), 7.40 (t, *J* = 7.8 Hz, 3H), 7.23 (dd, *J* = 5.2, 1.7 Hz, 3H), 7.16 (dd, *J* = 6.9, 2.8 Hz, 2H), 5.48 (dd, *J* = 2.7, 1.6 Hz, 1H), 5.40 (dd, *J* = 2.9, 1.6 Hz, 1H), 4.43 (s, 2H), 3.75 (s, 3H), 3.66 (ddd, *J* = 14.6, 4.8, 2.4 Hz, 1H), 3.53 (t, *J* = 4.3 Hz, 2H), 2.84 – 2.72 (m, 1H), 2.68 (ddt, *J* = 8.9, 5.9, 2.7 Hz, 1H). **^{13}C NMR** (101 MHz) *δ* 191.3, 170.2, 143.8, 138.0, 134.4, 133.1, 129.9, 129.3, 128.6, 128.3, 128.2, 127.5, 127.4, 112.8, 90.9, 79.9, 77.3, 73.2, 71.1, 53.0, 35.2. **HRMS** (ESI) *m/z* calcd for $C_{22}H_{22}O_5$ ([M+Na]$^+$) 389.1357; found 389.1365.

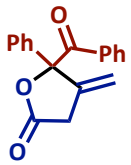

5-Benzoyl-4-methylene-5-phenyldihydrofuran-2(3*H*)-one (5q). Prepared from 2-diazo-1,2-diphenylethan-1-one and but-3-ynoic acid using general procedure **EI**. Clear oil (19 mg,

87%). **TLC**: R_f 0.54 (7:3 hexanes/EtOAc). **^{1}H NMR** (400 MHz) δ 7.56–7.29 (m, 10H), 5.45 (d, J = 2.5 Hz, 1H), 5.28 (t, J = 2.8 Hz, 1H), 3.50 – 3.22 (m, 2H). **^{13}C NMR** (101 MHz) δ 194.5, 172.9, 134.9, 133.3, 132.9, 130.7, 129.9, 129.0, 128.9, 128.8, 128.7, 128.3, 124.9, 115.2, 34.7, 29.7. **HRMS** (ESI) *m/z* calcd for $C_{18}H_{14}O_3$ ([M+H]$^+$) 279.1002; found 279.1003.

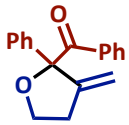

(3-Methylene-2-phenyltetrahydrofuran-2-yl)(phenyl)methanone (5r). Prepared from 2-diazo-1,2-diphenylethan-1-one and but-3-yn-1-ol using general procedure **EI**. Clear oil (70 mg, 86%). **TLC**: R_f 0.85 (7:3 hexanes/EtOAc). **^{1}H NMR** (400 MHz) δ 7.71–7.62 (m, 1H), 7.56–7.41 (m, 5H), 7.40–7.24 (m, 4H), 5.36 (t, J = 2.1 Hz, 1H), 5.05 (t, J = 2.3 Hz, 1H), 4.22–4.08 (m, 1H), 3.98 (td, J = 8.2, 6.8 Hz, 1H), 2.93–2.58 (m, 2H). **^{13}C NMR** (101 MHz) δ 198.4, 148.6, 140.3, 135.2, 134.9, 130.5, 129.9, 129.0, 128.5, 128.4, 128.3, 127.8, 127.7, 125.4, 111.5, 92.6, 66.7, 32.7. **HRMS** (ESI) *m/z* calcd for $C_{15}H_{16}O_3$ ([M+Na]$^+$) 287.1048; found 287.1038.

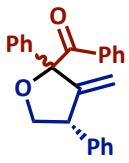

(3-Methylene-2,4-diphenyltetrahydrofuran-2-yl)(phenyl)methanone (5s). Prepared from 2-diazo-1,2-diphenylethan-1-one and 2-phenylbut-3-yn-1-ol using general procedure **EI**. Clear oil (19 mg, 82%). **TLC**: R_f 0.84 (7:3 hexanes/EtOAc). **^{1}H NMR** (400 MHz) δ 7.71–7.62 (m, 1H), 7.57–7.21 (m, 11H), 7.24–7.12 (m, 3H), 5.11 (d, J = 2.7 Hz, 1H), 5.03 (d, J = 2.4 Hz, 1H), 4.40 (t, J = 8.1 Hz, 1H), 4.13 (t, J = 8.1 Hz, 1H), 4.07 (tt, J = 7.8, 2.5 Hz, 1H). **^{13}C NMR** (101 MHz) δ 197.8, 153.2, 140.0, 134.9, 132.6, 130.6, 129.9, 129.0, 128.7, 128.6, 128.5,

127.9, 127.8, 126.9, 125.4, 113.9, 109.9, 77.3, 74.5, 50.3, 29.7. **HRMS** (ESI) *m/z* calcd for $C_{24}H_{20}O_2$ ([M+Na]$^+$) 363,1360; found 363.1350.

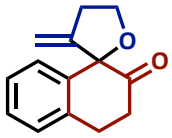

3-Methylene-3',4,4',5-tetrahydro-2'*H*,3*H*-spiro[furan-2,1'-naphthalen]-2'-one (5t). Prepared from 1-diazo-3,4-dihydronaphthalen-2(1*H*)-one and but-3-yn-1-ol using general procedure **EI**. Clear oil (28 mg, 71%). **TLC**: R_f 0.52 (8:2 hexanes/EtOAc). **^{1}H NMR** (400 MHz) δ 7.41–7.11 (m, 4H), 5.19 (d, *J* = 2.2 Hz, 1H), 4.67 (d, *J* = 2.2 Hz, 1H), 4.42 (td, *J* = 8.3, 5.6 Hz, 1H), 4.23 (q, *J* = 7.6 Hz, 1H), 3.16 (qd, *J* = 16.1, 7.9 Hz, 2H), 3.01 – 2.91 (m, 1H), 2.92 – 2.83 (m, 1H), 2.78 (ddd, *J* = 15.2, 7.7, 5.7 Hz, 1H), 2.64 (dt, *J* = 15.4, 6.5 Hz, 1H). **^{13}C NMR** (101 MHz) δ 208.1, 151.1, 138.9, 136.4, 128.1, 128.0, 127.6, 127.2, 110.8, 67.9, 35.9, 32.6, 28.7. **HRMS** (ESI) *m/z* calcd for $C_{14}H_{14}O_2$ ([M+Na]$^+$) 237.0892; found 237.0896.

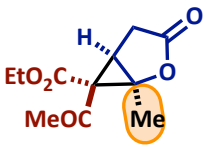

Ethyl 6-acetyl-1-methyl-3-oxo-2-oxabicyclo[3.1.0]hexane-6-carboxylate (7). Prepared from ethyl 2-diazo-3-oxobutanoate and pent-3-ynoic acid using general procedure **3**. Clear thick oil (17 mg, 64%). **TLC**: R_f 0.47 (7:3 hexanes/EtOAc). **^{1}H NMR** (400 MHz) δ 4.26 – 4.15 (m, 2H), 3.63 – 3.57 (m, 1H), 2.95 (d, *J* = 8.7 Hz, 1H), 2.91 (d, *J* = 8.7 Hz, 1H), 2.86 (d, *J* = 2.5 Hz, 1H), 2.81 (d, *J* = 2.5 Hz, 1H), 2.23 (d, *J* = 1.7 Hz, 3H), 1.75 (s, 3H), 1.29 (t, *J* = 7.1 Hz, 3H). **^{13}C NMR** (101 MHz) δ 173.8, 166.6, 164.3, 134.3, 134.1, 129.3, 129.2, 115.1, 109.9, 105.9,

77.3, 77.0, 76.7, 60.1, 47.1, 34.4, 23.7, 14.3, 14.2, 14.0. **ESI-MS** *m/z* calcd for $C_{11}H_{14}O_5$ ($[M+Na]^+$) 249.6; found 249.1.

APPENDIX 1

Spectra Relevant to Chapter 2

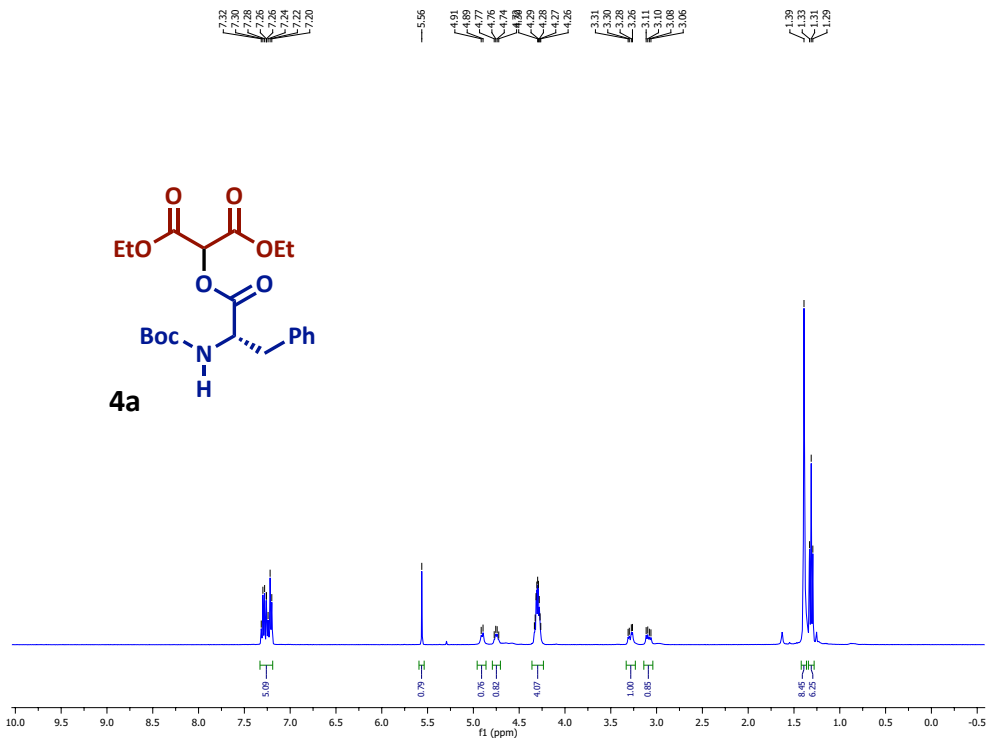
7.32
7.30
7.28
7.26
7.24
7.22
7.20
5.56
4.91
4.89
4.77
4.76
4.74
4.29
4.28
4.27
4.26
3.31
3.30
3.28
3.26
3.11
3.10
3.08
3.06
1.39
1.33
1.31
1.29
O
O
EtO
OEt
O
O
Boc
N
H
Ph
4a
5.09
0.79
0.76
0.82
4.07
1.00
0.85
8.45
6.25
f1 (ppm)

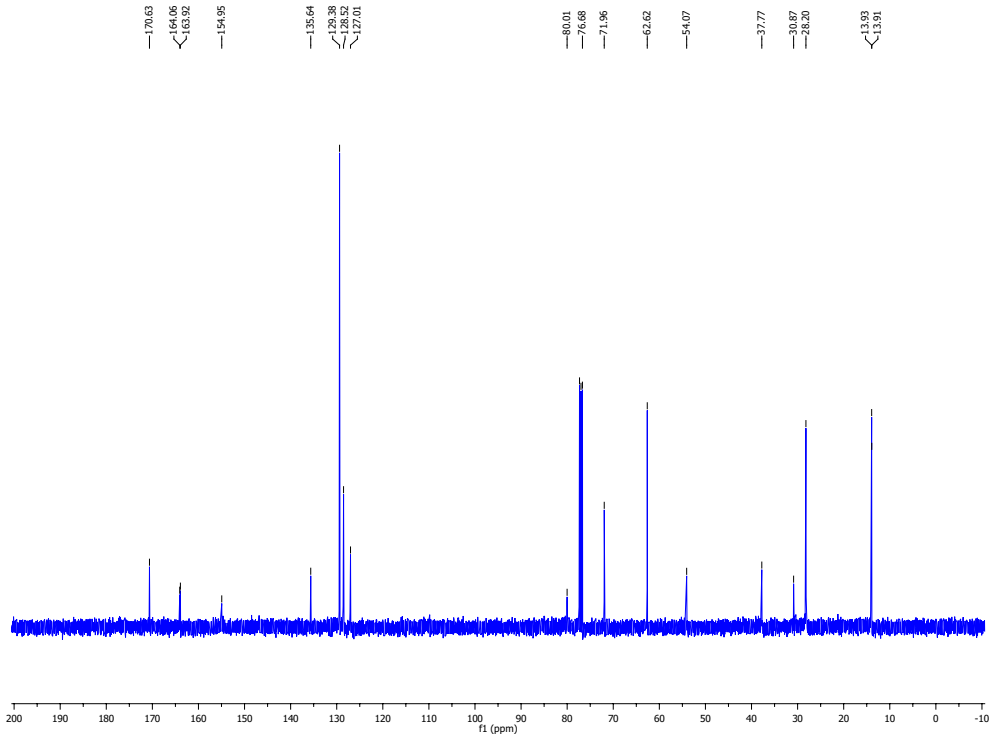
170.63
164.06
163.92
154.95
135.64
129.38
128.52
127.01
80.01
76.68
71.96
62.62
54.07
37.77
30.87
28.20
13.93
13.91
f1 (ppm)

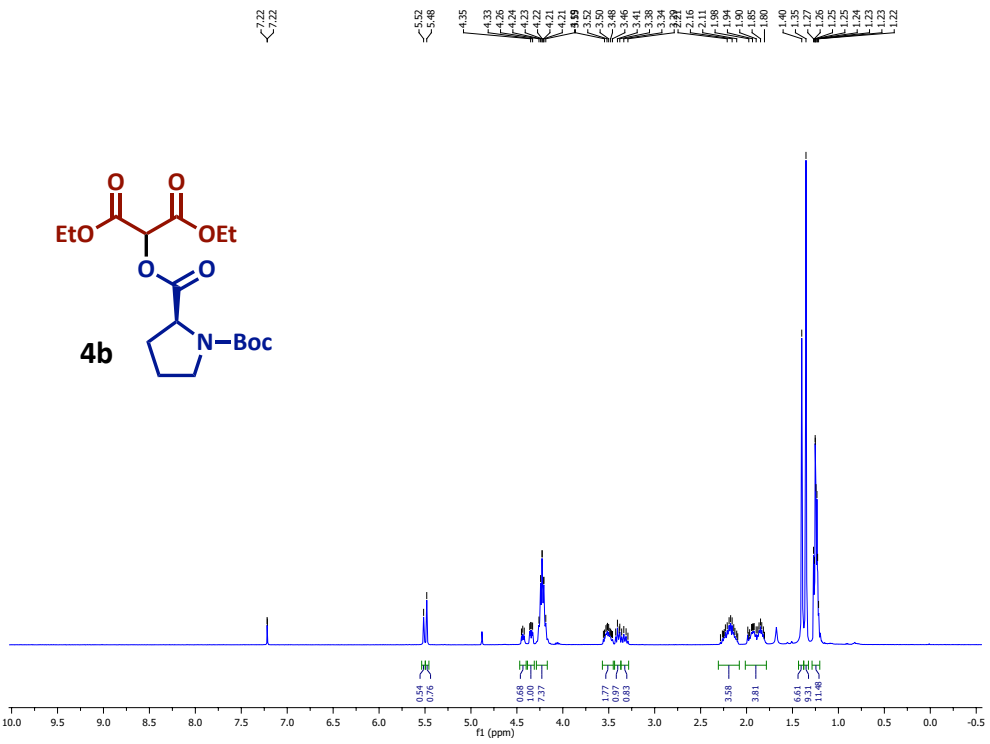
EtO
OEt
O
O
O
O
N–Boc
4b
f1 (ppm)

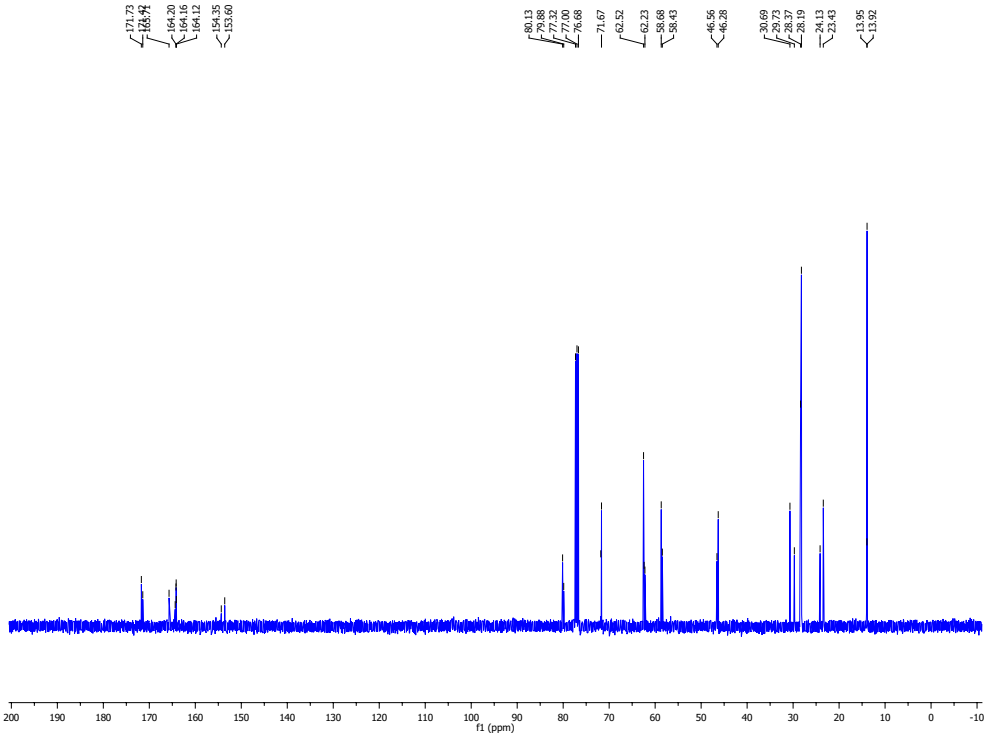
f1 (ppm)

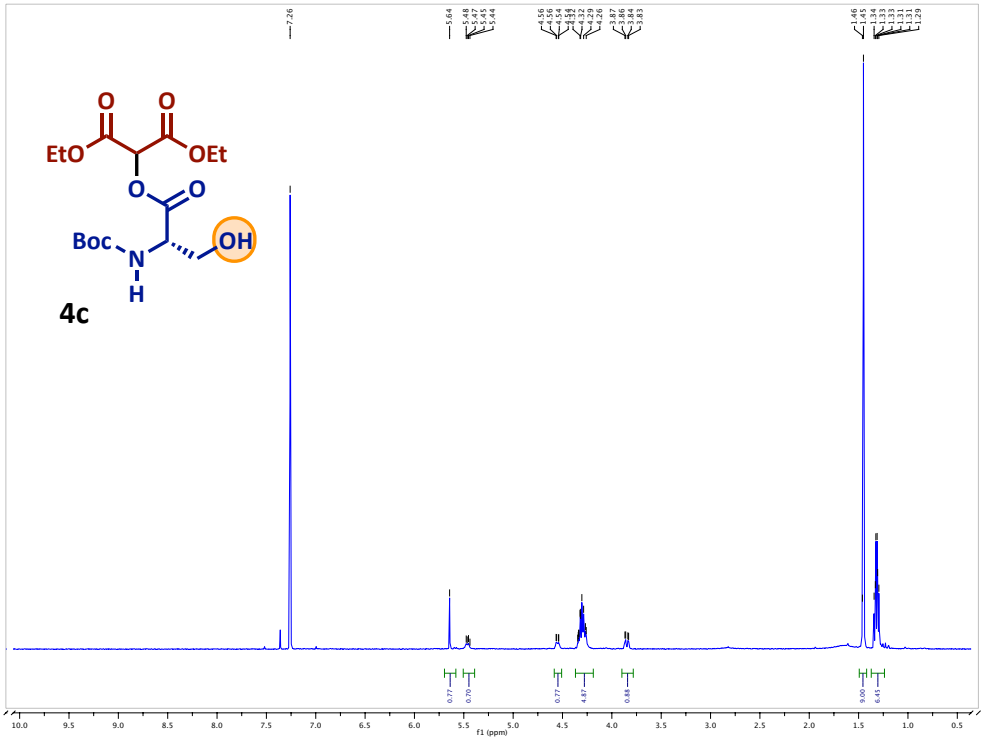
EtO
OEt
Boc
N
H
OH
4c

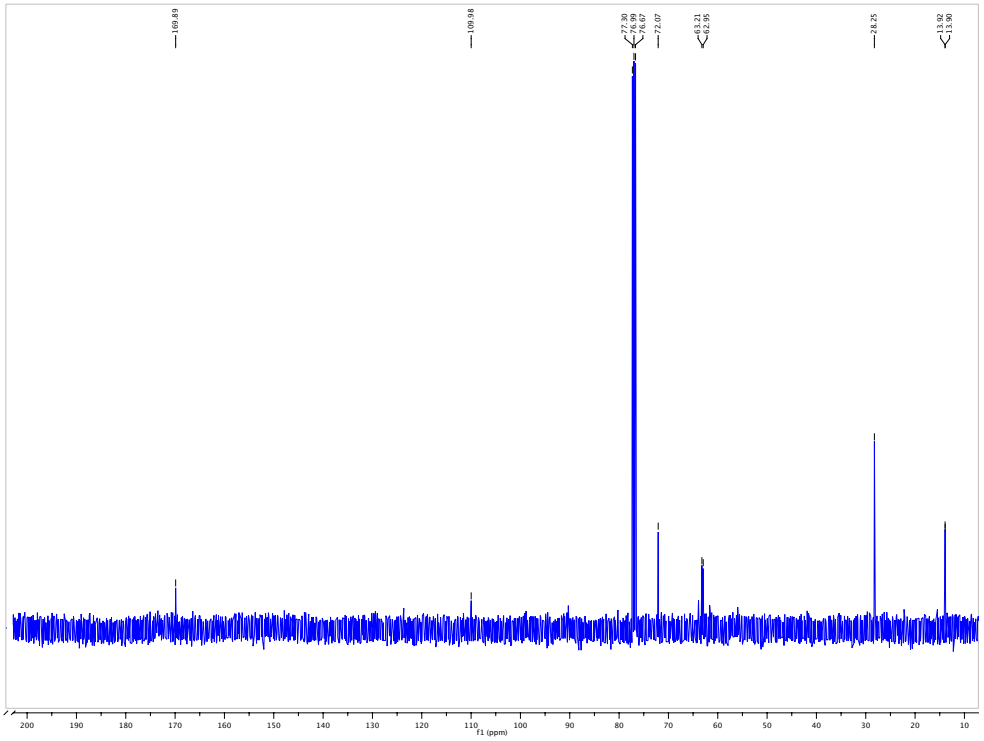

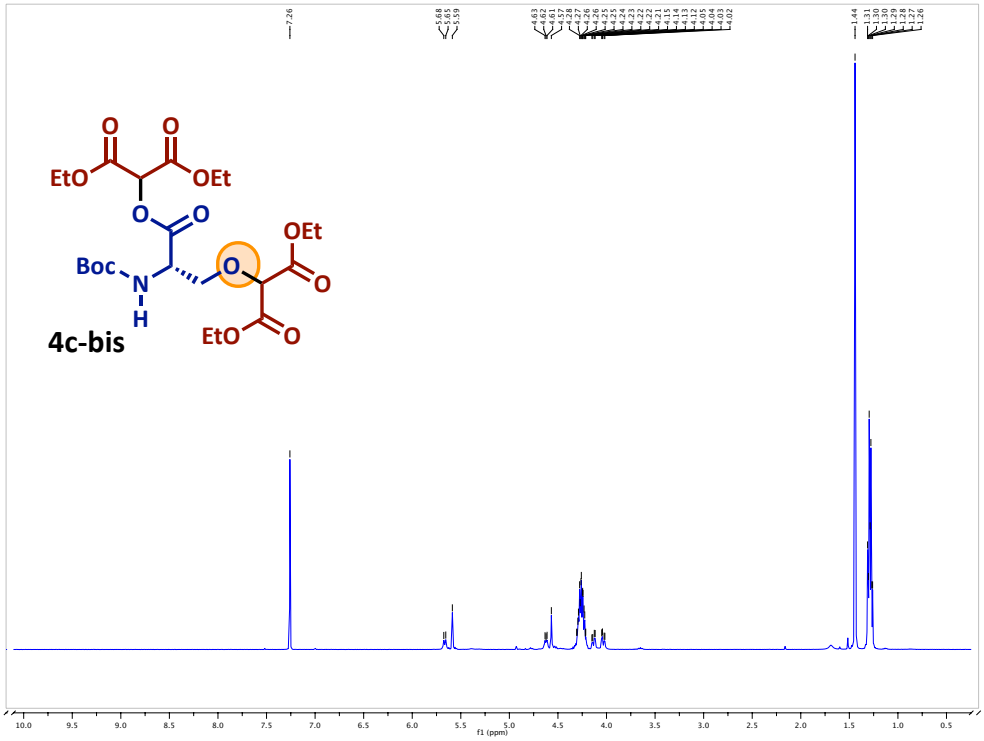
EtO
OEt
O
O
Boc
N
H
O
OEt
O
EtO
O
4c-bis
f1 (ppm)

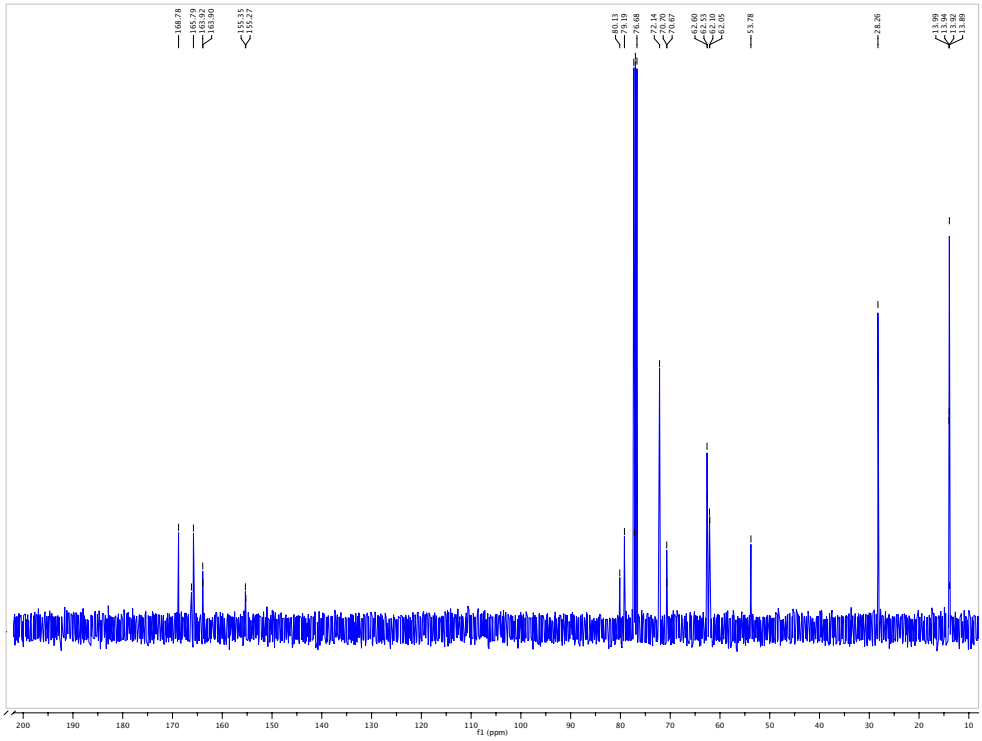
f1 (ppm)

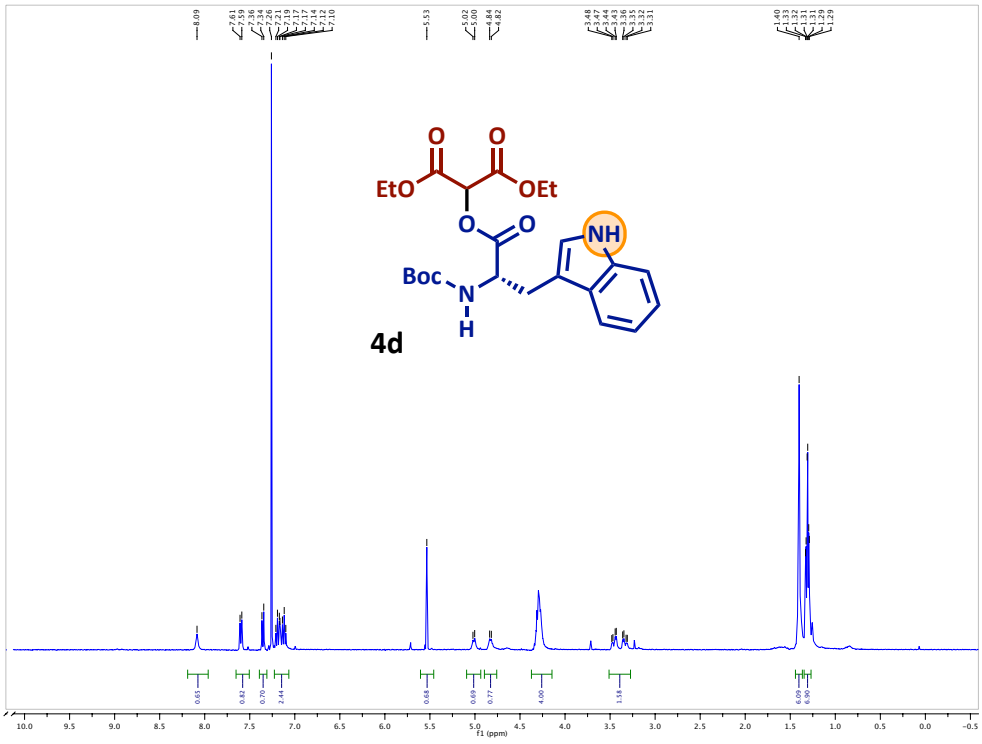
EtO
OEt
Boc
NH
4d

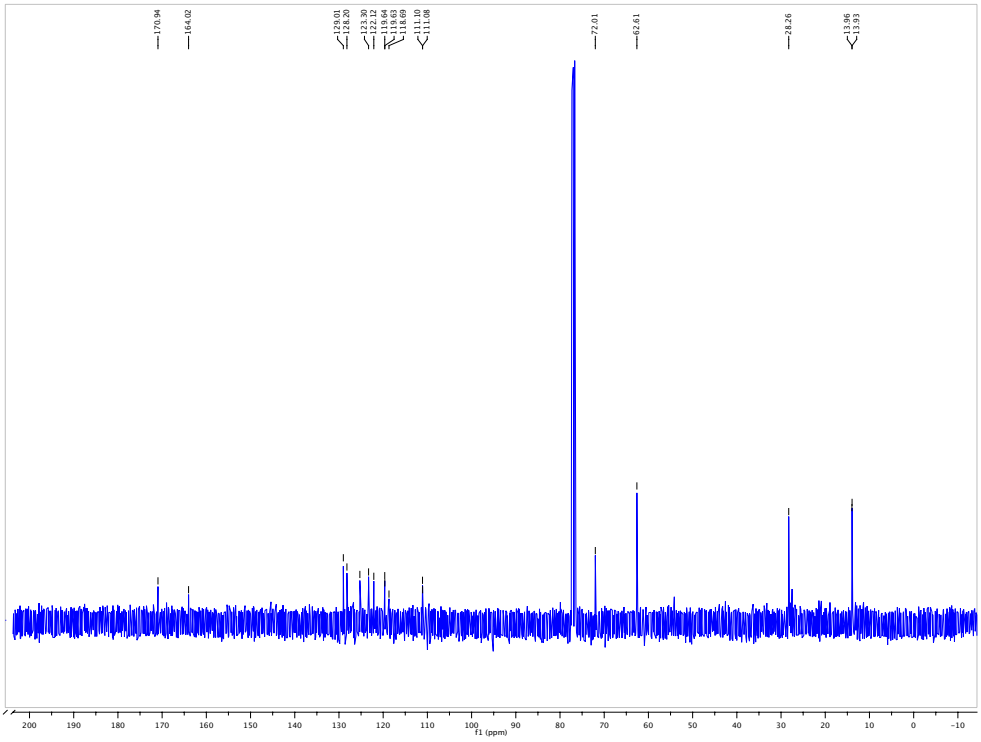

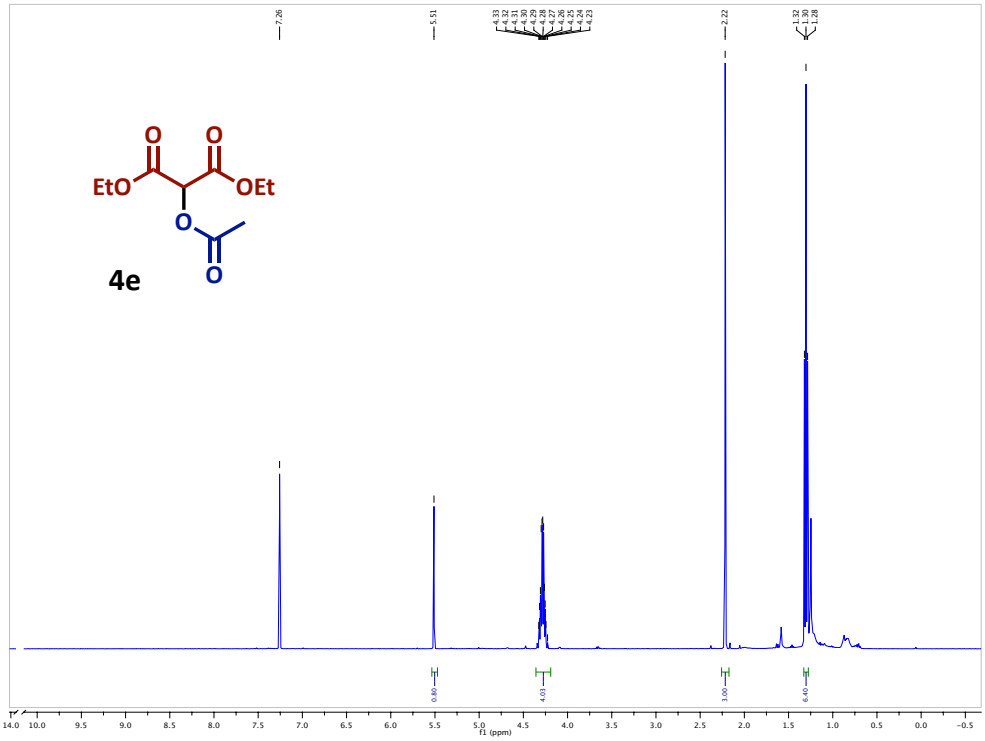
7.26
5.51
4.33
4.32
4.31
4.30
4.29
4.28
4.27
4.26
4.25
4.24
4.23
2.22
1.32
1.30
1.28
O
O
EtO
OEt
O
O
4e
0.80
4.01
3.00
6.40
f1 (ppm)

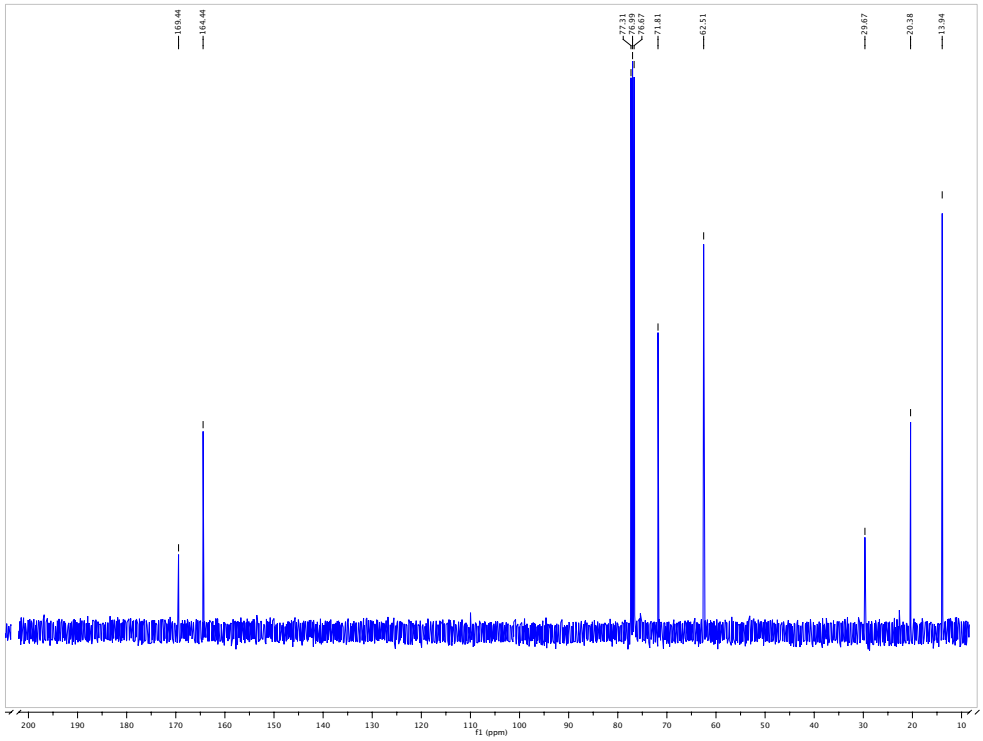
169.44
164.44
77.31
76.99
76.67
71.81
62.51
29.67
20.38
13.94
f1 (ppm)

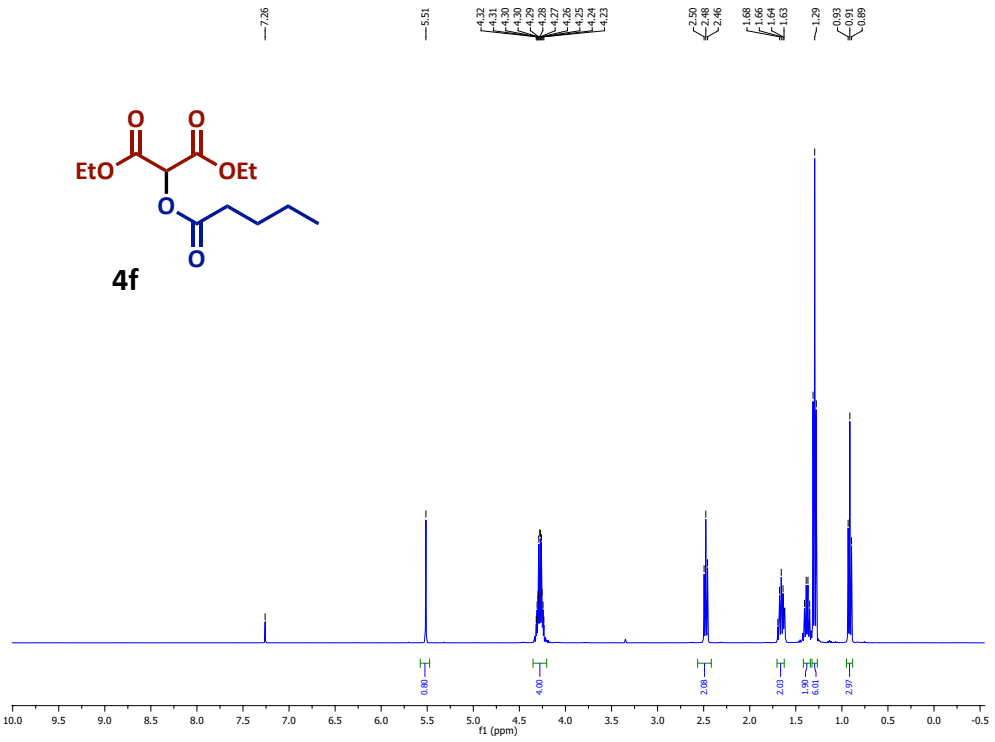
7.26
5.51
4.32
4.31
4.30
4.29
4.28
4.27
4.26
4.25
4.24
4.23
2.50
2.48
2.46
1.68
1.66
1.64
1.63
1.29
0.93
0.91
0.89
O
O
EtO
OEt
O
O
0.80
4.00
2.08
2.03
1.90
6.01
2.97
f1 (ppm)

4f

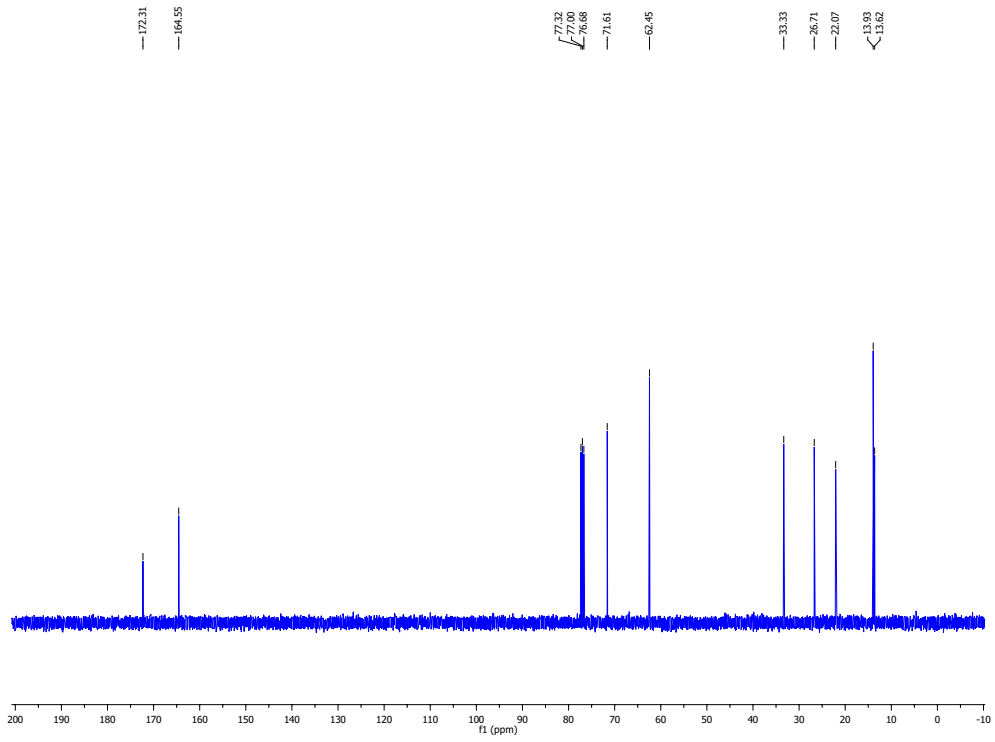
172.31
164.55
77.32
77.00
76.68
71.61
62.45
33.33
26.71
22.07
13.93
13.62
f1 (ppm)

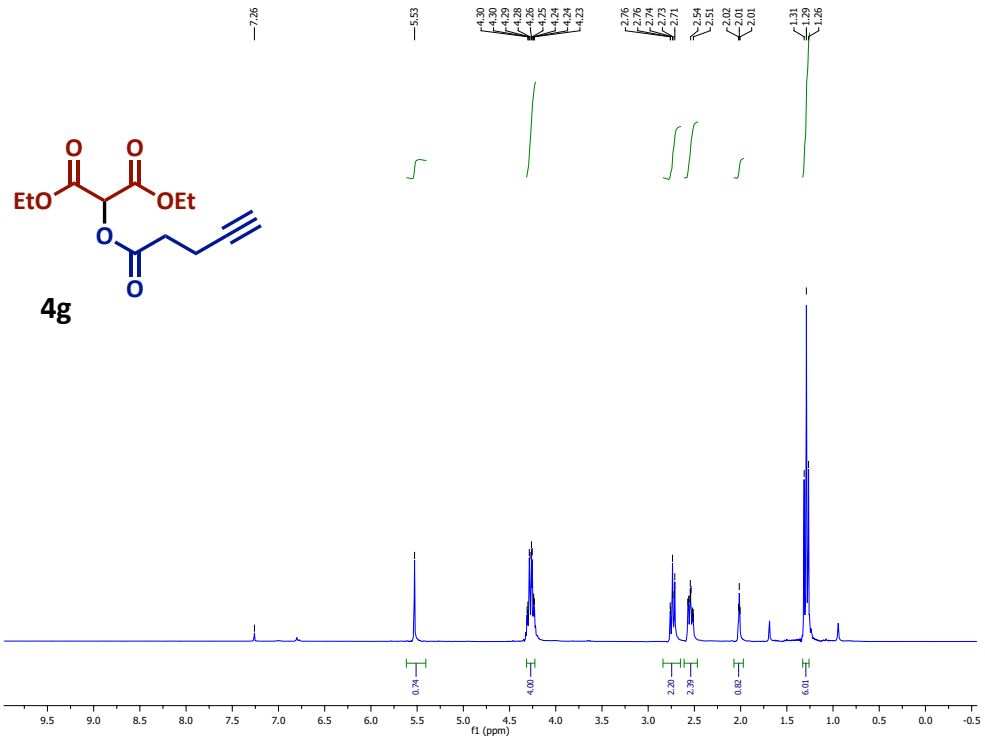
7.26
5.53
4.30
4.30
4.29
4.28
4.26
4.25
4.24
4.24
4.23
2.76
2.76
2.74
2.73
2.71
2.54
2.51
2.02
2.01
2.01
1.31
1.30
1.26
O
O
EtO
OEt
O
O
0.74
4.00
2.20
2.39
0.82
6.01
f1 (ppm)

4g

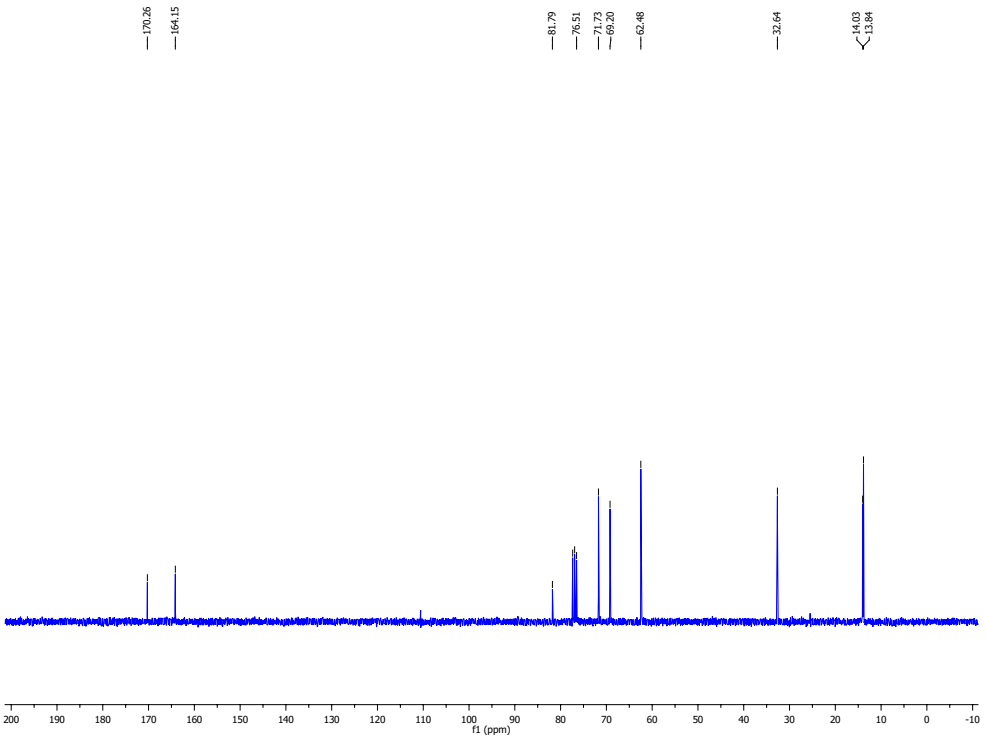
170.26
164.15
81.79
76.51
71.73
69.20
62.48
32.64
14.03
13.84
f1 (ppm)

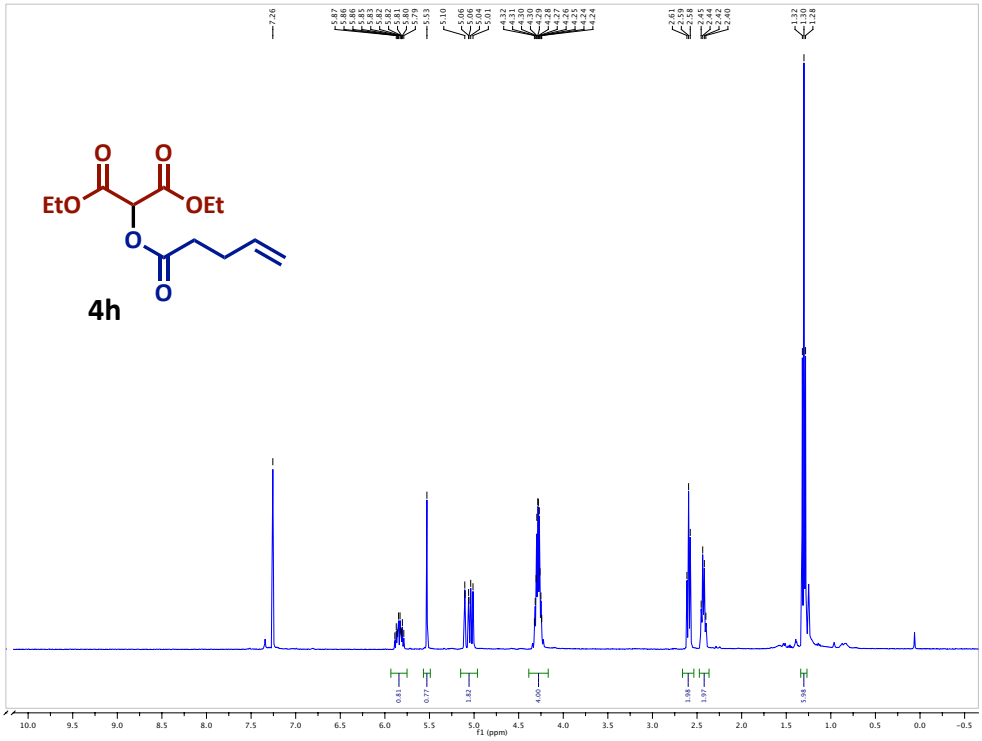
EtO
OEt
4h
f1 (ppm)

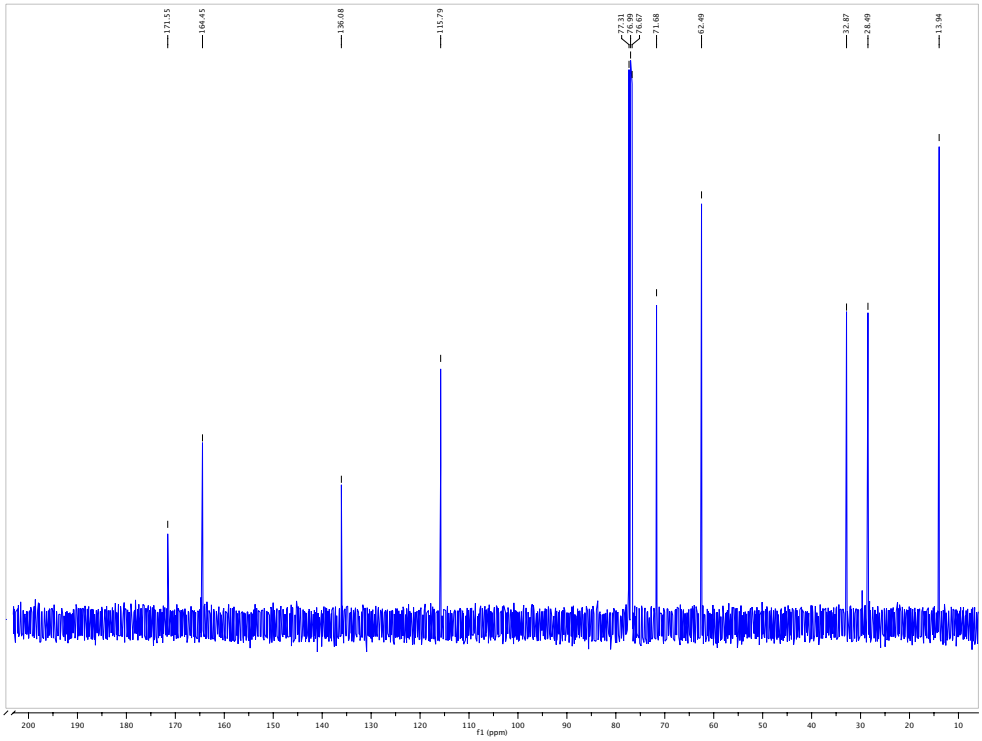
f1 (ppm)

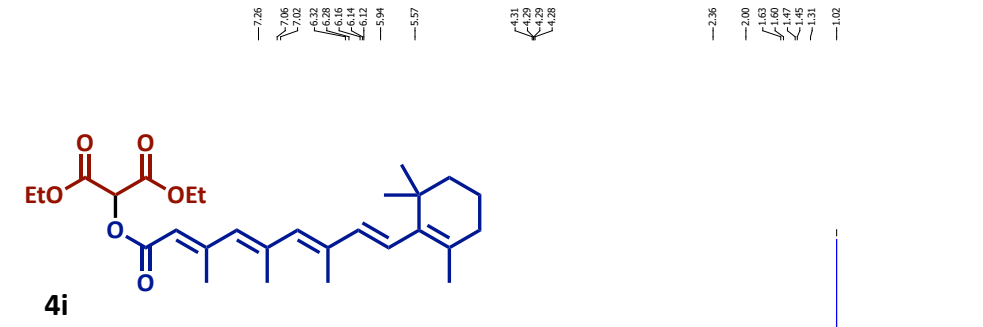
7.26
7.06
7.02
6.32
6.28
6.16
6.14
6.12
5.94
5.57
4.31
4.30
4.29
4.28
2.36
2.00
1.63
1.60
1.47
1.45
1.31
1.02
O
O
EtO
OEt
O
O

4i

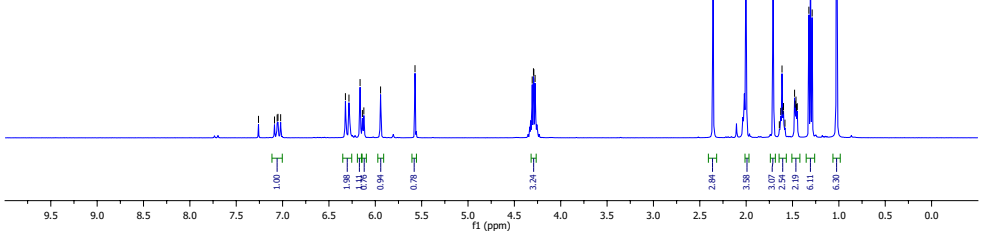
1.00
1.98
0.78
0.94
0.78
3.24
2.84
3.58
3.07
2.54
2.19
6.11
6.30
f1 (ppm)


165.13
164.89
155.90
140.47
137.12
134.54
132.16
130.19
129.33
129.12
116.02
77.32
77.00
76.68
71.39
62.38
39.58
34.23
33.09
28.93
21.72
19.18
14.15
13.96
12.91

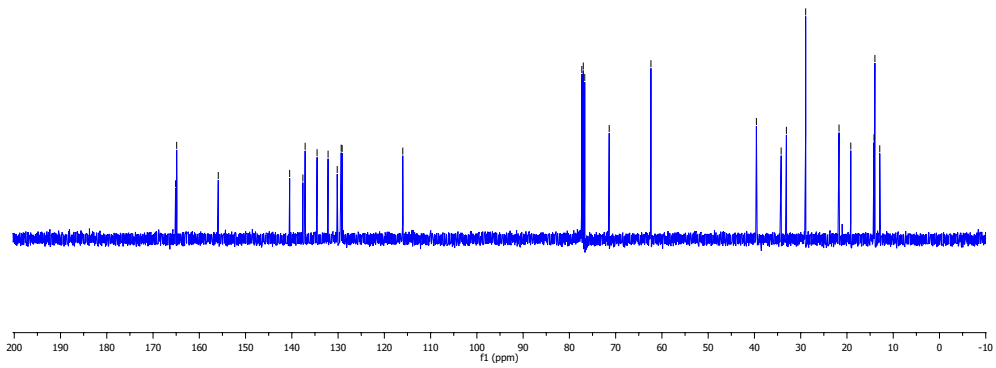
f1 (ppm)

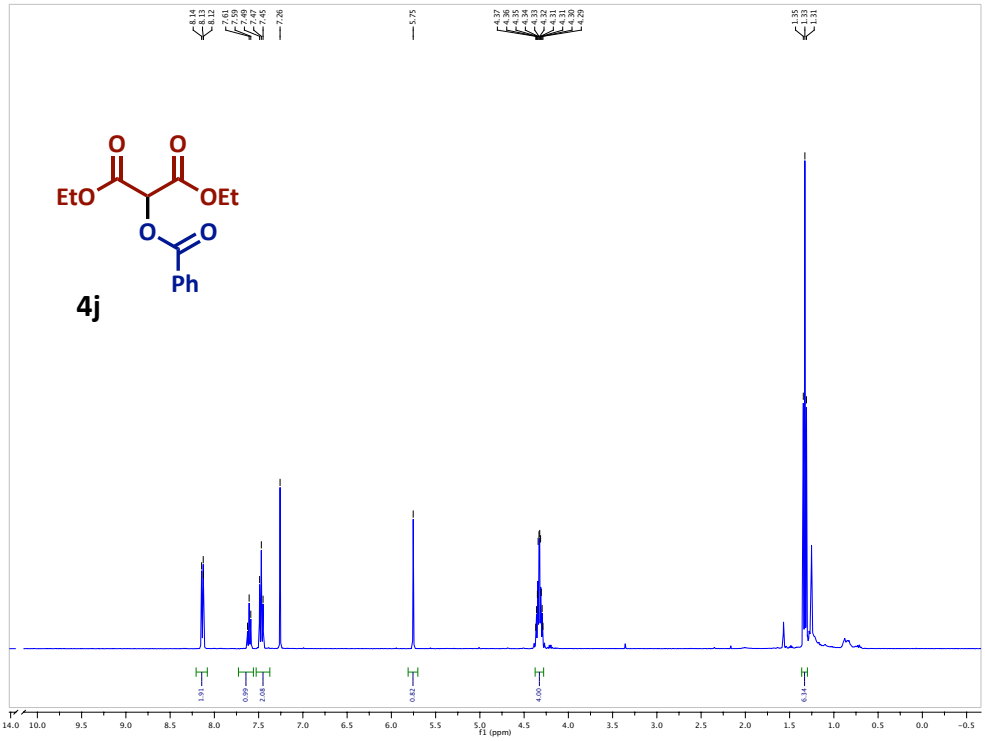
EtO
OEt
O
O
O
O
Ph
4j
f1 (ppm)

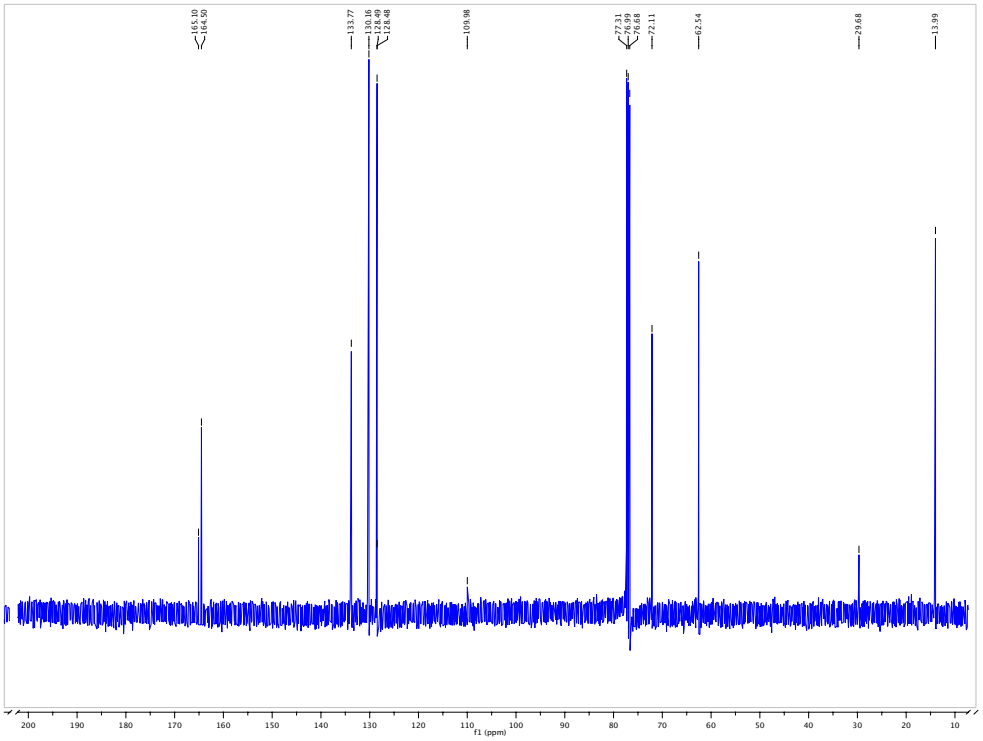
f1 (ppm)

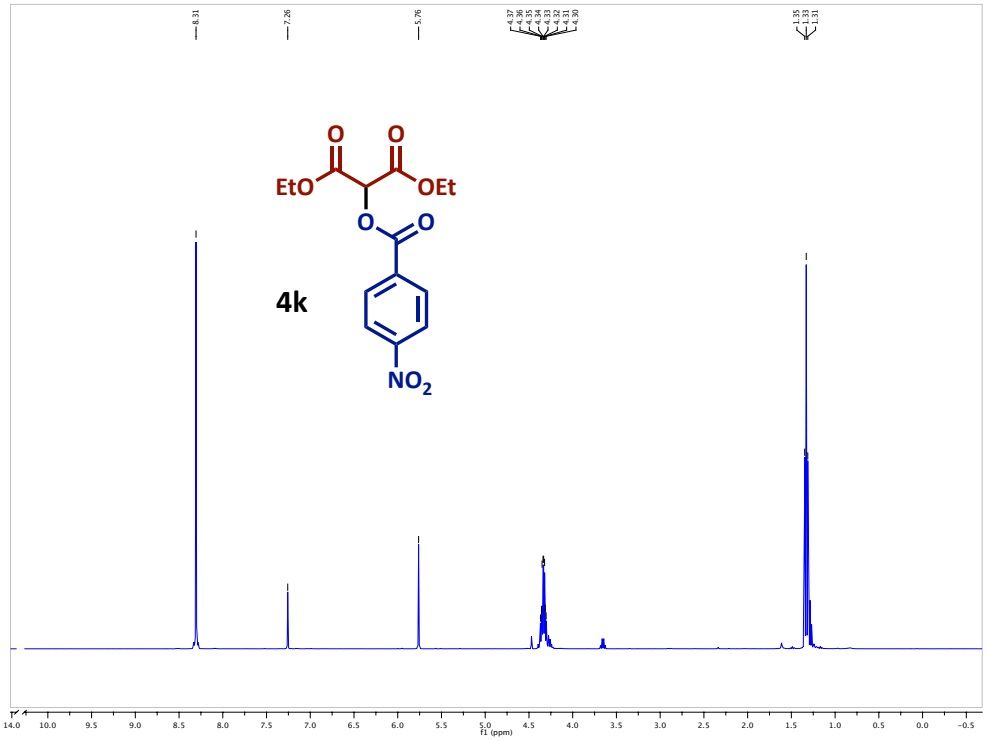
8.31
7.26
5.76
4.37
4.36
4.35
4.34
4.33
4.32
4.31
4.30
1.35
1.33
1.31
O
O
EtO
OEt
O
O
4k
NO2
f1 (ppm)

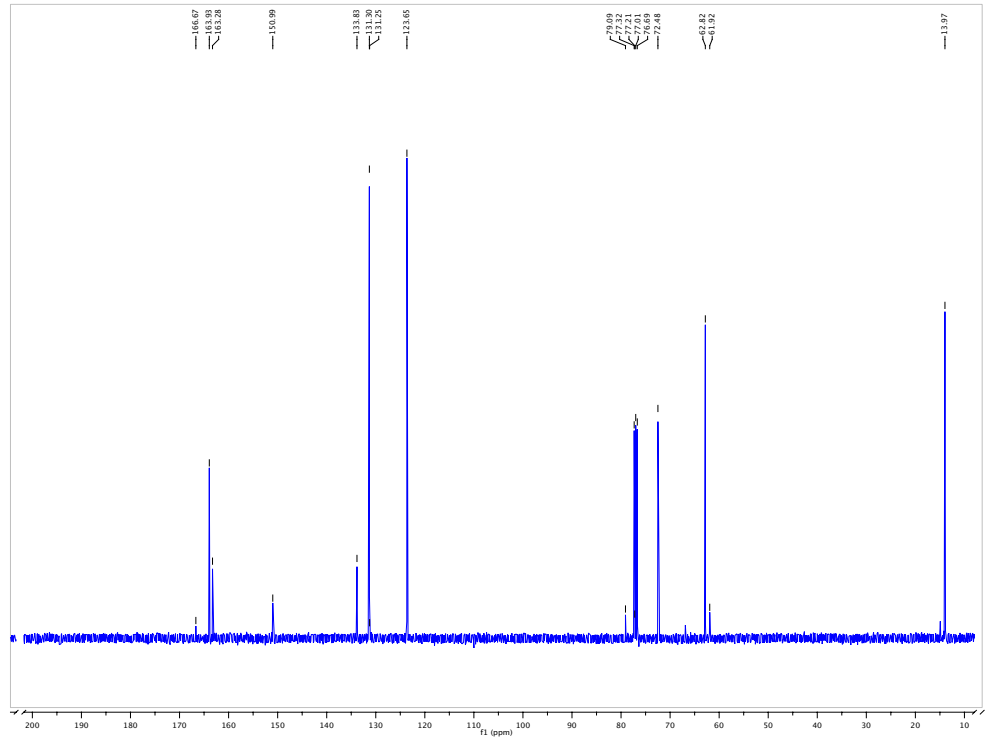
166.67
163.93
163.28
150.99
133.83
131.30
131.25
123.65
79.09
77.32
77.22
77.01
76.69
72.48
62.82
61.92
13.97
f1 (ppm)

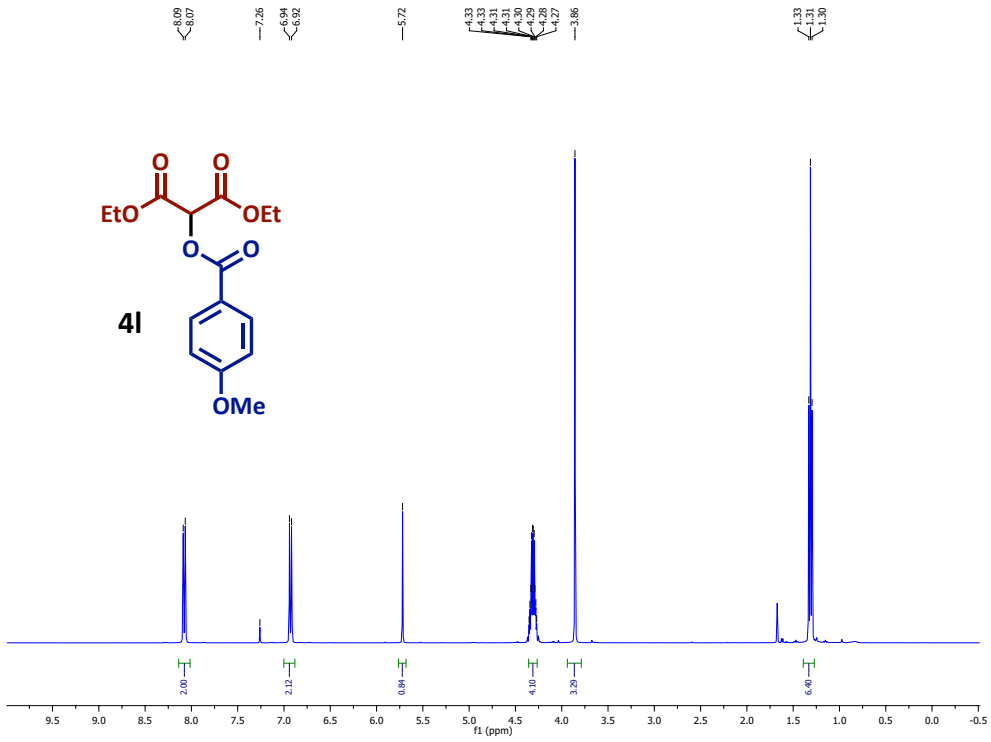
8.09
8.07
7.26
6.94
6.92
5.72
4.33
4.33
4.31
4.31
4.30
4.29
4.28
4.27
3.86
1.33
1.31
1.30
O
O
EtO
OEt
O
O
4l
OMe
2.00
2.12
0.84
4.10
3.29
6.40
f1 (ppm)

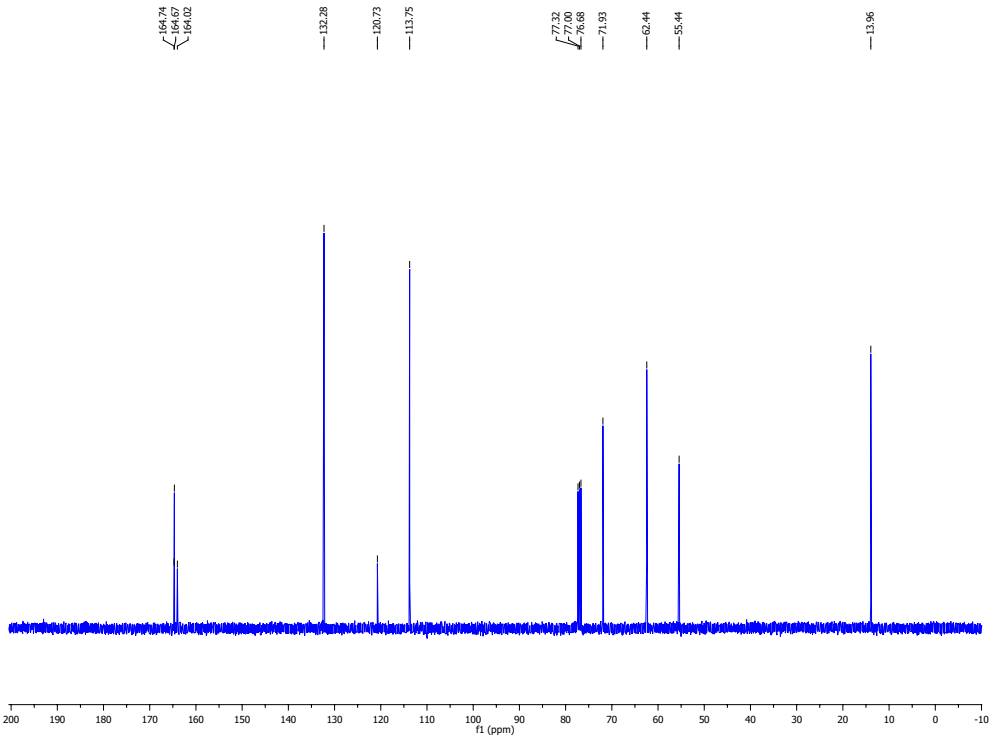
164.74
164.67
164.02
132.28
120.73
113.75
77.32
77.00
76.68
71.93
62.44
55.44
13.96
f1 (ppm)

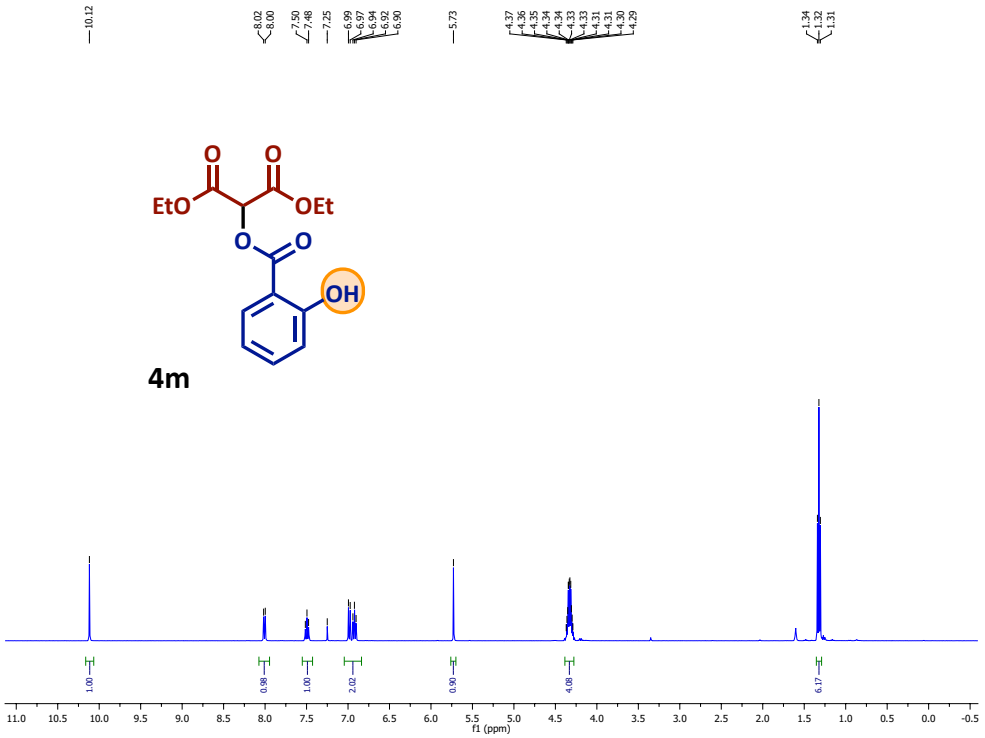
10.12
8.02
8.00
7.50
7.48
7.25
6.99
6.97
6.94
6.92
6.90
5.73
4.37
4.36
4.35
4.34
4.34
4.33
4.33
4.31
4.31
4.30
4.29
1.34
1.32
1.31
EtO
OEt
O
O
O
O
OH
4m
1.00
0.98
1.00
2.02
0.90
4.08
6.17
f1 (ppm)

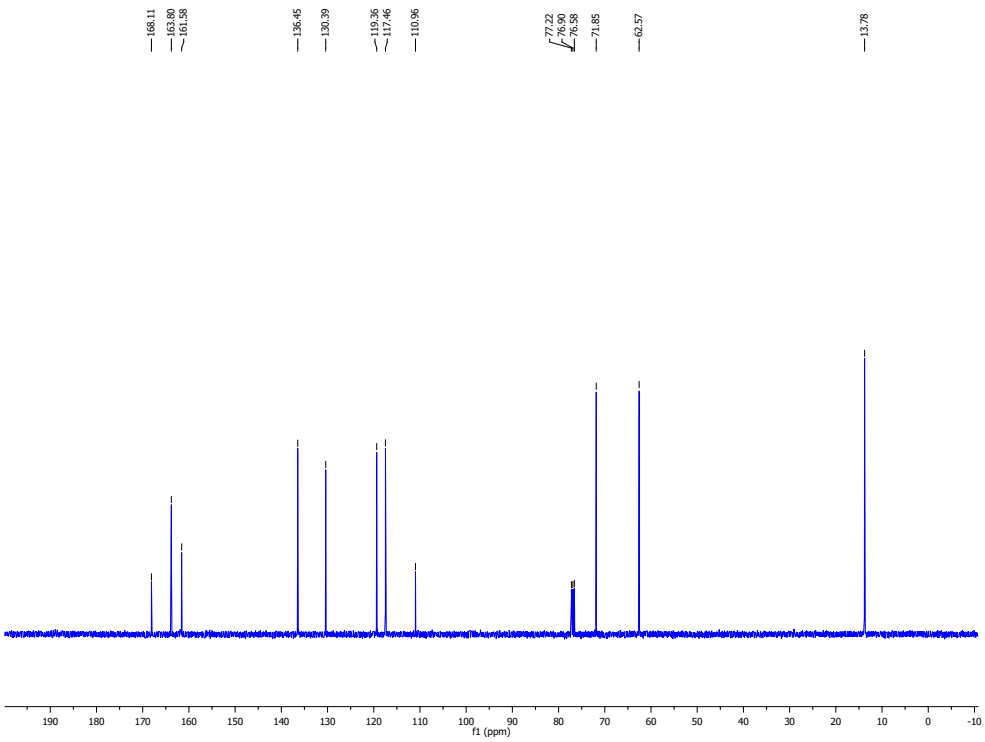
168.11
163.80
161.58
136.45
130.39
119.36
117.46
110.96
77.22
76.90
76.58
71.85
62.57
13.78
f1 (ppm)

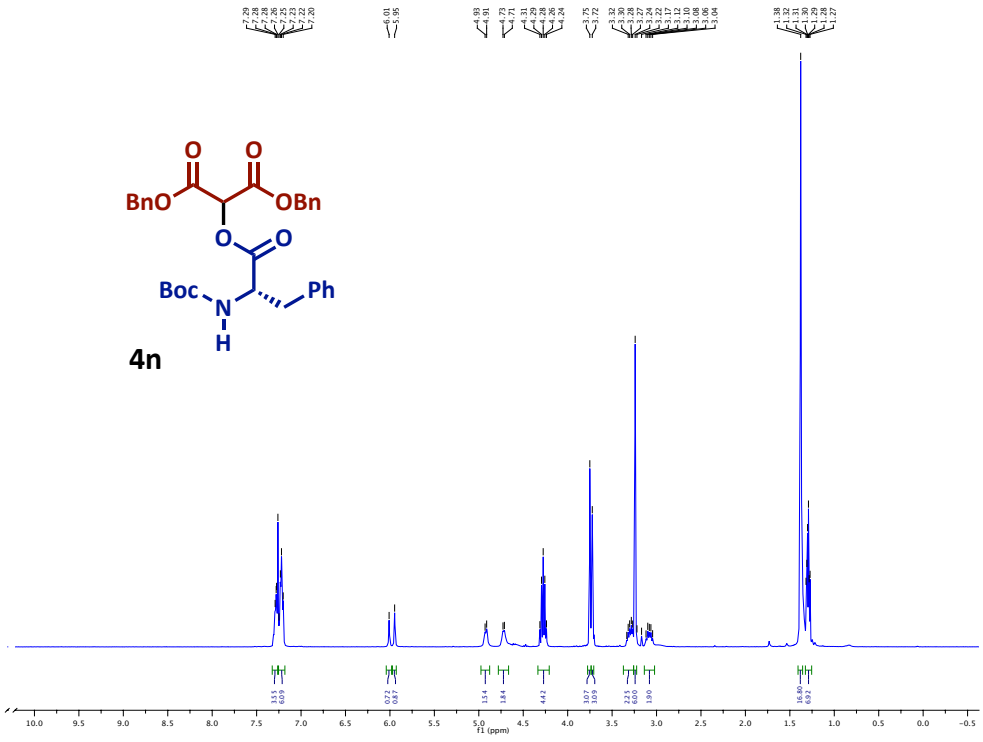
BnO
OBn
Boc
N
H
Ph
4n

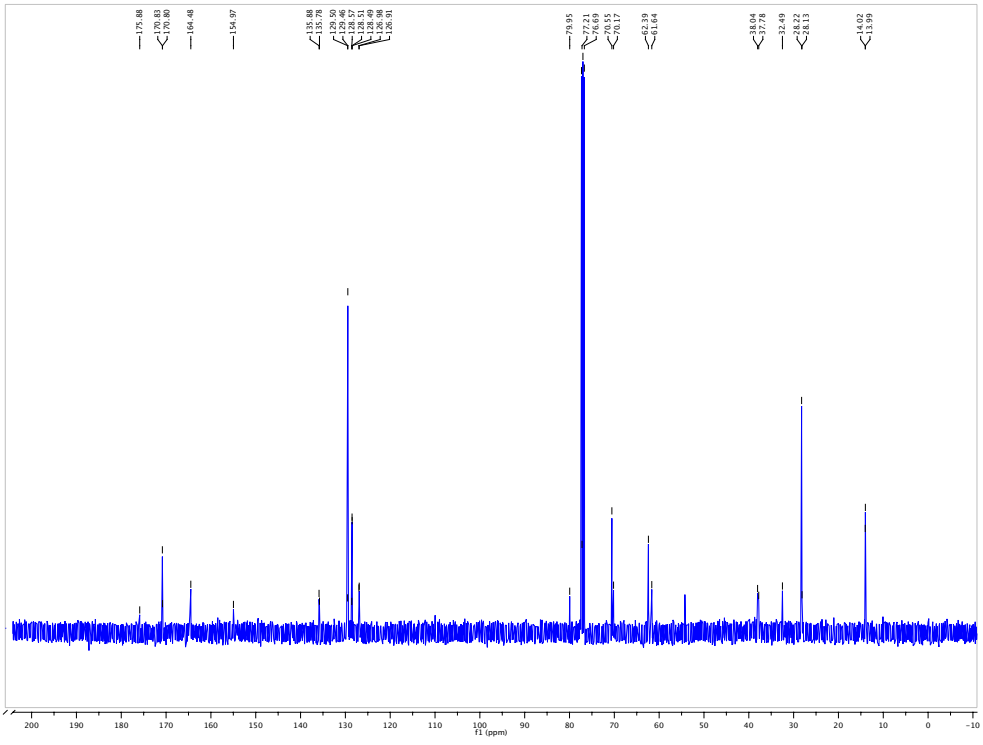

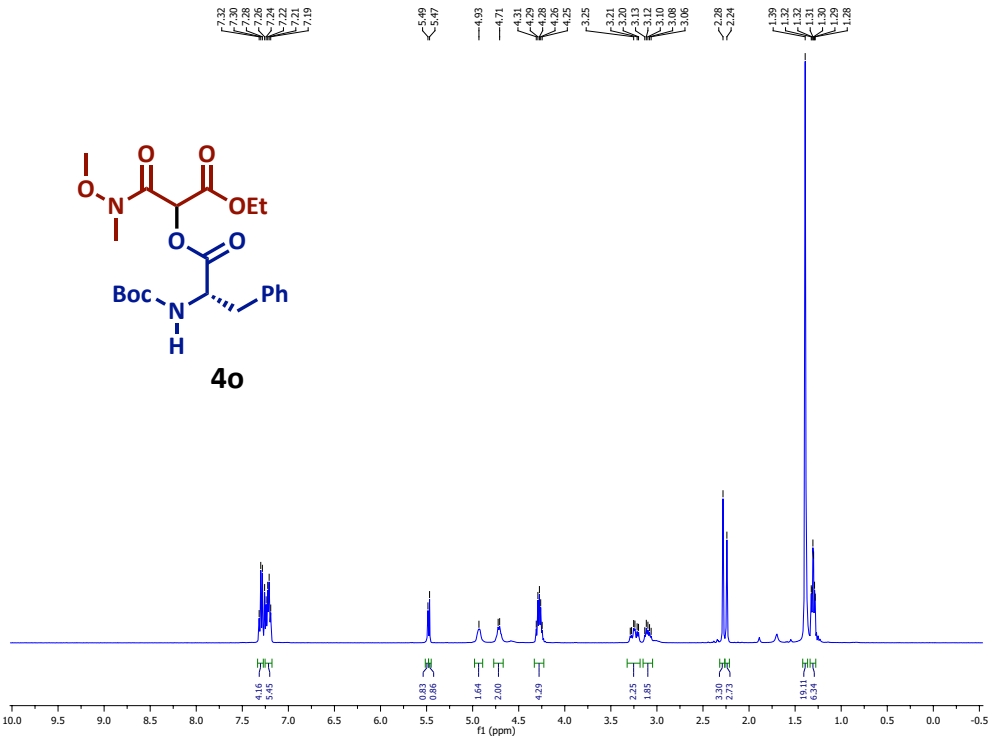
7.32
7.30
7.28
7.26
7.24
7.22
7.21
7.19
5.49
5.47
4.93
4.71
4.31
4.29
4.28
4.26
4.25
3.25
3.21
3.20
3.13
3.12
3.10
3.08
3.06
2.28
2.24
1.39
1.32
1.32
1.31
1.30
1.29
1.28
O
O
O
N
OEt
O
O
Boc
N
H
Ph
4.16
5.45
0.83
0.86
1.64
2.00
4.29
2.25
1.85
3.30
2.73
19.11
6.34
10.0
9.5
9.0
8.5
8.0
7.5
7.0
6.5
6.0
5.5
5.0
4.5
4.0
3.5
3.0
2.5
2.0
1.5
1.0
0.5
0.0
-0.5
f1 (ppm)

4o

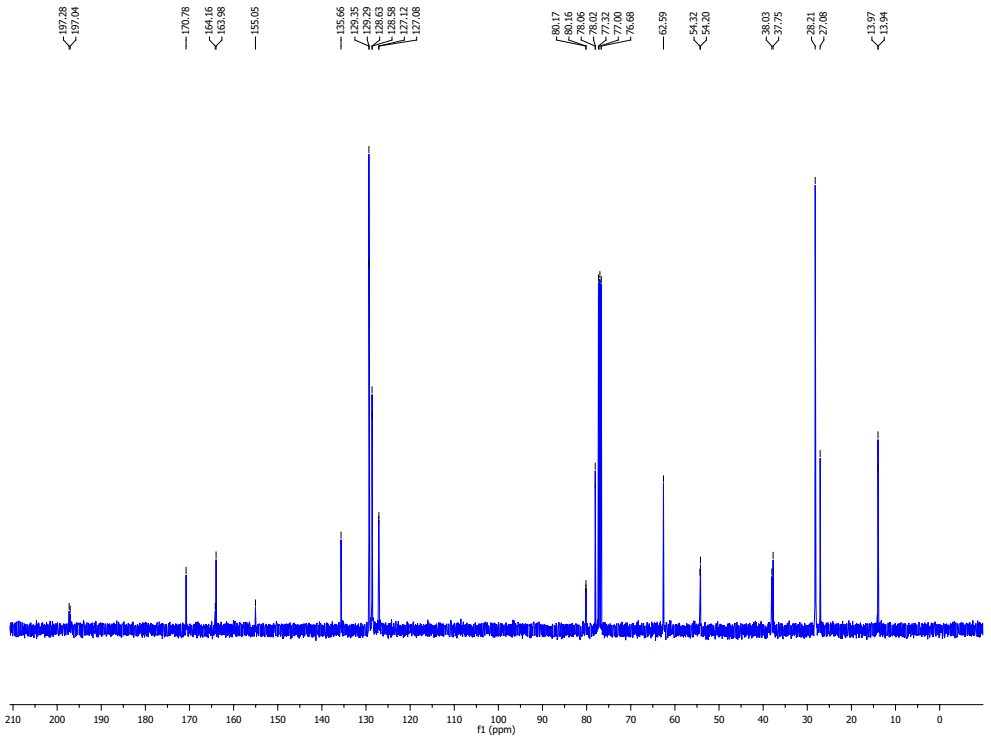
197.28
197.04
170.78
164.16
163.98
155.05
135.66
129.35
129.29
128.93
128.58
127.12
127.08
80.17
80.16
78.06
78.02
77.32
77.00
76.68
62.59
54.32
54.20
38.03
37.75
28.21
27.08
13.97
13.94
210
200
190
180
170
160
150
140
130
120
110
100
90
80
70
60
50
40
30
20
10
0
f1 (ppm)

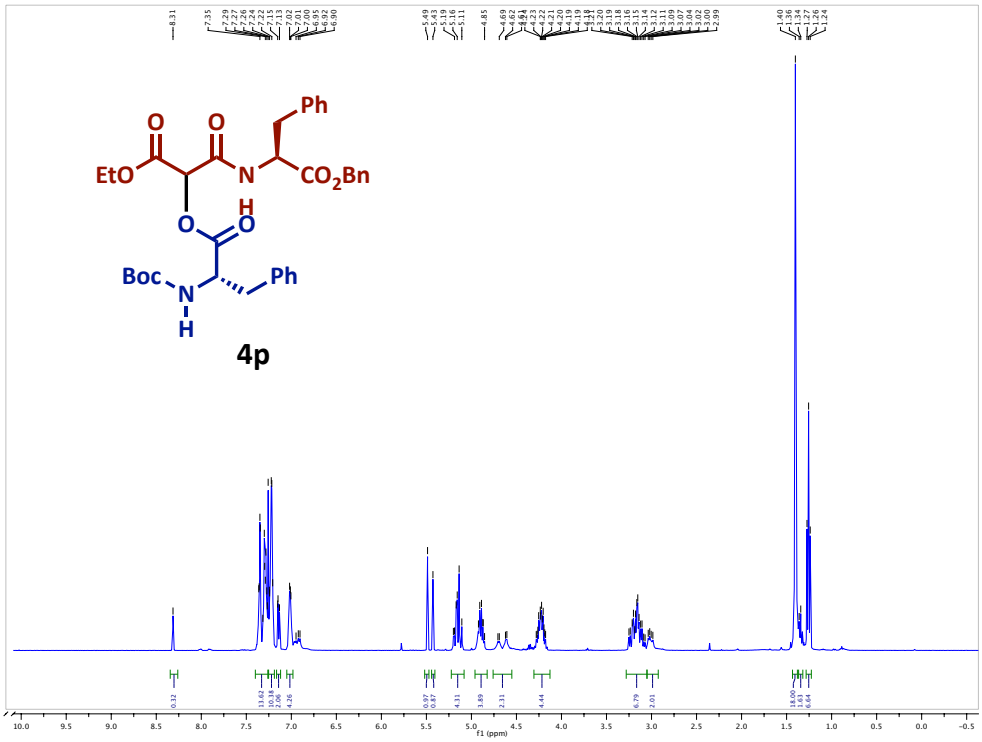
Ph
O
O
EtO
N
CO2Bn
O
H
O
Boc
N
Ph
H
4p

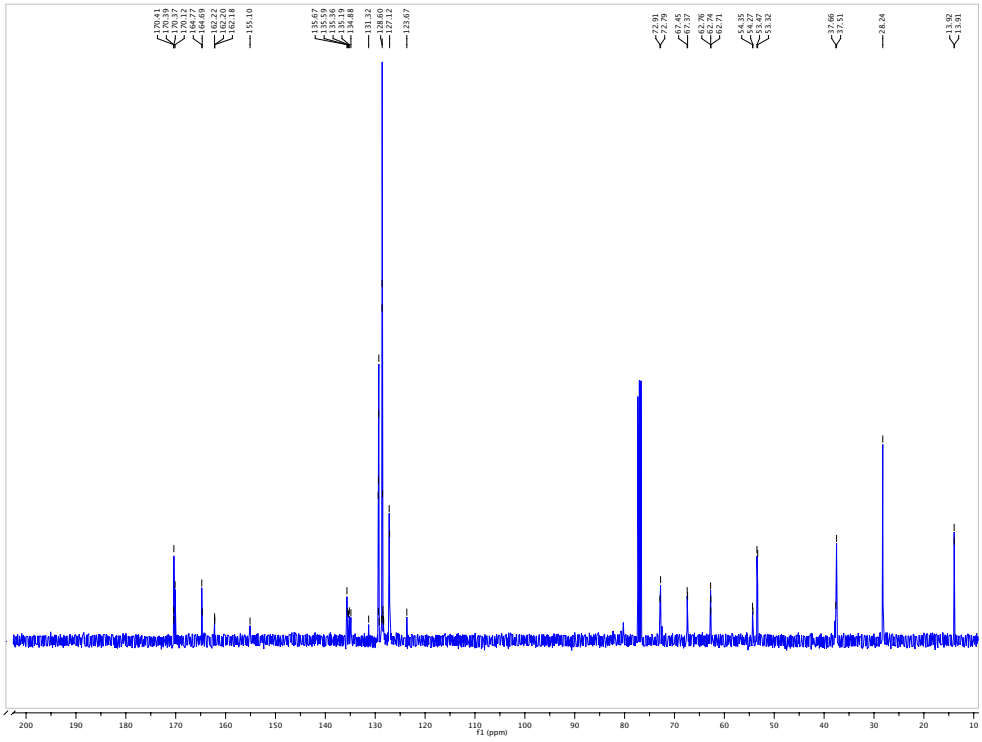

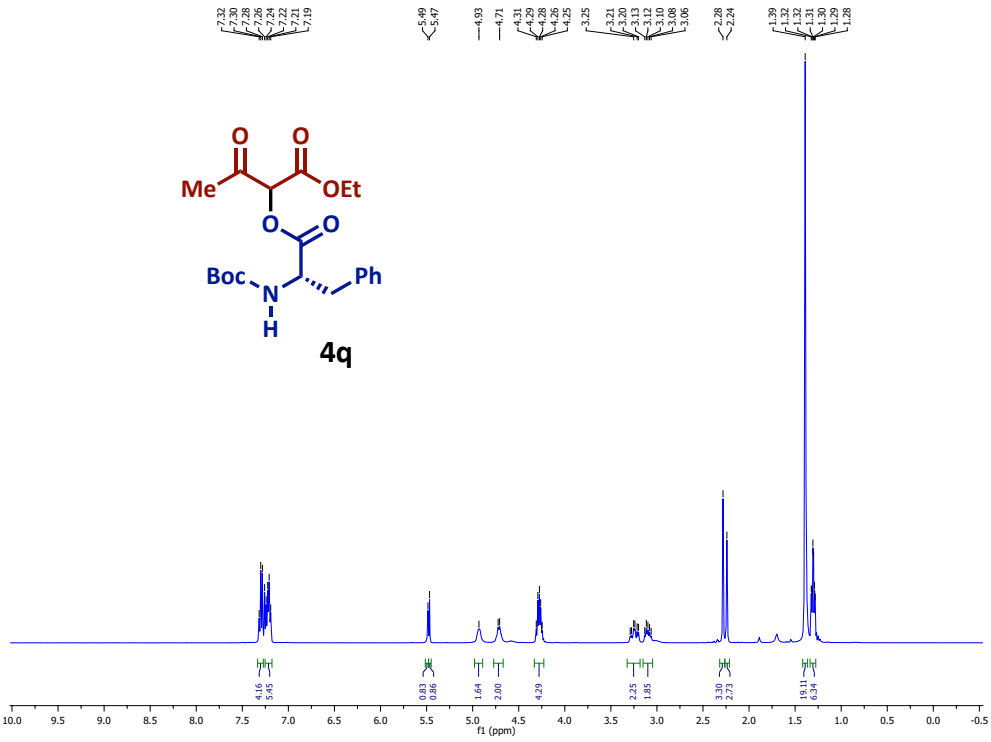
Me
OEt
Boc
Ph
N
H
4q
f1 (ppm)

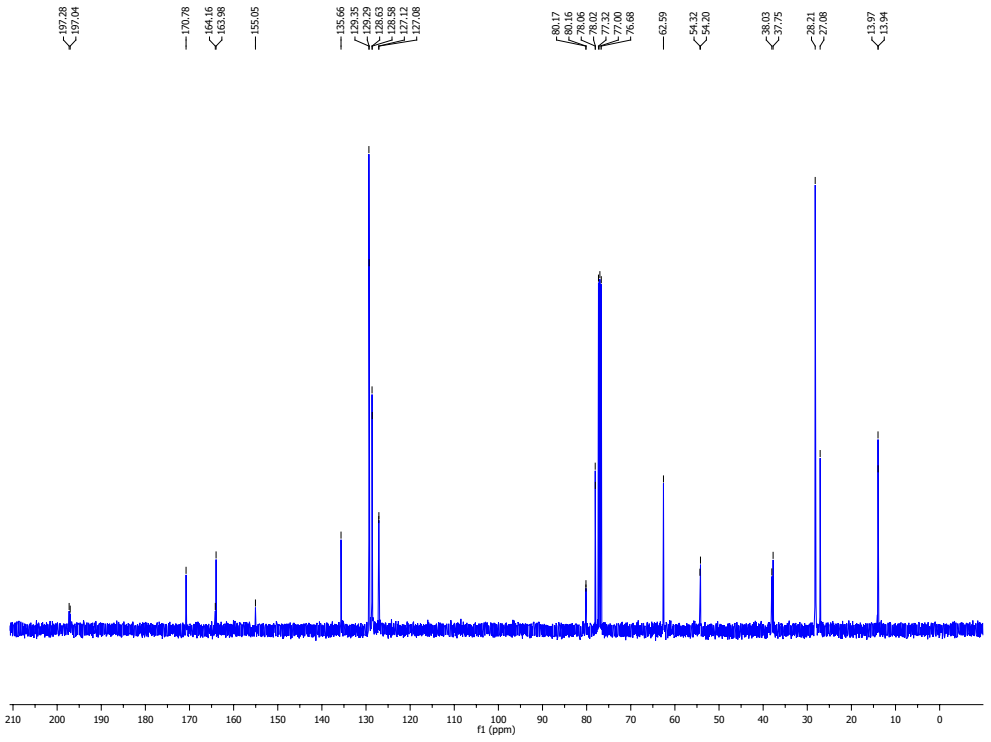
f1 (ppm)

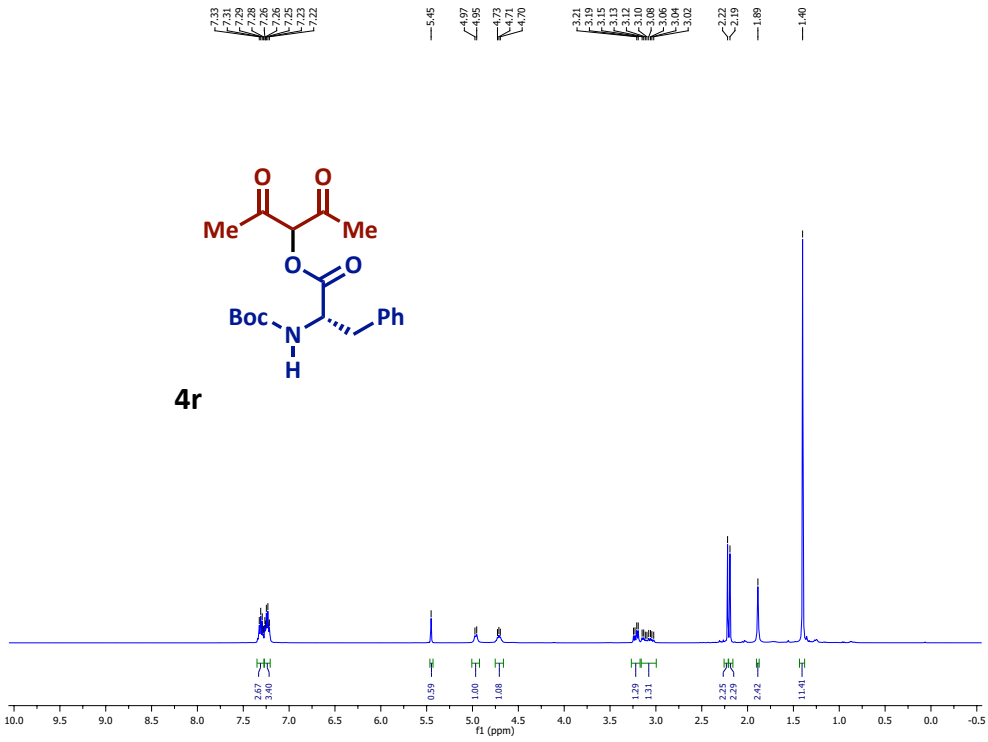
7.33
7.31
7.29
7.28
7.26
7.26
7.25
7.23
7.22
5.45
4.97
4.95
4.73
4.71
4.70
3.21
3.19
3.15
3.13
3.12
3.10
3.08
3.06
3.04
3.02
2.22
2.19
1.89
1.40
O
O
Me
Me
O
O
Boc
N
H
Ph
2.67
3.40
0.59
1.00
1.08
1.29
1.31
2.25
2.29
2.42
11.41
f1 (ppm)

4r

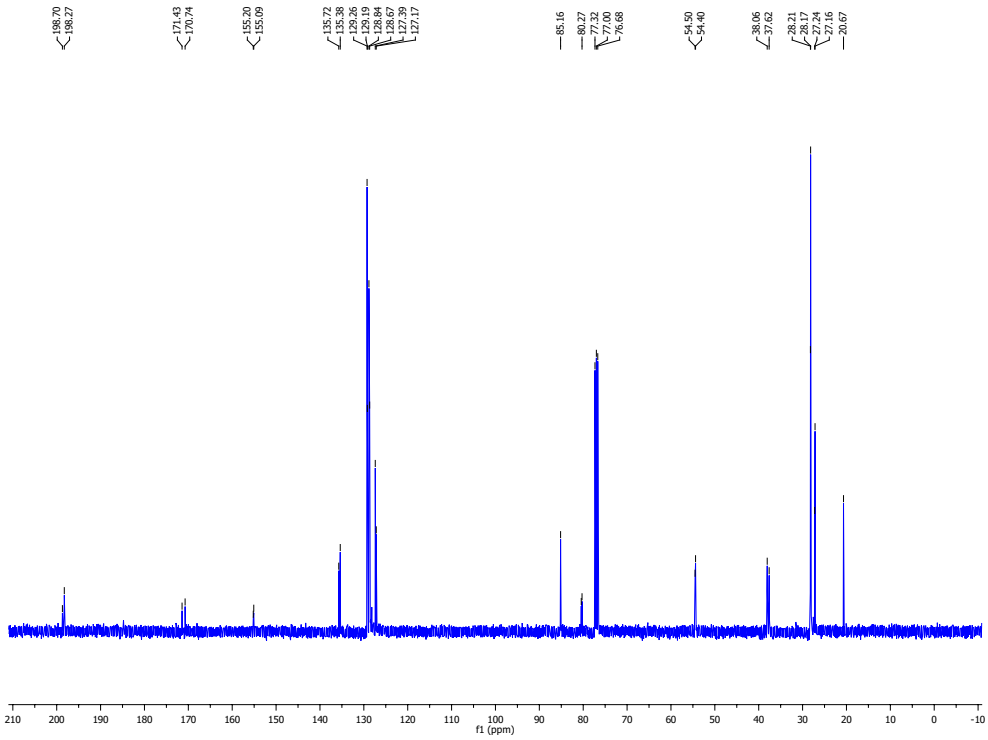
198.70
198.27
171.43
170.74
155.20
155.09
135.72
135.38
129.26
129.19
128.84
128.67
127.39
127.17
85.16
80.27
77.32
77.00
76.68
54.50
54.40
38.06
37.62
28.21
28.17
27.24
27.16
20.67
f1 (ppm)

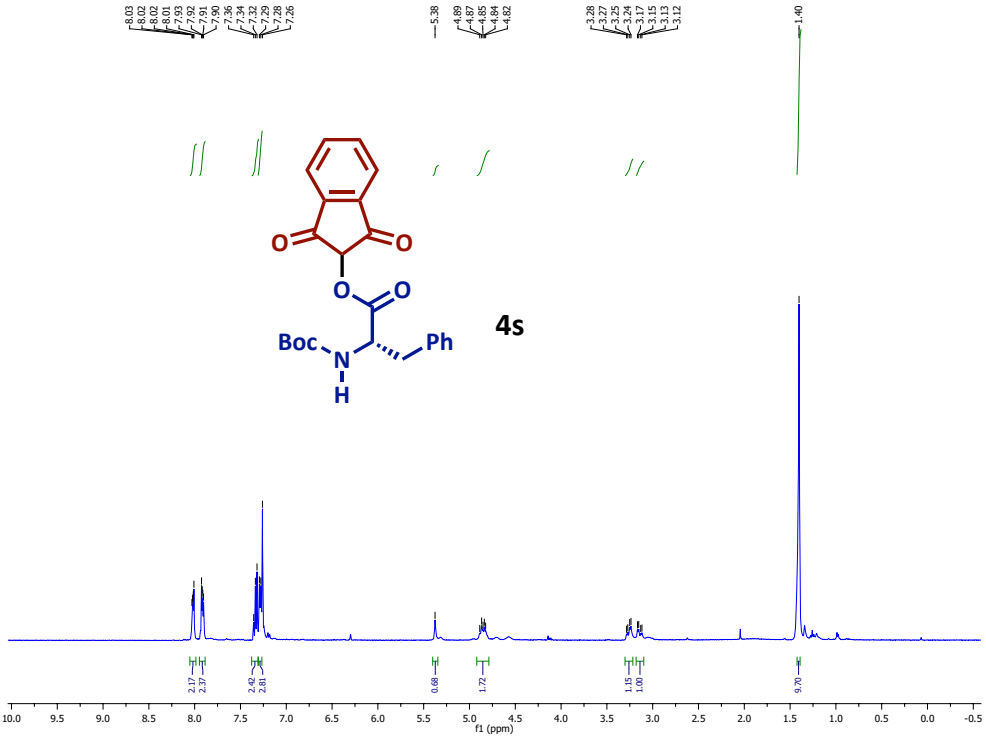
8.03
8.02
8.02
8.01
7.93
7.92
7.91
7.90
7.36
7.34
7.32
7.29
7.28
7.26
5.38
4.89
4.87
4.85
4.84
4.82
3.28
3.27
3.25
3.24
3.17
3.15
3.13
3.12
1.40
O
O
O
O
O
Boc
N
H
Ph
4s
2.17
2.37
2.42
2.81
0.68
1.72
1.15
1.00
9.70
f1 (ppm)

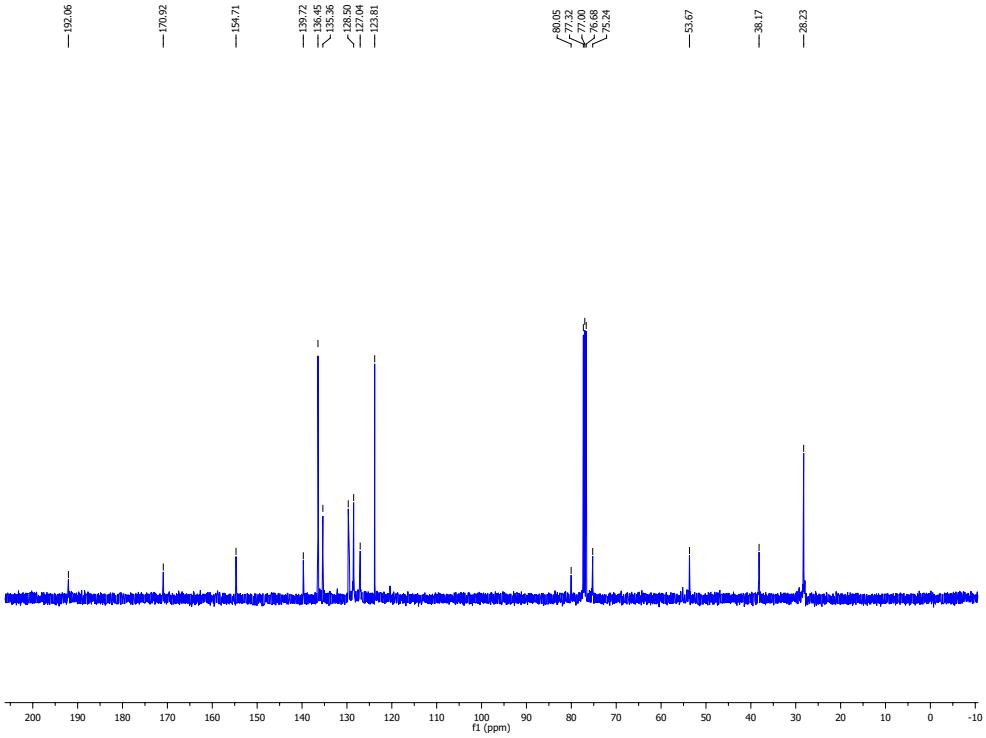
192.06
170.92
154.71
139.72
136.45
135.36
128.50
127.04
123.81
80.05
77.32
77.00
76.68
75.24
53.67
38.17
28.23
f1 (ppm)

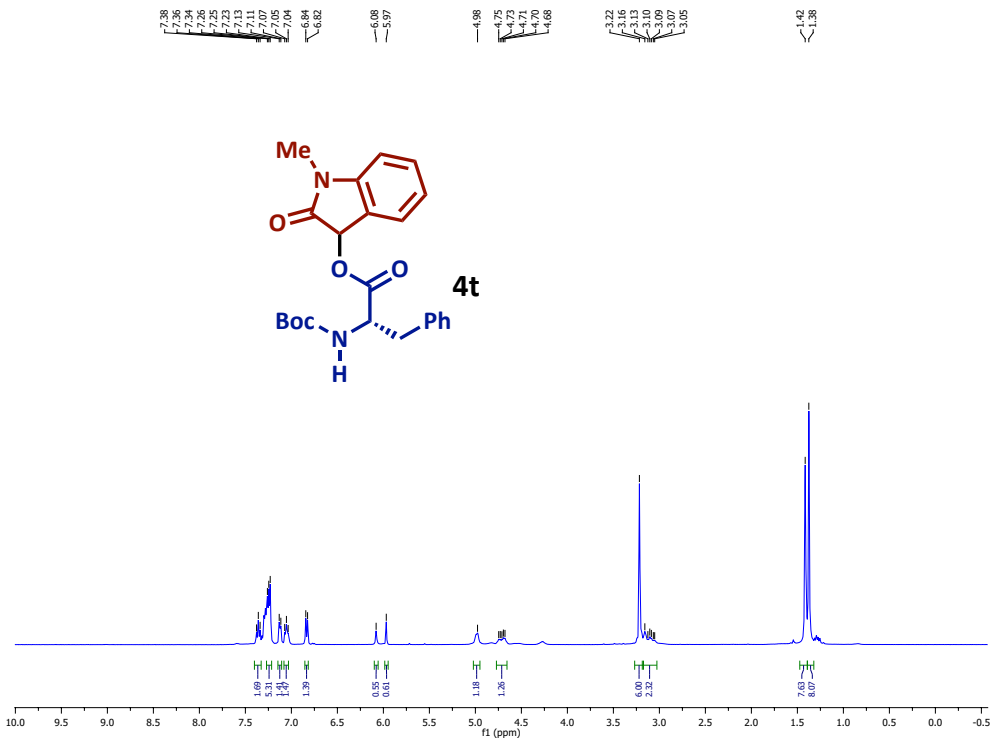
7.38
7.36
7.34
7.26
7.25
7.23
7.13
7.11
7.07
7.05
7.04
6.84
6.82
6.08
5.97
4.98
4.75
4.73
4.71
4.70
4.68
3.22
3.16
3.13
3.10
3.09
3.07
3.05
1.42
1.38
Me
N
O
O
O
Boc
N
H
Ph
4t
1.69
5.31
1.47
1.39
0.55
0.61
1.18
1.26
6.00
2.32
7.63
8.07
f1 (ppm)

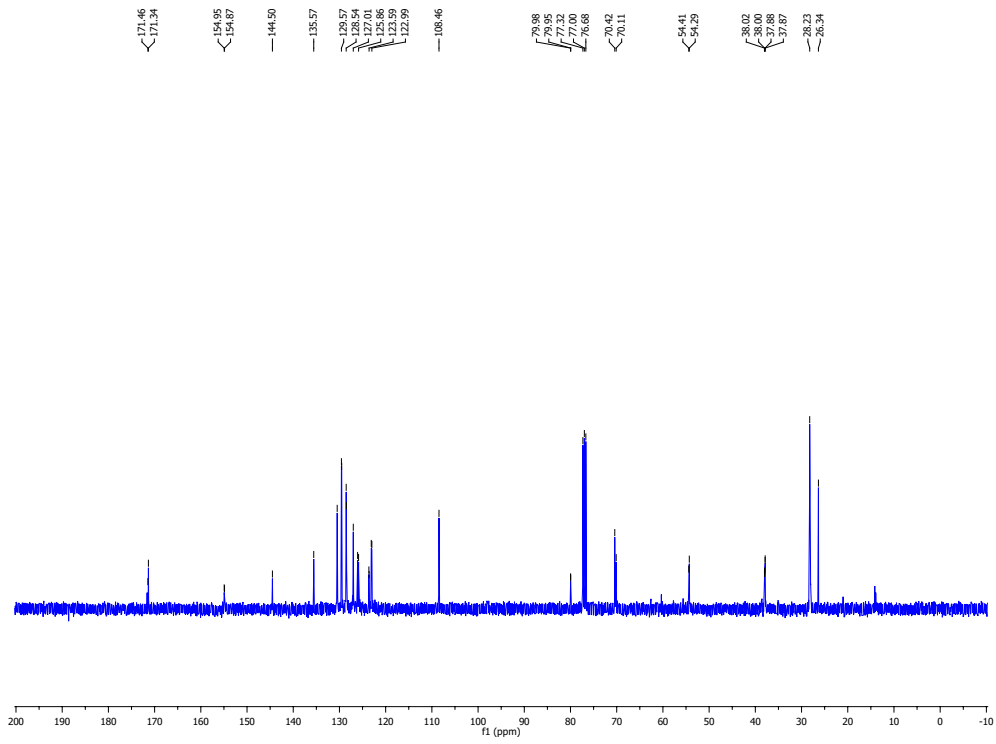
171.46
171.34
154.95
154.87
144.50
135.57
129.57
128.54
127.01
125.86
123.59
122.99
108.46
79.98
79.95
77.32
77.00
76.68
70.42
70.11
54.41
54.29
38.02
38.00
37.88
37.67
28.23
26.34
f1 (ppm)

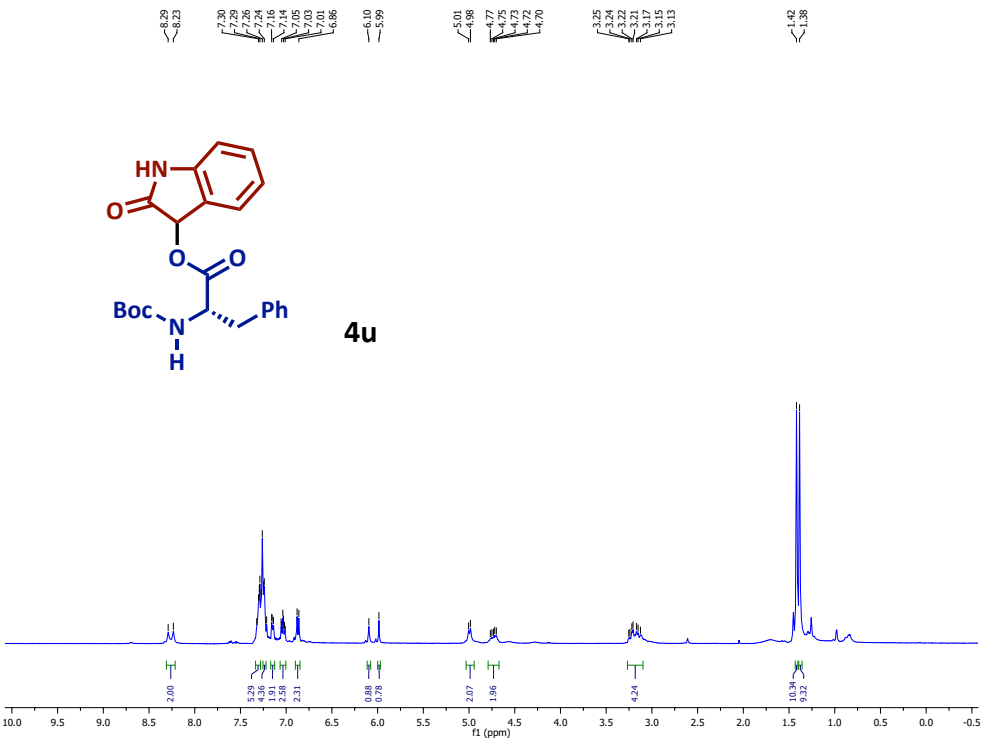
8.29
8.23
7.30
7.29
7.26
7.24
7.16
7.14
7.05
7.03
7.01
6.86
6.10
5.99
5.01
4.98
4.77
4.75
4.73
4.72
4.70
3.25
3.24
3.22
3.21
3.17
3.15
3.13
1.42
1.38
HN
O
O
O
Boc
N
H
Ph
4u
2.00
5.29
4.16
1.91
2.58
2.31
0.88
0.78
2.07
1.96
4.24
10.34
9.32
f1 (ppm)

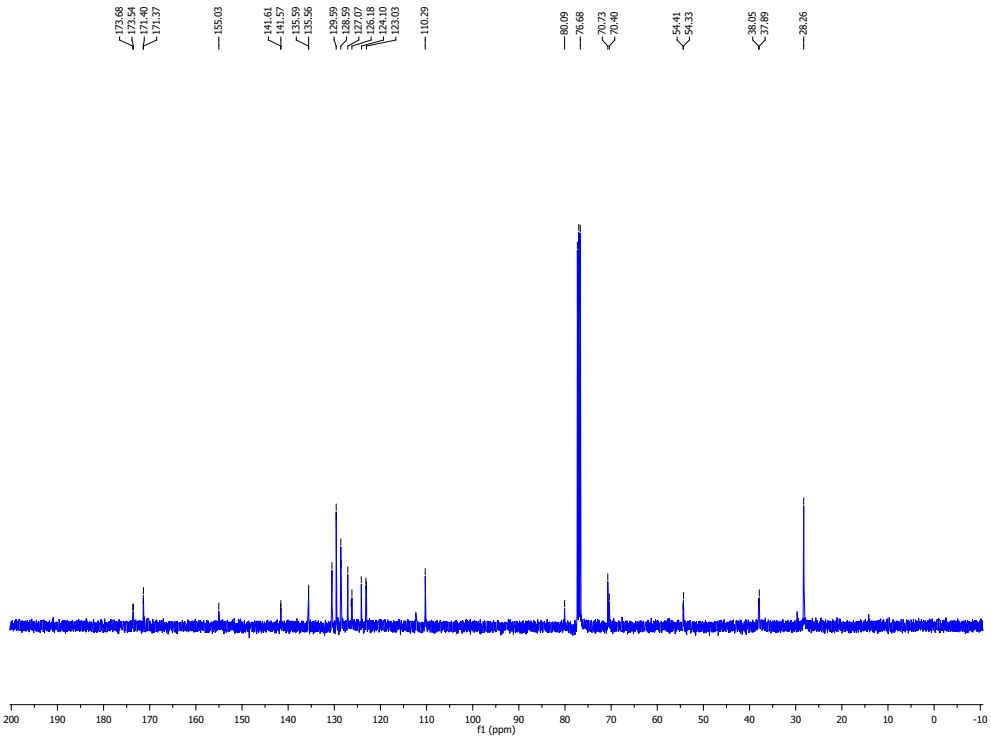
173.68
173.54
171.40
171.37
155.03
141.61
141.57
135.99
135.56
129.59
128.59
127.07
126.18
124.10
123.03
110.29
80.09
76.68
70.73
70.40
54.41
54.33
38.05
37.89
28.26
f1 (ppm)

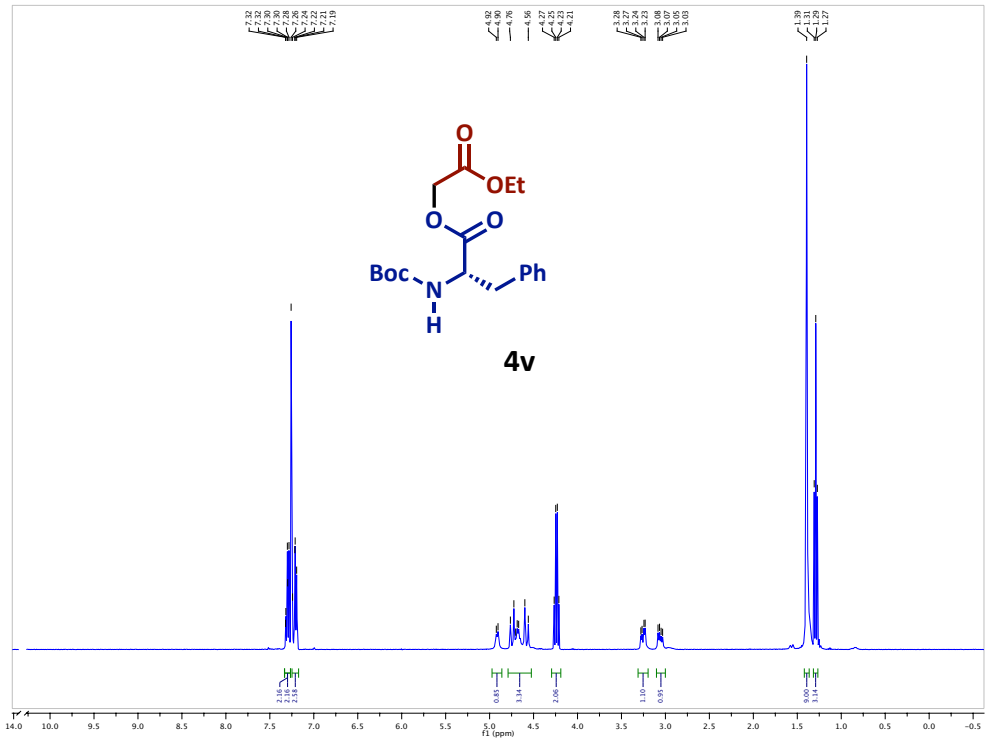

4v

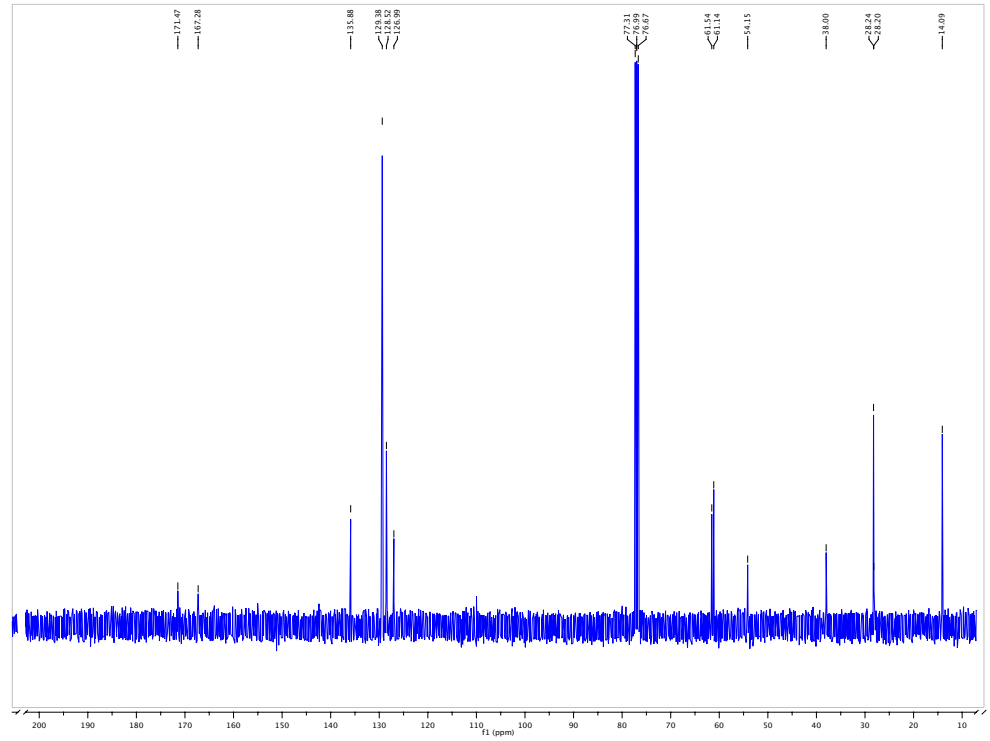

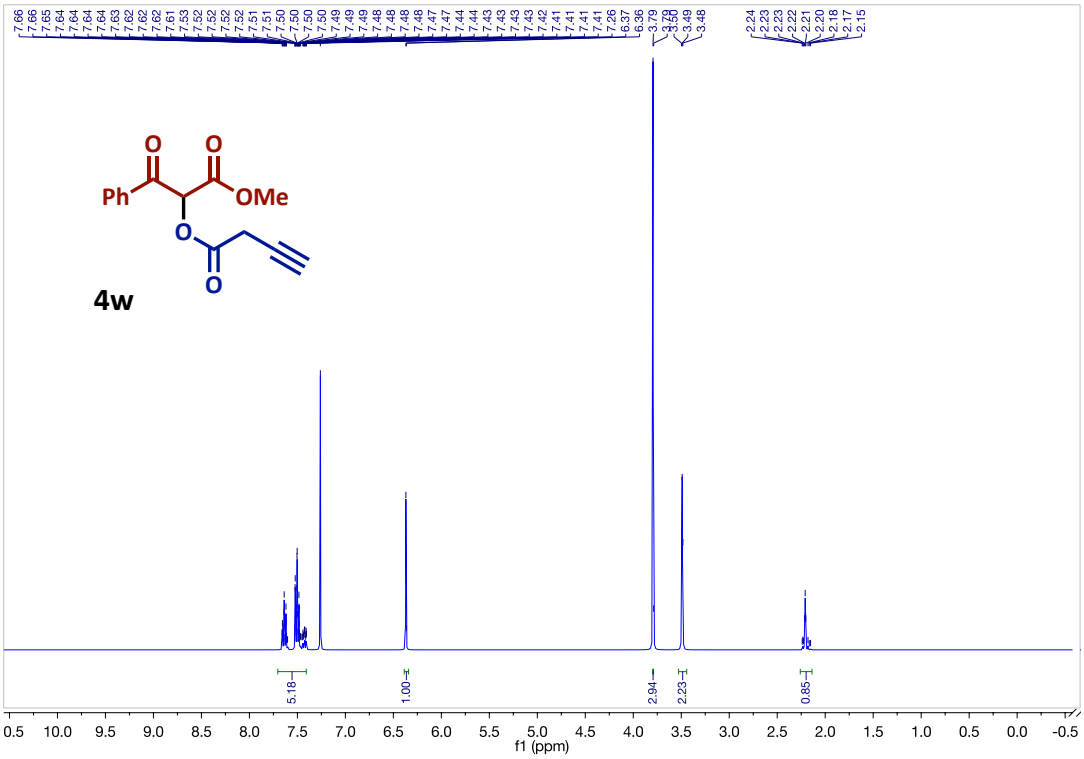
Ph
OMe
O
O
O
O
4w
5.18
1.00
2.94
2.23
0.85
f1 (ppm)

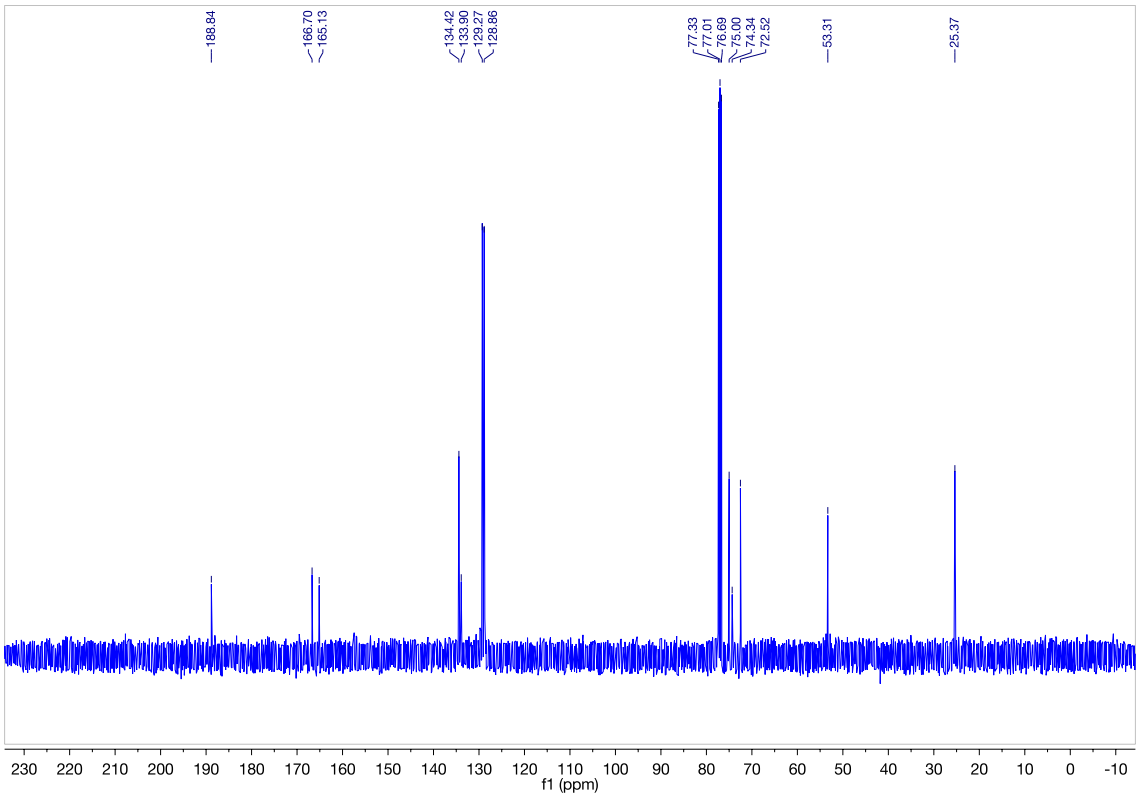
188.84
166.70
165.13
134.42
133.90
129.27
128.86
77.33
77.01
76.69
75.00
74.34
72.52
53.31
25.37
f1 (ppm)

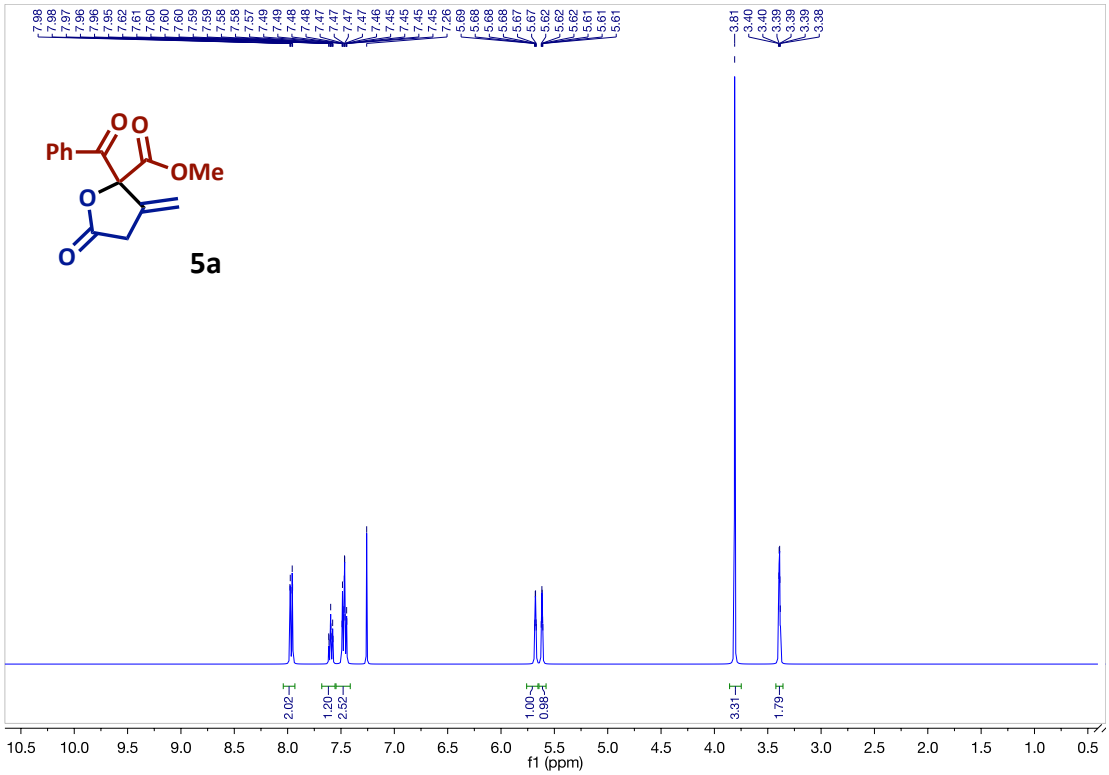
7.98
7.98
7.97
7.96
7.96
7.95
7.62
7.61
7.60
7.60
7.60
7.59
7.59
7.58
7.58
7.57
7.49
7.49
7.48
7.48
7.47
7.47
7.47
7.47
7.46
7.45
7.45
7.45
7.26
5.69
5.68
5.68
5.68
5.67
5.67
5.62
5.62
5.62
5.61
5.61
5.61
3.81
3.40
3.40
3.39
3.39
3.39
3.38
Ph
O
O
OMe
O
O
5a
2.02
1.20
2.52
1.00
0.98
3.31
1.79
10.5 10.0 9.5 9.0 8.5 8.0 7.5 7.0 6.5 6.0 5.5 5.0 4.5 4.0 3.5 3.0 2.5 2.0 1.5 1.0 0.5
f1 (ppm)

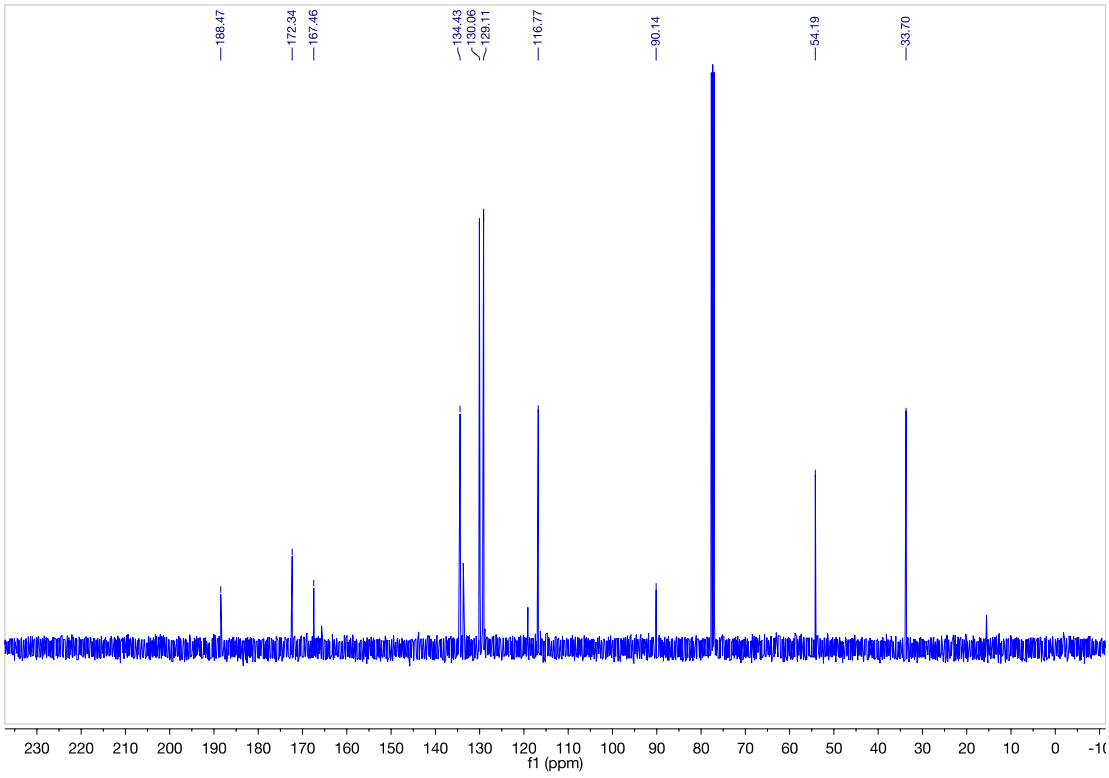
188.47
172.34
167.46
134.43
130.06
129.11
116.77
90.14
54.19
33.70
230 220 210 200 190 180 170 160 150 140 130 120 110 100 90 80 70 60 50 40 30 20 10 0
f1 (ppm)

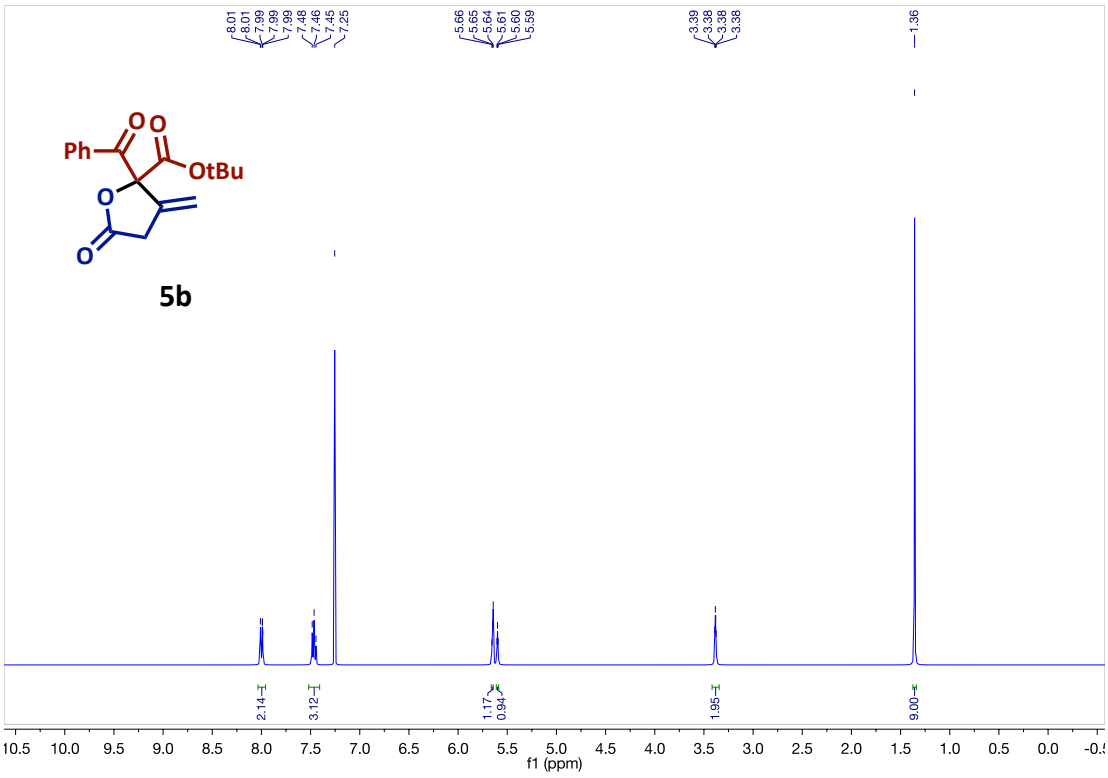
8.01
8.01
7.99
7.99
7.99
7.48
7.46
7.45
7.25
5.66
5.65
5.64
5.61
5.60
5.59
3.39
3.38
3.38
3.38
1.36
Ph
O
O
OtBu
O
O
5b
2.14
3.12
1.17
0.94
1.95
9.00
10.5 10.0 9.5 9.0 8.5 8.0 7.5 7.0 6.5 6.0 5.5 5.0 4.5 4.0 3.5 3.0 2.5 2.0 1.5 1.0 0.5 0.0 -0.5
f1 (ppm)

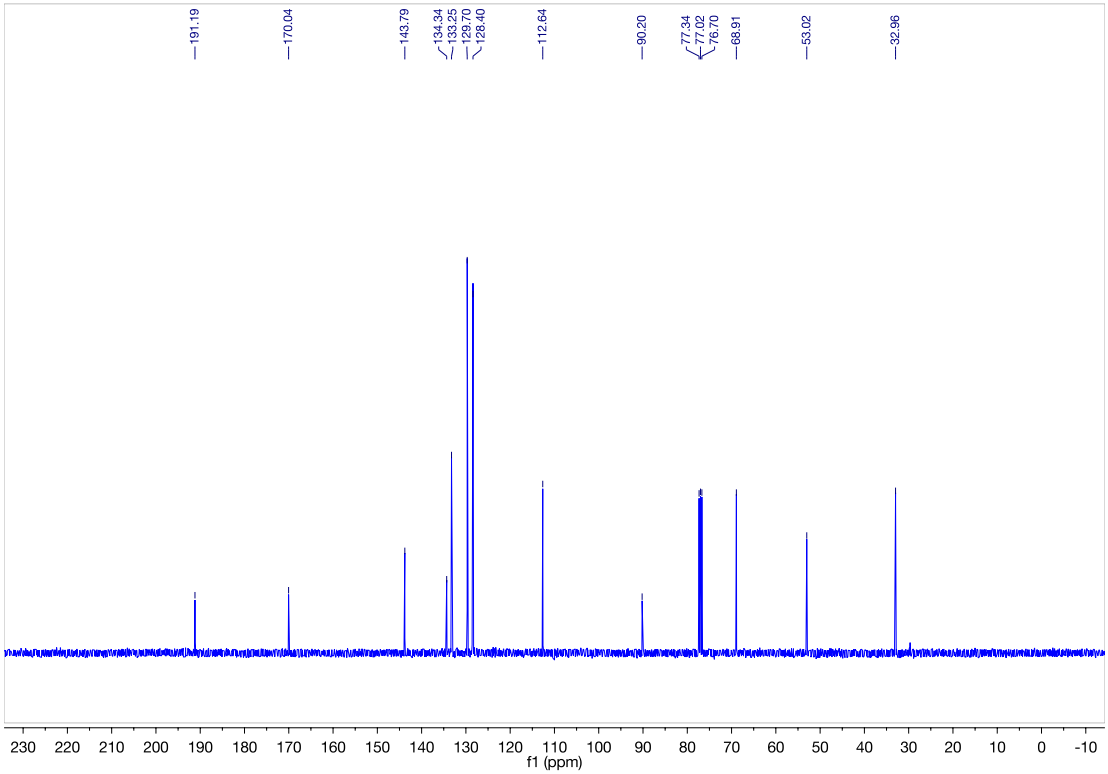
191.19
170.04
143.79
134.34
133.25
129.70
128.40
112.64
90.20
77.34
77.02
76.70
68.91
53.02
32.96
230 220 210 200 190 180 170 160 150 140 130 120 110 100 90 80 70 60 50 40 30 20 10 0 -10
f1 (ppm)

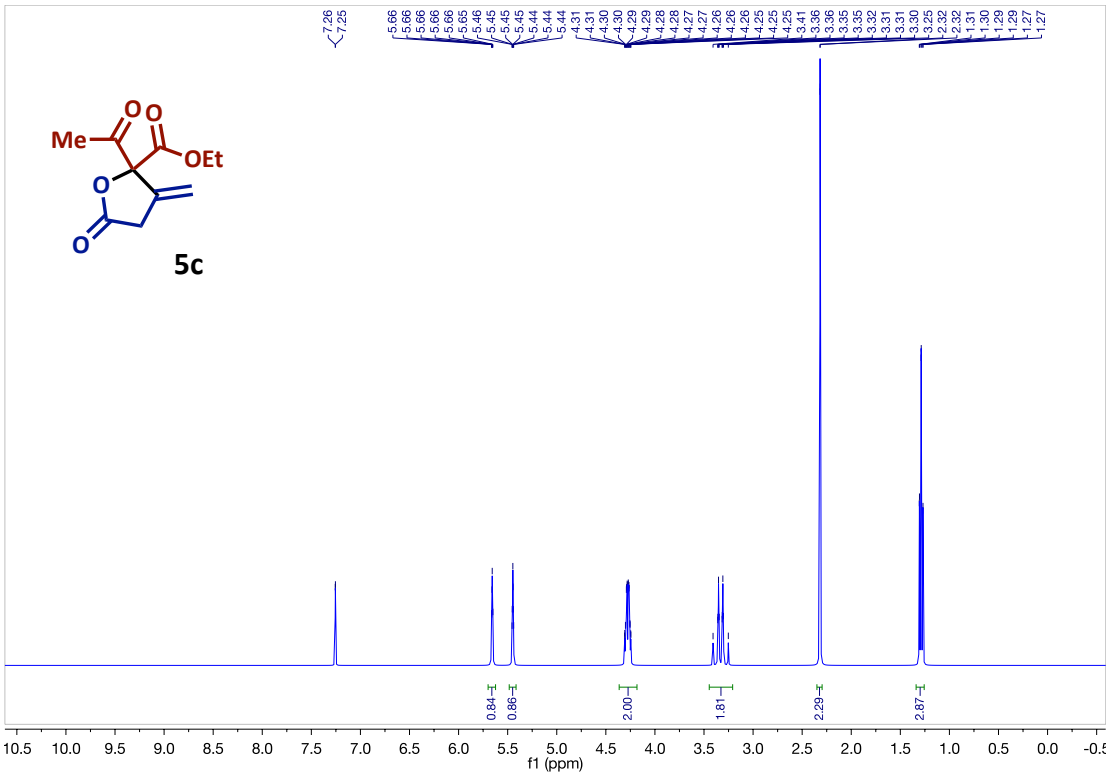
Me
O
O
OEt
O
O
5c
7.26
7.25
5.66
5.66
5.66
5.66
5.65
5.46
5.45
5.45
5.44
5.44
4.31
4.30
4.29
4.28
4.28
4.27
4.27
4.26
4.26
4.25
4.25
4.25
4.25
3.41
3.36
3.36
3.35
3.35
3.32
3.31
3.31
3.30
3.25
2.32
2.32
1.31
1.30
1.29
1.29
1.27
1.27
0.84
0.86
2.00
1.81
2.29
2.87
10.5 10.0 9.5 9.0 8.5 8.0 7.5 7.0 6.5 6.0 5.5 5.0 4.5 4.0 3.5 3.0 2.5 2.0 1.5 1.0 0.5 0.0
f1 (ppm)

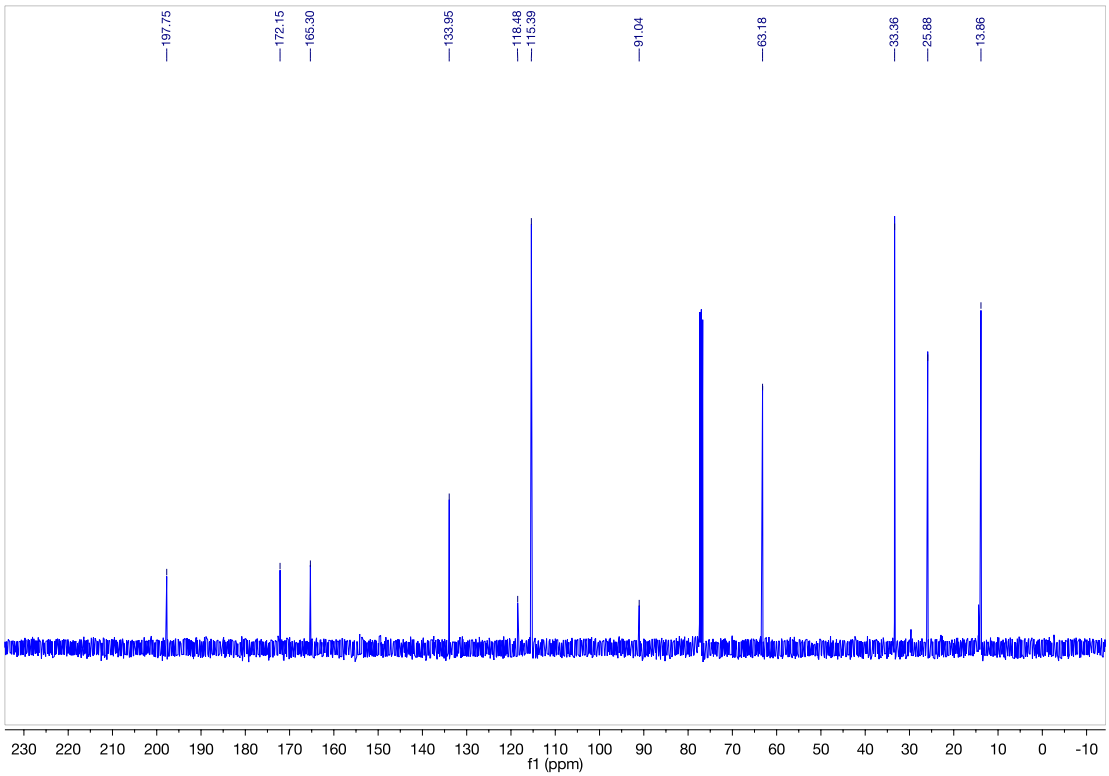
197.75
172.15
165.30
133.95
118.48
115.39
91.04
63.18
33.36
25.88
13.86
230 220 210 200 190 180 170 160 150 140 130 120 110 100 90 80 70 60 50 40 30 20 10 0 -10
f1 (ppm)

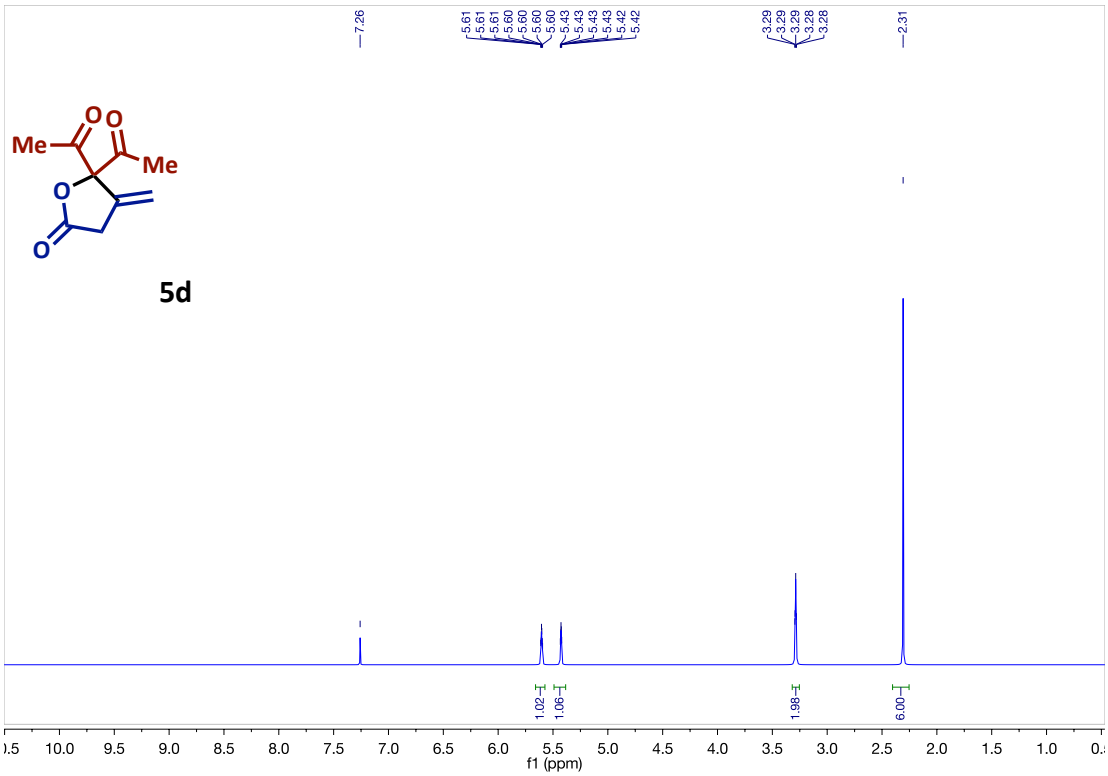
7.26
5.61
5.61
5.61
5.60
5.60
5.60
5.60
5.43
5.43
5.43
5.42
5.42
5.42
3.29
3.29
3.29
3.28
3.28
2.31
Me
O
O
Me
O
O
5d
1.02
1.06
1.98
6.00
f1 (ppm)

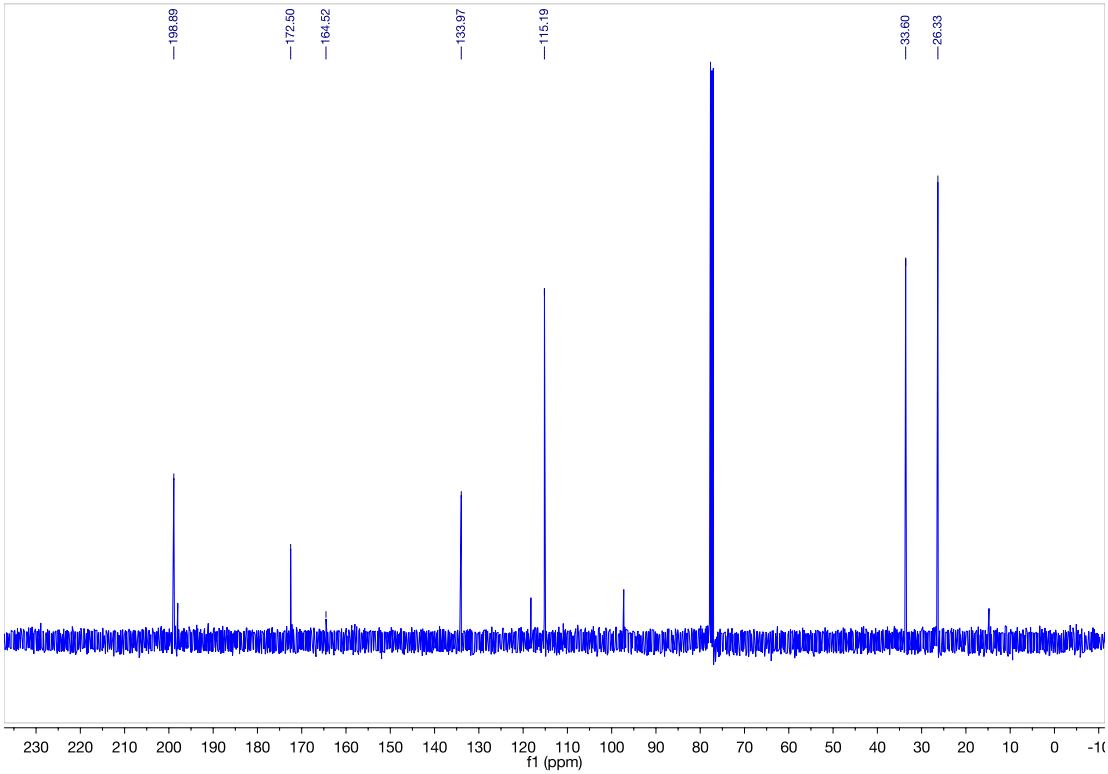
198.89
172.50
164.52
133.97
115.19
33.60
26.33
f1 (ppm)

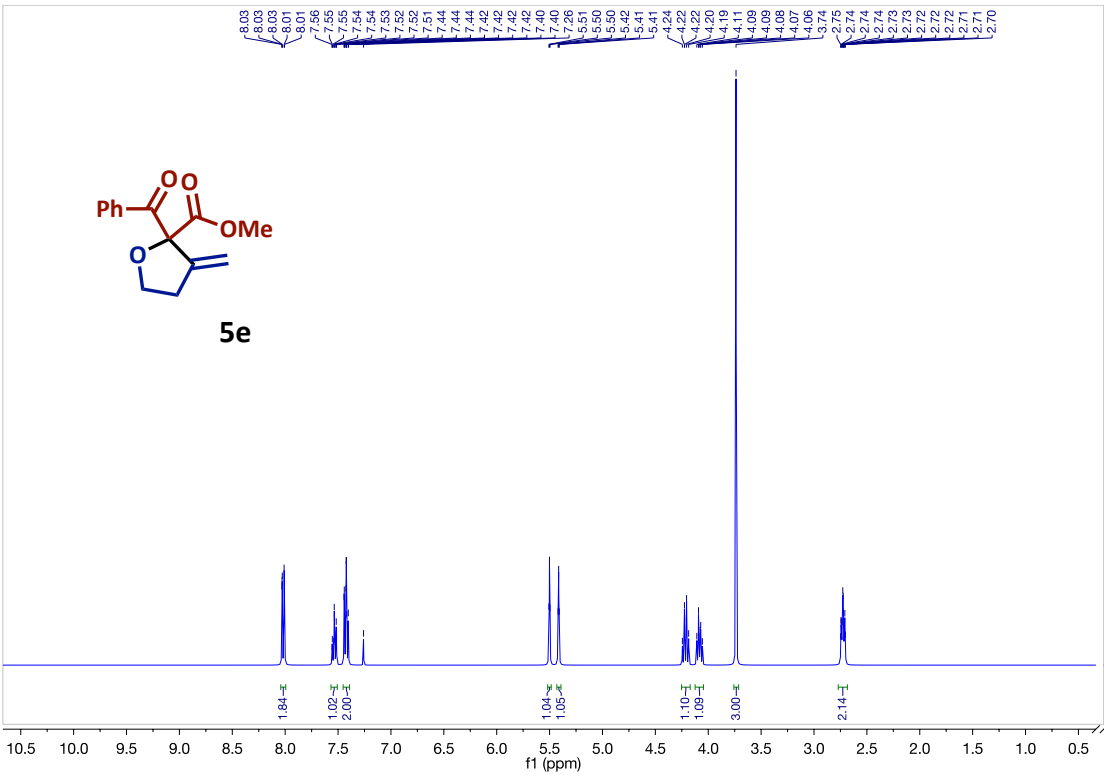
Ph
O
O
OMe
O
5e
f1 (ppm)

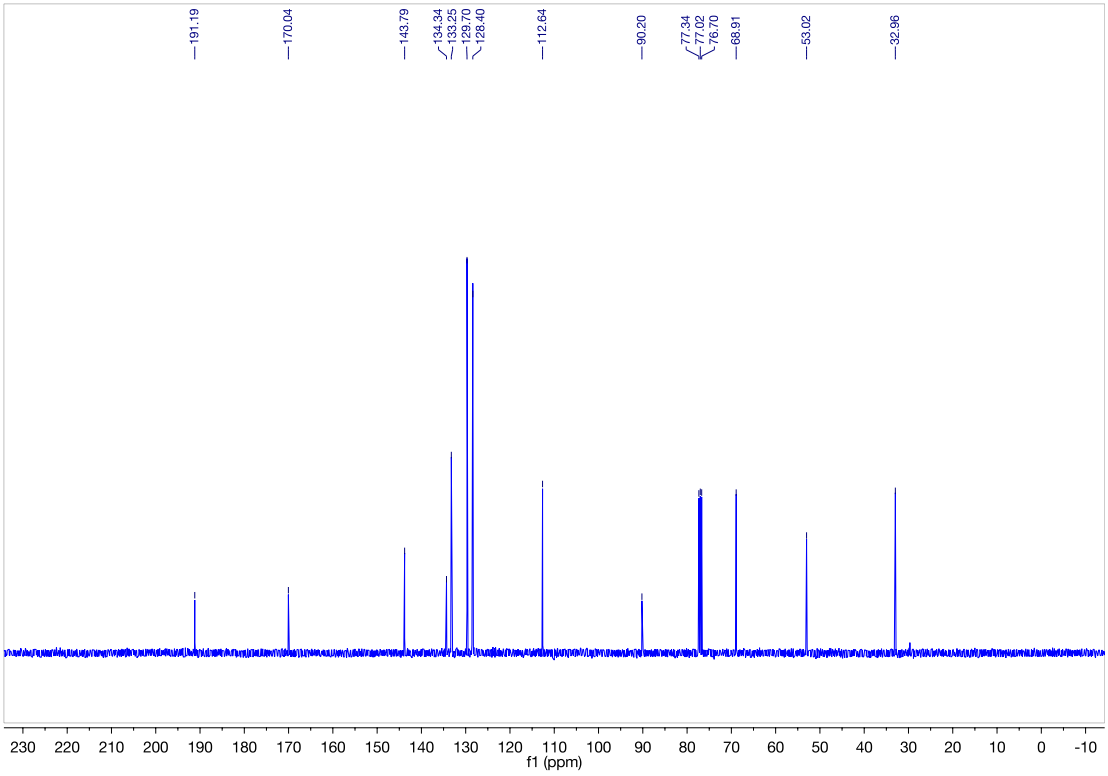
191.19
170.04
143.79
134.34
133.25
129.70
128.40
112.64
90.20
77.34
77.02
76.70
68.91
53.02
32.96
f1 (ppm)

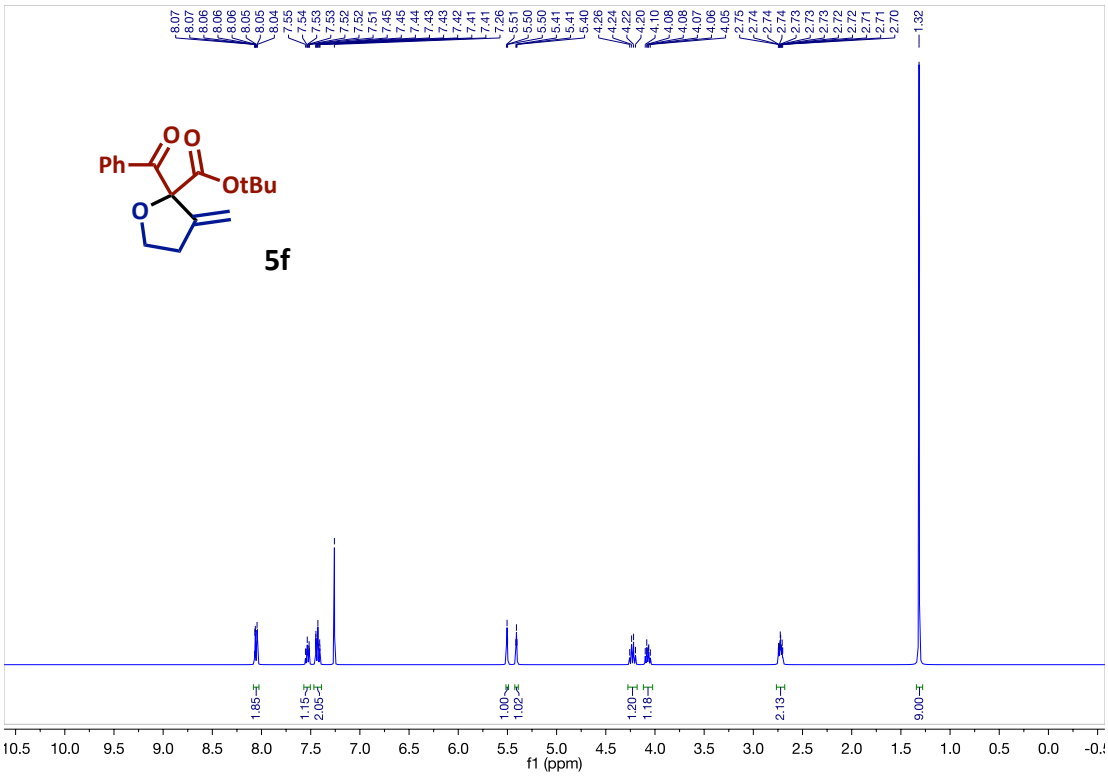
Ph
O
O
OtBu
O
5f
f1 (ppm)

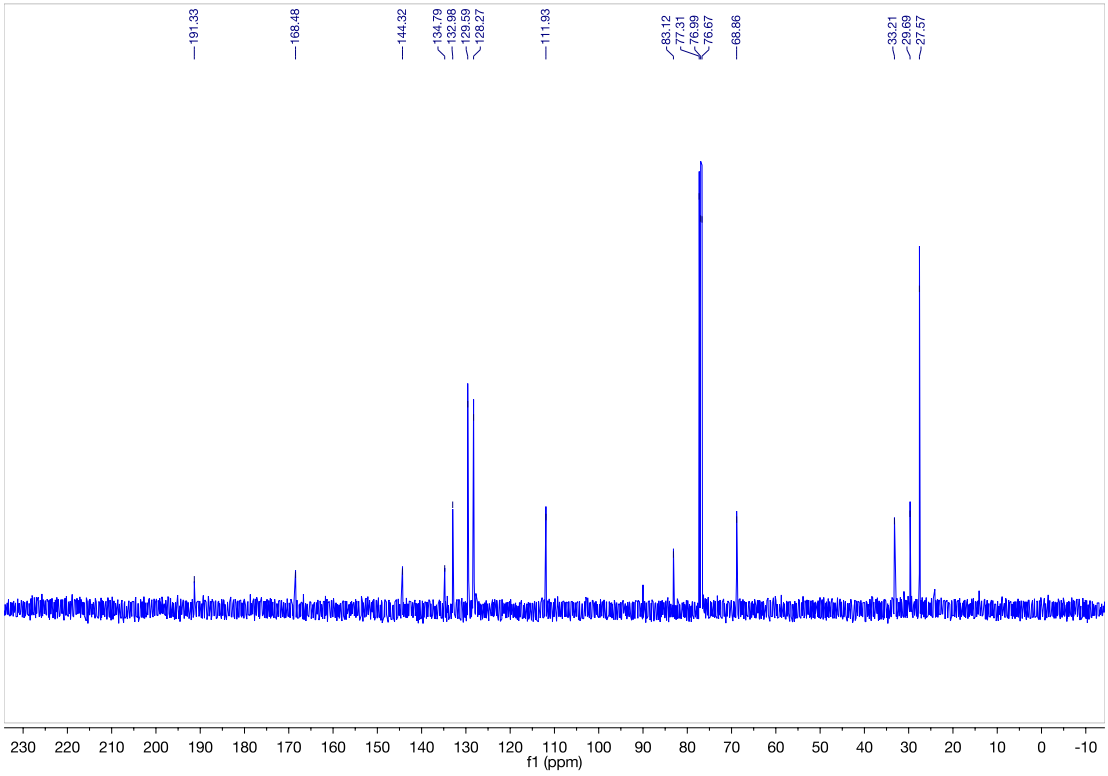
f1 (ppm)

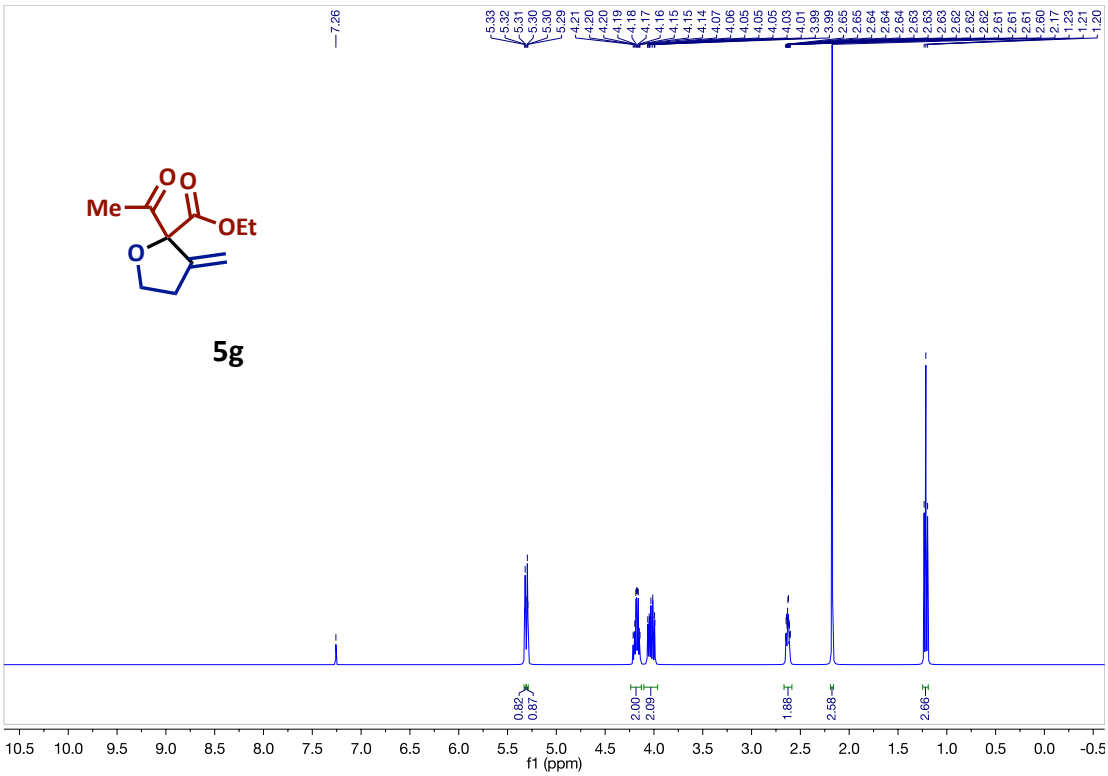
Me
O
O
OEt
O
5g
f1 (ppm)

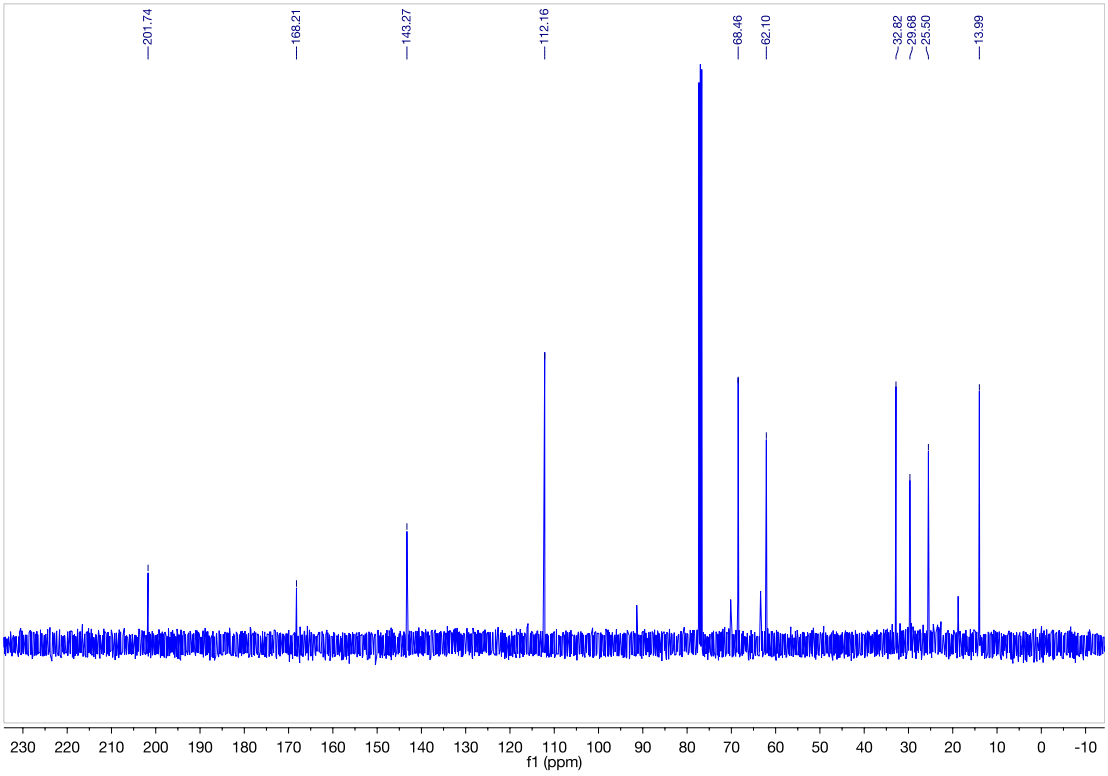
201.74
168.21
143.27
112.16
68.46
62.10
32.82
29.68
25.50
13.99
f1 (ppm)

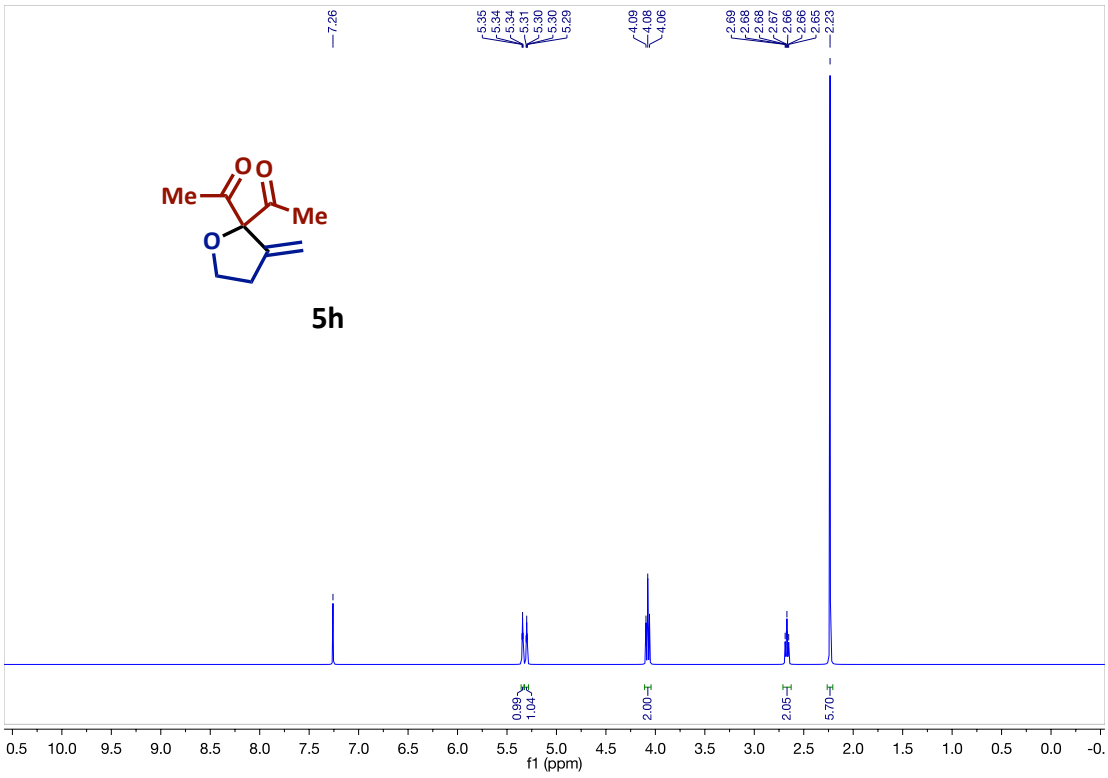
7.26
5.35
5.34
5.34
5.31
5.30
5.30
5.29
4.09
4.08
4.06
2.69
2.68
2.68
2.67
2.66
2.66
2.65
2.23
Me
O
O
Me
O
5h
0.99
1.04
2.00
2.05
5.70
f1 (ppm)

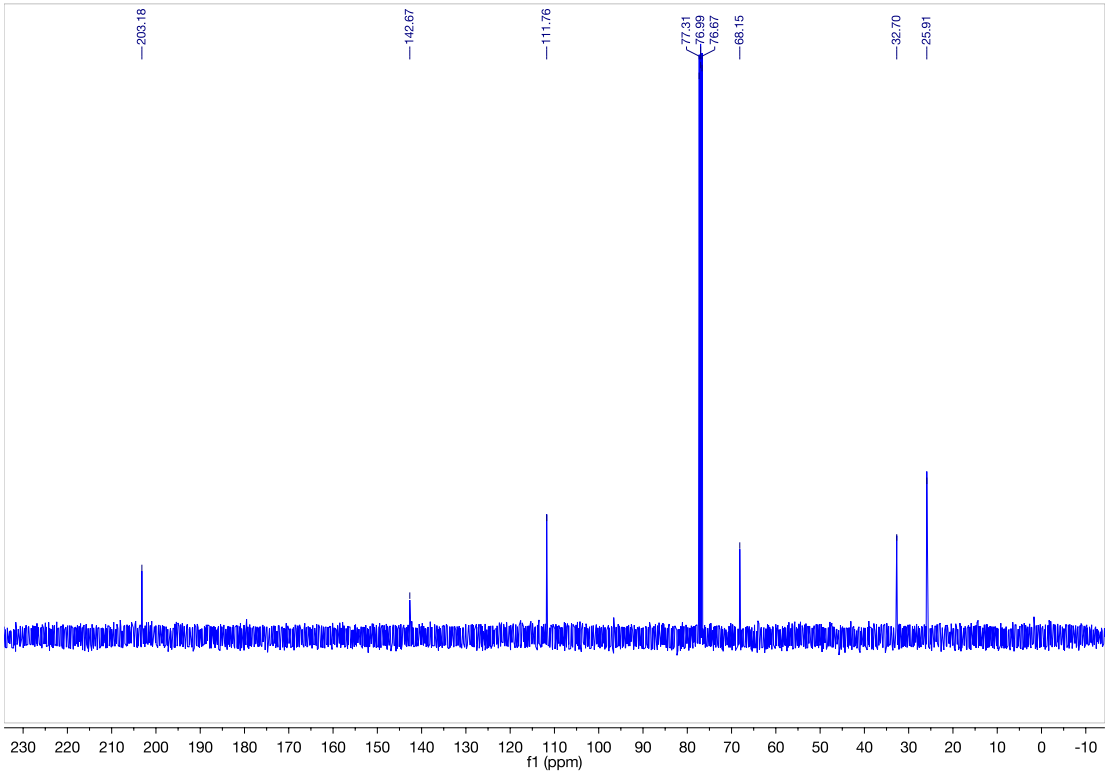
203.18
142.67
111.76
77.31
76.99
76.67
68.15
32.70
25.91
f1 (ppm)

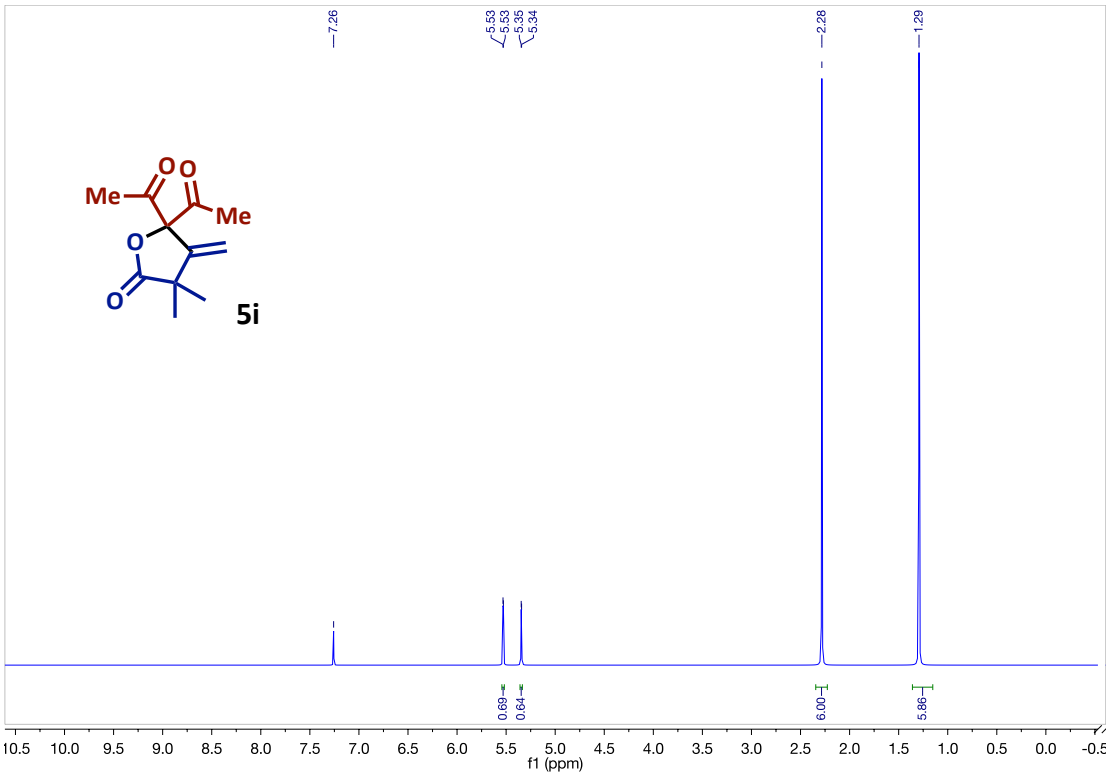
7.26
5.53
5.53
5.35
5.34
2.28
1.29
Me
O
O
Me
O
O
5i
0.69
0.64
6.00
5.86
f1 (ppm)

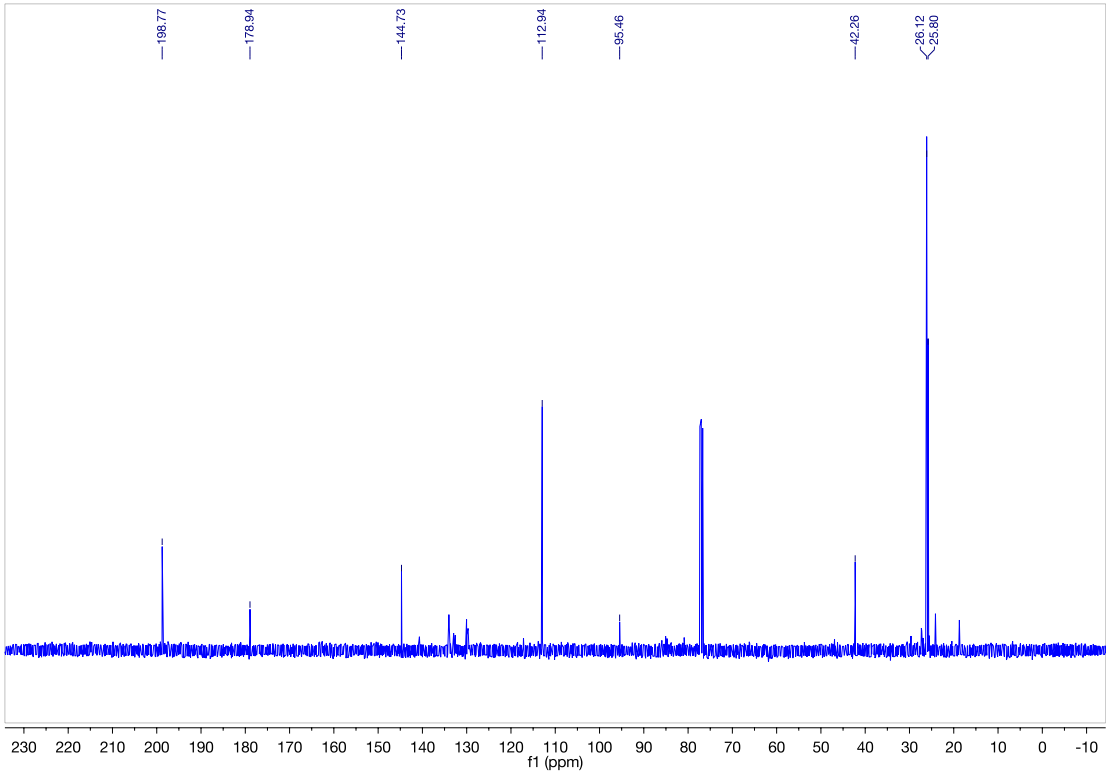
198.77
178.94
144.73
112.94
95.46
42.26
26.12
25.80
f1 (ppm)

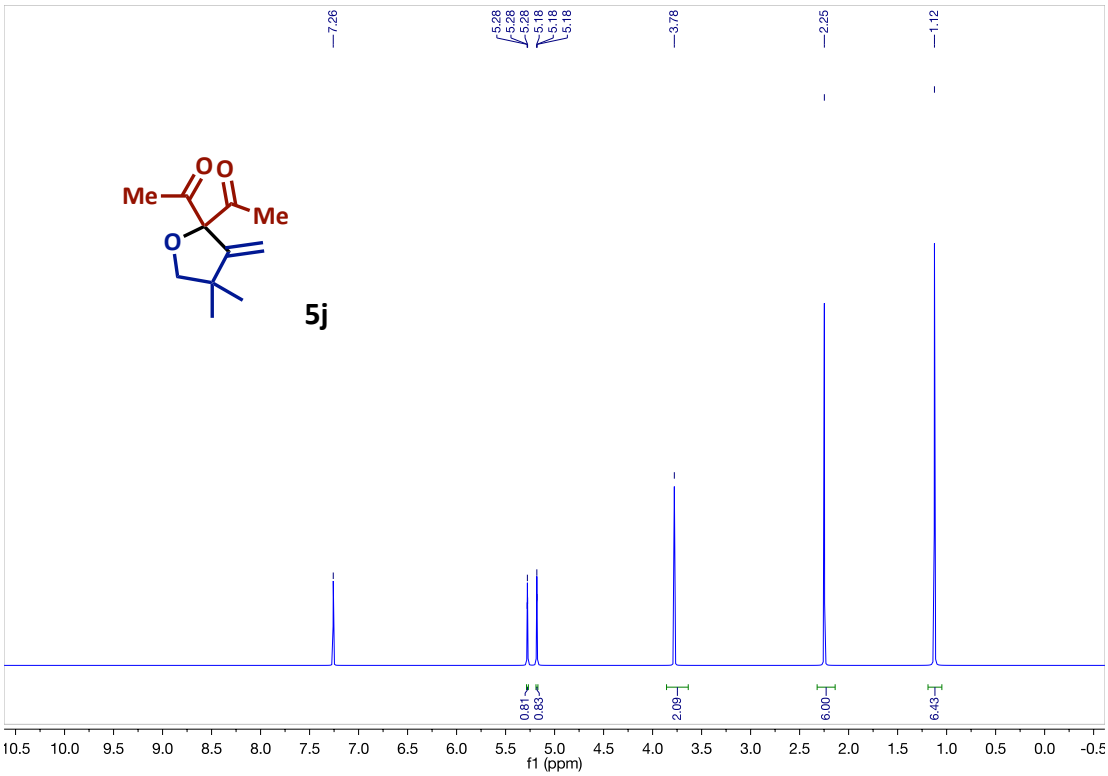
7.26
5.28
5.28
5.28
5.18
5.18
5.18
3.78
2.25
1.12
Me
O
O
Me
O
5j
0.81
0.83
2.09
6.00
6.43
f1 (ppm)

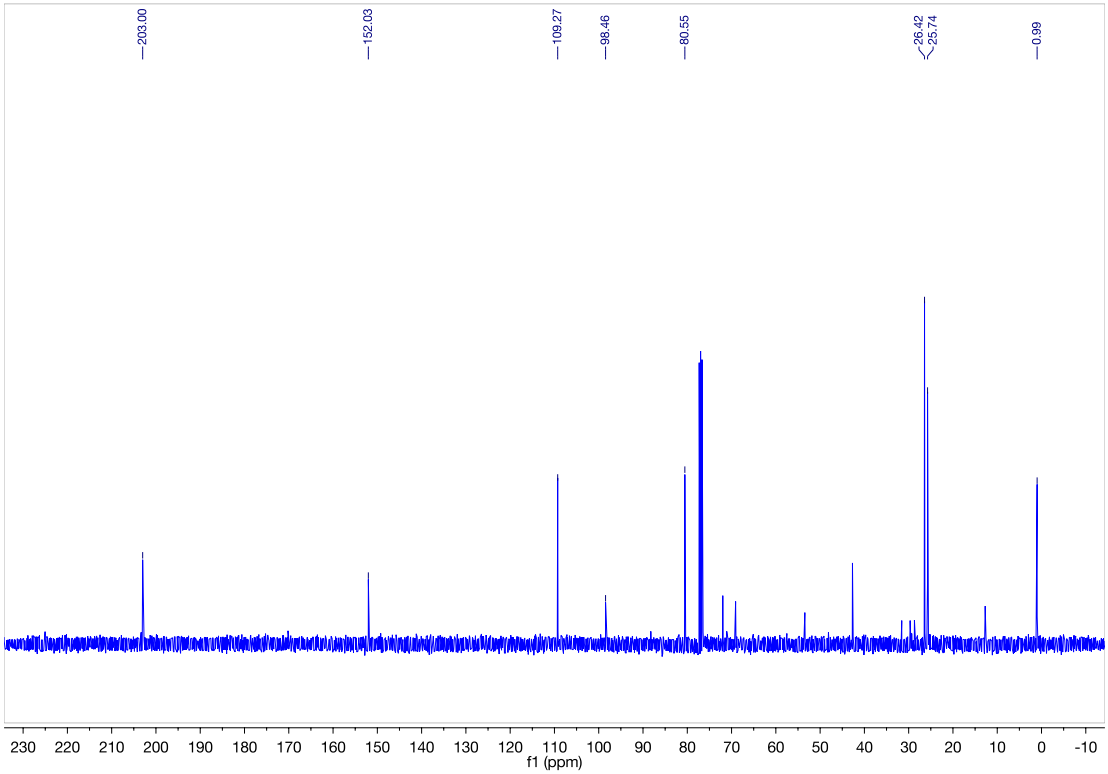
203.00
152.03
109.27
98.46
80.55
26.42
25.74
0.99
f1 (ppm)

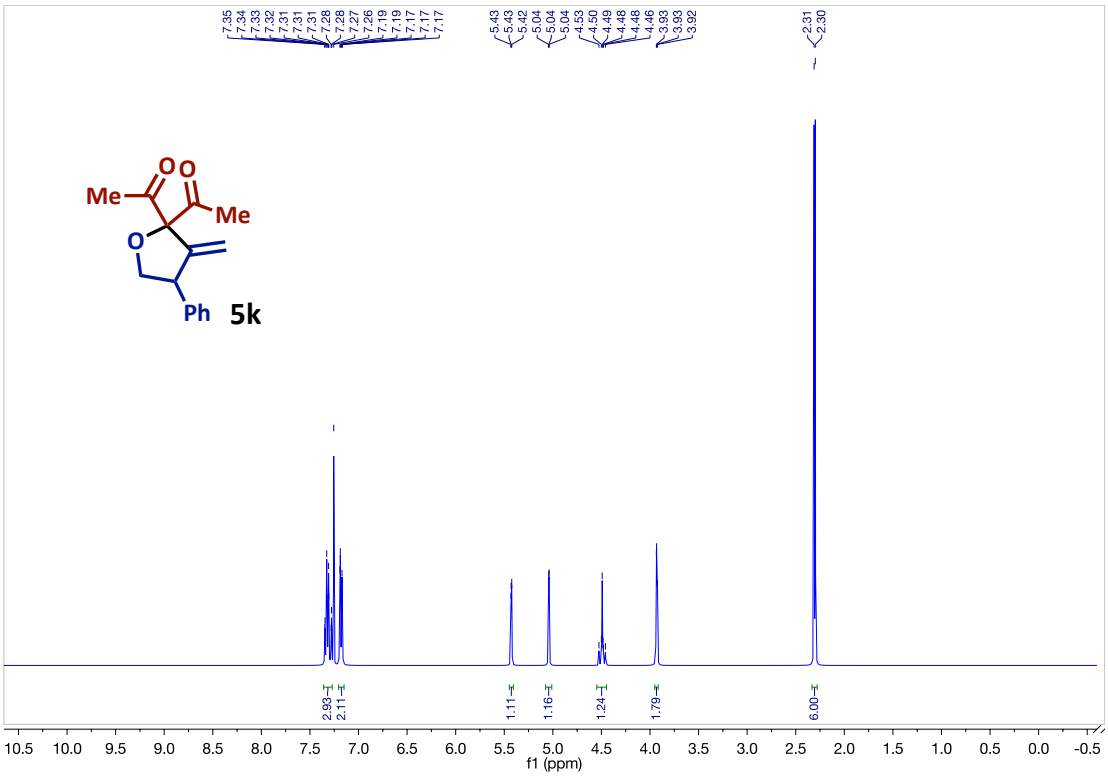
Me
O
O
Me
O
Ph
5k
f1 (ppm)

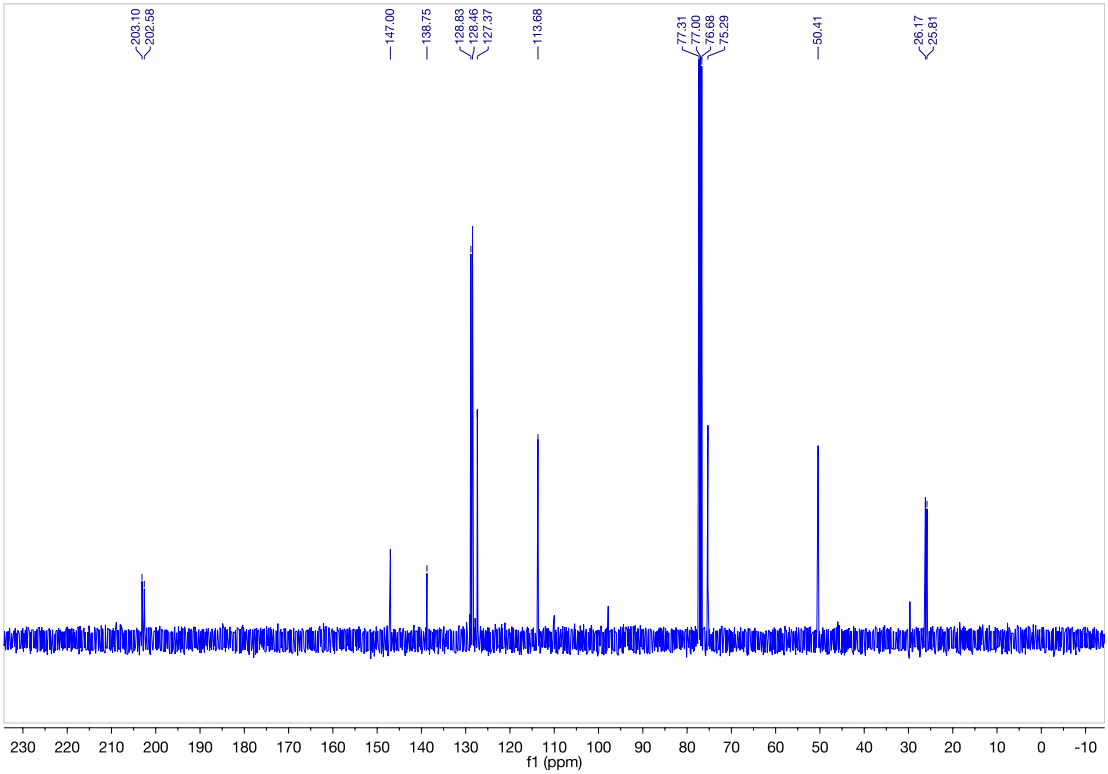
f1 (ppm)

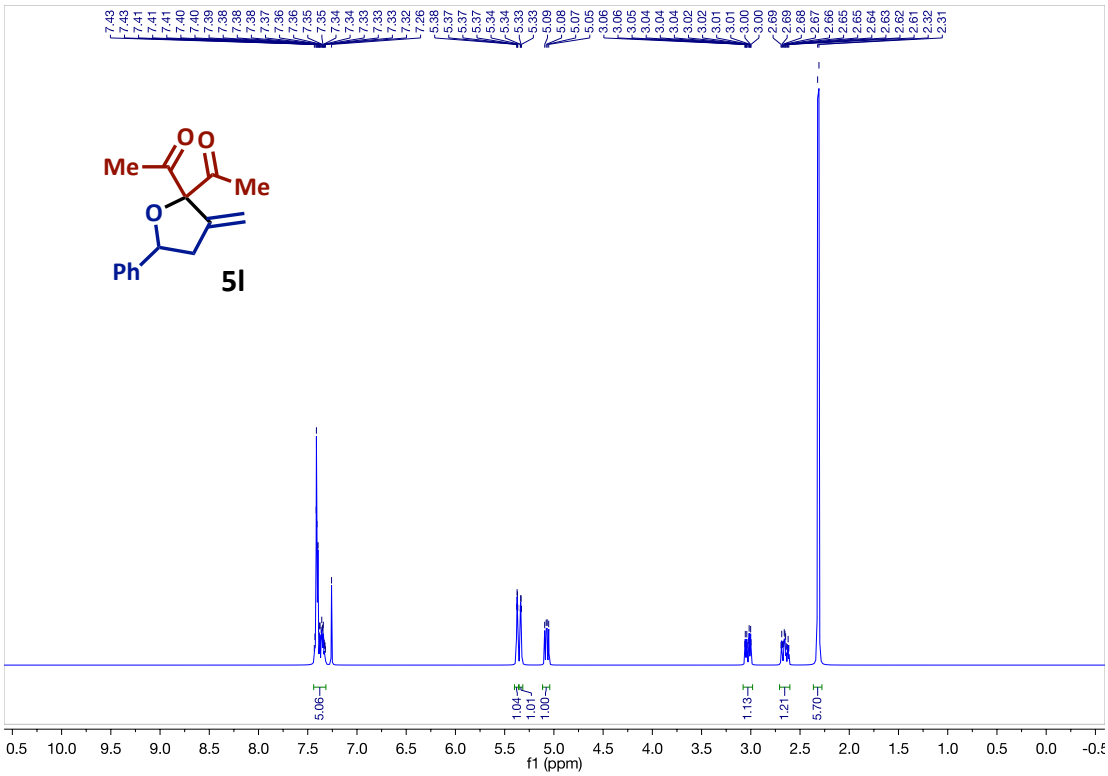
Me
O
O
Me
O
Ph
5l
f1 (ppm)

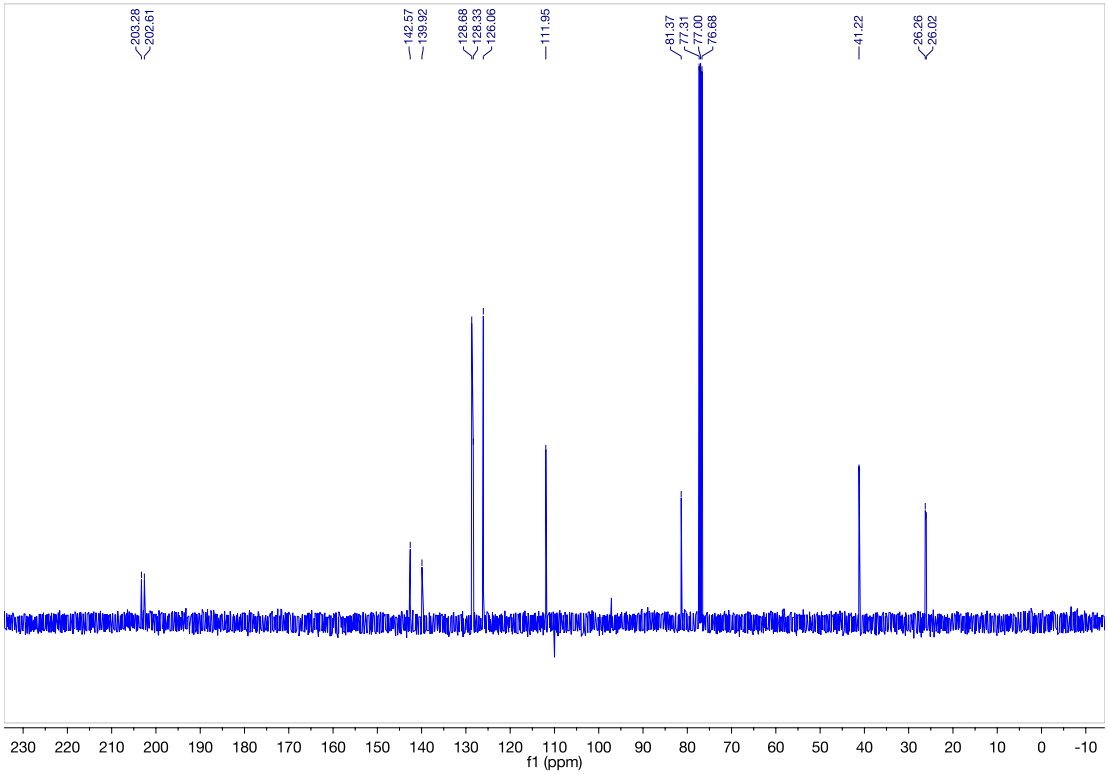
203.28
202.61
142.57
139.92
128.68
128.33
126.06
111.95
81.37
77.31
77.00
76.68
41.22
26.26
26.02
f1 (ppm)

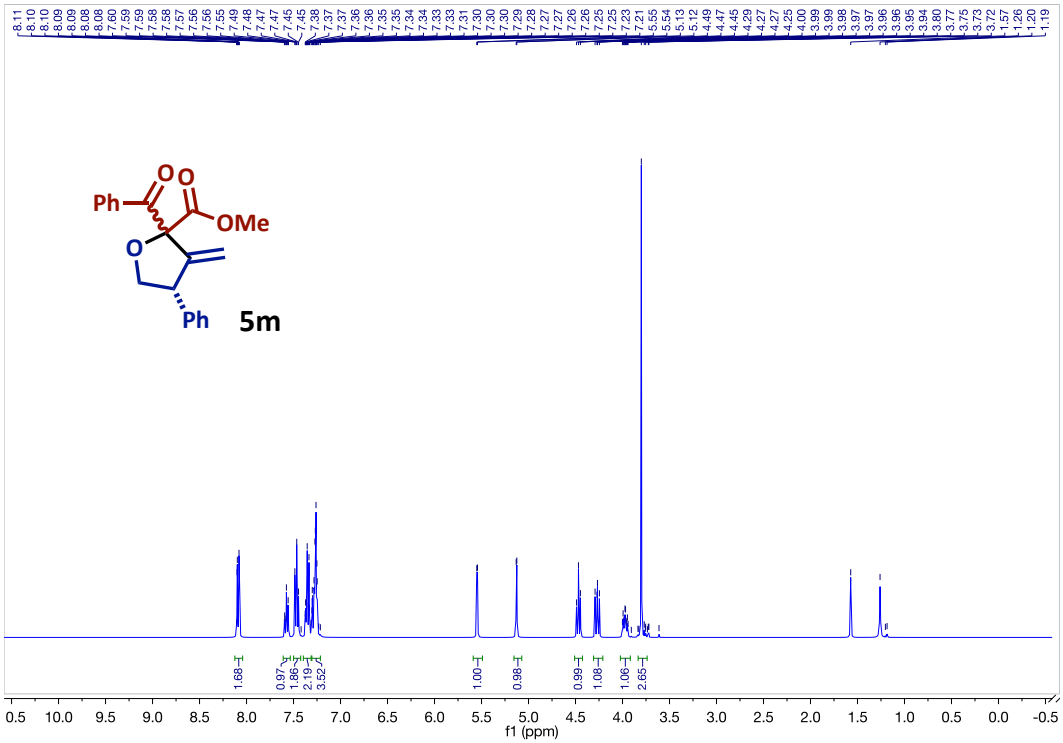
Ph
O
O
OMe
O
Ph
5m
f1 (ppm)

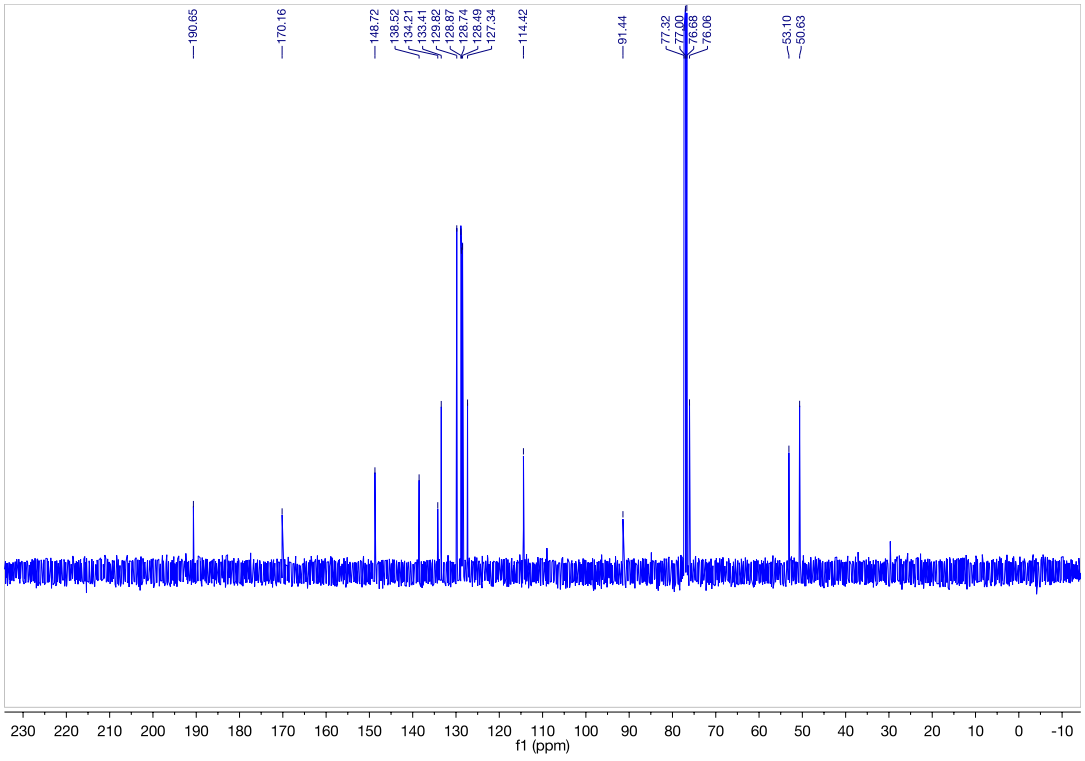
190.65
170.16
148.72
138.52
134.21
133.41
129.82
128.87
128.74
128.49
127.34
114.42
91.44
77.32
77.00
76.68
76.06
53.10
50.63
f1 (ppm)

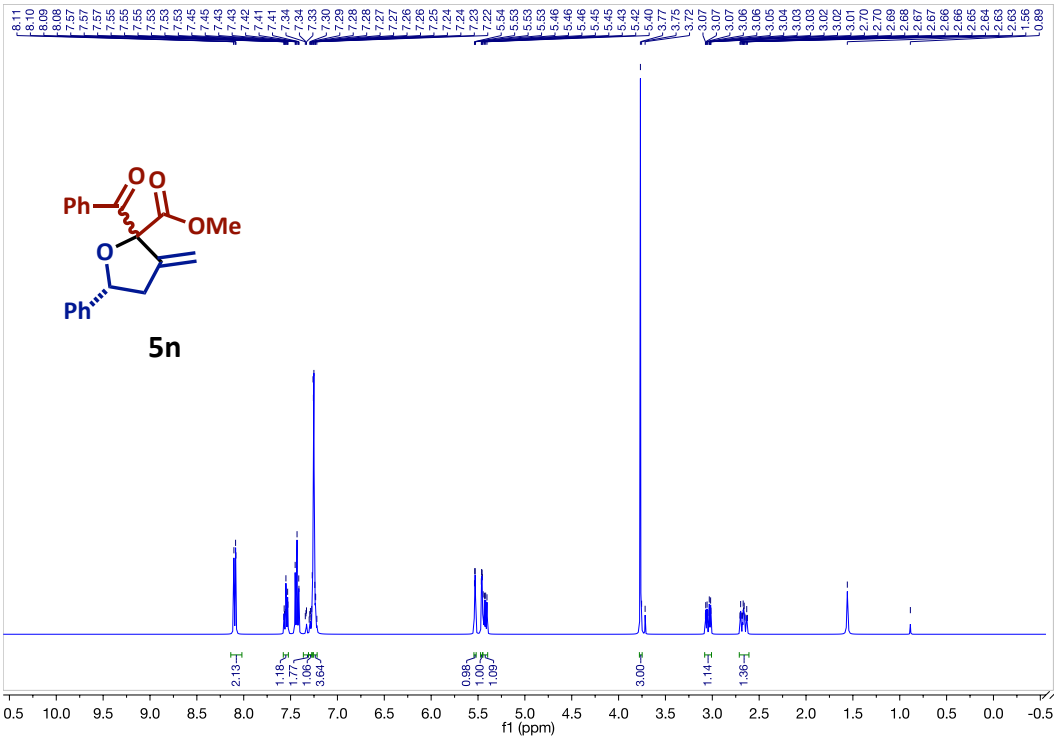
Ph
O
O
OMe
O
Ph
5n
f1 (ppm)

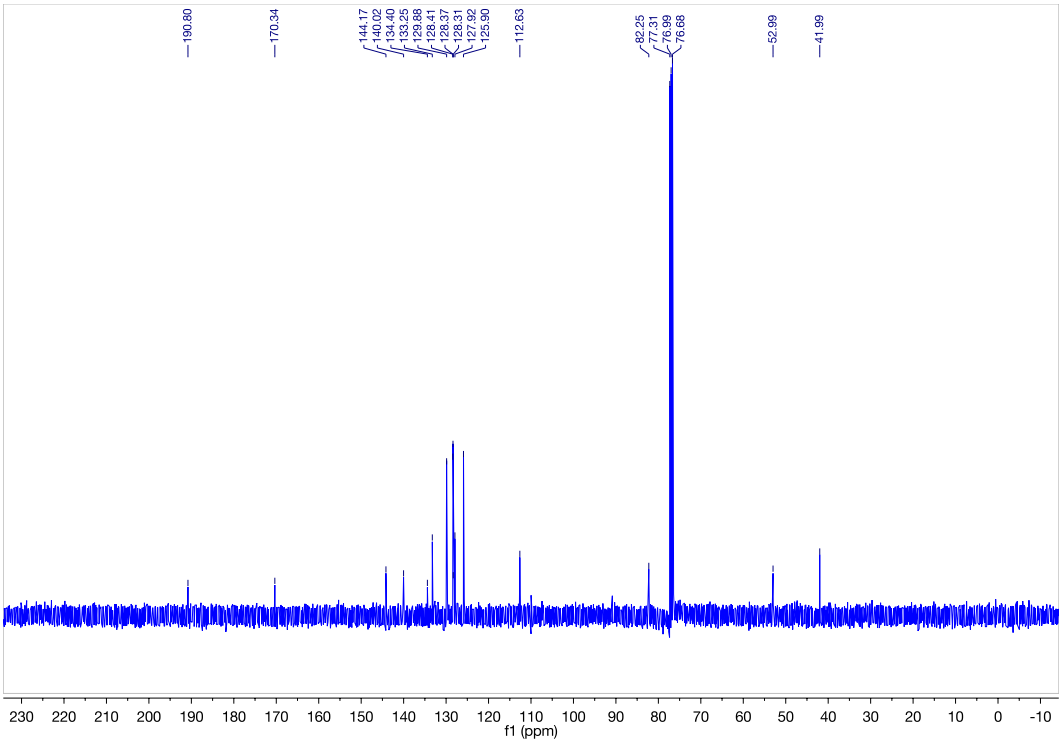
190.80
170.34
144.17
140.02
134.40
133.25
129.88
128.41
128.37
128.31
127.92
125.90
112.63
82.25
77.31
76.99
76.68
52.99
41.99
f1 (ppm)

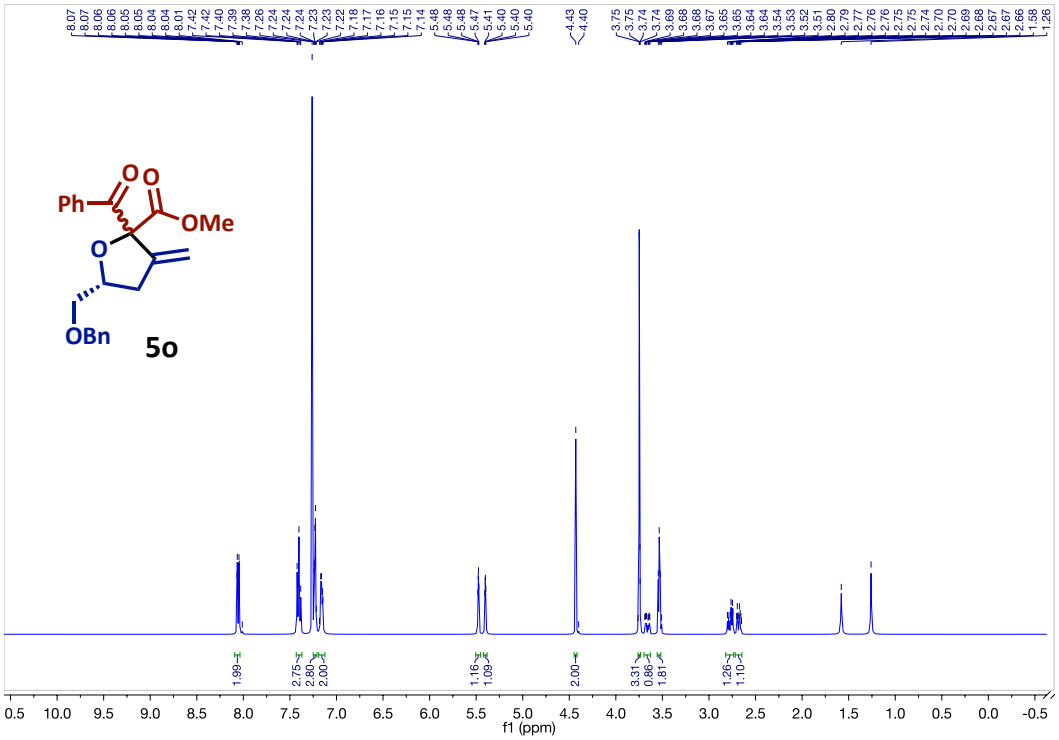
Ph
O
O
OMe
O
OBn
5o
f1 (ppm)

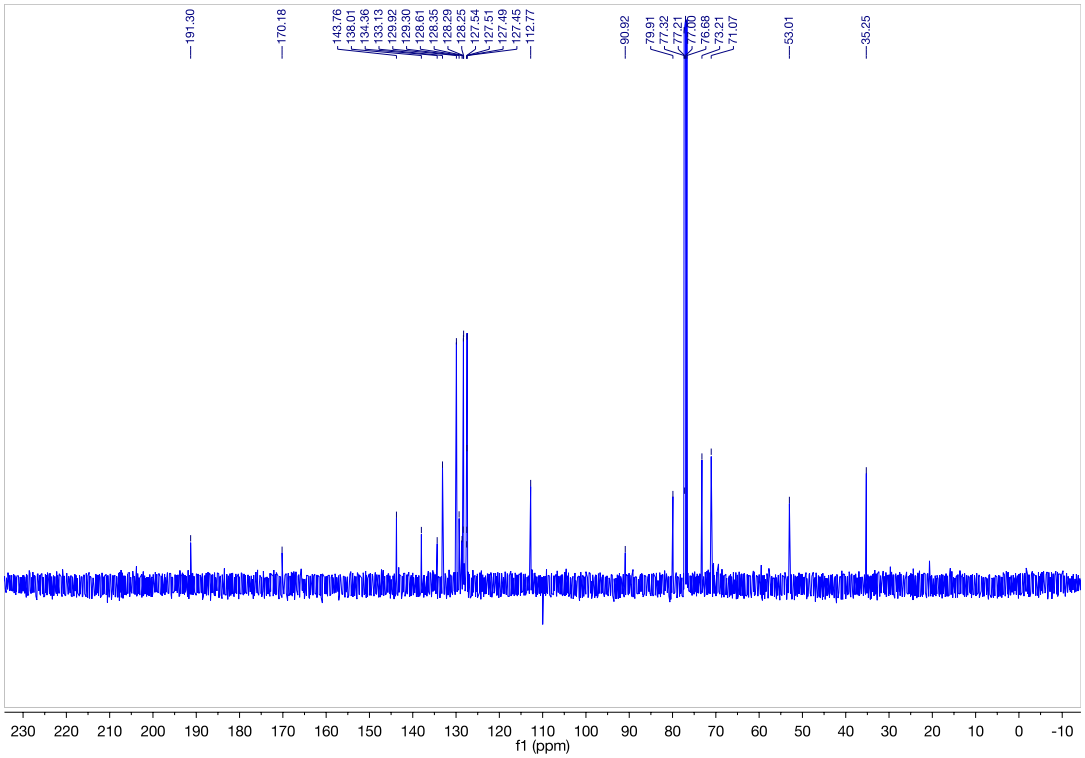
191.30
170.18
143.76
138.01
134.36
133.13
129.92
129.30
128.61
128.35
128.29
128.25
127.54
127.51
127.49
127.45
112.77
90.92
79.91
77.32
77.21
77.00
76.68
73.21
71.07
53.01
35.25
f1 (ppm)

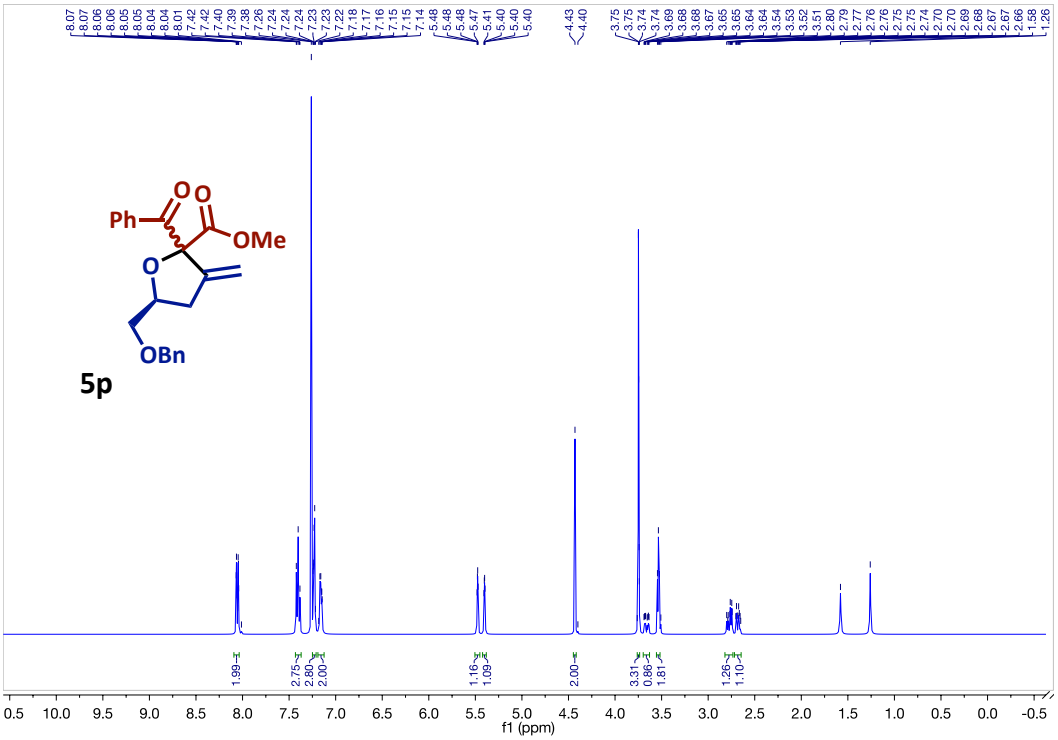
Ph
O
O
OMe
O
OBn
5p
f1 (ppm)

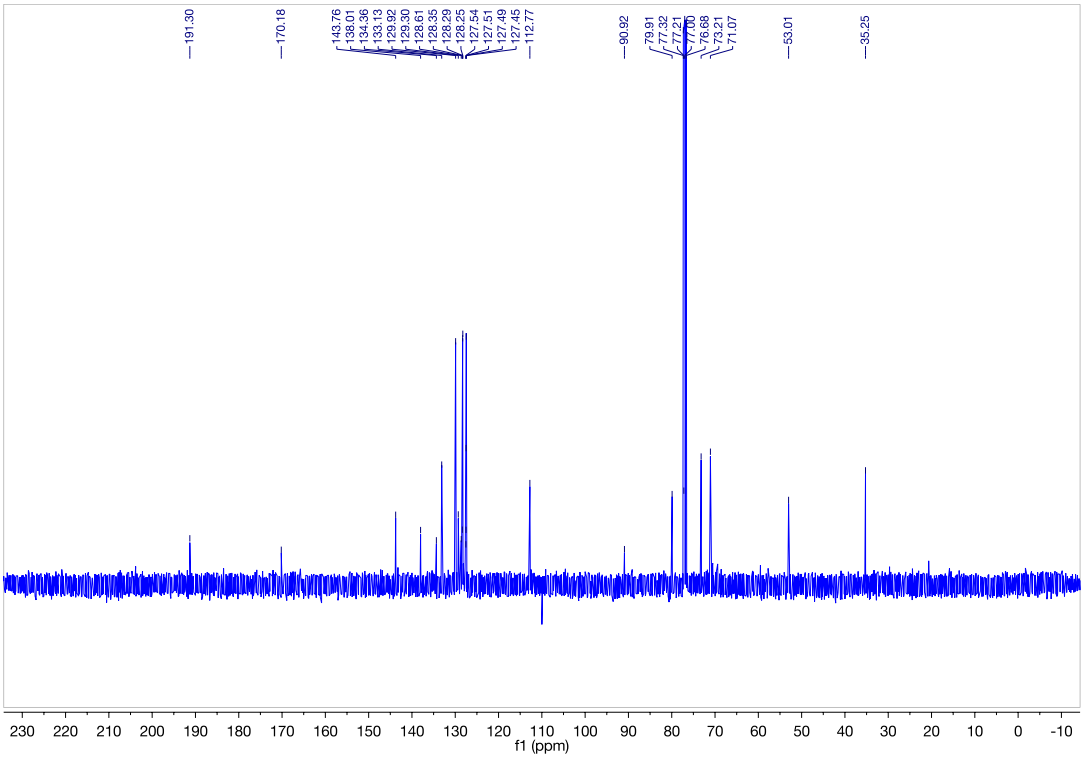
191.30
170.18
143.76
138.01
134.36
133.13
129.92
129.30
128.61
128.35
128.29
128.25
127.54
127.51
127.49
127.45
112.77
90.92
79.91
77.32
77.21
77.00
76.68
73.21
71.07
53.01
35.25
f1 (ppm)

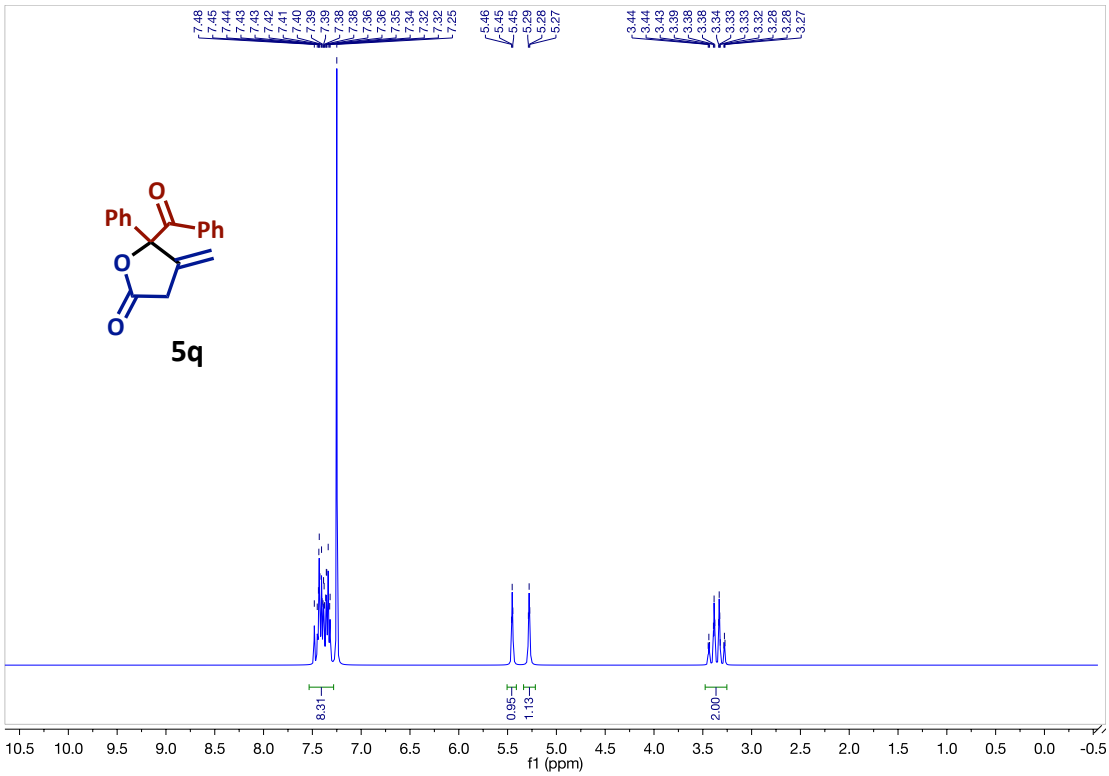
7.48
7.45
7.44
7.43
7.43
7.42
7.41
7.40
7.39
7.39
7.38
7.38
7.36
7.36
7.35
7.34
7.32
7.32
7.25
5.46
5.45
5.45
5.29
5.28
5.27
3.44
3.44
3.43
3.39
3.38
3.34
3.33
3.33
3.32
3.28
3.27
Ph
Ph
O
O
O
5q
8.31
0.95
1.13
2.00
10.5 10.0 9.5 9.0 8.5 8.0 7.5 7.0 6.5 6.0 5.5 5.0 4.5 4.0 3.5 3.0 2.5 2.0 1.5 1.0 0.5 0.0 -0.5
f1 (ppm)

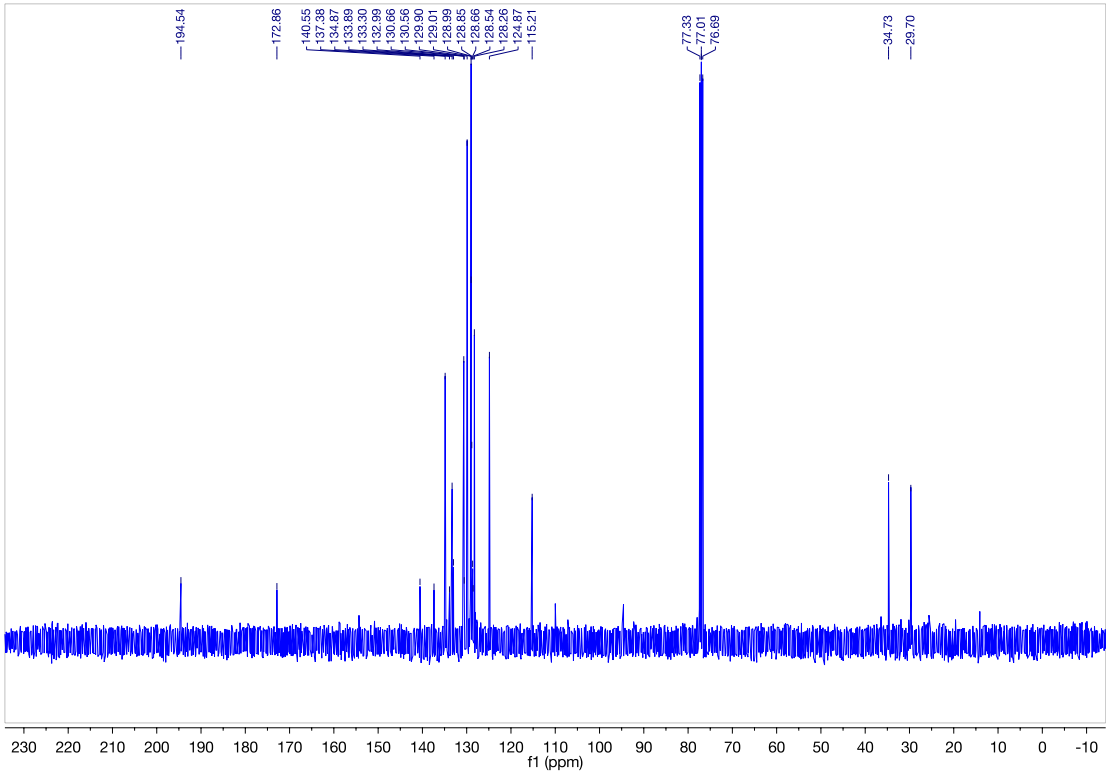
194.54
172.86
140.55
137.38
134.87
133.89
133.30
132.99
130.66
130.56
129.90
129.01
128.99
128.85
128.66
128.54
128.26
124.87
115.21
77.33
77.01
76.69
34.73
29.70
230 220 210 200 190 180 170 160 150 140 130 120 110 100 90 80 70 60 50 40 30 20 10 0 -10
f1 (ppm)

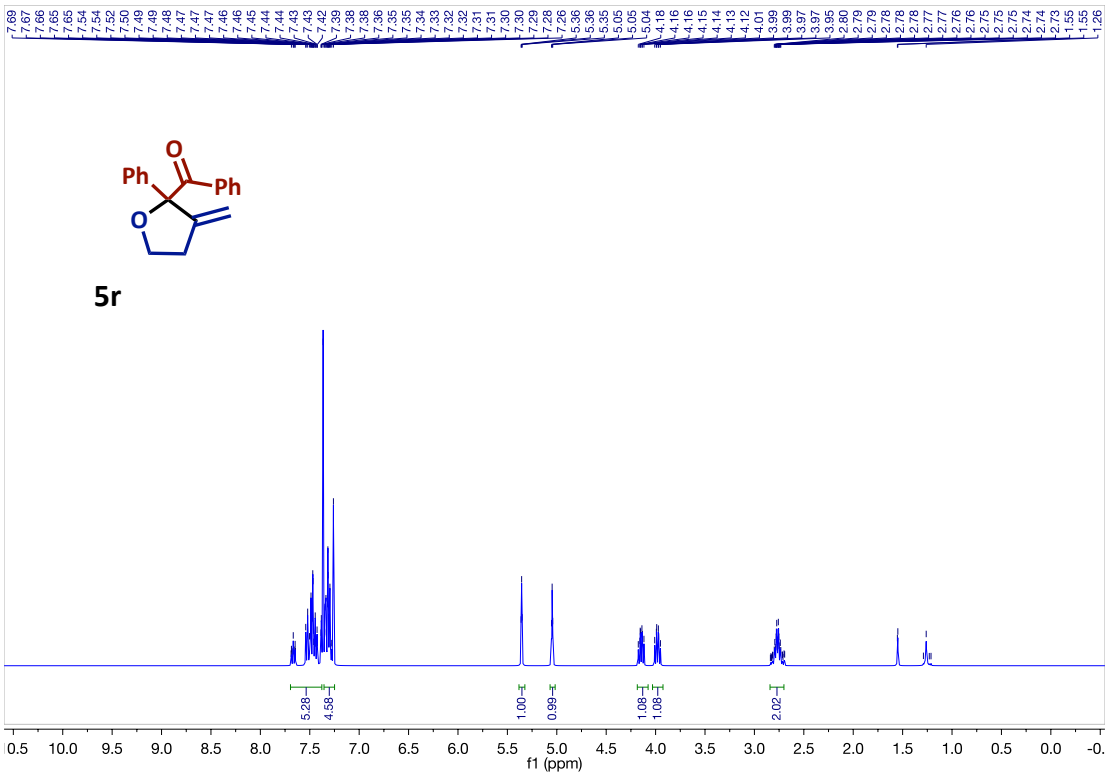
Ph
O
Ph
O
5r
5.28
4.58
1.00
0.99
1.08
1.08
2.02
f1 (ppm)

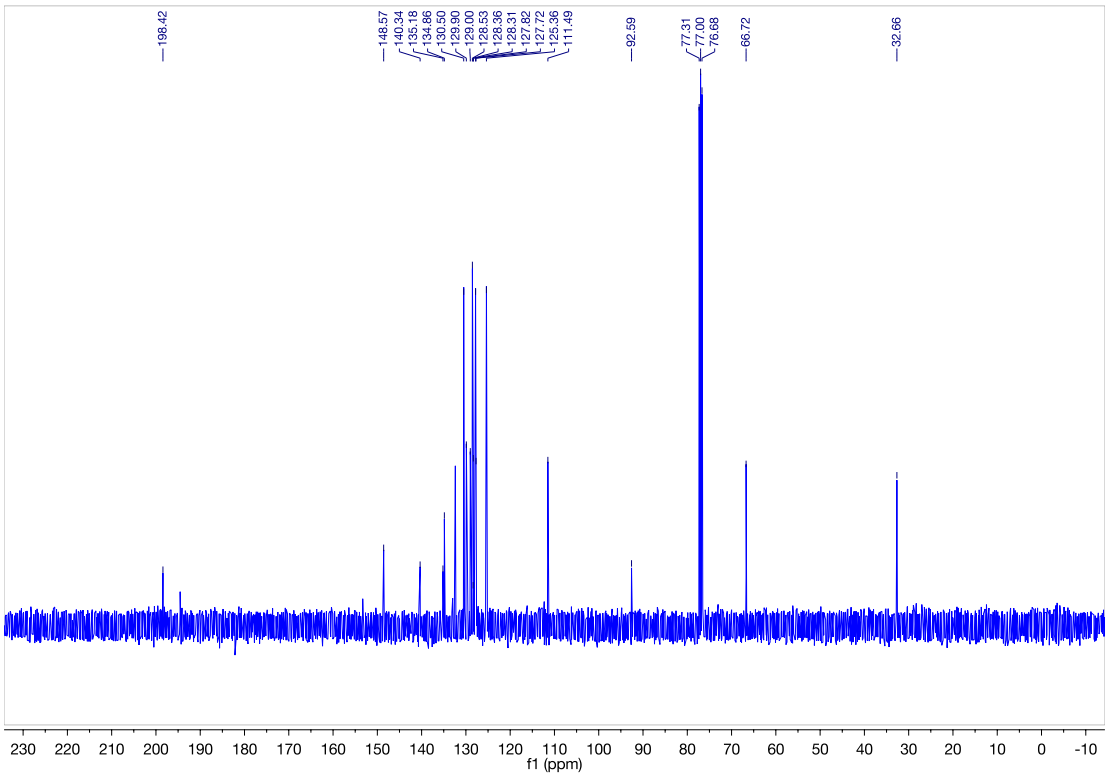
198.42
148.57
140.34
135.18
134.86
130.50
129.90
129.00
128.53
128.36
128.31
127.82
127.72
125.36
111.49
92.59
77.31
77.00
76.68
66.72
32.66
f1 (ppm)

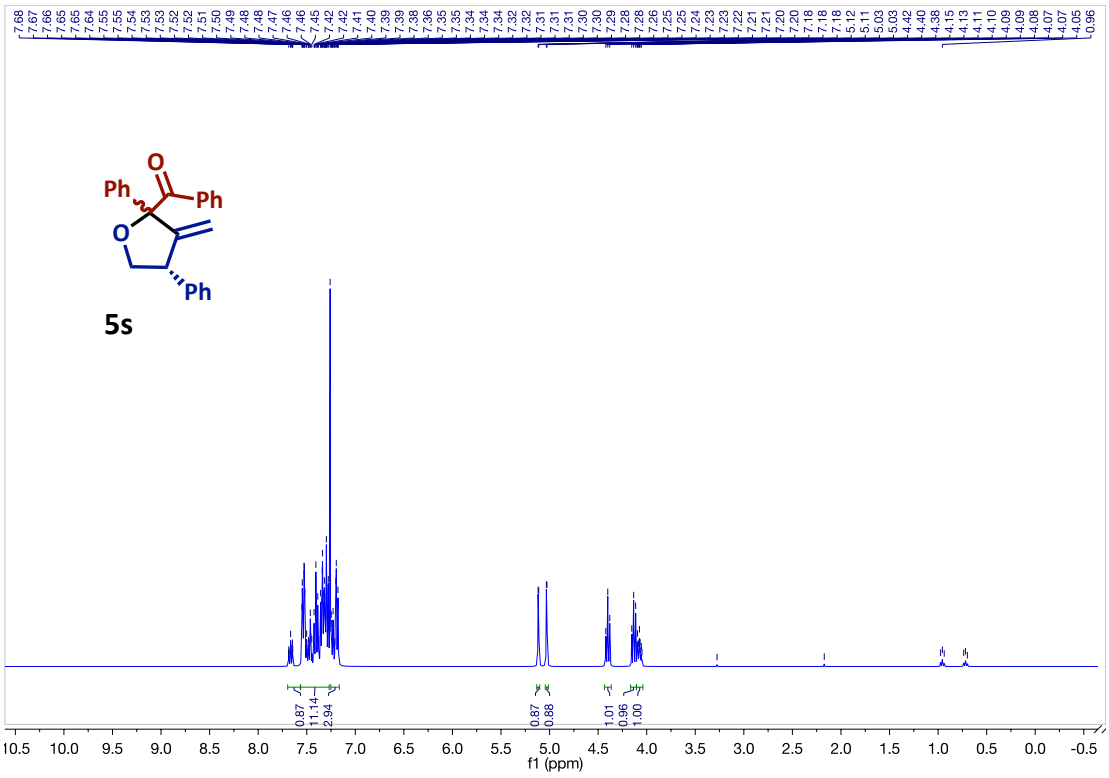
Ph
O
Ph
O
Ph
5s
f1 (ppm)

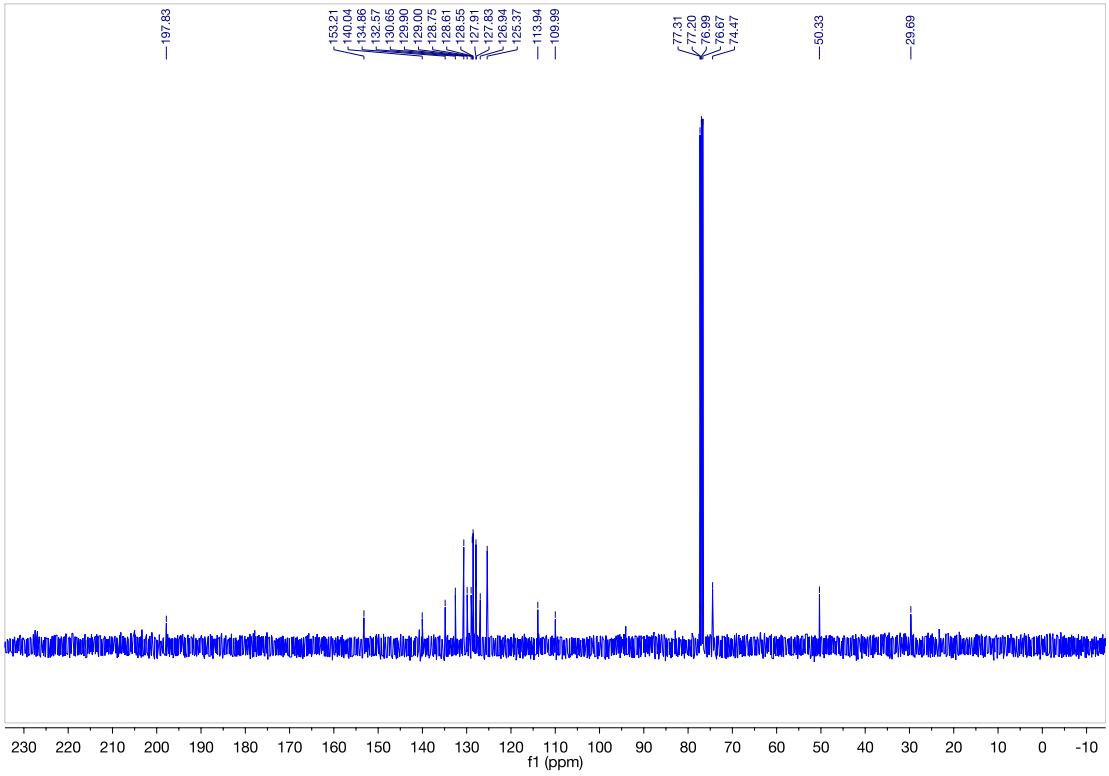
f1 (ppm)

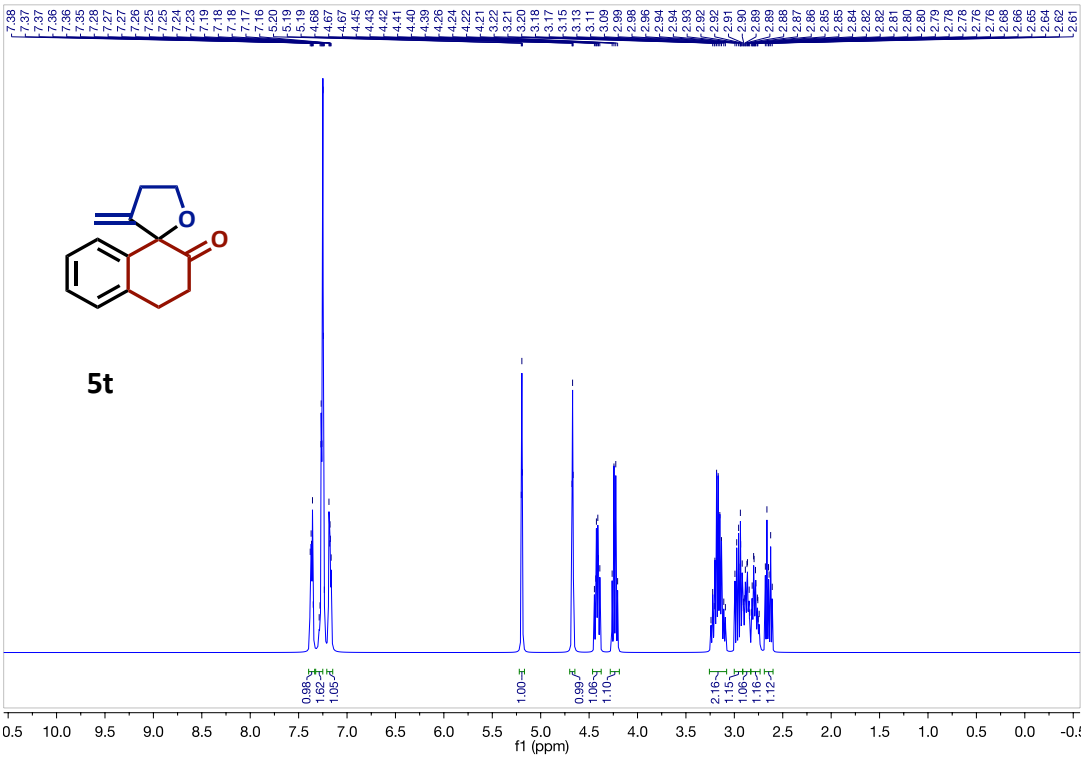
O
O
5t
0.98
1.62
1.05
1.00
0.99
1.06
1.10
2.16
1.15
1.06
1.16
1.12
f1 (ppm)

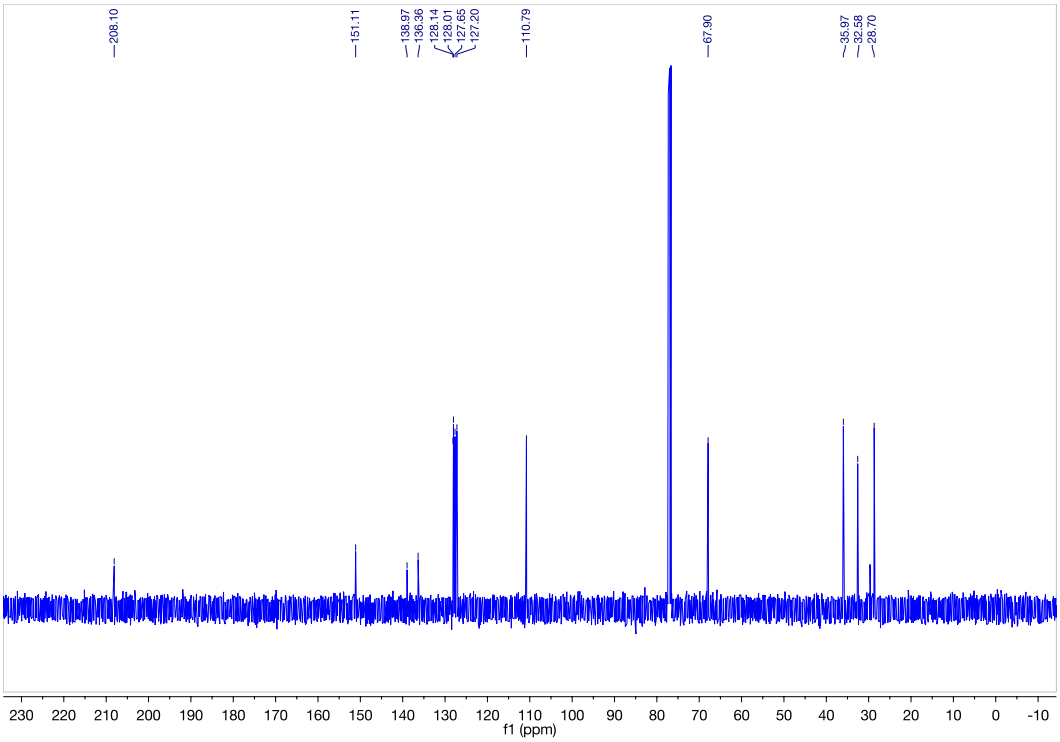
208.10
151.11
138.97
136.36
128.14
128.01
127.65
127.20
110.79
67.90
35.97
32.58
28.70
f1 (ppm)

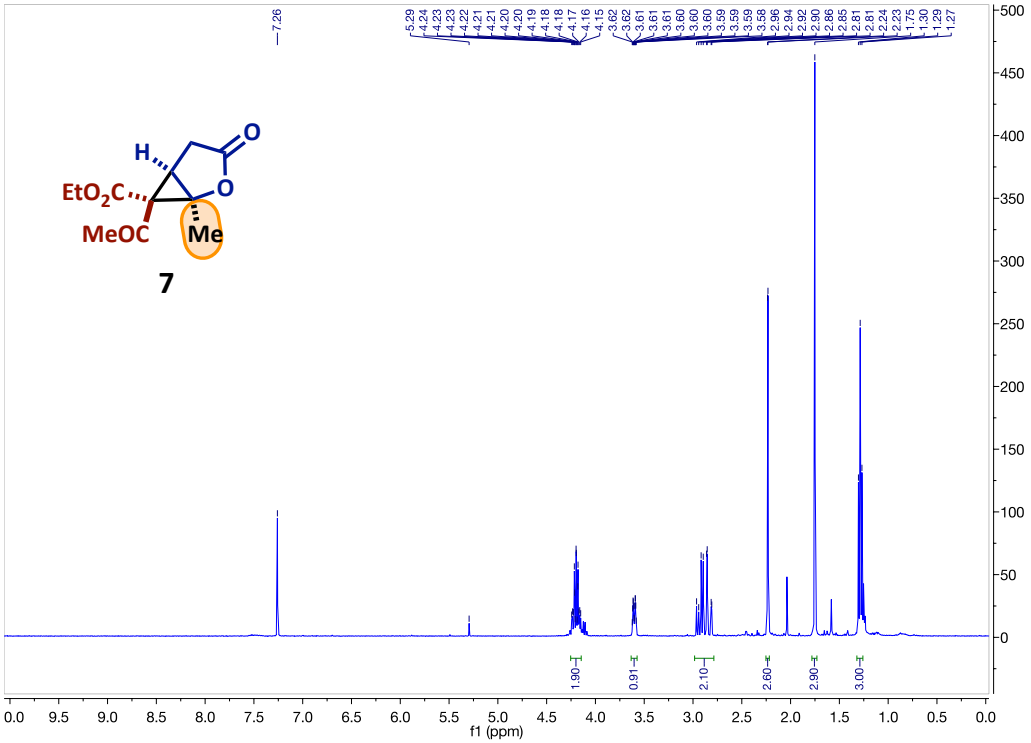
7.26
5.29
4.24
4.23
4.23
4.22
4.21
4.21
4.20
4.20
4.19
4.18
4.18
4.17
4.16
4.15
3.62
3.61
3.61
3.61
3.60
3.60
3.60
3.59
3.59
3.59
3.58
2.96
2.94
2.92
2.90
2.86
2.85
2.81
2.81
2.24
2.23
1.75
1.30
1.29
1.27
H
O
O
EtO2C
MeOC
Me
7
1.90
0.91
2.10
2.60
2.90
3.00
f1 (ppm)

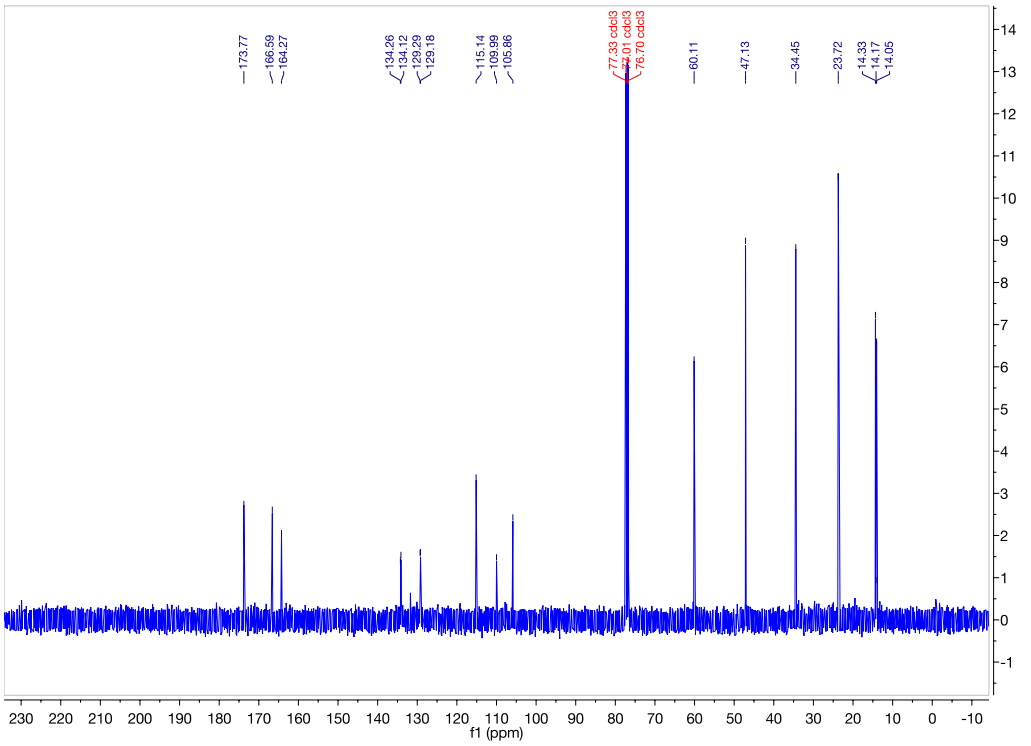
173.77
166.59
164.27
134.26
134.12
129.29
129.18
115.14
109.99
105.86
77.33 cdcl3
77.01 cdcl3
76.70 cdcl3
60.11
47.13
34.45
23.72
14.33
14.17
14.05
f1 (ppm)

CHAPTER 3

Rh(II)/Au(I) Catalyzed Synthesis of

Spiroethers and Azaspiro-Ring Systems

3.1 INTRODUCTION

The stereoselective synthesis of spiroethers, which are found in a wide range of bioactive natural products and drug molecules (**Figure 3.1**), is of great importance to the field of synthetic chemistry.[1] Examples of naturally occurring spiroethers include the pseurotins and spirooxindoles. Due to the biological importance of spiroethers, the synthesis of this scaffold remains an area of current interest to the chemical community.

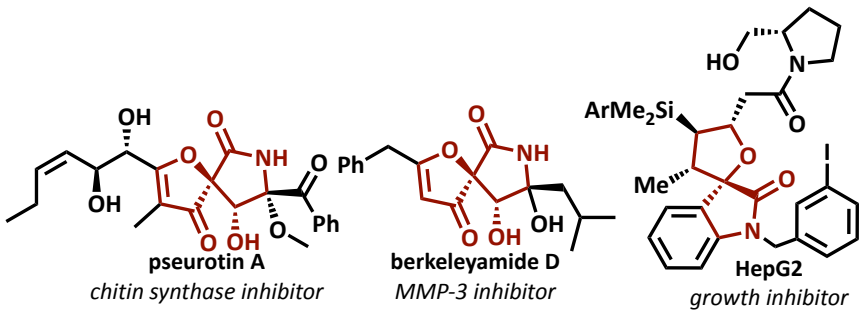

Figure 3.1. *Representative examples of biologically active spiroethers as natural products and synthetically derived drug molecules.*

Most existing methods to access spiroethers rely heavily on intramolecular cyclization/rearrangement reactions of appropriate linear precursors which require multiple synthetic steps for preparation. For example, in 2012 Jiao et al. identified a direct C(sp^3)–H functionalization of tetrahydrofurans to access spiroethers (**Scheme 3.1**).[2] In this work it was necessary to start with a tetrahydrofuran that contained both an α,β-unsaturated aldehyde and a diethylmalonate moiety. When this highly functionalized substrate was placed in the presence of a strong Lewis acid and organocatalyst, an iminium ion mediated C–H functionalization occurred. Although this method provided access to a variety of spiroethers with differing substituents and ring sizes, the method is not ideal because of the four synthetic steps needed to access the linear precursor for intramolecular cyclization.

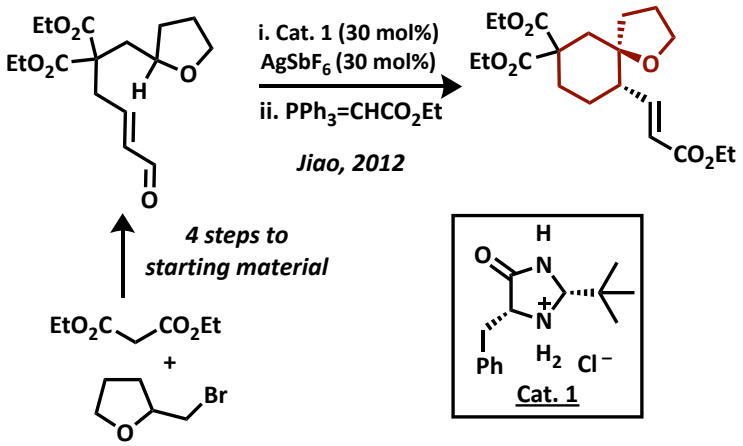

Scheme 3.1. *Previous approach to spiroethers showing the general need to synthesize a complex linear precursor prior to setting spirocenter.*

Also of great value are azaspiro-ring systems which uniquely possess an aza-substituted quaternary center.[3] This motif is frequently found in many biologically active natural alkaloids such as cylindricine A, lepadeformine A, TAN1251A, and FR901483 (**Figure 3.2**).[3a] Azaspiro-ring systems are also found in a variety of highly valuable ligand scaffolds. These types of ligands have been proven to be especially powerful due to their ability to induce impeccable stereocontrol because of the proximity of the spiro-backbone to the nitrogen center which coordinates catalysts. Although azaspiro-ring systems such as spiropyrollidines are of great value, their associated synthetic challenges cause syntheses for accessing them to be limited, similar to spiroethers.

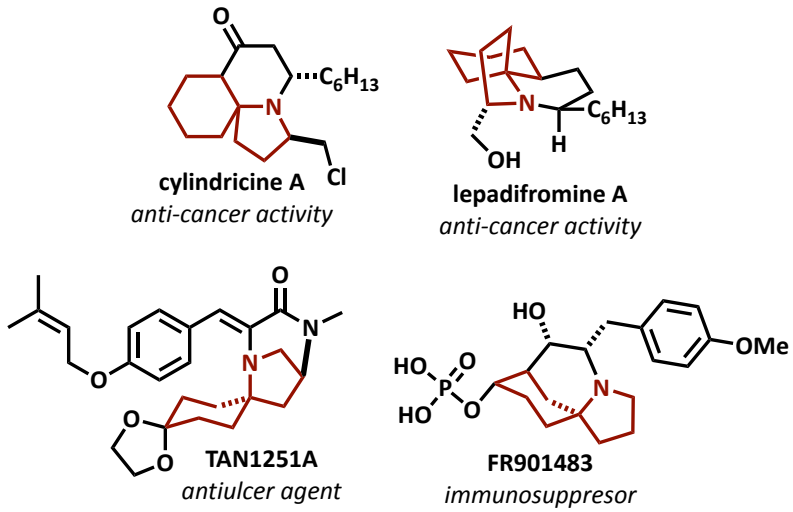

Figure 3.2. *Biologically active azaspiro-ring systems found in natural products*

In 2015 Zhang et al. designed a spiropyrollidine organocatalyst and applied it to a catalytic asymmetric Michael addition for the construction of all-carbon quaternary centers (**Scheme 3.2**).[3b] During the design of this organocatalyst the authors had to complete eight

synthetic steps from a complex linear precursor to obtain their spiropyrollidine ligand scaffolds for screening. This eight-step sequence had to be repeated for each different ligand scaffold for screening.

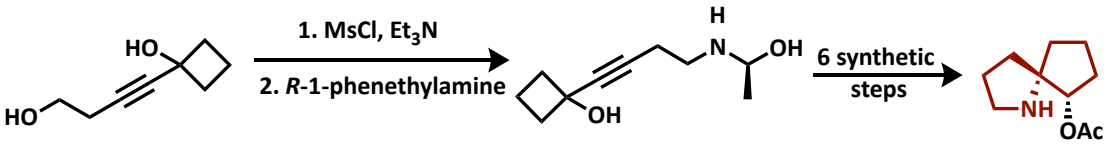

Zhang, 2015

Scheme 3.2. *Biologically active azaspiro-ring systems found in natural products*

When analyzing the structures of spiroethers and spiropyrollidines, one's attention is immediately drawn to the daunting task of forming the quaternary stereocenter stereoselectively, and this feat is increasingly difficult because the quaternary stereocenter is incorporated into a spirocycle. Despite this obvious challenge, we were intrigued by the uniqueness, usefulness, and lack of representation of these scaffolds. Therefore, to overcome the aforementioned challenge and avoid the application of complex linear precursors, we decided to dissect the molecule in a simple yet unique manner: *by splitting it down the middle*. This disconnection would provide convergent access to spiroethers and azaspiro-ring systems. After splitting this scaffold down the middle, we see that it is necessary to have two substrates that possess both nucleophilic and electrophilic reactivity, which is better known as "ambiphilic reactivity" (**Figure 3.3**). This ambiphilicity can be found within a tethered molecule having both an electrophile and nucleophile and also within a singlet carbene that can be directly accessed through diazo compounds.[4]

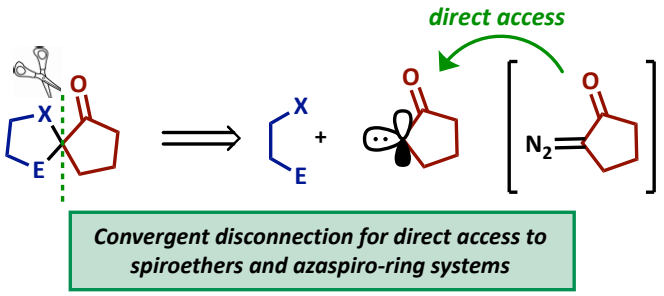

Figure 3.3. *Novel disconnection to spirocycles developed by Sharma Lab*

3.2 STEREOSELECTIVE TRAPPING OF Rh(II) CARBENES WITH Au(I) ACTIVATED ALKYNOLS FOR THE SYNTHESIS OF SPIROETHERS

In the preceding chapter, we reported the identification and application of $Rh_2(esp)_2$ and PPh_3AuOTf as a synergistic catalytic cocktail to access γ-butyrolactones and tetrahydrofurans.[5] Within this work, our diazocarbonyls were often linear substrates. However, there was one example where we implemented a cyclic diazocarbonyl derived from 2-tetralone (**Scheme 3.3**). When diazo **1a** was exposed to our catalytic conditions in the presence of 3-butynol, we were able to obtain the corresponding spiroether **3a** in 71% yield.

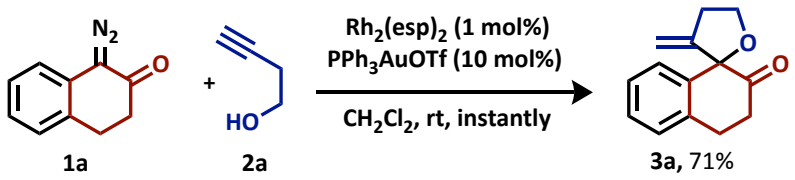

Scheme 3.3. *Preliminary results to help justify synthetic approach.*

With this preliminary result in hand, we hypothesized that we could split spiroethers "down the middle" into a corresponding cyclic diazocarbonyl and alkynol derivative, the hydroxyl group being our nucleophile and the alkyne being our electrophile. When these two substrates are exposed to our $Rh_2(esp)_2$/PPh_3AuOTf catalytic cocktail, the desired spiroether would be rapidly and efficiently obtained. This approach would eliminate the need to synthesize highly functionalized linear precursors, thereby making our method highly convergent.

3.2.1 INITIAL SCREENING OF CATALYTIC CONDITIONS

Inspired by the initial synthesis of spiroether **3a** using our $Rh_2(esp)_2$/PPh_3AuOTf catalytic conditions, we decided to focus our attention on optimizing this transformation using *N*-methyl isatin diazo **1b**. This diazo would provide highly relevant spirooxindole scaffolds which are privileged skeletons due to their broad and promising biological activities and prevalence in naturally occurring molecules.[6]

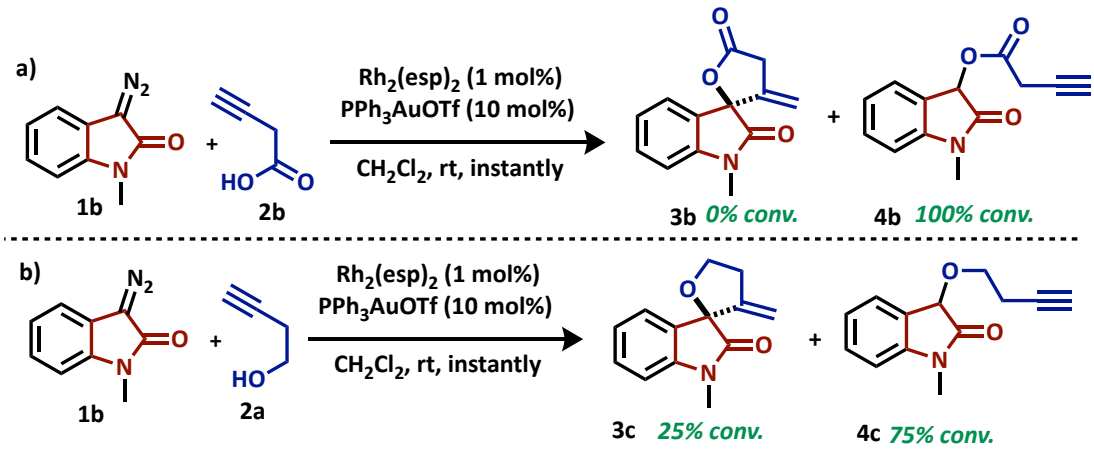

Scheme 3.4. *Preliminary results for cascade spirocyclization*

We initiated our work by attempting the carboxylic acid O–H insertion/Conia-ene cyclization using diazo **1b** and 3-butynoic acid (**Scheme 3.4a**). Surprisingly, this reaction yielded only the corresponding insertion product **4b** and no trace of the cyclized product **3b** was detected. The incompatibility of the carboxylic acid in this cascade reaction may be attributed to the low p*K*a value of the protonated carboxylic acid in the zwitterionic intermediate (approximated –7.4).[7] This low p*K*a value would thereby favor a higher rate of proton transfer over the trapping of the activated alkyne. Undeterred by this failed reaction, we next decided to screen the reaction with 3-butynol, as it was just as efficient as 3-butynoic acid in our O–H insertion/Conia-ene cyclization methodology (**Scheme 3.4b**). Upon completion of this reaction we observed a 25:75 ratio of the desired spiroether **3c** to the competing insertion product **4c**. Encouraged by the results in hand, we began to optimize the reaction in order to obtain a higher conversion to spiroether **3c** (**Table 3.1**).

When examining the mechanism of this transformation it is understood that in order to have a higher probability of the active Rh(II)-bound zwitterionic intermediate being trapped by the Au(I)-activated alkynol, the lifetime of the Rh(II)–bound zwitterionic intermediate must be increased.[8] One obvious way to increase the lifetime is to limit the amount of diazocarbonyl present in the reaction mixture, consequently the Rh(II) will not be influenced to leave the zwitterionic intermediate to go decompose another diazocarbonyl. To test this hypothesis, we added a solution of **1b** in dichloromethane via syringe pump to a mixture of the catalytic solution and 3-butynol. When this reaction was complete, we observed a significant increase in conversion to a 40:60 ratio of the desired spiroether **3c** to the competing insertion product **4c** (**Table 3.1,** entry 2). Next, we decided

to test the influence of a decreased temperature, however, when the reaction was conducted at 0 ºC with a syringe pump addition of **1b** no significant change in conversion was observed (**Table 3.1,** entry 3). Lastly, we hypothesized that an increase in Lewis-acidity of the Rh(II) catalyst could extend the lifetime of the Rh(II)-bound zwitterionic intermediate.[8a, 9] To test this hypothesis, we conducted the reaction in the presence of highly electrophilic $Rh_2(TFA)_4$ instead of $Rh_2(esp)_2$. This change proved to be exceedingly successful, providing almost exclusively the desired spiroether in an 80% conversion (**Table 3.1**, entry 4).

Table 3.1. *Optimization of O–H Insertion/Conia-ene Cascade for Spiroether Synthesis*

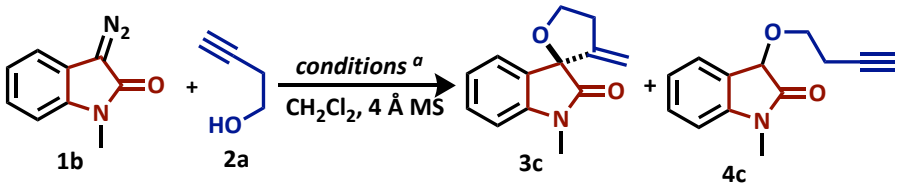

entry	Rh(II)/Lewis acid	time[b](temp)	3c:4c[c]
1	$Rh_2(esp)_2$/AgOTf/PPh_3AuCl	Instant(rt)	25:75
2	$Rh_2(esp)_2$/AgOTf/PPh_3AuCl[d]	1hr addition(rt)	40:60
3	$Rh_2(esp)_2$/AgOTf/PPh_3AuCl[d]	1hr addition(0 ºC)	40:60
4	$Rh_2(TFA)_4$[e]/AgOTf/PPh_3AuCl[d]	1hr addition(0 ºC)	80:20

[a]All optimization reactions were performed in 0.1 M CH_2Cl_2 with **1b** (1.20 equiv.), **2a** (1 equiv.), Rh_2L_4 (1 mol%), and Lewis acids (10 mol%) along with 4 Å molecular sieves; [b]time required for the complete consumption of **1b**; [c]Conversion (%) was determined from the crude ^1H NMR spectrum;[d]**1b** was added via syringe pump addition as a solution in CH_2Cl_2; [e]TFA = trifluoroacetate.

3.2.2 APPLICATION TO SUBSTRATE SCOPE

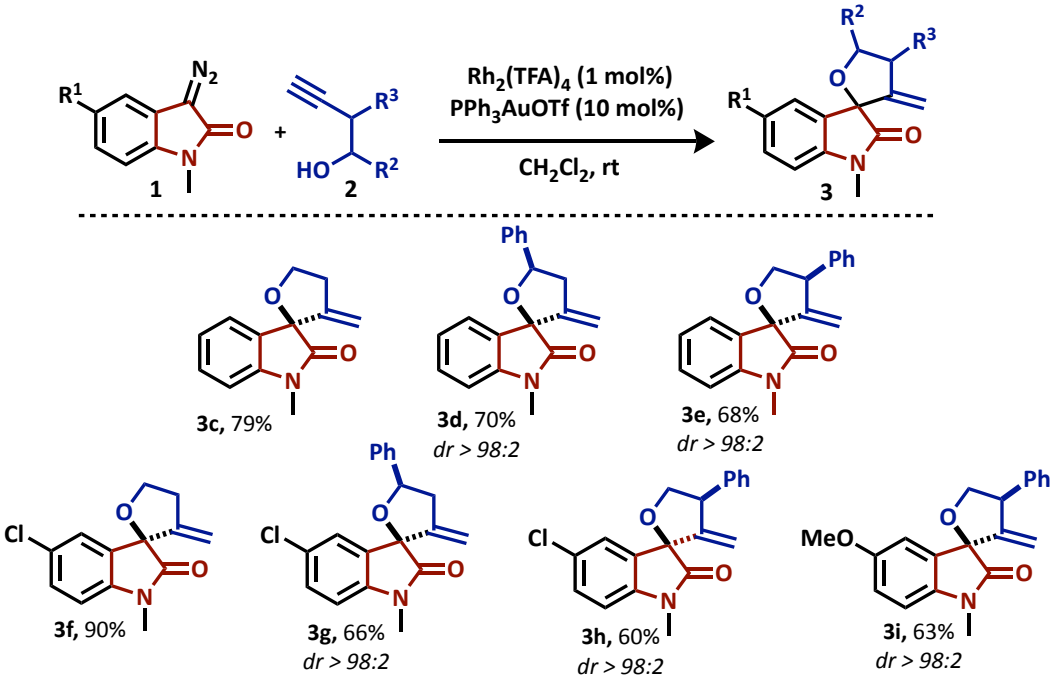

Scheme 3.5. *Representative substrate scope of oxindole spiroethers accessed through O–H Insertion/Conia-ene cyclization with $Rh_2(TFA)_4$/PPh_3AuOTf*

With optimized conditions in hand, we undertook a thorough study of the substrate scope of this transformation in hopes of accessing a variety of functionalized spiroethers (**Scheme 3.5**). When the reaction was conducted with a sterically hindered secondary benzyl alkynol the desired product **3d** was produced in a good 68% yield. Next, a phenyl-substituted primary alkynol provided **3e** in 70% yield. Interested in the electronic effects of the isatin diazo, we conducted the reaction using a 6-chloro substituent on the oxindole core. This electron-deficient species did not have a pronounced effect on the yield of any of the isolated substrates (**3f–3h**). Lastly, we screened the effect of an electron rich

oxindole core, and this perturbation in electronics also did not have an effect on the transformation (**3i**).

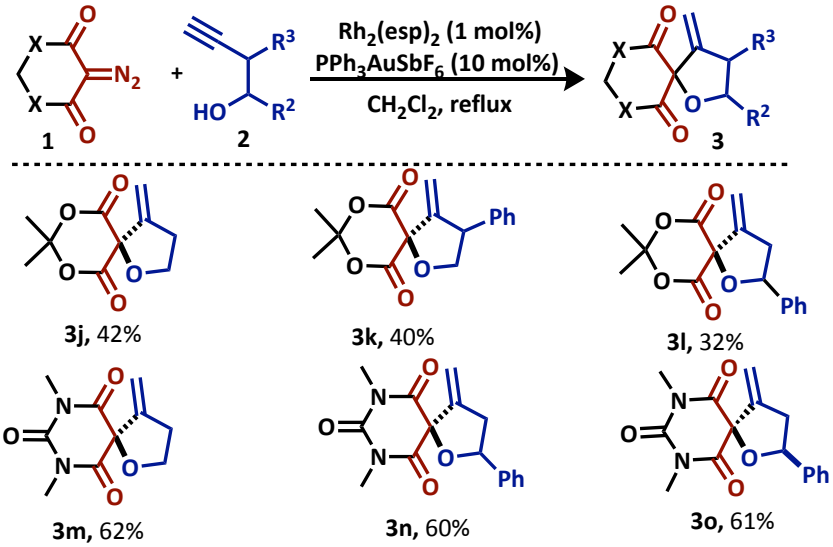

Scheme 3.6. *Representative substrate scope of spiroethers accessed through O–H Insertion/Conia-ene cyclization with $Rh_2(esp)_2/PPh_3AuSbF_6$*

To further expand the application of this method, we began to focus on highly stable A/A cyclic diazocarbonyls, such as the diazocarbonyls derived from Meldrum's acid and barbituric acid. When these substrates were exposed to a mixture of $Rh_2(TFA)_4/PPh_3AuOTf$ no decomposition of the diazo-moiety was observed. Therefore, we decided to return to the more active mixture of $Rh_2(esp)_2/PPh_3AuOTf$ at room temperature, however the diazo-moiety persisted and was completely stable at room temperature. Next, we decided to reflux the reaction in dichloromethane and diazo decomposition finally occurred but the desired Meldrum's acid spiroether **3j** was produced in a very low isolated yield. This was presumably due to the effect of the silver triflate, as metal triflates have been known to be

a mild source of triflic acid which could cause decomposition of the desired spiroether product.[10] With this problem in hand, we thought to screen a more stable silver salt with a less active counter ion and our silver salt of choice was $AgSbF_6$. Delightfully, this change increased the yield of the desired product **3j** to 42%.

With our newly modified conditions, we expanded the substrate scope of this reaction to A/A cyclic diazocarbonyls (**Scheme 3.6**). The Meldrum's acid diazo was compatible with substituted primary and secondary alcohols giving the desired substrates **3k** and **3l** in 40% yield and 32% yield, respectively. We believe the moderate yields observed in these transformations with Meldrum's acid diazocarbonyl can be attributed to molecular instability of the corresponding spiroether in the presence of Lewis acids.[11] These substrates have a high level of entropic driving force for fragmentation. Next, we decided to screen the diazocarbonyl derived from barbituric acid which would not have the entropic driving force for fragmentation. When this diazo was reacted with 3-butynol under the optimized conditions the desired compound **3m** was produced in a 62% yield, validating our hypothesis. As expected, this diazo also accommodated primary and secondary alcohol substituents (**3n**–**3o**).

3.2.3 MECHNISTIC INSIGHTS

To probe the reaction mechanism, deuterium labeling experiments were conducted with both the donor/acceptor and acceptor/acceptor cyclic diazocarbonyls. To conduct this study, it was necessary to synthesize a deuterated 3-butynol derivative (**Scheme 3.5**). Initially, we explored a kinetic deprotonation and exposed our parent 3-butynol to 2.5

equivalents of *n*-butyllithium and proceeded to quench the reaction with D_2O, however, this was proven to be unsuccessful. Next, we decided to exploit the relative acidity of the alkyne proton and explored thermodynamic deprotonation conditions. We exposed a TBS-protected 3-butynol derivative to 1.2 equivalents of trithethylamine in a 1:1 mixture of D_2O and THF, hoping to facilitate a proton/deuterium exchange within the reaction. This solution was stirred overnight and the next morning the desired compound was isolated with 95% deuterium incorporation. To complete the synthesis of the desired deuterated alkynol, a TBS-deprotection was needed, however when this compound was exposed *tetra*-butylammonium fluoride (TBAF) and isolation was attempted, the desired compound was

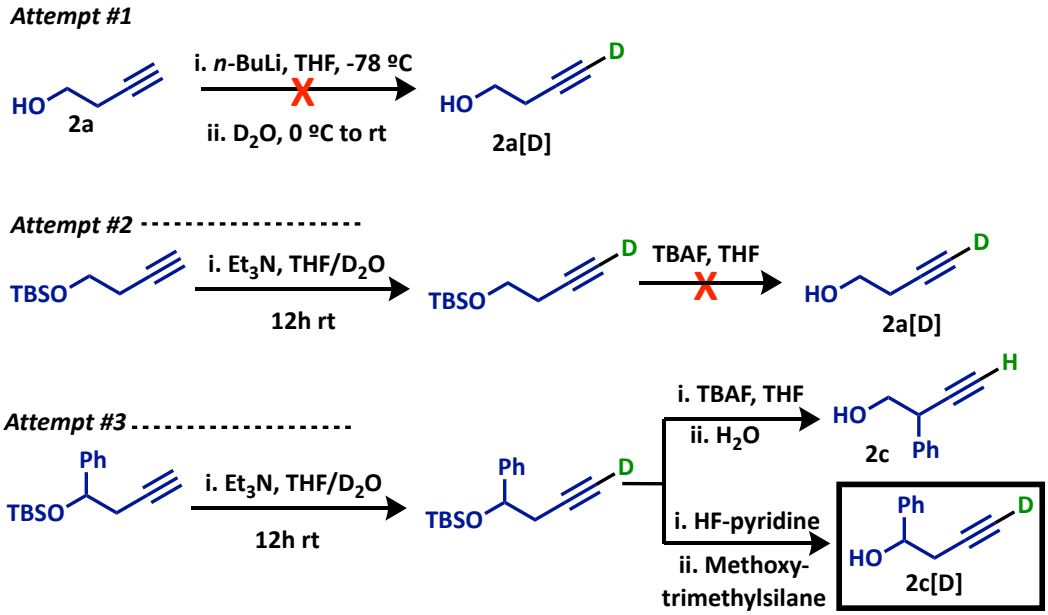

Scheme 3.7. *Insights into the synthesis of deuterated 3-butynol derivative*

lost during isolation due to its extremely low boiling point. This observation caused us to synthesize the phenyl-substituted derivative of 3-butynol in hopes of increasing the boiling

point of the desired compound. However, when the deuterated derivative was synthesized and exposed to TBAF, ^{1}H NMR showed reincorporation of the proton at the alkyne. This caused us to explore an alternative method of TBS-deprotection, HF-pyridine which was quenched with methoxytrimethylsilane instead of water upon completion of the reaction. This method produced the desired substrate **2c[D]** in a 33% yield.

Once our deuterated alkynol was obtained, it was exposed to both the donor/acceptor and acceptor/acceptor cyclic diazocarbonyls under their respective optimized reaction conditions (**Scheme 3.8**). In both cases, no deuterium scrambling was observed, and the deuterium was found to be syn to the carbonyl functionality using 1D nOe experiments. This observation was in accordance with results published by Toste et al. in his previous Au(I)-catalyzed Conie-ene cyclization.[12] These results suggest a mechanism involving the trapping of an enol-intermediate with a gold-alkyne π-coordinated complex, ruling out the formation of a gold acetylide.[13]

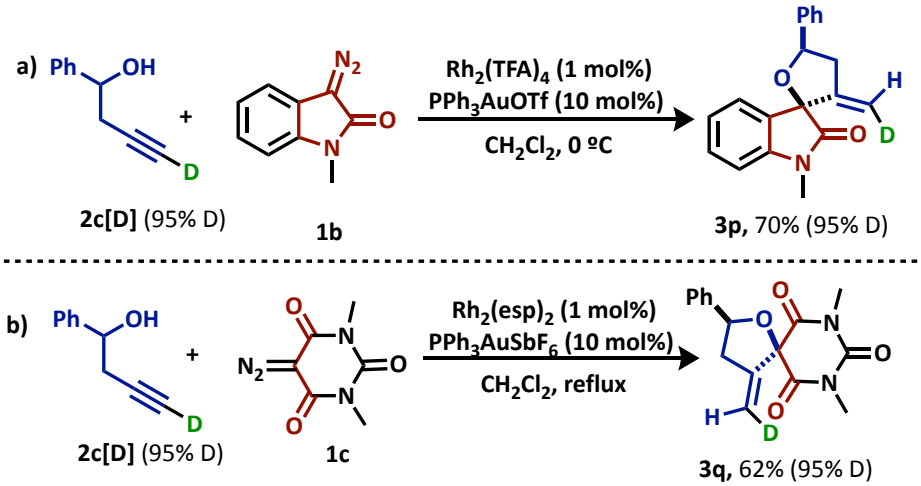

Scheme 3.8. *Deuterium labeling studies using deueterated alkynol*

For further insights we conducted the reaction with isatin diazo **1b** and 3-butynol in the presence of D_2O in order to determine a possible mode of proto-demetalation for this transformation (**Scheme 3.9**). Upon completion of the reaction a 47:53 ratio of spirother **3c/3c[D]** to insertion byproduct **4c/4c[D]** was observed. For the spiroether, there was a 38% deuterium incorporation at the alkene and for the insertion compound there was a 55% deuterium incorporation at the α-center of the isatin and no deuterium incorporation at the alkyne. These observations suggest that there is a high likelihood the proto-demetalation step for this transformation occurs intermoleculary through trace amount of water present in the reaction.

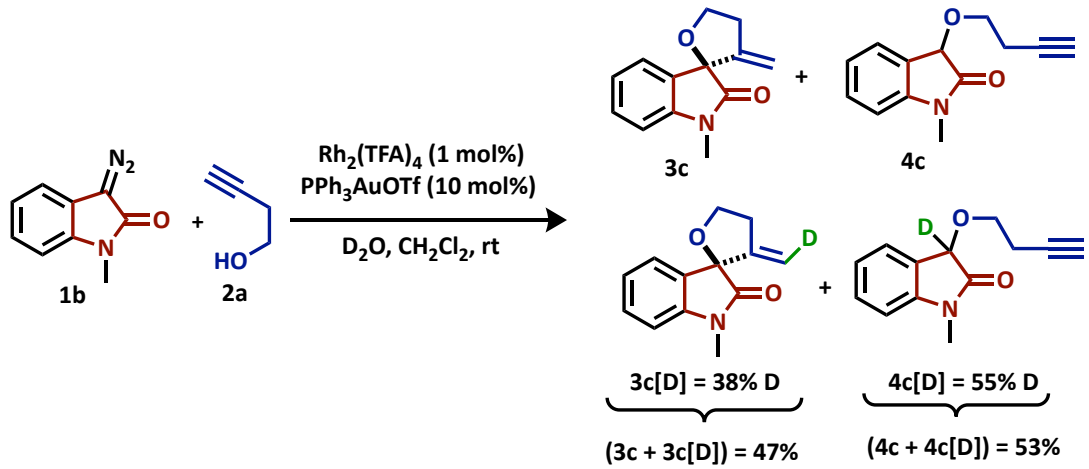

Scheme 3.9. *Deuterium labeling studies using D_2O as an additive*

Once the deuterium labeling experiments were complete, we wanted to validate the synergy of this transformation and whether these substrates could be accessed in a stepwise fashion. To do this, we synthesized the insertion products with the

donor/acceptor and acceptor/acceptor cyclic diazocarbonyls using $Rh_2(TFA)_4$ and $Rh_2(esp)_2$ as catalysts, respectively. When the insertion compounds were subjected to the Au(I) catalyzed Conia-ene cyclizatin condition, we did not observe any cyclized products even

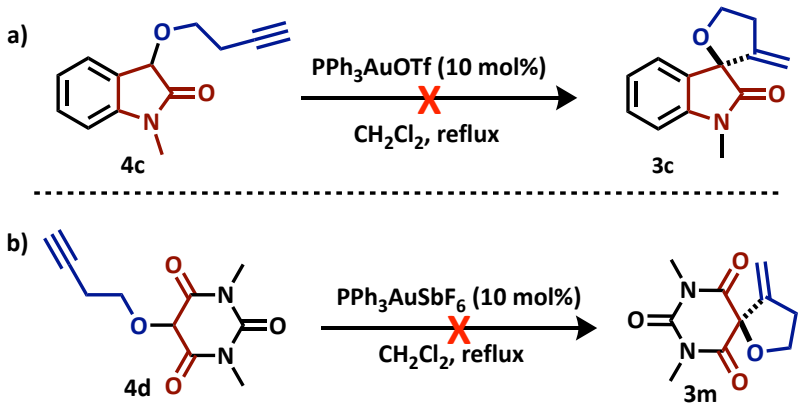

Scheme 3.10. *Probing stepwise transformation for validation of synergy*

after 12 hours in refluxing dichloromethane (**Scheme 3.8**). We also exposed the insertion products to a mixture of Rh(II) and cationic Au(I), in order to probe whether the catalyst mixture is able to induce the stepwise transformation. However, no cyclized products were observed under these conditions also, even after 12 hours in refluxing dichloromethane. This study supports the complete synergy of Rh(II) and Au(I) in this catalytic cascade.

As a final effort to obtain mechanistic understanding, we conducted studies to probe whether this transformation could be conducted asymmetrically (**Table 3.2**). Initially, we attempted the cascade reaction with chiral Rh(II) catalysts, Rh_2(*S*-DOSP)$_4$ and Rh_2(*S*-PTAD)$_4$ with isatin diazo **1b**. We also screened the optimized reaction with the incorporation of *R*-BINAP$(AuCl)_2$. Nevertheless, after screening these conditions no enantiomeric excess (ee) was observed. This observation was in accordance with literature

Table 3.2. *Optimization of Asymmetric Transformation with Isatin Diazo*

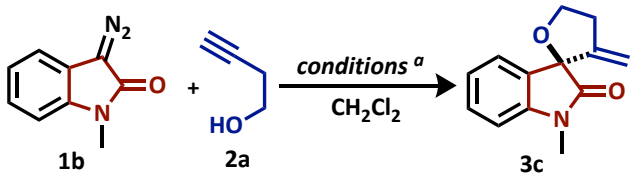

entry	Condition	time[b](temp)	%ee(yield%)
1	Rh_2(*S*-DOSP)$_4$/AgOTf/PPh_3AuCl	1hr addition(0 ºC)	0 (52)
2	Rh_2(*S*-PTAD)$_4$/AgOTf/PPh_3AuCl	1hr addition(0 ºC))	0 (43)
3	Rh_2(TFA)$_4$[c]/AgOTf/*R*-BINAP(AuCl)$_2$	1hr addition(0 ºC)	0 (61)

[a]All optimization reactions were performed in 0.1 M CH_2Cl_2 with **1b** (1.20 equiv.), **2a** (1 equiv.), Rh_2L_4 (1 mol%), and Lewis acids (10 mol%) along with 4 Å molecular sieves; [b]time required for the complete consumption of **1b**; [c]TFA = trifluoroacetate.

reports of inducing negligible enantioselectivity with chiral Rh(II) catalysts when the reaction centralized around the trapping of electrophiles with oxonium and ammonium zwitterionic intermediates that are formed in situ. Subsequently, we probed whether we could induce asymmetry using a chiral Au(I) catalyst. After completing the reaction with Rh_2(TFA)$_4$/*R*-BINAP(AuCl)$_2$/AgOTf the desired compound **3c** was isolated in a 53% yield, but no enantiomeric excess was induced.

Next, we decided to change the diazocarbonyl for optimization to the 2-tetralone diazocarbonyl due to a hypothesis that the reactivity of an α-ketone diazocarbonyl would differ from the amide of isatin diazocarbonyl (**Table 3.3**). Whenever we exposed **1a** to 3-butynol in the presence of Rh_2(esp)$_2$/*R*-BINAP(AuCl)$_2$/AgOTf we obtained the desired spiroether **3a** in a 73% yield with 33% ee. Subsequently we replaced Rh_2(esp)$_2$ with Rh_2(OAc)$_4$ and the ee dropped to 28%. However, when Rh_2(TFA)$_4$ was used the yield increased to 96% and the ee also increased to 39%. It is well known that decreasing the

temperature of the reaction can increase the corresponding ee, therefore we lowered the temperature to 0 ºC and the ee increased to 42%. A further drop to -40 ºC increased the ee to 66%, however, conducting the reaction at -78 ºC was ineffective due to the inability of the diazocarbonyl to be decomposed.

Table 3.3. *Optimization of Asymmetric Transformation with 2-Tetralone Diazo*

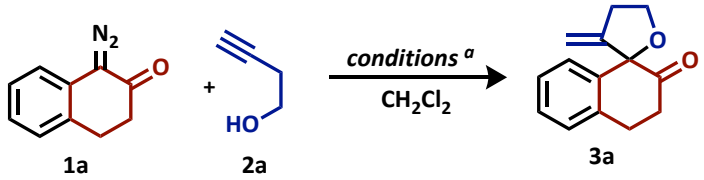

entry	Condition	time[b](temp)	%ee(yield%)
1	Rh_2(*S*-DOSP)$_4$/AgOTf/PPh_3AuCl	1hr addition(rt)	0 (65)
2	Rh_2(*S*-PTAD)$_4$/AgOTf/PPh_3AuCl	1hr addition(rt)	0 (63)
3	Rh_2(esp)$_2$/AgOTf/*R*-BINAP(AuCl)$_2$	1hr addition(rt)	33 (73)
4	Rh_2(OAc)$_4$/AgOTf/*R*-BINAP(AuCl)$_2$	1hr addition(rt)	28 (62)
5	Rh_2(TFA)$_4$/AgOTf/*R*-BINAP(AuCl)$_2$	1hr addition(rt)	39 (96)
6	Rh_2(TFA)$_4$/AgOTf/*R*-BINAP(AuCl)$_2$	1hr addition(0 ºC)	42 (95)
7	Rh_2(TFA)$_4$/AgOTf/*R*-BINAP(AuCl)$_2$	1hr addition(-40 ºC)	66 (96)
8	Rh_2(TFA)$_4$/AgOTf/*R*-BINAP(AuCl)$_2$	1hr addition(-78 ºC)	– [d]

[a]All optimization reactions were performed in 0.1 M CH_2Cl_2 with **1b** (1.20 equiv.), **2a** (1 equiv.), Rh_2L_4 (1 mol%), and Lewis acids (10 mol%) along with 4 Å molecular sieves; [b]time required for the complete consumption of **1a**; [c]TFA = trifluoroacetate; [d]Diazo **1a** did not decompose at -78 ºC.

With these mechanistic insights we were able to propose a mechanism for this transformation (**Scheme 3.11**). When added in a stepwise fashion, Rh(II)/Au(I) work independently without exerting any synergistic effect on each other. Specifically, Rh(II) decomposes the diazocarbonyl compound to form a Rh(II)-carbene **5** that undergoes

oxygen insertion to provide a zwitterionic intermediate **6** which undergoes keto–enol tautomerism to provide a reactive, dually activated intermediate **7**. The reactive enol form enables the Conia-ene cyclization with the cyclic diazocarbonyl compound. The enol-intermediate also explains the lack of enantioinduction with chiral Rh(II) salts. The stereoselectivity of the Conia-ene cyclization is influenced by the steric bulk as well as the Au(I)-coordinated alkynol substrate, where the enol form approaches the Au(I)-activated alkyne from the opposite face of the steric bulk.

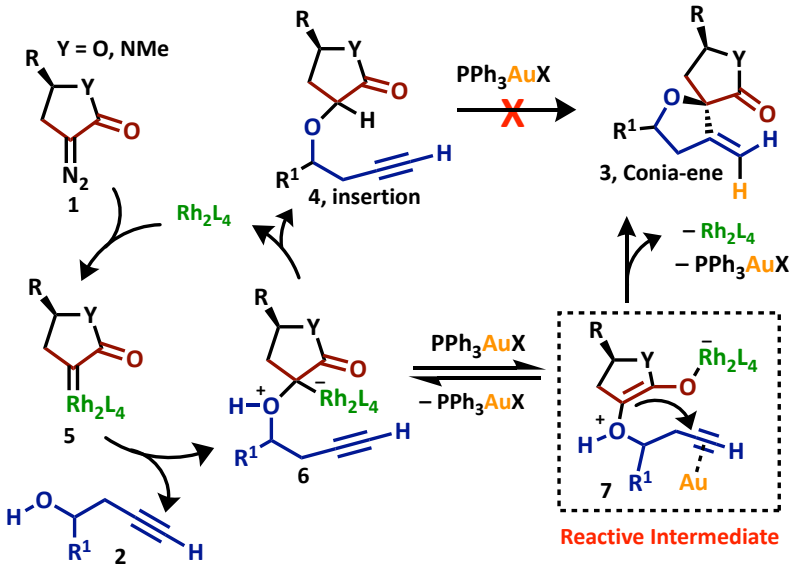

Scheme 3.11. *Probing stepwise transformation for validation of synergy*

The newly identified conditions for the synthesis of spiroethers are mild, selective, and provide a general and convergent route to diverse spiroethers. An important feature of this transformation is the high stereoselectivity and success of new Conia-ene cyclizations that are inaccessible using traditional mono-catalytic systems. The next goal

for our Rh(II)/Au(I) synergistic catalytic cocktail was its application to a corresponding N–H insertion/Conia-ene cascade to access various azaspiro-ring systems such as spiropyrollidines.

3.3 STEREOSELECTIVE TRAPPING OF Rh(II) CARBENES WITH Au(I) ACTIVATED AMINOALKYNES FOR THE SYNTHESIS OF SPIROPYROLLIDINES

As one has seen thus far, diazocarbonyl derived rhodium carbenes are versatile synthetic intermediates that offer sequential reactions with a nucleophile and electrophile. In continuation with our interest in accessing diverse spirocyclic scaffolds, we focused our efforts on the development of a synergistic cascade reaction that would provide direct access to five membered azaspiro heterocycles which are common structural motifs in bioactive natural products and pharmaceuticals. Inspired by our previous work[14], in which we efficiently trapped rhodium carbenes with a variety of Au(I)-activated alkynoic acids and alkynols, we envisioned trapping rhodium carbenes with aminoalkynes using the same Rh(II)/Au(I) catalytic cocktail.

3.3.1 INITIAL SCREENING OF CATALYTIC CONDITIONS

To initiate our study, aminoalkyne **5a** and 2-tetralone diazo **1a** were selected as model substrates. The addition of 2-tetralone diazo **1a** to aminoalkyne **5a** in the presence of our previously optimized $Rh_2(esp)_2$/PPh_3AuCl/$AgSbF_6$ catalyst cocktail in

dichloromethane at room temperature provided the major spiropyrollidine product **6a** in 75% conversion with an isolated 60% yield (**Table 3.4,** entry 1). Encouraged by the initial results of this cascade reaction, we examined the effect of different Lewis acids known for synthesizing *N*-heterocycles through alkyne cyclization.[15] We screened $ZnCl_2$, $In(OTf)_3$, PPh_3AuCl (alone), $AgSbF_6$ (alone) and no conversion to the desired spiro compound was observed (**Table 3.4,** entry 2–5). Next, we decided to examine the effect of different dirhodium carboxylates known to decompose diazocarbonyls. Surprisingly, a mixture of $Rh_2(OAc)_4/PPh_3AuSbF_6$ was completely ineffective and produced none of the desired

Table 3.4. *Optimization of N–H insertion/Conia-ene Cascade*

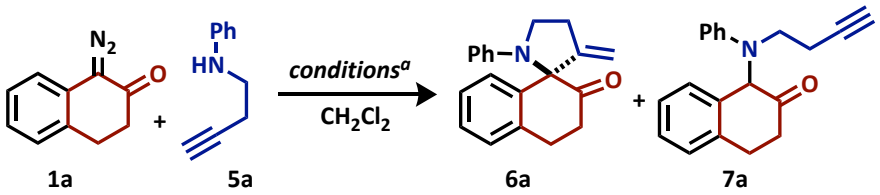

entry	Rh(II)	Lewis Acid	6a:7a
1	$Rh_2(esp)_2$	PPh_3AuSbF_6	75:25
2	$Rh_2(esp)_2$	$ZnCl_2$	0:100
3	$Rh_2(esp)_2$	$In(OTf)_3$	0:100
4	$Rh_2(esp)_2$	PPh_3AuCl	0:100
5	$Rh_2(esp)_2$	$AgSbF_6$	0:100
6	$Rh_2(OAc)_4$	PPh_3AuSbF_6	0:100
7	$Rh_2(TFA)_4$	PPh_3AuSbF_6	40:60

[a]All optimization reactions were performed by adding diazo **1a** (1 equiv.) dropwise via syringe to a solution of **5a** (1 equiv.), Rh_2L_4 (1 mol%), and Lewis acids (10 mol%) along with 4 Å molecular sieves in 0.3 M CH_2Cl_2.

spiropyrollidine (**Table 3.4,** entry 6). Subsequently we screened a mixture of $Rh_2(TFA)_4/PPh_3AuSbF_6$, which were the optimal conditions for the O–H insertion/Conia-ene cyclization of donor/acceptor cyclic diazocarbonyls, but only 40% conversion to the desired spiroether was observed (**Table 3.4,** entry 7).

3.3.2 APPLICATION TO SUBSTRATE SCOPE

With the optimized conditions in hand, we investigated the applicability of this cascade reaction to a wide variety of substrates (**Scheme 3.12**). The fused aromatic phenanthrenone diazocarbonyl also participated in the cascade under the optimized conditions to provide spiropyrollidine **6b** in a 62% yield. To demonstrate the utility of the transformation, it was necessary to identify a removable protecting group that would provide access to the free N–H spiropyrollidine, a functionality necessary for many ligand scaffolds. Using an aminoalkyne that was synthesized from *para*-anisidine, we were able to obtain the PMP (*para*-methoxy phenyl) protected spiropyrollidine **6c** in 65% yield. This substrate was then taken forward and exposed to CAN (ceric ammonium nitrate) to give the free spiropyrollidine **8** in 83% yield.

Next, we hoped to apply these conditions to the more stable acceptor/acceptor diazocarbonyls. To initiate these efforts, methyl-benzoylacetate diazocarbonyl was exposed to aminoalkyne **5a** in the presence of our optimized catalytic cocktail. At room temperature this electron deficient A/A diazocarbonyl did not decompose because of preferred complexation of $Rh_2(esp)_2$ with the Lewis-basic aminoalkyne. Due to the ineffectiveness of the catalyst at room temperature the reaction was refluxed in order to

initiate the desired transformation. However, **6d** was obtained in a very low yield because the aminoalkyne **5a** favored the 5-*endo*-dig self-cyclization when heated in the presence of PPh_3AuSbF_6. To optimize the yield of **6d**, the A/A diazocarbonyl was added to the aminoalkyne in the presence of $Rh_2(esp)_2$ alone in refluxing dichloromethane. After the desired insertion product was visualized via thin layer chromatography PPh_3AuCl and $AgSbF_6$ were added to the same reaction vial and provided **6d** in 92% yield. This modified protocol was also used to synthesize pyrollidine **6e** in 90% yield and **6f** in 94% yield.

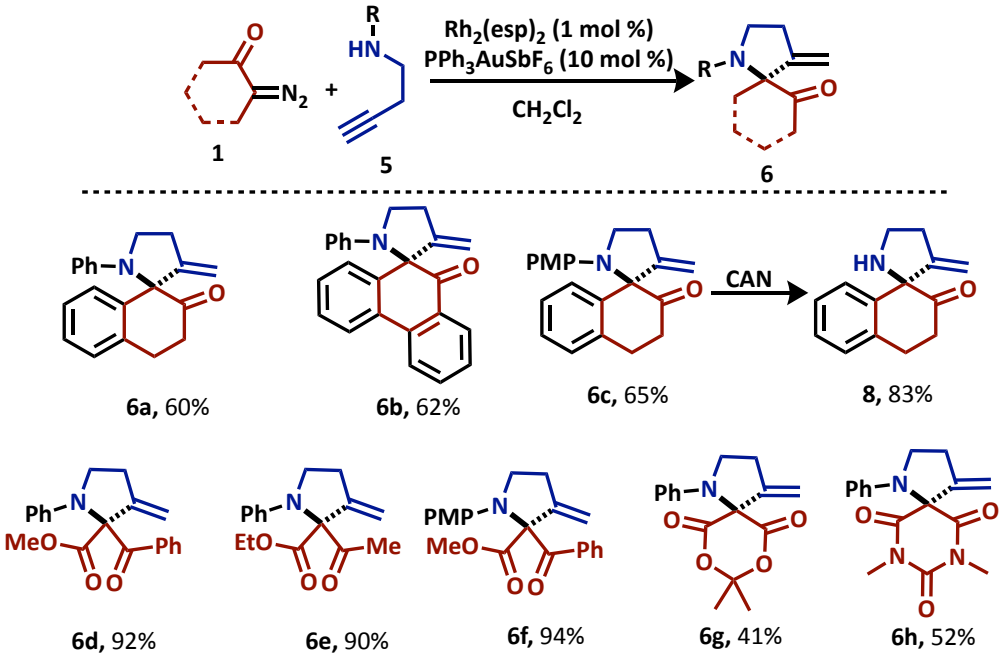

Scheme 3.12. *Substrate scope of $Rh_2(esp)_2/PPh_3AuSbF_6$ catalyzed N–H insertion/Conia-ene cascade reaction to access spiropyrollidines/pyrollidines*

As seen in the synthesis of spiroethers, A/A cyclic diazocarbonyls are extremely stable substrates and required modified conditions to obtain their corresponding

spiroether products. This observation persisted with the aminoalkynes, also. When attempting to extend the aforementioned modified protocol to A/A cyclic diazocarbonyls such as Meldrum's acid and barbituric acid diazos, it was observed that the stepwise Conia-ene reaction was unsuccessful. Therefore, to synthesize substrates **6g–6h**, the cyclic diazocarbonyl was added to the aminoalkyne and $Rh_2(esp)_2$/PPh_3AuSbF_6 then refluxed until complete. The method produced **6g** and **6h** in lower yields due to the competing self-cyclization of the aminoalkyne **5a**.

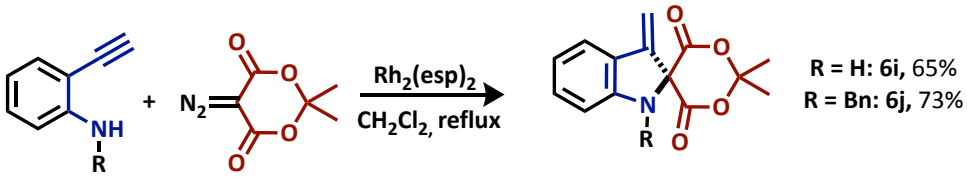

Scheme 3.13. *Applicaton of 2-ethynlaniline to access spiro-indoles*

Next, we desired to expand our system to accommodate other aminoalkynes. Easily accessible 2-ethynylaniline was synthesized and exposed to Meldrum's acid diazocarbonyl. In the presence of our catalytic cocktail the desired product **6i** was produced in a mediocre yield. However, the self-cyclization of 2-ethynylaniline under Au(I) catalysis cannot occur due to geometrical restraints. Therefore, the decreased yield in this transformation is presumable attributed to the thermal decomposition of the desired product in the presence of Lewis acids. Nevertheless, we hypothesized that aromatic constraint found within 2-ethynylaniline could facilitate the Conia-ene cyclization step with $Rh_2(esp)_2$ alone, exploiting the inherent reactivity of the zwitterionic intermediate. Our hypothesis was

proven correct and spiro-indoline **6i** was produced in 65% yield. The benzyl protected compound **6j** was also successfully synthesized using this modified method (**Scheme 3.13**).

3.3.3 MECHANISTIC INSIGHTS

To gain further insight into the mechanism of this transformation insertion products were synthesized with both the donor/acceptor 2-tetralone diazocarbonyl (**7a**) and the acceptor/acceptor methylbenzoylacetate diazocarbonyl (**7b**) using $Rh_2(esp)_2$ as a catalyst (**Scheme 3.14a**). When the insertion products were subjected to the Au(I)-catalyzed Conia-ene cyclization we did not observe any cyclization for the 2-tetralone insertion compound **7a** even after refluxing for 12 hours in dichloromethane. However, for the methylbenzoylacetate insertion product **7b**, cyclization occurred with equal efficiency as observed in our one pot, tandem cyclization protocol.

Next, we examined if non-terminal alkynes were tolerated in this transformation (**Scheme 3.14b**). When insertion product **7c** was exposed to PPh_3AuSbF_6 no cyclization occurred even after the reaction was refluxed for 12 hours. Lastly in an attempt to access piperidines, insertion product **7d** was synthesized and exposed to PPh_3AuSbF_6, however no cyclization occurred with this substrate either (**Scheme 3.14b**).

Given the results from the control experiments, we decided to probe the reaction mechanism using deuterium labeling experiments with 2-tetralone diazocarbonyl **1a** and methylbenzoylacetate diazocarbonyl **1c** (**Scheme 3.15**). When the deuterium labeling experiment was completed with 2-tetralone diazocarbonyl and the deuterated aminoalkyne, the desired product **3k** was obtained in 62% yield, proving there was no effect

of deuterium on the overall reaction efficiency. However, deuterium scrambling was observed with only 67% deuterium incorporation in the final product **3k**. This observation

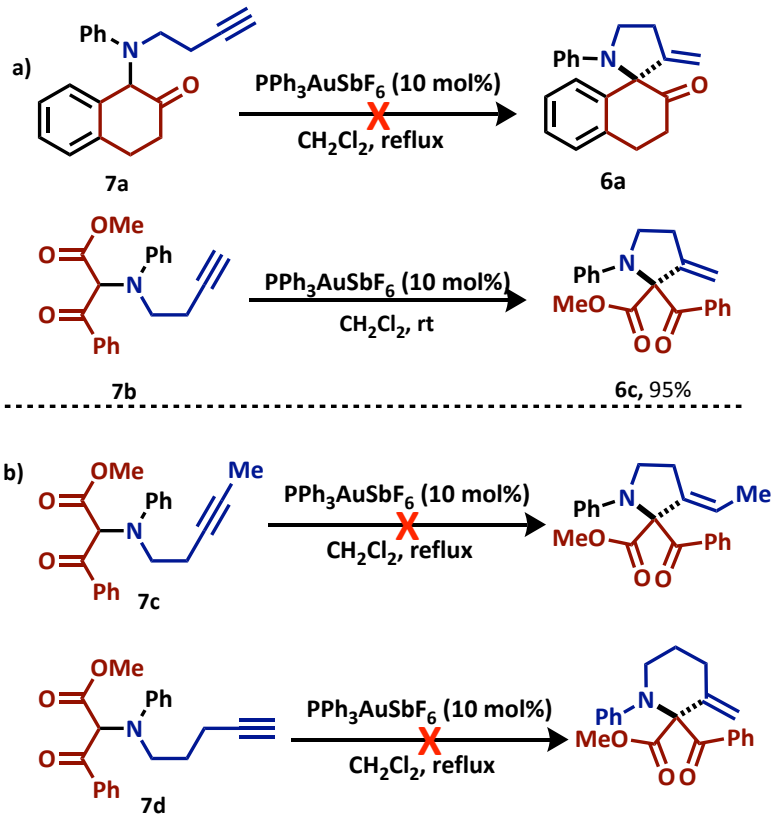

Scheme 3.14. *a) Insertion products exposed to Conia-ene cyclization conditions; b) Attempted cyclizations for non-terminal and 6-membered alkynes.*

was inconsistent with studies in our synthesis of spiroethers conducted earlier within this chapter and also studies completed by Toste et al. in their original identification of cationic Au(I) catalysis for Conia-ene cyclizations.[12b] When the experiment was conducted using diazocarbonyl **1c**, deuterium scrambling was also observed, although in a lessened manner with 80% deuterium incorporation in the final product **3l**. The results of these experiments

suggest the possibility of a Au(I)-acetylide as a reactive intermediate that is in equilibrium with an alkyne-π-complex with Au(I), and the equilibrium prefers the alkyne-π-complex with Au(I).

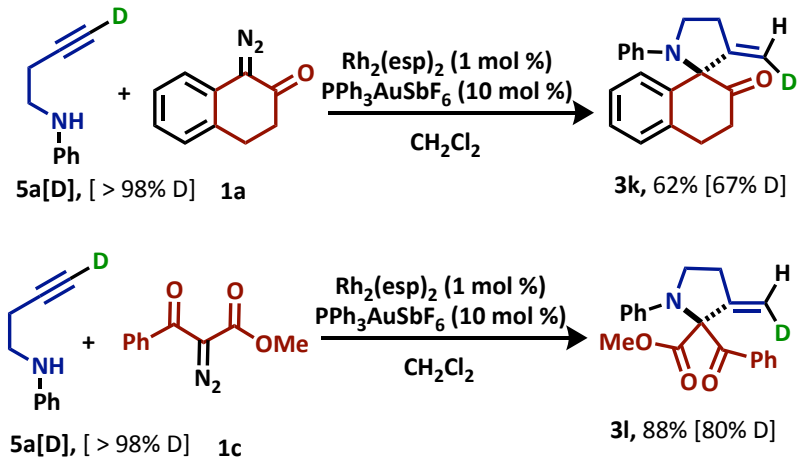

Scheme 3.15. *Deuterium labeling studies.*

These findings allow us to propose a reaction mechanism that is similar to the mechanism observed with spiroethers (**Scheme 3.16**). Specifically, Rh(II) decomposes the diazocarbonyls to form a Rh(II)-carbene **1** that undergoes nitrogen addition to provide a zwitterionic intermediate **9**, which proceeds to undergo keto–enol tautomerism to provide a reactive dually activated zwitterionic intermediate **11**. This active zwitterionic intermediate proceeds to undertake a Conia-ene cyclization with the diazocarbonyl compounds when in the presence of a Au(I)-activated alkyne. In the stepwise mechanism, the zwitterionic intermediate undergoes 1,2-proton transfer to provide the insertion product **7** and only when this insertion product is derived from an A/A diazo will a stepwise Conia-ene cyclization ensue in the presence of cationic Au(I).

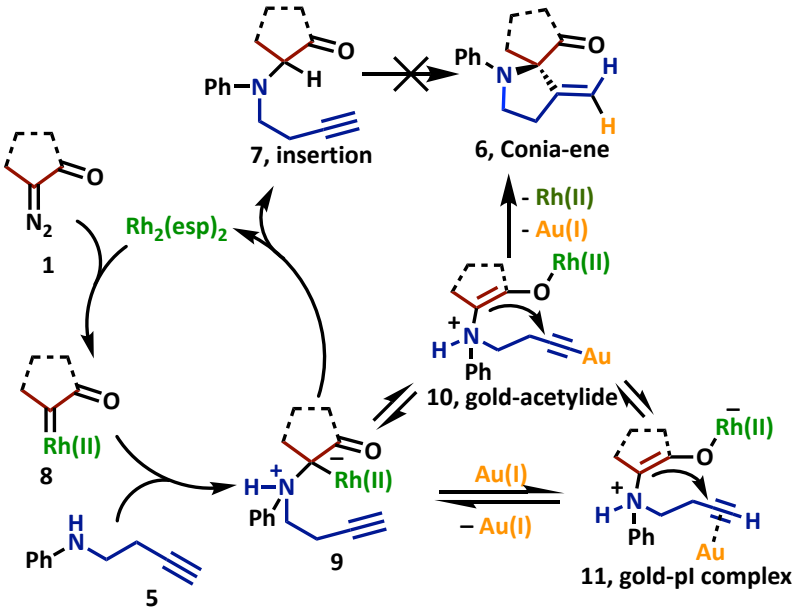

Scheme 3.16. *Plausible mechanism for the stepwise and synergistic Rh(II)/Au() catalyzed diazo N–H insertion/Conia-ene cascade.*

This new method for trapping rhodium carbenes with aminoalkynes is convergent in nature and uses readily available starting materials for the synthesis of a variety of *N*-heterocycles. An important feature of this transformation is its high chemo- and regio-selectivity. Upon completion of this work we were able to fulfill our goal of developing a general method to access azaspiro-ring systems using our Rh(II)/Au(I) synergistic catalytic cocktail.

3.4 STEPWISE ASYMMETRIC CONIA-ENE CYCLIZATION

A pronounced challenge during the development of the previously mentioned methodologies was their respective applications to an asymmetric transformation. During a literature survey it was realized that there were no reports of enantioselective Conia-ene

cyclizations for the synthess of tetrahydrofurans and pyrrolidines, although there have been several reports of enantioselective Conia-ene cyclizations for the synthesis of cyclopentanes.[16]

Due to the fact that the asymmetric Conia-ene cyclization has been employed in the synthesis of a variety of complex molecules[17], we believed the development of an asymmetric Conia-ene oxo- (to access tetrahydrofurans) and aza- (to access pyrrolidines) cyclization would be of great value to the chemical community, even if it could not be accessed through a derivative of our synergistic Rh(II)/Au(I) synergistic catalytic cocktail. Our synergistic cocktail is dependent on an expeditious activation of our corresponding reactive intermediates; consequentially, this method of reactivity is not conducive to an enantioselective transformation. Also, non-asymmetric Conia-ene cyclizations that are catalyzed by metal-based Lewis acids are efficient because they proceed through pure alkyne activation and when asymmetric variants of these known transformations were investigated, it was realized that a lack of enantioselectivity is achieved due to the poor transmission of ligand chirality as a consequence of the linear geometry of the alkyne-metal complex.[16c] Therefore, to induce adequate levels of enatioselectivity in the Conia-ene cyclization of carbonyl and dicarbonyl compounds, it is necessary to create a chiral enolate that would attack the alkyne.[16b]

3.4.1 OPTIMIZATION OF ASYMMETRIC CATALYTIC CONDITIONS

Although there are many non-enantioselective protocols for the Conia-ene carbo-cyclization which use a wide range of Lewis acid metal complexes, asymmetric methods are

scarce and typically rely on the activation of a metallic complex with a chiral ligand. The first report of a transformation of this kind came from Toste et al. in which they developed an asymmetric Pd(II) DTBM-SegPhos complex with $Yb(OTf)_3$ as a co-catalyst.[16c] Subsequently, a system using $La(OiPr)_3$/AgOAc and a peptide-based ligand was developed by Shibasaki et al.[16e] Next, Enders et al. identified a $AgNTf_2$/quinidine combination and a $(CuOTf)_2$-tol/cinchona complex that both enabled the enantioselective Conia-ene cyclization, respectively.[16b] Lastly White et al. obtained excellent results with their application of an iron-salene complex to achieve the desired transformation.[16a]

Table 3.5. *Optimizatin of Asymmetric Stepwise Conia-ene Cyclization*

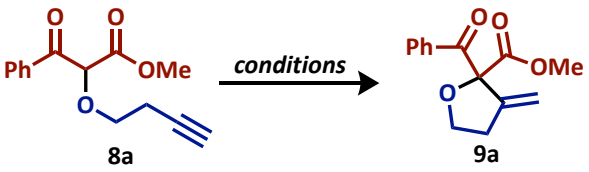

8a **9a**

entry	Lewis Acid/Chiral Ligand	solvent	Yield (% ee)
1	*R*-BINAP$(AuOTf)_2$	CH_2Cl_2	48 (24)
2	$(CuOTf)_2$-tol/cinchona ligand	CH_2Cl_2	76 (33)
3	*R*-DTBM-SegPhos[$Pd(OTf)_2$]	ether	95 (83)

All optimization reactions were performed by adding **8a** (1 equiv.) to a solution of the Lewis Acid (10 mol%) in 0.1 M of the appropriate solvent. The reaction was then stirred overnight until visualized as complete by thin layer chromatography.

Inspired by the reports in the literature, we set out determine the applicability of a select number of these systems with our insertion substrate **8a**, that was accessed through the $Rh_2(esp)_2$ catalyzed O–H insertion of 3-butynol into methylbenzoylacetate diazocarbonyl (**Table 3.5**). As a means of setting a proper basis for our initial studies, we

examined chiral Au(I) catalysis through the use of *R*-BINAP(AuOTf)$_2$. This chiral Au(I) complex gave us the desired cyclization in a 48% yield and a mediocre 24% ee (**Table 3.5**, entry 1). Next, we applied the (CuOTf)$_2$-tol/cinchona complex reported by Enders et al., these conditions increased the yield to 77% but the ee remained mediocre at 33% (**Table 3.5**, entry 2). Lastly, we applied the Pd(II) DTBM-SegPhos complex with Yb(OTf)$_3$ in ether that was developed by Toste et al. (**Table 3.5**, entry 3). This system provided great results with a 95% yield and 83% ee. When this system was applied to the corresponding N–H insertion product, the desired compound was isolated in a 64% yield and 81% ee (**Scheme 3.17**).

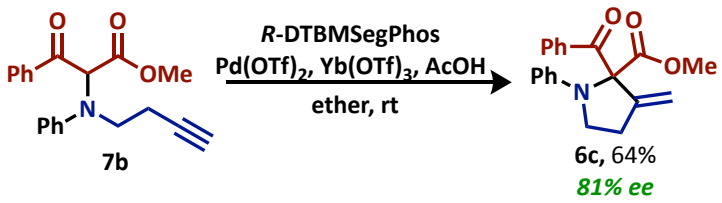

Scheme 3.17. *Asymmetric synthesis of pyrollidine* ***6c*** *using chiral Pd(II) catalysis.*

Excited by these results and the ability to induce ee in our system, we desired to design a new asymmetric catalytic system that was cheaper, easier to access, and was not known for any prior Conia-ene type cyclizations. Although Toste's conditions were effective they required a palladium complex that necessitated 5 synthetic steps to obtain. Inspired by the development of an asymmetric cross-dehydrogenative coupling reaction that was dependent on the formation of a chrial enolate and developed by the Schiedt group, we decided to investigate Cu(I) catalysis with readily available bisoxazoline (BOX) ligands that

Schiedt applied in their system.[18] BOX ligands are ideal ligands for asymmetric catalysis because they are accessed through a chiral amino acids, allowing them to be readily accessible.

Table 3.6. *Optimization of Cu(I)/BOX Ligand Catalyzed Conia-ene Cyclization*

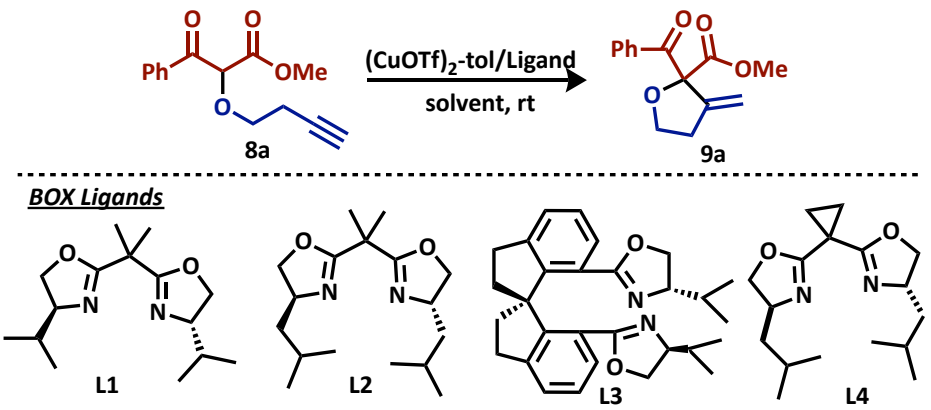

entry	BOX Ligand	solvent	Yield (% ee)
1	Ligand 1 (**L1**)	CH_2Cl_2	84 (47)
2	Ligand 2 (**L2**)	CH_2Cl_2	81 (83)
3	Ligand 3 (**L4**)	CH_2Cl_2	44 (34)
4	Ligand 4 (**L4**)	CH_2Cl_2	86 (91)
5	Ligand 4 (**L4**)	toluene	47 (28)
6	Ligand 4 (**L4**)	ether	25 (43)
7	Ligand 4 (**L4**)	$CHCl_3$	87 (93)

All optimization reactions were performed by adding **8a** (1 equiv.) to a solution of the $(CuOTf)_2$-tol (10 mol%) and Ligand (12 mol%) in 0.1 M of the appropriate solvent. The reaction was then stirred overnight until visualized as complete by thin layer chromatography.

To initiate our studies we synthesized a variety of BOX ligands using known synthetic protocols.[18-19] First, we complexed ligand **L1** with $(CuOTf)_2$-tol in dicholoromethane and allowed that solution to stir for 15 minutes before adding our

insertion compound **8a**. After stirring overnight, the desired compound **9a** was obtained in 87% yield but only 47% ee. Next, we used the same conditions with ligand **L2** that has more steric bulk, this ligand increased the ee to 83%. Inspired by previous works showing the impeccable stereo-induction of spiro-BOX ligands such as **L3**[19b, 19c], we applied this ligand to our system. However, the reaction was extremely sluggish and provided the desired product in a mediocre 34% ee. Lastly, we were curious about the impact of a cyclopropane backbone on our optimal ligand. The inclusion of this scaffold would decrease the "bite-angle" of our catalyst/ligand complex and thereby increase the steric crowding of the system. Gratifyingly, when ligand **L4** was applied in our system the ee increased to 91%. Next, we screened the effect of different solvents and chloroform increased the ee to 93%. When this system was applied to the corresponding N–H insertion product **7b**, the desired compound was isolated in 81% yield and 94% ee (**Scheme 3.18)**.

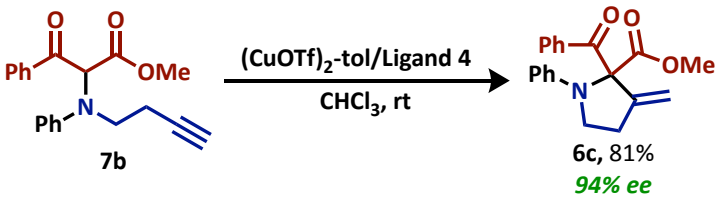

Scheme 3.18. *Asymmetric synthesis of pyrollidine* ***6c*** *using chiral Cu(I) catalysis.*

In conclusion, we have identified a $(CuOTf)_2$/BOX ligand complex that effectively induces asymmetry in the Conia-ene oxo- and aza-cyclizations to provide chiral tetrahydrofurans and pyrollidines. This catalytic system allows for the asymmetric installation of quaternary centers and generates an alkene that can be further manipulated

for valuable transformations. Further applications of this system will be reported in due course.

3.5 SUMMARY

After completion of the work within this chapter, we developed strategies to prepare spiroethers[14] and azaspiro-ring systems[20] from readily available starting materials and easily accessible diazocarbonyl compounds. Difficulties in preparing certain substrates led us to explore different catalytic conditions, temperatures, and reagent addition methods. Prompted by several mechanistic probing experiments, we were able to identify a differing mode of reactivity for O–H insertion/Conia-ene cyclizations as compared to N–H insertion/Conia-ene cyclizations. Enantioselective variants of this transformation were also explored. Results from the asymmetric experiments for the synthesis of spiroethers provided insight into the difficulty of inducing ee using chiral Rh(II) salts, however, the use of chiral Au(I) complexes provided preliminary ee data and valuable understanding of the transition state involved in this transformation. Due to our desire to synthesize chiral tetrahydrofurans and pyrrolidines, we were able to identify a Cu(I)/chiral bisoxazoline catalytic combination that enabled the stepwise enantioselective Conia-ene cyclization in ee's as high as 93%.

3.6 REFERENCES FOR CHAPTER 3

[1] **For insights into the importance of spiroethers and methods for their synthesis:** a) S. Aoki, Y. Watanabe, M. Sanagawa, A. Setiawan, N. Kotoku, M. Kobayashi, *J. Am. Chem. Soc.* **2006**, *128*, 3148–3149; b) P. Bloch, C. Tamm, *Helv. Chim. Acta* **1981**, *64*, 304–315; c) P. Bloch, C. Tamm, P. Bollinger, T. J. Petcher, H. P. Weber, *Helv. Chim. Acta* **1976**, *59*, 133–137; d) M. Entzeroth, A. J. Blackman, J. S. Mynderse, R. E. Moore, *J. Org. Chem.* **1985**, *50*, 1255–1259; e) Y. Hirasawa, H. Morita, M. Shiro, J. i. Kobayashi, *Org. Lett.* **2003**, *5*, 3991–3993; f) M. Ishikawa, T. Ninomiya, *J. Antibiot.* **2008**, *61*, 692–695; g) M. Ishikawa, T. Ninomiya, H. Akabane, N. Kushida, G. Tsujiuchi, M. Ohyama, S. Gomi, K. Shito, T. Murata, *Bioorg. Med. Chem. Lett.* **2009**, *19*, 1457–1460; h) I. A. Katsoulis, G. Kythreoti, A. Papakyriakou, K. Koltsida, P. Anastasopoulou, C. I. Stathakis, I. Mavridis, T. Cottin, E. Saridakis, D. Vourloumis, *Chem. Biochem.* **2011**, *12*, 1188–1192; i) F. A. Macias, J. L. G. Galindo, R. M. Varela, A. Torres, J. M. G. Molinillo, F. R. Fronczek, *Org. Lett.* **2006**, *8*, 4513–4516; j) S. Nozoe, M. Morisaki, K. Tsude, Y. Iitaka, N. Tokahashi, S. Tamura, K. Ishibashi, M. Shirasaka, *J. Am. Chem. Soc.* **1965**, *87*, 4968–4970.

[2] Z. W. Jiao, S. Y. Zhang, C. He, Y. Q. Tu, S. H. Wang, F. M. Zhang, Y. Q. Zhang, H. Li, *Angew. Chem. Int. Ed.* **2012**, *51*, 8811–8815.

[3] **For insights into the importance of azaspiro-ring systems:** a) X.-H. Ding, W.-C. Cui, X. Li, X. Ju, D. Liu, S. Wang, Z.-J. Yao, *Tetrahedron Lett.* **2013**, *54*, 1956–1959; b) J. M. Tian, Y. H. Yuan, Y. Q. Tu, F. M. Zhang, X. B. Zhang, S. H. Zhang, S. H. Wang, X. M. Zhang, *Chem. Commun.* **2015**, *51*, 9979–9982.

[4] D. Bourissou, O. Guerret, F. P. Gabbaï, G. Bertrand, *Chem. Rev.* **1999**, *100*, 39–91.

[5] a) A. C. Hunter, K. Chinthapally, I. Sharma, *Eur. J. Org. Chem.* **2016**, *2016*, 2260–2263; b) A. C. Hunter, S. C. Schlitzer, I. Sharma, *Chem. Eur. J.* **2016**, *22*, 16062–16065.

[6] **For insights into the importance of spiroxindoles:** a) Z. Y. Cao, X. Wang, C. Tan, X. L. Zhao, J. Zhou, K. Ding, *J. Am. Chem. Soc.* **2013**, *135*, 8197–8200; b) P. Drouhin, T. E. Hurst, A. C. Whitwood, R. J. Taylor, *Org. Lett.* **2014**, *16*, 4900–4903; c) C. V. Galliford, K. A. Scheidt, *Angew. Chem. Int. Ed. Engl.* **2007**, *46*, 8748–8758; d) C. Marti, Erick M. Carreira, *Eur. J. Org. Chem.* **2003**, *2003*, 2209–2219; e) W. Ren, X.-Y. Wang, J.-J. Li, M. Tian, J. Liu, L. Ouyang, J.-H. Wang, *RSC Adv.* **2017**, *7*, 1863–1868; f) J. W. Yang, X.Z.; Le Quesne, P.W.; Deschamps, J.R.; Cook, J.M., *J. Nat. Prod.* **2008**, *71*, 1431–1440.

[7] N. P. Massaro, J. C. Stevens, A. Chatterji, I. Sharma, *Org. Lett.* **2018,** 20, 7585–7589.

[8] **For insights into Au(I) activated intermediates:** a) H. Qiu, M. Li, L. Q. Jiang, F. P. Lv, L. Zan, C. W. Zhai, M. P. Doyle, W. H. Hu, *Nat. Chem.* **2012**, *4*, 733–738; b) D. Xing, W. Hu, *Tetrahedron Lett.* **2014**, *55*, 777–783; c) J.-B. Xi, M.-L. Ma, W. Hu, *Tetrahedron* **2016**, *72*, 579–583; d) Y. Zhang, Y. Yao, L. He, Y. Liu, L. Shi, *Adv. Synth. Catal.* **2017**, *359*, 2754–2761.

[9] **For insights into Rh(II) bound zwitterionic intermediates:** a) A. Padwa, *Chem. Soc. Rev.* **2009**, *38*, 3072–3081; b) X.-Y. Guan, L.-P. Yang, W. Hu, *Angew. Chem. Int. Ed.* **2010**, *49*, 2190–2192.

[10] a) M. J. L. Tschan, C. M. Thomas, H. Strub, J.-F. Carpentier, *Adv. Synth. Catal.* **2009**, *351*, 2496–2504; b) B. Bouguerne, P. Hoffmann, C. Lherbet, *Synth. Commun.* **2010**, *40*, 915–926.

[11] E. L. Armstrong, H. K. Grover, M. A. Kerr, *J. Org. Chem.* **2013**, *78*, 10534–10540.

[12] a) X.-Z. Shu, S. C. Nguyen, Y. He, F. Oba, Q. Zhang, C. Canlas, G. A. Somorjai, A. P. Alivisatos, F. D. Toste, *J. Am. Chem. Soc.* **2015**, *137*, 7083–7086; b) J. J. Kennedy-Smith, S. T. Staben, F. D. Toste, *J. Am. Chem. Soc.* **2004**, *126*, 4526–4527.

[13] a) A. S. K. P. Hashmi, M., *Chem. Rev.* **2007**, *107*, 3180–3211; b) A. S. K. W. Hashmi, J.P.; Frey, W.; Bats, J.W., *Org Lett* **2004**, *6*, 4391–4394; c) A. S. K. P. Hashmi, M., *J. Chem. Theory Comput.* **2009**, *5*, 2717–2725; d) J. Bucher, T. Wurm, K. S. Nalivela, M. Rudolph, F. Rominger, A. S. K. Hashmi, *Angew. Chem., Int. Ed.* **2014**, *53*, 3854–3858; e) M. M. Hansmann, F. Rominger, A. S. K. Hashmi, *Chem. Sci.* **2013**, *4*, 1552–1559.

[14] A. C. Hunter, S. C. Schlitzer, J. C. Stevens, B. Almutwalli, I. Sharma, *J. Org. Chem.* **2018**, *83*, 2744–2752.

[15] a) W. B. Hess, J.W., *Adv. Synth. Catal.* **2011**, *353*, 2966–2970; b) K. M. Takahashi, M.; Kawano, K.; Ishihara, J.; Hatakeyama, S., *Angew. Chem. Int. Ed. Engl.* **2008**, *47*, 6244–6246.

[16] a) S. Shaw, J. D. White, *J. Am. Chem. Soc.* **2014**, *136*, 13578–13581; b) M. Blumel, D. Hack, L. Ronkartz, C. Vermeeren, D. Enders, *Chem. Commun.* **2017**, *53*, 3956–3959; c) B. K. Corkey, F. D. Toste, *J. Am. Chem. Soc.* **2005**, *127*, 17168–17169; d) F. Sladojevich, A. L. Fuentes de Arriba, I. Ortin, T. Yang, A. Ferrali, R. S. Paton, D. J.

Dixon, *Chem. Eur. J.* **2013**, *19*, 14286–14295; e) A. Matsuzawa, T. Mashiko, N. Kumagai, M. Shibasaki, *Angew. Chem. Int. Ed. Engl.* **2011**, *50*, 7616–7619.

[17] a) K. Eto, M. Yoshino, K. Takahashi, J. Ishihara, S. Hatakeyama, *Org. Lett.* **2011**, *13*, 5398–5401; b) M. Yang, F. Yin, H. Fujino, S. A. Snyder, *J. Am. Chem. Soc.* **2019**; c) N. Huwyler, E. M. Carreira, *Angew. Chem. Int. Ed.* **2012**, *51*, 13066–13069.

[18] A. Lee, R. C. Betori, E. A. Crane, K. A. Scheidt, *J. Am. Chem. Soc.* **2018**, *140*, 6212–6216.

[19] a) W. D. Chu, L. Zhang, Z. Zhang, Q. Zhou, F. Mo, Y. Zhang, J. Wang, *J. Am. Chem. Soc.* **2016**, *138*, 14558–14561; b)S. F. Zhu, Y. Cai, H. X. Mao, J. H. Xie, Q. L. Zhou, *Nat. Chem.* **2010**, *2*, 546–551; c) B. Liu, S.-F. Zhu, L.-X. Wang, Q.-L. Zhou, *Tetrahedron: Asymmetry* **2006**, *17*, 634–641.

[20] A. C. Hunter, B. Almutwalli, A. I. Bain, I. Sharma, *Tetrahedron* **2018**, *74*, 5451–5457.

3.7 EXPERIMENTAL SECTION

3.7.1 GENERAL PRODCEDURE OF O–H INSERTION/CONIA ENE FOR A/D DIAZOS

In a 15 mL round bottom flask, powdered 4Å molecular sieves (100 mg/mmol of diazo) were activated via heat and cooled to room temperature under vacuum. $Rh_2(TFA)_4$ (1 mol%), AgOTf (5 mol%), and PPh_3AuCl (5 mol%) were added, and dissolved in a solution of dry dichloromethane (0.2M). The flask was sealed and cooled to 0 ºC in an ice water bath. In a separate 4 mL vial, alkynol (1 equiv.) and *N*-methylisatin diazo (1.2 equiv.) were dissolved together in dry dichloromethane (0.1M) and taken into a syringe. The diazo/alkynol solution was then added to the catalytic mixture dropwise via syringe pump at a rate of 1 mL/hr. Once addition was complete, the reaction was diluted with dichloromethane (20 mL) and quenched with a saturated solution of sodium bicarbonate. The aqueous layer was extracted, and combined organics were dried over sodium sulfate, filtered, and concentrated. Crude NMR was analyzed, and the mixture was purified by flash chromatography with the designated solvent system as listed below.

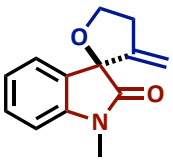

1'-methyl-3-methylene-4,5-dihydro-3*H*-spiro[furan-2,3'-indolin]-2'-one (3c). Prepared from 3-diazo-1-methylindolin-2-one and but-3-yn-1-ol using general procedure **G**. orange oil (30 mg, 79%). **TLC**: R_f 0.38 (20% EtOAc in hexanes). **IR** (NaCl): 3059.10, 2922.16, 2362.80, 2339.65, 1724.36, 1614.42. **^{1}H NMR** (400 MHz) δ 7.34 – 7.32 (td, *J* = 7.7, 1.3 Hz, 1H), 7.21 – 7.18 (dd, *J* = 7.5, 1.3 Hz, 1H), 7.09 – 7.05 (t, *J* = 7.5 Hz, 1H), 6.82 – 6.80 (d, *J* = 7.8

Hz, 1H), 5.11 – 5.10 (t, *J* = 2.2 Hz, 1H), 4.58 – 4.57 (t, *J* = 2.4 Hz, 1H), 4.53 – 4.49 (td, *J* = 8.1, 6.7 Hz, 1H), 4.28 – 4.23 (td, *J* = 7.9, 5.9 Hz, 1H), 3.16 (s, 3H), 3.13 – 3.07 (m, 1H), 2.93 – 2.85 (m, 1H). **^{13}C NMR** (101 MHz) δ 169.5, 149.4, 144.6, 129.9, 129.5, 125.3, 124.8, 123.2, 123.0, 108.6, 108.2, 68.1, 32.9, 26.2 **HRMS** (ESI) *m/z* calcd for $C_{13}H_{13}NO_2Na$ ([M+Na]$^+$) 238.0844; found 238.0835.

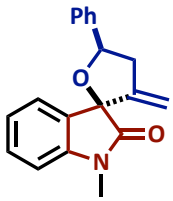

1'-methyl-3-methylene-5-phenyl-4,5-dihydro-3*H*-spiro[furan-2,3'-indolin]-2'-one (3d). Prepared from 3-diazo-1-methylindolin-2-one and 1-phenylbut-3-yn-1-ol using general procedure **G**. Orange oil (55 mg, 70%). **TLC**: R_f 0.59 (20% EtOAc in hexanes). **IR** (NaCl): 3062, 2953, 2926, 2854, 2594, 2358, 2341, 1728, 1614, 1558, 1494, 1571, 1373, 1255, 1097, 1026, 1004, 937, 777, 754, 698. **^{1}H NMR** (500 MHz) δ 7.67 – 7.66 (m, 1H), 7.42 – 7.35 (m, 2H), 7.13 – 7.10 (t, *J* = 7.5 Hz, 0H), 6.85 – 6.83 (d, *J* = 7.8 Hz, 1H), 5.33 – 5.30 (dd, *J* = 11.0, 5.3 Hz, 1H), 5.15 – 5.14 (d, *J* = 2.7 Hz, 1H), 4.58 – 4.57 (d, *J* = 2.9 Hz, 1H), 3.33 –3.27 (ddt, *J* = 14.2, 11.0, 2.9 Hz, 1H), 3.21 (s) 3.13 – 3.07 (dd, *J* = 14.7, 5.3 Hz, 1H). **^{13}C NMR** (126 MHz) δ 168.5, 145.6, 134.8, 129.9, 128.1, 126.9, 125.0, 123.2, 108.9, 108.1, 82.2, 42.5, 26.4. **LRMS** (ESI) *m/z* calcd for $C_{19}H_{17}NO_2Na$ ([M+Na]$^+$) 314.1157; found 314.1151.

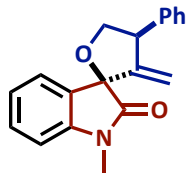

1'-methyl-3-methylene-4-phenyl-4,5-dihydro-3*H*-spiro[furan-2,3'-indolin]-2'-one (3e). Prepared from 3-diazo-1-methylindolin-2-one and 2-phenylbut-3-yn-1-ol using general procedure **G**. Orange oil (25 mg, 68%). **TLC**: R_f 0.41 (20% EtOAc in hexanes). **IR** (NaCl): 3057, 3028, 2920, 2893, 2850, 2360, 2343, 1722, 1614, 1492, 1469, 1369, 1348, 1246, 1095, 1039, 1018, 906, 754, 700. **^{1}H NMR** (500 MHz) δ 7.41 – 7.30 (m, 7H), 7.12 – 7.08 (td, *J* = 7.5, 1.0 Hz, 1H), 6.85 – 6.83 (dt, *J* = 7.7, 0.7 Hz, 1H), 4.87 – 4.84 (t, *J* = 8.4 Hz, 1H), 4.77 – 4.76 (d, *J* = 2.5 Hz, 1H), 4.66 – 4.65 (d, *J* = 2.8 Hz, 1H), 4.51 – 4.47 (tt, *J* = 8.2, 2.7 Hz, 1H), 4.27 – 4.25 (t, *J* = 8.1 Hz, 1H), 3.19 (s, 3H). **^{13}C NMR** (126 MHz) δ 167.2, 153.7, 144.6, 140.0, 130.1, 128.8, 128.6, 127.9, 127.1, 125.2, 123.3, 110.6, 108.3, 77.3, 75.4, 49.9, 26.3. **HRMS** (ESI) *m/z* calcd for $C_{19}H_{17}NO_2Na$ ([M+Na]$^+$) 314.1157; found 314.1152.

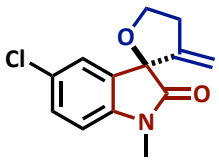

5'-chloro-1'-methyl-3-methylene-4,5-dihydro-3H-spiro[furan-2,3'-indolin]-2'-one (3f). Prepared from 5-chloro-3-diazo-1-methylindolin-2-one and 3-butyn-1-ol using general procedure **G**. Orange oil (27 mg, 90%). **TLC**: R_f 0.25 (30% EtOAc in hexanes). **IR** (NaCl): 2958,

2920, 2891, 2358, 2331, 1780, 1610, 1489, 1429, 1359, 1342, 1263, 1195, 1103, 1033, 981, 900, 812, 742. **^{1}H NMR** (500 MHz) δ 7.31 (dd, *J* = 8.3, 2.1 Hz, 1H), 7.19 (dd, *J* = 2.1, 0.4 Hz, 1H), 6.75 (d, *J* = 8.3 Hz, 1H), 5.15 (t, *J* = 2.2 Hz, 1H), 4.60 (t, *J* = 2.3 Hz, 1H), 4.51 (td, *J* = 8.1, 6.6 Hz, 1H), 4.26 (td, *J* = 7.9, 5.9 Hz, 1H), 3.16 (s, 3H), 3.11 (dddt, *J* = 15.5, 8.3, 6.0, 2.4 Hz, 1H), 2.89 (dddt, *J* = 15.4, 7.7, 6.6, 2.1 Hz, 1H).**^{13}C NMR** (126 MHz) δ 176.3, 148.9, 143.1, 134.2, 134.1, 131.1, 129.8, 129.3, 129.2, 128.5, 125.3, 109.2, 109.0, 68.4, 32.8, 26.3. **HRMS** (ESI) *m/z* calcd for $C_{13}H_{12}ClNNaO_2$ ($[M+Na]^+$) 272.0454; found .

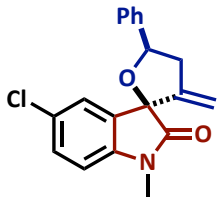

5'-chloro-1'-methyl-3-methylene-5-phenyl-4,5-dihydro-3*H*-spiro[furan-2,3'-indolin]-2'-one (3g). Prepared from 5-chloro-3-diazo-1-methylindolin-2-one and 1-phenylbut-3-yn-1-ol using general procedure **G**. Orange oil (18 mg, 66%). **TLC**: R_f 0.71 (30% EtOAc in hexanes). **IR** (NaCl): 3427.5, 3298.3, 3049.5, 2926.01, 2353.2, 1728.2, 1612.5. **^{1}H NMR** (500 MHz) δ 7.66 – 7.63 (m, 2H), 7.42 – 7.36 (m, 4H), 7.34 – 7.33 (p, *J* = 1.5 Hz, 3H), 6.78 – 6.76 (d, *J* = 8.2 Hz, 1H), 5.32 – 5.29 (dd, *J* = 11.0, 5.3 Hz, 1H), 5.18 – 5.17 (dd, *J* = 2.9, 1.1 Hz, 1H), 4.60 (dd, *J* = 3.0, 0.8 Hz, 1H), 3.32 – 3.25 (ddt, *J* = 14.1, 11.0, 2.9 Hz, 1H), 3.20 (s, 3H), 3.12 – 3.07 (ddt, *J* = 14.7, 5.4, 1.0 Hz, 1H). **^{13}C NMR** (126 MHz) δ 171.8, 149.1, 143.2, 140.6, 131.3, 129.9, 128.5, 128.3, 128.2, 128.0, 126.9, 125.7, 125.5, 109.9, 109.3, 109.2, 82.4, 72.3, 70.9, 42.4, 29.5, 26.5. **HRMS** (ESI) *m/z* calcd for $C_{19}H_{16}ClNO_2Na$ ($[M]^+$) 325.0870; found 326.0949.

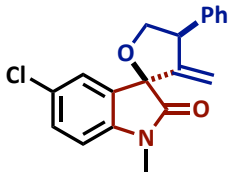

5'-chloro-1'-methyl-3-methylene-4-phenyl-4,5-dihydro-3*H*-spiro[furan-2,3'-indolin]-2'-one (3h). Prepared from 5-chloro-3-diazo-1-methylindolin-2-one and 2-phenylbut-3-yn-1-ol using general procedure **G**. Orange oil (14 mg, 60%). **TLC**: R_f 0.52 (20% EtOAc in hexanes). **IR** (NaCl): 2931.8, 2858.5, 2362.8, 2349.3, 1728.2. **^{1}H NMR** (500 MHz) δ 7.44 – 7.30 (m, 5H), 7.25 (d, *J* = 2.1 Hz, 1H), 6,80 – 6.78 (d, *J* = 8.3 Hz, 1H), 4.88 – 4.84 (t, *J* = 8.4 Hz, 1H), 4.80 – 4.79 (d, *J* = 2.5 Hz, 1H), 4.69 – 4.68 (d, *J* = 2.8 Hz, 1H), 4.52 – 4.49 (tt, *J* = 8.3, 2.7 Hz, 1H), 4.27 – 4.24 (t, *J* = 8.2 Hz, 1H), 3.19 (s, 3H). **^{13}C NMR** (126 MHz) δ 175.8, 153.2, 143.1, 139.4, 130.9, 130.0, 128.8, 128.6, 128.5, 127.2, 125.6, 110.9, 109.2, 75.5, 49.8, 29.7, 26.4. **HRMS** (ESI) *m/z* calcd for $C_{19}H_{16}ClNO_2Na$ ([M+Na]$^+$) 348.0767; found 348.0753.

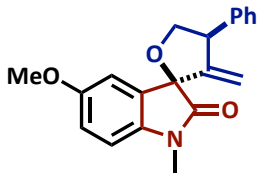

5'-methoxy-1'-methyl-3-methylene-4-phenyl-4,5-dihydro-3*H*-spiro[furan-2,3'-indolin]-2'-one (3i). Prepared from 3-diazo-5-methoxy-1-methylindolin-2-one and 2-phenylbut-3-yn-1-ol using general procedure **G**. Orange oil (5 mg, 63%). **TLC**: R_f 0.42 (20% EtOAc in hexanes). **IR** (NaCl): 3429.4, 3400.5, 2922.2, 2856.6, 2366.6, 2341.6, 1724.4. **^{1}H NMR** (500

MHz) δ 7.44 – 7.26 (m, 5H), 6.89 – 6.87 (m, 2H), 6.79 – 6.73 (m, 1H), 4.88 – 4.86 (t, *J* = 8.4 Hz, 1H), 4.79 – 4.78 (d, *J* = 2.5 Hz, 1H), 4.69 – 4.68 (d, *J* = 2.8 Hz, 1H), 4.52 – 4.48 (tt, *J* = 8.3, 2.7 Hz, 1H), 4.28 – 4.25 (t, *J* = 8.0 Hz, 1H), 3.81 (s, 3H), 3.18 (s, 2H). **^{13}C NMR** (126 MHz) δ 176.1, 156.4, 139.8, 134.0, 114.3, 112.3, 109.9, 108.6, 75.3, 65.8, 55.8, 49.8, 29.7, 26.3, 15.2. **HRMS** (ESI) *m/z* calcd for $C_{23}H_{19}NO_3Na$ ([M+Na]$^+$) 344.1263; found 344.1246.

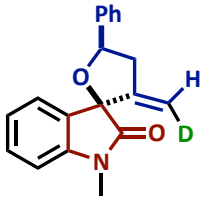

1'-methyl-3-(methylene-*d*)-5-phenyl-4,5-dihydro-3*H*-spiro[furan-2,3'-indolin]-2'-one (3p). Prepared from 3-diazo-1-methylindolin-2-one and 1-phenylbut-3-yn-4-*d*-1-ol using general procedure **H**. Orange oil (14 mg, 70%). **TLC**: R_f 0.59 (20% EtOAc in hexanes). **IR** (NaCl): 3057, 3028, 2924, 2981, 2854, 2358, 2339, 1722, 1614, 1558, 1539, 1494, 1469, 1369, 1346, 1240, 1093, 1035, 958, 848, 754, 698. **^{1}H NMR** (500 MHz) δ 7.67 – 7.66 (m, 1H), 7.42 – 7.35 (m, 2H), 7.13 – 7.10 (t, *J* = 7.5 Hz, 0H), 6.85 – 6.83 (d, *J* = 7.8 Hz, 1H), 5.33 – 5.30 (dd, *J* = 11.0, 5.3 Hz, 1H), 5.15 – 5.14 (d, *J* = 2.7 Hz, 1H), 4.58 – 4.57 (d, *J* = 2.9 Hz, 0.06 H), 3.33 –3.27 (ddt, *J* = 14.2, 11.0, 2.9 Hz, 1H), 3.21 (s) 3.13 – 3.07 (dd, *J* = 14.7, 5.3 Hz, 1H). **^{13}C NMR** (126 MHz) δ 168.5, 145.6, 134.8, 129.9, 128.1, 126.9, 125.0, 123.2, 108.9, 108.1, 82.2, 42.5, 26.4. **HRMS** (ESI) *m/z* calcd for $C_{19}H_{16}DNO_2Na$ ([M+Na]$^+$) 315.1220; found 314.1219.

3.7.2 GENERAL PRODCEDURE OF O–H INSERTION/CONIA ENE FOR A/A DIAZOS

To a 4.0 mL vial equipped with a magnetic stir bar was added powdered 4Å molecular sieves (70 mg/ mL solvent). The molecular sieves were activated via heat and allowed to cool to room temperature under vacuum. $Rh_2(esp)_2$ (1 mol %), $AuClPPh_3$ (10 mol %), and $AgSbF_6$ (10 mol %) were then measured directly into the reaction vessel. A solution of alkynol (1.2 equiv.) and diazo (1.0 equiv.) in dichloromethane (0.3M) was added, and the mixture was sonicated for 30 seconds. The reaction vessel was sealed, and heated to 60 ºC. The reaction was monitored by TLC until complete consumption of diazo was observed (between 30 minutes – 5 h). The crude reaction mixture was then cooled to room temperature, filtered through a pad of celite, concentrated, and analyzed via ^{1}H NMR. The crude mixture was then purified via flash chromatography to furnish spirocyclic compounds.

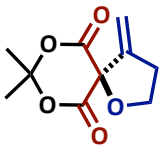

8,8-dimethyl-4-methylene-1,7,9-trioxaspiro[4.5]decane-6,10-dione (3j). Prepared from 5-diazo-2,2-dimethyl-1,3-dioxane-4,6-dione and but-3-yn-1-ol using general procedure **F** (Conversion of Diazo observed in 30 minutes). Clear oil (20 mg, 42%). **TLC**: R_f 0.6 (20% EtOAc in hexanes). **IR** (NaCl): 2957, 2918, 2850, 2359, 2340, 1732, 1714, 1633, 1608, 1558, 1539, 1489, 1456, 1384, 1211, 1097, 1010, 939. **^{1}H NMR** (500 MHz) δ 5.37 – 5.35 (q, *J* = 2.0

Hz, 1H), 5.27 – 5.26 (q, *J* = 2.1 Hz, 1H), 4.44 – 4.41 (t, *J* = 7.1 Hz, 2H), 2.92 – 2.89 (tt, *J* = 7.1, 2.2 Hz, 2H), 1.83 – 1.82 (d, *J* = 4.5 Hz, 6H). **^{13}C NMR** (126 MHz) δ 167.3, 149.5, 109.9, 106.0, 71.4, 32.6, 30.5, 27.3. **HRMS** (ESI) *m/z* calcd for $C_{10}H_{12}O_5Na$ ([M+Na]$^+$) 235.0582; found 235.0578.

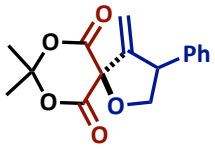

8,8-dimethyl-4-methylene-3-phenyl-1,7,9-trioxaspiro[4.5]decane-6,10-dione (3k). Prepared from 5-diazo-2,2-dimethyl-1,3-dioxane-4,6-dione and 2-phenylbut-3-yn-1-ol using general procedure **F** (Conversion of Diazo observed in 30 minutes). Clear oil (12 mg, 40%). **TLC**: R_f 0.75 (20% EtOAc in hexanes). **IR** (NaCl): 3004, 2980, 2918, 2950, 2359, 2341, 1791, 1761, 1683, 1558, 1494, 1394, 1292, 1199, 1118, 1029, 999, 914, 700. **^{1}H NMR** (500 MHz) δ 7.39 – 7.30 (m, 5H), 5.36 – 5.35 (ddd, *J* = 3.1, 1.9, 0.6 Hz, 1H), 4.96 – 4.95 (dd, *J* = 2.8, 1.9 Hz, 1H), 4.76 – 4.74 (td, *J* = 8.3, 0.5 Hz, 1H), 4.43 – 4.42 (dd, *J* = 10.4, 8.2 Hz, 1H), 4.27 – 4.22 (ddt, *J* = 10.6, 8.5, 2.9 Hz, 1H), 1.87 – 1.85 (m, 6H). **^{13}C NMR** (126 MHz) δ 167.6, 166.9, 154.2, 129.1, 128.9, 127.7, 111.4, 106.2, 78.2, 50.4, 30.6, 27.3. **HRMS** (ESI) *m/z* calcd for $C_{16}H_{16}O_5Na$ ([M+Na]$^+$) 311.0895; found 311.0894.

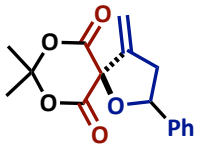

8,8-dimethyl-4-methylene-2-phenyl-1,7,9-trioxaspiro[4.5]decane-6,10-dione (3l). Prepared from 5-diazo-2,2-dimethyl-1,3-dioxane-4,6-dione and 1-phenylbut-3-yn-1-ol

using general procedure **F** (Conversion of Diazo observed in 30 minutes). Clear oil (24 mg, 32%). **TLC**: R_f 0.80 (20% EtOAc in hexanes). **IR** (NaCl): 3052, 2920, 2850, 2358, 2341, 1791, 1759, 1683, 1558, 1456, 1394, 1386, 1284, 1197, 1118, 1012, 916, 700. **^{1}H NMR** (500 MHz) δ 7.57 – 7.55 (m, 2H), 7.42 – 7.33 (m, 3H), 5.55 – 5.52 (dd, *J* = 10.5, 5.8 Hz, 1H), 5.38 – 5.37 (dt, *J* = 2.9, 1.5 Hz, 1H), 5.30 – 5.29 (dt, *J* = 3.1, 1.5 Hz, 1H), 3.18 – 3.13 (ddt, *J* = 15.5, 5.7, 1.4 Hz, 1H), 2.99 – 2.93 (ddt, *J* = 15.4, 10.5, 2.9 Hz, 1H), 1.85 – 1.83 (d, *J* = 9.9 Hz, 6H). **^{13}C NMR** (126 MHz) δ 167.8, 167.0, 149.5, 139.3, 128.6, 128.6, 126.7, 109.9, 109.9, 106.1, 84.6, 82.1, 41.5, 30.6, 27.4. **HRMS** (ESI) *m/z* calcd for $C_{16}H_{16}O_5Na$ ([M+Na]$^+$) 311.0895; found 311.0895.

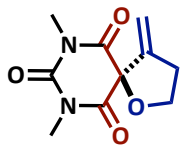

7,9-dimethyl-4-methylene-1-oxa-7,9-diazaspiro[4.5]decane-6,8,10-trione (3m). Prepared from 5-diazo-1,3-dimethylpyrimidine-2,4,6(1*H*,3*H*,5*H*)-trione and 3-butyn-1-ol using general procedure **F** (Conversion of Diazo observed in 40 minutes). cloudy oil (40 mg, 55%). **TLC**: R_f 0.43 (30% EtOAc in hexanes). **IR** (NaCl): 2858.5, 2358.9, 2339.7, 1670.6. **^{1}H NMR** (400 MHz) δ 5.25 – 5.24 (q, *J* = 2.1, 1.5 Hz, 1H), 5.00 – 4.99 (q, *J* = 2.2 Hz, 1H), 4.47 – 4.43 (td, *J* = 7.1, 1.2 Hz, 2H), 3.47 – 3.40 (d, *J* = 1.0 Hz, 6H), 2.86 – 2.81 (tdd, *J* = 6.9, 2.5, 1.6 Hz, 2H). **^{13}C NMR** (101 MHz) δ 168.1, 159.4, 155.0, 149.0, 108.3, 78.9, 70.9, 32.4, 31.5, 29.4, 29.2. **HRMS** (ESI) *m/z* calcd for $C_{16}H_{16}N_2O_4Na$ ([M+Na]$^+$) 247.0695; found 247.0698.

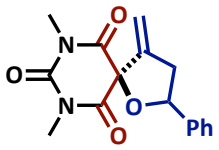

7,9-dimethyl-4-methylene-3-phenyl-1-oxa-7,9-diazaspiro[4.5]decane-6,8,10-trione (3n). Prepared from 5-diazo-1,3-dimethylpyrimidine-2,4,6(1*H*,3*H*,5*H*)-trione and 2-phenylbut-3-yn-1-ol using general procedure **F** (Conversion of Diazo observed in 40 minutes). Cloudy oil (75 mg, 62%). **TLC**: R_f 0.63 (30% EtOAc in hexanes). **IR** (NaCl): 3061, 3030, 2958, 2899, 2852, 2361, 2342, 1759, 1693, 1681, 1602, 1446, 1377, 1280, 1163, 1068, 908, 754 **^{1}H NMR** (500 MHz) δ 7.35– 7.17 (m, 5H), 5.11 – 5.10 (ddd, *J* = 2.9, 2.1, 0.5 Hz, 1H), 4.85 – 4.84 (dd, *J* = 2.8, 2.1 Hz, 1H), 4.81 – 4.78 (t, *J* = 8.4 Hz, 1H), 4.51 – 4.47 (dd, *J* = 10.3, 8.2 Hz, 1H), 4.21 – 4.16 (m, 1H), 3.39 (s 3H), 3.37 (s 3H). **^{13}C NMR** (126 MHz) δ 168.5, 167.4, 153.8, 150.9, 137.1, 128.9, 128.9, 128.3, 127.6, 109.7, 84.2, 77.7, 72.6, 67.5, 50.2, 29.4, 29.1. **HRMS** (ESI) *m/z* calcd for $C_{16}H_{16}N_2O_4Na$ ([M+Na]$^+$) 323.1008; found 323.1013.

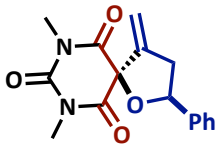

7,9-dimethyl-4-methylene-2-phenyl-1-oxa-7,9-diazaspiro[4.5]decane-6,8,10-trione (3o). Prepared from 5-diazo-1,3-dimethylpyrimidine-2,4,6(1H,3H,5H)-trione and (S)-1-phenylbut-3-yn-1-ol using general procedure **F** (Conversion of Diazo observed in 1 hour). Faint yellow oil (21 mg, 60%). $[\alpha]^{21}_D$ –2.4 (c = 0.005, $CHCl_3$). **TLC :** R_f 0.73 (50% Ethyl acetate in hexanes). **IR (NaCl):** 3056, 2920, 2850, 2360, 2330, 1732, 1693, 1681, 1558, 1435, 1375, 1281, 1068, 985, 754, 700. **^{1}H NMR** (500 MHz) δ 7.65 – 7.61 (m, 2H), 7.42 – 7.31 (m, 3H), 5.57 (dd, *J* = 10.5, 5.7 Hz, 1H), 5.26 (m, 1H), 5.02 (m, 1H), 3.38 (d, *J* = 2.7 Hz, 6H), 3.12 – 3.05

(m, 1H), 2.88 (ddt, *J* = 15.4, 10.5, 2.9 Hz, 1H). **^{13}C NMR** (126 MHz) δ 168.7, 149.3, 139.9, 128.6, 128.4, 126.6, 108.3, 83.9, 41.5, 29.4, 29.2. **HRMS** (ESI) m/z calcd for $C_{16}H_{16}N_2O_4Na$ ($[M+Na]^+$) 323.1008; found 323.1014.

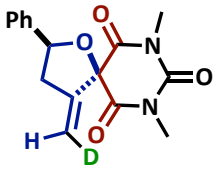

7,9-dimethyl-4-methylene-2-phenyl-1-oxa-7,9-diazaspiro[4.5]decane-6,8,10-trione (3q). Prepared from 5-diazo-1,3-dimethylpyrimidine-2,4,6(1H,3H,5H)-trione and (R)-1-phenylbut-3-yn-1-ol using general procedure **F** (Conversion of Diazo observed in 1 hour). Faint yellow oil (22 mg, 61%). $[\alpha]^{21}_D$ –2.3 (c = 0.007, $CHCl_3$). **TLC :** R_f 0.73 (50% Ethyl acetate in hexanes). **IR (NaCl):** 3042, 2956, 2922, 2852, 2358, 2339, 1693, 1579, 1454, 1438, 1375, 1280, 1134, 1068, 985, 754, 731, 700. **^{1}H NMR** (400 MHz) δ 7.63 (d, *J* = 7.4 Hz, 2H), 7.44 – 7.24 (m, 3H), 5.58 (d, *J* = 12.4 Hz, 1H), 5.26 (s, 1H), 5.03 (s, 1H), 3.38 (d, *J* = 2.2 Hz, 6H), 3.10 (dd, *J* = 15.3, 5.7 Hz, 1H), 2.94 – 2.83 (m, 1H). **^{13}C NMR** (126 MHz) δ 168.7, 167.7, 151.0, 149.3, 139.9, 128.6, 128.4, 128.3, 126.6, 108.3, 83.9, 41.5, 29.4, 29.2. **HRMS** (ESI) m/z calcd for $C_{16}H_{16}N_2O_4Na$ ($[M+Na]^+$) 323.1008; found 323.0992.

3.7.3 GENERAL PRODCEDURE FOR PYRROLIDINES 6a–6c, 6k

To a 4.0 mL vial equipped with a magnetic stir bar was added $Rh_2(esp)_2$ (1 mol %), PPh_3AuCl (10 mol %), and $AgSbF_6$ (10 mol %) directly into the reaction vessel. A solution of (but-3-yn-1-yl)-aniline (1.1 equiv.) was then added. Lastly, the diazo (1.0 equiv.) in dichloromethane (0.3M) was added. The reaction vessel was sealed, and allowed to stir at

room temperature until bubbling ceased and the diazo was consumed via TLC (approximately 30 minutes). Once the reaction was complete, the crude reaction mixture was filtered through a slurry of celite/silica gel, concentrated, and analyzed via crude ^{1}H NMR. The crude mixture was then purified via flash chromatography to furnish functionalized spiropyrrolidines**.**

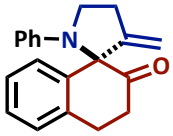

3'-methylene-1'-phenyl-3,4-dihydro-2H-spiro[naphthalene-1,2'-pyrrolidin]-2-one (6a). Prepared from 1-diazo-3,4-dihydronaphthalen-2(1H)-one and N-(but-3-yn-1-yl)aniline (Reaction time = 10 minutes) Yellow oil (32 mg, 60%). TLC : R_f 0.52 (20% ethyl acetate in hexanes). IR (NaCl): 3289, 3065, 2922, 2859, 2367, 2320, 1719. ^{1}H NMR (500 MHz, $CDCl_3$) δ 7.23 (td, J = 7.3, 1.5 Hz, 1H), 7.18 – 7.12 (m, 1H), 7.10 (dd, J = 7.9, 1.5 Hz, 1H), 7.06 – 6.99 (m, 2H), 6.59 (tt, J = 7.3, 1.0 Hz, 1H), 6.29 (dt, J = 7.8, 1.0 Hz, 2H), 5.15 (dd, J = 2.6, 1.3 Hz, 1H), 4.61 (dd, J = 2.9, 1.2 Hz, 1H), 3.95 – 3.85 (m, 2H), 3.49 – 3.16 (m, 4H), 3.03 – 2.88 (m, 1H), 2.84 – 2.75 (m, 1H), 2.74 – 2.62 (m, 1H). ^{13}C NMR (151 MHz, $CDCl_3$) δ 207.6, 152.9, 145.1, 140.0, 135.6, 128.6 (2C), 128.1, 127.8, 127.7, 127.3 (2C), 116.7, 113.7 (2C), 111.6, 49.02, 36.73, 29.89, 28.62. LRMS (ESI) m/z calcd for $C_{20}H_{19}NONa$ ($[M+Na]^+$) 312.13; found 312.14.

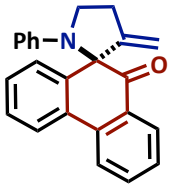

3'-methylene-1'-phenyl-10H-spiro[phenanthrene-9,2'-pyrrolidin]-10-one (6b). Prepared from 10-diazophenanthren-9(10H)-one and N-(but-3-yn-1-yl)aniline (Reaction time = 10 minutes). Yellow oil (33 mg, 62%). TLC : R_f 0.55 (20% ethyl acetate in hexanes). IR (NaCl): 3065, 3036, 2959, 2926, 2363, 2350, 1684. ^{1}H NMR (600 MHz, $CDCl_3$) δ 8.13 (d, J = 8.1 Hz, 1H), 8.10 – 8.05 (m, 2H), 7.73 (td, J = 7.7, 1.5 Hz, 1H), 7.46 – 7.40 (m, 1H), 7.37 (td, J = 8.0, 7.6, 1.4 Hz, 1H), 7.31 (dd, J = 7.9, 1.3 Hz, 1H), 7.23 (d, J = 7.0 Hz, 1H), 7.00 (dd, J = 8.5, 7.2 Hz, 2H), 6.61 – 6.53 (m, 1H), 6.26 (d, J = 8.1 Hz, 2H), 4.86 (t, J = 2.1 Hz, 1H), 4.54 (t, J = 2.1 Hz, 1H), 4.03 (td, J = 8.2, 6.8 Hz, 1H), 3.99 (td, J = 8.9, 4.9 Hz, 1H), 3.06 – 2.97 (m, 1H), 2.89 – 2.82 (m, 1H). ^{13}C NMR (151 MHz, $CDCl_3$) δ 197.1, 150.1, 145.2, 141.4, 137.4, 134.8 (2C), 129.9, 129.8, 128.7, 128.5 (2C), 128.2, 127.9, 127.0, 124.0, 123.1, 116.7, 114.4 (2C), 109.8, 76.6, 49.0, 29.5. LRMS (ESI) m/z calcd for $C_{24}H_{19}NONa$ ($[M+Na]^+$) 360.13; found 360.14.

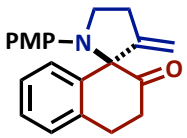

1'-(4-methoxyphenyl)-3'-methylene-3,4-dihydro-2H-spiro[naphthalene-1,2'-pyrrolidin]-2-one (6c). Prepared from 1-diazo-3,4-dihydronaphthalen-2(1H)-one and N-(but-3-yn-1-yl)-4-methoxyaniline (Reaction time = 10 minute). Yellow oil (70 mg, 65%). TLC : R_f 0.60 (30% ethyl acetate in hexanes). IR (NaCl): 2926, 2859, 2359, 2324, 2124, 1792, 1753. ^{1}H NMR (500 MHz, $CDCl_3$) δ 7.29 – 7.21 (m, 2H), 7.17 – 7.15 (m, 2H), 6.70 – 6.61 (m, 2H), 6.31

– 6.19 (m, 2H), 5.13 (dd, J = 2.6, 1.4 Hz, 1H), 4.60 (dd, J = 2.9, 1.3 Hz, 1H), 3.90 – 3.84 (m, 2H), 3.66 (s, 3H), 3.39 – 3.30 (m, 1H), 3.27 – 3.14 (m, 2H), 2.93 (dddt, J = 15.0, 10.1, 7.6, 2.7 Hz, 1H), 2.82 – 2.74 (m, 1H), 2.69 – 2.61 (m, 1H). ^{13}C NMR (126 MHz, $CDCl_3$) δ 208.4, 153.2, 151.3, 140.3, 139.8, 135.7, 128.3, 128.1, 128.0, 127.7, 127.3, 114.7 (2C), 114.4 (2C), 111.4, 55.6, 49.4, 37.1, 30.0, 28.6. LRMS (ESI) m/z calcd for $C_{21}H_{21}NO_2Na$ ([M+Na]$^+$]) 342.14; found 342.16.

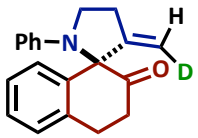

3'-(methylene-d)-1'-phenyl-3,4-dihydro-2H-spiro[naphthalene-1,2'-pyrrolidin]-2-one (6k). Prepared from 1-diazo-3,4-dihydronaphthalen-2(1H)-one and N-(but-3-yn-1-yl-4-d)aniline (Reaction time = 10 minutes). Faint yellow oil (43 mg, 67%). TLC: R_f 0.77 (30% ethyl acetate in hexanes). IR (NaCl): 3032, 2922, 2849, 1719, 1600. ^{1}H NMR (600 MHz, $CDCl_3$) δ 7.26 (t, J = 6.7 Hz, 1H), 7.21 (t, J = 7.4 Hz, 1H), 7.13 (t, J = 7.5 Hz, 1H), 7.08 (d, J = 7.9 Hz, 1H), 7.02 (t, J = 7.9 Hz, 2H), 6.58 (t, J = 7.3 Hz, 1H), 6.27 (d, J = 8.0 Hz, 2H), 5.15 – 5.10 (m, 1H), 4.59 (t, J = 1.8 Hz, 0.44H), 3.91 – 3.84 (m, 2H), 3.35 (dt, J = 13.8, 6.7 Hz, 1H), 3.29 – 3.15 (m, 2H), 2.97 – 2.87 (m, 1H), 2.76 (dt, J = 15.2, 5.6 Hz, 1H), 2.72 – 2.63 (m, 1H). ^{13}C NMR (151 MHz, $CDCl_3$) δ 207.6, 152.8, 152.7, 145.1, 140.0, 135.6, 135.6, 128.6, 128.3, 128.0, 127.7, 127.7, 127.4, 116.7, 113.7, 111.6, 111.37, 111.2, 49.4, 36.7, 29.9. LRMS (ESI) m/z calcd for $C_{21}H_{21}NONa$ ([M+Na]$^+$) 313.14; found 313.06.

3.7.4 GENERAL PRODCEDURE FOR PYRROLIDINES 6d–6f, 6l

To a 4.0 mL vial equipped with a magnetic stir bar was added $Rh_2(esp)_2$ (1 mol %) and a solution of (but-3-yn-1-yl)-aniline (1.1 equiv.). The diazo (1.0 equiv.) in dichloromethane (0.3M) was added and the reaction vessel was sealed, and allowed to stir at reflux until bubbling ceased and the diazo was consumed via TLC (approximately 5 minutes). Once the insertion product had formed PPh_3AuCl (10 mol %), and $AgSbF_6$ (10 mol %) were added directly into the reaction vessel and this solution was allowed to stir an additional 30 minutes until the insertion product was no longer visible on TLC and a new, more polar spot had formed (the cyclization product). Once the reaction was complete, the crude reaction mixture was filtered through a slurry of celite/silica gel, concentrated, and analyzed via crude ^{1}H NMR. The crude mixture was then purified via flash chromatography to furnish functionalized pyrrolidines

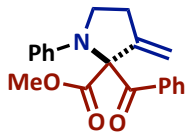

methyl-2-benzoyl-3-methylene-1-phenylpyrrolidine-2-carboxylate (6d). Prepared from methyl 2-diazo-3-oxo-3-phenylpropanoate and N-(but-3-yn-1-yl)aniline (Reaction time = 20 minutes). Yellow oil (54 mg, 92%). TLC : R_f 0.41 (20% ethyl acetate in hexanes). IR (NaCl): 3059, 2949, 2916, 2849, 2320, 1740, 1678. ^{1}H NMR (600 MHz, $CDCl_3$) δ 7.68 (dd, J = 8.4, 1.4 Hz, 2H), 7.35 (ddt, J = 8.8, 7.3, 1.3 Hz, 1H), 7.24 – 7.19 (m, 2H), 7.11 – 7.05 (m, 2H), 6.67 (td, J = 7.3, 1.0 Hz, 1H), 6.61 (dq, J = 7.3, 1.5, 1.0 Hz, 2H), 5.31 – 5.24 (m, 2H), 3.87 (dt, J = 8.9, 7.5 Hz, 1H), 3.73 (s, 3H), 3.64 (dt, J = 8.7, 7.2 Hz, 1H), 2.98 (tt, J = 7.3, 2.3 Hz, 2H). ^{13}C NMR

(151 MHz, $CDCl_3$) δ 197.2, 169.2, 146.4, 145.1, 136.0, 132.2, 128.8 (2C), 128.7 (2C), 127.9 (2C), 118.2, 113.7, 112.8, 80.3, 74.8, 52.7, 47.8, 30.0. LRMS (ESI) m/z calcd for $C_{20}H_{19}NO_3Na$ ($[M+Na]^+$) 344.12; found 344.15.

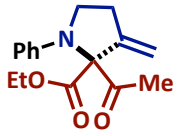

ethyl-2-acetyl-3-methylene-1-phenylpyrrolidine-2-carboxylate (6e). Prepared from ethyl 2-diazo-3-oxobutanoate and N-(but-3-yn-1-yl)aniline (Reaction time = 20 minutes). Faint yellow oil (50 mg, 90%). TLC : R_f 0.44 (20% ethyl acetate in hexanes). IR (NaCl): 2978, 2926, 2855, 2363, 2324, 1751, 1734, 1601. ^1H NMR (500 MHz, $CDCl_3$) δ 7.25 – 7.14 (m, 2H), 6.78 (tt, J = 7.3, 1.0 Hz, 1H), 6.56 (dt, J = 7.9, 1.0 Hz, 2H), 5.34 (td, J = 2.3, 0.7 Hz, 1H), 5.27 (td, J = 2.2, 0.7 Hz, 1H), 4.19 – 4.01 (m, 2H), 3.80 (ddd, J = 8.6, 7.3, 6.0 Hz, 1H), 3.64 (dt, J = 8.6, 7.5 Hz, 1H), 2.93 – 2.83 (m, 2H), 2.13 (s, 3H), 1.07 (t, J = 7.1 Hz, 3H). ^{13}C NMR (151 MHz, $CDCl_3$) δ 202.8, 168.5, 145.4, 129.1 (2C), 118.2, 113.2 (2C), 111.4, 80.3, 61.4, 48.1, 30.6, 26.1, 13.8. LRMS (ESI) m/z calcd for $C_{16}H_{19}NO_3Na$ ($[M+Na]^+$) 296.12; found 296.14.

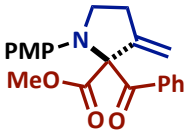

methyl-2-benzoyl-1-(4-methoxyphenyl)-3-methylenepyrrolidine-2-carboxylate (6f). Prepared from methyl 2-diazo-3-oxo-3-phenylpropanoate and N-(but-3-yn-1-yl)-4-methoxyaniline (Reaction time = 20 minutes). Vibrant yellow oil (80 mg, 94%). TLC: R_f 0.47 (30% ethyl acetate in hexanes). IR (NaCl): 2955, 2835, 1740, 1682. ^1H NMR (600 MHz, $CDCl_3$) δ 7.78 – 7.71 (m, 2H), 7.41 – 7.33 (m, 1H), 7.25 – 7.22 (m, 2H), 6.71 – 6.62 (m, 2H), 6.61 –

6.53 (m, 2H), 5.25 (qd, J = 2.3, 0.8 Hz, 2H), 3.82 (ddd, J = 8.7, 7.9, 6.2 Hz, 1H), 3.71 (s, 3H), 3.66 (s, 3H), 3.58 (td, J = 8.5, 6.6 Hz, 1H), 2.99 – 2.91 (m, 2H). ^{13}C NMR (151 MHz, $CDCl_3$) δ 197.3, 169.3, 152.3, 146.7, 139.3, 136.1, 132.2, 128.9 (2C), 127.9 (2C), 115.0 (2C), 114.3 (2C), 112.8, 80.8, 55.5, 52.6, 48.2, 30.1. LRMS (ESI) m/z calcd for $C_{21}H_{21}NO_4Na$ ($[M+Na]^+$) 374.13; found 374.52.

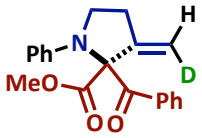

methyl-2-benzoyl-3-(methylene-d)-1-phenylpyrrolidine-2-carboxylate (6l). Prepared from methyl 2-diazo-3-oxo-3-phenylpropanoate and N-(but-3-yn-1-yl-4-d)aniline (Reaction time = 20 minutes). Yellow oil (50 mg, 95%). TLC: R_f 0.59 (30% ethyl acetate in hexanes). IR (NaCl): 3059, 2949, 2855, 2363, 1748, 1680. ^{1}H NMR (500 MHz, benzene d^6) δ 7.85 – 7.74 (m, 2H), 7.06 – 6.99 (m, 2H), 6.94 – 6.84 (m, 3H), 6.83 – 6.77 (m, 2H), 6.61 (ddt, *J* = 8.4, 7.4, 1.1 Hz, 1H), 5.34 (t, *J* = 2.2 Hz, 0H), 4.93 – 4.88 (m, 1H), 3.44 (dq, *J* = 11.4, 4.3, 2.4 Hz, 1H), 3.37 (s, 3H), 3.29 (td, *J* = 9.0, 5.3 Hz, 1H), 2.54 (ddt, *J* = 10.9, 8.6, 4.3 Hz, 1H), 2.46 – 2.36 (m, 1H). ^{13}C NMR (151 MHz, $CDCl_3$) δ 197.2, 169.2, 146.3, 145.1, 136.0, 132.2, 128.8, 128.7, 127.9, 118.2, 113.7, 112.7, 112.6, 112.4, 80.3, 53.4, 52.7, 47.8, 30.1, 30.0. LRMS (ESI) *m/z* calcd for $C_{20}H_{18}DNO_3Na$ ($[M+Na]^+$) 345.13; found 345.61.

3.7.5 GENERAL PRODCEDURE FOR PYRROLIDINES 6g–6h

To a 4.0 mL vial equipped with a magnetic stir bar was added $Rh_2(esp)_2$ (1 mol %), PPh_3AuCl (10 mol %), and $AgSbF_6$ (10 mol %) directly into the reaction vessel. A solution of (but-3-

yn-1-yl)-aniline (1.1 equiv.) was then added. Lastly, the diazo (1.0 equiv.) was added. The reaction vessel was sealed and allowed to stir at reflux for 16 hours. After this time, the crude reaction mixture was filtered through a slurry of celite/silica gel, concentrated, and analyzed via crude ^{1}H NMR. The crude mixture was then purified via flash chromatography to furnish functionalized spiropyrrolidines.

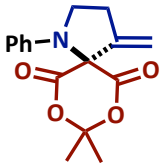

8,8-dimethyl-4-methylene-1-phenyl-7,9-dioxa-1-azaspiro[4.5]decane-6,10-dione (6g). Prepared from 5-diazo-2,2-dimethyl-1,3-dioxane-4,6-dione and N-(but-3-yn-1-yl)aniline (Reaction time = 16 hours). Yellow oil (24 mg, 41%). TLC : R_f 0.26 (20% ethyl acetate in hexanes). IR (NaCl): 2926, 2845, 2359, 2162, 1684. ^{1}H NMR (600 MHz, $CDCl_3$) δ 7.23 (d, J = 8.0 Hz, 2H), 6.85 (t, J = 7.3 Hz, 1H), 6.61 (d, J = 8.1 Hz, 2H), 5.37 (t, J = 2.1 Hz, 2H), 3.79 (t, J = 6.9 Hz, 2H), 2.96 (tt, J = 6.9, 2.0 Hz, 2H), 1.91 (s, 6H). ^{13}C NMR (151 MHz, $CDCl_3$) δ 165.6, 148.8, 144.3, 134.2, 132.0, 129.3, 129.2, 119.9, 114.6, 111.1, 107.1, 72.1, 48.8, 31.3, 30.5, 29.2. LRMS (ESI) m/z calcd for $C_{16}H_{17}NO_4Na$ ($[M+Na]^+$) 310.10; found 310.12.

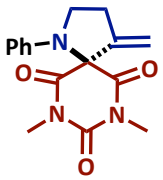

7,9-dimethyl-4-methylene-1-phenyl-1,7,9-triazaspiro[4.5]decane-6,8,10-trione (6h). Prepared from 5-diazo-1,3-dimethylpyrimidine-2,4,6(1H,3H,5H)-trione and N-(but-3-yn-1-yl)aniline (Reaction time = 16 hours). Yellow oil (33 mg, 52%) TLC : R_f 0.22 (20% ethyl

acetate in hexanes). ^{1}H NMR (600 MHz, $CDCl_3$) δ 7.19 (dd, J = 8.7, 7.4 Hz, 2H), 6.79 – 6.75 (m, 1H), 6.32 (dt, J = 7.7, 1.0 Hz, 2H), 5.20 (q, J = 2.1 Hz, 1H), 5.01 (q, J = 2.2 Hz, 1H), 3.86 (t, J = 7.0 Hz, 2H), 3.40 (s, 6H), 2.96 (tt, J = 6.9, 2.2 Hz, 2H). ^{13}C NMR (151 MHz, $CDCl_3$) δ 168.4 (2C), 149.3, 144.3, 129.5 (2C), 118.7 (2C), 112.9 (2C), 108.5, 90.0, 48.5, 31.0, 29.7, 29.5. LRMS (ESI) m/z calcd for $C_{16}H_{17}N_3O_3Na$ ([M+Na]$^+$); 322.11; found 322.12.

3.7.6 GENERAL PRODCEDURE FOR PYRROLIDINES 6i–6j

To a 4.0 mL vial equipped with a magnetic stir bar was added $Rh_2(esp)_2$ (1 mol %) directly into the reaction vessel. A solution of 2-ethynylaniline (1.1 equiv.) was then added. Lastly, the diazo (1.0 equiv.) was added. The reaction vessel was sealed and allowed to stir at reflux for 16 hours. After this time, the crude reaction mixture was filtered through a slurry of celite/silica gel, concentrated, and analyzed via crude ^{1}H NMR. The crude mixture was then purified via flash chromatography to furnish functionalized spiropyrrolidines

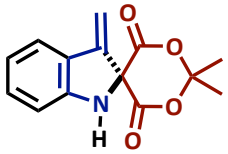

2',2'-dimethyl-3-methylenespiro[indoline-2,5'-[1,3]dioxane]-4',6'-dione (6i). prepared from 2,2-dimethyl-1,3-dioxane-4,6-dione and 2-ethynylaniline (Reaction time = 16 hours). Faint yellow oil (50 mg, 65%). TLC : R_f 0.14 (20% ethyl acetate in hexanes). IR (NaCl): 3327, 2922, 2855, 2363, 2324, 1790, 1740. ^{1}H NMR (600 MHz, $CDCl_3$) δ 7.35 – 7.32 (m, 1H), 7.25 – 7.22 (m, 1H), 6.91 (t, J = 7.3 Hz, 2H), 5.65 (d, J = 2.3 Hz, 1H), 5.37 (d, J = 2.4 Hz, 1H), 4.66

(s, 1H), 1.90 (s, 3H), 1.78 (s, 3H). ^{13}C NMR (126 MHz, $CDCl_3$) δ 166.7 (2C), 152.3, 147.8, 131.4 (2C), 123.5, 121.6, 112.8, 106.1, 104.2, 71.6, 31.1, 27.3. LRMS (ESI) m/z calcd for $C_{14}H_{13}NO_4Na$ ($[M+Na]^+$) 282.07; found 282.11.

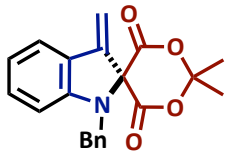

1-benzyl-2',2'-dimethyl-3-methylenespiro[indoline-2,5'-[1,3]dioxane]-4',6'-dione (6j). Prepared from 5-diazo-2,2-dimethyl-1,3-dioxane-4,6-dione and N-benzyl-2-ethynylaniline (Reaction time = 16 hours). Faint yellow oil (30 mg, 73%). TLC : R_f 0.38 (20% ethyl acetate in hexanes). IR (NaCl): 2926, 2855, 2359, 2324, 2124, 1792, 1753. ^{1}H NMR (600 MHz, $CDCl_3$) δ 7.55 – 7.51 (m, 2H), 7.37 – 7.33 (m, 2H), 7.29 (t, J = 6.7 Hz, 2H), 7.12 – 7.08 (m, 1H), 6.76 (td, J = 7.5, 0.9 Hz, 1H), 6.40 (d, J = 8.1 Hz, 1H), 5.62 (d, J = 2.3 Hz, 1H), 5.34 (d, J = 2.3 Hz, 1H), 4.47 (s, 2H), 1.85 (s, 3H), 1.52 (s, 3H). ^{13}C NMR (151 MHz, $CDCl_3$) δ 164.8 (2C), 153.5, 147.0, 136.2, 131.4, 128.7, 128.2 (2C), 127.8 (2C), 123.2, 121.2, 119.4, 109.0, 106.2, 103.4, 51.6, 31.1, 29.7, 28.0. LRMS (ESI) m/z calcd for $C_{21}H_{19}NO_4Na$ ($[M+Na^+]$) 372.12; found 372.13.

APPENDIX 2

Spectra Relevant to Chapter 3

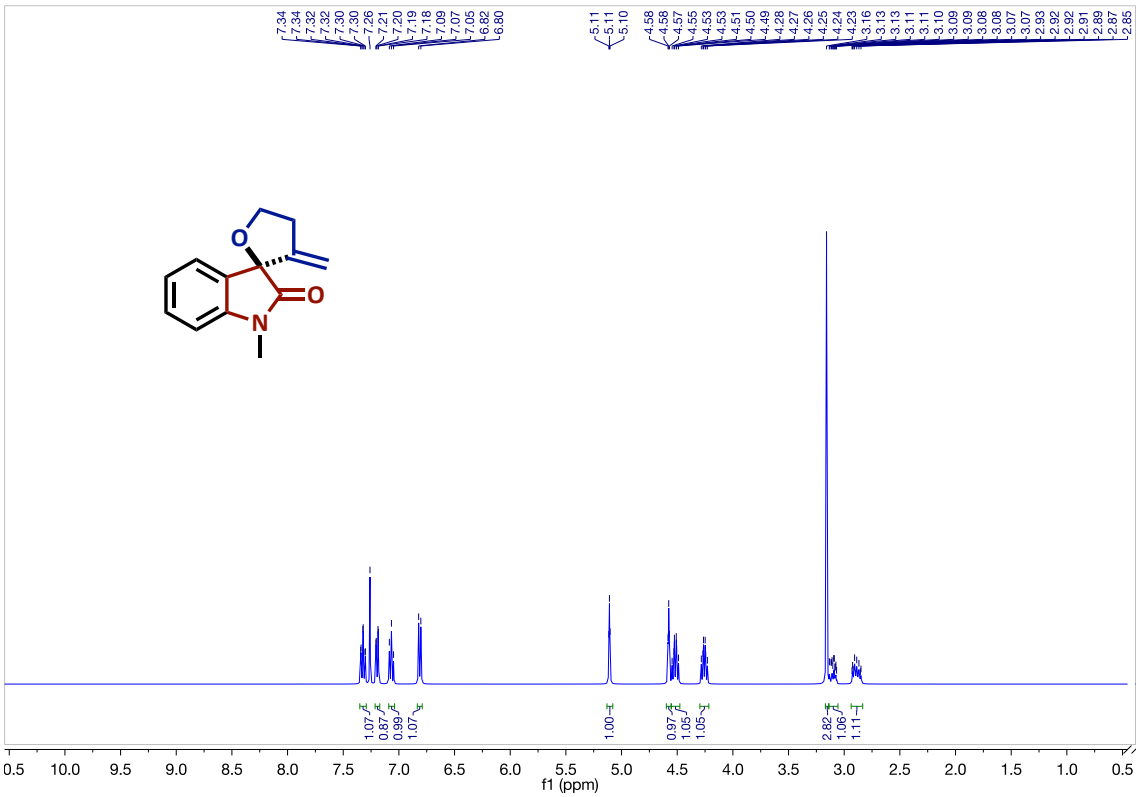
7.34
7.34
7.32
7.32
7.30
7.30
7.26
7.21
7.20
7.19
7.18
7.09
7.07
7.05
6.82
6.80
5.11
5.10
4.58
4.58
4.57
4.55
4.53
4.53
4.51
4.50
4.49
4.28
4.27
4.26
4.25
4.24
4.23
3.16
3.13
3.13
3.11
3.11
3.10
3.09
3.09
3.09
3.08
3.08
3.07
3.07
2.93
2.92
2.92
2.91
2.89
2.87
2.85
O
O
N
1.07
0.87
0.99
1.07
1.00
0.97
1.05
1.05
2.82
1.06
1.11
0.5 10.0 9.5 9.0 8.5 8.0 7.5 7.0 6.5 6.0 5.5 5.0 4.5 4.0 3.5 3.0 2.5 2.0 1.5 1.0 0.5
f1 (ppm)

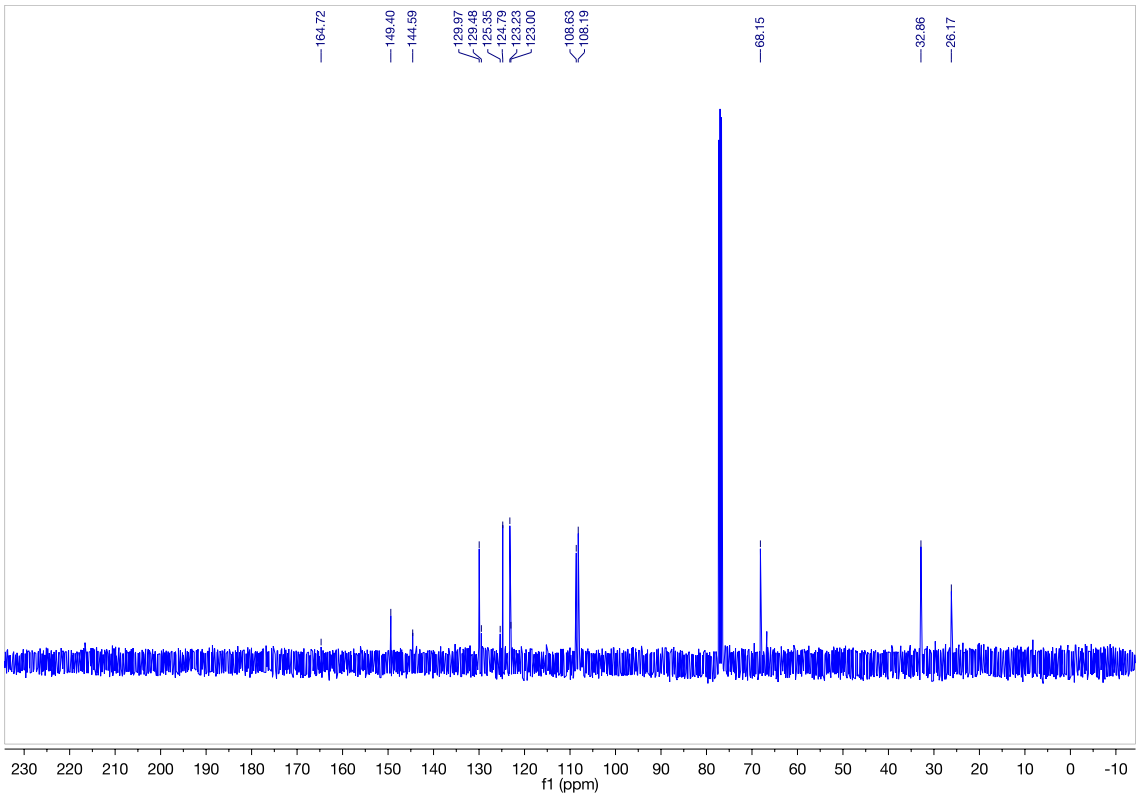
164.72
149.40
144.59
129.97
129.48
125.35
124.79
123.23
123.00
108.63
108.19
68.15
32.86
26.17
230 220 210 200 190 180 170 160 150 140 130 120 110 100 90 80 70 60 50 40 30 20 10 0 -10
f1 (ppm)

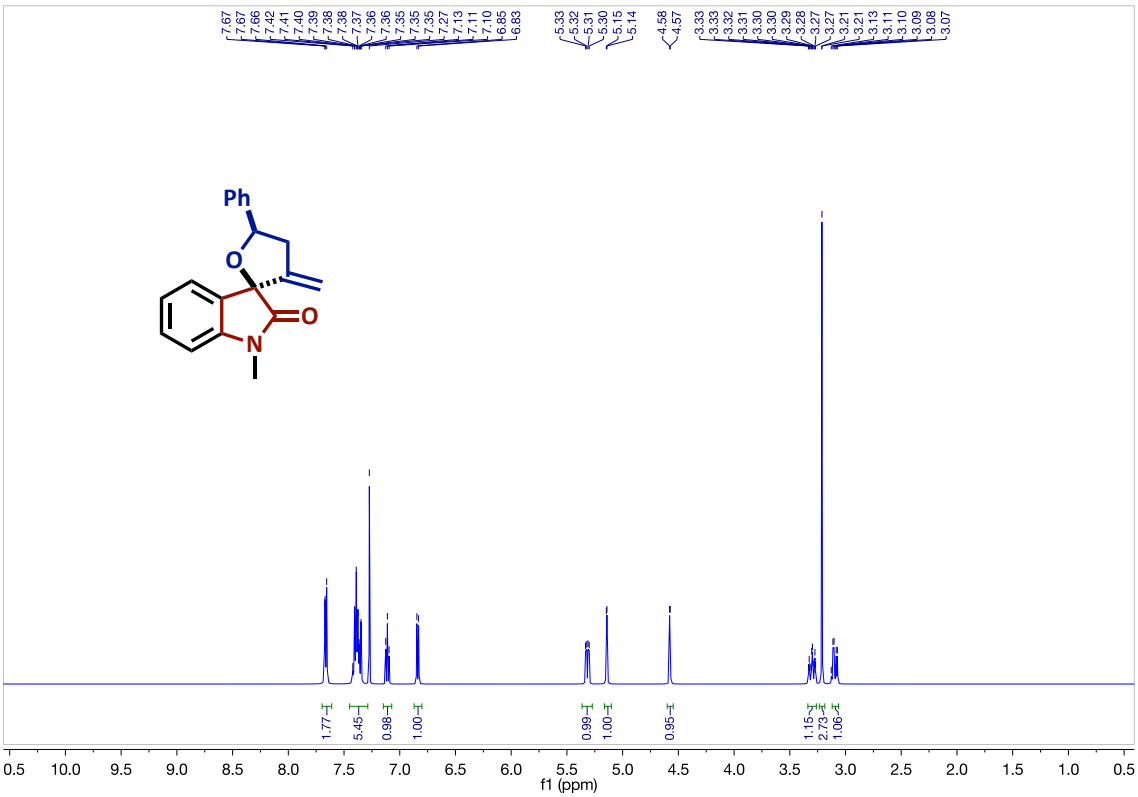
7.67
7.67
7.66
7.42
7.41
7.40
7.39
7.38
7.38
7.37
7.36
7.36
7.35
7.35
7.35
7.27
7.13
7.11
7.10
6.85
6.83
5.33
5.32
5.31
5.30
5.15
5.14
4.58
4.57
3.33
3.33
3.32
3.31
3.30
3.30
3.29
3.28
3.27
3.27
3.21
3.21
3.13
3.11
3.10
3.09
3.08
3.07
Ph
O
O
N
1.77
5.45
0.98
1.00
0.99
1.00
0.95
1.15
2.73
1.06
f1 (ppm)

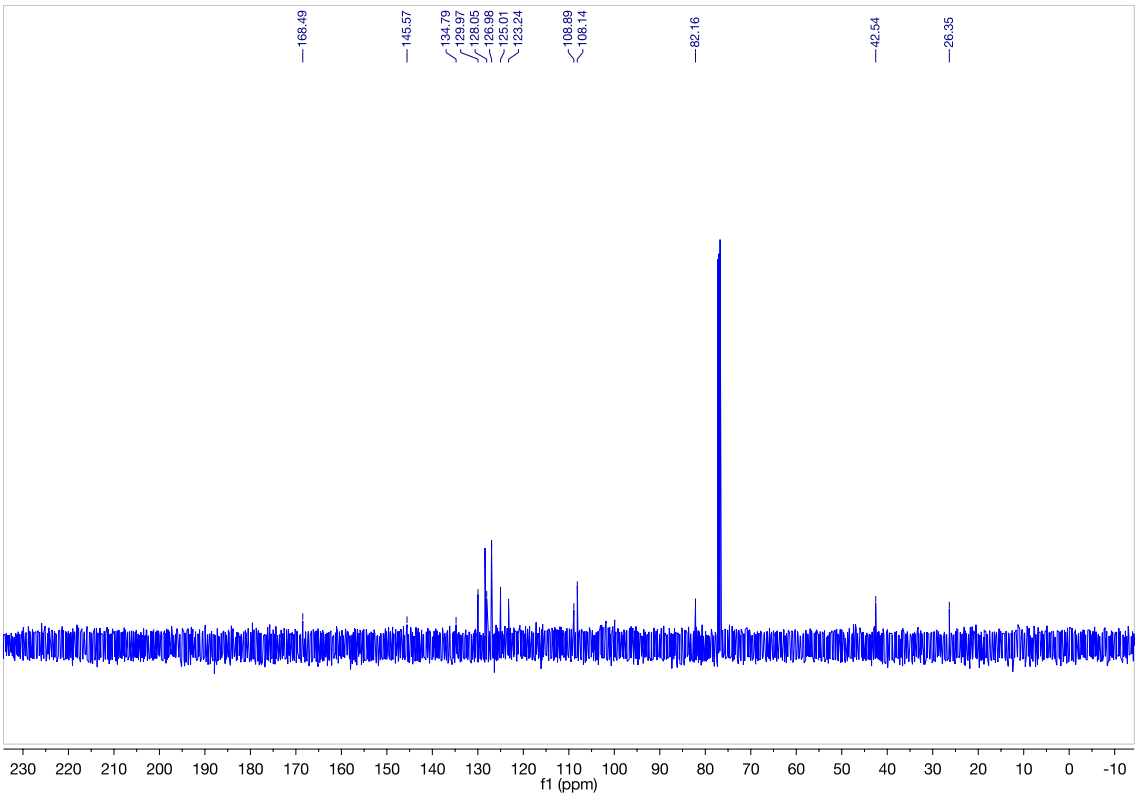
168.49
145.57
134.79
129.97
128.05
126.98
125.01
123.24
108.89
108.14
82.16
42.54
26.35
f1 (ppm)

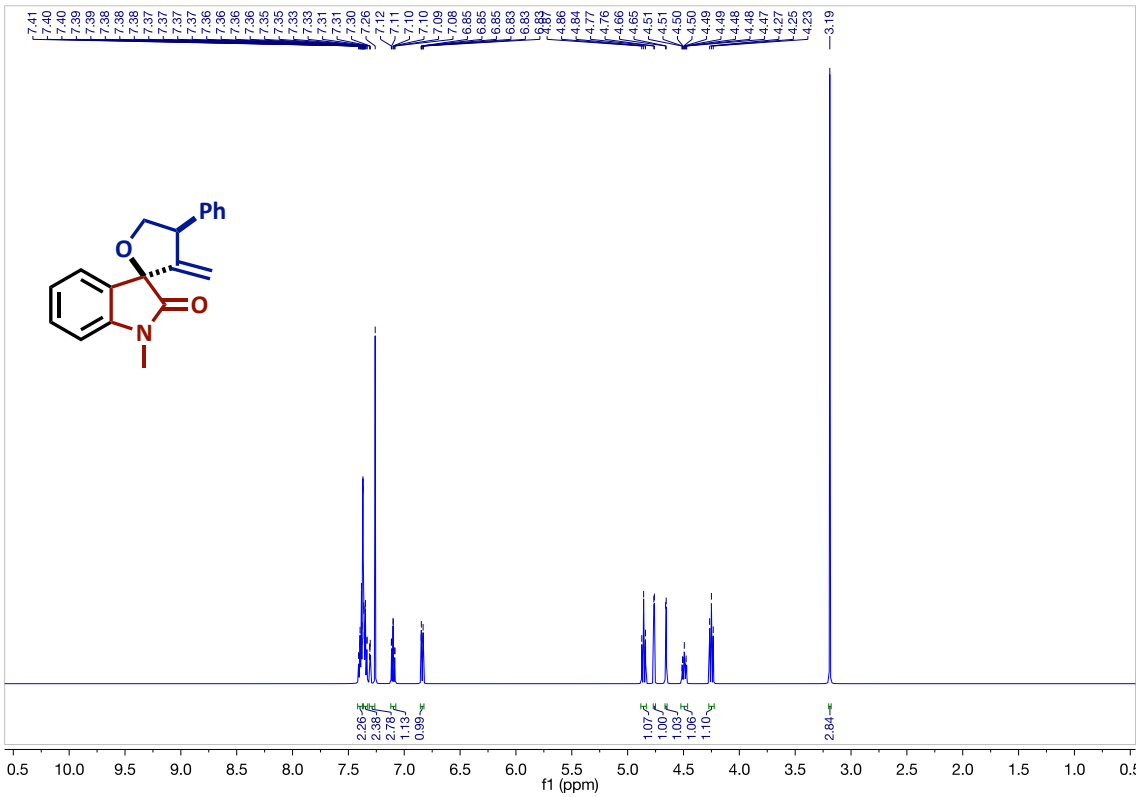
Ph
O
O
N
7.41 7.40 7.40 7.39 7.39 7.38 7.38 7.38 7.37 7.37 7.37 7.36 7.36 7.36 7.35 7.35 7.33 7.33 7.31 7.31 7.30 7.26 7.12 7.11 7.10 7.10 7.09 7.08 6.85 6.85 6.83 6.83 4.86 4.84 4.77 4.76 4.66 4.65 4.51 4.51 4.50 4.50 4.49 4.49 4.48 4.48 4.47 4.27 4.25 4.23 3.19
2.26 2.38 2.78 1.13 0.99 1.07 1.00 1.03 1.06 1.10 2.84
0.5 10.0 9.5 9.0 8.5 8.0 7.5 7.0 6.5 6.0 5.5 5.0 4.5 4.0 3.5 3.0 2.5 2.0 1.5 1.0
f1 (ppm)

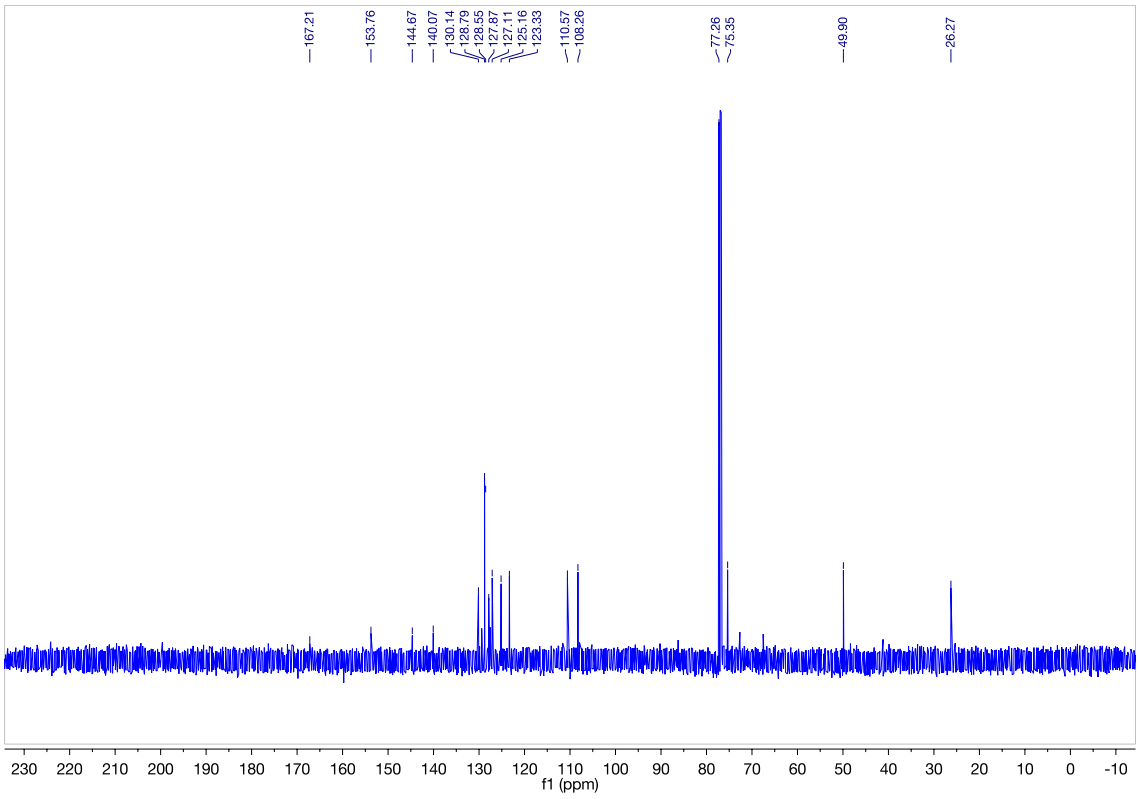
167.21 153.76 144.67 140.07 130.14 128.79 128.55 127.87 127.11 125.16 123.33 110.57 108.26 77.26 75.35 49.90 26.27
230 220 210 200 190 180 170 160 150 140 130 120 110 100 90 80 70 60 50 40 30 20 10 0 -10
f1 (ppm)

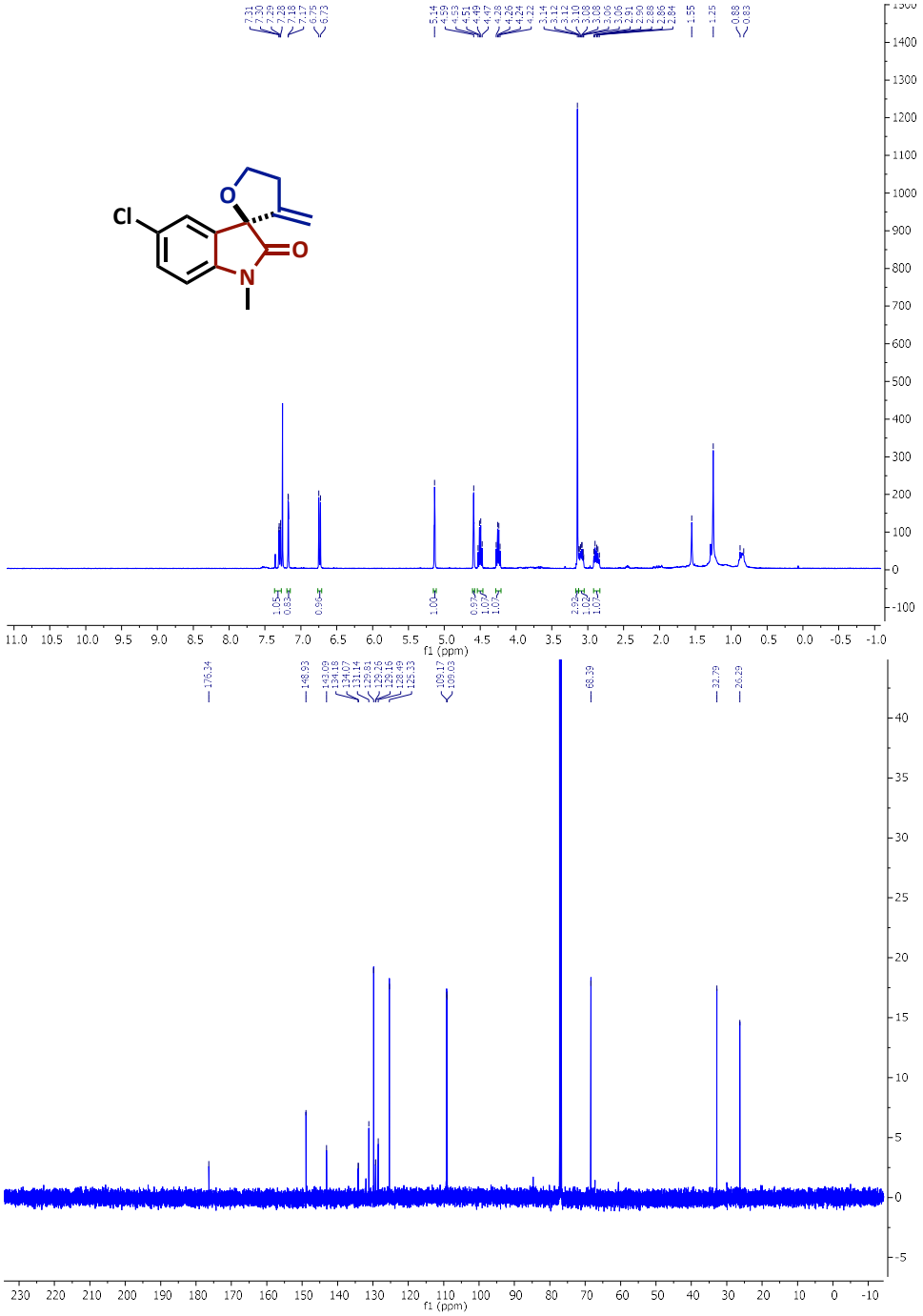
Cl
O
O
N
f1 (ppm)
f1 (ppm)

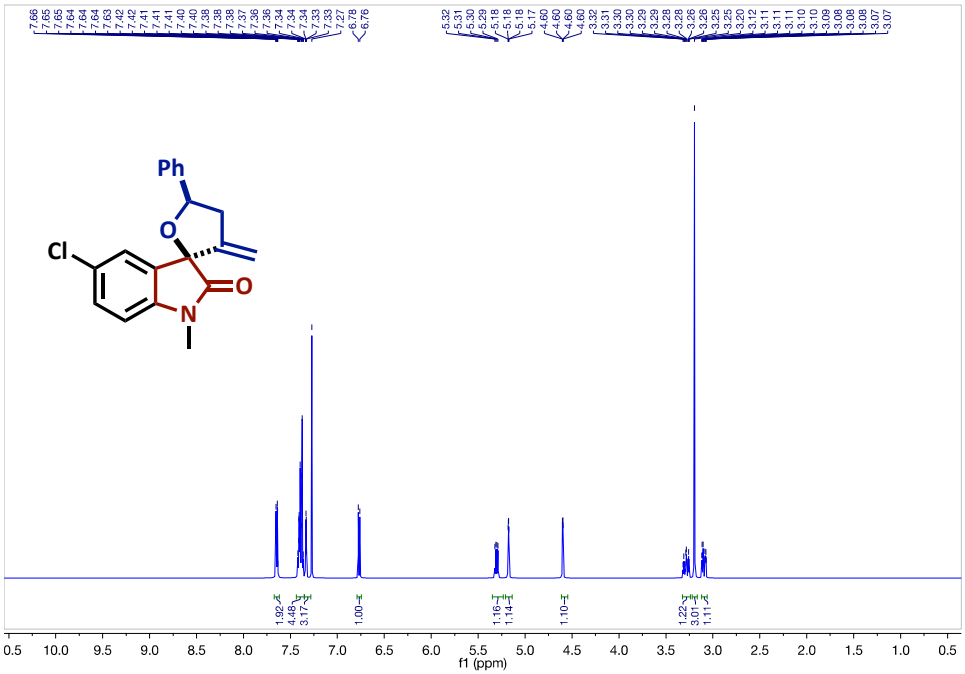
Ph
O
Cl
O
N
f1 (ppm)

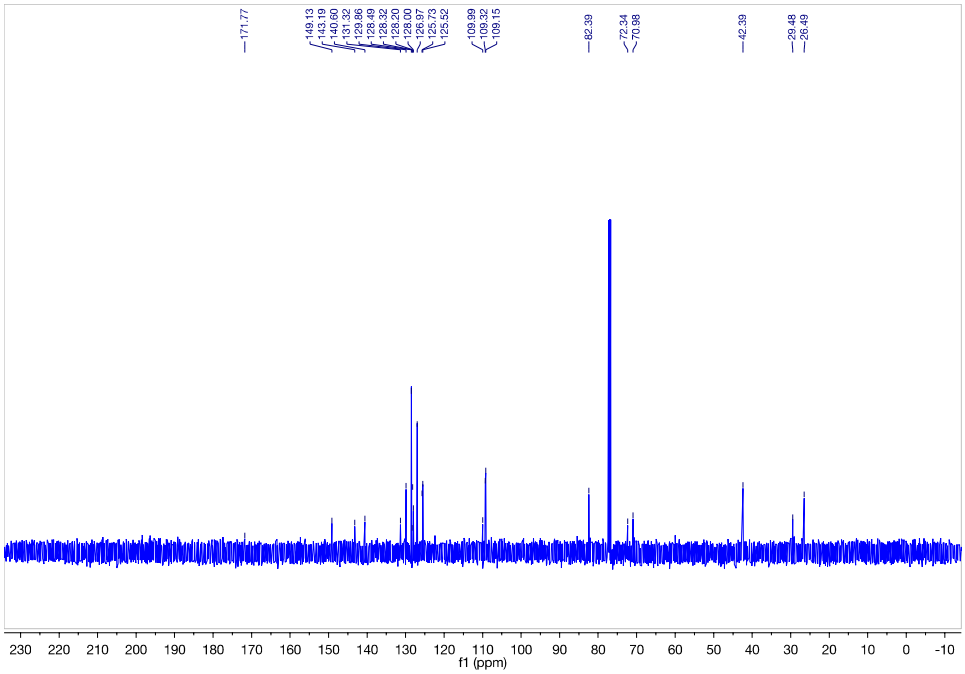
f1 (ppm)

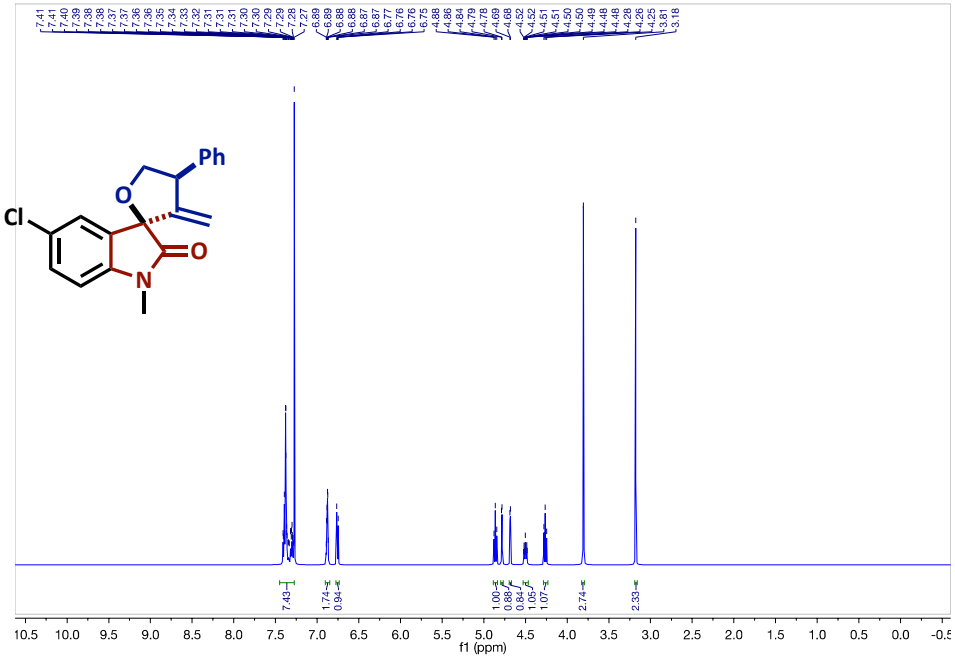
Ph
O
Cl
O
N
f1 (ppm)

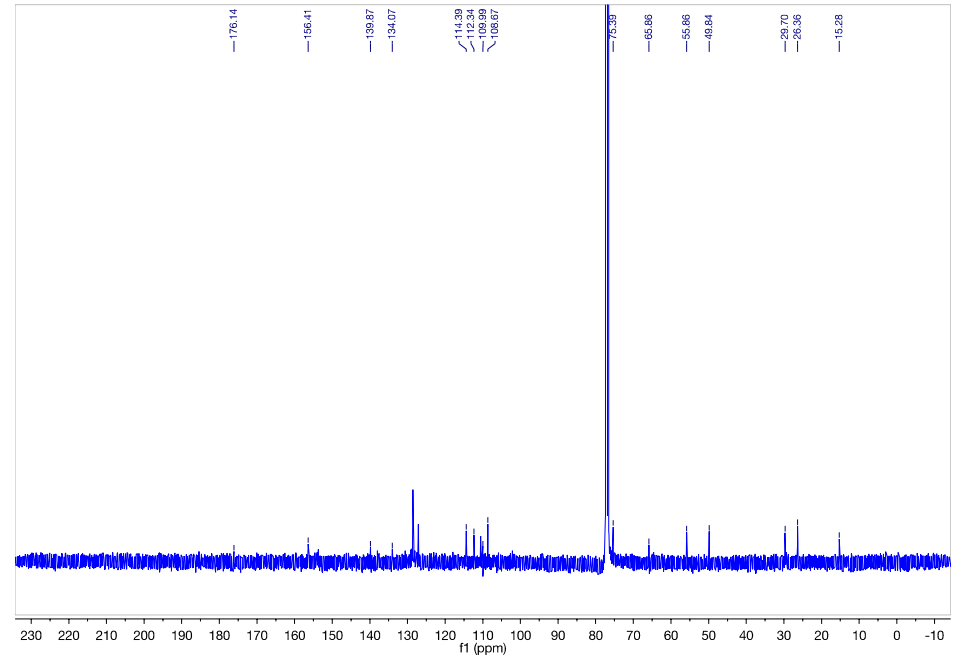
f1 (ppm)

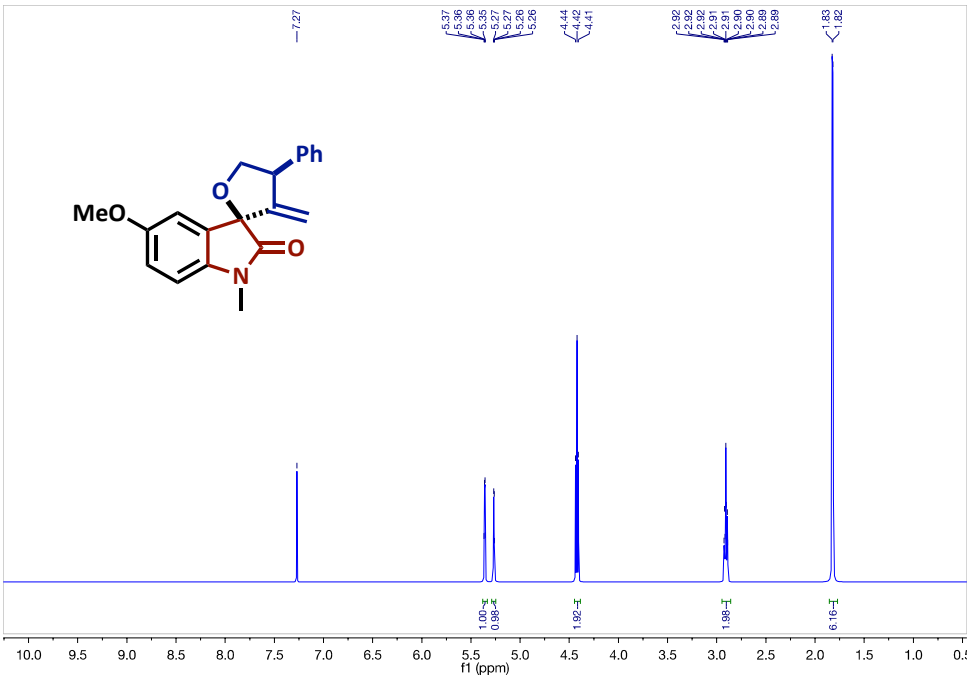
7.27
5.37
5.36
5.36
5.35
5.27
5.27
5.26
5.26
4.44
4.42
4.41
2.92
2.92
2.92
2.91
2.91
2.90
2.90
2.89
2.89
1.83
1.82
Ph
O
MeO
O
N
1.00
0.98
1.92
1.98
6.16
10.0 9.5 9.0 8.5 8.0 7.5 7.0 6.5 6.0 5.5 5.0 4.5 4.0 3.5 3.0 2.5 2.0 1.5 1.0
f1 (ppm)

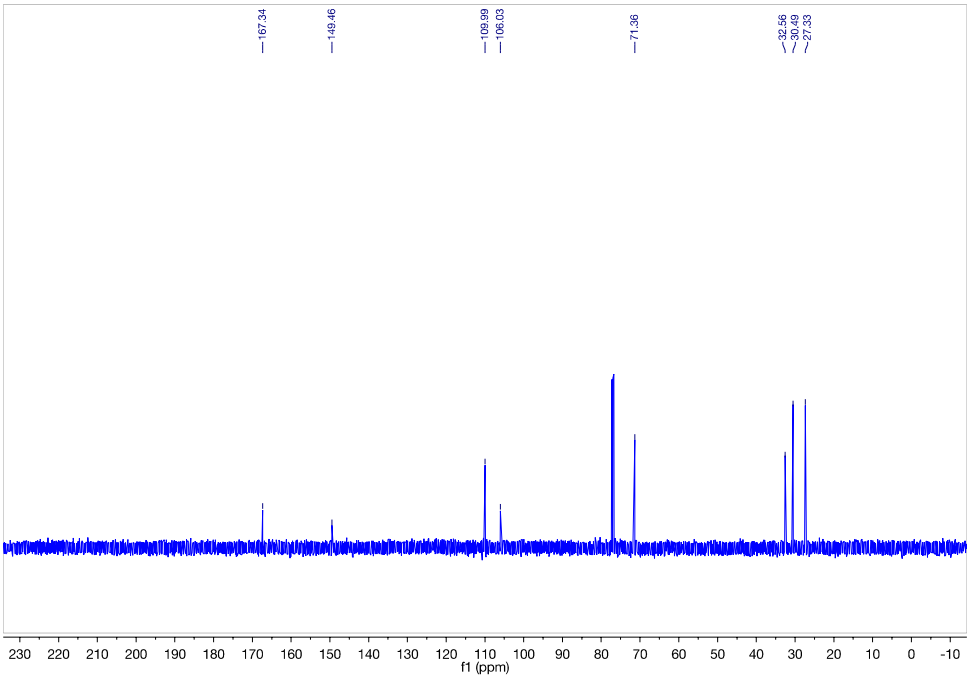
167.34
149.46
109.99
106.03
71.36
32.56
30.49
27.33
230 220 210 200 190 180 170 160 150 140 130 120 110 100 90 80 70 60 50 40 30 20 10 0 -10
f1 (ppm)

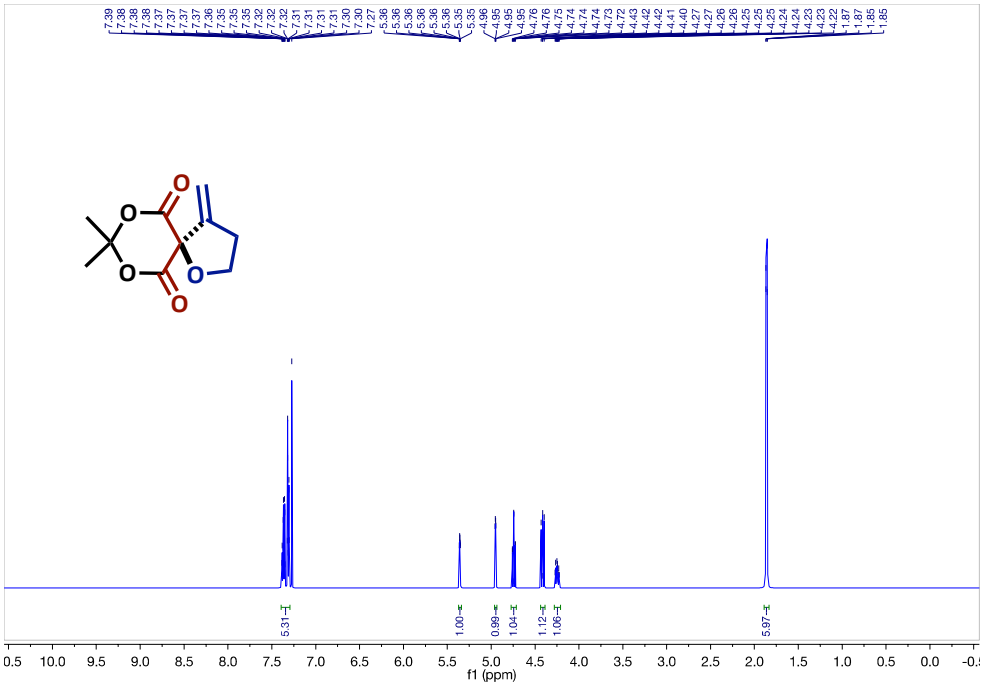
7.39 7.38 7.38 7.38 7.37 7.37 7.37 7.37 7.36 7.35 7.35 7.32 7.32 7.32 7.31 7.31 7.31 7.31 7.30 7.27
5.36 5.36 5.36 5.36 5.36 5.35 5.35
4.96 4.95 4.95 4.95 4.76 4.76 4.75 4.74 4.74 4.74 4.73 4.72 4.43 4.42 4.42 4.41 4.40 4.27 4.27 4.26 4.26 4.25 4.25 4.25 4.24 4.24 4.23 4.23 4.22 1.87 1.87 1.85 1.85
O
O
O
O
O
5.31
1.00
0.99
1.04
1.12
1.06
5.97
0.5 10.0 9.5 9.0 8.5 8.0 7.5 7.0 6.5 6.0 5.5 5.0 4.5 4.0 3.5 3.0 2.5 2.0 1.5 1.0 0.5 0.0
f1 (ppm)

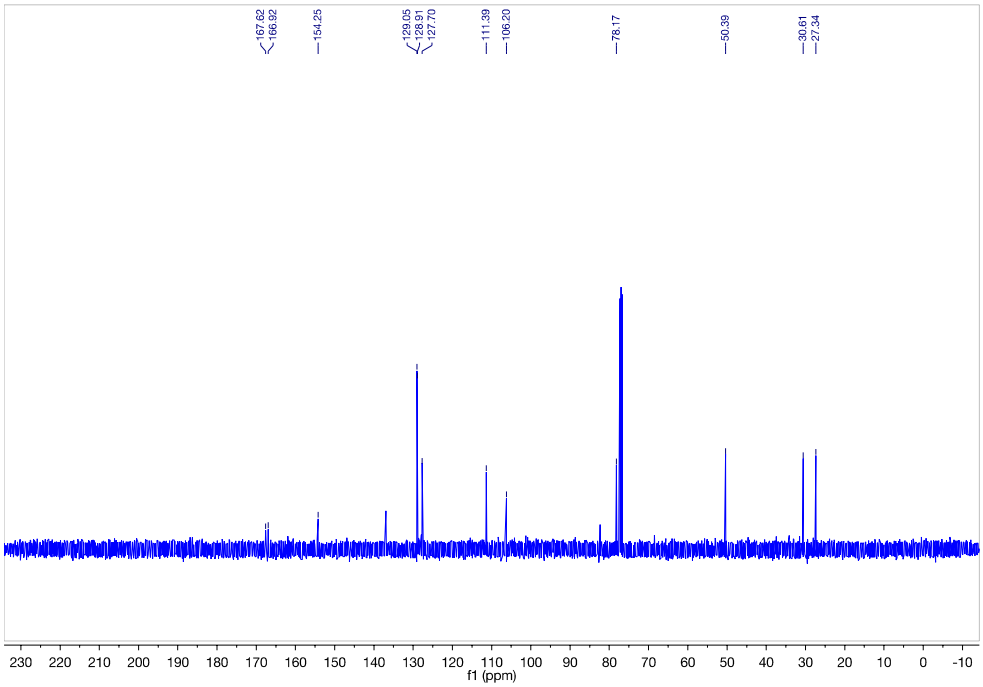
167.62
166.92
154.25
129.05
128.91
127.70
111.39
106.20
78.17
50.39
30.61
27.34
230 220 210 200 190 180 170 160 150 140 130 120 110 100 90 80 70 60 50 40 30 20 10 0 -10
f1 (ppm)

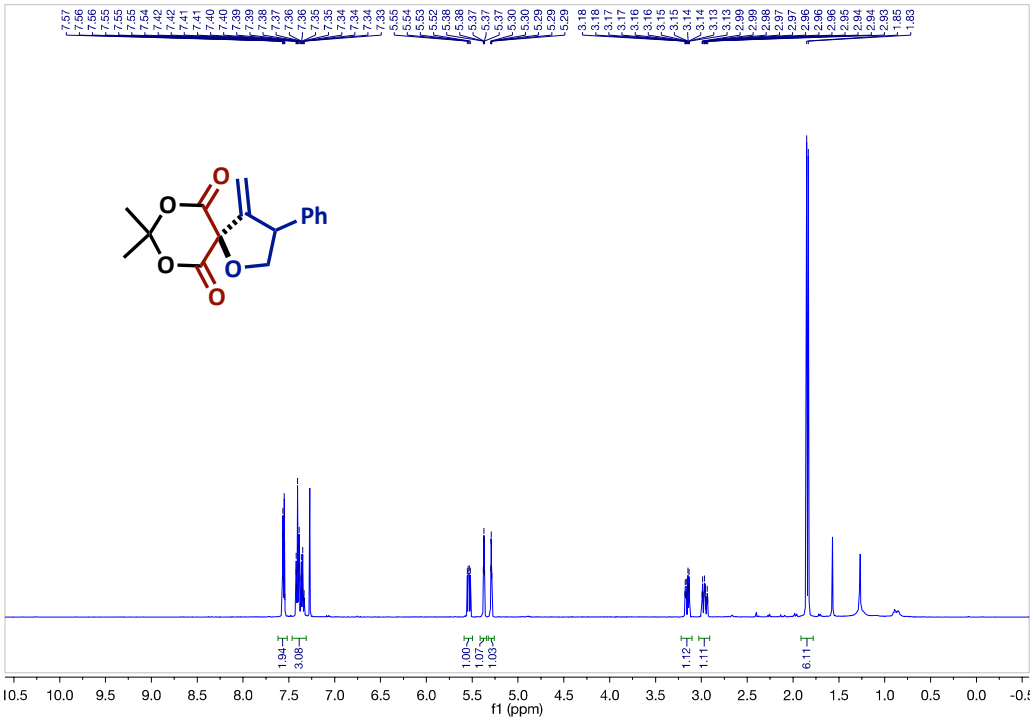
O
O
O
O
O
Ph
7.57 7.56 7.56 7.55 7.55 7.55 7.54 7.42 7.42 7.41 7.41 7.40 7.40 7.39 7.39 7.38 7.37 7.36 7.36 7.35 7.35 7.34 7.34 7.34 7.33
5.55 5.54 5.53 5.52 5.38 5.38 5.37 5.37 5.30 5.30 5.29 5.29 5.29
3.18 3.18 3.17 3.17 3.16 3.16 3.15 3.15 3.14 3.14 3.13 3.13 2.99 2.99 2.98 2.98 2.97 2.96 2.96 2.96 2.95 2.94 2.94 2.93 1.85 1.83
1.94 3.08 1.00 1.07 1.03 1.12 1.11 6.11
f1 (ppm)

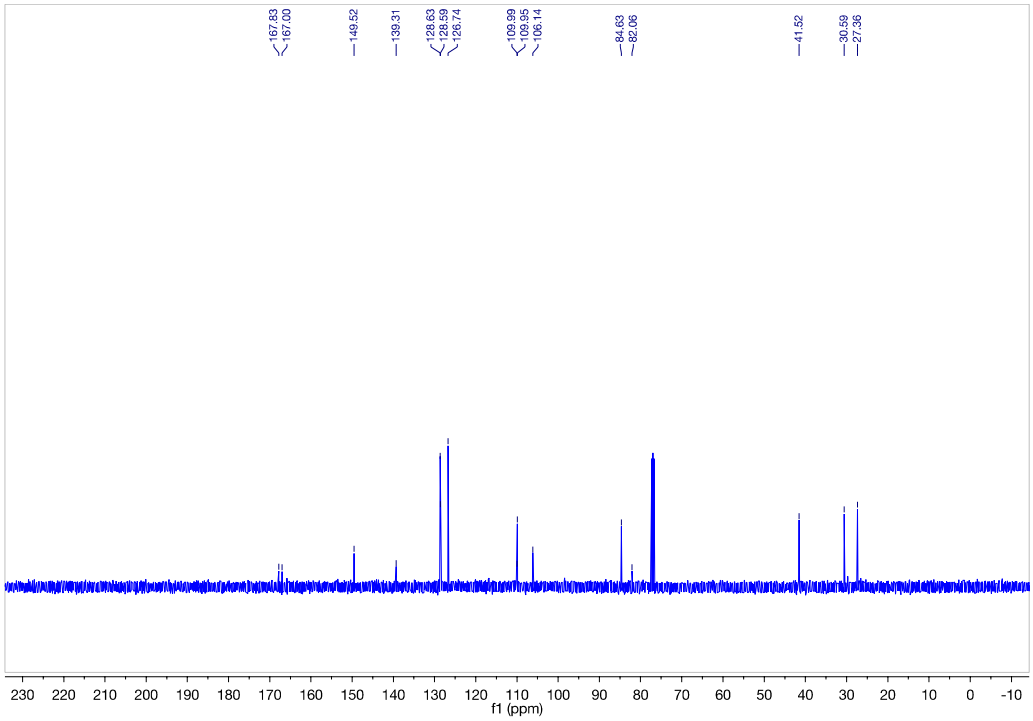
167.83 167.00 149.52 139.31 128.63 128.59 126.74 109.99 109.95 106.14 84.63 82.06 41.52 30.59 27.36
f1 (ppm)

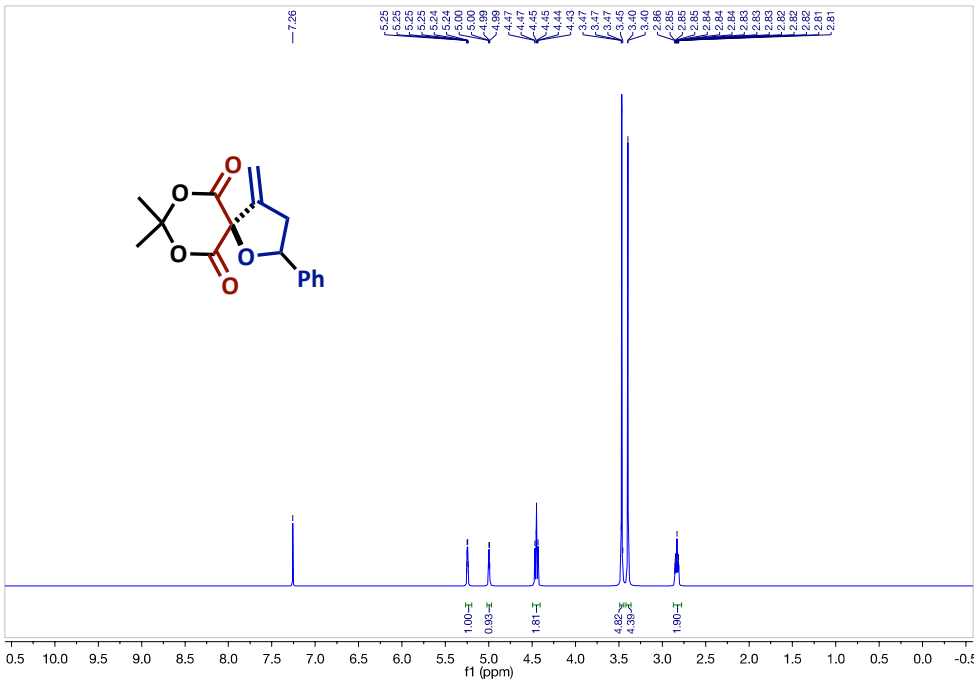
7.26
5.25
5.25
5.25
5.25
5.24
5.24
5.00
5.00
4.99
4.99
4.47
4.47
4.45
4.45
4.44
4.44
4.43
3.47
3.47
3.47
3.45
3.40
3.40
2.86
2.85
2.85
2.84
2.84
2.84
2.83
2.83
2.83
2.82
2.82
2.82
2.81
2.81
O
O
O
O
O
Ph
1.00
0.93
1.81
4.82
4.39
1.90
0.5 10.0 9.5 9.0 8.5 8.0 7.5 7.0 6.5 6.0 5.5 5.0 4.5 4.0 3.5 3.0 2.5 2.0 1.5 1.0 0.5 0.0
f1 (ppm)

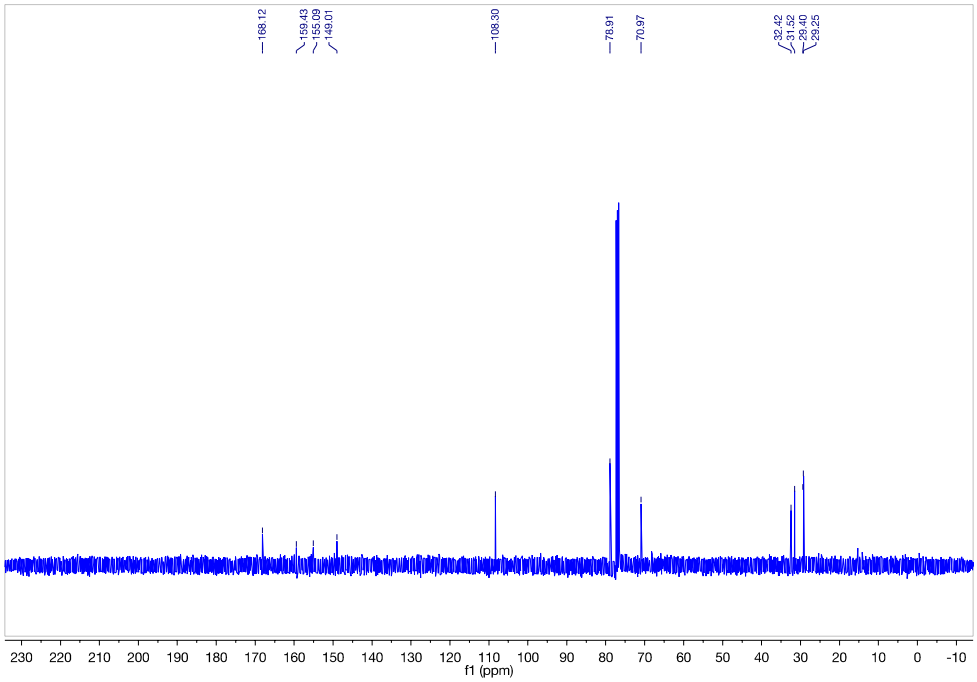
168.12
159.43
155.09
149.01
108.30
78.91
70.97
32.42
31.52
29.40
29.25
230 220 210 200 190 180 170 160 150 140 130 120 110 100 90 80 70 60 50 40 30 20 10 0 -10
f1 (ppm)

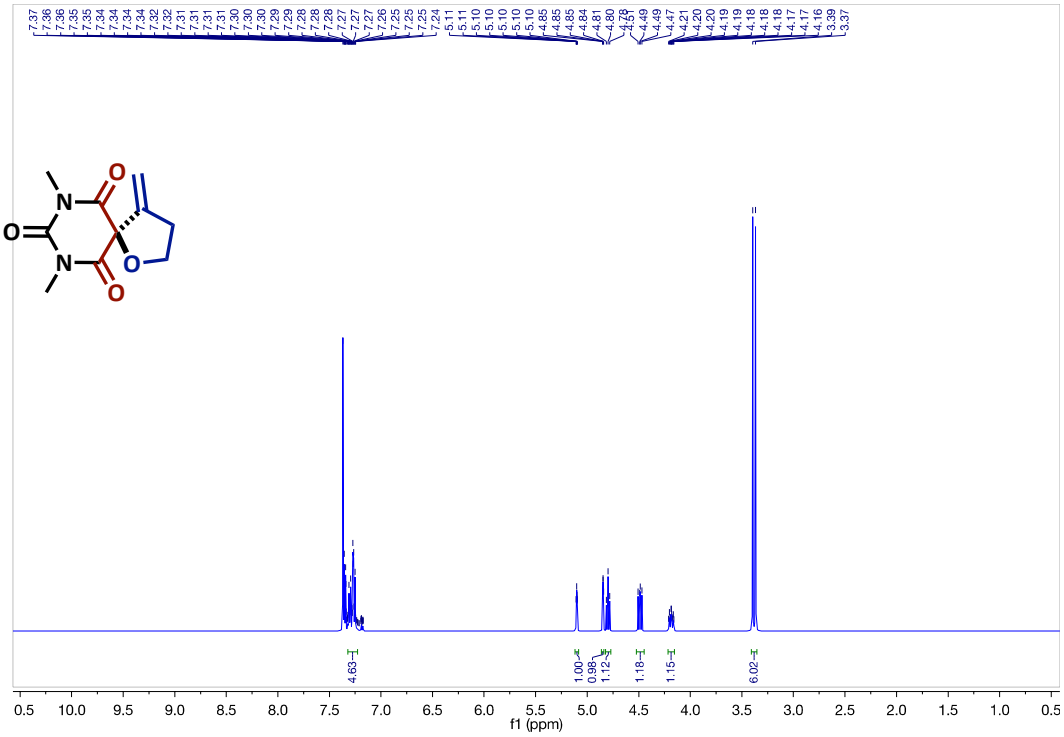
7.37 7.36 7.36 7.35 7.34 7.34 7.34 7.34 7.32 7.32 7.31 7.31 7.31 7.31 7.30 7.30 7.30 7.29 7.29 7.28 7.28 7.28 7.27 7.27 7.27 7.26 7.25 7.25 7.25 7.24 5.11 5.11 5.10 5.10 5.10 5.10 4.85 4.85 4.85 4.84 4.81 4.80 4.51 4.49 4.49 4.47 4.21 4.20 4.20 4.19 4.19 4.18 4.18 4.18 4.17 4.17 4.16 3.39 3.37
O
N
O
N
O
O
O
4.63
1.00
0.98
1.12
1.18
1.15
6.02
0.5 10.0 9.5 9.0 8.5 8.0 7.5 7.0 6.5 6.0 5.5 5.0 4.5 4.0 3.5 3.0 2.5 2.0 1.5 1.0 0.5
f1 (ppm)

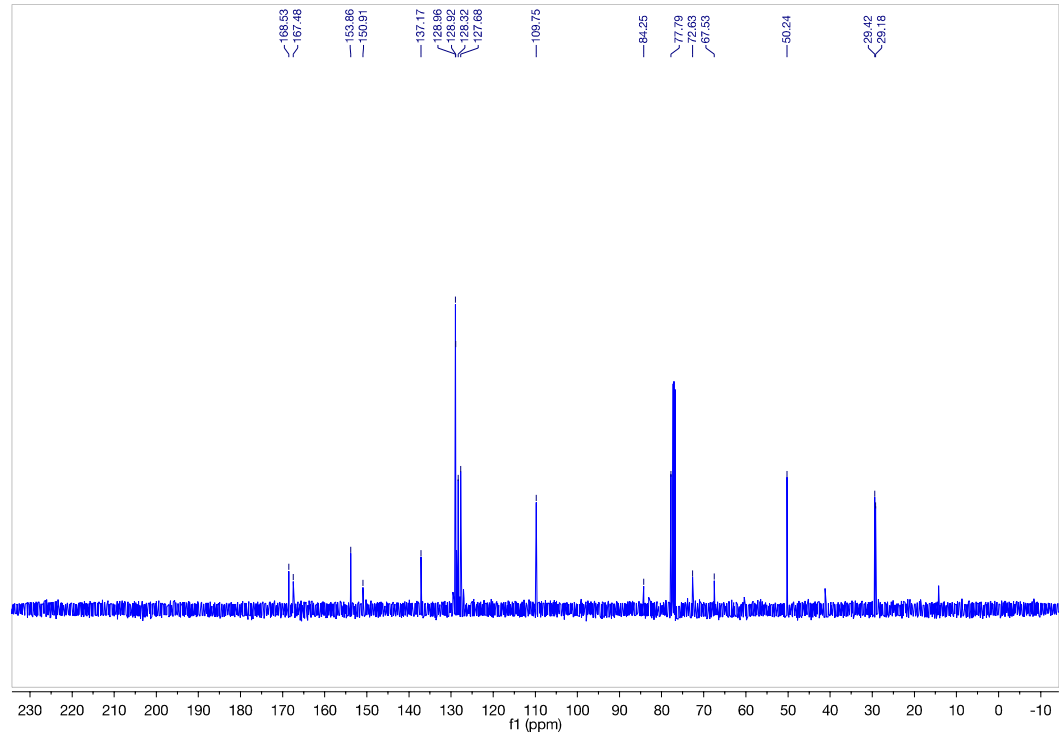
168.53
167.48
153.86
150.91
137.17
128.96
128.92
128.32
127.68
109.75
84.25
77.79
72.63
67.53
50.24
29.42
29.18
230 220 210 200 190 180 170 160 150 140 130 120 110 100 90 80 70 60 50 40 30 20 10 0 -10
f1 (ppm)

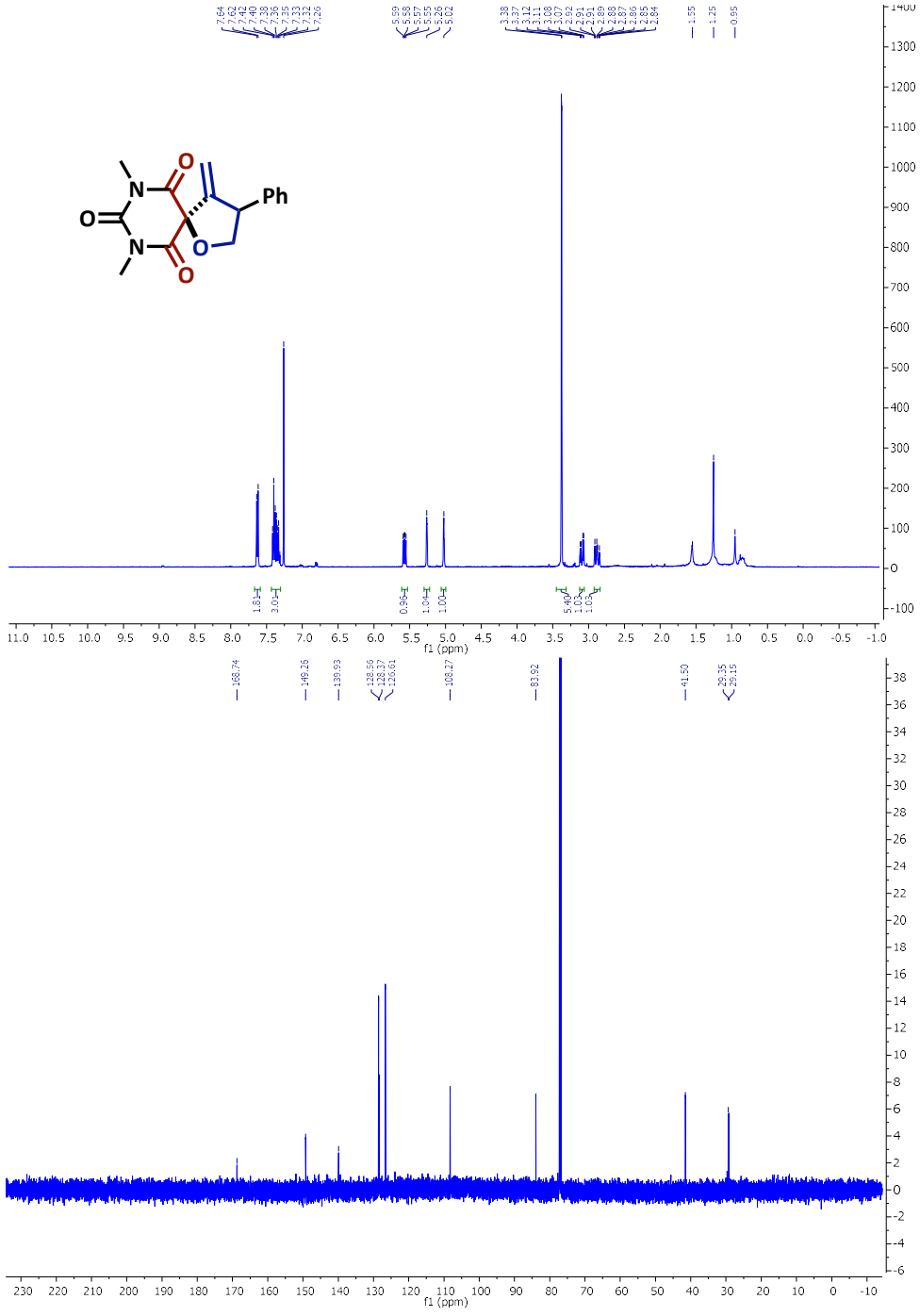
Ph
f1 (ppm)
f1 (ppm)

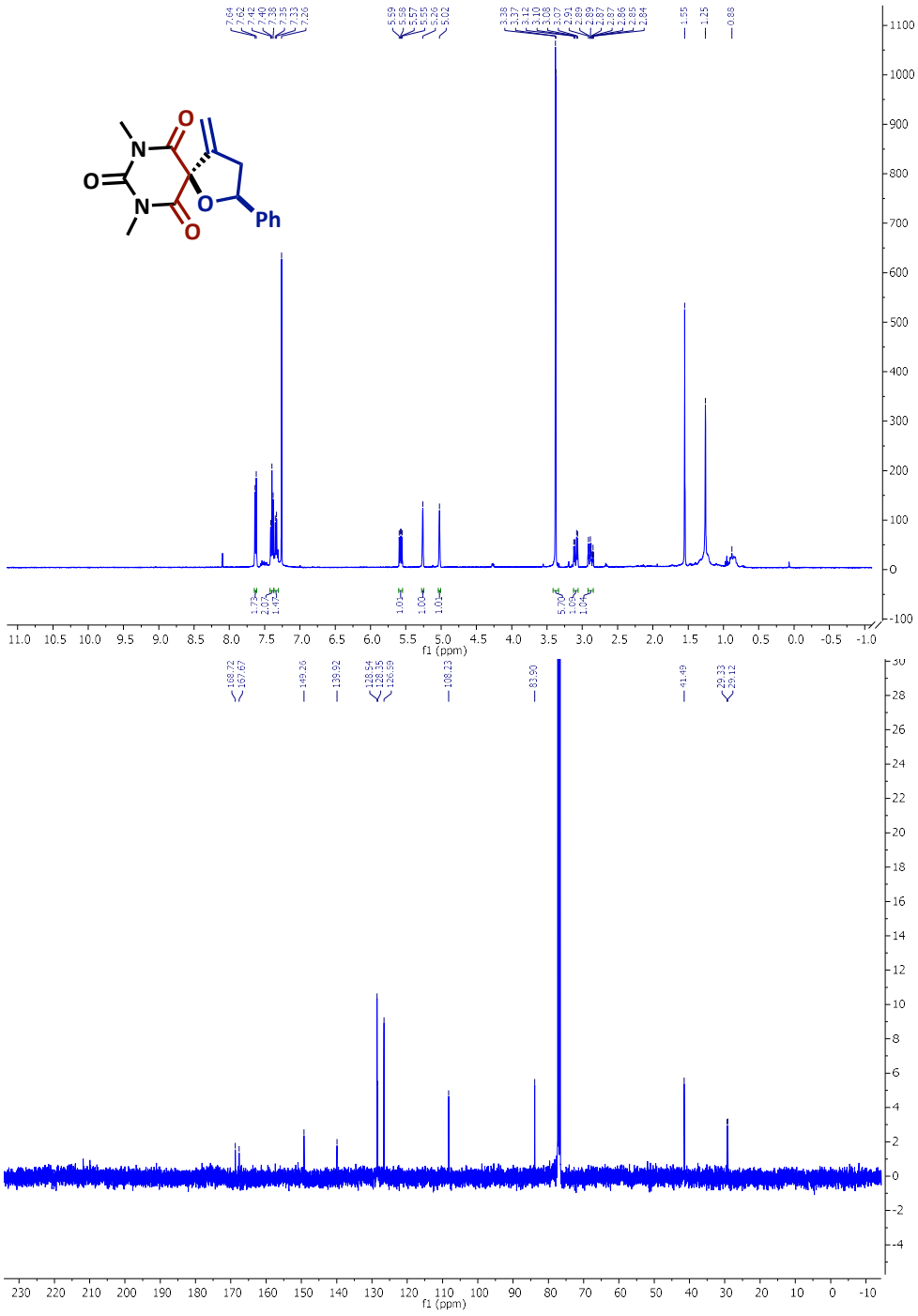
O
N
O
N
O
O
O
Ph
f1 (ppm)
f1 (ppm)

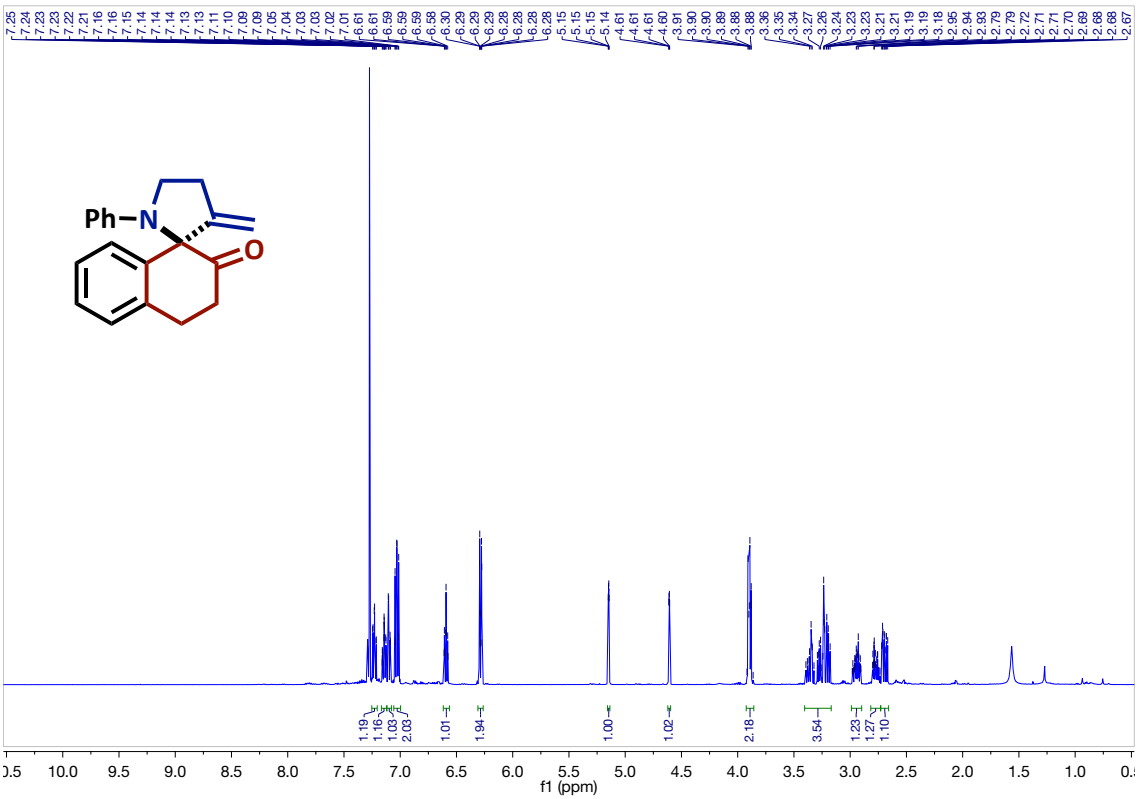
Ph–N
O
f1 (ppm)

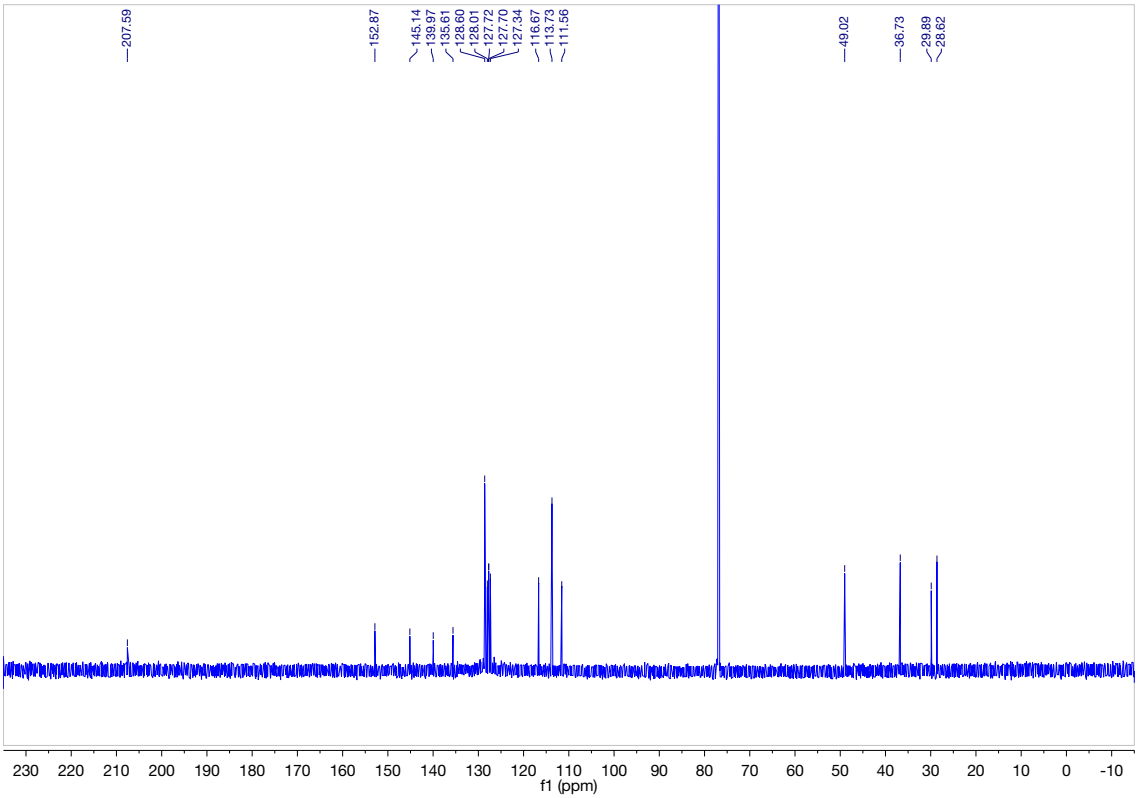
207.59
152.87
145.14
139.97
135.61
128.60
128.01
127.72
127.70
127.34
116.67
113.73
111.56
49.02
36.73
29.89
28.62
f1 (ppm)

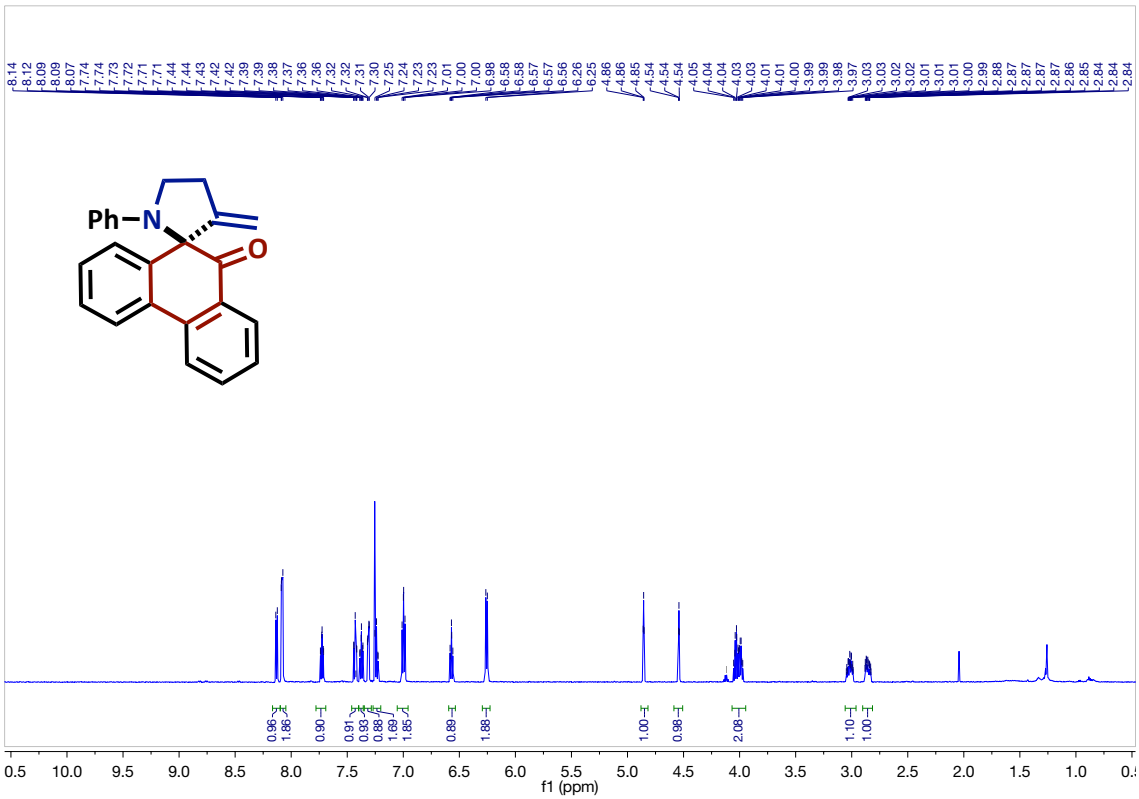
Ph–N
O
f1 (ppm)

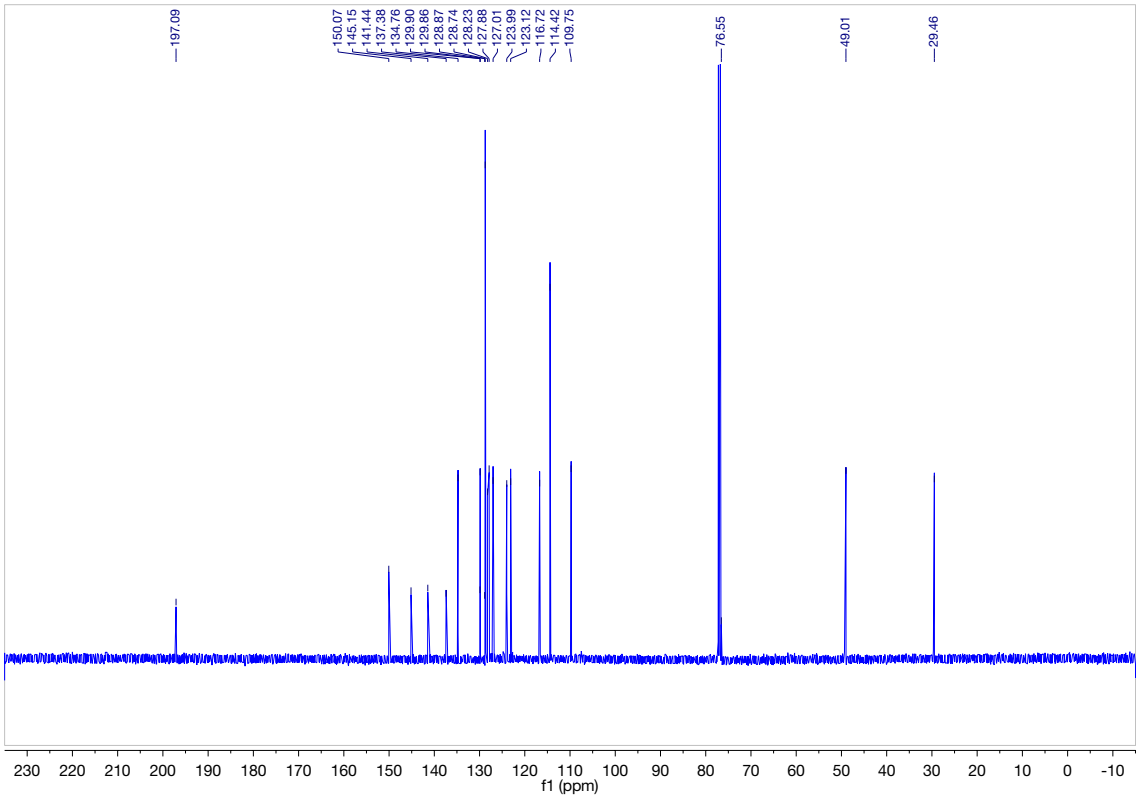
197.09
150.07
145.15
141.44
137.38
134.76
129.90
129.86
128.87
128.74
128.23
127.88
127.01
123.99
123.12
116.72
114.42
109.75
76.55
49.01
29.46
f1 (ppm)

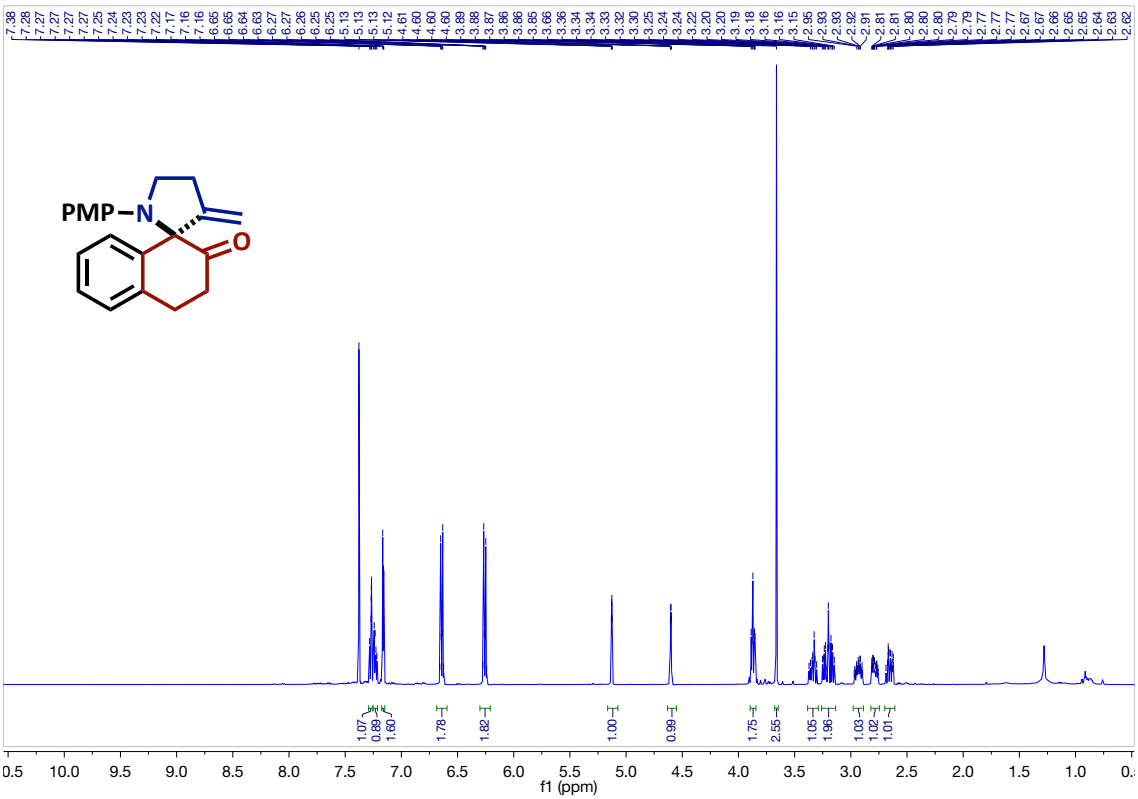
PMP–N
O
1.07
0.89
1.60
1.78
1.82
1.00
0.99
1.75
2.55
1.05
1.96
1.03
1.02
1.01
f1 (ppm)

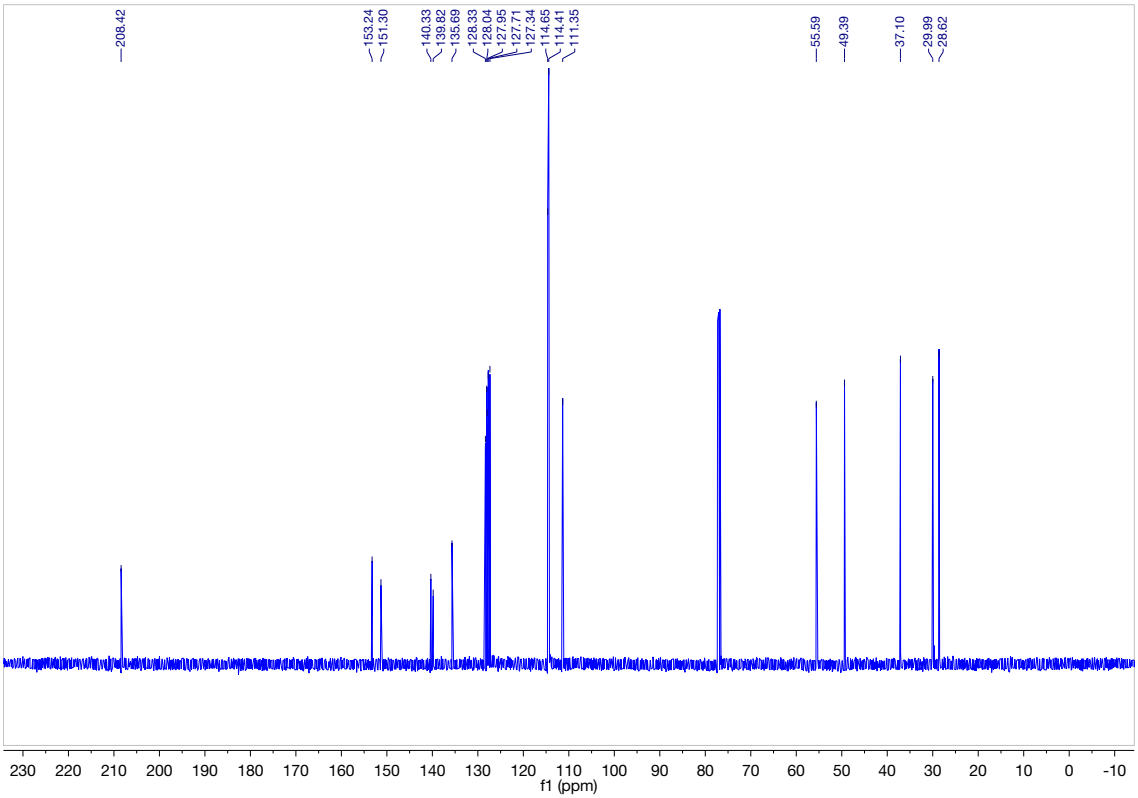
208.42
153.24
151.30
140.33
139.82
135.69
128.33
128.04
127.95
127.71
127.34
114.65
114.41
111.35
55.59
49.39
37.10
29.99
28.62
f1 (ppm)

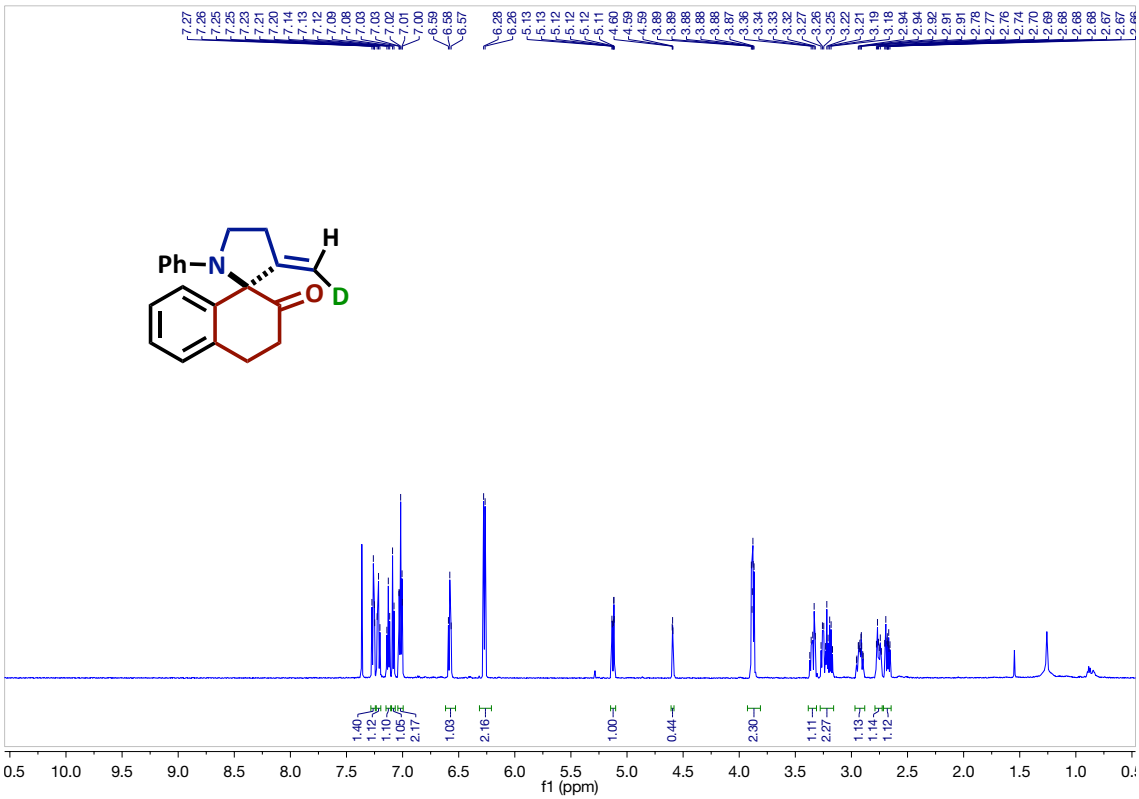
Ph–N
H
O
D
f1 (ppm)

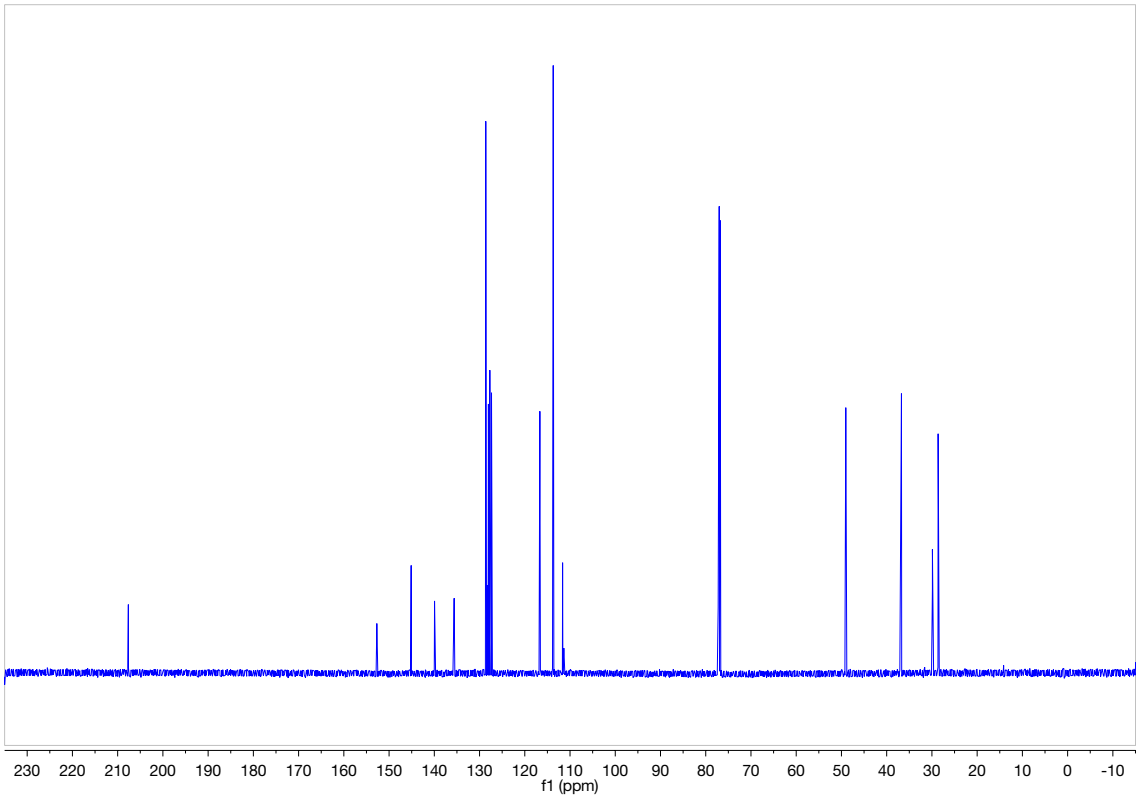
f1 (ppm)

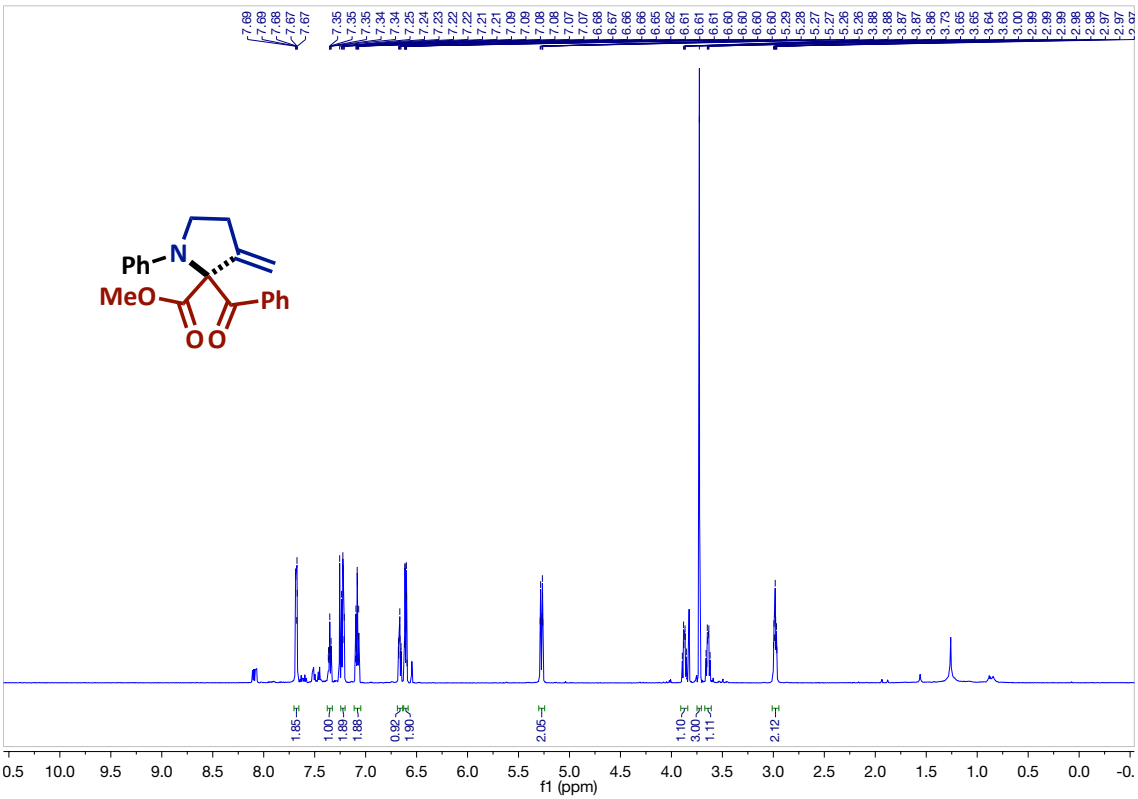
Ph
N
MeO
Ph
O O
f1 (ppm)

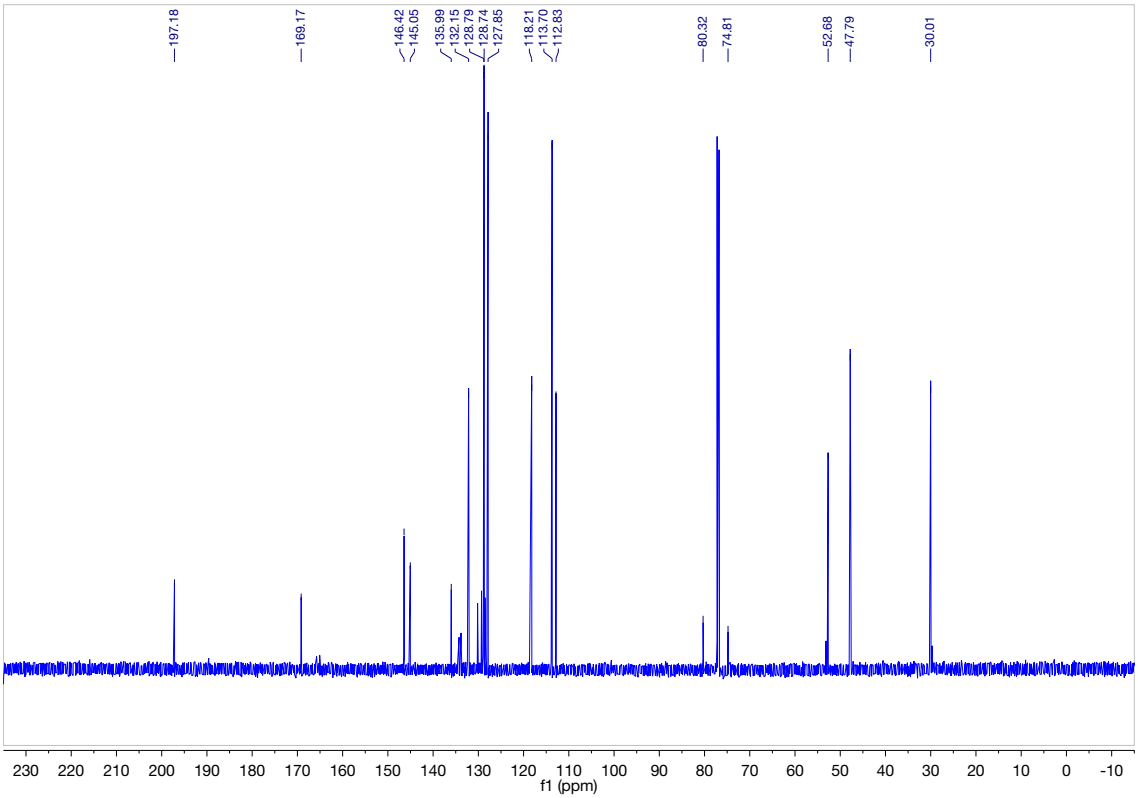
197.18
169.17
146.42
145.05
135.99
132.15
128.79
128.74
127.85
118.21
113.70
112.83
80.32
74.81
52.68
47.79
30.01
f1 (ppm)

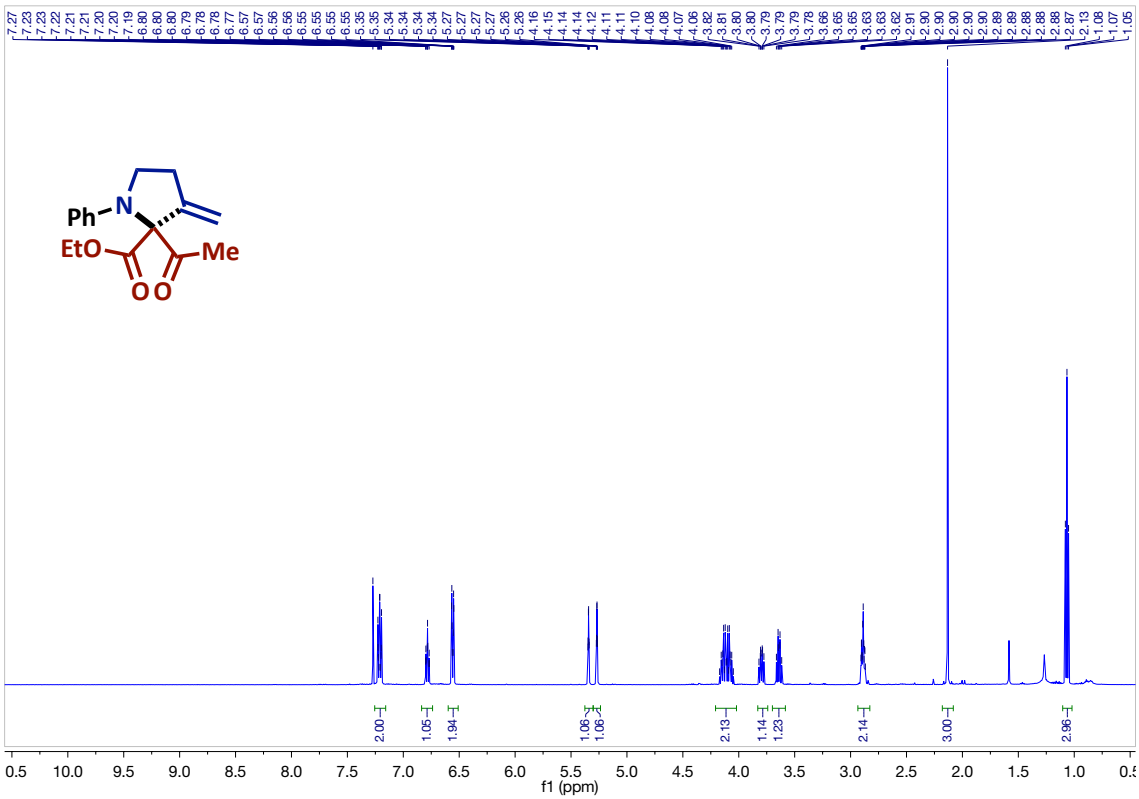
Ph
N
EtO
Me
O
O
2.00
1.05
1.94
1.06
1.06
2.13
1.14
1.23
2.14
3.00
2.86
f1 (ppm)

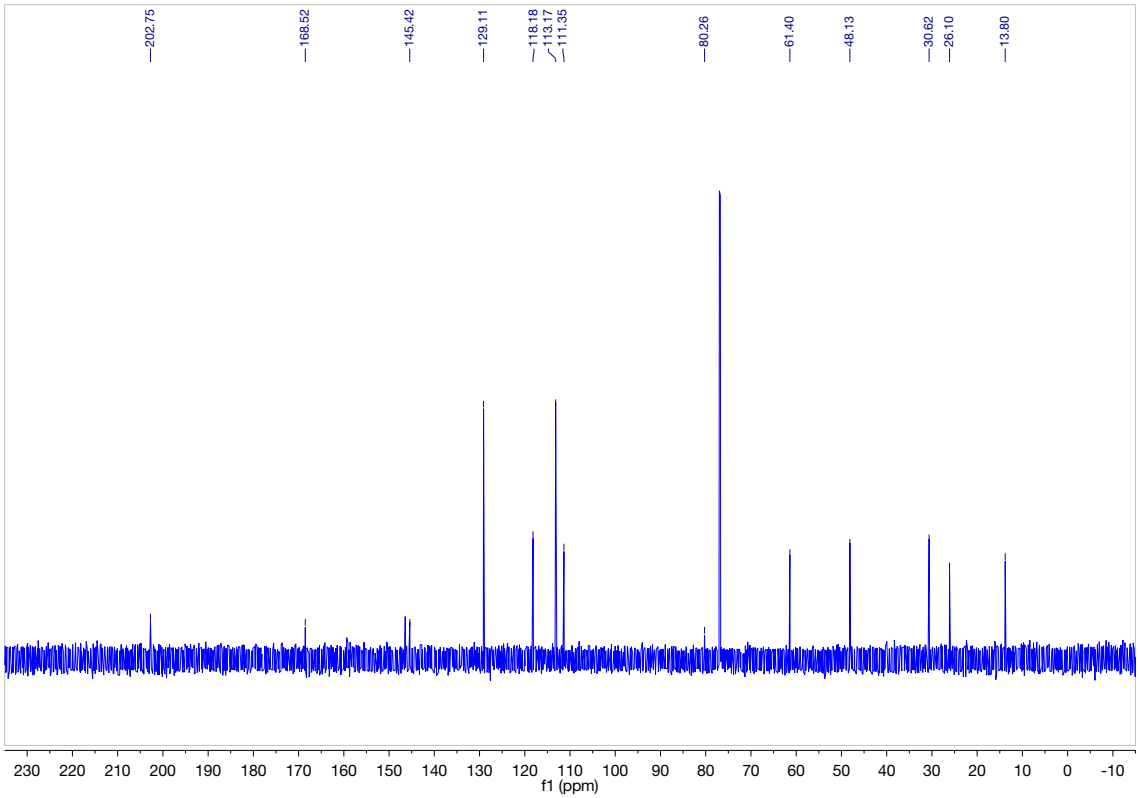
202.75
168.52
145.42
129.11
118.18
113.17
111.35
80.26
61.40
48.13
30.62
26.10
13.80
f1 (ppm)

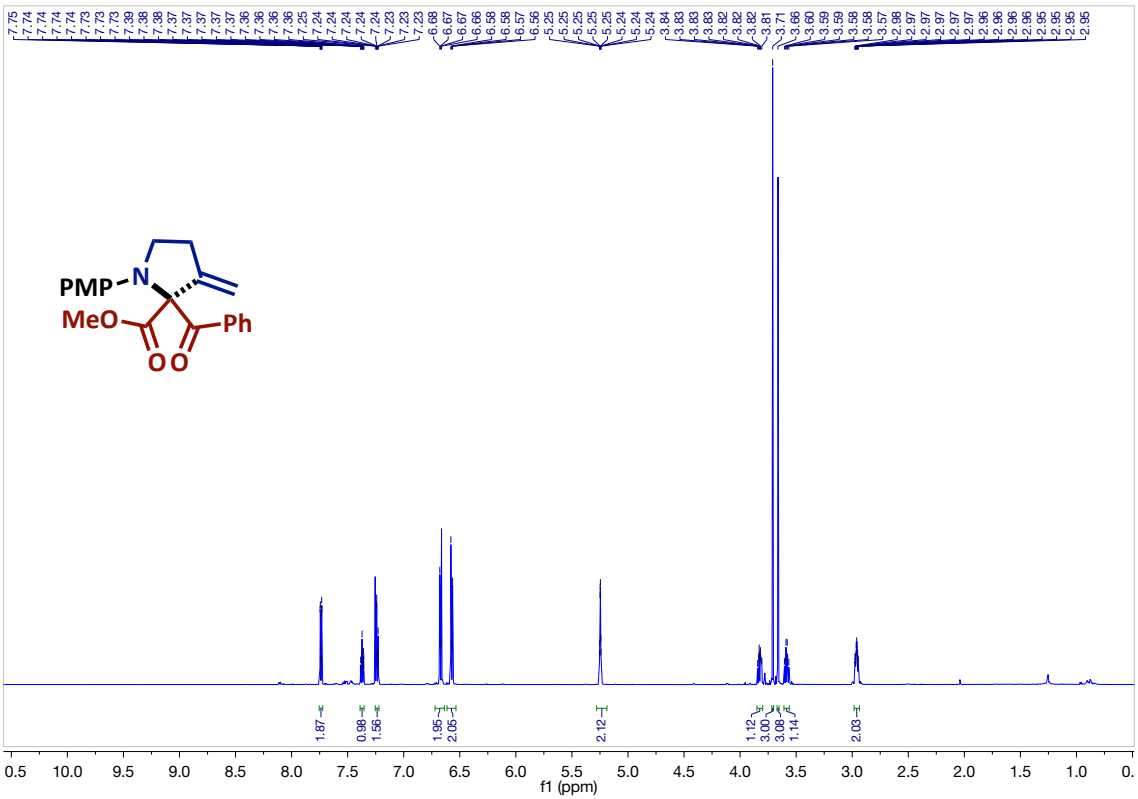
PMP
N
MeO
Ph
O
O
f1 (ppm)

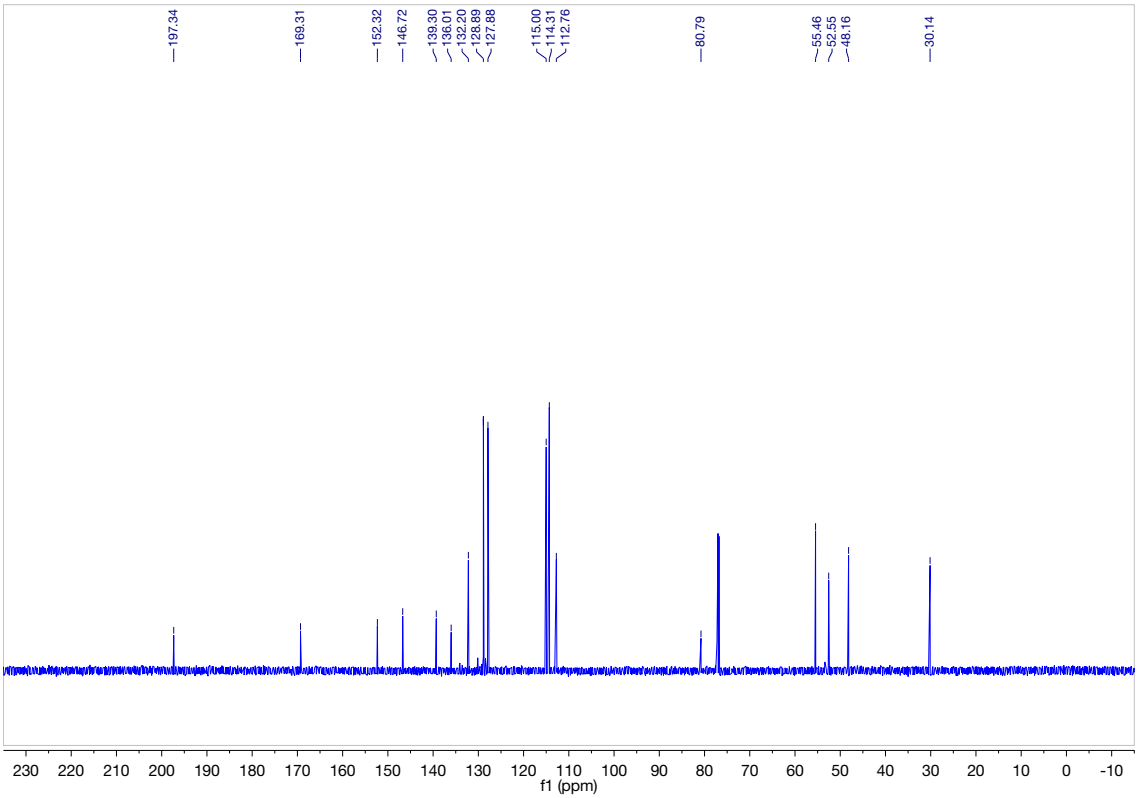
197.34
169.31
152.32
146.72
139.30
136.01
132.20
128.89
127.88
115.00
114.31
112.76
80.79
55.46
52.55
48.16
30.14
f1 (ppm)

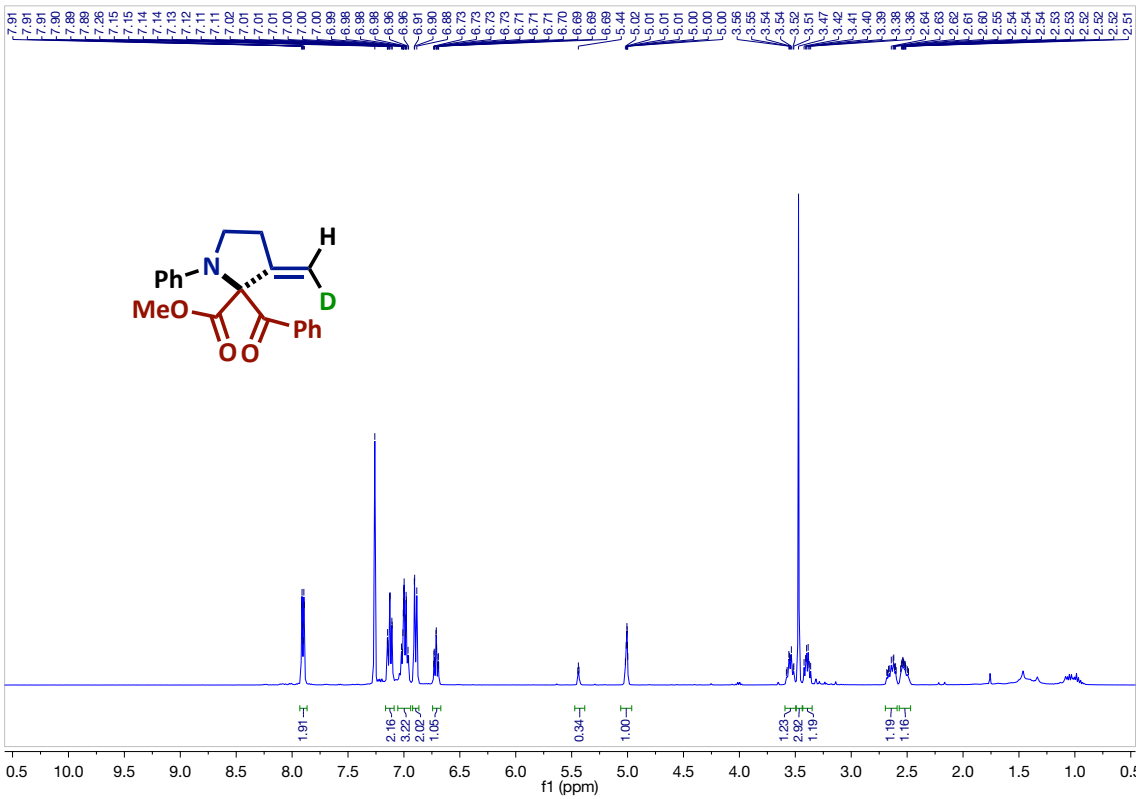
Ph
N
MeO
O O
H
D
Ph
f1 (ppm)

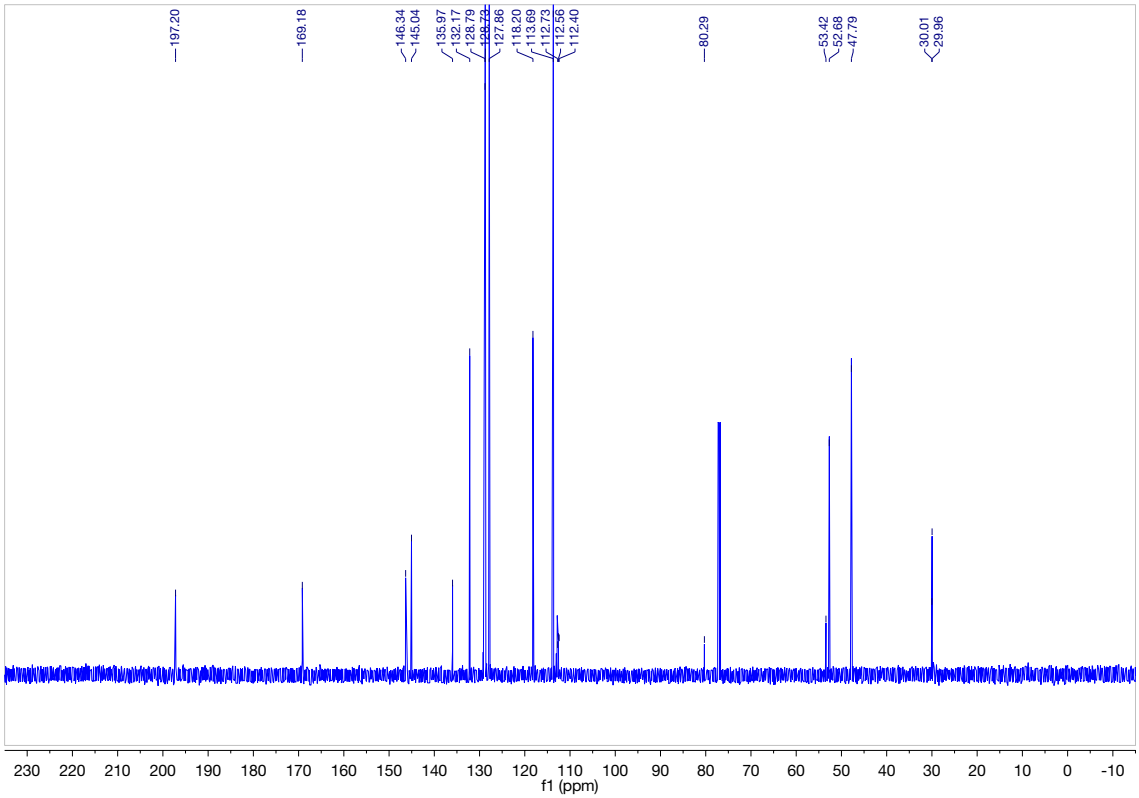
197.20
169.18
146.34
145.04
135.97
132.17
128.79
128.73
127.86
118.20
113.69
112.73
112.56
112.40
80.29
53.42
52.68
47.79
30.01
29.96
f1 (ppm)

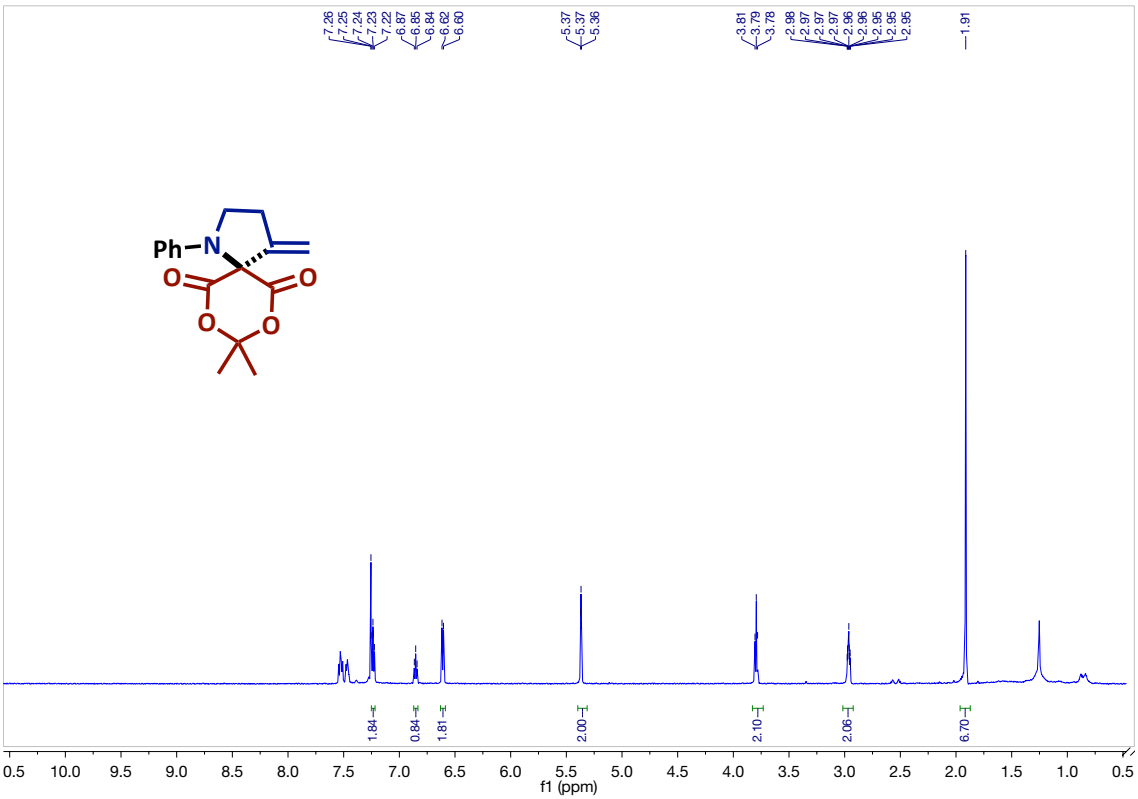
7.26
7.25
7.24
7.23
7.22
6.87
6.85
6.84
6.62
6.60
5.37
5.37
5.36
3.81
3.79
3.78
2.98
2.97
2.97
2.97
2.96
2.96
2.95
2.95
2.95
1.91
Ph–N
O
O
O
O
1.84
0.84
1.81
2.00
2.10
2.06
6.70
0.5 10.0 9.5 9.0 8.5 8.0 7.5 7.0 6.5 6.0 5.5 5.0 4.5 4.0 3.5 3.0 2.5 2.0 1.5 1.0 0.5
f1 (ppm)

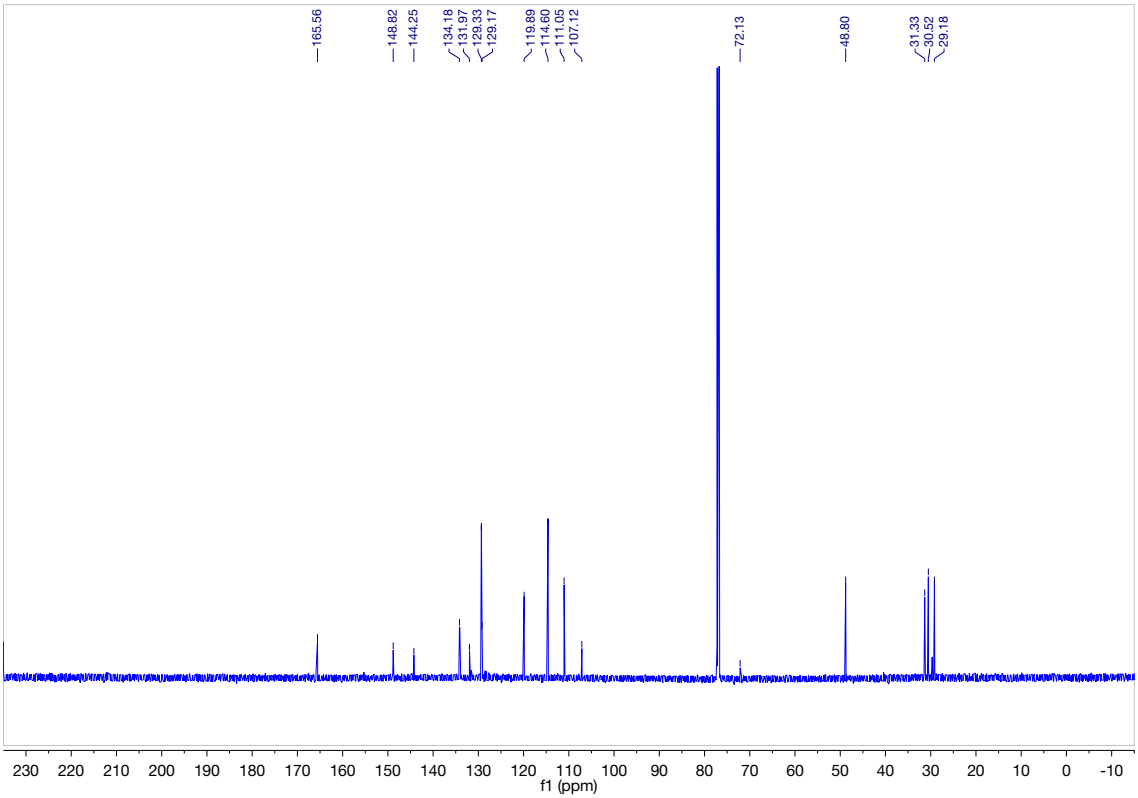
165.56
148.82
144.25
134.18
131.97
129.33
129.17
119.89
114.60
111.05
107.12
72.13
48.80
31.33
30.52
29.18
230 220 210 200 190 180 170 160 150 140 130 120 110 100 90 80 70 60 50 40 30 20 10 0 -10
f1 (ppm)

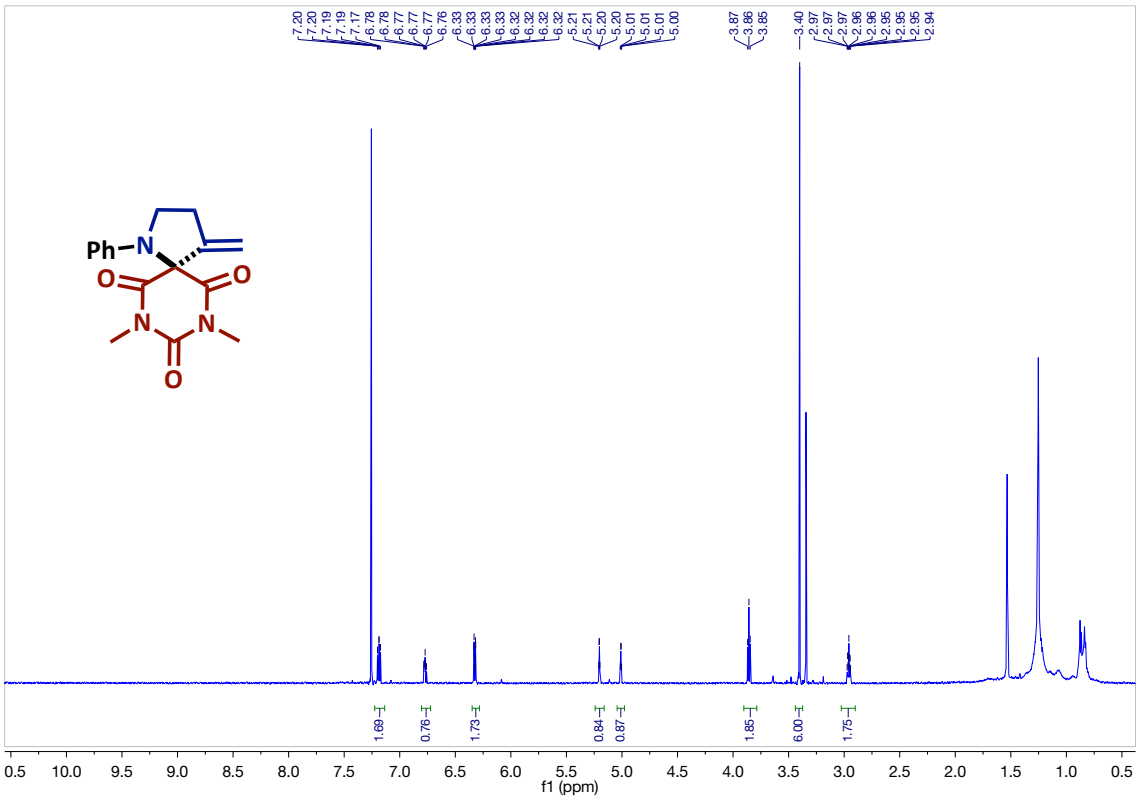
7.20
7.20
7.19
7.19
7.17
6.78
6.78
6.77
6.77
6.76
6.33
6.33
6.33
6.32
6.32
6.32
5.21
5.20
5.20
5.01
5.01
5.00
3.87
3.86
3.85
3.40
2.97
2.97
2.96
2.96
2.95
2.95
2.94
Ph
N
O
O
N
N
O
1.69
0.76
1.73
0.84
0.87
1.85
6.00
1.75
f1 (ppm)

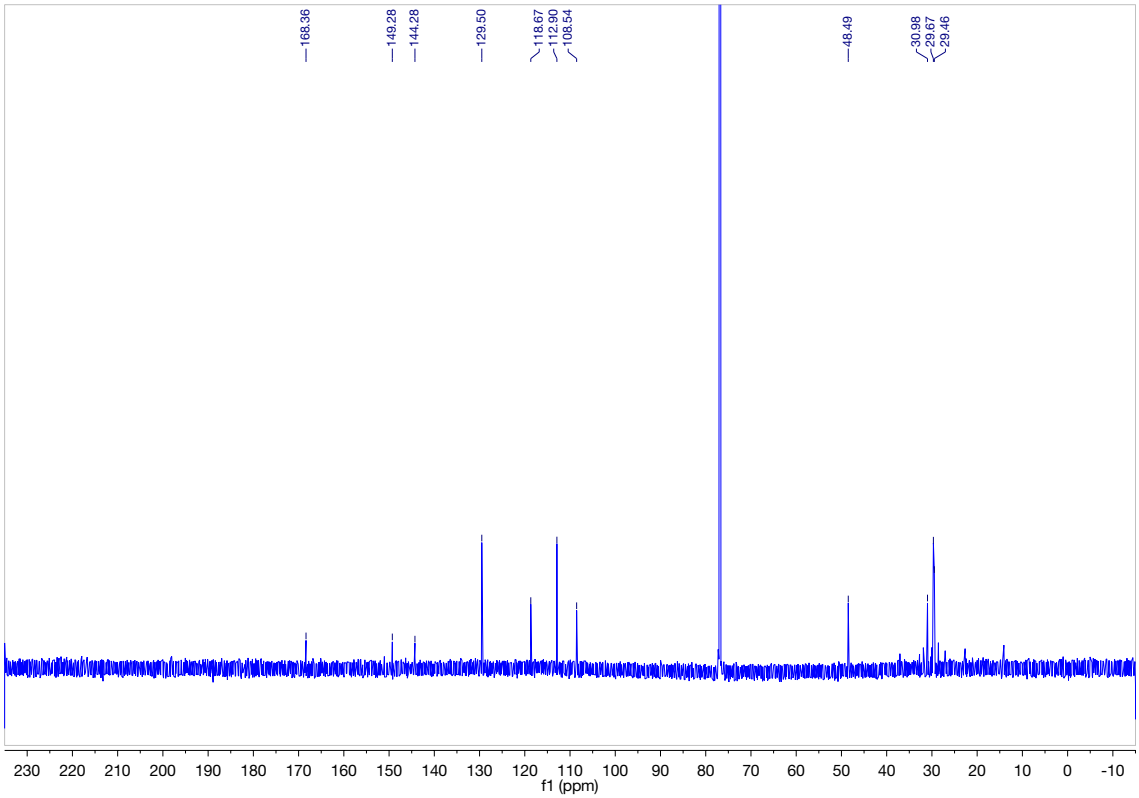
168.36
149.28
144.28
129.50
118.67
112.90
108.54
48.49
30.98
29.67
29.46
f1 (ppm)

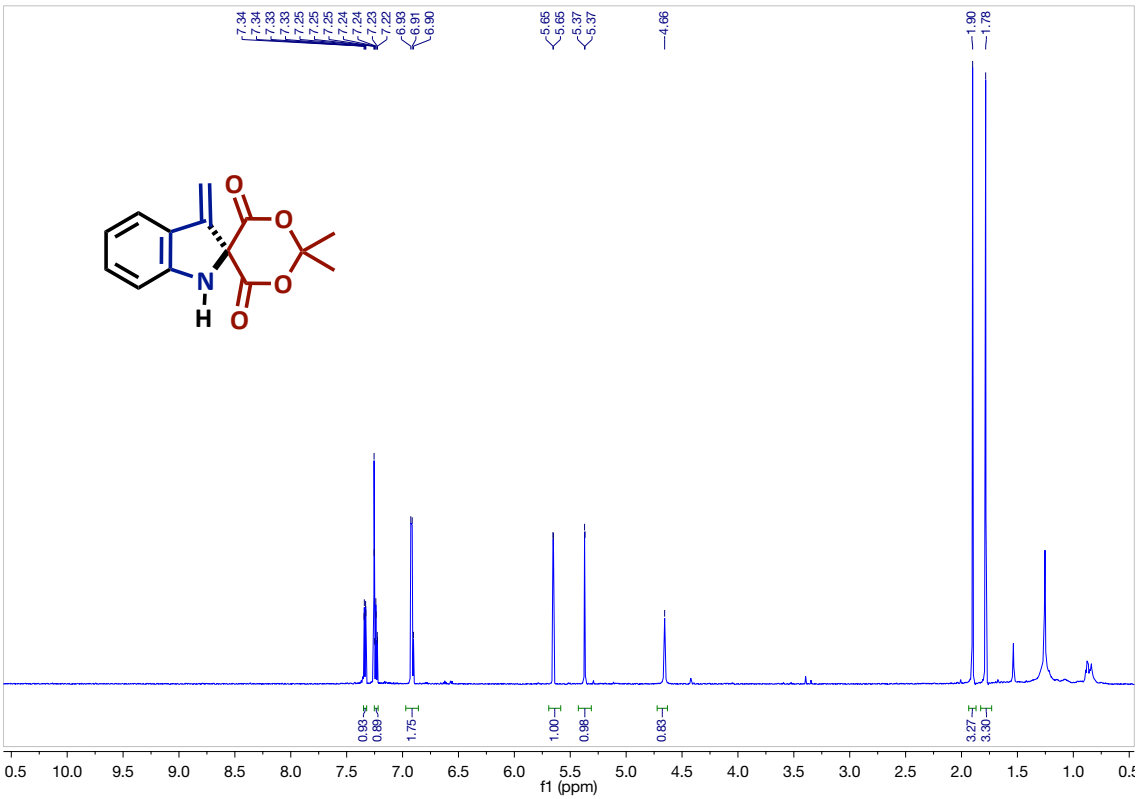
7.34
7.34
7.33
7.33
7.25
7.25
7.25
7.24
7.24
7.23
7.22
6.93
6.91
6.90
5.65
5.65
5.37
5.37
4.66
1.90
1.78
O
O
O
O
N
H
0.93
0.89
1.75
1.00
0.98
0.83
3.27
3.30
0.5 10.0 9.5 9.0 8.5 8.0 7.5 7.0 6.5 6.0 5.5 5.0 4.5 4.0 3.5 3.0 2.5 2.0 1.5 1.0 0.5
f1 (ppm)

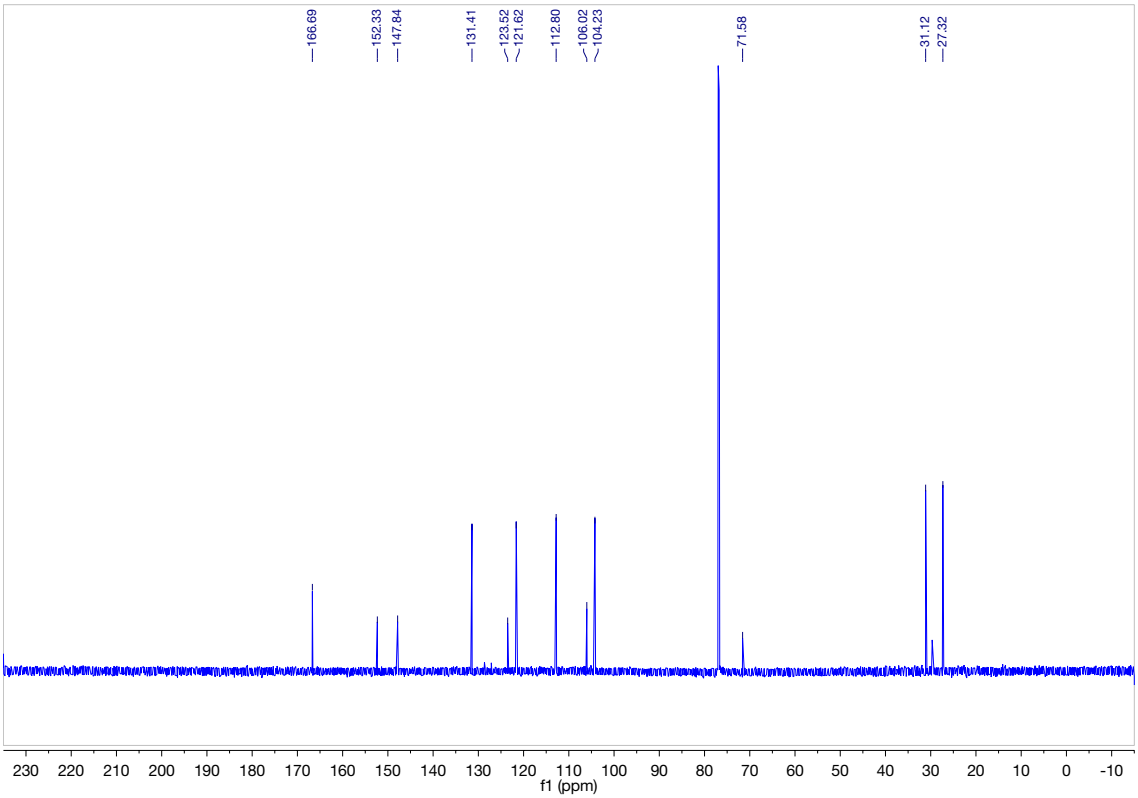
166.69
152.33
147.84
131.41
123.52
121.62
112.80
106.02
104.23
71.58
31.12
27.32
230 220 210 200 190 180 170 160 150 140 130 120 110 100 90 80 70 60 50 40 30 20 10 0 -10
f1 (ppm)

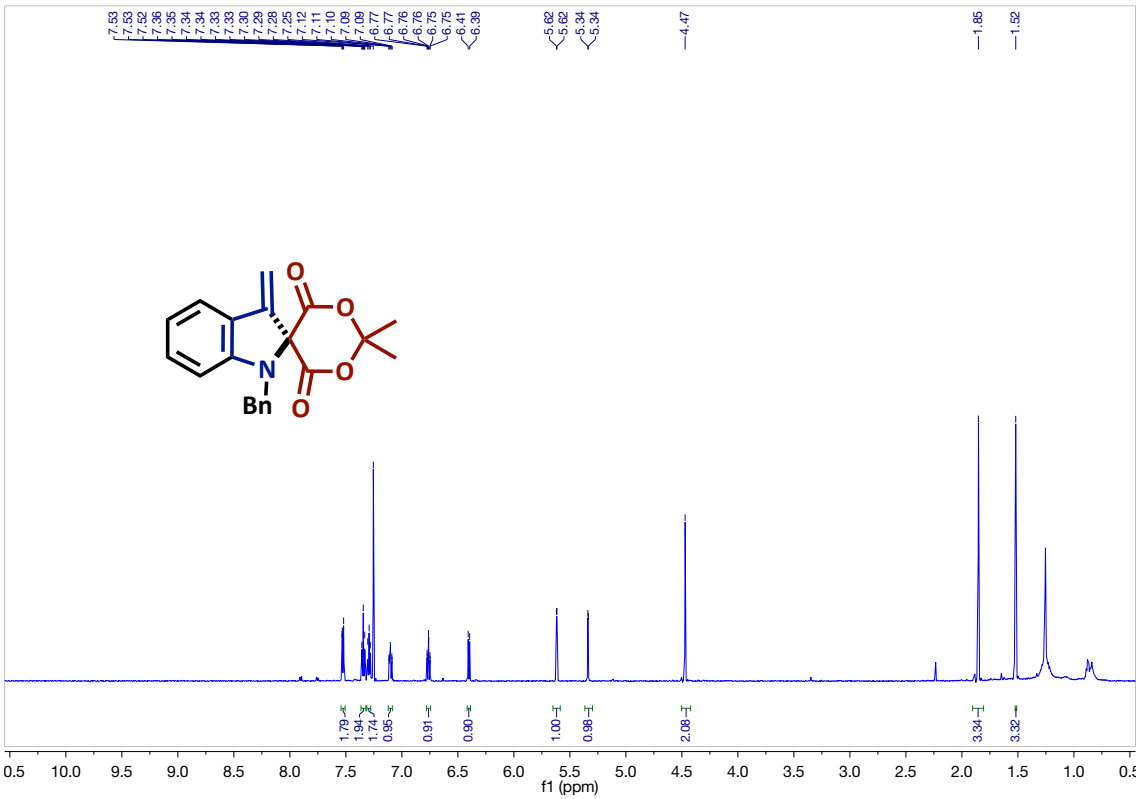
7.53
7.53
7.52
7.36
7.35
7.34
7.34
7.33
7.33
7.30
7.29
7.28
7.25
7.12
7.11
7.10
7.09
7.09
6.77
6.76
6.76
6.75
6.75
6.41
6.39
5.62
5.62
5.34
5.34
4.47
1.85
1.52
O
O
O
O
N
Bn
1.79
1.94
1.74
0.95
0.91
0.90
1.00
0.98
2.08
3.34
3.32
f1 (ppm)

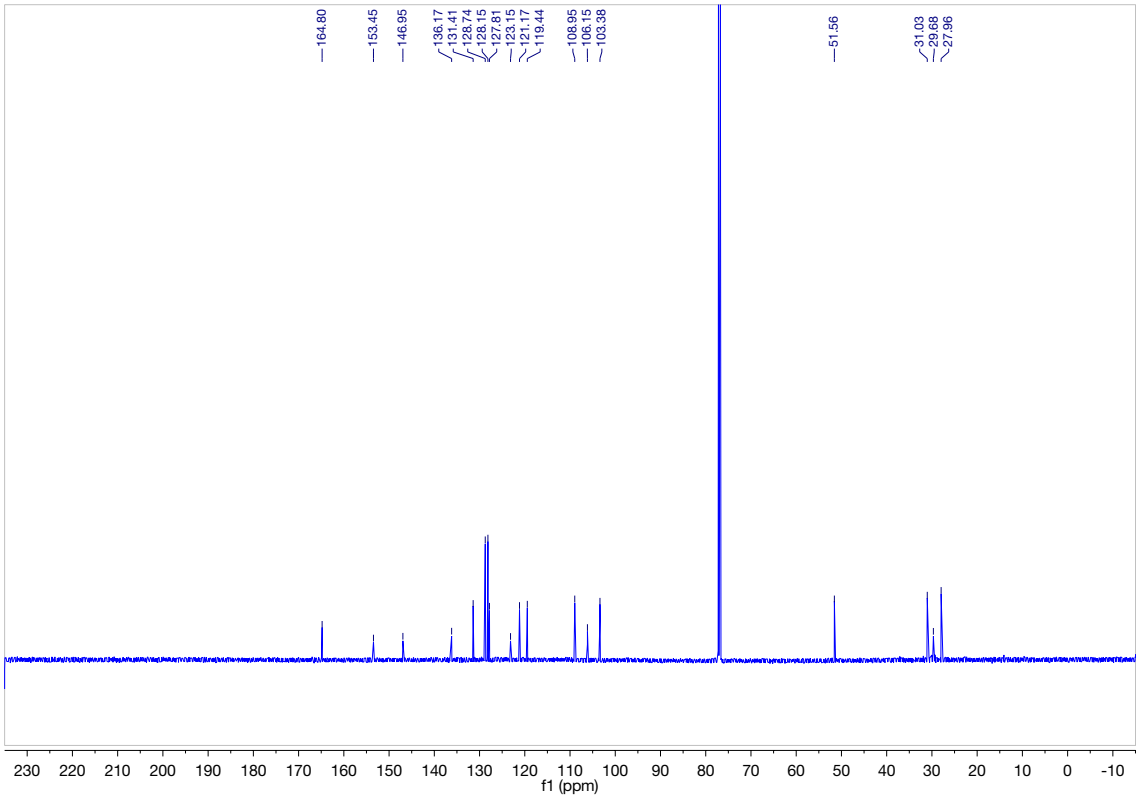
164.80
153.45
146.95
136.17
131.41
128.74
128.15
127.81
123.15
121.17
119.44
108.95
106.15
103.38
51.56
31.03
29.68
27.96
f1 (ppm)

CHAPTER 4

Metal Carbene Initiated Synthesis of

5-, 6-, and 7-membered Spirocarbocycles

4.1 INTRODUCTION

Research groups throughout the field of synthetic chemistry have focused great efforts on the stereoselective synthesis of spirocarbocycles with multiple stereocenters.[1] In particular, their focus has been centralized around the synthesis of six-membered spirocarbocycles, which are found in many biologically active natural and synthetic compounds, with one of the most well-known examples being gelsemine (**Figure 4.1**).

A common strategy for synthesizing all carbon spirocycles, such as the one found in gelsemine, involves the cyclization of the ends of two substituents on a fully-substituted carbon center that was previously installed on a pre-formed ring system (**Figure 4.2)**.[1] In very few cases are the both rings on the spirocarbocycle formed in the same step, thereby

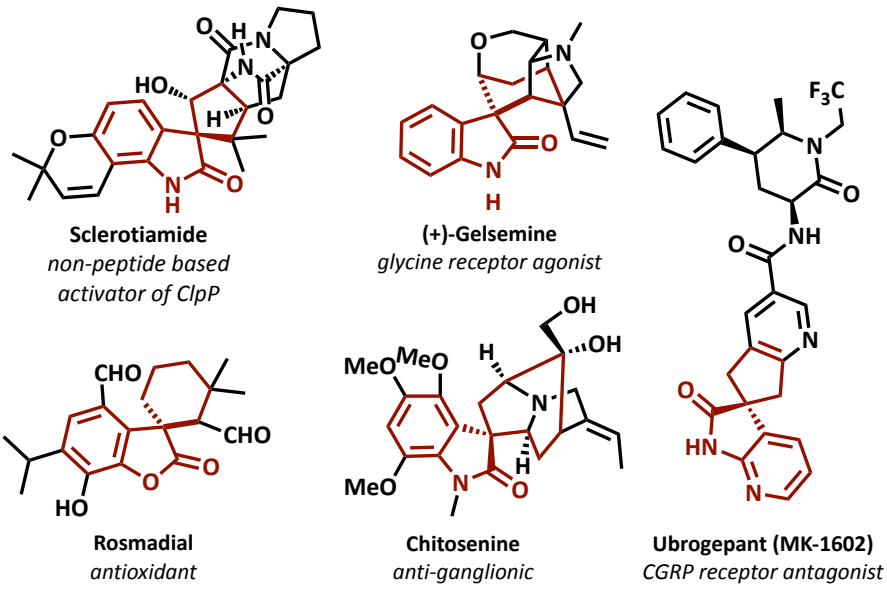

Figure 4.1. *Biologically active natural products and drug molecules containing 5-, 6-, and 7-membered spirocarbocycle core*

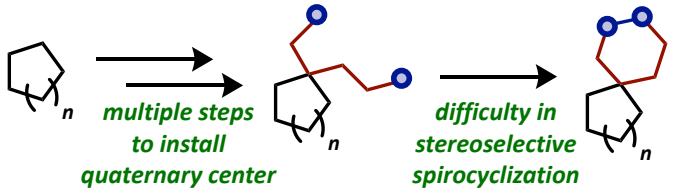

Figure 4.2. *Current synthetic challenges in synthesis all-carbon spirocycles*

making it extremely difficult to maintain stereocontrol in the desired product. With this challenge in mind, it was of great interest to our research group to induce de novo formation of both ring systems of the spirocarbocycle in a single step in hopes of maintaining control of the stereochemistry in the spirocenter bond forming process.

As previously mentioned, dual catalysis is a powerful way to assemble molecular complexity, such as the spirocarbocyclic motif, from readily available starting materials due

to the fact that multiple bonds, that are often difficult to install, are formed in one pot by simultaneous yet discrete catalytic events.[2] Other than being synthetically appealing, this approach allows for price efficiency in terms of reagents, solvents, and waste management as well as in time and effort.[3] Recently, significant efforts have been devoted to developing one-pot dual catalytic methods to achieve carbon-carbon bond formations[4], and we believed that dual catalysis would enable us to complete the task of forming both rings of the spirocarbocycle in one pot.

Given the success of our Rh(II)/Au(I) synergistic catalytic cocktail for the synthesis of γ-butyrolactones, tetrahydrofurans, spiroethers, and azaspiro-ring systems[5] we envisioned the possibility of using this catalytic system to synthesize oxindole hybridized spirocarbocycles, which are found in a wide range of bioactive natural products and pharmaceuticals such as sclerotiamide, gelsemine, chitosenine, and ubrogepant (**Figure 4.1**).[6] Spriocyclic hybrids containing oxindole units exhibit higher interaction with biological receptors by protein inhibition or ezymatic pathways.[6j] These hybrids have been recognized as having promising anticancer activity.[6j]

Our proposed retrosynthetic design for the synthesis of oxindole hybridized spirocarbocycles involved an intramolecular carbene sp^2 C–H functionalization/Conia-ene cascade as visualized in **Scheme 4.1b**. As seen in previous chapters, we have had great success with the Conia-ene cyclization, however, the generation of a masked "carbon nucleophile" that would insert into an active Rh(II) carbene and create our desired zwitterionic intermediate was a new challenge. Within the literature there are various types of C–H insertion reactions in which diazocarbonyl compounds participate, however,

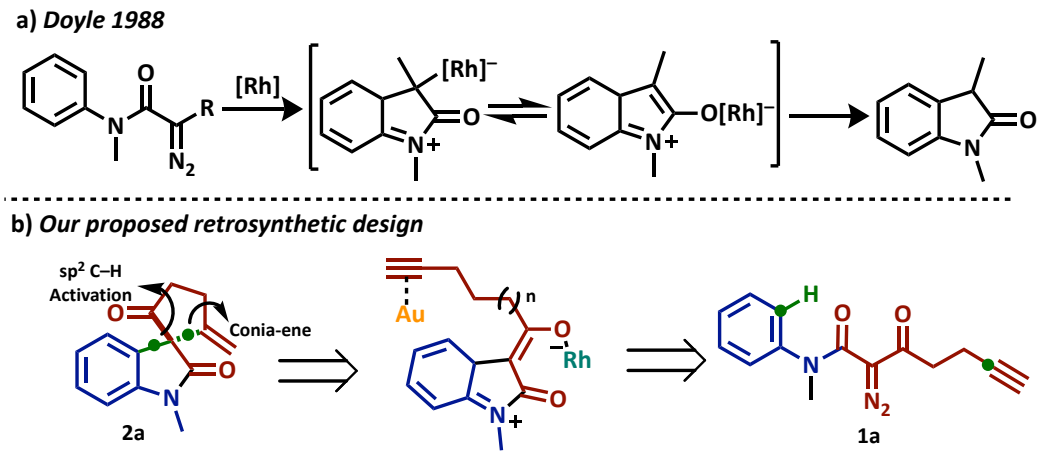

Scheme 4.1. *a) Initial development of sp² C–H functionalization by Doyle et al.*

b) Our retrosynthetic design using sp² C–H functionalization/Conia-ene cascade.

in 1998 Doyle et al. proposed the formation of a zwitterionic intermediate during the aromatic C–H insertion of *N*-aryl diazoamide into a Rh(II)-carbene (**Scheme 4.1a**).[7] This zwitterionic intermediate is electronically favorable because the positive charge of the intermediate is stabilized by the electron-rich oxindole resonance stabilization. This zwitterionic intermediate typically undergoes rapid proton transfer to generate C–H functionalized products, conversely, we desired to trap this intermediate with an alkyne.

With these insights from the literature in mind, we decided to design a substrate that linked an alkyne substituted acceptor/acceptor diazocarbonyl to an electron rich aniline to access a derivative of the *N*-aryl diazoamide that Doyle used in his initial 1988 study.[7] It is important to note that there were no previous reports of an intramolecular cascade reaction utilizing both sp² C–H functionalization[8] and a Conia-ene cascade[9]. This may be attributed to selectivity issues caused by the alkyne functionality in the carbene sp² C–H functionalization step, such as cyclopropenation[10] or carbene/alkyne metathesis.[11]

For the initial investigation, we took our newly synthesized diazo-acetoacetamide **1a** as a model substrate and exposed it to our previously developed Rh(II)/Au(I) synergistic catalytic cocktail that was used for our carbene heteroatom insertion/Conia-ene cyclizations. This reaction proceeded very cleanly, however, it provided a major product in which the characteristic ketone peak (~200 ppm) in ^{13}C NMR spectrum was missing. Further structural analysis revealed the formation of an unexpected *exo*-glycal product in 67% yield (**Scheme 4.2**). With this finding we quickly realized that application of our prolific Rh(II)/Au(I) synergistic catalytic cocktail would not be as direct when applying it to the synthesis of spirocarbocycles.

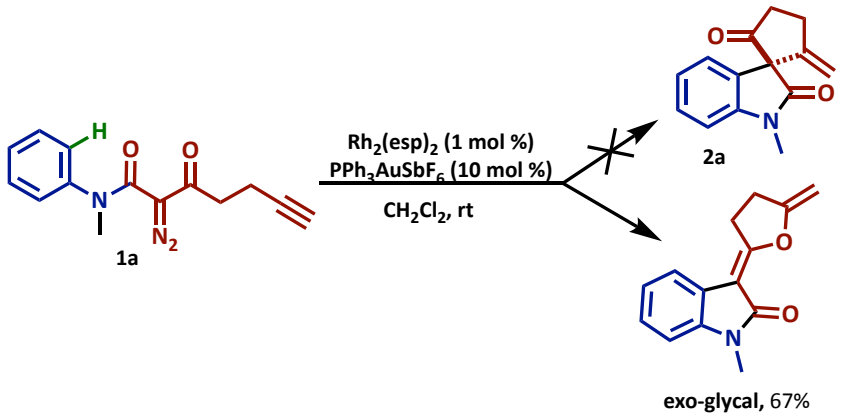

Scheme 4.2. *Unexpected results that provided an undesired exo-glycal via O-alkylation of alkyne instead of C-alkylation.*

4.2 Rh(II)/Au(I) DUAL CATALYSIS IN CARBENE sp^2 C–H FUNCTIONALIZATION/CONIA-ENE CASCADE

a) enol-*endo* Baldwin Rules

	enol-*endo*				
ring size	3	4	5	6	7
exo-tet	✖	✖	✖	✔	✔
exo-trig	✖	✖	✖	✔	✔
exo-dig			?	?	?

b) *O*- vs. *C*- Alkylation

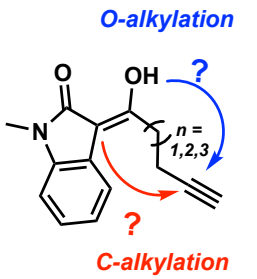

Figure 4.3. *a) Baldwin rules for enol-endo cyclizations; b) Visualization of two different modes of attack possible within our designed system*

Given the results from our initial experiment with **1a** in **Scheme 4.2**, we looked into the literature to examine enol*endo* intramolecular ring cyclizations.[12] After a survey of literature, we observed that while there were indeed few reports of 5–enol*endo*–*exo* dig cyclizations known in literature, it was only obtained in a trace amount as a byproduct with the more favorable 6-enol*endo*-*endo* dig cyclization.[12a–c] Next, we looked into Sir Jack E. Baldwin's original work in which he derived a different set of rules for enol*endo* cyclizations (**Figure 4.3a**).[12d–f] In these studies, Baldwin investigated the ring closure reactions of enol*endo*-*exo*-tet/trig systems; however, there was no report of enol*endo*-*exo*-dig cyclizations in his work.[10f] Keeping in mind the Baldwin rules for enol*endo*-*exo*-tet/trig systems and examples from literature of 6-enol*endo*-*exo* dig cyclizations, we hypothesized that through extension of the hydrocarbon chain length we would create a substrate with

a better trajectory to favor *C*-alkylation over *O*-alkylation to provide the desired spirocarbocycle (**Figure 4.3b**).[13]

4.2.1 INITIAL SCREENING OF CATALYTIC CONDITIONS

For the initial optimization, diazo-acetoacetamide **1b** was selected as the model substrate. The addition of **1b** to our previously optimized synergistic $Rh_2(esp)_2$/AgOTf/PPh_3AuCl and $Rh_2(esp)_2$/$AgSbF_6$/PPh_3AuCl catalytic conditions for carbene heteroatom insertion/Conia-ene cascades provided the sp^2 C–H functionalization product with instantaneous alkyne hydration to give a 1,5-dione **4b** at room temperature (**Table 4.1**, entry 1–2). This Markovnikov addition of water across a triple bond to generate ketones is a well-known practice and is generally initiated by strong Brønsted and Lewis acids.[12j–12l] In particular, the generation of the 1,5-dione is highly favorable due to the stabilized 6-membered transition state found in **intermediate-A** that promotes hydration.[12l] It is important to note this is the same type of intermediate that led to the formation of the undesired *exo*-glycal in our initial studies in **Scheme 4.2**.

As we have seen in previous chapters, Au(I)-catalyzed reactions involve [LAu][Y] as an active species, where L = any type of phosphine ligand and Y = TfO^-, SbF_6^- or a variety of other counter anions.[14] These electrophilic species are generated by the metal–ion exchange between PPh_3AuCl and AgY (Y = TfO^- or SbF_6^-) and are typically not isolated after formation due to their highly active nature, even though there is a risk of interference of silver with the catalytic process.[14] Assuming the highly cationic nature of a Ag(I) activated Au(I) salt was not ideal for this transformation, we decided to examine other Lewis acids

Table 4.1. *Optimization for the Synthesis of 6-Membered Spirocarbocycle*

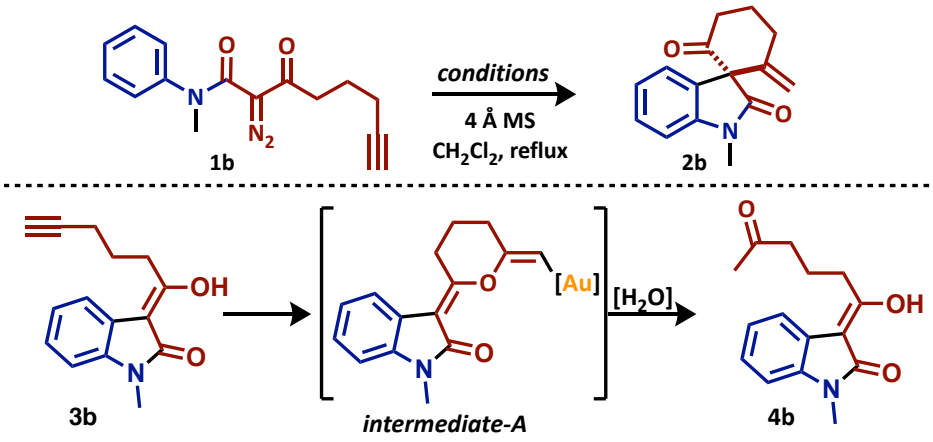

entry	catalysts	temp, t	yield (%)[b]
1	$Rh_2(esp)_2$/AgOTf/PPh_3AuCl	rt, 30 min	0[c]
2	$Rh_2(esp)_2$/$AgSbF_6$/PPh_3AuCl	rt, 30 min	0[c]
3	$Rh_2(esp)_2$/PPh_3AuCl/$(CuOTf)_2$-tol	reflux, 3 h	57
4	$Rh_2(esp)_2$/$(CuOTf)_2$-tol	reflux, 12 h	45
5	$Rh_2(esp)_2$/PPh_3AuCl	reflux, 12 h	32
6	$Rh_2(esp)_2$/$ZnCl_2$	reflux, 12 h	43
7	$Rh_2(OAc)_4$/PPh_3AuCl/$(CuOTf)_2$-tol	reflux, 3 h	31
8	$Rh_2(HFB)_4$[d]/PPh_3AuCl/$(CuOTf)_2$-tol	reflux, 3 h	63
9	**$Rh_2(HFB)_4$[d]/PPh_3AuCl/$(CuOTf)_2$-tol**	**reflux, 3 h**	**68**[e]
10	PPh_3AuCl/ $(CuOTf)_2$-tol	reflux, 12h	0[f]

[a] All optimization reactions were performed by adding a 0.5 M solution of **1b** (1.0 equiv.) into a 0.2 M solution of Rh(II) (1 mol %) and Lewis acid(s) (10 mol %) *via* syringe, unless otherwise noted all reactions were refluxed until starting material diazo was consumed. [b] Isolated yields after column chromatography. [c] Reaction conditions instantaneously hydrated the alkene to provide the 1,5-dione alkyne hydration product derived from **4a**. [d] HFB = heptafluorobutyrate. [e] Reaction ran with the addition of heat activated 4 Å MS (100 mg/1 mmol of **1b**).[f]Reaction conditions did not decompose **1b**, starting material remained.

known to promote Conia-ene cyclizations[9] in hopes of attenuating the level of activation of our active intermediate (**Table 4.1**). Recently hit has been shown that Cu(I) triflate can activate Au(I) salts to form stable cationic Au(I) complexes at elevated temperatures.[14] In 2013 Guérinot et al. hypothesized that a gradual, and possibly reversible, delivery of cationic Au(I) from a reservoir of stable PPh_3AuCl would create a more controlled reaction environment for their respective transformation.[14] The authors stated that the quick precipitation of AgCl makes any source of silver salt undesirable for this catalytic method, however within their study they. showed that Cu(I) triflate provided the desired attenuated reactivity. [14] With these insights in mind, we exposed diazo **1b** to a catalytic cocktail of $Rh_2(esp)_2/PPh_3AuCl/(CuOTf)_2$-tol at room temperature and only obtained the C–H functionalization product **3b** and no spirocarbocycle **2b**. However, in refluxing dichloromethane, the desired product **2b** was obtained in 57% yield after 3 hours (**Table 4.1**, entry 3).

Next, we wanted to determine if this reactivity was due to the Au(I)/Cu(I) Lewis acids acting in synergism, therefore we screened Au(I) and Cu(I) salts individually (**Table 4.1**, entry 4–5). When diazo **1b** was exposed to $Rh_2(esp)_2/(CuOTf)_2$-tol in refluxing dichloromethane, the reaction was found to be sluggish and spirocarbocycle **2b** was formed in 45% yield after refluxing for 12 hours. We also observed a sluggish reaction with the $Rh_2(esp)_2/PPh_3AuCl$ combination. It is well known that $ZnCl_2$ can efficiently catalyze Conia-ene cyclizations[15], therefore we screened a mixture of $Rh_2(esp)_2/ZnCl_2$ but did not achieve any significant improvement, only a 43% of the desired spirocarbocycle formed

after 12h refluxing in dichloromethane with a mixture of the undesired endo-alkene rearrangement product (**Table 4.1**, entry 6).

With our best Au(I)/Cu(I) Lewis acid combination, we then examined different dirhodium carboxylates known to decompose diazocarbonyls in our attempt to increase the yield of **2b** (**Table 4.1**, entry 7–9).[16] In a thorough study by Doyle et al. in 1998, he proposed that the process of aromatic C–H functionalization is more accurately described mechanistically as electrophilic aromatic substitution[7], therefore a more electrophilic Rh(II)-carbene would be most ideal for this transformation. With this insight in mind, we first screened $Rh_2(OAc)_4$, which creates a *less* electrophilic carbene as compared to $Rh_2(esp)_2$.[16] This Rh(II) salt decreased the yield of the desired transformation to 31%, providing solid evidence for validation of our hypothesis. Next, we screened the highly electrophilic $Rh_2(HFB)_4$ catalyst and the yield of the desired product increased to 63%, thereby validating the hypothesis of the need for an electrophilic carbene. Subsequently, we repeated these conditions in the presence of heat activated 4Å molecular sieves and the reaction yield was increased to 68%. Lastly, to ensure the necessity of Rh(II) in the system, we exposed **1b** to the Au(I)/Cu(I) catalytic conditions (**Table 4.1**, entry 10). However, under these conditions **1b** did not undergo decomposition to initiate the desired sp^2 C–H functionalization.

4.2.2 SYNTHESIS OF 5/6 OXINDOLE HYBRIDIZED SPIROCARBOCYCLES

With optimized conditions in hand, we then investigated the scope of this cascade sequence (**Scheme 4.3**). For our initial studies, we decided to probe the diastereoselectivity of the transformation. A phenyl substituted diazo was exposed to the optimized conditions

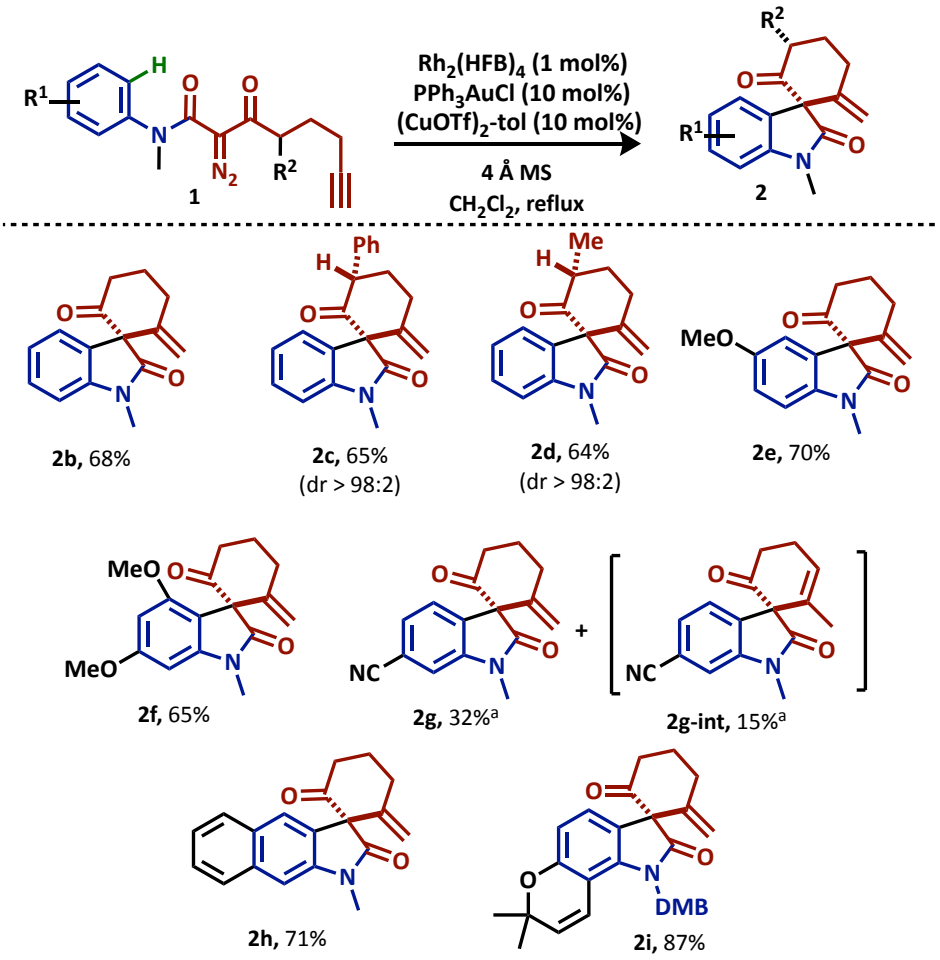

Scheme 4.3. *Scope of Rh(II)/Au(I)/Cu(I) catalyzed cascade for the synthesis of functionalized 6-membered oxindole hybridized spirocarbocycles.*

and underwent the desired transformation smoothly to obtain the corresponding spirocarbocycle **2c** in 65% yield with high diastereoselectivity. The aryl component of the

oxindole ring is trans to the side chain substituent on the ring formed during the Conia-ene cyclization. The stereochemical arrangement of the substituents was determined based on the coupling constants of the protons of interest (**Figure 4.4**). The coupling constant for the benzylic proton to the neighboring diastereotopic protons was J = 12.8 Hz for the axial-axial interaction and J = 6.4 Hz for the axial-equatorial interaction. This high diastereoselectivity was also maintained for the less bulky methyl substituted spirocarbocycle **2d**.

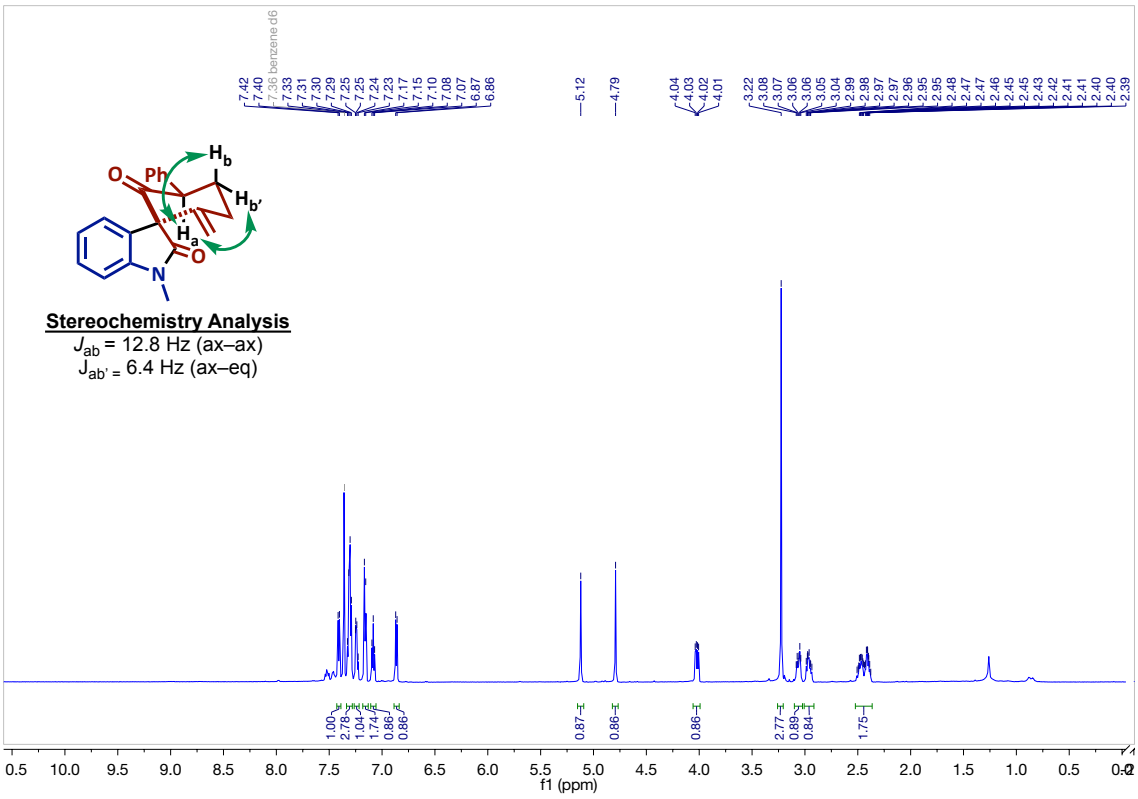

Figure 4.4. *Stereochemical analysis of* ***2c*** *via calculated coupling constants.*

Next, we looked into the electronic effects of the cascade transformation. Electron rich substrates were equally efficient as the non-electronically perturbed substrates,

producing the desired compounds **2e** and **2f** in 70% and 65% yields. Next, an electron poor diazo-acetoacetamide was synthesized and exposed to the optimized conditions. This substrate underwent the desired transformation to provide **2g**, albeit in a significantly lower 32% yield showing that electron withdrawing substituents on the aromatic ring have a substantial effect on the efficiency of the reaction. An extended reaction time of 14 hours was necessary for this substrate and caused alkene isomerization to the more thermodynamically favored product. which also contributed to the decreased yield of **2g**. Next, diazo-acetoacetamide derived from the corresponding naphthalenamine was examined and it gave the desired product **2h** in 71% yield with high regioselectivity for C–H functionalization. Subsequently, we synthesized a benzopyran substituted diazo-acetoacetamide and exposed it to our optimized reaction conditions. The desired spirocarbocycle **2i** was synthesized in 87% yield and afforded a scaffold which is found in many biologically active oxindole hybridized spirocarbocycles. [6e]

Lastly, we hypothesized our optimized conditions could be extended to the synthesis of spirobenzofuranones, a scaffold that is found in the biologically active natural product rosmadial (**Figure 4.1**). A phenol substituted diazo-acetoacetate was synthesized and exposed to the $Rh_2(HFB)_4$/PPh_3AuCl/$(CuOTf)_2$-tol catalytic cocktail and a complex mixture was obtained. Upon a literature survey, it was discovered that sp^2 C–H functionalization of phenol substituted diazo-acetates is highly dependent on the nature of the ligand (therefore the corresponding electronics) of the Rh(II) catalyst.[17] In literature, Rh(II) perfluorobutyrate catalysts provide a cycloheptatrienyl ring expanded product over sp^2 C–H functionalization.[17] Therefore, $Rh_2(OAc)_4$ was used instead of $Rh_2(HFB)_4$ to obtain

the desired sp^2 C–H functionalization and intramolecular Conia-ene cyclization to provide **2j** in 72% yield (**Scheme 4.4**).

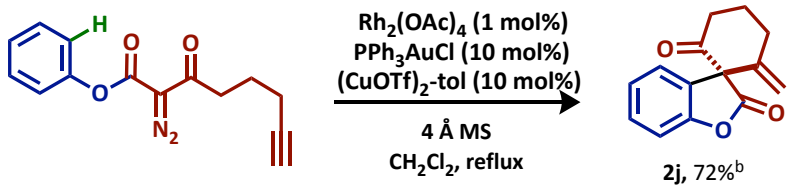

Scheme 4.4. *Syntheis of spriobenzofuranone through modified conditions using $Rh_2(OAc)_4$.*

4.2.3 SYNTHESIS OF 5/7 OXINDOLE HYBRIDIZED SPIROCARBOCYCLES

In order to expand the applicability of this methodology to larger ring cyclizations, we decided to synthesize a diazo-acetoacetamide with an extended carbon chain which would provide a seven-membered spirocarbocyle. Carbocyclic seven-membered rings are common structural units that can be found in a variety of polycyclic natural products that are of considerable medicinal interest. [6j] However, unlike smaller ring sizes, the construction of seven-membered rings is more challenging, and their syntheses are limited in literature. [6j]

We hypothesized that the application to seven-membered scaffolds would not be simple, typically seven-membered rings are much more difficult to form than the corresponding five- and six-membered rings. This is due to two factors: entropy and enthalpy. Entropy favors the formation of smaller rings; however, our model substrate would only give access to either a seven-membered (7-*exo*-dig) cyclization or an eight-membered (8-*endo*-dig) cyclization. Therefore, we knew entropic barriers would not be an

issue. Nevertheless, overcoming enthalpic barriers would play a major role. When we consider the strain in the transition state leading to our desired ring cyclization, we see that transannular repulsion through the unfavorable "flagpole" interactions becomes an issue. With these thermodynamic insights in mind, we set out to apply our methodology to the synthesis of seven-membered spirocarbocycles.

When the extended diazo-acetoacetamide was exposed to the optimized reaction conditions identified in **Table 4.1**, the reaction stalled at the C–H functionalization step to provide the corresponding insertion compound, proving that the seven-membered ring formation needed more energy to proceed. Therefore, we increased the catalytic loading of PPh_3AuCl and $(CuOTf)_2$-tol to 20 mol% and allowed a longer reaction time and the desired product **2k** was isolated in a 49% yield. Next, we looked into the diastereoselectivity of this reaction with a phenyl-substituted seven-membered diazo-acetoacetamide. The desired product **2l** was isolated in 54% yield as a single diastereomer. The relative stereochemistry of the phenyl substituent and spiro-junction in **2l** was determined based on the nuclear Overhauser effect (nOe) correlations and was further confirmed by the single crystal structure using X-Ray crystallography (**Figure 4.5**). Similar to the six-membered spirocarbocycle, the aryl component of the oxindole is trans to the stereo-center substituent on the ring formed during the Conia-ene cyclization. Lastly, **2m** was synthesized in a 47% yield and the high stereoselectivity was also maintained with the less bulky methyl substituent on the side chain.

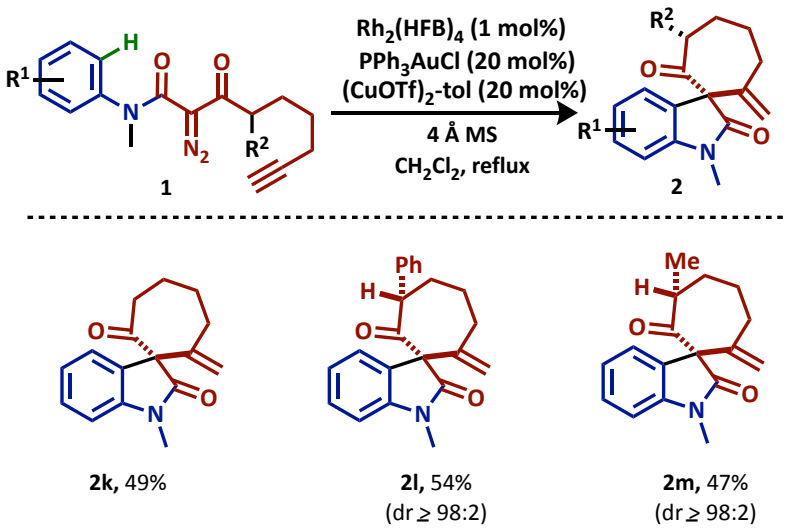

Scheme 4.5. *Synthesis of 7-membered spirocarbocycle oxindole hybrids*

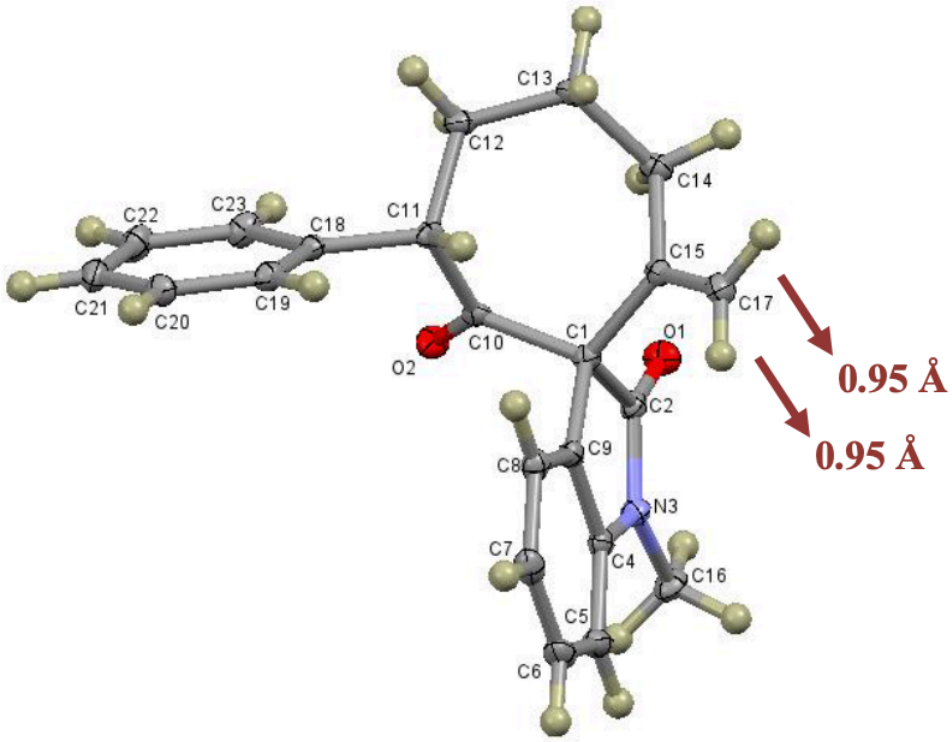

Figure 4.5. *Cyrstal structure of* ***2l****;*

C–H bond lengths in resulting alkene functionality = 0.95 Å.

4.2.4 SYNTHESIS OF 5/5 OXINDOLE HYBRIDIZED SPIROCARBOCYCLES

After the successful formation of the 6- and 7-membered oxindole hybridized spirocarbocycles, we turned our attention to the synthesis of 5-membered hybrids. Scaffolds of this type are found in a variety of biologically active natural products. [6a, 6e, 6f] Due to the prevalence of this core in nature, it was a great desire of ours to access the corresponding spirocyclization through our optimized methodology. Because of our failed attempt at a 5-membered spirocyclization with diazo **1a** in **Scheme 4.2**, we hypothesized that by synthesizing mono-carbonyl diazo **1n** we would create a substrate that has a more favorable trajectory to prefer *C*-alkylation over the undesired *O*-alkylation. We would also avoid the possibility of forming **intermediate**-**A** as seen in **Table 4.1** that promotes the undesired *O*-alkylation by excluding the additional carbonyl ketone. Our newly designed substrate would proceed through a well-known 5-*exo*-dig cyclization that is similar to work published by the Toste group.[18] Furthermore, all enol*exo* cyclizations for the tet/trig/dig systems follow the original Baldwin rules as seen in our previous work[5, 19] with Rh(II)-carbene initiated heteroatom insertion/Conia-ene cascade cyclizations, therefore this substrate possessed the ideal design to achieve a successful reaction.

For the initial optimization we exposed **1n** to our optimized conditions that provided the 6- and 7-membered spirocarbocycles. After refluxing in dichloromethane for three hours, this catalytic combination of $Rh_2(HFB)_4$/PPh_3AuCl/$(CuOTf)_2$-tol provided the sp^2 C–H functionalization product **3n** only (**Table 4.2**, entry 1). We hypothesized that the mild activation of PPh_3AuCl with $(CuOTf)_2$-tol was not enough to catalyze this reaction, therefore we decided to attempt this transformation with our previously developed

Table 4.2. *Optimization for the Synthesis of 5-Membered Spirocarbocycle*

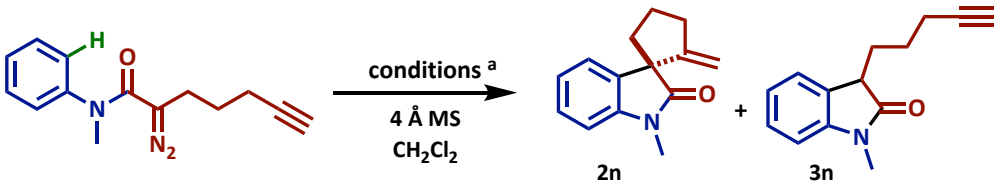

entry	catalysts	temp, t	yield (%)[b]
1	$Rh_2(HFB)_4/PPh_3AuCl/(CuOTf)2\text{-}tol$	reflux, 3 h	0[c]
2	$Rh_2(HFB)_4/PPh_3AuCl/AgSbF_6$	rt, 2 h	53
3[d]	**$PPh_3AuCl/AgSbF_6$**	**rt, 12 h**	**67**

[a] For entries 1 and 2: reactions were performed by adding a 0.5 M solution of **1n** (1.0 equiv) into a 0.2 M solution of Rh(II) (1 mol %) and Lewis acid(s) (10 mol %), and heat activated 4 Å MS (100 mg/mmol) via syringe; Reactions were stirred at the designated temperature until **1n** was consumed. [b] Isolated yields. [c] Reaction provided only the sp^2 C–H activation product. [d] For entry 3: reaction was performed by adding a 0.5 M solution of **1n** (1.0 equiv.) into a 0.2 M solution of PPh_3AuCl (20 mol %) and $AgSbF_6$ (20 mol %) via syringe, and was stirred at rt until desired product formed.

Rh(II)/Au(I)/Ag(I) conditions (**Table 4.2**, entry 2). This combination provided the desired compound **2n** in a 53% isolated yield after reacting for two hours. Interestingly, we did not observe any hydration product of the alkyne functionality as previously observed for the corresponding six-membered Conia-ene cyclization.

In an attempt to increase the yield of **2n** we conducted a literature survey and found that mono-carbonyl diazos such as **1n** can readily decompose under gold-catalyzed conditions to generate a gold-carbenoid.[20] With this insight, we hypothesized that the entire transformation of **1n** to **2n** could be catalyzed with Au(I) alone. When **1n** was added to a solution of $PPh_3AuCl/AgSbF_6$ and stirred at room temperature for 12 hours, the

diazocarbonyl was consumed to provide complete conversion to **2n** without any uncyclized sp^2 C–H functionalization product **3n** present.

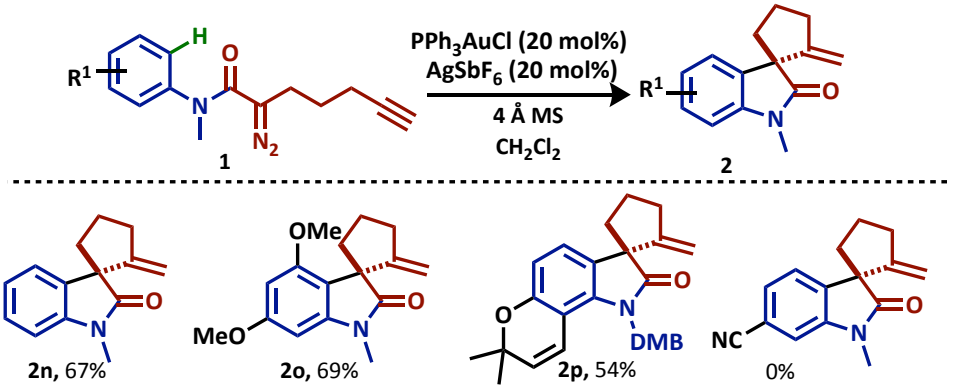

Scheme 4.6. *Scope of Au(I)/Ag(I) catalyzed cascade for the synthesis of functionalized 5-membered oxindole hybridized spirocarbocycles.*

With these newly optimized conditions in hand we decided to look into the electronic effects for this transformation (**Scheme 4.6**). Electron rich aromatics were accommodated with equal efficiency as the parent compound (**2o**). Furthermore, the benzopyran fused spirocarbocycle **2p** was also obtained in a moderate 54% yield under these reaction conditions. The core of **2p** can be found in the natural product, sclerotiamide, which has recently been identified by Duerfeldt et al. as the first non-peptide-based natural product activator of bacterial caseinolytic protease P (ClpP) (**Figure 4.1**).[6a] It is important to note that the electron deficient substrate could not be accessed with this methodology. The reaction stalled at the sp^2 C–H functionalization presumably due to the decreased nucleophilicity of the oxindole in the intramolecular Conia-ene cyclization.

4.2.5 MECHANISTIC INSIGHTS

To probe the mechanism of this transformation and determine if synergy was necessary to obtain the desired oxindole hybridized spirocarbocycles, we synthesized insertion compound **3b** and isolated it as the enol tautomer of the β-keto amide. We exposed this substrate to $PPh_3AuCl/(CuOTf)_2$-tol in refluxing dichloromethane and **2b** was isolated in 84% yield. This suggests the possibility of a non-synergistic stepwise transformation involving a carbene sp^2 C–H functionalization and subsequent Conia-ene cyclization (**Scheme 4.7**).

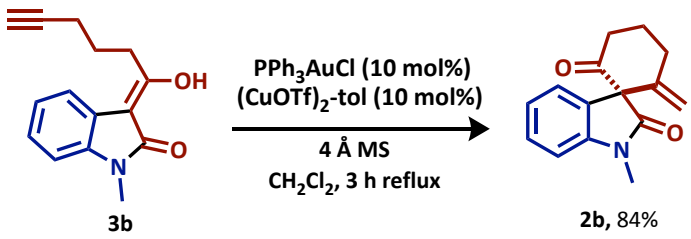

3b **2b,** 84%

Scheme 4.7. *Synthesis of **2b** from isolated insertion compound.*

To further probe the mechanism, we synthesized a variety of deuterium labeled diazo compounds. Diazo acetoacetamide **1q** was synthesized to examine the kinetic isotope effect of the reaction and validate whether the transformation was through a cyclopropanation or electrophilic aromatic substitution mechanism (**Scheme 4.8**). In the literature, it has been stated that typical k_H/k_D values for electrophilic aromatic substitution mechanisms are less than 1.3 unless the formation of the initial sigma-complex from nucleophilic attack of the aromatic ring onto the electrophile is reversible. [17] Therefore, when we observed a $k_H/k_D = 1$ in this experiment we were able to conclude that the

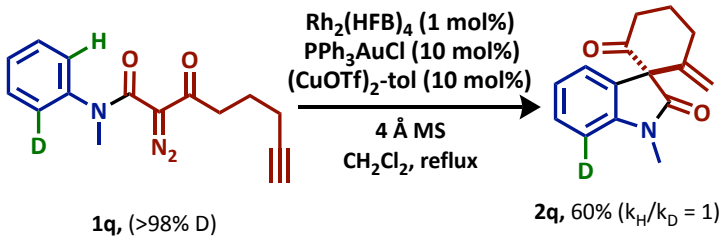

Scheme 4.8. *Deuterium labeling experiment probing kinetic isotope effect for C–H functionalization.*

mechanism is proceeding through electrophilic aromatic substitution as originally proposed by Doyle in 1998 and also Hu et al. in their work featuring a similar sp^2 C–H functionalization intermediate.

Next, the penta-deuterated diazo **1r** was synthesized and exposed to the optimized reaction conditions to provide **2r** (**Scheme 4.9**). Interestingly no deuterium incorporation was observed in the resulting alkene functionality of **2r**, suggesting the possibility of an intermolecular 1,2-proton transfer. As seen in **Scheme 4.7**, the transformation has a high likelihood of proceeding through an enol-intermediate where the corresponding deuterium transferred during the C–H functionalization can now be exchanged at a high

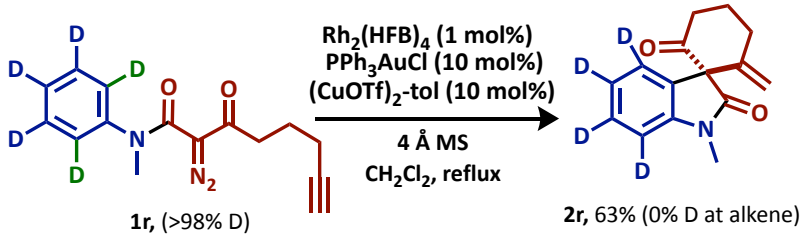

Scheme 4.9. *Deuterium labeling experiment probing inter- vs intra- molecular deuterium transfer.*

rate as a deuterated enol. This exchange is likely occurring with the minimal moisture present in the reaction medium. Therefore, in the resultant Conia-ene cyclization we are not observing any deuterium incorporation on the alkene. This experiment provided additional conclusive evidence of the stepwise transformation.

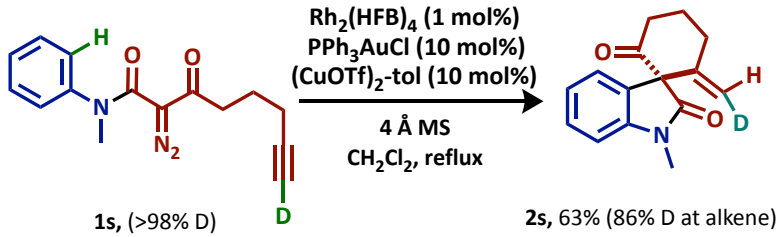

Scheme 4.10. *Deuterium labeling experiment giving insight into gold complexation.*

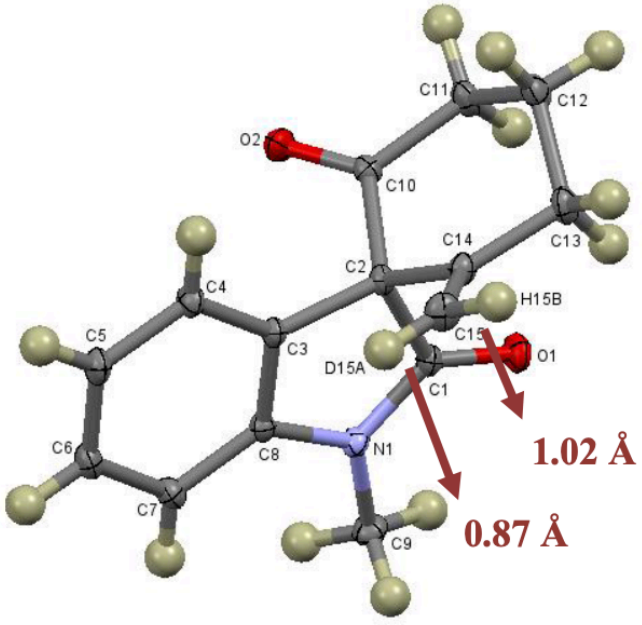

Figure 4.6. *Crystal structure of* ***2s****; C–D bond length = 0.87 Å; C–H bond length = 1.02 Å.*

Lastly diazo-acetoacetamide **1s** was synthesized with a deuterium incorporated on the alkyne. When this substrate was exposed to the optimized conditions, the desired product **2s** was obtained in good yield with 86% deuterium incorporation at the resulting alkene functionality (**Scheme 4.10)**. The deuterium was found to be syn to the carbonyl functionality as observed in our previous spiroether work and by the Toste group. [9a] The deuterium orientation was further confirmed by the single crystal structure using X-ray crystallography (**Figure 4.6**). Upon analysis, the C–D bond length, which was 0.87 Å, was found to be significantly shorter than the C–H bond length, which was 1.02 Å. [21] The results from this deuterium labeling experiment suggest the possibility of an equilibrium between an alkyne-π complex with gold and a gold acetylide.[22]

Table 4.3. *Attempted Optimization of Asymmetric Spirocyclization*

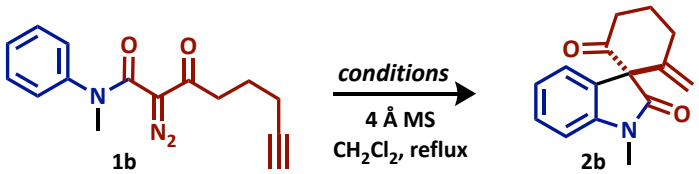

Entry	Catalysts[a]	Ligand	Yield (%)	% ee
1	Rh_2(*R*-DOSP)$_4$ /PPh_3AuCl/$(CuOTf)_2$⋅tol	–	52	0
2	$Rh_2(HFB)_4$/L1$(AuCl)_2$/$(CuOTf)_2$⋅tol	L1	44	0
3	$Rh_2(HFB)_4$/PPh_3AuCl/$(CuOTf)_2$⋅tol/L2	L2	< 5	0

[a] Catalyst loading: 1 mol% of Rh(II), 10 mol % of Au(I), 10 mol % of Cu(I), 11 mol% ligand

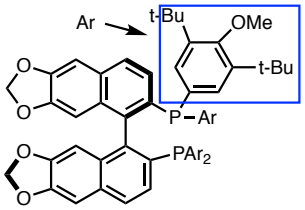

L1 = (*R*)-DTBM-SEGPHOS

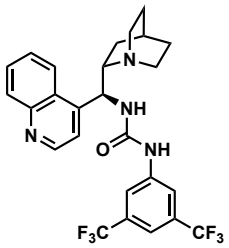

L2 = Urea-Cinchona Ligand[6]

In an attempt to induce asymmetry in our methodology (**Table 4.3**), we attempted the cascade reaction with chiral rhodium salt Rh_2(*S*-DOSP)$_4$, PPh_3AuCl, $(CuOTf)_2$-tol, and our model six-membered diazo-acetoacetamide. Unfortunately no enantiomeric excess (ee) was observed using chiral Rh(II) salts. We also attempted the cascade reaction with gold and copper bearing chrial ligands but did not induce ee in the resulting spirocarbocycle.

The findings identified by our mechanistic probing experiments in combination with evidence found during the development of our substrate scope allowed us to propose a mechanism depicted in **Scheme 4.11**. First the diazo is decomposed by the metal catalyst

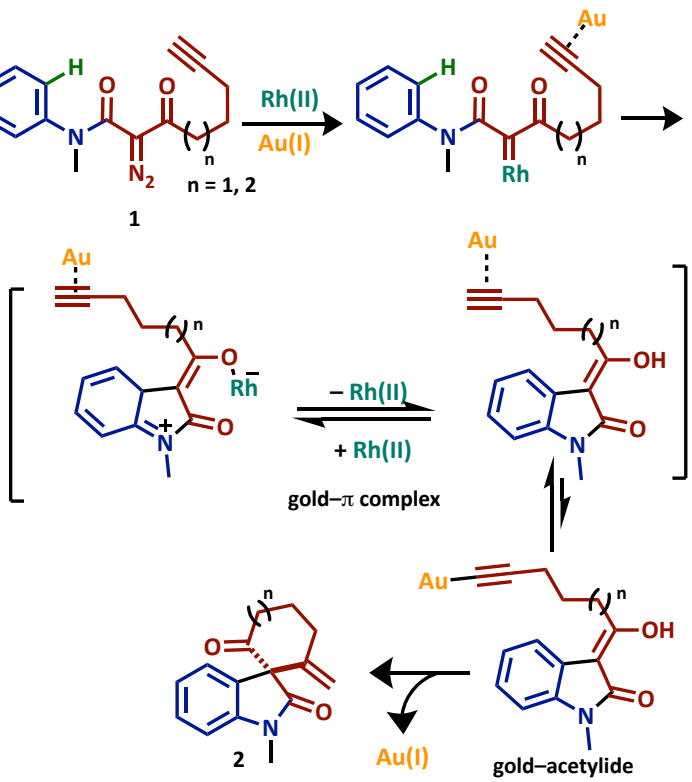

Scheme 4.11. *Proposed mechanism through a stepwise C–H functionalization and Conia-ene cascade cyclization.*

to form a metal carbene that undergoes a sp^2 C–H functionalization to provide an alkyne-gold activated oxindole zwitterionic intermediate. This substrate then undergoes a gold(I) activated Conia-ene cyclization to provide the desired spirocarbocycle. As seen through the deuterium loss in **Scheme 4.10**, gold activation of the alkyne is in equilibrium between the gold-acetylide and gold-π complex, with the equilibrium favoring the π-complex.

4.3 SUMMARY

Upon completion of this work, a general approach to the stereoselective synthesis of 5-, 6-, and 7-memebered oxindole hybridized spirocarbocycles was developed. Extension of our previously identified Rh(II)/Au(I) catalytic cocktail was proven to be successful, although a modification to the activation of Au(I) by Cu(I) was needed to obtain the desired reactivity. The experimental findings within this work led to the development of a novel bond disconnection in the synthesis of a variety of spirocarbocycles. The next logical step in building upon this methodology is to complete computational analyses to provide insight into how one could effectively induce asymmetry in the system.

4.4 REFERENCES

[1] S. D. Karyakarte, C. Um, I. A. Berhane, S. R. Chemler, *Angew. Chem. Int. Ed.* **2018**, *57*, 12921–12924.

[2] For reviews on dual catalysis, see: a) A. E. Allen, D. W. C Macmillan, *Chem. Sci.* **2012**, *3,* 633−658. b) D. –F. Chen, Z. –Y. Han, X. –L. Zhou, L. –Z. Gong, *Acc. Chem. Res.* **2014**, *47*, 2365−2377. c) S. Matsunaga, M. Shibasaki, *Chem. Commun.* **2014**, *50,* 1044−1057. d) M. H. Wang, K. A. Scheidt, *Angew. Chem. Int., Ed.* **2016**, *55*, 14912−14922. e) Y. Y. Ren, S. F. Zhu, Q. L. Zhou, *Org. Biomol. Chem.* **2018**, *16*, 3087–3094. f) B. Zimmerman, J. Burkhard, M. Beller, *Angew. Chem. Int. Ed.* **1999**, *38*, 2372–2375. g) N. Jeong, S. D. Seo, J. Y. Sin, *J. Am. Chem. Soc.* **2000**, *122*, 10220–10221.

[3] For the importance of efficiency in organic synthesis, see: a) B. M. Trost, *Science,* **1991**, *254*, 1471−1477. b) P. A. Wender, V. A. Verma, T. J. Paxton, T. H. Pillow, *Acc. Chem. Res.* **2008**, *41*, 40−49. c) N. Z. Burns, P. S. Baran, R. W. Hoffmann, *Angew. Chem. Int., Ed.* **2009**, *48*, 2854−2867. d) K. C. Nicolaou, J. S. Chen, *Chem. Soc. Rev.* **2009**, *38*, 2993–3009.

[4] For recent examples of dual transition metal catalysis with rhodium, see: a) Ö. Aksın-Artok, N. Krause, *Adv. Synth. Catal.* **2011**, *353*, 385–391. b) J. J. Hirner, Y. Shi, S. A. Blum, *Acc. Chem. Res.* **2011**, *44*, 603–613. c) Z.-S. Chen, L.-Z. Huang, H. J. Jeon, Z. Xuan, S. Lee, *ACS Catal.* **2016**, *6*, 4914–4919. d) Z. S. Chen, X. Y. Huang, J. M. Gao, K. Ji, *Org. Lett.* **2016**, *18*, 5876–5879. e) Y. N. Wu, T. Xu, R. Fu, N. N. Wang, W. J. Hao, S. L. Wang, G. Li, S. J. Tu, B. Jiang, *Chem. Commun.* **2016**, *52*, 11943–11946. f) Y. Li, R. Zhang, A. Ali, J.

Zhang, X. Bi, J. Fu, *Org. Lett.* **2017**, *19*, 3087–3090. g) Z.-S. Chen, X.-Y. Huang, L.-H. Chen, J.-M. Gao, K. Ji, *ACS Catal.* **2017**, *7*, 7902–7907. h) L.-Z. Huang, Z. Xuan, H. J. Jeon, Z.-T. Du, J. H. Kim, S.-G. Lee, *ACS Catal.* **2018**, *8*, 7340–7345. i) L. Jiang, W. Jin, W. Hu, *ACS Catal.* **2016**, *6*, 6146–6150. j) W. Hengbin, J. R. Denton, H. M. Davies, *Org. Lett.* **2011**, *13*, 4316–4319. k) M. M. Hansmann, A. S. K. Hashmi, M. Lautens, *Org. Lett.* **2013**, *15*, 3226–3229. l) X. Xu, P. Y. Zavalij, W. Hu, M. P. Doyle, *J. Org. Chem.* **2013**, *78*, 1583–1588. m) K. Liu, C. Zhu, J. Min, S. Peng, G. Xu, J. Sun, *Angew. Chem. Int., Ed.* **2015**, *54*, 12962–12967.

[5] a) A. C. Hunter, S. C. Schlitzer, I. Sharma, *Chem. Eur. J.* **2016**, *22*, 16062–16065. b) A. C. Hunter, S. C. Schlitzer, J. C. Stevens, B. Almutwalli, I. Sharma, *J. Org. Chem.* **2018**, *83*, 2744–2752. c) A. C. Hunter, B. Almutwalli, A. Bain, I. Sharma, *Tetrahedron* **2018**, *74*, 5451–5457.

[6] For examples of biologically active spirocarbocycles and their importance, see: a) N. P. Lavey, J. A. Coker, E. A. Ruben, A. S. Duerfeldt, *J. Nat. Prod.* **2016**, *79*, 1193–1197. b) A. Madin, C. J. O'Donnell, T. Oh, D. W. Old, L. E. Overman, M. Sharp, *J. Am. Chem. Soc*. **2005**, *127*, 18054–18065. c) T. Harada, J. Shimokawa, T. Fukuyama, *Org. Lett.* **2016**, *18*, 4622–4625. d) M. R. Stephen, M. T. Rahman, V. Tiruveedhula, G. O. Fonseca, J. R. Deschamps, J. M. Cook, *Chem. Eur. J.* **2017**, *23*, 15805–15819. e) E. V. Mercado-Marin, R. Sarpong, *Chem. Sci.*, **2015**, *6*, 5048–5052. f) E. V. Mercado-Marin, P. Garcia-Reynaga, S. Romminger, E. F. Pimenta, D. K. Romney, M. W. Lodewyk, D. E. Williams, R. J. Andersen, S. J. Miller, D. J. Tantillo, R. G. Berlinck, R. Sarpong, *Nature*, **2014**, *509*, 318–324. g) Y.-J. Zheng, C. M. Tice, *Expert Opin. Drug Discov.* **2016**, *11*, 831–834. h) Y. Zheng,

C. M. Tice, S. B Singh, *Bioorg. Med. Chem. Lett.* **2014,** *24*, 3673–3682. i) Phase 2 clinical trials of MK-1602. Available from: https://clinicaltrials.gov/ct2/results?term=MK-1602&pg=1 j) X. Li, R. E. Kyne, T. V. Ovaska, *J. Org. Chem.* **2007**, *72*, 6624–6627.

[7] M. P. Doyle, M. A. McKervey, T. Ye, *Modern Catalytic Methods for Organic Synthesis with Diazo Compounds: From Cyclopropanes to Ylides*, Wiley, **1998**.

[8] a) M. Kischkewitz, C. G. Daniliuc, A. Studer, *Org. Lett.* **2016**, *18*, 1206–1209. b) H. M. L. Davies, S. J. Hedley, *Chem. Soc. Rev*. **2007**, *36*, 1109–1119. c) H. Qiu, M. Li, L.-Q. Jiang, F.-P. Lv, L. Zan, C.-W. Zhai, M. P. Doyle, W.-H. Hu, *Nat. Chem*. **2012**, *4*, 733–738. d) A. G. H. Wee, B. Liu, L. Zhang, *J. Org. Chem.* **1992**, *57*, 4404–4414. e) K. Yamamoto, Z. Qureshi, J. Tsoung, G. Pisella, M. Lautens, *Org. Lett.* **2016**, *18*, 2016.

[9] a) J. J. Kennedy-Smith, S. T. Staben, F. D. Toste, *J. Am. Chem. Soc.* **2004**, *126*, 4526–4527. b) B. K. Corkey, F. D. Toste, *J. Am. Chem. Soc.* **2005**, *127*, 17168–17169. c) D. Hack, M. Bluemel, P. Chauhan, A. R. Philipps, D. Enders, *Chem. Soc. Rev.* **2015**, *44*, 6059–6093. d) M. L. Clarke, M. B. France, *Tetrahedron*, **2008**, *64*, 9003–9031.

[10] a) J. F. Briones, J. Hansen, K. I. Hardcastle, J. Autschbach, H. M. L. Davies, *J. Am. Chem. Soc.* **2010**, *132*, 17211–17215. b) T. Goto, K. Takeda, N. Shimada, H. Nambu, M. Anada, M. Shiro, K. Ando, S.-I. Hashimoto, *Angew. Chem. Int., Ed.* **2011**, *50*, 6803–6808.

[11] a) S. Jansone-Popova, J. A. May, *J. Am. Chem. Soc.* **2012**, *134*, 17877–17880. b) H. Qiu, Y. Deng, K. O. Marichev, M. P. Doyle, *J. Org. Chem.* **2017**, *82*, 1584–1590.

[12] For examples of 5 and 6 enolendo cyclizations see: a) C.-L. Deng, R.-J. Song, S.-M. Guo, Z.-Q. Wang, J.-H. Li, *Org. Lett.* **2007**, *9*, 5111–5114. b) N. Huwyler, E. M. Carreira, *Angew. Chem. Int. Ed.* **2012**, *51*, 13066–13069. c) X. Xiong, Y. Li, Z. Lu, M. Wan, J. Deng, S. Wu,

H. Shao, A. Li, *Chem. Commun.* **2014**, *50*, 5294–5297. For more references on Baldwin rules, see: d) J. E. Baldwin, *J. Chem. Soc., Chem. Commun.* **1976**, 734−736; e) J. E. Baldwin, L. I. Kruse, *J. Chem. Soc., Chem. Commun*. **1977**, 233–235. f) J. E. Baldwin, M. J. Lusch, *Tetrahedron*, **1982**, *38*, 2939–2947. g) C. D. Johnson, *Acc. Chem. Res*. **1993**, *26*, 476–482. h) I. V. Alabugin, V. I. Timokhin, J. N. Abrams, M. Manoharan, I. Ghiviriga, R. Abrams, *J. Am. Chem. Soc*. **2008**, *130*, 10984−10995. i) K. Gilmore, I. V. Alabugin, *Chem. Rev*. **2011**, *111*, 6513–6556. j) Q. Peng, R. S. Paton, *Acc. Chem. Res.* **2016**, *49*, 1042–1051. For insights into alkyne hydration see: k) K. Imi, K. Imai, K. Utimoto, *Tetrahedron Lett.* **1987**, *28*, 3127–3130. l) F. Chevallier, B. Breit, *Angew. Chem. Int. Ed.* **2006**, *45*, 1599–1602.

[13] a) M. Kodpinid, Y. Thebtaranonth, *Tetrahedron Lett*. **1984**, *25*, 2509–2512. b) I. V. Alabugin, K. Gilmore, *Chem. Commun.* **2013**, *49*, 11246–11250. c) K. Gilmore, R. K. Mohamed, I. V. Alabugin, *WIREs Comput. Mol. Sci.* **2016**, *6*, 487–514. d) M. Blümel, D. Hack, L. Ronkartz, C. Vermeeren, D. Enders, *Chem. Commun.* **2017**, *53*, 3956–3959.

[14] A. Guerinot, W. Fang, M. Sircoglou, C. Bour, S. Bezzenine-Lafollee, V. Gandon, *Angew. Chem. Int., Ed.* **2013**, *52*, 5848–5852.

[15] F. Urabe, S. Miyamoto, K. Takahashi, J. Ishihara, S. Hatakeyama, *Org. Lett.* **2014**, *16*, 1004–1007.

[16] A. C. Hunter, K. Chinthapally, I. Sharma, *Eur. J. Org. Chem.* **2016**, 2260–2263.

[17] M. Hrytsak, T. J. Durst, *Chem. Soc., Chem. Commun*. **1987**, 1150–1151.

[18] B. K. Corkey, F. D. Toste, *J. Am. Chem. Soc*. **2007**, *129*, 2764–2765.

[19] a) K. Chinthapally, N. P. Massaro, I. Sharma, *Org. Lett.* **2016**, *18*, 6340–6343. b) K. Chinthapally, N. P. Massaro, H. L. Padgett, I. Sharma, *Chem. Commun.* **2017**, *53*, 12205–12208. c) N.P. Massaro, J. C. Stevens, A. Chatterji, I. Sharma, *Org. Lett.* **2018**, *20*, 7585–7589.

[20] a) B. Ma, Z. Wu, B. Huang, L. Liu, J. Zhang, *Chem. Commun.* **2016**, *52*, 9351–9354. b) Z. Yu, H. Qiu, L. Liu, J. Zhang, *Chem. Commun.* **2016**, *52*, 2257–2260.

[21] a) L. S. Bartell, K. Kuchitsu, R. J. De Neui, *J. Chem. Phys.* **1960**, *33*, 1254–1255. b) E. A. Halevi, *New J. Chem.* **2014**, *38*, 3840–3852.

[22] J. Bucher, T. Wurm, K. S. Nalivela, M. Rudolph, F. Rominger, A. S. K. Hashmi, *Angew. Chem., Int. Ed.* **2014**, *53*, 3854–3858.

[23] W-W. Chan, T-L. Kwong, W-Y. Yu, *Org. Biomol. Chem*., **2012**, *10*, 3749–3755.

4.5 EXPERIMENTAL SECTION

4.5.1 MATERIALS AND METHODS

Reagents: Reagents and solvents were obtained from Sigma-Aldrich (www.sigma-aldrich.com), Chem-Impex (www.chemimpex.com) or Acros Organics (www.fishersci.com) and used without further purification unless otherwise indicated. Dry solvents (acetonitrile) were obtained from Acros Organics (www.fishersci.com), and dichloromethane was distilled over CaH under N_2 unless otherwise indicated. THF purchased from Sigma-Aldrich was distilled over Na metal with benzophenone indicator. Toluene was obtained from Sigma-Aldrich. **Reactions:** All reactions were performed in flame-dried glassware under positive N_2 pressure with magnetic stirring unless otherwise noted. Liquid reagents and solutions were transferred through rubber septa *via* syringes flushed with N_2 prior to use. Cold baths were generated as follows: 0 °C with wet ice/water and −78 °C with dry ice/acetone. **Chromatography:** TLC was performed on 0.25 mm E. Merck silica gel 60 F254 plates and visualized under UV light (254 nm) or by staining with potassium permanganate ($KMnO_4$), cerium ammonium molybdenate (CAM), phosphomolybdic acid (PMA), and ninhydrin. Silica flash chromatography was performed on Sorbtech 230–400 mesh silica gel 60. **Analytical Instrumentation:** IR spectra were recorded on a Thermo Scientific Nicolet 6700 FTIR spectrometer with peaks reported in cm^{-1}. NMR spectra were recorded on a Varian VNMRS 400, 500 and 600 MHz NMR spectrometer in $CDCl_3$ unless otherwise indicated. Chemical shifts are expressed in ppm relative to solvent signals: $CDCl_3$ (^1H, 7.26 ppm, ^{13}C, 77.0 ppm); coupling constants are

expressed in Hz. NMR spectra were processed using Mnova (www.mestrelab.com/software/mnova-nmr). Mass spectra were obtained on an Advion Expression^{L} CMS Mass Spectrometer or at the OU Analytical Core Facility on an Agilent 6538 High-Mass-Resolution QTOF Mass Spectrometer and an Agilent 1290 UPLC. X-ray crystallography analysis was carried out at the University of Oklahoma using a Bruker APEX ccd area detector (1) and graphite-monochromated Mo Kα radiation (λ = 0.71073 Å) source. Crystal structures were visualized using CCDC Mercury software (http://www.ccdc.cam.ac.uk/products/mercury/). **Nomenclature:** *N.B.*: Atom numbers shown in chemical structures herein correspond to IUPAC nomenclature, which was used to name each compound.

4.5.2 GENERAL PROCEDURE FOR 6-MEMBERED SPIROCARBOCYCLES

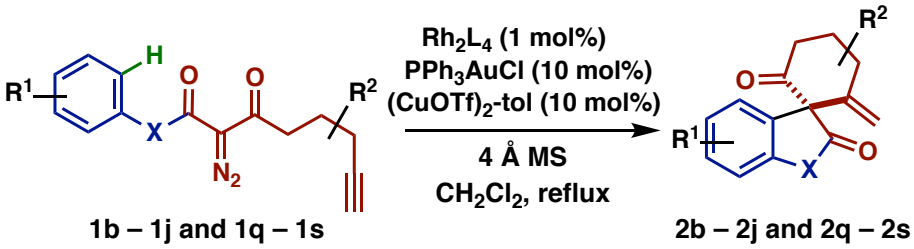

1b – 1j and 1q – 1s **2b – 2j and 2q – 2s**

To a teflon coated 20 mL vial was added heat activated 4 Å molecular sieves (100 mg/mmol of starting material), $Rh_2(HFB)_4$ (1 mol %), PPh_3AuCl (10 mol %), and $(CuOTf)_2$-toluene (10 mol %). This mixture was dissolved in 0.2 M dichloromethane and allowed to stir for 5 minutes at room temperature. The corresponding diazo compound **1** (0.55 mmol) was dissolved in 0.5 M dicholoromethane and then added to the catalyst solution stirring at room temperature. The 20 mL vial was sealed and

placed on a heating mantle and allowed to stir at reflux for 5 hours. Once the reaction was completed, the crude mixture was filtered over a celite pad to remove the 4 Å molecular sieves. The filtrate was directly loaded to a silica gel column and purified using flash column chromatography eluting with 10% EtOAc in Hex to afford spirocarbocycle product **2b–2j** and **2q–2s**.

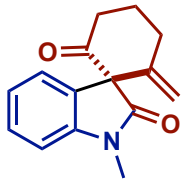

2b, 68%

1'-methyl-2-methylenespiro[cyclohexane-1,3'-indoline]-2',6-dione (2b). White solid (39 mg, 68%, mp 141-142 °C). **TLC**: R_f 0.71 (40% EtOAc in Hex). **IR** (NaCl): 3055, 2941, 2644, 2367, 1730. **^{1}H NMR** (500 MHz, , Chloroform-*d*) δ 7.36 (t, *J* = 5.0, 1H), 7.19 (t, *J* = 5.0, 1H), 7.15 (t, *J* = 5.0, 1H), 6.88 (d, *J* = 7.8 Hz, 1H), 4.88 (s, 1H), 4.51 (s, 1H), 3.35 – 3.24 (m, 2H), 3.18 (s, 3H), 2.66–2.55 (m, 2H), 2.26–2.20 (m, 1H), 1.86 (qt, *J* = 13.2, 4.2 Hz, 1H). **^{13}C NMR** (126 MHz, Chloroform-*d*) δ 203.0, 171.2, 145.7, 143.7, 128.8, 127.1, 126.4, 122.6, 111.6, 108.5, 72.3, 39.1, 30.9, 26.6, 24.6. **HRMS** (ESI) *m/z* calcd for $C_{15}H_{16}NO_2$ ($[M+H]^+$) 242.1181; found 242.1184.

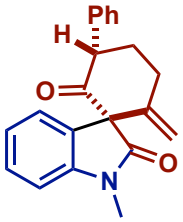

2c, 65%
(dr > 98:2)

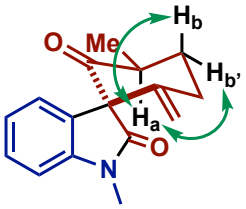

Stereochemistry Analysis[5]
J_{ab} = 12.8 Hz (ax–ax)
$J_{ab'}$ = 6.4 Hz (ax–eq)

1'-methyl-6-methylene-3-phenylspiro[cyclohexane-1,3'-indoline]-2,2'-dione (2c). Orange solid (31.0 mg, 65%, mp 155-156 °C). **TLC**: R_f 0.54 (20% EtOAc in Hex). **IR** (NaCl): 2934, 2113, 1729, 1697. **^{1}H NMR** (600 MHz, Chloroform-*d) δ* 7.41 (d, *J* = 7.5 Hz, 1H), 7.31 (q, *J* = 7.4 Hz, 3H), 7.25–7.23 (m, 1H), 7.16 (d, *J* = 7.5 Hz, 2H), 7.08 (t, *J* = 7.6 Hz, 1H), 6.86 (d, *J* = 7.8 Hz, 1H), 5.12 (s, 1H), 4.79 (s, 1H), 4.02 (dd, *J* = 12.8, 6.4 Hz, 1H), 3.22 (s, 3H), 3.08–3.04 (m, 1H), 2.99–2.93 (m, 1H), 2.51–2.38 (m, 2H). **^{13}C NMR** (151 MHz, Chloroform-*d*) *δ* 203.5, 173.3, 144.1, 143.7, 137.7, 129.3, 129.0, 128.8 (2C), 128.3 (2C), 127.2, 123.4, 122.6, 113.9, 108.9, 77.1, 70.6, 54.6, 31.1, 29.6. **HRMS** (ESI) *m/z* calcd for $C_{21}H_{21}NO_3Na$ ($[M+Na+H_2O]^+$) 336.1600; found 336.1598.

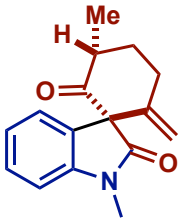

2d, 64%
(dr > 98:2)

1',3-dimethyl-6-methylenespiro[cyclohexane-1,3'-indoline]-2,2'-dione (2d). White solid (98 mg, 64%, mp 139-138 °C). **TLC**: R_f 0.84 (40% EtOAc in Hex). **IR** (NaCl): 3069, 2936, 1732, 1657. **^{1}H NMR** (600 MHz, , Chloroform-*d*) *δ* 7.32–7.28 (m, 2H), 7.04 (t, *J* = 7.8 Hz, 1H), 6.86 (d, *J* = 7.8 Hz, 1H), 5.01 (s, 1H), 4.70 (s, 1H), 3.25 (s, 3H), 2.91–2.81 (m, 3H), 2.23–2.18 (m,

1H), 1.85–1.78 (m, 1H), 1.13 (d, *J* = 6.5 Hz, 3H). **^{13}C NMR** (151 MHz, Chloroform-*d*) *δ* 206.1, 173.5, 144.4, 143.9, 134.1, 128.8, 123.3, 122.4, 113.1, 108.9, 70.5, 42.6, 30.9, 30.3, 26.5, 14.9. **HRMS** (ESI) *m/z* calcd for $C_{16}H_{17}NO_2Na$ ([M+Na]$^+$) 278.1157; found 278.1163.

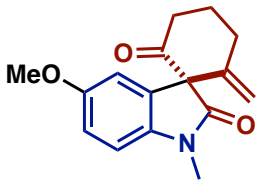

2e, 70%

5'-methoxy-1'-methyl-2-methylenespiro[cyclohexane-1,3'-indoline]-2',6-dione (2e). Yellow oil (30 mg, 70%). **TLC**: R_f 0.68 (40% EtOAc in Hex). **IR** (NaCl): 2367, 1701, 1638, 1603. **^{1}H NMR** (600 MHz, Chloroform-*d*) *δ* 6.86 (dd, *J* = 8.5, 2.6 Hz, 1H), 6.79–6.73 (m, 2H), 4.86 (s, 1H), 4.51 (s, 1H), 3.79 (s, 3H), 3.33–3.23 (m, 2H), 3.13 (s, 3H), 2.63–2.51 (m, 2H), 2.23–2.18 (m, 1H), 1.86–1.77 (m, 1H). **^{13}C NMR** (151 MHz, Chloroform-*d*) *δ* 203.1, 170.9, 155.7, 145.7, 137.2, 131.9, 127.6, 114.2, 113.5, 111.6, 108.8, 72.7, 55.8, 39.2, 26.8, 24.5. **HRMS** (ESI) *m/z* calcd for $C_{16}H_{17}NO_3Na$ ([M+Na]$^+$) 294.1106; found 294.1113.

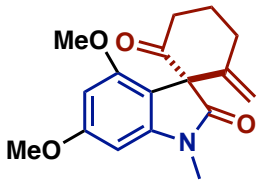

2f, 65%

4',6'-dimethoxy-1'-methyl-2-methylenespiro[cyclohexane-1,3'-indoline]-2',6-dione (2f). Yellow oil (33 mg, 65%). **TLC**: R_f 0.61 (40% EtOAc in Hex). **IR** (NaCl): 3007, 2945, 2363, 1703, 1620. **^{1}H NMR** (600 MHz, Chloroform-*d*) *δ* 6.22 (d, *J* = 2.0 Hz, 1H), 6.10 (d, *J* = 2.0 Hz, 1H), 4.80 (d, *J* = 1.9 Hz, 1H), 4.42 (s, 1H), 3.84 (s, 3H), 3.75 (s, 3H), 3.22–3.14 (m, 1H), 3.10 (s, 3H), 3.03 (ddd, *J* = 15.2, 13.3, 6.1 Hz, 1H), 2.66–2.55 (m, 2H), 2.18–2.13 (m, 1H), 1.81 (qt, *J*

= 13.2, 4.0 Hz, 1H). **^{13}C NMR** (151 MHz, Chloroform-*d*) δ 202.5, 172.2, 162.3, 156.3, 145.8, 143.5, 110.3, 106.6, 93.1, 88.7, 70.5, 55.6, 55.5, 39.6, 31.0, 26.8, 23.3. **HRMS** (ESI) *m/z* calcd for $C_{17}H_{19}NO_4Na$ ([M+Na]$^+$) 324.1212; found 324.1209.

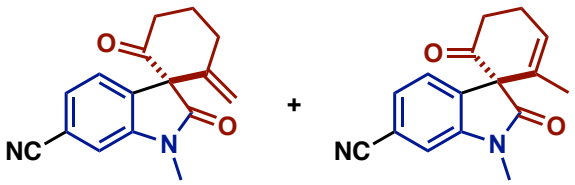

2g (2:**1**) **S1** (**2**:1)

1'-methyl-2-methylene-2',6-dioxospiro[cyclohexane-1,3'-indoline]-6'-carbonitrile (2g). Yellow oil (17 mg, 32% combined yield). **TLC**: R_f 0.52 (40% EtOAc in Hex). **IR** (NaCl): 3075, 2926, 2324, 2224, 1699. **^{1}H NMR** (600 MHz, Chloroform-*d*) [external alkene] δ 7.45 (t, *J* = 7.9 Hz, 1H), 7.34 (dd, *J* = 7.8, 1.1 Hz, 1H), 6.98 (dd, *J* = 7.9, 1.1 Hz, 1H), 5.08 (d, *J* = 4.5 Hz, 1H), 3.55 (t, *J* = 7.1 Hz, 3H), 3.27 (s, 5H), 2.26 – 2.17 (m, 6H), 2.16 (q, *J* = 1.6 Hz, 4H).**1',2-dimethyl-2',6-dioxospiro[cyclohexane-1,3'-indolin]-2-ene-6'-carbonitrile** (**S1**) (600 MHz, Chloroform-*d*) [internal alkene] (600 MHz, Chloroform-*d*) [internal alkene] δ 7.39 (dd, *J* = 7.9, 1.0 Hz, 1H), 7.26–7.24 (m, 1H), 7.05 (dd, *J* = 7.9, 1.0 Hz, 1H), 4.96 (d, *J* = 2.0 Hz, 1H), 4.33 (d, *J* = 1.8 Hz, 1H), 3.17 (s, 3H), 3.17–3.11 (m, 2H), 2.75–2.60 (m, 2H), 2.26–2.17 (m, 1H), 1.95 (qt, *J* = 13.7, 3.9 Hz, 1H). **^{13}C NMR** (101 MHz) (151 MHz, Chloroform-*d*) δ 200.7, 169.8, 149.7, 143.2, 141.0, 129.7, 127.9, 126.5, 126.3, 126.1, 123.4, 123.3, 119.7, 116.3, 112.2, 111.8, 111.1, 110.7, 109.5, 106.3, 101.9, 101.4, 71.9, 39.3, 31.0, 29.7, 26.9, 26.0, 23.3, 22.4, 19.1, 16.8. **HRMS** (ESI) *m/z* calcd for $C_{16}H_{15}N_2O_2$ ([M+H]$^+$) 267.1133; found 267.1137.

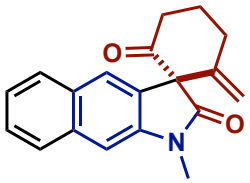

2h, 71%

1-methyl-2'-methylenespiro[benzo[f]indole-3,1'-cyclohexane]-2,6'(1H)-dione (2h). Clear oil (25 mg, 71%). **TLC**: R_f 0.79 (40% EtOAc in Hex). **IR** (NaCl): 3055, 2941, 1707, 1639. **^{1}H NMR** (600 MHz, Chloroform-*d*) δ 7.81 (dd, *J* = 17.8, 8.1 Hz, 2H), 7.62 (s, 1H), 7.49 (ddd, *J* = 8.1, 6.9, 1.2 Hz, 1H), 7.40 (ddd, *J* = 8.2, 6.9, 1.2 Hz, 1H), 7.15 (s, 1H), 4.91 (d, *J* = 1.8 Hz, 1H), 4.57 (s, 1H), 3.37–3.29 (m, 2H), 3.28 (s, 3H), 2.71–2.59 (m, 2H), 2.29–2.24 (m, 1H), 1.95–1.87 (m, 1H). **^{13}C NMR** (151 MHz, Chloroform-*d*) δ 203.0, 171.1, 145.9, 141.8, 133.9, 130.2, 128.5, 127.0, 126.9, 126.8, 126.7, 124.3, 112.0, 104.2, 71.7, 39.4, 31.2, 26.9, 24.6. **HRMS** (ESI) *m/z* calcd for $C_{19}H_{18}NO_2$ ($[M+H]^+$) 292.1337; found 292.1344.

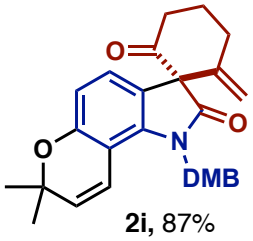

2i, 87%

1'-(2,4-dimethoxybenzyl)-7',7'-dimethyl-2-methylene-1',7'-dihydro-2'H-spiro[cyclohexane-1,3'-pyrano[2,3-g]indole]-2',6-dione (2i). Bright yellow oil (92 mg, 87%). **TLC**: R_f 0.74 (40% EtOAc in Hex). **IR** (NaCl): 2968, 2941, 2868, 1699. **^{1}H NMR** (500 MHz, Chloroform-*d*) δ 6.93 (d, *J* = 8.1 Hz, 1H), 6.69 (d, *J* = 8.4 Hz, 1H), 6.62 (d, *J* = 8.2 Hz, 1H), 6.48 (d, *J* = 2.4 Hz, 1H), 6.35 (dd, *J* = 8.4, 2.4 Hz, 1H), 6.27 (d, *J* = 10.1 Hz, 1H), 5.45 (d, *J* = 10.1 Hz, 1H), 5.01–4.89 (m, 3H), 4.65 (s, 1H), 3.86 (s, 3H), 3.76 (s, 3H), 3.34–3.24 (m, 2H),

2.69–2.57 (m, 2H), 2.25–2.19 (m, 1H), 1.91–1.81 (m, 1H), 1.38 (s, 3H), 1.34 (s, 3H). **^{13}C NMR** (101 MHz, Chloroform-*d*) δ 203.8, 172.9, 160.2, 157.2, 153.9, 138.9, 134.1, 130.5, 126.9, 126.3, 119.2, 117.1, 116.4, 110.9, 107.3, 104.1, 98.6, 74.9, 71.3, 60.4, 55.4, 40.9, 39.3, 31.1, 27.5, 27.1, 24.4, 14.2. **HRMS** (ESI) *m/z* calcd for $C_{28}H_{29}NO_5Na$ ([M+Na]$^+$) 482.1944; found. 482.1945.

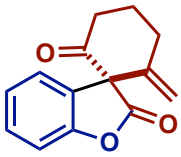

2j, 72%[b]

2'-methylene-2H-spiro[benzofuran-3,1'-cyclohexane]-2,6'-dione (2j). Clear oil (32 mg, 72%). **TLC**: R_f 0.60 (20% EtOAc in Hex). **IR** (NaCl): 2924, 2852, 1712, 1608. **^{1}H NMR** (600 MHz, Chloroform-*d*) δ 7.39 (ddd, *J* = 8.1, 5.7, 3.4 Hz, 1H), 7.28–7.23 (m, 2H), 7.15 (dt, *J* = 8.1, 0.8 Hz, 1H), 5.00 (d, *J* = 1.8 Hz, 1H), 4.60 (d, *J* = 1.4 Hz, 1H), 3.27–3.18 (m, 2H), 2.70–2.58 (m, 2H), 2.28–2.23 (m, 1H), 1.87 (qt, *J* = 13.1, 4.2 Hz, 1H). **^{13}C NMR** (151 MHz, Chloroform-*d*) δ 200.4, 170.4, 153.4, 144.3, 129.8, 127.5, 124.5, 124.2, 113.4, 110.8, 70.5, 38.4, 30.3, 24.7. **HRMS** (ESI) *m/z* calcd for $C_{14}H_{13}O_3$ ([M+H]$^+$) 229.0864; found 229.0876.

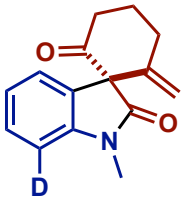

2q, 60% (k_H/k_D = 1)

1'-methyl-2-methylenespiro[cyclohexane-1,3'-indoline]-2',6-dione-7'-d (2q). White solid (15 mg, 60%, mp 140-141 °C). **TLC**: R_f 0.71 (40% EtOAc in Hex). **IR** (NaCl): 3059, 2941, 2320, 1699. **^{1}H NMR** (500 MHz, Chloroform-*d* δ 7.38 – 7.34 (m, 1H), 7.21 – 7.14 (m, 2H), 6.88 (dt, *J* = 7.8, 0.8 Hz, 0.47H), 4.88 (d, *J* = 2.1 Hz, 1H), 4.51 (d, *J* = 1.6, 1H), 3.36 – 3.25 (m, 2H), 3.18 (s, 3H), 2.66 – 2.55 (m, 2H), 2.27 – 2.21 (m, 1H), 1.86 (qt, *J* = 13.1, 4.1 Hz, 1H). **^{13}C NMR** (101 MHz, Chloroform-*d*) δ 203.1, 171.2, 145.7, 128.7, 127.1, 126.4, 122.6, 121.2, 111.6, 108.5, 72.3, 39.2, 30.9, 26.7, 24.6. **HRMS** (ESI) *m/z* calcd for $C_{15}H_{14}DNO_2Na$ ($[M+Na]^+$) 265.1064; found 265.1060.

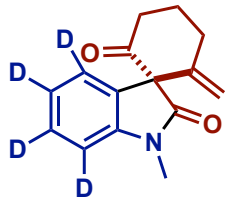

2r, 63% (0% D at alkene)

1'-methyl-2-methylenespiro[cyclohexane-1,3'-indoline]-2',6-dione-4',5',6',7'-d$_4$ (2r). White solid (23 mg, 63%, mp 141-142 °C). **TLC**: R_f 0.71 (40% EtOAc in Hex). **IR** (NaCl): 3059, 2936, 1703, 1600. **^{1}H NMR** (400 MHz, Chloroform-*d*) δ 4.86 (s, 1H), 4.49 (s, 1H), 3.34–3.22 (m, 2H), 3.16 (s, 3H), 2.64–2.53 (m, 2H), 2.25–2.21 (m, 1H), 1.89–1.82 (m, 1H). **^{13}C NMR** (101 MHz) (101 MHz, Chloroform-*d*) δ 203.1, 171.2, 145.7, 143.6, 126.9, 126.7, 126.3,

111.6, 109.9, 108.2, 72.3, 39.2, 30.9, 26.7, 24.6. **HRMS** (ESI) *m/z* calcd for $C_{15}H_{11}D_4NO_2$ ($[M+H]^+$) 246.1432; found 246.1437.

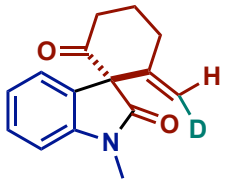

2s, 63% (86% D at alkene)

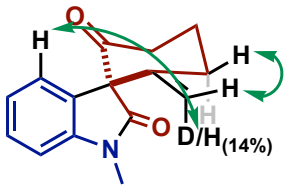

2s, nOe Analysis

1'-methyl-2-(methylene-d)spiro[cyclohexane-1,3'-indoline]-2',6-dione (2s). White solid (80 mg, 63%). Recrystallization from 1:1 dichloromethane/hexanes (slow evaporation method) yielded colorless block crystals (mp 140-141 °C). **TLC**: R_f 0.71 (40% EtOAc in Hex). **IR** (NaCl): 3052, 2939, 1696, 1610. **^{1}H NMR** (600 MHz, Chloroform-*d*) δ 7.33 (td, *J* = 7.6, 1.3 Hz, 1H), 7.17 (dd, *J* = 7.5, 1.4 Hz, 1H), 7.13 (t, *J* = 7.5 Hz, 1H), 6.86 (d, *J* = 7.8 Hz, 1H), 4.84 (d, *J* = 1.9 Hz, 1H), 4.49 (d, *J* = 1.5 Hz, 0.16H), 3.32–3.23 (m, 2H), 3.15 (s, 3H), 2.63–2.52 (m, 2H), 2.23–2.18 (m, 1H), 1.83 (qt, *J* = 13.1, 4.1 Hz, 1H). **^{13}C NMR** (151 MHz, Chloroform-*d*) δ 203.1, 171.2, 145.6, 143.7, 128.8, 127.1, 126.4, 122.6, 111.4 (t, *J* = 24.17 Hz, 1C), 108.5, 72.3, 39.2, 30.9, 26.7, 24.6. **HRMS** (ESI) *m/z* calcd for $C_{15}H_{14}DNO_2Na$ ($[M+Na]^+$) 265.0987; found 265.0984.

4.5.3 GENERAL PROCEDURE FOR 7-MEMBERED SPIROCARBOCYCLES

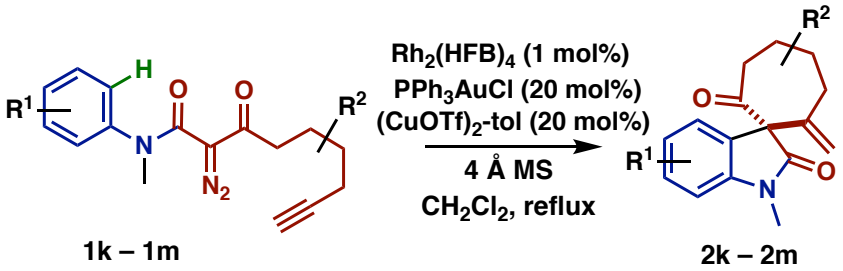

To a teflon coated 20 mL vial was added heat activated 4 Å molecular sieves (100 mg/mmol of starting material), $Rh_2(HFB)_4$ (1 mol %), PPh_3AuCl (20 mol %), and $(CuOTf)_2$·toluene (20 mol %). This mixture was dissolved in 0.2 M dichloromethane and allowed to stir for 5 minutes at room temperature. The corresponding diazo compound **1** (0.55 mmol) was dissolved in 0.5 M CH_2Cl_2 and then added to the catalyst solution stirring at room temperature. The 20 mL vial was sealed and placed on a heating mantle and allowed to stir at reflux for 5 hours. Once the reaction was completed, the crude mixture was filtered over a celite pad to remove the 4 Å molecular sieves. The filtrate was directly loaded to a silica gel column and purified using flash column chromatography eluting with 10% EtOAc in Hex to afford spirocarbocycle product **2k–2m**.

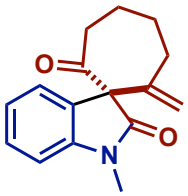

2k, 49%

1'-methyl-2-methylenespiro[cycloheptane-1,3'-indoline]-2',7-dione (2k). White sticky oil (30.5 mg, 49%). **TLC**: R_f 0.74 (40% EtOAc in Hex). **IR** (NaCl): 3059, 2932, 1734, 1632. **^{1}H NMR** (600 MHz, Chloroform-*d*) δ 7.32 (td, J = 7.7, 1.3 Hz, 1H), 7.23 (dd, J = 7.5, 1.2 Hz, 1H), 7.07

(td, *J* = 7.6, 1.1 Hz, 1H), 6.88–6.85 (m, 1H), 5.16 (d, *J* = 0.9 Hz, 1H), 4.79 (d, *J* = 0.9 Hz, 1H), 3.20 (s, 3H), 2.87 (ddd, *J* = 11.8, 10.7, 2.6 Hz, 1H), 2.79–2.66 (m, 2H), 2.65–2.52 (m, 1H), 2.14–1.96 (m, 2H), 1.87–1.65 (m, 2H). **^{13}C NMR** (151 MHz, Chloroform-*d*) *δ* 206.3, 173.6, 146.1, 144.1, 132.0, 129.1, 124.3, 122.5, 116.7, 108.8, 71.7, 42.6, 35.6, 32.4, 27.7, 26.4. **HRMS** (ESI) *m/z* calcd for $C_{16}H_{17}NO_2Na$ ($[M+Na]^+$) 278.1157; found 278.1165.

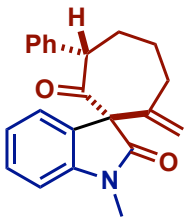

2l, 54%
(dr > 98:2)

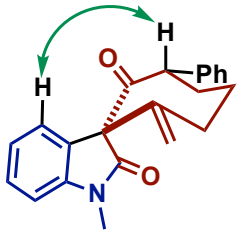

2l, nOe Analysis

1'-methyl-7-methylene-3-phenylspiro[cycloheptane-1,3'-indoline]-2,2'-dione (2l). White solid (80 mg, 54%). Recrystallization from 1:1 dichloromethane/hexanes (slow evaporation method) yielded colorless block crystals (mp 153-154 °C) **TLC**: R_f 0.67 (40% EtOAc in Hex). **IR** (NaCl): 3069, 2936, 1732, 1657. **^{1}H NMR** (400 MHz, Chloroform-*d*) *δ* 7.49 (dd, *J* = 7.5, 1.2 Hz, 1H), 7.30 (td, *J* = 7.8, 1.3 Hz, 1H), 7.24 (d, *J* = 4.3 Hz, 4H), 7.17 (h, *J* = 4.4 Hz, 1H), 7.11 (td, *J* = 7.6, 1.1 Hz, 1H), 6.82 (d, *J* = 7.8 Hz, 1H), 5.29 – 5.26 (m, 1H), 4.91 (s, 1H), 4.37 (dd, *J* = 10.5, 3.6 Hz, 1H), 3.16 (s, 3H), 2.97–2.84 (m, 1H), 2.76 (dt, *J* = 14.1, 4.0 Hz, 1H), 2.29–2.13 (m, 3H), 1.94–1.71 (m, 1H). **^{13}C NMR** (101 MHz, Chloroform-*d*) *δ* 204.4, 173.8, 145.5, 144.6, 139.9, 129.4, 128.2 (2C), 128.1 (2C), 126.9, 125.7, 124.4, 122.3, 117.2, 109.0, 72.0, 56.4, 36.2, 35.2, 31.8, 26.3. **HRMS** (ESI) *m/z* calcd for $C_{22}H_{22}NO_2$ ($[M+H]^+$) 332.1650; found 332.1655.

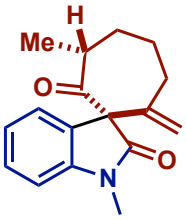

2m, 47%
(dr > 98:2)

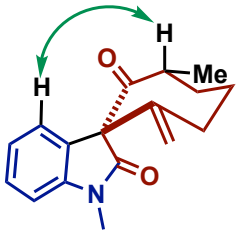

2m, nOe Analysis

1',3-dimethyl-7-methylenespiro[cycloheptane-1,3'-indoline]-2,2'-dione (2m). White sticky oil (30.5 mg, 47%). **TLC**: R_f 0.74 (40% EtOAc in Hex). **IR** (NaCl): 3059, 2936, 2363, 1734, 1638. **^{1}H NMR** (600 MHz, Chloroform-*d*) δ 7.31 (td, *J* = 7.8, 1.2 Hz, 1H), 7.22 (dd, *J* = 7.6, 1.2 Hz, 1H), 7.05 (td, *J* = 7.6, 1.0 Hz, 1H), 6.86 (d, *J* = 8.2 Hz, 1H), 5.16 (q, *J* = 0.8 Hz, 1H), 4.76 (t, *J* = 1.0 Hz, 1H), 3.20 (s, 3H), 3.19–3.15 (m, 1H), 2.82–2.71 (m, 1H), 2.69–2.60 (m, 1H), 2.12–2.06 (m, 1H), 1.86–1.78 (m, 1H), 1.70–1.58 (m, 2H), 1.04 (d, *J* = 6.6 Hz, 3H). **^{13}C NMR** (101 MHz, Chloroform-*d*) δ 207.9, 173.9, 145.9, 144.5, 134.2, 129.2, 123.9, 122.4, 116.6, 108.9, 71.8, 45.8, 36.6, 35.2, 31.8, 26.3, 17.8. **HRMS** (ESI) *m/z* calcd for $C_{17}H_{19}NO_2Na$ ([M+Na]$^+$) 292.1314; found 292.1322.

4.5.3 GENERAL PROCEDURE FOR 5-MEMBERED

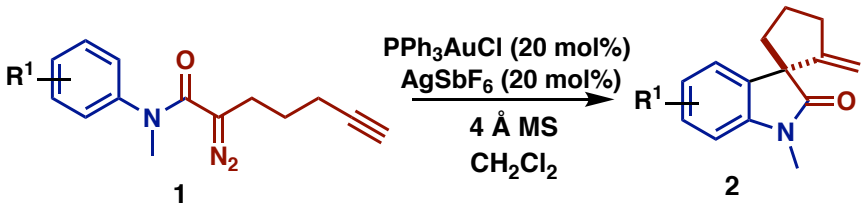

To a teflon coated 20 mL vial was added heat activated 4 Å molecular sieves (100 mg/mmol of starting material), PPh_3AuCl (20 mol %), and $AgSbF_6$ (20 mol %). This mixture was dissolved in 0.2 M dichloromethane and allowed to stir for 5 minutes at room temperature. The corresponding diazo compound **1** (0.55 mmol) was dissolved in 0.5 M CH_2Cl_2 and then

added to the catalyst solution stirring at room temperature. The 20 mL vial was sealed and allowed to stir at room temperature overnight. Once the reaction was completed, the crude mixture was filtered over a celite pad to remove the 4 Å molecular sieves. The filtrate was directly loaded to a silica gel column and purified using flash column chromatography eleuting with 10% EtOAc in Hex to afford spirocarbocycle product **2n–2p**.

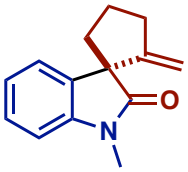

2n, 67%

1'-methyl-2-methylenespiro[cyclopentane-1,3'-indolin]-2'-one (2n). Faint yellow oil (32 mg, 67%). **TLC**: R_f 0.71 (40% EtOAc in Hex). **IR** (NaCl): 3055, 2922, 2849, 1713, 1611. **^{1}H NMR** (600 MHz, Chloroform-*d*) δ 7.25 (t, *J* = 6.0 Hz, 3H), 7.10 (d, *J* = 7.5, 1H), 7.04 (t, *J* = 7.5, 1H), 6.83 (d, *J* = 7.8 Hz, 1H), 4.94 (t, *J* = 2.1 Hz, 1H), 4.39 (t, *J* = 2.3 Hz, 1H), 3.20 (s, 3H), 2.83–2.72 (m, 1H), 2.67–2.58 (m, 1H), 2.33–2.19 (m, 2H), 2.07–1.91 (m, 2H). **^{13}C NMR** (151 MHz, Chloroform-*d*) δ 179.9, 154.5, 143.7, 135.2, 123.0, 122.9, 108.2, 107.7, 58.4, 38.5, 33.7, 29.7, 26.3, 24.3. **HRMS** (ESI) *m/z* calcd for $C_{14}H_{16}NO$ ($[M+H]^+$) 214.1232; found 214.1229.

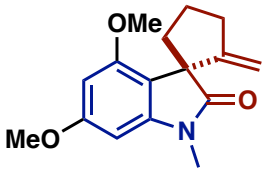

2o, 69%

4',6'-dimethoxy-1'-methyl-2-methylenespiro[cyclopentane-1,3'-indolin]-2'-one (2o). Faint yellow oil (55 mg, 69%, mp 136-137 °C). **TLC**: R_f 0.61 (40% EtOAc in Hex). **IR** (NaCl): 3075, 2936, 2849, 1709. **^{1}H NMR** (600 MHz, Chloroform-*d*) δ 6.16 (d, *J* = 2.0 Hz, 1H), 6.10

(d, *J* = 2.0 Hz, 1H), 4.87 (t, *J* = 2.2 Hz, 1H), 4.37 (t, *J* = 2.2 Hz, 1H), 3.84 (s, 3H), 3.78 (s, 3H), 3.15 (s, 3H), 2.70 (dt, *J* = 14.9, 7.2 Hz, 2H), 2.61 (dt, *J* = 15.6, 7.3 Hz, 2H), 2.30 (dt, *J* = 12.2, 7.0 Hz, 1H), 2.18–2.07 (m, 2H), 2.04–1.96 (m, 1H). **^{13}C NMR** (151 MHz, Chloroform-*d*) *δ* 181.1, 161.3, 155.6, 154.0, 145.8, 112.6, 106.1, 92.6, 88.0, 57.2, 55.6 (2C), 35.3, 34.2, 26.4, 24.7. **HRMS** (ESI) *m/z* calcd for $C_{16}H_{20}NO_3$ ([M+H]$^+$) 274.1443; found 274.1442.

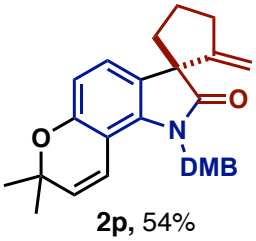

2p, 54%

1'-(3,4-dimethylbenzyl)-7',7'-dimethyl-2-methylene-1',7'-dihydro-2'H-spiro[cyclopentane-1,3'-pyrano[2,3-g]indol]-2'-one (2p). Faint yellow oil (53 mg, 54%). **TLC**: R_f 0.71 (30% EtOAc in Hex). **IR** (NaCl): 2955, 2924, 2852, 1712, 1608. **^{1}H NMR** (600 MHz, Chloroform-*d*) *δ* 6.87 (d, *J* = 8.1 Hz, 1H), 6.78 (d, *J* = 8.4 Hz, 1H), 6.51 (d, *J* = 8.0 Hz, 1H), 6.48 (d, *J* = 2.3 Hz, 1H), 6.36 (dd, *J* = 8.4, 2.3 Hz, 1H), 6.32 (d, *J* = 10.1 Hz, 1H), 5.46 (d, *J* = 10.1 Hz, 1H), 5.04 (d, *J* = 17.4 Hz, 1H), 5.00 (t, *J* = 2.3 Hz, 1H), 4.92 (d, *J* = 17.3 Hz, 1H), 4.55 (t, *J* = 2.3 Hz, 1H), 3.87 (s, 3H), 3.76 (s, 3H), 2.33 (td, *J* = 13.1, 7.3 Hz, 1H), 2.29–2.23 (m, 1H), 2.07 (dt, *J* = 12.0, 7.2 Hz, 1H), 1.95 (dp, *J* = 13.9, 7.4 Hz, 1H), 1.36 (s, 3H), 1.33 (s, 3H). **^{13}C NMR** (151 MHz, Chloroform-*d*) *δ* 181.4, 160.0, 157.2, 155.2, 153.0, 138.8, 130.4, 127.6, 126.5, 123.1, 117.4, 117.1, 110.7, 108.2, 106.8, 104.1, 98.7, 74.8, 57.5, 55.4, 40.3, 40.0, 33.6, 29.7, 27.5, 27.0, 24.0. **HRMS** (ESI) *m/z* calcd for $C_{27}H_{30}NO_4$ ([M+H]$^+$) 432.2175; found 432.2138.

APPENDIX 3

Spectra Relevant to Chapter 4

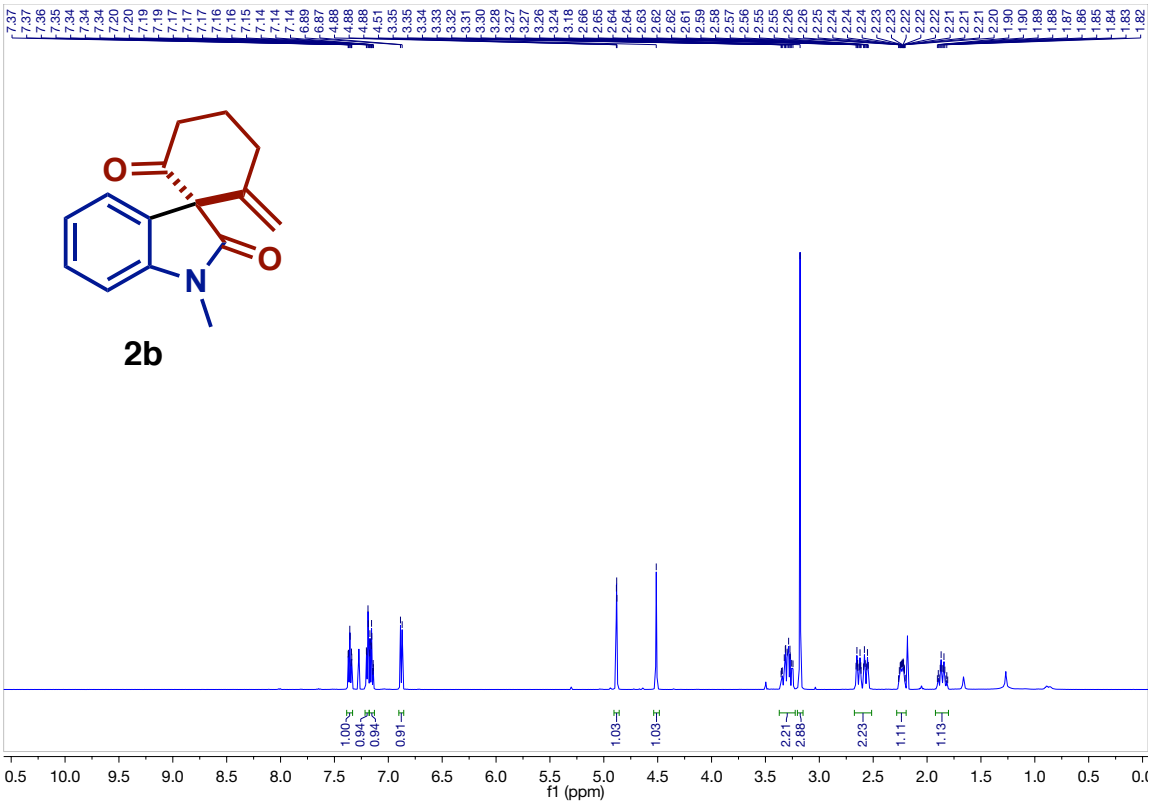
O
O
N
2b
1.00
0.94
0.94
0.91
1.03
1.03
2.21
2.88
2.23
1.11
1.13
f1 (ppm)

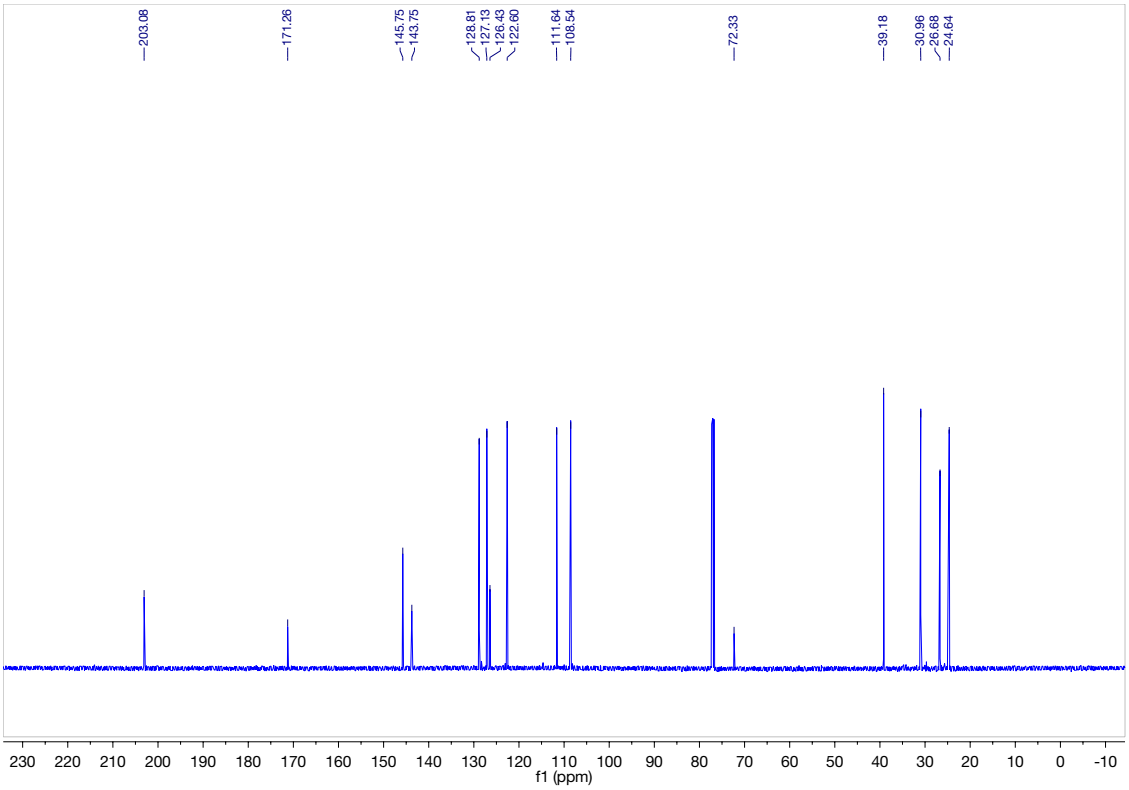
203.08
171.26
145.75
143.75
128.81
127.13
126.43
122.60
111.64
108.54
72.33
39.18
30.96
26.68
24.64
f1 (ppm)

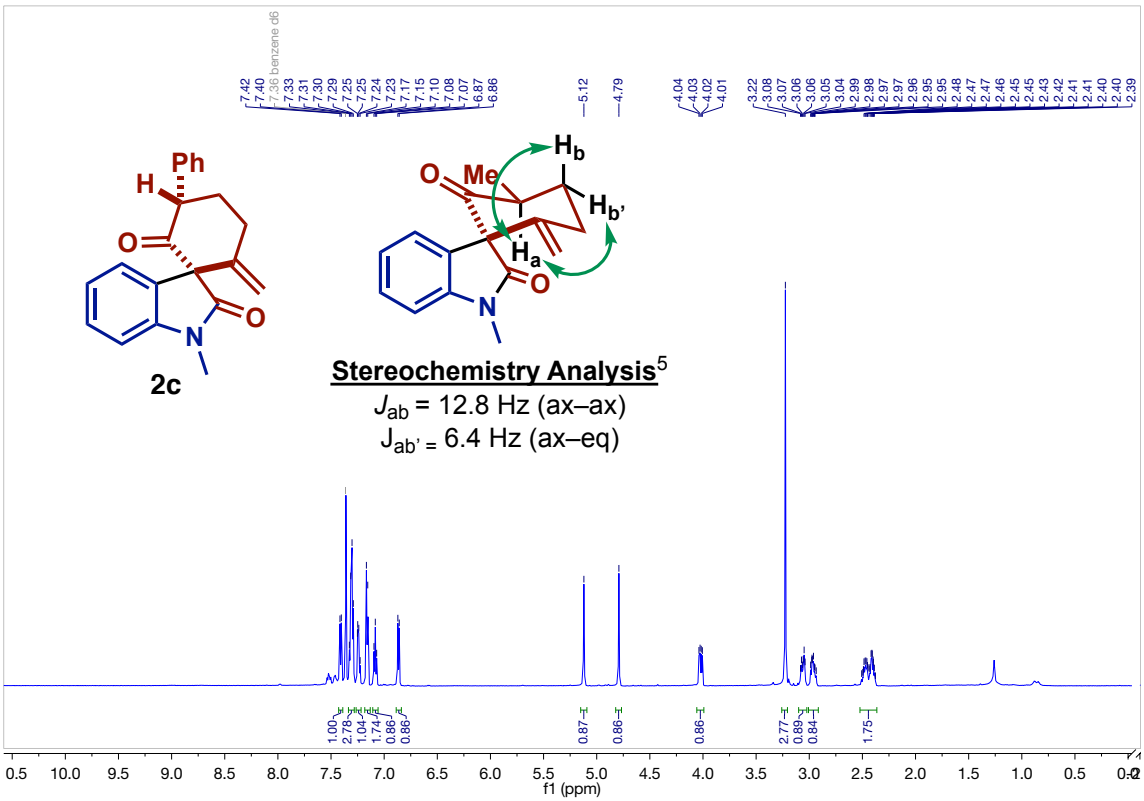
Ph
H
O
O
N
2c
Me
O
H_b
$H_{b'}$
H_a
O
N
Stereochemistry Analysis[5]
J_{ab} = 12.8 Hz (ax–ax)
$J_{ab'}$ = 6.4 Hz (ax–eq)
f1 (ppm)

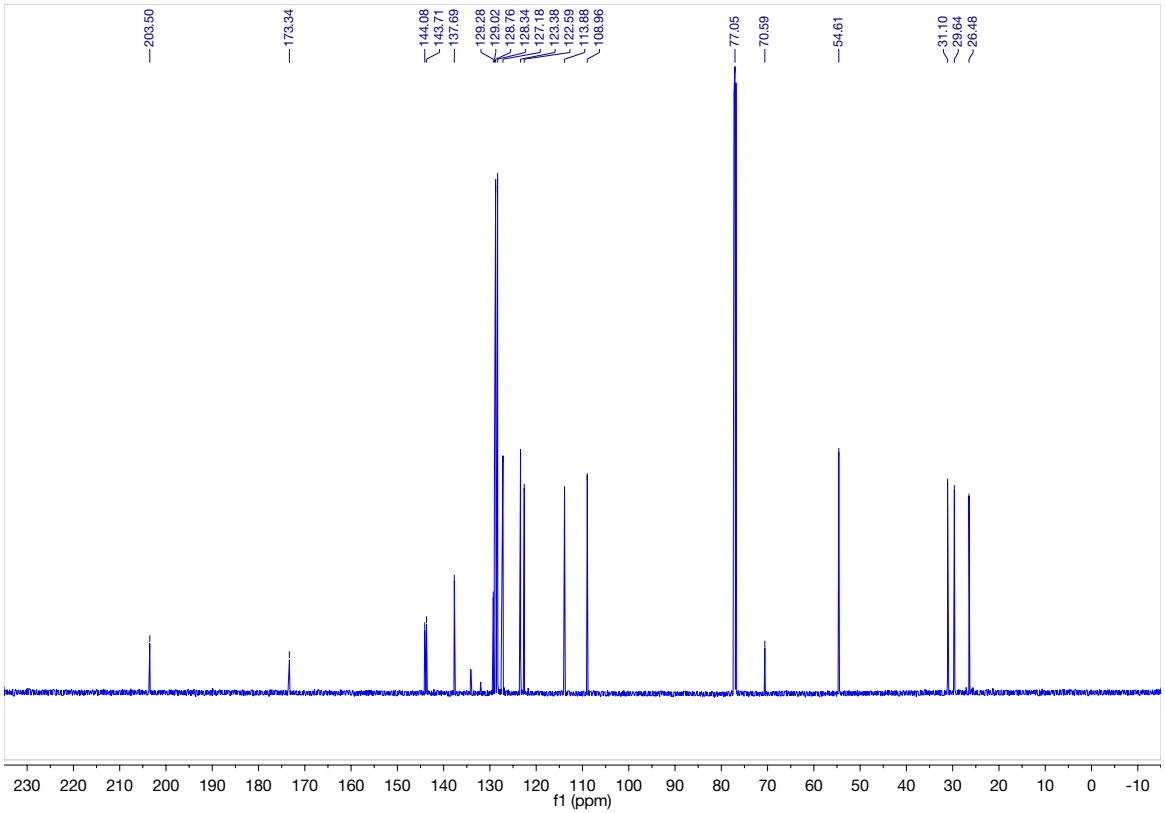
f1 (ppm)

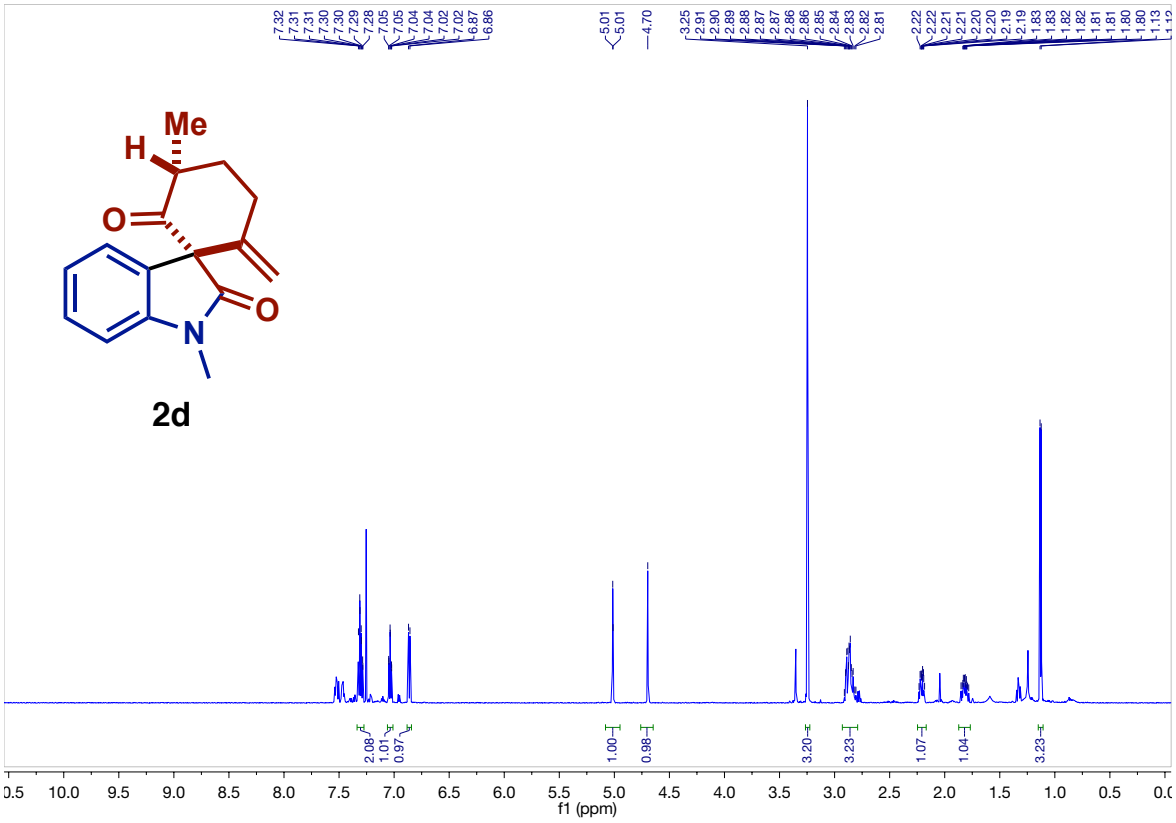
Me
H
O
O
N
2d
f1 (ppm)

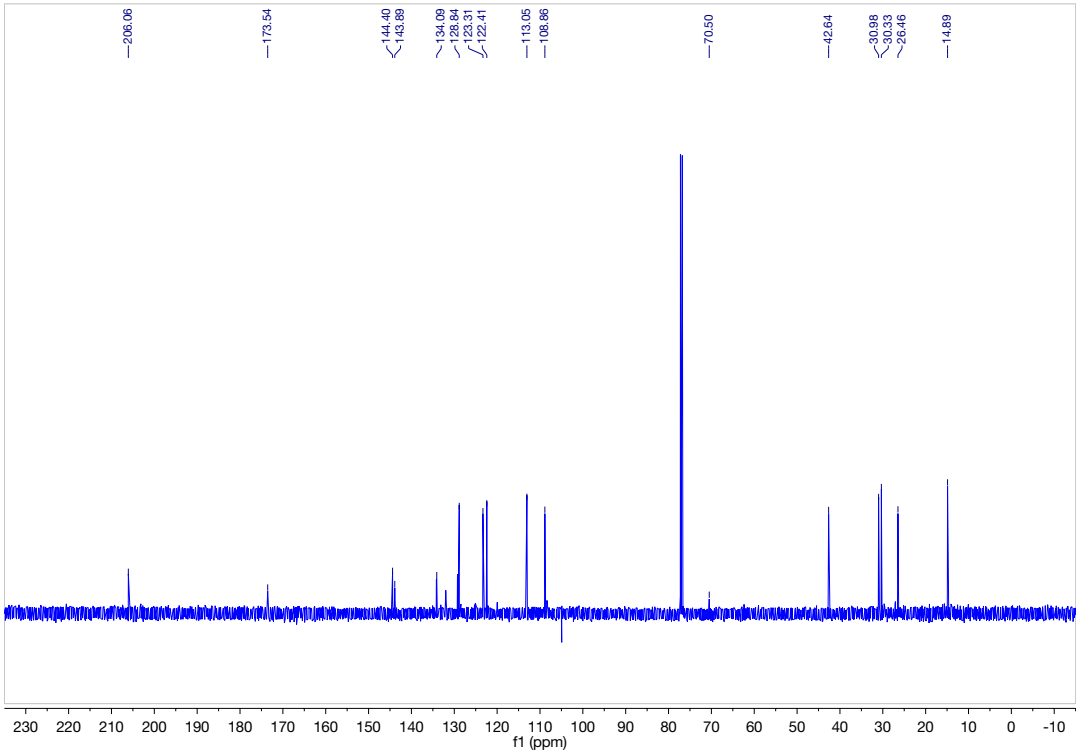
f1 (ppm)

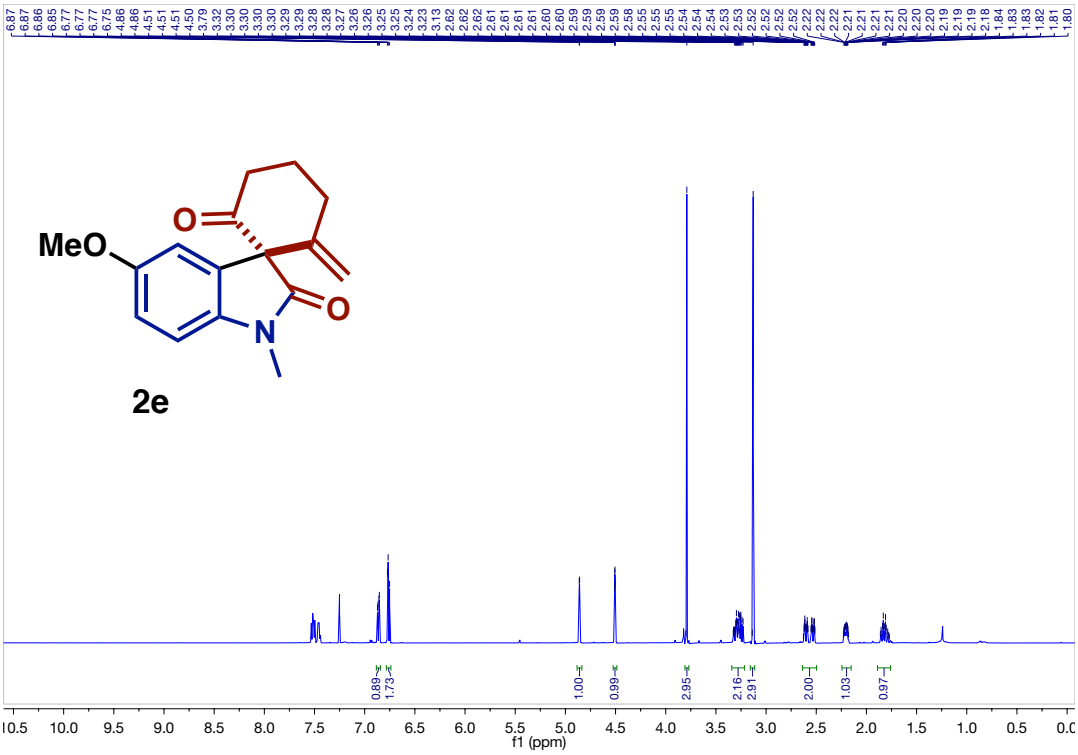
MeO
O
O
N
2e
f1 (ppm)

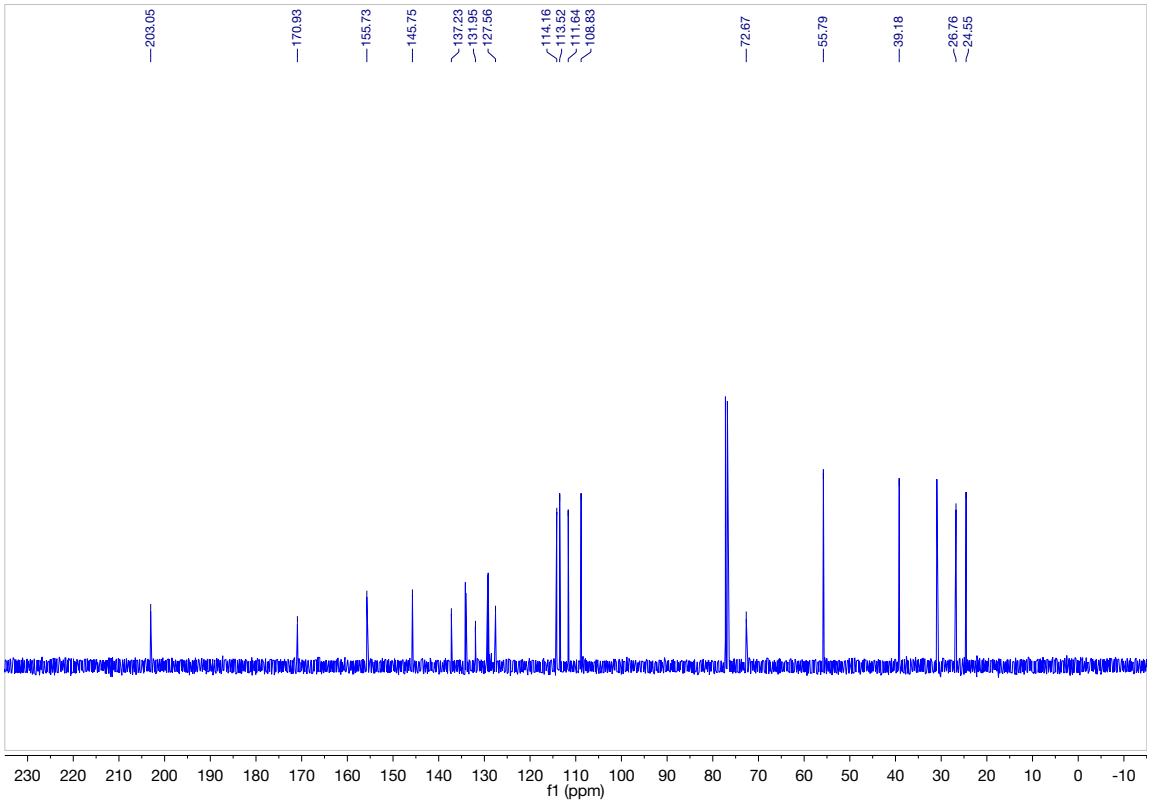
203.05
170.93
155.73
145.75
137.23
131.95
127.56
114.16
113.52
111.64
108.83
72.67
55.79
39.18
26.76
24.55
f1 (ppm)

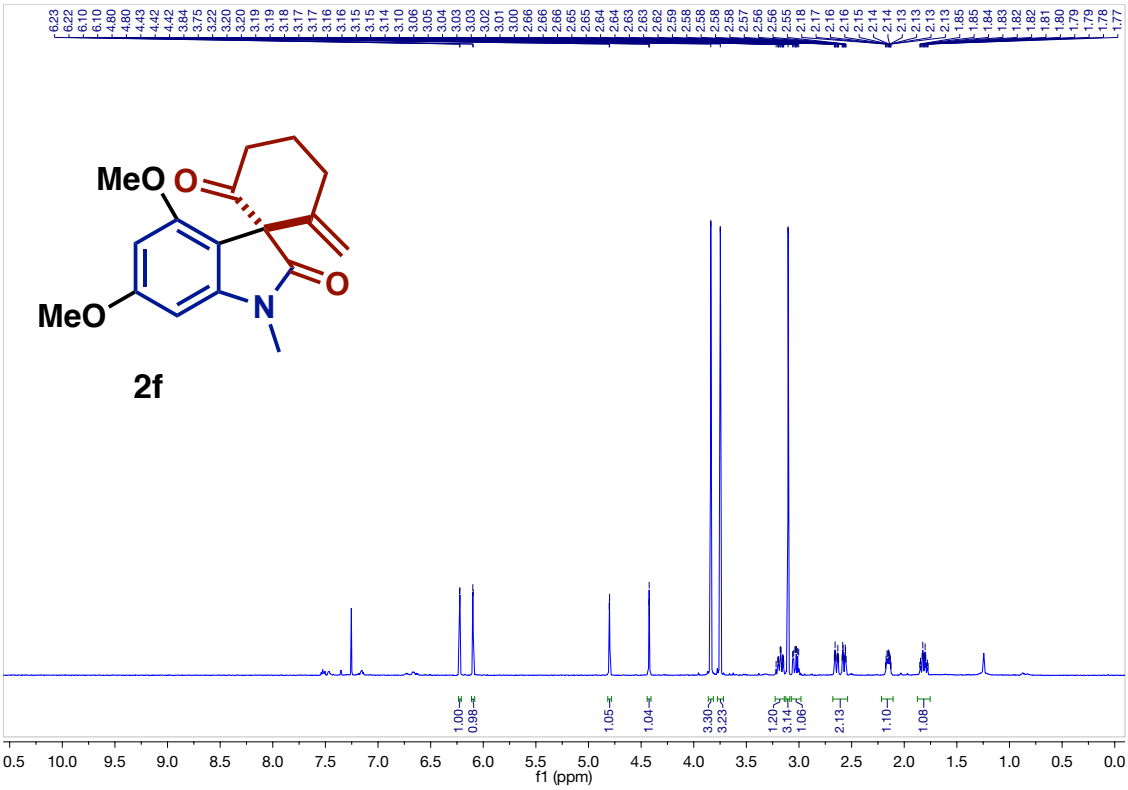
MeO
O
MeO
N
O
2f
f1 (ppm)

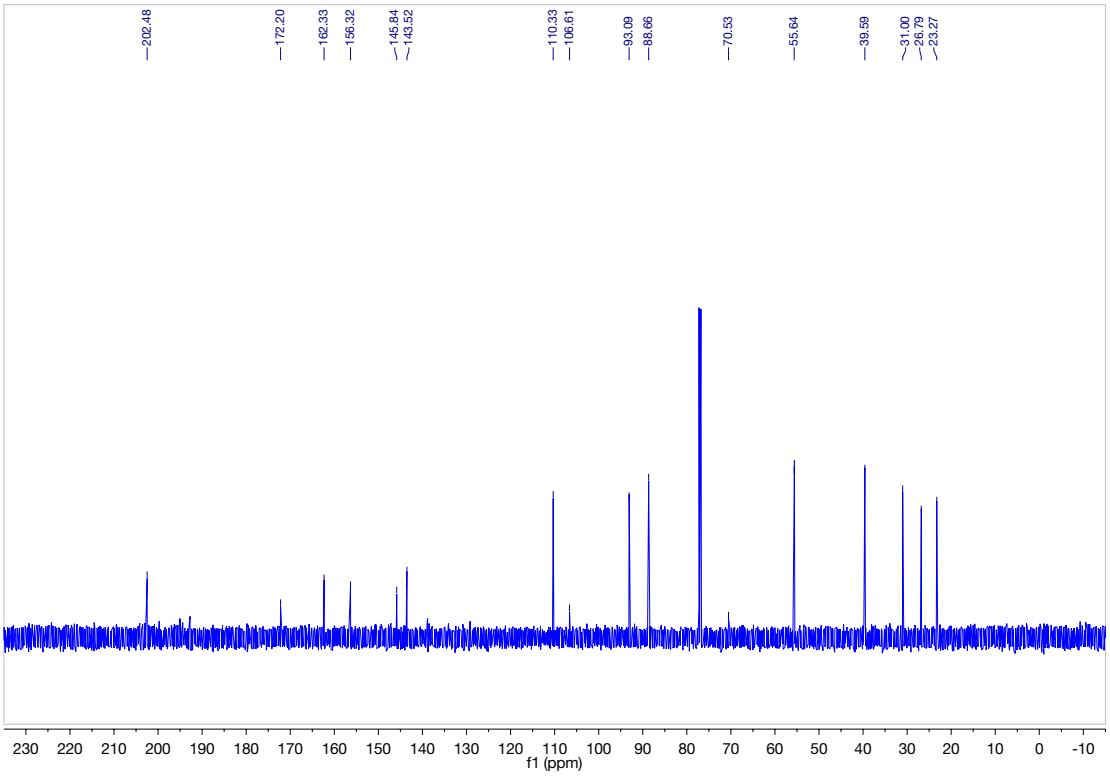
202.48
172.20
162.33
156.32
145.84
143.52
110.33
106.61
93.09
88.66
70.53
55.64
39.59
31.00
26.79
23.27
f1 (ppm)

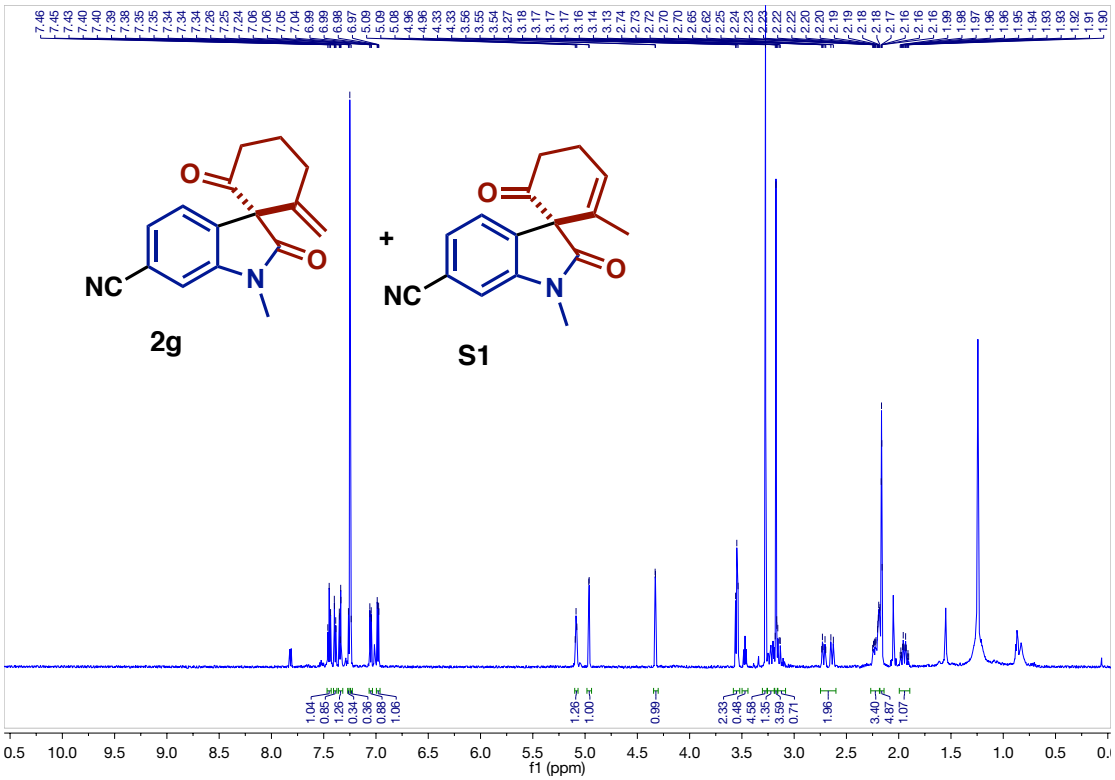
NC
2g
+
NC
S1
f1 (ppm)

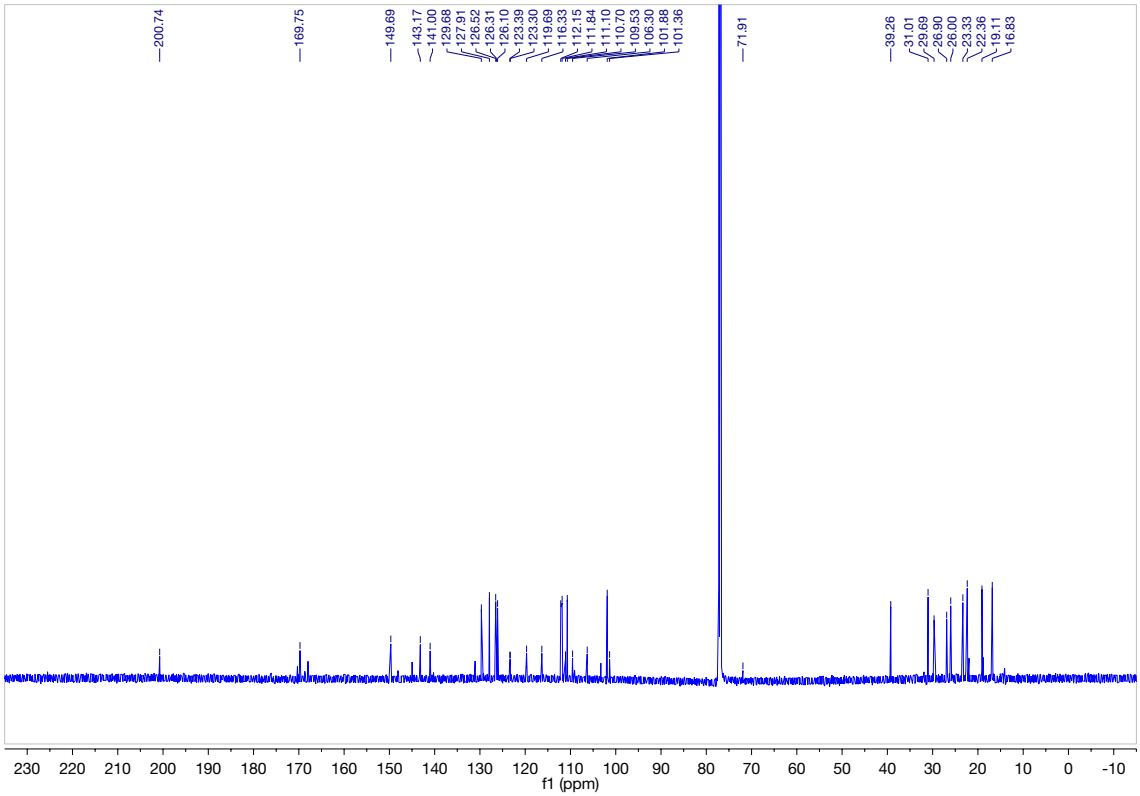
f1 (ppm)

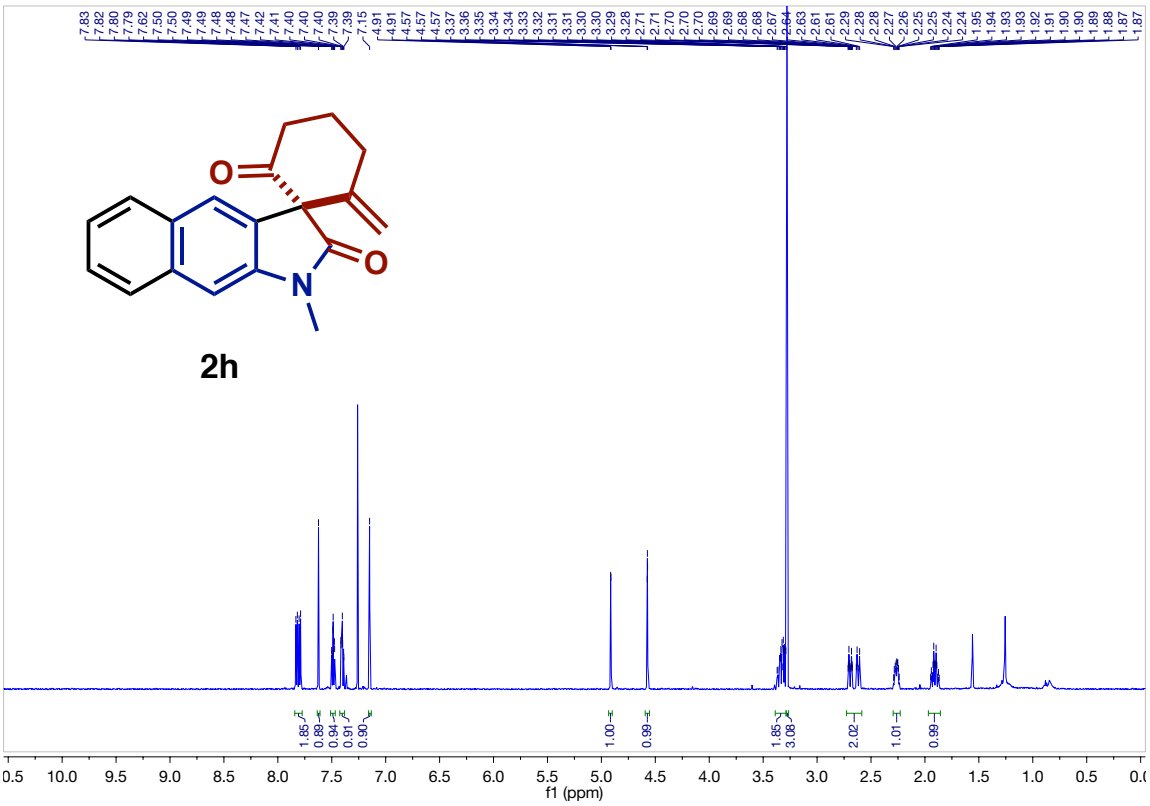
O
O
N
2h
f1 (ppm)

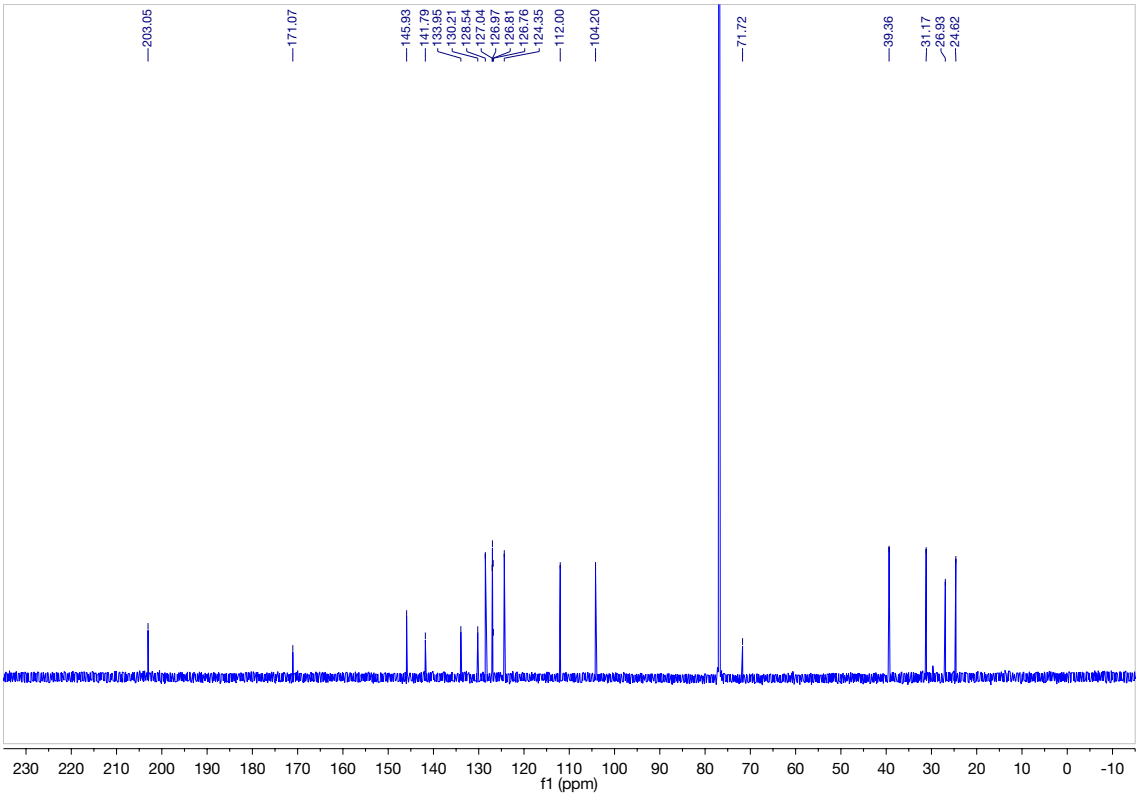
203.05
171.07
145.93
141.79
133.95
130.21
128.54
127.04
126.97
126.81
126.76
124.35
112.00
104.20
71.72
39.36
31.17
26.93
24.62
f1 (ppm)

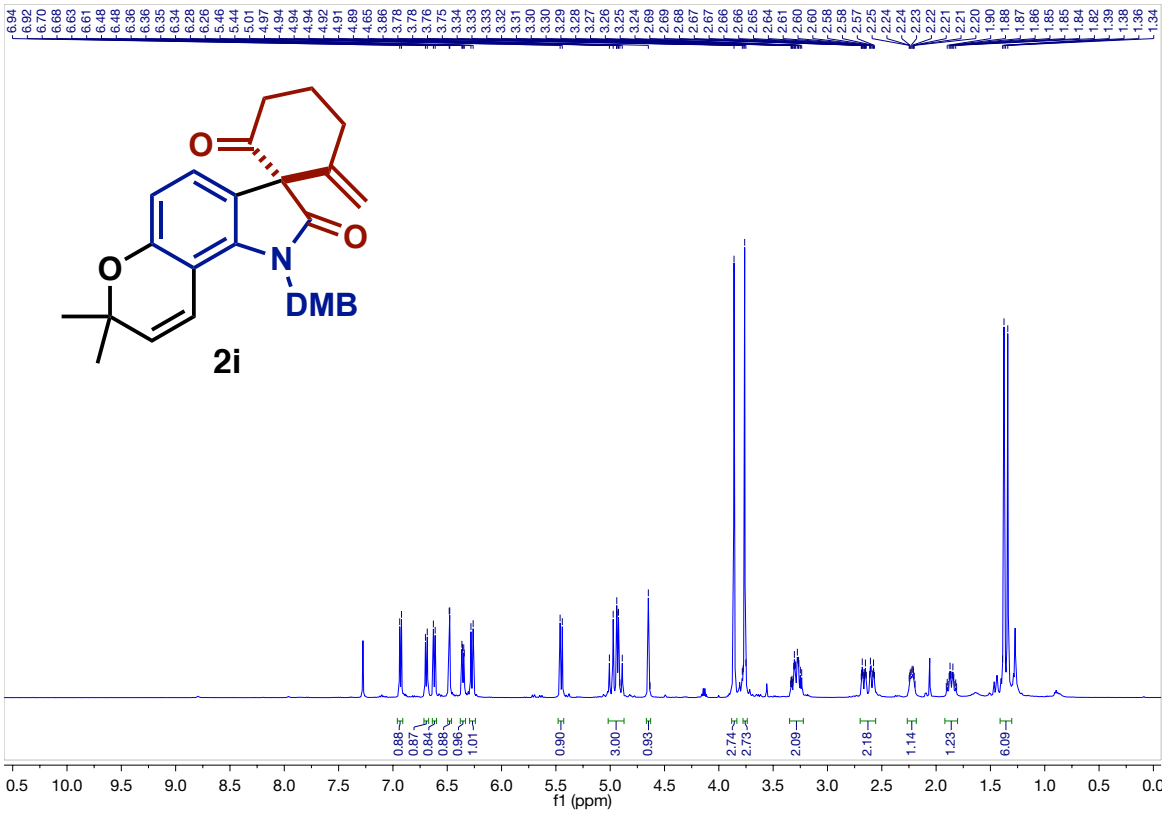
O
O
O
N
DMB
2i
f1 (ppm)

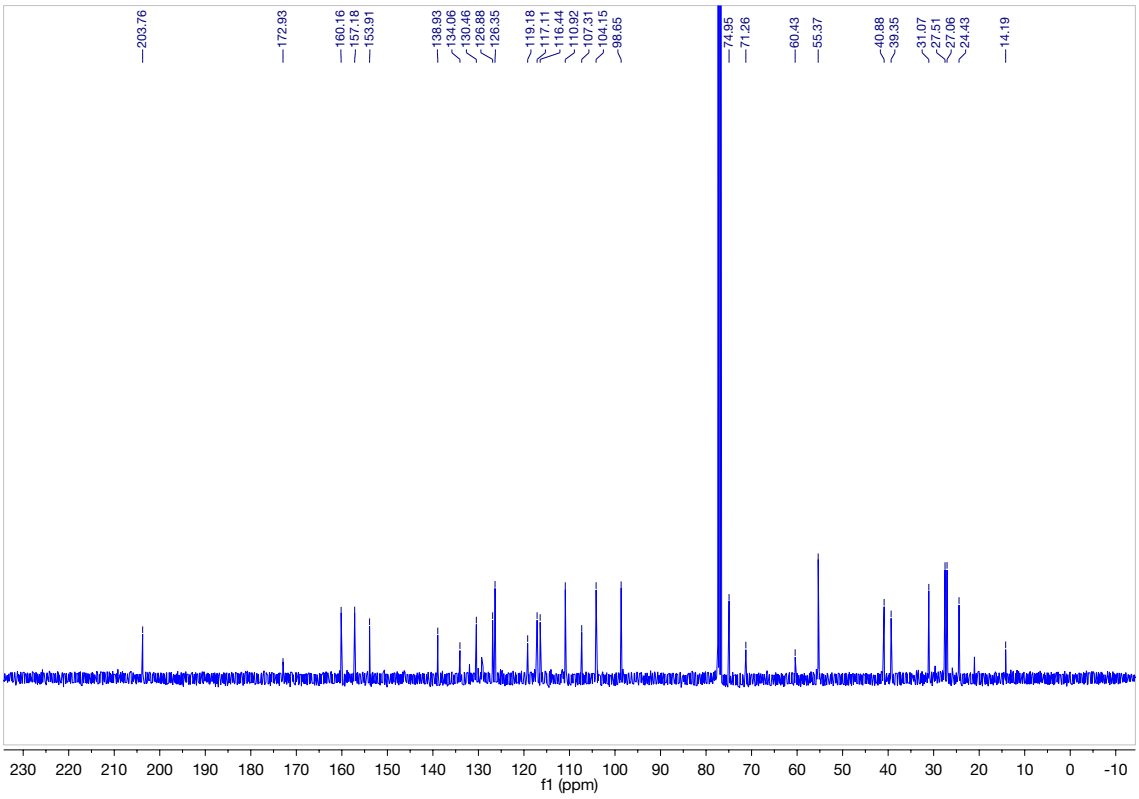
203.76
172.93
160.16
157.18
153.91
138.93
134.06
130.46
126.88
126.35
119.18
117.11
116.44
110.92
107.31
104.15
98.65
74.95
71.26
60.43
55.37
40.88
39.35
31.07
27.51
27.06
24.43
14.19
f1 (ppm)

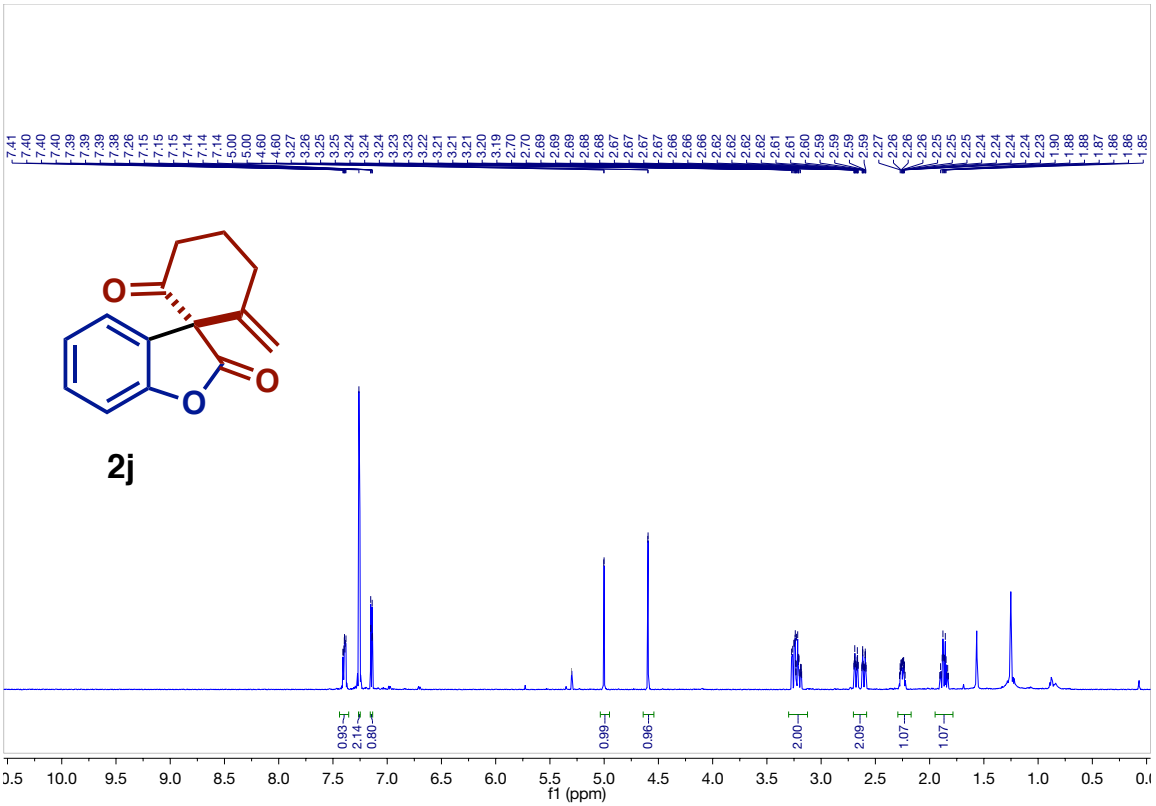
2j
0.93
2.14
0.80
0.99
0.96
2.00
2.09
1.07
1.07
f1 (ppm)

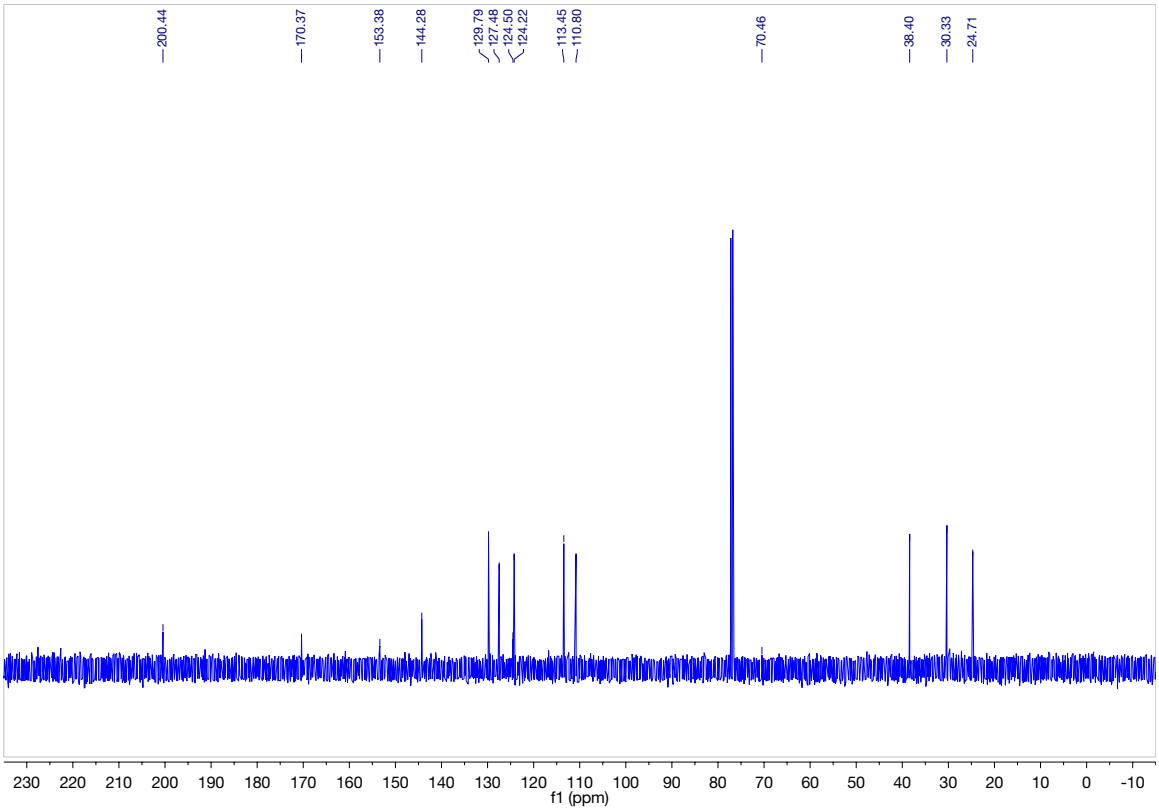
200.44
170.37
153.38
144.28
129.79
127.48
124.50
124.22
113.45
110.80
70.46
38.40
30.33
24.71
f1 (ppm)

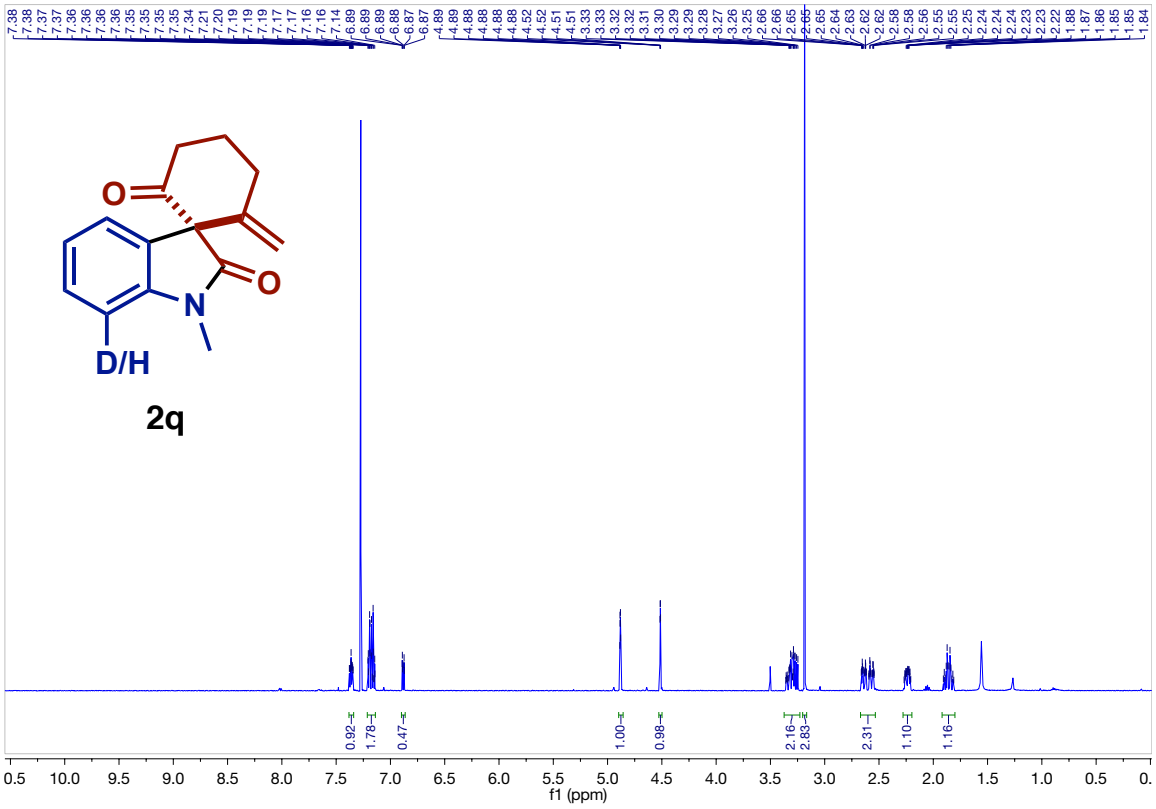
O
O
N
D/H
2q
0.92
1.78
0.47
1.00
0.98
2.16
2.83
2.31
1.10
1.16
f1 (ppm)

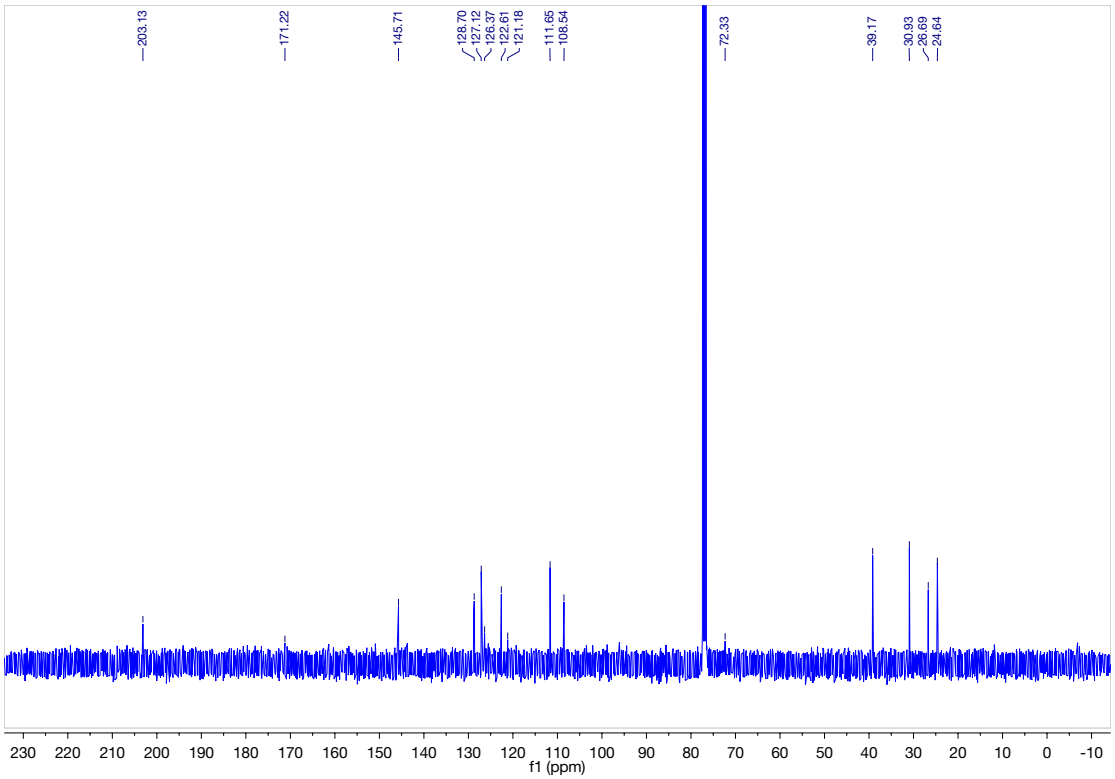
203.13
171.22
145.71
128.70
127.12
126.37
122.61
121.18
111.65
108.54
72.33
39.17
30.93
26.69
24.64
f1 (ppm)

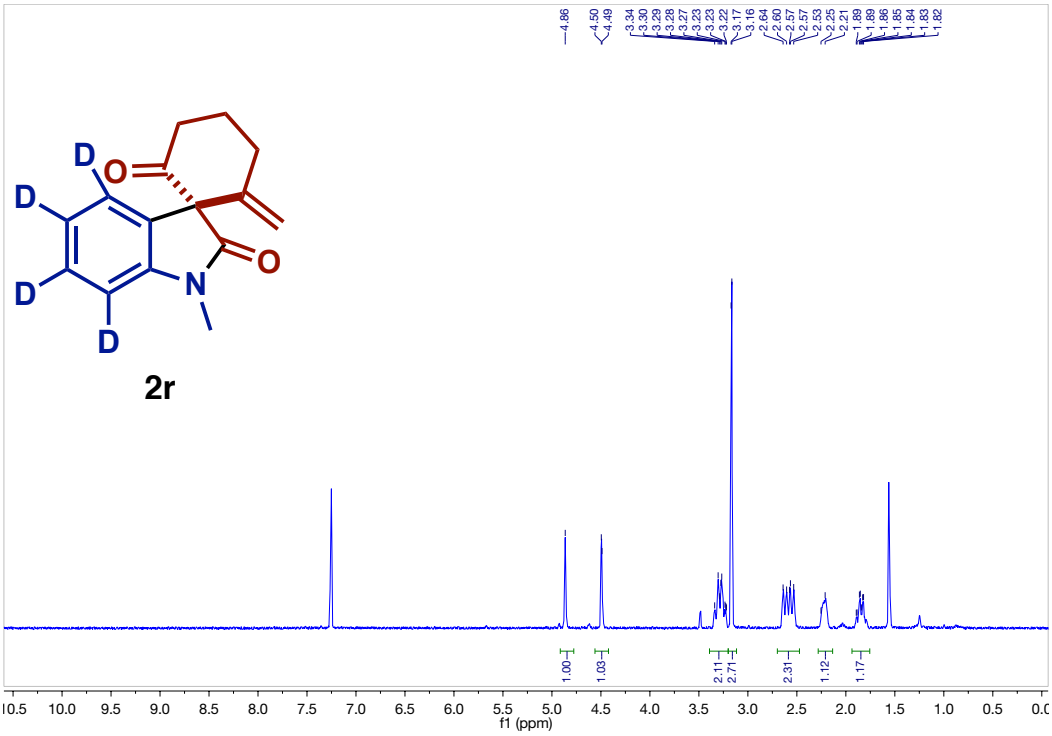
D
O
D
D
N
O
D
2r
4.86
4.50
4.49
3.34
3.30
3.29
3.28
3.27
3.23
3.22
3.17
3.16
2.64
2.60
2.57
2.57
2.53
2.25
2.21
1.89
1.89
1.86
1.85
1.84
1.83
1.82
1.00
1.03
2.11
2.71
2.31
1.12
1.17
f1 (ppm)

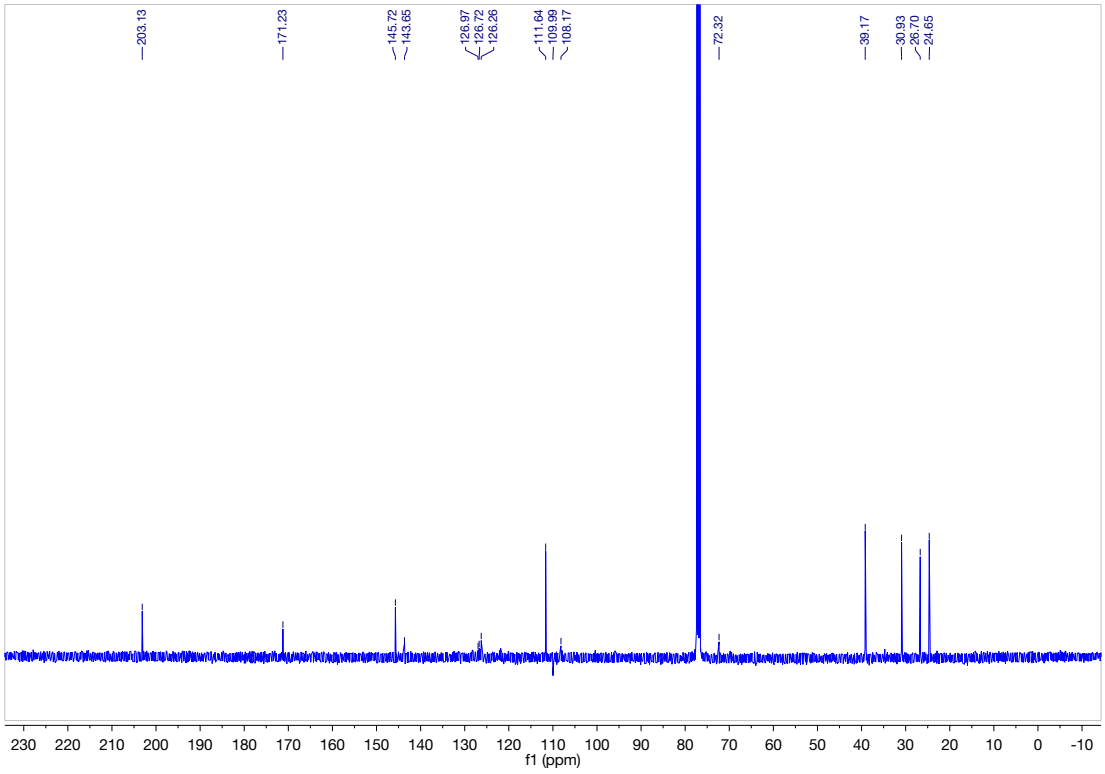
203.13
171.23
145.72
143.65
126.97
126.72
126.26
111.64
109.99
108.17
72.32
39.17
30.93
26.70
24.65
f1 (ppm)

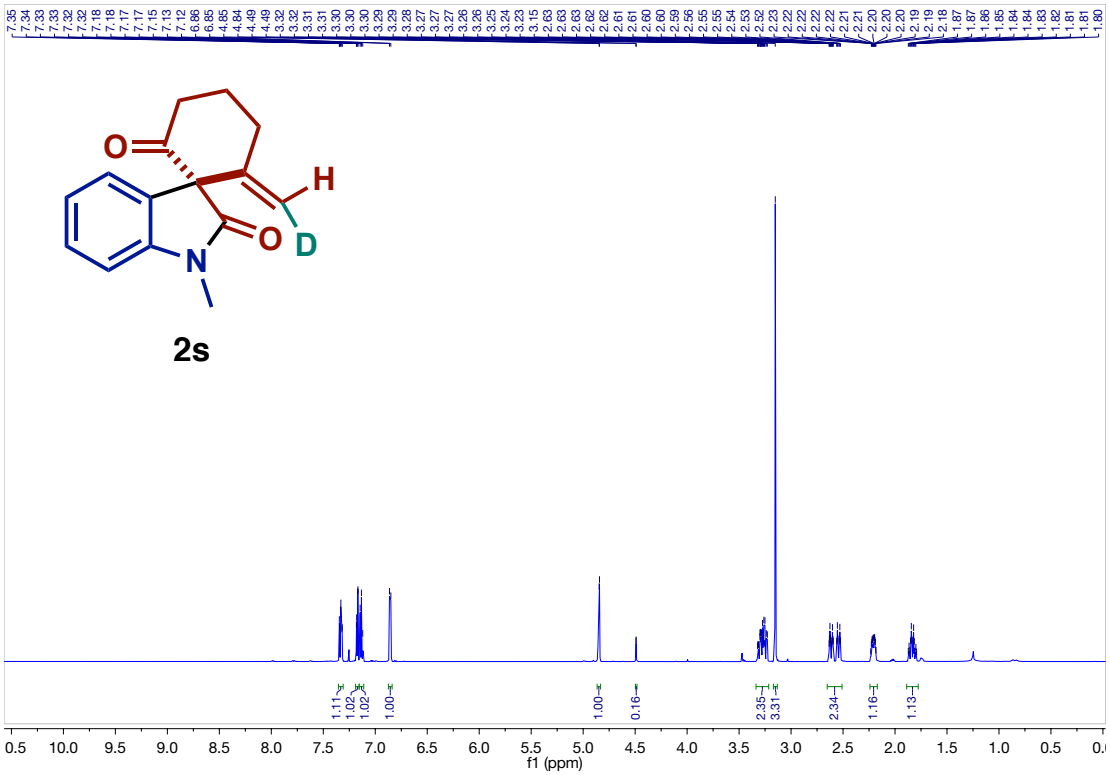
O
H
O
D
N
2s
f1 (ppm)

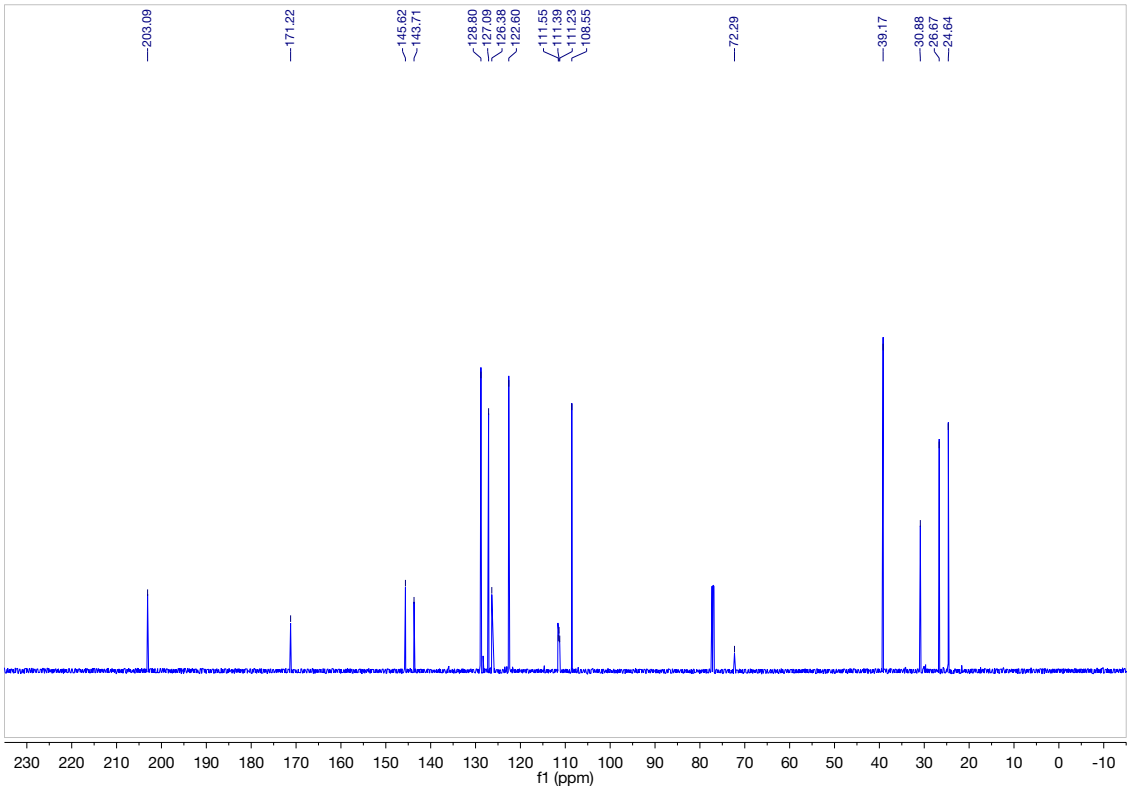
203.09
171.22
145.62
143.71
128.80
127.09
126.38
122.60
111.55
111.39
111.23
108.55
72.29
39.17
30.88
26.67
24.64
f1 (ppm)

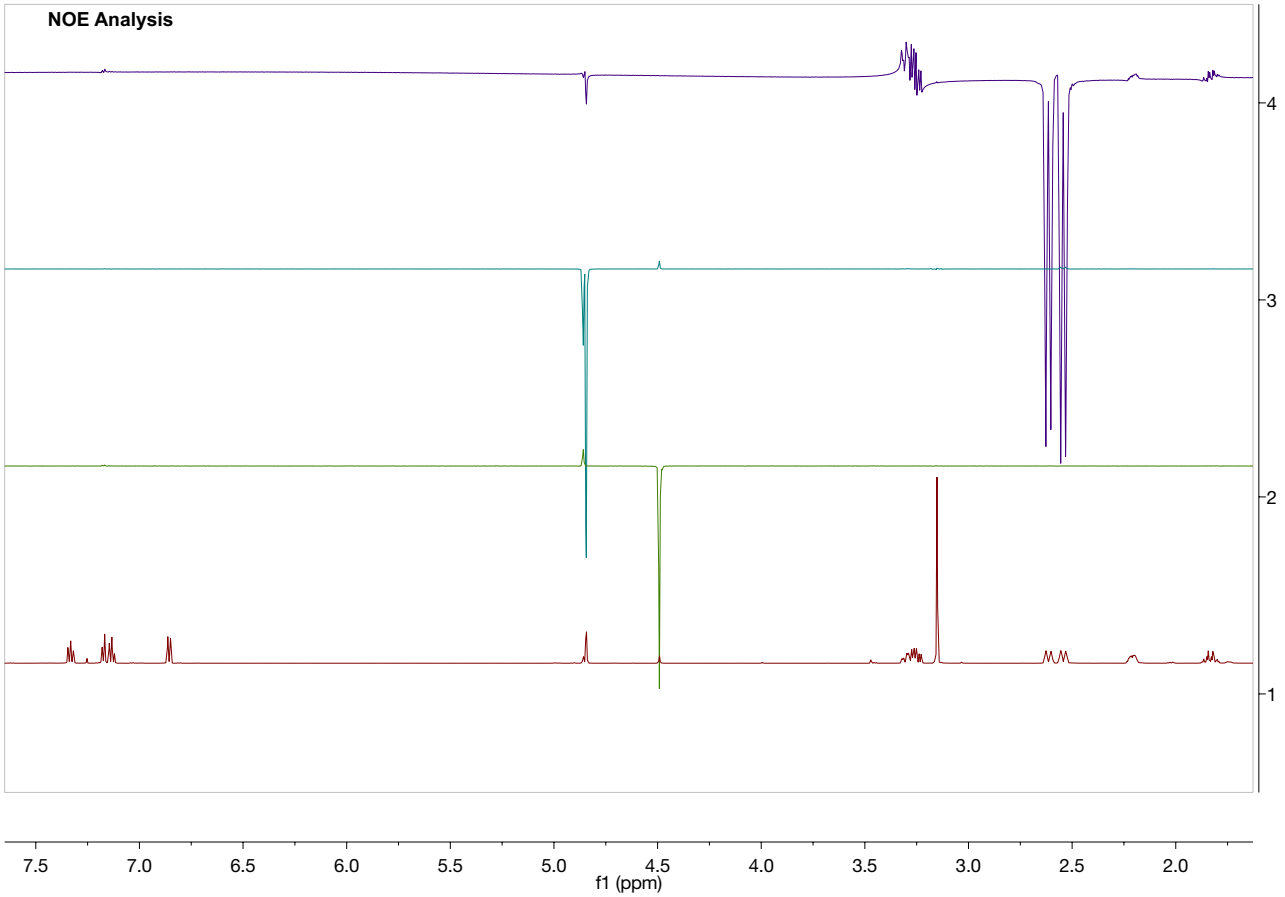

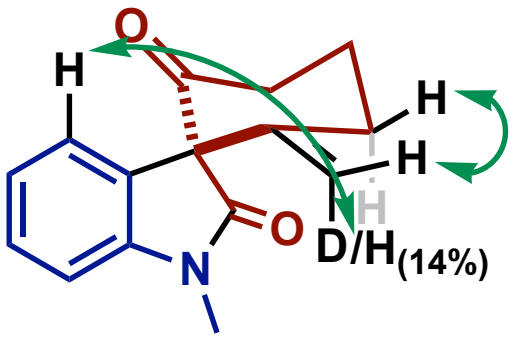

2s, nOe Analysis

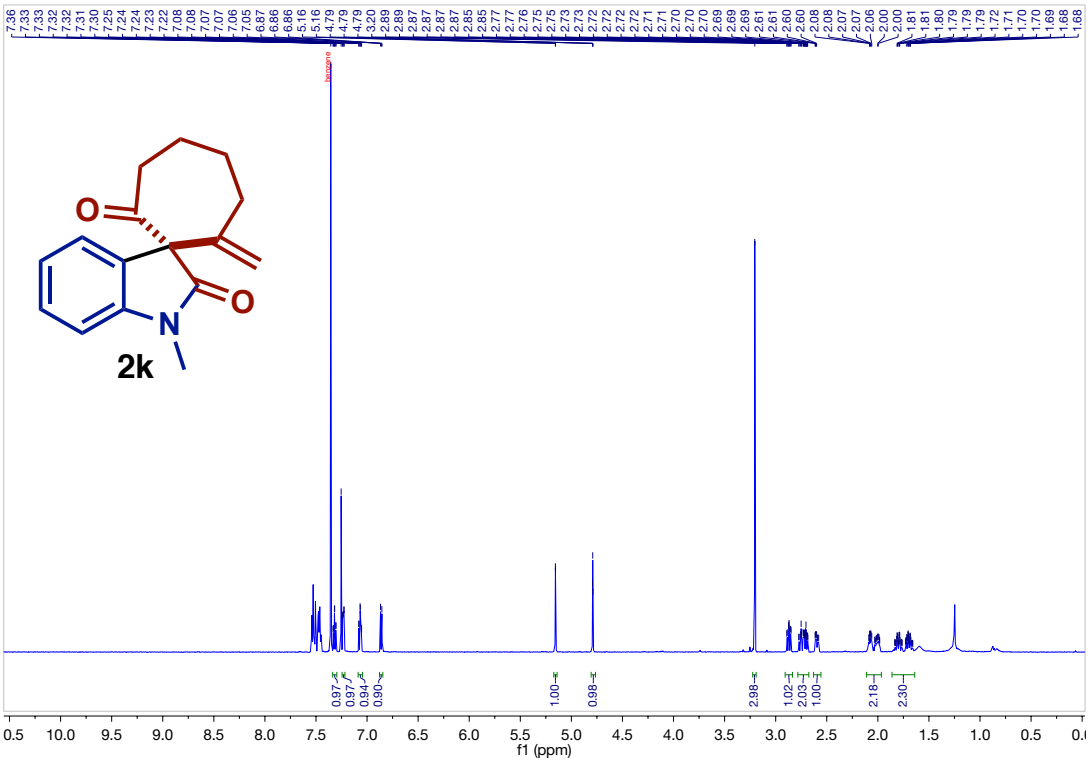
O
O
N
2k
f1 (ppm)

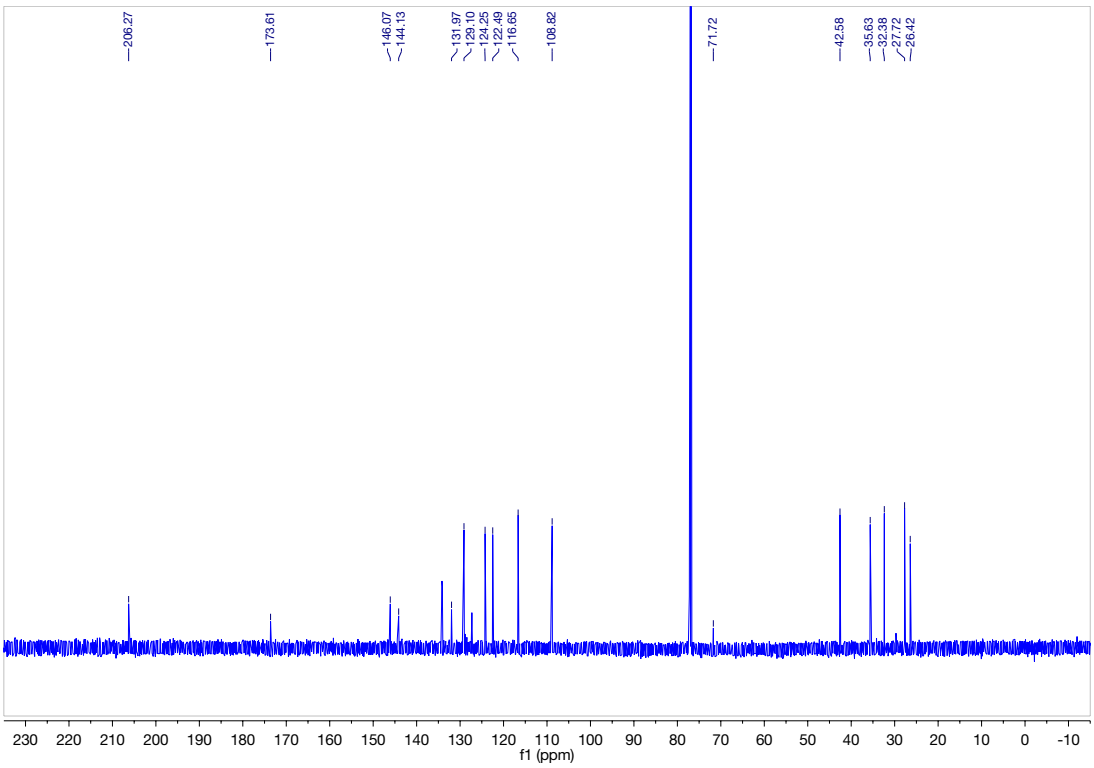
206.27
173.61
146.07
144.13
131.97
129.10
124.25
122.49
116.65
108.82
71.72
42.58
35.63
32.38
27.72
26.42
f1 (ppm)

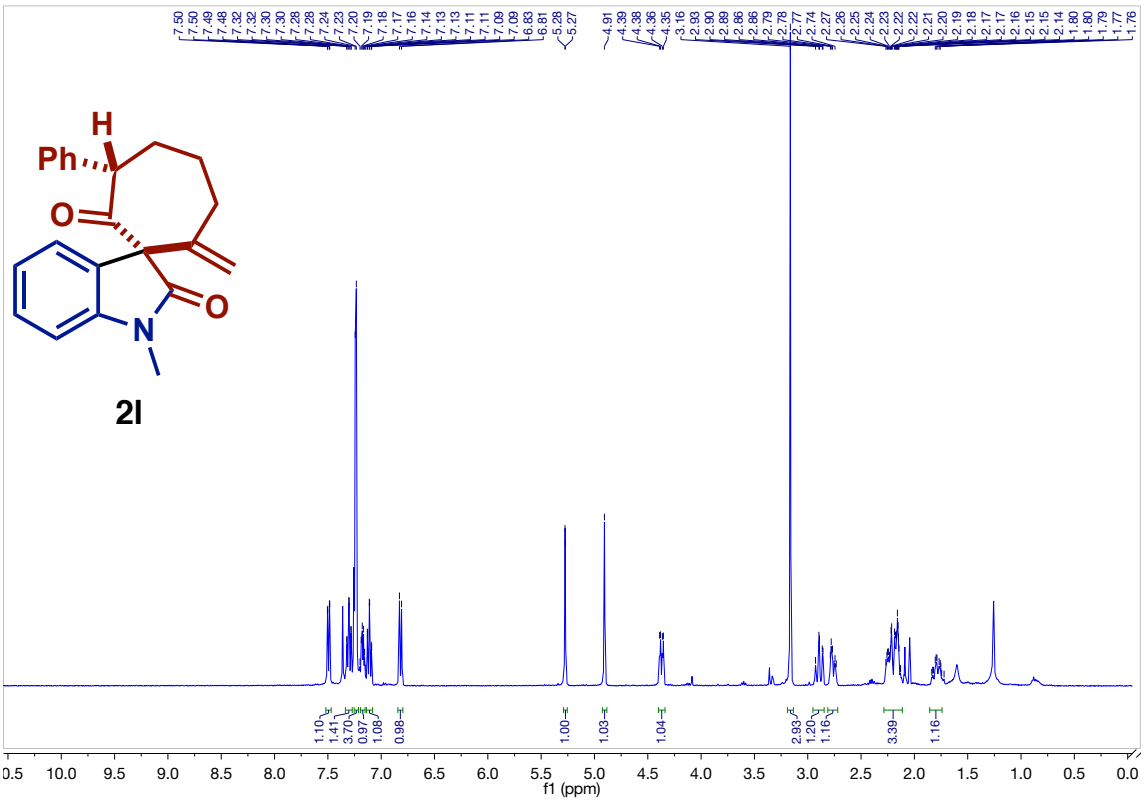
H
Ph
O
O
N
2l
f1 (ppm)

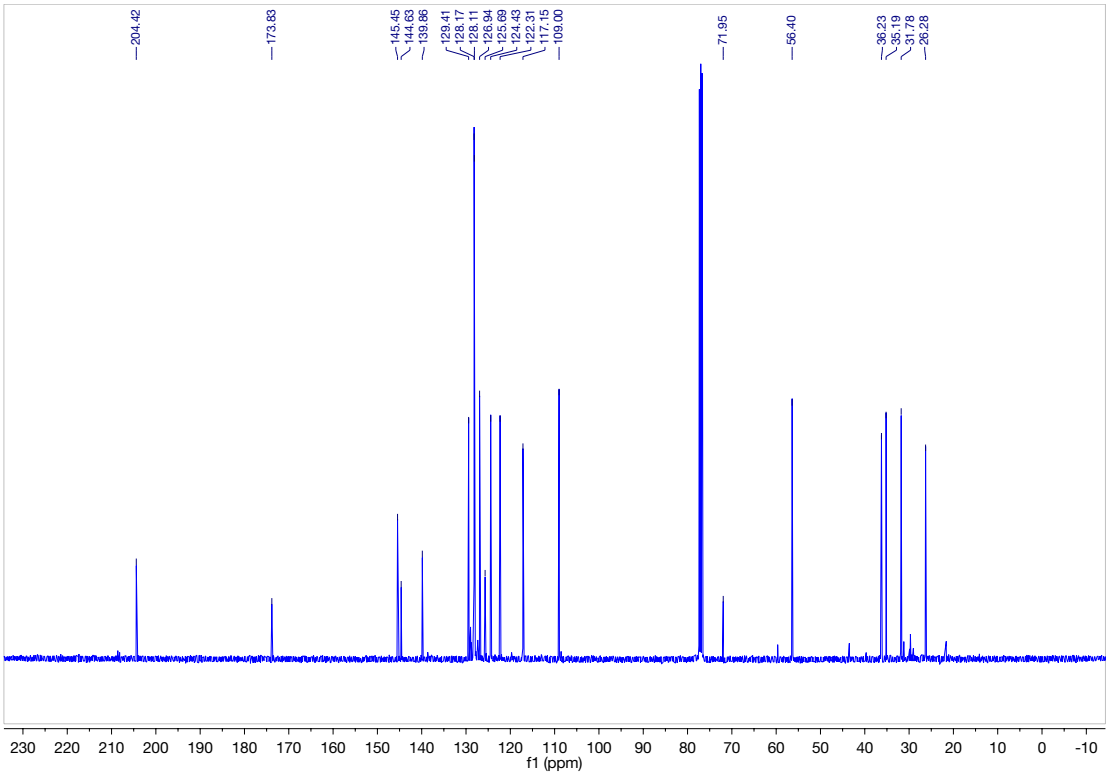
f1 (ppm)

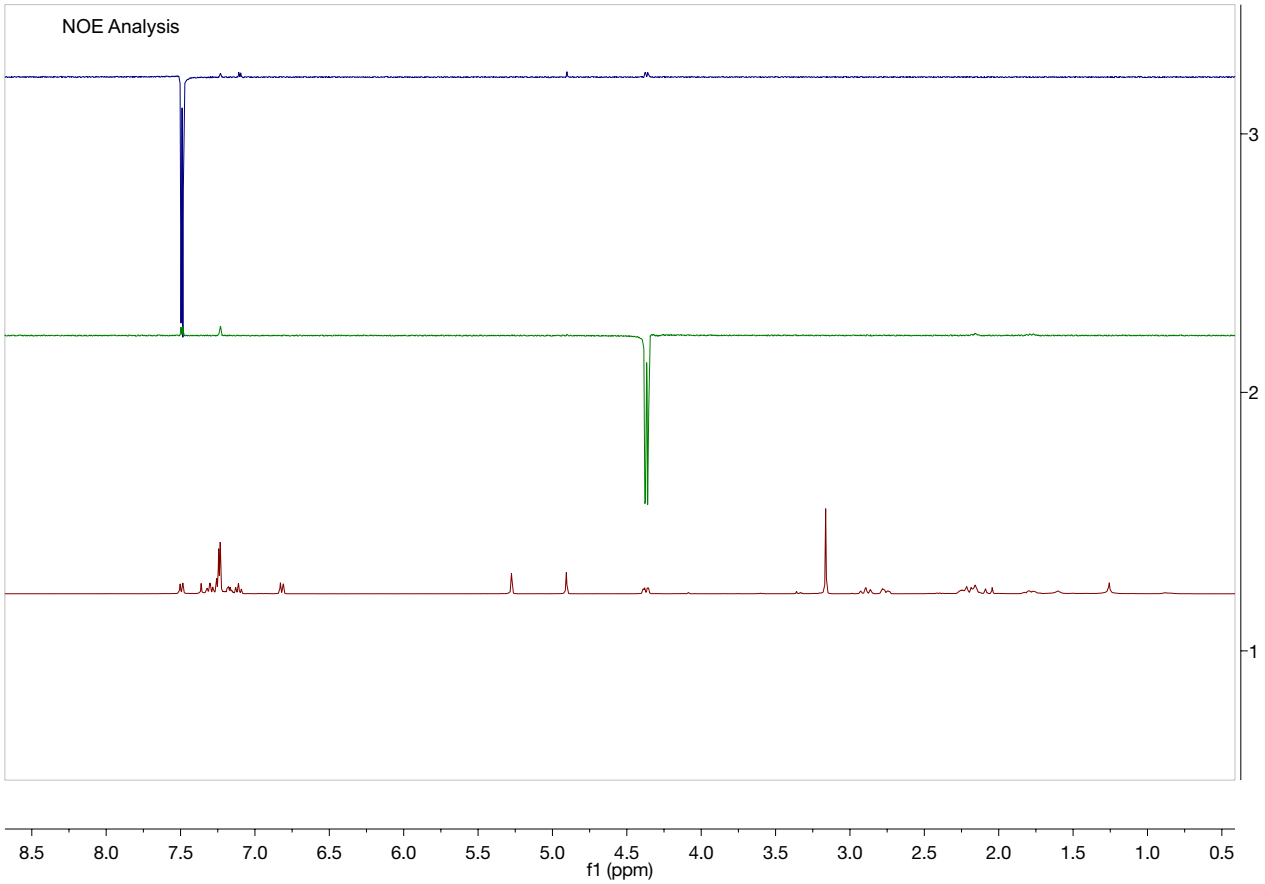

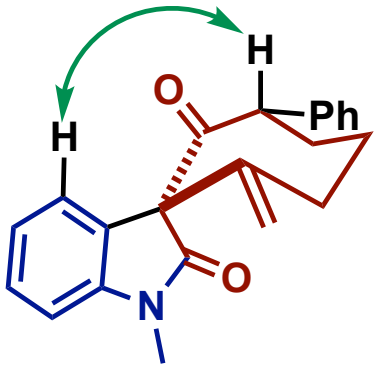

2l, nOe Analysis

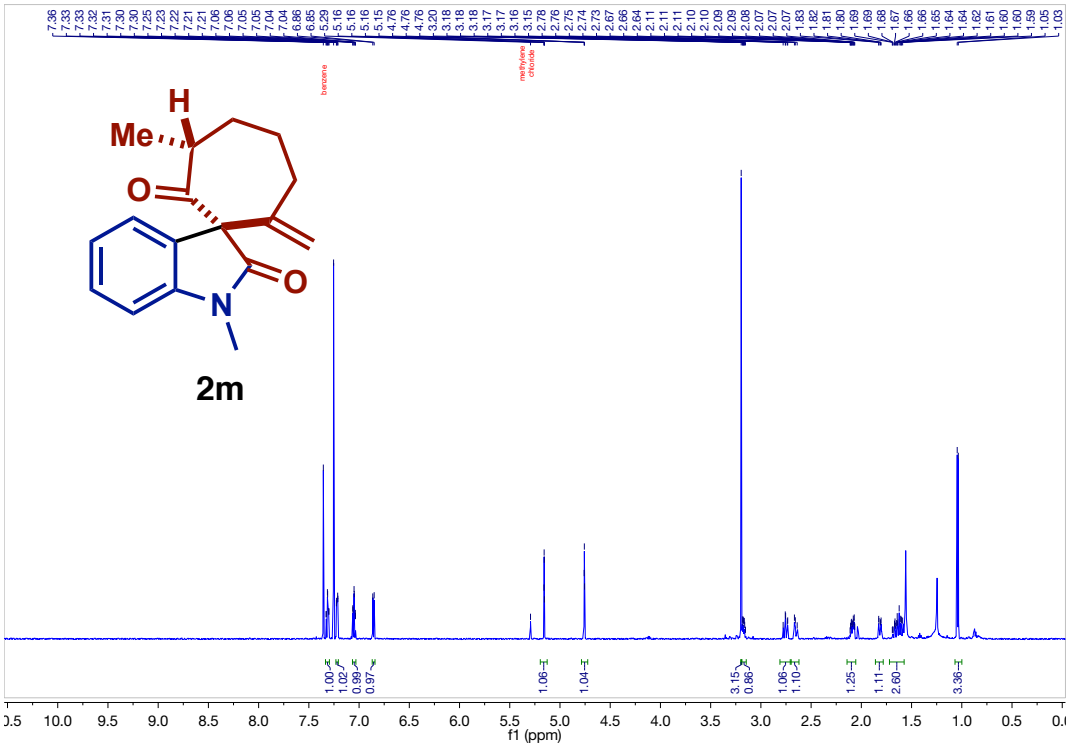
H
Me
O
O
N
2m
benzene
methylene chloride
1.00
1.02
0.99
0.97
1.06
1.04
3.15
0.86
1.06
1.10
1.25
1.11
2.60
3.36
f1 (ppm)

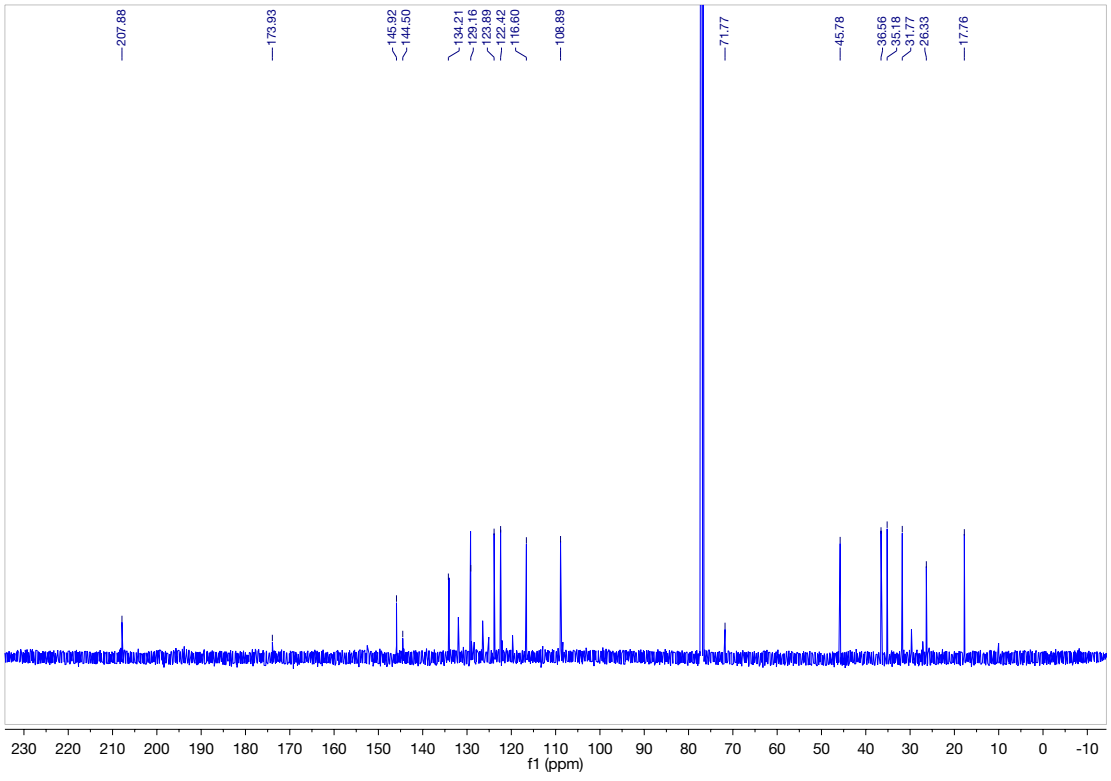
207.88
173.93
145.92
144.50
134.21
129.16
123.89
122.42
116.60
108.89
71.77
45.78
36.56
35.18
31.77
26.33
17.76
f1 (ppm)

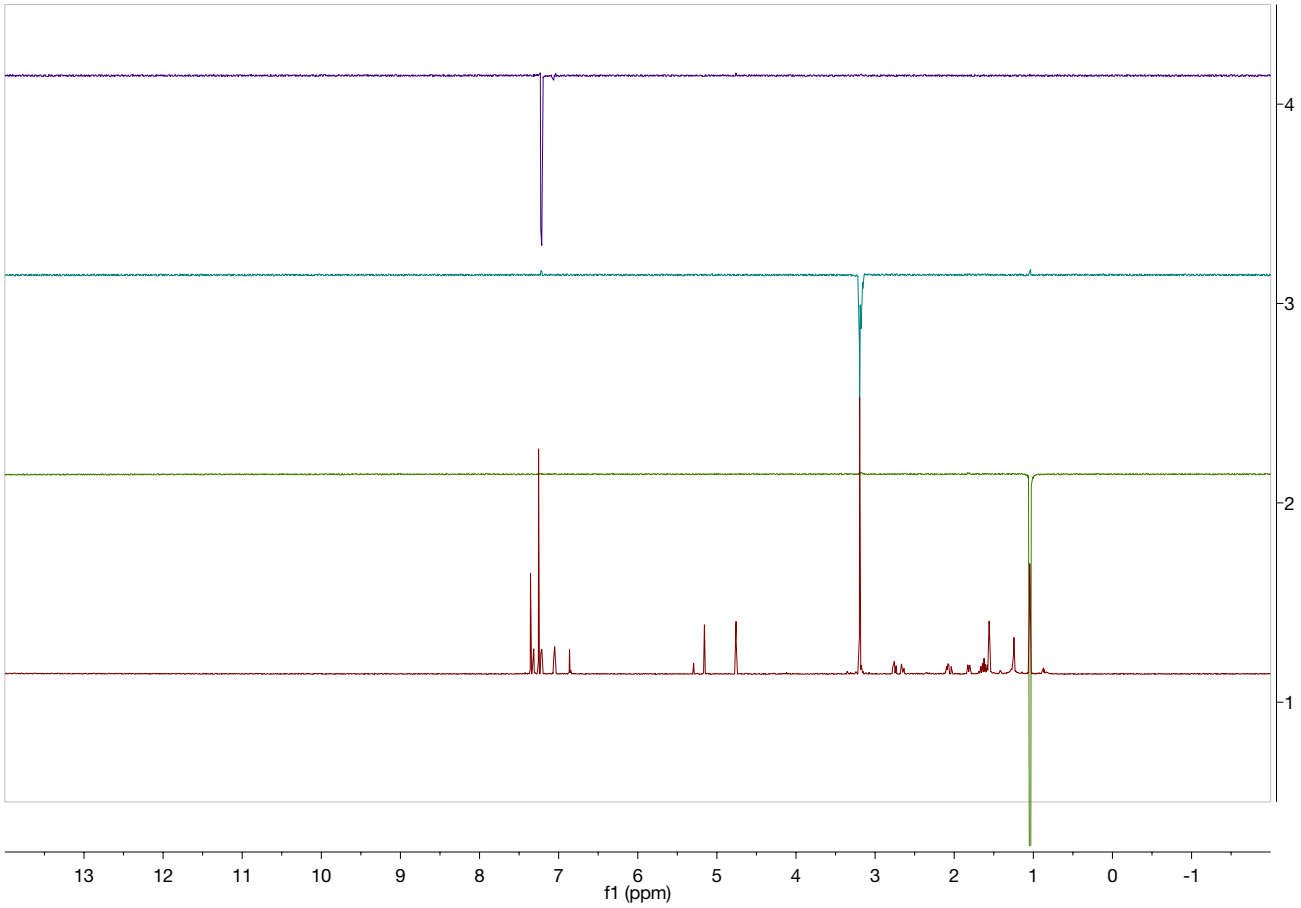

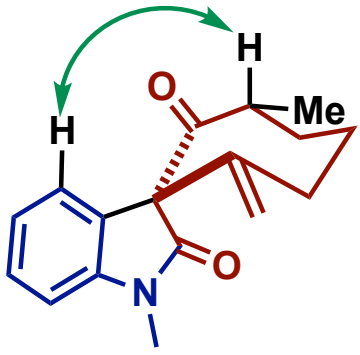

2m, nOe Analysis

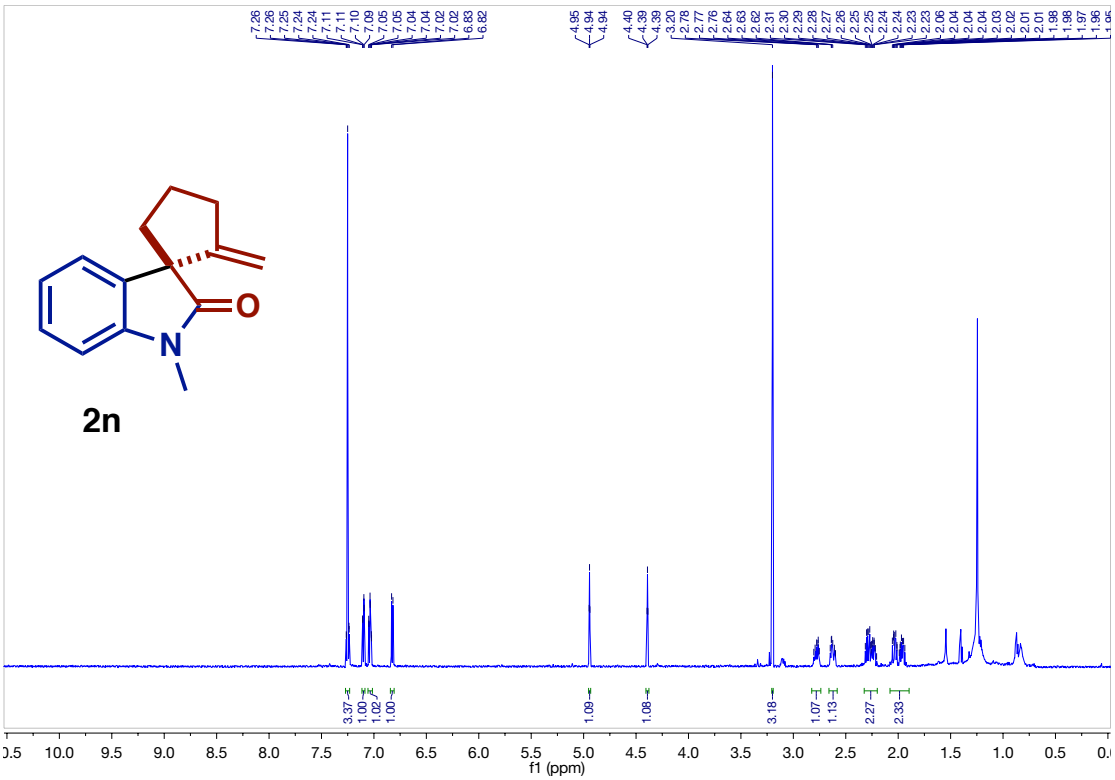
O
N
2n
f1 (ppm)

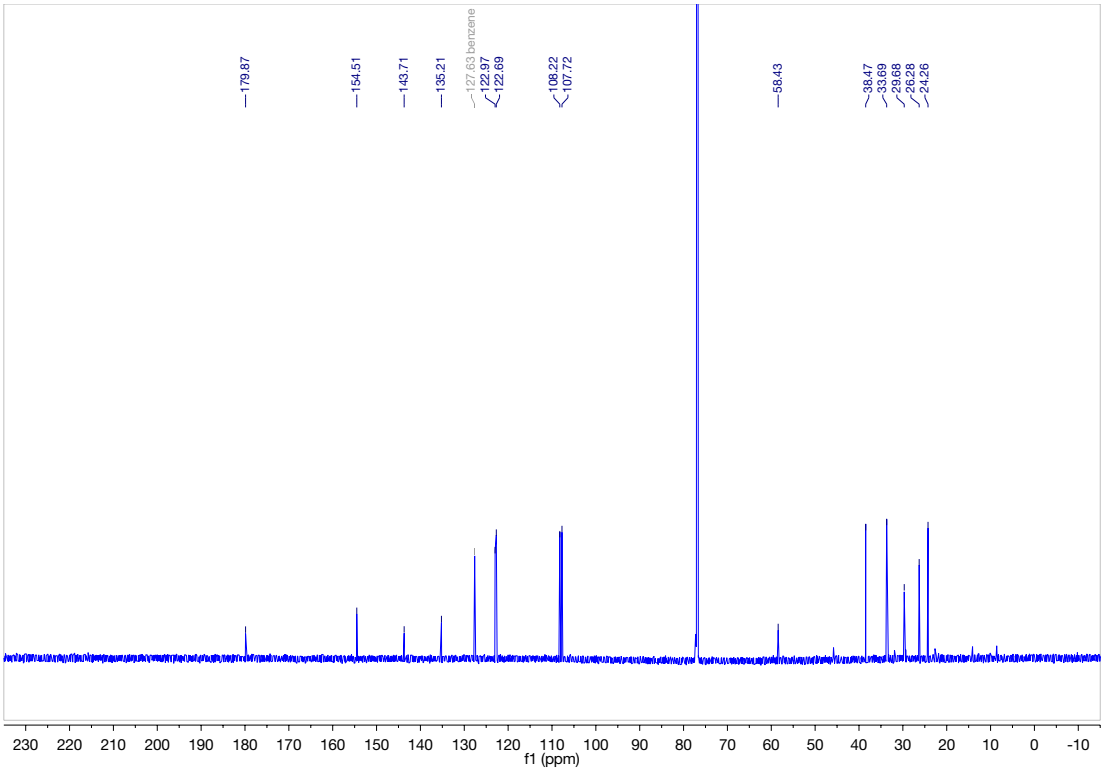
179.87
154.51
143.71
135.21
127.63 benzene
122.97
122.69
108.22
107.72
58.43
38.47
33.69
29.68
26.28
24.26
f1 (ppm)

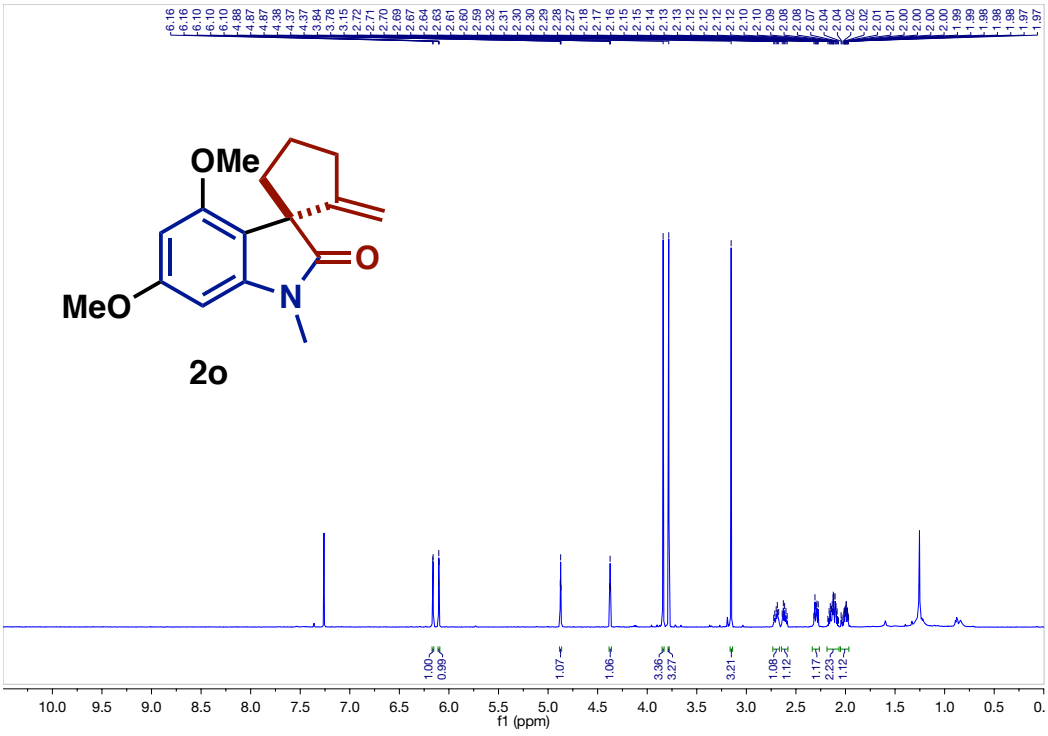
OMe
MeO
O
N
2o
f1 (ppm)

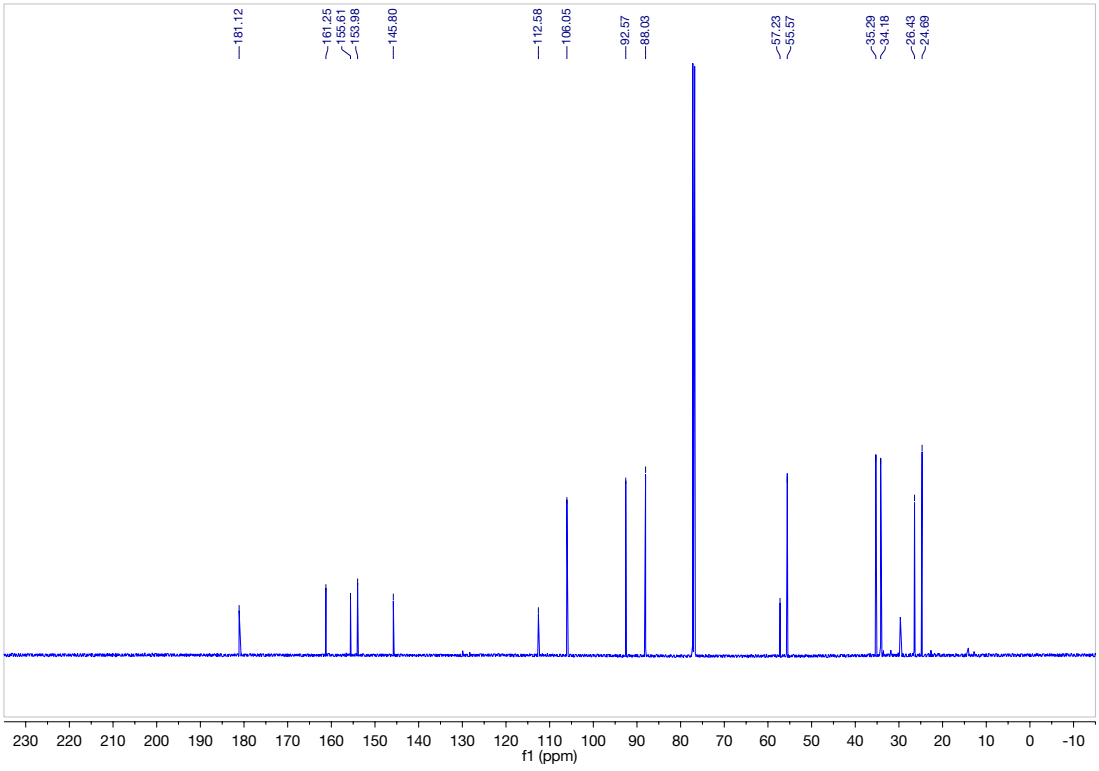
181.12
161.25
155.61
153.98
145.80
112.58
106.05
92.57
88.03
57.23
55.57
35.29
34.18
26.43
24.69
f1 (ppm)

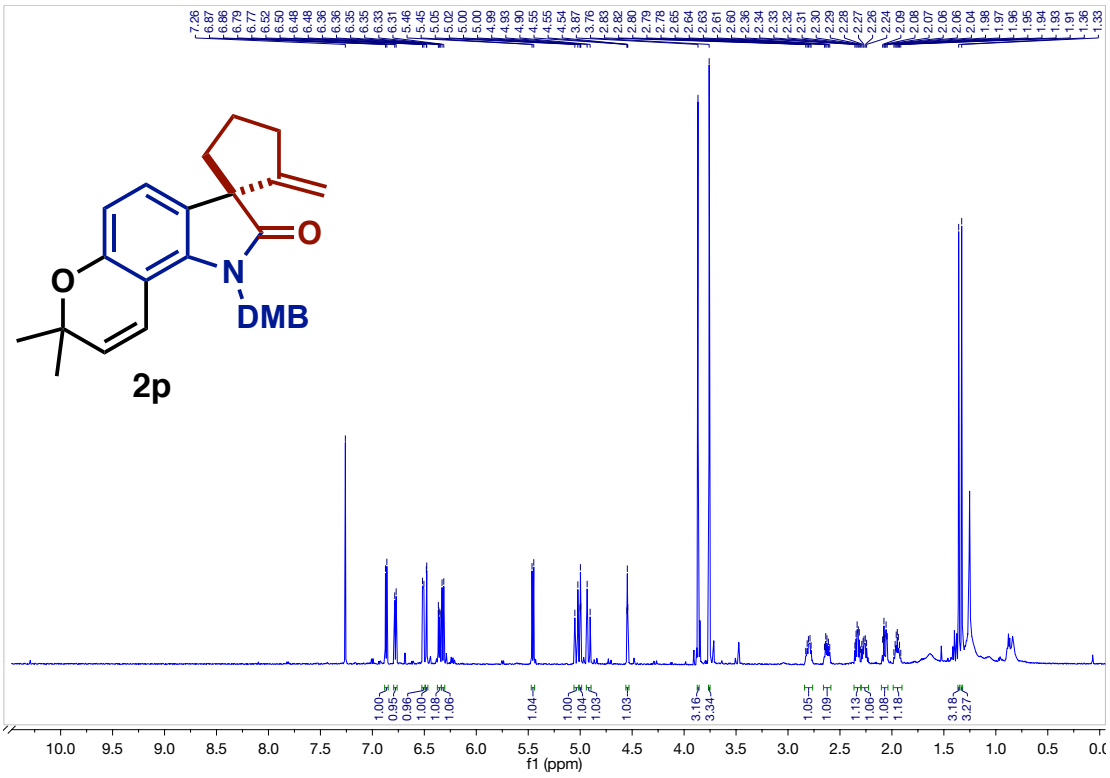
O
N
DMB
O
2p
f1 (ppm)

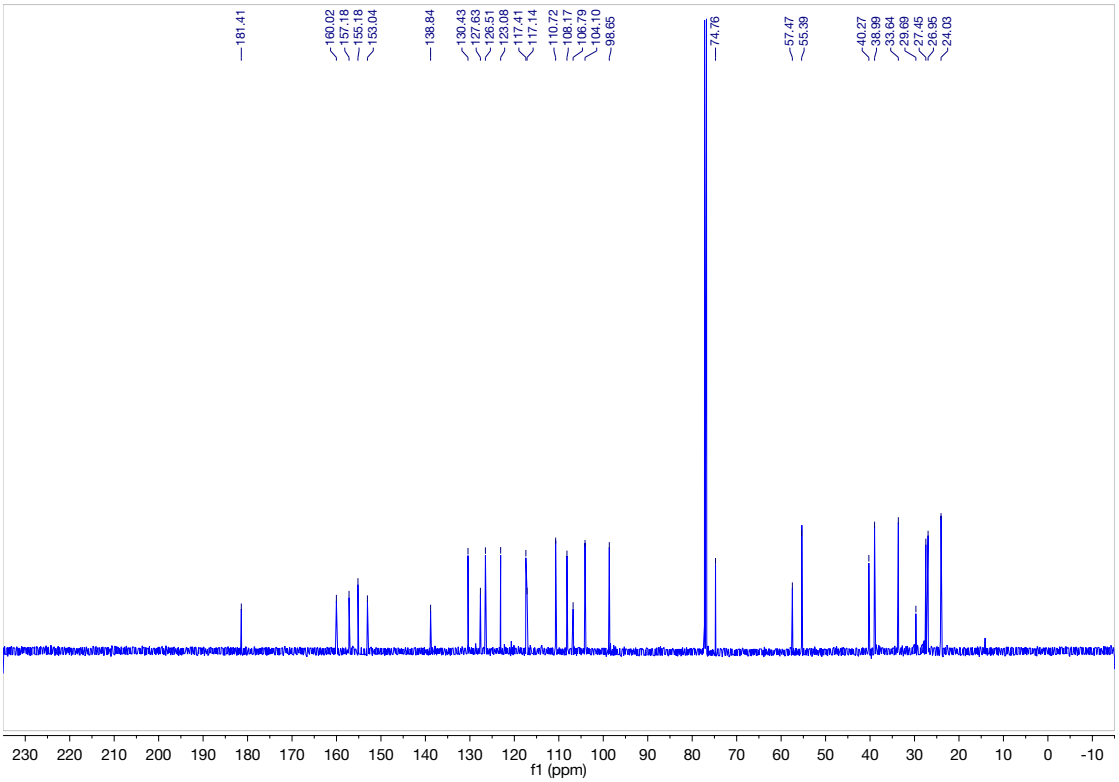
f1 (ppm)

CHAPTER 5

[3+2] Annulations of α-Diazoketones for the Synthesis of Spiroketals and Spiroaminals

5.1 INTRODUCTION

The spiroketal moiety is considered a highly privileged scaffold that is found in numerous natural products and drugs (**Figure 5.1**).[1] Molecules that contain the spiroketal

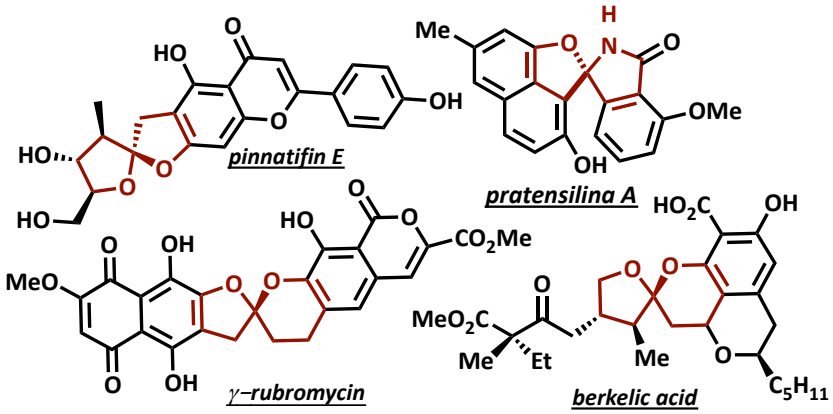

Figure 5.1. *Biologically active natural products and drug molecules containing spiroketals/aminals*

backbone have at least two oxacyclic rings in which the oxygen atoms, that belong to their own respective rings, share a common spiro-carbon atom. Currently, the isolation and characterization of new spiroketals is a continually growing field, therefore new methods for the laboratory synthesis of these scaffolds is highly appreciated by the chemical community.[1b] Synthetic efforts completed by laboratories can provide insight into possible biosynthetic pathways that lead to the natural synthesis of spiroketal containing natural products.

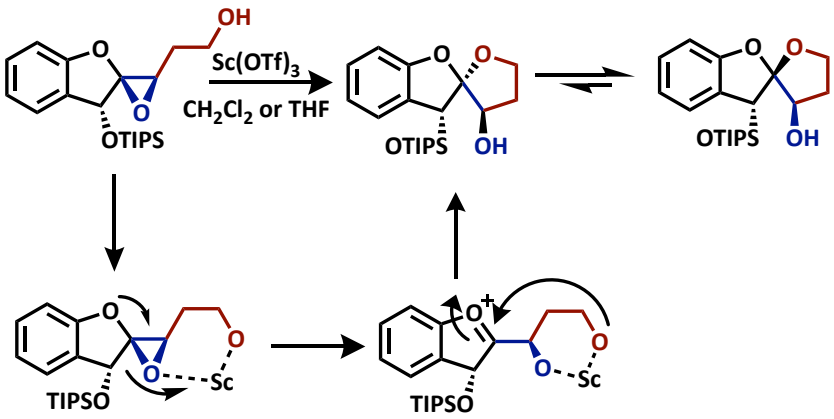

Scheme 5.1. *Synthesis of benzannulated spiroketals developed by Sharma et al.*

Recently in 2014, Sharma et al. developed a solvent-dependent stereoselective spiroketalization using $Sc(OTf)_3$ and *exo*-glycal epoxides having alcohol side chains (**Scheme 5.1**).[2] The reaction proceeds through a Sc(III) mediated epoxide opening which forms a stabilized oxocarbenium ion that undergoes *O*-alkylation by the flanking hydroxyl group to provide the desired benzannulated spiroketals (**Scheme 5.1**). Subsequently in 2017, Liang et al. developed a $Sc(OTf)_3/PPh_3AuOTf$ catalyzed spiroketalization using *exo*-enol ethers and *ortho*-quinone methides.[3] The authors propose this reaction proceeds through a Au(I)

catalyzed cyclization of an alkyne to form an *exo*-enol ether. Simultaneously, Sc(III) generates the *ortho*-quinone methide through a dehydration sequence. When these two intermediates react, they undergo a [4+2] annulation to form the desired benzannulated spiroketals (**Scheme 5.2**).

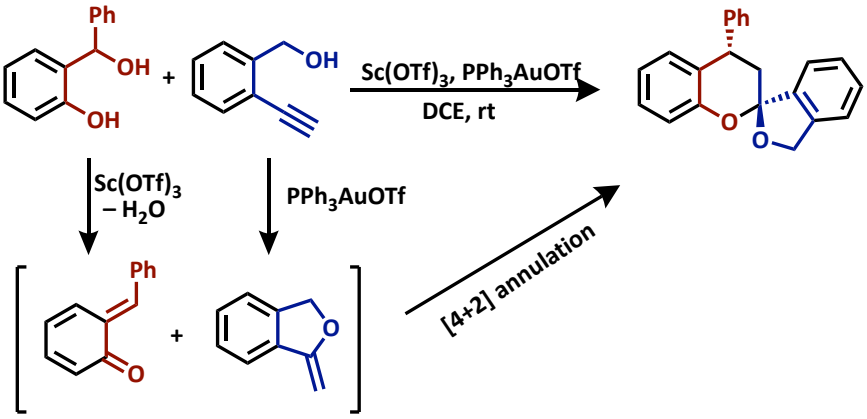

Scheme 5.2. *Synthesis of benzannulated spiroketals developed by Liang et al.*

Given these insights into spiroketal synthesis from the literature, we began to hypothesize different methods to access this scaffold using our previously developed Rh(II)/Au(I) catalytic cocktail and taking inspiration from the systems developed by Sharma et al. and Liang et al in **Schemes 5.1** and **5.2**. As stated in Chapter 3, when analyzing spiroethers and azaspiro-ring systems, we dissected these molecules in half to create two ambiphilic reacting partners that would combine to form our desired spirocenter. However, when we applied this dissection to spiroketals it was determined that a cyclic diazo whose diazo substituted-carbon was directly bound to a heteroatom would be needed (**Figure 5.2**). No known syntheses of diazos of this nature can be found in literature,

presumably due to a lack of stability of the desired compound.[4] After many failed attempts at developing a synthesis for a diazo compound of this nature, it was determined that this retrosynthetic design would be unsuccessful.

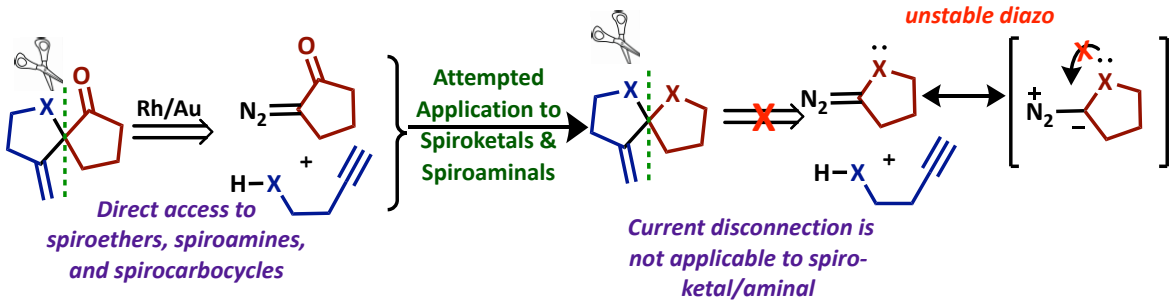

Figure 5.2. *Attempted retrosynthetic disconnection of spiroketals*

5.1.1 PRELIMINARY IDENTIFICATION OF REACTIVITY OF α-DIAZOKETONES

With the limitation of this unique diazo synthesis consistently in our minds, we came across a serendipitous discovery that was based on the reactivity of α-diazoketones. As previously mentioned in Chapter 2, during the substrate scope expansion of the carboxylic acid O–H insertion/Conia-ene cascade we identified the formation of a [3.1.0]-fused ring system when non-terminal alkynes were applied in our Rh(II)/Au(I) catalytic system (**Scheme 5.3a**).[5] This product was confirmed to form through a cyclopropanation of the resulting furanone produced during the premixing of 3-pentynoic acid with the Rh(II)/Au(I) catalytic cocktail via a 5-*endo*-dig self-lactonization. Interested in expanding the scope of this serendipitous finding, we exposed α-diazoketone **1a** to these conditions, however an unexpected rearrangement occurred to form dihydropyranone **2a** in 28% yield. We decided to further optimize this transformation through screening different Lewis acids

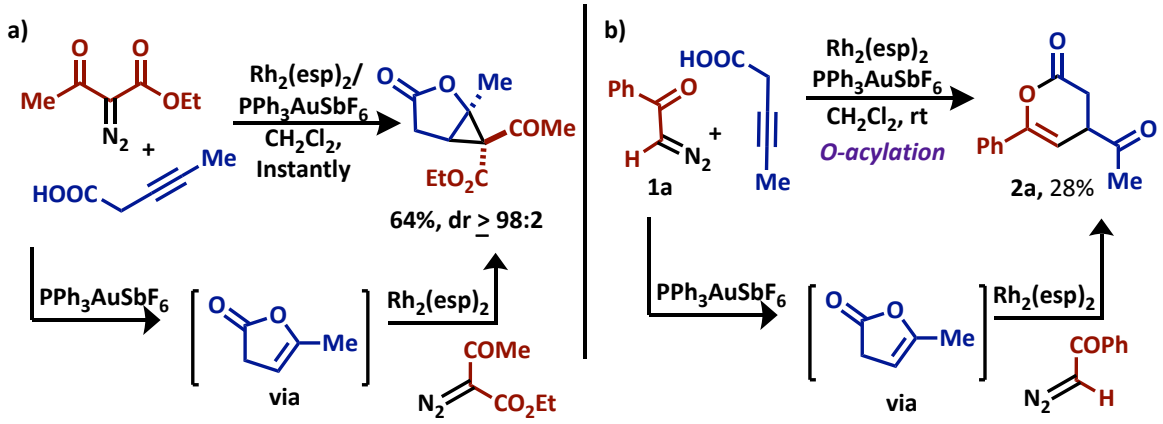

Scheme 5.3. *a) Synthesis of [3.1.0]-fused ring system through Rh(II)/Au(I) catalyzed cyclopropanation; b) Serendipitous finding in system when α-diazoketones were used.*

Table 5.1. *Optimization of Dihydropyranone Synthesis*

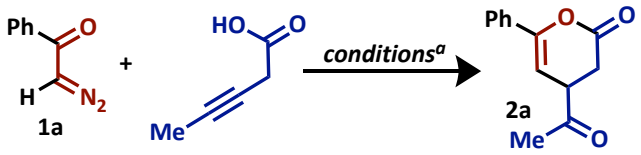

entry	catalysts	temp, t	yield (%)[b]
1	$Rh_2(esp)_2$/AgOTf/PPh_3AuCl	rt, 15 min	28%
2	$Rh_2(esp)_2$/$AgSbF_6$/PPh_3AuCl	rt, 15 min	29%
3	$Rh_2(esp)_2$/PPh_3AuCl/$(CuOTf)_2$-tol	rt, 15 min	55%
4	**$Rh_2(esp)_2$/PPh_3AuCl/$(CuOTf)_2$-tol**	**0 ºC, 30 min**	**72%**
5	$Rh_2(esp)_2$/PPh_3AuCl	rt, 24 h	0%
6	$Rh_2(esp)_2$/$(CuOTf)_2$-tol	rt, 24 h	0%

All optimization reactions were performed by adding **3-pentynoic acid** (2.5 equiv.) to a solution of the Lewis Acid (10 mol%) and $Rh_2(esp)_2$ (1 mol%) in 0.1 M of the appropriate CH_2Cl_2. Once the furanone was visualized on TLC, diazo **1a** (1 equiv.) was added dropwise via syringe pump. Once the addition was complete the desired product was isolated by column chromatography.

(**Table 5.1**). Switching the silver salt to $AgSbF_6$ had little effect on increasing the yield of the transformation, therefore we decided to screen the mixture of $PPh_3AuCl/(CuOTf)_2$-tol that was used in Chapter 4 for a more controlled activation of the alkyne in our system. This change significantly increased the yield of **2a** to 55% (**Table 5.1**, entry 3). Next, we decreased the temperature of the reaction to 0 ºC and the yield increased to 72% (**Table 5.1**, entry 4). Lastly, we screened PPh_3AuCl and $(CuOTf)_2$-tol separately in the presence of $Rh_2(esp)_2$ and neither Lewis acid was able to cyclize 3-pentynoic acid into the corresponding furanone, therefore diazo **1a** underwent carboxylic acid O–H insertion into 3-pentynoic acid.

Once the optimized conditions were identified we investigated the applicability of this method to different substrates (**Scheme 5.4**). The electron rich *para*-methoxy ketone diazocarbonyl participated in the reaction and the desired compound **2b** was isolated in 92% yield. Next, the *para*-bromo ketone diazocarbonyl was exposed to the optimized reaction conditions and the desired compound **2c** was isolated in a 68% yield.

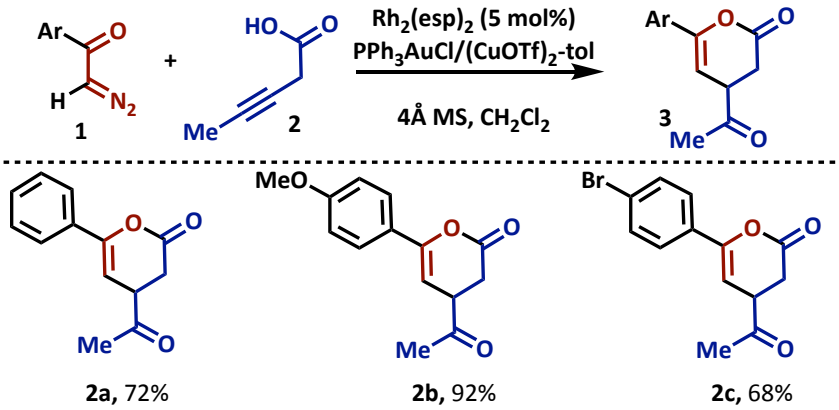

Scheme 5.4. *Substrate scope of dihydropyranones*

After extending the substrate scope to different α-diazoketones, we were able to propose a possible reaction mechanism as illustrated in **Scheme 5.5**. When exposed to a mixture of $PPh_3AuCl/(CuOTf)_2$-tol, 3-pentynoic acid undergoes a 5-*endo*-dig self-lactonization to form furanone **4**. Next, the Rh(II)-carbene of the α-diazoketone is attacked

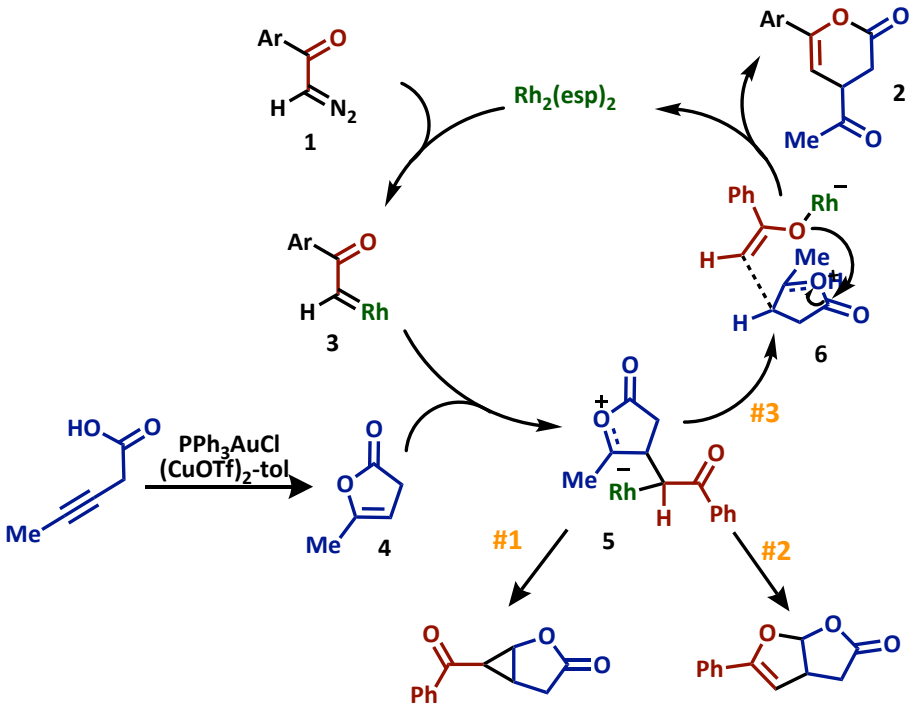

Scheme 5.5 *Proposed mechanism of dihydropyranone synthesis providing insight into 3 possible pathways of reactivity*

by the electron-rich furanone to form the active zwitterionic intermediate **5**. This intermediate has the ability to pursue three differing pathways: 1) *C*-alkylation to form a cyclopropane, 2) *O*-alkylation to form a furano-furan derivative, or 3) *O*-acylation to form a six-membered lactone, kicking out a methyl-ketone as a leaving group. The latter pathway

is the favored mode of reactivity for this transformation, leading to a variety of dihydropyranone derivatives. Further experimentation is needed to provide thorough justification for the preference for *O*-acylation/6-membered lactonization.

With preliminary insights into the differing reactivity of α-diazoketones, we wanted to extend the reaction seen in **Scheme 5.5** to electron-rich alkenes that would not be prone to pursue pathway #3 as seen in the mechanism. To initiate our studies, we exposed commercially available dihydrofuran to the parent α-diazoketone **1a**, however only cyclopropanation was observed (**Scheme 5.6**). We postulated that a change in our α-diazoketone was needed that would prefer *O*-alkylation of an oxo-carbenium ion over *C*-alkylation, therefore we decided to peruse the literature in search of a different α-diazoketone.

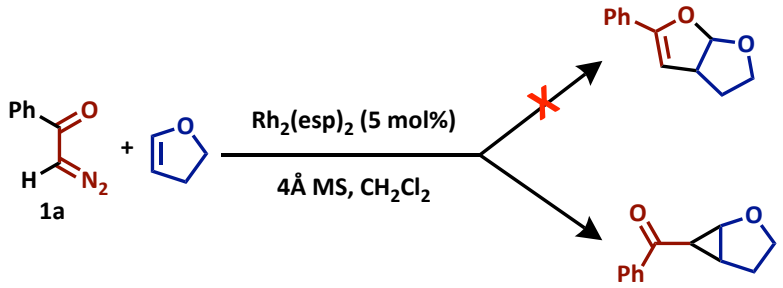

Scheme 5.6. *Attempted extension to dihydrofuran endo-alkene*

Recently in 2013, Kitamura et al. found that diazonaphthoquinones can react with enol ethers to provide dihydronaphthoruans through an *O*-alkylation of an oxo-carbenium ions (**Scheme 5.7**).[6] The authors propose that diazonaphthoquinones (**7**) form a Rh(II) carbene complex in the presence of $Rh_2(OAc)_4$ that reacts with enol ethers to form the

active zwitterionic intermediate **9**. This intermediate aromatizes to form a Rh(II)-bound phenolate **10** that proceeds to undergo *O*-alkylation to form the desired dihydronaphthofuran **11**. Taking these findings as inspiration, we decided to use phenanthrenone diazo **12a**, which has many similarities to the diazo used by Kitamura et

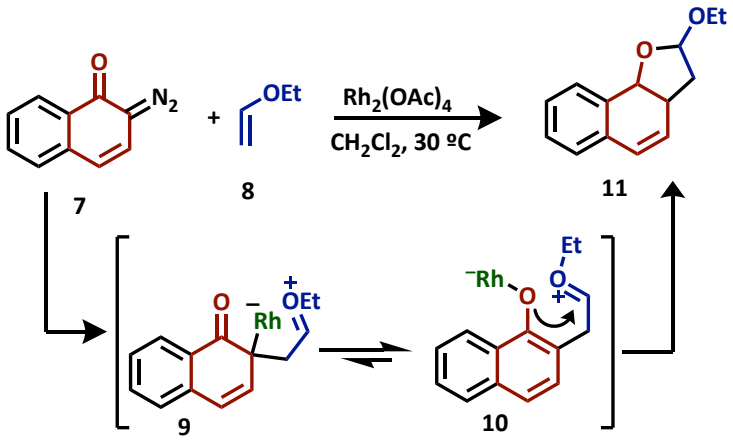

Scheme 5.7. *Synthesis of dihydronapthofurans by Kitamura et al.*

al., and expose it to dihydrofuran in the presence of $Rh_2(esp)_2$ alone (the Au(I)/Cu(I) mixture was not needed due to a pre-cyclized endo-alkene being used). Once the reaction was complete, the desired benzannulated furano-furan **13a** was isolated in 76% yield.

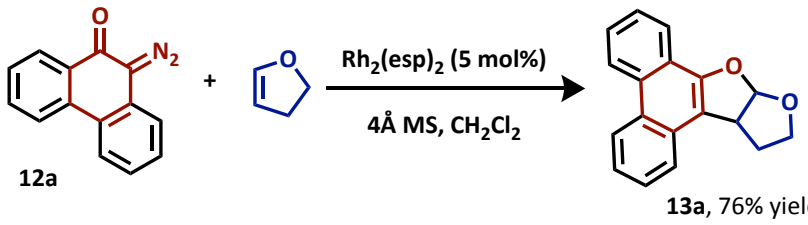

Scheme 5.8. *Synthesis of benzannulated furano-furans through [3+2] annulation*

Inspired by these results, we sought to identify a variety of quinone-type diazocarbonyls that would provide similar reactivity as identified with phanenthrenone diazo **12a**. Recently in literature, diazo quinones synthesized from 2-aminophenol derivatives have been shown to form metal-quinoid carbenes when in the presence of varying metal catalysis.[7] These active metal-quinoid carbenes have been shown to undergo aromatic C–H arylations with electron rich arenes[7b] and C–H functionalizations with arylphosphine oxides[7a], however no report of the corresponding C–H functionalization followed by *O*-alkylation of oxo-carbenium ions to form furan-derivatives with these types

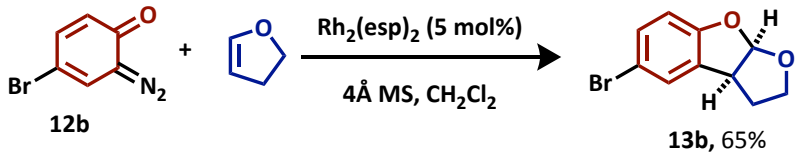

Scheme 5.9. *Application of diazo quinone in developed methodology*

of diazo quinones has been reported. With this insight, we exposed diazo quinone **12b** to commercially available dihydropyran in the presence of $Rh_2(esp)_2$ in refluxing dichloromethane, upon completion of the reaction benzannulated furano-furan **13b** was isolated in 61% yield (**Scheme 5.9**). We proceeded to extend this methodology to a variety of electron rich alkenes (**Scheme 5.10**). Dihydropyran performed similarly to dihydrofuran

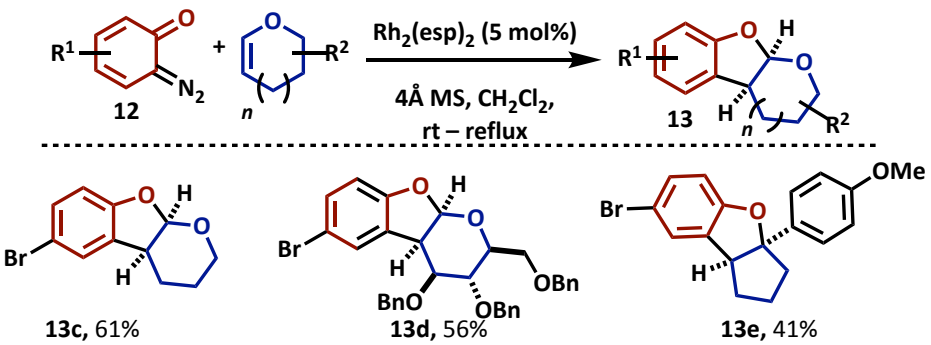

Scheme 5.10. *Substrate scope of benzannulated furano-furans*

to provide **13c** in 65% yield. Next, we exposed the electron rich endo-alkene synthesized from glucose to our optimized conditions and obtained the desired compound **13d** in 56% yield. Lastly, we applied our method to an endo-alkene which was electron rich due to a *para*-methoxy aryl substituent. This alkene underwent the desired transformation to provide **13e** in 41% yield.

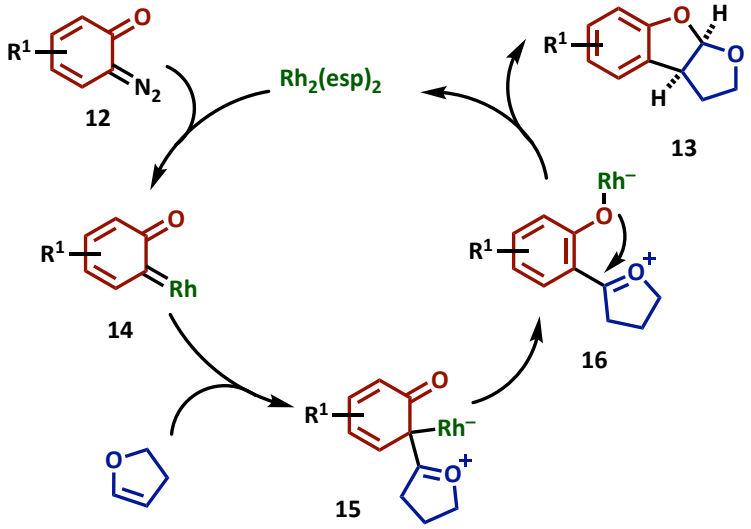

Scheme 5.11. *Proposed mechanism of furano-furan sysnthesis mediated by metal-quinoid carbenes to provide thermodynamically favored cis-junction*

A plausible mechanism for the formation of the benzannulated furan-ring systems is shown in **Scheme 5.11**. When in the presence of $Rh_2(esp)_2$ the diazo quinones form active Rh(II)-quinoid carbenes **14** that undergo C–H functionalization with the electron-rich alkenes to form a zwitterionic intermediate **15** that quickly aromatizes to give the metal-bound phenolate complex **16**. This complex undergoes *O*-alkylation onto the oxo-carbenium ion to form the thermodynamically stable *cis*-ring junction in **13**.

Through a thorough understanding of the reactivity of α-diazoketones in hand, a new retrosynthesis was designed that "splits" spiroketals in a different manner (**Figure 5.3**). We hypothesized that by applying this newly identified mode of reactivity of metal carbenes derived from α-diazoketones and also metal-quinoid carbenes to electron-rich *exo*-alkenes, we could access a variety of spiroketals and spiroaminals through stereoselective [3+2] annulations.

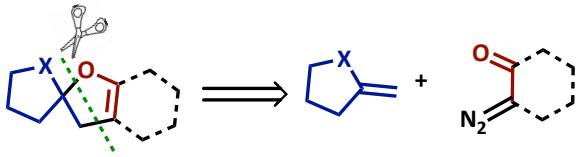

New disconnection exploits character of electron rich alkenes in spirocyclizations

Figure 5.3. *New retrosynthetic disconnection for spiroketals*

5.2 SYNTHESIS OF SPIROKETALS AND SPIROAMINALS

5.2.1 OPTIMIZATION OF CATALYTIC CONDITIONS

With our interest intently set on the development of a mild and efficient method that provides access to a variety of spiroketals using metal-carbene mediated methodology, we proceeded to synthesize electron-rich exo-alkene **17a** from readily available 2-iodobenzoic acid using literature known protocols. Once this alkene was obtained it was exposed to a variety of metal catalysts in the presence of α-diazoketone **1a**. When the reaction was conducted in the with of $Rh_2(esp)_2$ a 7:3 ratio of the desired product **19a** to the cyclopropane **18a** was isolated in a total 37% yield (**Table 5.2**). The

Table 5.2 *Optimization of [3+2] Annulation of Exo-Alkene*

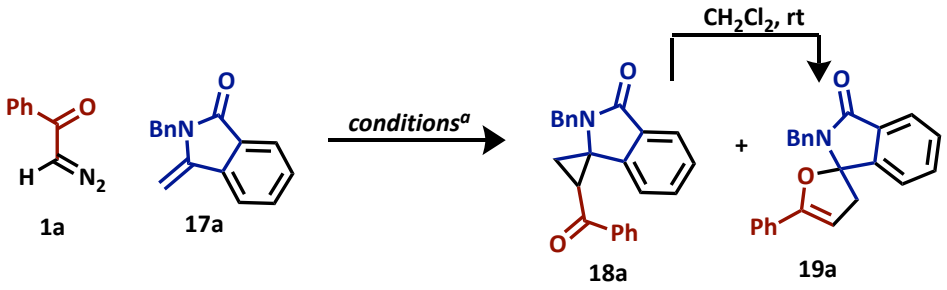

entry	catalysts	temp, t	**18a**:**19a**	**19a** %yield
1	$Rh_2(esp)_2$	rt, 30 min	30:70	26%
2	$Rh_2(esp)_2$	rt, 4 hr	0:100	43%
3	$Rh_2(OAc)_4$	rt, 4 hr	0:100	35%
4	Rh_2(*R*-DOSP)$_4$	rt, 4hr	0:100	42%
5	$Rh_2(esp)_2$	reflux, 2 hr[b]	0:100	64%

All optimization reactions were performed by adding **1a** (2.5 equiv.) to a solution of Rh(II)(5 mol%) in 0.2 M of CH_2Cl_2. [b] **1a** was added via syringe pump to a refluxing solution of **17a**, no cyclopropane intermediate was observed with this method of addition

reaction gave valuable insight into the possible reaction mechanism; however, we were curious whether the highly substituted polarized cyclopropane could undergo rearrangement to the desired product **19a**. Therefore, **18a** was stirred at room temperature overnight and the next day clean conversion to **19a** was observed. With these insights, we repeated the reaction with $Rh_2(esp)_2$ and increased the reaction time to 4 hours, assuming this would be enough time for any necessary rearrangement, and isolated **19a** in 43% yield (**Table 5.2**, entry 2). Next, we repeated these conditions in the presence of $Rh_2(OAc)_4$ and the desired product was isolated in 35% yield (**Table 5.2**, entry 3). Subsequently, we screened the chiral Rh(II)-salt, Rh_2(*R*-DOSP)$_4$, in hopes of inducing enantiomeric excess (ee) in the transformation but no ee was induced (**Table 5.2**, entry 4). Lastly, we revisted $Rh_2(esp)_2$ but added the α-diazoketone dropwise via syringe pump to a refluxing solution of exo-alkene **17a** and $Rh_2(esp)_2$ in hopes of increasing the yield of the desired product. These conditions provided the desired compound **19a** in a 64% isolated yield.

5.2.2 APPLICATION TO SUBSTRATE SCOPE

With the optimal conditions in hand we proceeded to extend the substrate scope to access a variety of spirocyces. When a non-terminal electron-rich alkene was used the desired spiroketal **19c** was isolated as a single diastereomer in 47% yield (**Scheme 5.12a**). The yield of this reaction was low despite all attempts at optimization. This was presumably

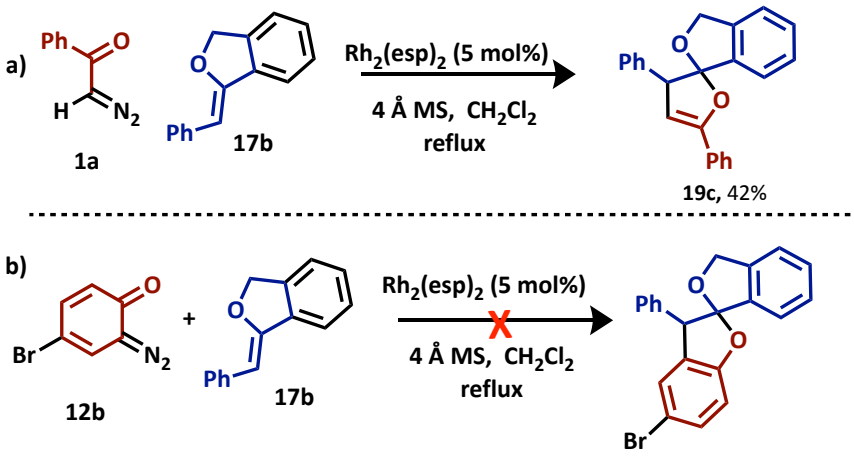

Scheme 5.12. *a) Synthesis of spiroketal* ***19c****; b) Non-terminal exo-alkene was not able to react with diazo quinone.*

due to the electron-rich alkene that was formed in the final product that is of equal reactivity to the alkene found in the starting material. To solve this problem, we believed the use of diazo quinones in this transformation would increase the yield because there would be no reactive alkenes present in the final product. However, when diazo quinone **12b** was reacted with the non-terminal alkene **17b** under our optimized conditions the [3+2] annulation was not successful and the diazo quinone instead underwent hydration to form *para*-bromo phenol (**Scheme 5.12b**). We theorized that the steric hindrance of alkene **17b** was not ideal for this transformation with diazo quinones, therefore we screened terminal electron-rich *exo*-alkenes **17a** and **17c** with the diazo quinone. These substrates successfully underwent the desired transformation to form benzannulated spiroaminal **19d** and sprioketal **19e** in 68% yield and 63% yields respectively (**Scheme 5.13**).

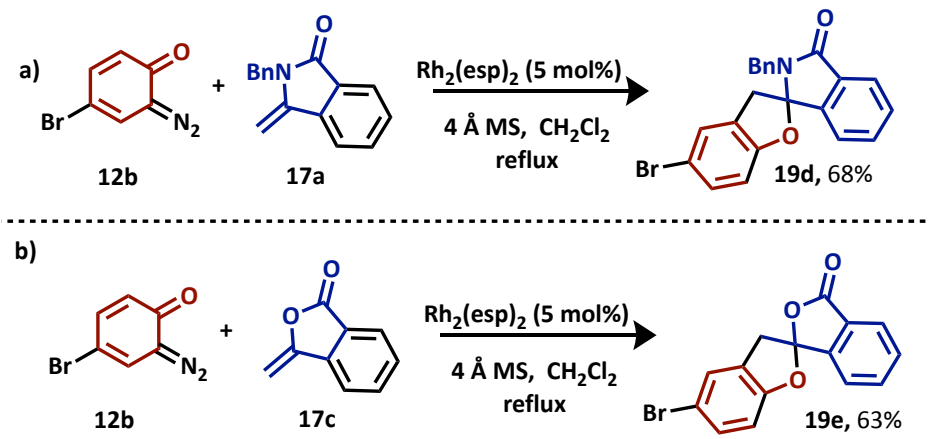

Scheme 5.13. *a) Synthesis of benzannulated spiroaminal* ***19d****; b) Synthesis of benzannulated spiroketal* ***19e****.*

5.2.3 PROPOSED MECHANISM

After applying the methodology to a brief substrate scope, we were able to propose a plausible reaction pathway for the Rh(II)-carbene catalyzed spirocyclization (**Scheme 5.14**). Decomposition of the α-diazoketone or diazo quinone in the presence of $Rh_2(esp)_2$ forms their respective carbene species. In the case of α-diazoketone carbenes (**Scheme 5.14a**), a cyclopropanation is presumed to occur initially, however this polarized cyclopropane **20** is highly susceptible to fragmentation to form a zwitterionic species consisting of an enolate and oxo/aza-carbenium ion (**21**). This intermediate undergoes *O*-alkylation to form the desired spiroketal/spiroaminal. Comparatively, in the case of Rh(II)-quinoid carbenes (**Scheme 5.14b**), the initial C–H functionalization by the electron rich alkene occurs to form a reactive zwitterionic intermediate **22** that immediately undergoes aromatization to form intermediate **23** thereby prohibiting cyclopropanation. This

phenolate-zwitterionic intermediate then undergoes *O*-alkylation to provide the desired spiroketal/spiroaminal.

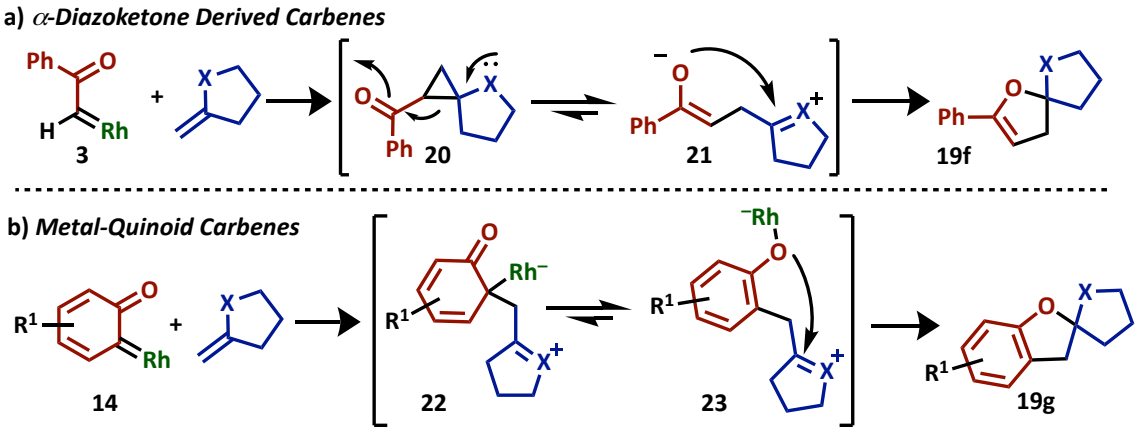

Scheme 5.14. *a) Mechanism of spiroketalization using α-diazoketones; b) Mechanism of spiroketalization using diazo quinones*

5.3 SUMMARY

In conclusion, we have developed methodology to access a variety of heterocyclic scaffolds, including dihydropyranones, benzannulated furano-furans, spiroketals, and spiroaminals, through use of α-diazoketones and electron-rich alkenes. The unique reactivity of metal carbenes derived from α-diazoketones and metal-quinoid carbenes to prefer *O*-alkylation over *C*-alkylation and the thermal rearrangement of polarized cyclopropanes was crucial to the success of these efforts. Further application of this methodology to a wider range of scaffolds and optimization of enantioselective transformations are currently being pursued in the Sharma laboratory and will be reported in due time.

5.4 REFERENCES

[1] Insights into the importance of spiroketals: a) Q. Zheng, Z. Tian, W. Liu, *Curr. Opin. Chem. Biol.* **2016**, *31*, 95–102; b) F. M. Zhang, S. Y. Zhang, Y. Q. Tu, *Nat. Prod. Rep.* **2018**, *35*, 75–104.

[2] I. Sharma, J. M. Wurst, D. S. Tan, *Org. Lett.* **2014**, *16*, 2474–2477.

[3] M. Liang, S. Zhang, J. Jia, C.-H. Tung, J. Wang, Z. Xu, *Org. Lett.* **2017**, *19*, 2526–2529.

[4] For reviews on diazocarbonyls and their stability: a) M. P. Doyle, R. Duffy, M. Ratnikov, L. Zhou, *Chem. Rev.* **2010**, *110*, 704–724; bM. P. Doyle, M. A. McKervey, T. Ye, *Modern Catalytic Methods for Organic Synthesis with Diazo Compounds: From Cyclopropanes to Ylides*, Wiley, **1998**.

[5] A. C. Hunter, S. C. Schlitzer, I. Sharma, *Chem. Eur. J.* **2016**, *22*, 16062–16065.

[6] M. Kitamura, K. Araki, H. Matsuzaki, T. Okauchi, *Eur. J. Org. Chem.* **2013**, *2013*, 5045–5049.

[7] a) Z. Liu, J.-Q. Wu, S.-D. Yang, *Org. Lett.* **2017**, *19*, 5434–5437; b) K. Wu, B. Cao, C. Y. Zhou, C. M. Che, *Chem. Eur. J.* **2018**, *24*, 4815–4819.

5.5 EXPERIMENTAL SECTION

5.5.1 GENERAL PROCEDURE FOR SYNTHESIS OF DIHYDROPYRANS

To a teflon coated 20 mL vial was added heat activated 4 Å molecular sieves (100 mg/mmol of starting material), $Rh_2(esp)_2$ (1 mol %), PPh_3AuCl (10 mol %), and $(CuOTf)_2$-toluene (10 mol %). This mixture was dissolved in 0.2 M dichloromethane and allowed to stir for 5 minutes at room temperature before 3-pentynoic acid (2.5 equiv.) was added. The reaction was stirred for 15 minutes or until the acid was consumed via TLC and a more non-polar spot (the desired furanone) formed. The corresponding diazo compound **1** (1.0 equiv.) was dissolved in 0.5 M dicholoromethane and then added to the catalyst solution stirring at 0 ºC via syringe pump. Once the addition was completed, the crude mixture was filtered over a celite pad to remove the 4 Å molecular sieves. The filtrate was directly loaded to a silica gel column and purified using flash column chromatography eluting with 10%–25% EtOAc in Hex to afford the dihydropyran.

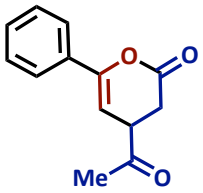

4-acetyl-6-phenyl-3,4-dihydro-2H-pyran-2-one (2a). **^{1}H NMR** (600 MHz, Chloroform-*d*) δ 7.61 (dd, *J* = 6.7, 2.9 Hz, 2H), 7.37 (dd, *J* = 5.3, 1.9 Hz, 3H), 5.91 (d, *J* = 5.6 Hz, 1H), 3.62 (q, *J* = 6.0 Hz, 1H), 3.00 (dd, *J* = 16.2, 5.7 Hz, 1H), 2.72 (dd, *J* = 16.2, 6.6 Hz, 1H), 2.29 (s, 3H). **^{13}C NMR** (151 MHz, Chloroform-*d*) δ 203.8, 166.7, 152.1, 128.6, 124.8, 96.8, 44.6, 29.5, 28.0.

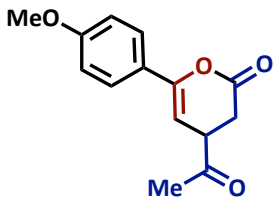

4-acetyl-6-(4-methoxyphenyl)-3,4-dihydro-2H-pyran-2-one (2b). **^{1}H NMR** (400 MHz, Chloroform-*d*) δ 7.99 – 7.93 (m, 2H), 6.99 – 6.93 (m, 2H), 3.89 (s, 3H), 3.08 (dd, *J* = 19.1, 6.4 Hz, 1H), 2.76 – 2.64 (m, 2H), 2.59 (dd, *J* = 6.4, 4.7 Hz, 1H), 1.64 (s, 3H). **^{13}C NMR** (101 MHz, Chloroform-*d*) δ 192.6, 175.4, 163.9, 130.5, 113.9, 72.7, 55.6, 55.6, 38.1, 33.7, 23.8, 12.9.

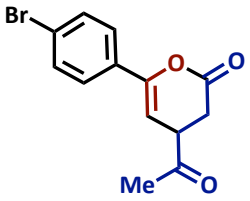

4-acetyl-6-(4-bromophenyl)-3,4-dihydro-2H-pyran-2-one (2c). **^{1}H NMR** (600 MHz, Chloroform-*d*) δ 7.50 (q, *J* = 8.5 Hz, 4H), 5.91 (d, *J* = 5.6 Hz, 1H), 3.62 (q, *J* = 6.1 Hz, 1H), 3.01 (dd, *J* = 16.2, 6.0 Hz, 1H), 2.74 (dd, *J* = 16.2, 6.6 Hz, 1H), 2.30 (s, 3H). **^{13}C NMR** (151 MHz, Chloroform-*d*) δ 203.5, 166.3, 151.3, 131.9, 126.3, 97.3, 44.6, 29.5.

5.5.2 GENERAL PROCEDURE FOR SYNTHESIS OF BENZANNULATED FURANO-FURANS

To a teflon coated 20 mL vial was added heat activated 4 Å molecular sieves (100 mg/mmol of starting material), $Rh_2(esp)_2$ (5 mol %), and the *endo*-alkene (3.0 equiv.). This mixture was dissolved in 0.2 M dichloromethane then the corresponding diazo compound **1** (1.0 equiv.) was added, the reaction was then heated to reflux until complete. Once complete, the crude mixture was filtered over a celite pad to remove the 4 Å molecular sieves. The

filtrate was directly loaded to a silica gel column and purified using flash column chromatography eluting with 5%–10% EtOAc in Hex to afford the benzannulated furano-furan.

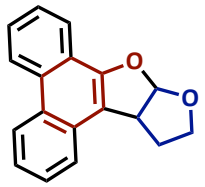

9a,11,12,12a-Tetrahydrofuro[2,3-b]phenanthro[9,10-d]furan (13a). **TLC**: R_f 0.5 (9:1 hexanes/EtOAc). **^{1}H NMR** (500 MHz, $CDCl_3$) δ 8.69 – 8.66 (m, 2H), 8.15 (dd, *J* = 7.8, 1.3 Hz, 1H), 7.77 (dd, *J* = 9.0, 1.0 Hz, 1H), 7.70 – 7.60 (m, 3H), 7.53 (ddd, *J* = 8.3, 7.0, 1.4 Hz, 1H), 6.67 (d, *J* = 5.9 Hz, 1H), 4.43 (dd, *J* = 8.3, 6.1 Hz, 1H), 4.17 (t, *J* = 8.5 Hz, 1H), 3.70 (ddd, *J* = 11.9, 8.8, 5.2 Hz, 1H), 2.43 (tdd, *J* = 11.9, 8.6, 7.6 Hz, 1H), 2.35 (dd, *J* = 12.0, 5.0 Hz, 1H); **^{13}C NMR** (125 MHz, $CDCl_3$) δ 152.7, 131.5, 129.4, 127.4, 127.2, 127.0, 126.7, 123.7, 123.6, 122.9, 122.6, 122.6, 121.3, 113.7, 112.0, 67.5, 46.9, 31.6.

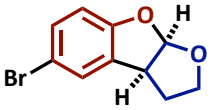

5-Bromo-2,3,3a,8a-tetrahydrofuro[2,3-b]benzofuran (13b). **TLC**: R_f 0.4 (9:1 hexanes/EtOAc). **^{1}H NMR** (400 MHz, $CDCl_3$) δ 7.29 – 7.30 (m, 1H), 7.24 (ddd, *J* = 6.7, 2.1, 0.7 Hz, 1H), 6.69 (d, *J* = 8.5 Hz, 1H), 6.31 (d, *J* = 5.7 Hz, 1H), 4.09 (t, *J* = 8.1 Hz, 1H), 3.99 (dd, *J* = 8.4, 5.9 Hz, 1H), 3.62 (ddd, *J* = 12.1, 8.8, 4.9 Hz, 1H), 2.30 (tdd, *J* = 12.2, 8.6, 7.7 Hz, 1H), 2.05 (ddd, *J* = 12.4, 4.8, 0.4 Hz, 1H); **^{13}C NMR** (101 MHz, $CDCl_3$) δ 158.6, 131.5, 130.1, 127.7, 112.8, 111.4, 110.8, 67.3, 46.5, 33.4.

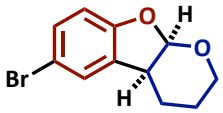

6-Bromo-3,4,4a,9a-tetrahydro-2H-pyrano[2,3-b]benzofuran (13c). **TLC**: R_f 0.3 (9:1 hexanes/EtOAc). **^{1}H NMR** (400 MHz, $CDCl_3$) δ 7.26 – 7.25 (m, 2H), 6.5 (d, *J* = 8.4 Hz, 1H), 5.89 (d, *J* = 6.3 Hz, 1H), 3.81 – 3.69 (m, 2H), 3.32 (q, *J* = 5.9 Hz, 1H), 2.11–2.02 (m, 1H), 1.90–1.83 (m, 1H), 1.68 – 1.62 (m, 1H), 1.57 – 1.50 (m, 1H); **^{13}C NMR** (101 MHz, $CDCl_3$) δ 157.5, 131.9, 131.1, 126.9, 112.9, 111.4, 104.5, 61.1, 38.8, 22.6, 19.9.

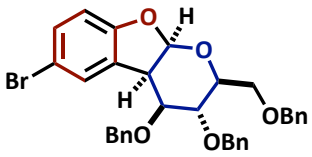

3,4-Bis(benzyloxy)-2-((benzyloxy)methyl)-6-bromo-3,4,4a,9a-tetrahydro-2H-pyrano[2,3-b]benzofuran (13d). **TLC**: R_f 0.5 (8:2 hexanes/EtOAc). **^{1}H NMR** (500 MHz, $CDCl_3$) δ 7.38 – 7.32 (m, 9H), 7.30 – 7.27 (m, 3H), 7.26 – 7.24 (m, 2H), 7.12 (d, *J* = 7.5 Hz, 2H), 6.72 (d, *J* = 8.5 Hz, 2H), 6.10 (d, *J* = 6.9 Hz, 1H), 4.76 (d, *J* = 11.6 Hz, 1H), 4.64 – 4.56 (m, 3H), 4.53 (d, *J* = 12.1 Hz, 1H), 4.45 (d, *J* = 11.4 Hz, 1H), 3.82 – 3.72 (m, 3H), 3.71 – 3.66 (m, 2H), 3.52 (t, *J* = 6.2 Hz, 1H); **^{13}C NMR** (125 MHz, $CDCl_3$) δ 157.3, 137.9, 137.7, 132.5, 131.6, 128.6 (2C), 128.5 (2C), 128.4 (2C), 128.1, 128.0 (2C), 127.9 (2C), 127.8, 127.8, 127.7, 127.6 (2C), 117.2, 111.2, 110.0, 104.8, 79.9, 76.1, 73.5, 73.5, 73.0, 72.5, 69.1, 44.6.

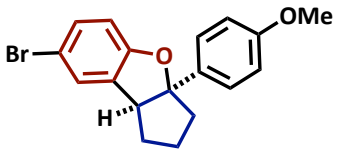

3a-(4-Methoxyphenyl)-2,3,3a,8b-tetrahydro-1H-cyclopenta[b]benzofuran (13e). **TLC**: R_f 0.5 (9:1 hexanes/EtOAc). **^{1}H NMR** (500 MHz, $CDCl_3$) δ 7.39 (d, *J* = 7.1 Hz, 1H), 7.35 (d, *J* = 8.8

Hz, 2H), 7.30 – 7.27 (m, 1H), 7.19 (d, *J* = 7.3 Hz, 1H), 7.06 – 7.02 (m, 1H), 6.86 (d, *J* = 8.7 Hz, 2H), 4.00 (d, *J* = 8.7 Hz, 1H), 3.78 (s, 3H), 2.53 (dd, *J* = 13.8, 5.7 Hz, 1H), 2.25 – 2.13 (m, 2H), 2.04 – 1.99 (m, 1H), 1.93 – 1.88 (m, 1H), 1.78 – 1.71 (m, 1H); **^{13}C NMR** (125 MHz, $CDCl_3$) *δ* 159.1, 153.9, 135.6, 131.7, 130.1, 126.1 (2C), 124.1, 121.1, 118.4, 113.9 (2C), 101.5, 55.3, 54.2, 41.8, 36.4, 25.0.

5.5.3 GENERAL PROCEDURE FOR SYNTHESIS OF SPIROKETALS/AMINALS

To a teflon coated 20 mL vial was added heat activated 4 Å molecular sieves (100 mg/mmol of starting material), $Rh_2(esp)_2$ (5 mol %), and the *exo*-alkene (1.0 equiv.). This mixture was dissolved in 0.2 M dichloromethane then the corresponding diazo compound **1** (2.0 equiv.) was added, the reaction was then heated to reflux until complete. Once complete, the crude mixture was filtered over a celite pad to remove the 4 Å molecular sieves. The filtrate was directly loaded to a silica gel column and purified using flash column chromatography eluting with 10%–20% EtOAc in Hex.

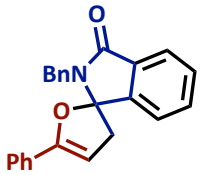

2'-benzyl-5-phenyl-3H-spiro[furan-2,1'-isoindolin]-3'-one (19a). **^{1}H NMR** (600 MHz, Chloroform-*d*) δ 7.95 – 7.83 (m, 2H), 7.31 (dq, *J* = 10.4, 3.6, 2.9 Hz, 5H), 7.16 (t, *J* = 7.3 Hz, 3H), 5.45 (t, *J* = 2.9 Hz, 1H), 4.80 (d, *J* = 15.4 Hz, 1H), 4.54 (d, *J* = 15.6 Hz, 1H), 3.28 (dd, *J* = 17.7, 2.5 Hz, 1H), 2.91 (dd, *J* = 17.8, 2.9 Hz, 1H).

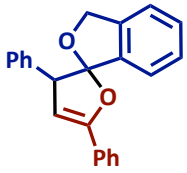

3,5-diphenyl-3H,3'H-spiro[furan-2,1'-isobenzofuran] (19c). **^{1}H NMR** (500 MHz, Benzene-d_6) δ 7.73 – 7.66 (m, 2H), 7.33 (dt, *J* = 7.6, 0.9 Hz,10H), 7.25 – 7.20 (m, 2H), 7.12 – 6.97 (m, 9H), 6.59 (dt, *J* = 7.5, 1.0 Hz, 1H), 5.55 (d, *J* = 2.3 Hz, 1H), 4.87 – 4.76 (m, 2H), 4.20 (d, *J* = 12.8 Hz, 1H).

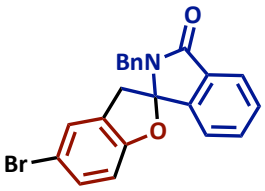

***2'-benzyl-5-bromo-3H-spiro[benzofuran-2,1'-isoindolin]-3'-one (19d*)**. **^{1}H NMR** (600 MHz, Chloroform-*d*) δ 7.92 – 7.85 (m, 1H), 7.64 – 7.53 (m, 2H), 7.44 (d, *J* = 7.3 Hz, 1H), 7.30 (dd, *J* = 8.4, 2.1 Hz, 1H), 7.23 – 7.17 (m, 3H), 7.09 – 7.04 (m, 2H), 6.60 (d, *J* = 8.5 Hz, 1H), 4.78 (d, *J* = 15.7 Hz, 1H), 4.37 (d, *J* = 15.4 Hz, 1H), 3.56 (d, *J* = 17.4 Hz, 1H), 3.24 (d, *J* = 17.4 Hz, 1H).

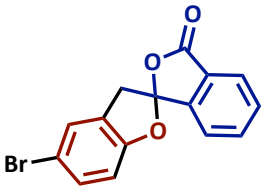

5-bromo-3H,3'H-spiro[benzofuran-2,1'-isobenzofuran]-3'-one (19e). **^{1}H NMR** (600 MHz, Chloroform-*d*) δ 7.96 – 7.91 (m, 1H), 7.81 – 7.75 (m, 1H), 7.68 (t, *J* = 7.5 Hz, 1H), 7.61 (d, *J* = 7.6 Hz, 1H), 7.44 (s, 1H), 7.37 (d, *J* = 2.2 Hz, 1H), 6.83 (d, *J* = 8.5 Hz, 1H), 3.80 – 3.74 (m, 1H), 3.64 (d, *J* = 17.3 Hz, 1H). **^{13}C NMR** (151 MHz, Chloroform-*d*) δ 166.95, 156.74, 145.69,

134.99, 131.62, 131.45, 128.31, 127.79, 126.82, 126.73, 125.62, 122.71, 114.50, 113.58, 111.72, 40.41.

APPENDIX 4

Spectra Revelant to Chapter 5

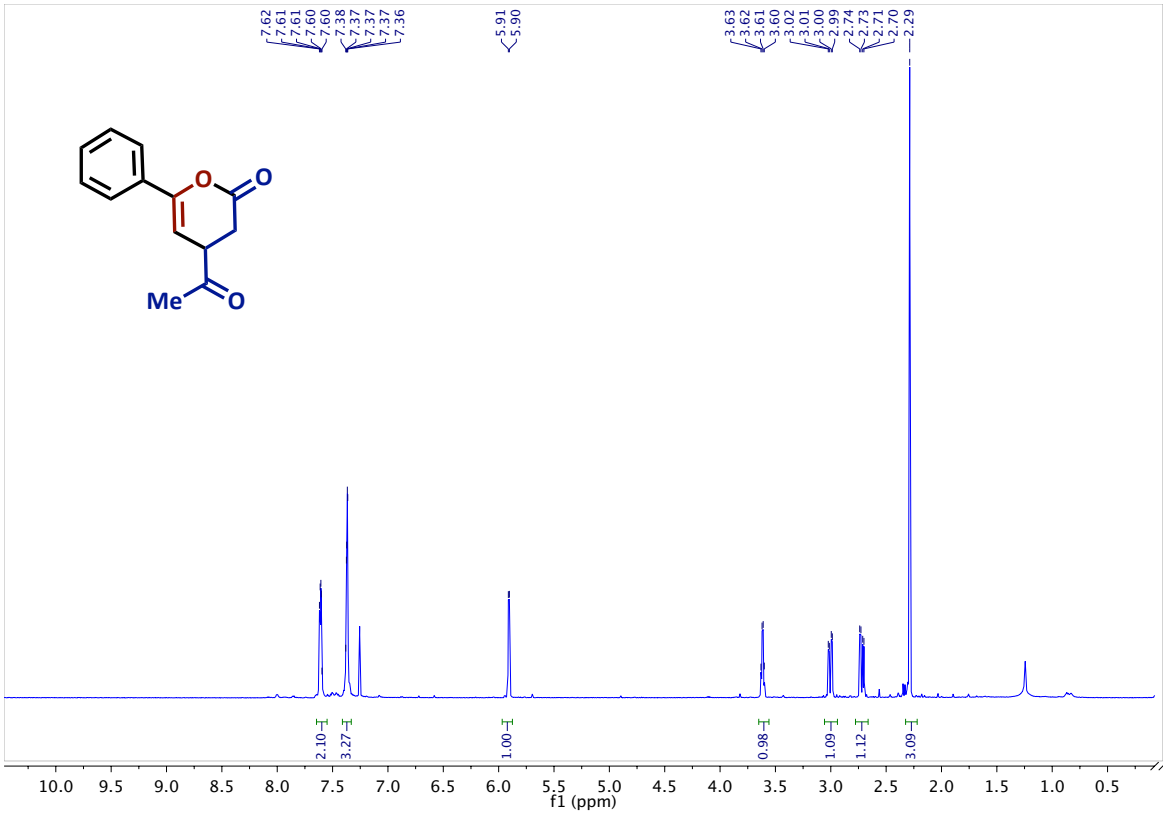
7.62
7.61
7.61
7.60
7.60
7.38
7.37
7.37
7.37
7.36
5.91
5.90
3.63
3.62
3.61
3.60
3.02
3.01
3.00
2.99
2.74
2.73
2.71
2.70
2.29
O
O
Me
O
2.10
3.27
1.00
0.98
1.09
1.12
3.09
10.0 9.5 9.0 8.5 8.0 7.5 7.0 6.5 6.0 5.5 5.0 4.5 4.0 3.5 3.0 2.5 2.0 1.5 1.0 0.5
f1 (ppm)

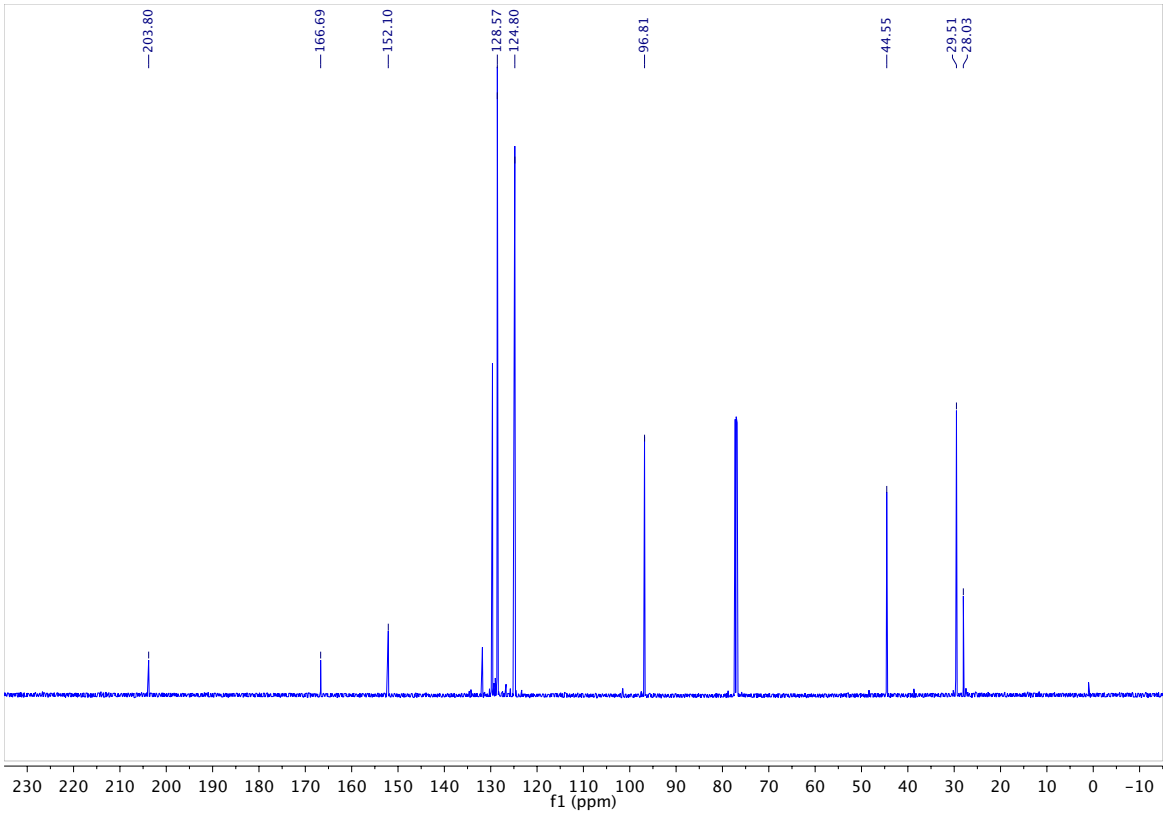
203.80
166.69
152.10
128.57
124.80
96.81
44.55
29.51
28.03
230 220 210 200 190 180 170 160 150 140 130 120 110 100 90 80 70 60 50 40 30 20 10 0 -10
f1 (ppm)

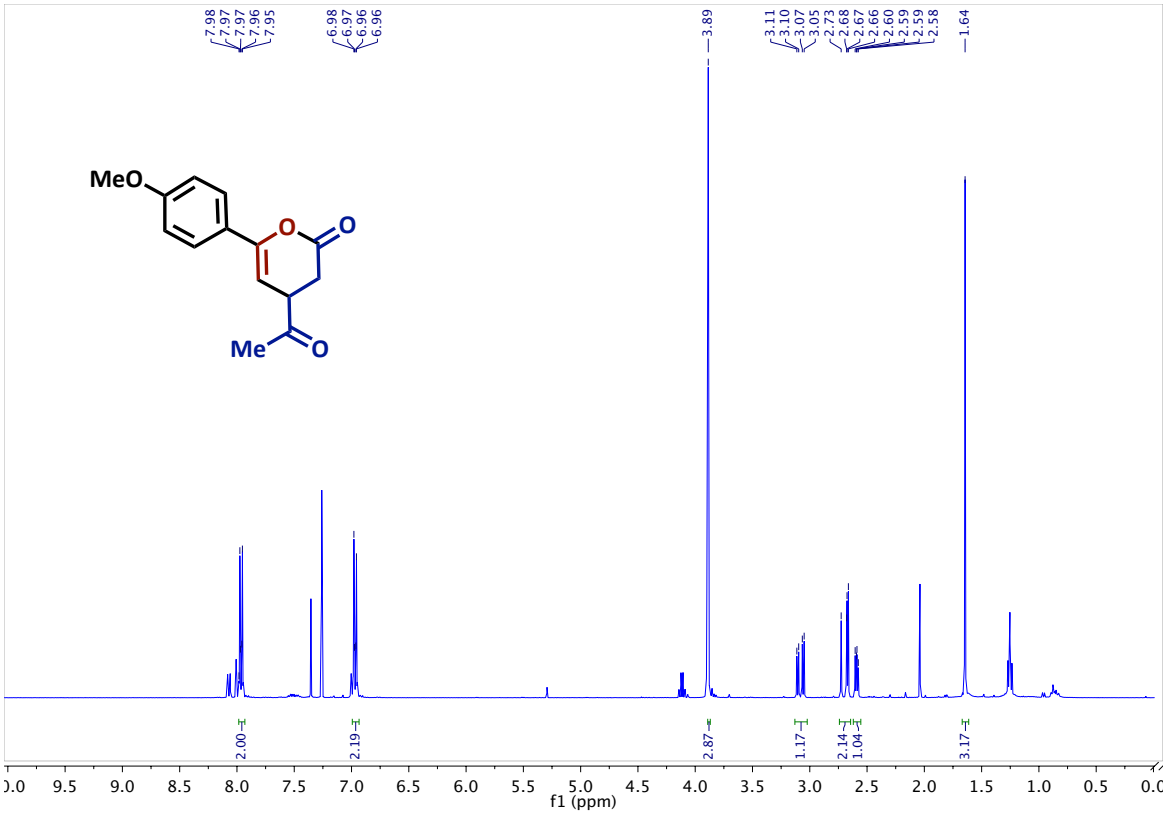
7.98
7.97
7.97
7.96
7.95
6.98
6.97
6.96
6.96
3.89
3.11
3.10
3.07
3.05
2.73
2.68
2.67
2.66
2.60
2.59
2.59
2.58
1.64
MeO
O
O
Me
O
2.00
2.19
2.87
1.17
2.14
1.04
3.17
f1 (ppm)

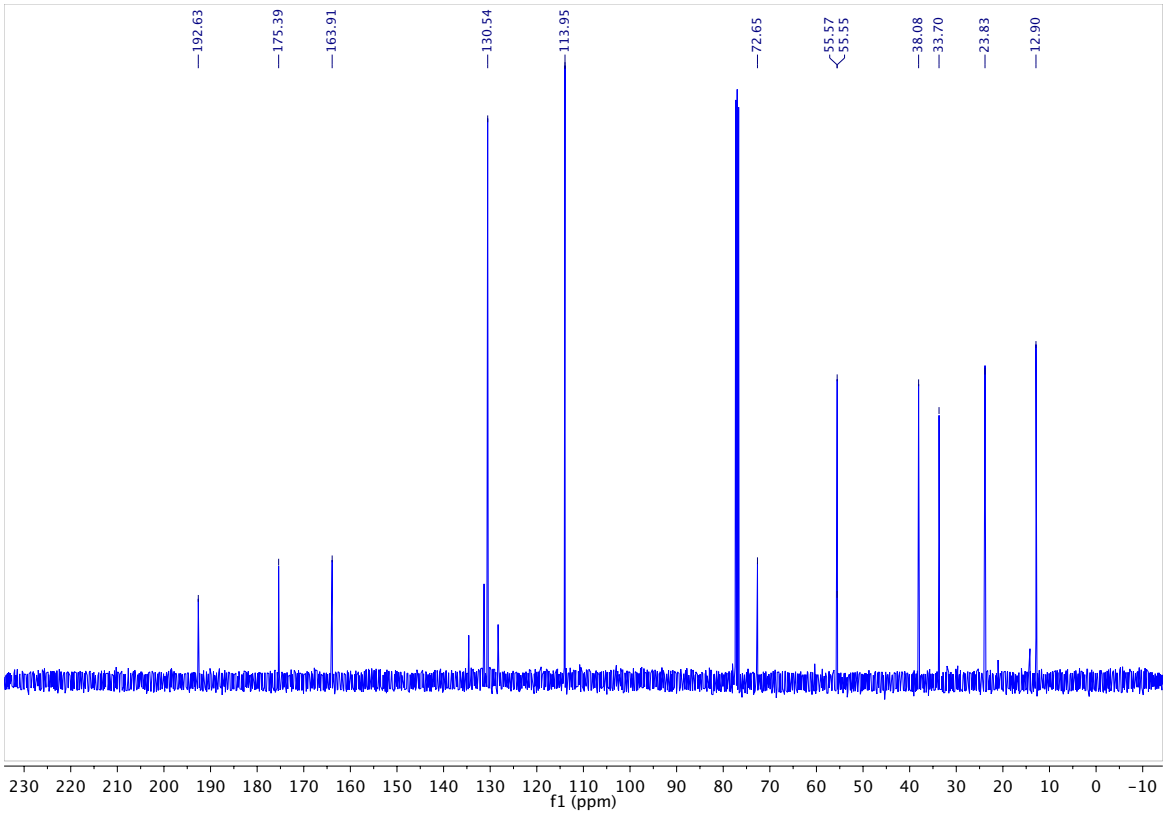
192.63
175.39
163.91
130.54
113.95
72.65
55.57
55.55
38.08
33.70
23.83
12.90
f1 (ppm)

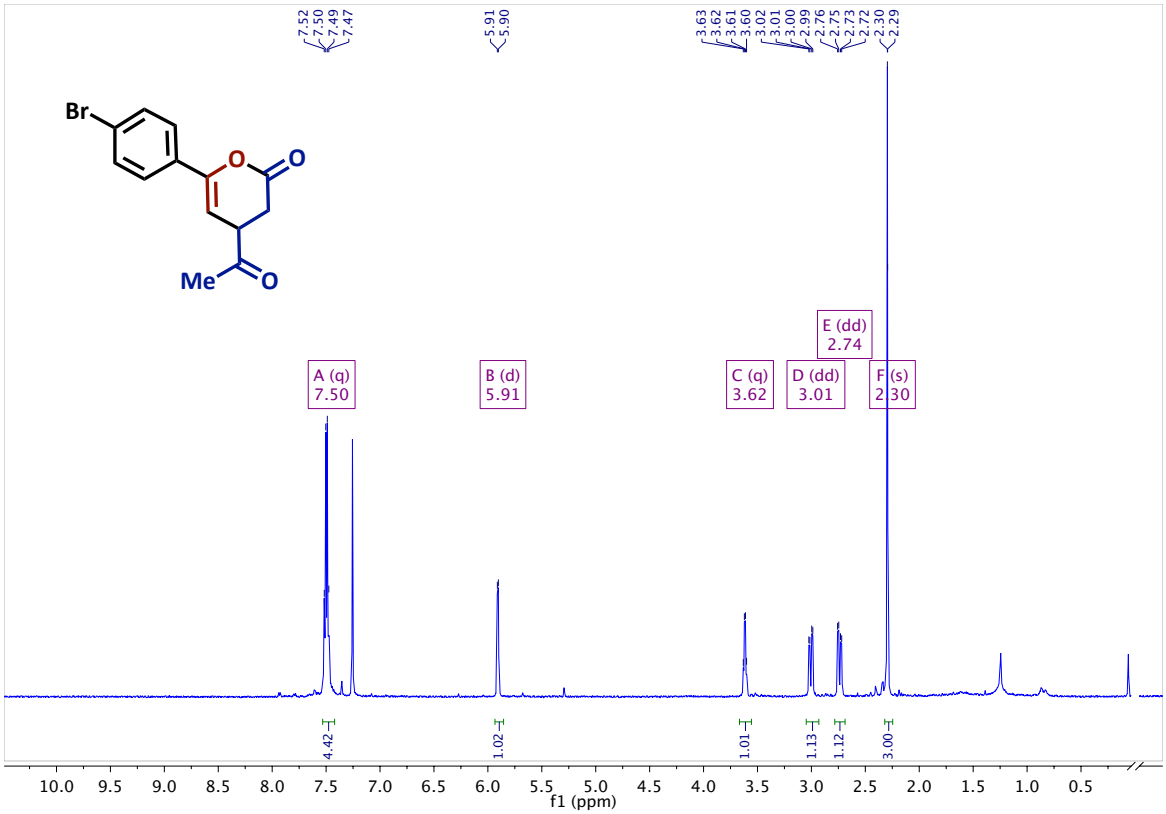
Br
O
O
Me
O
7.52
7.50
7.49
7.47
5.91
5.90
3.63
3.62
3.61
3.60
3.02
3.01
3.00
2.99
2.76
2.75
2.73
2.72
2.30
2.29
A (q) 7.50
B (d) 5.91
C (q) 3.62
D (dd) 3.01
E (dd) 2.74
F (s) 2.30
4.42
1.02
1.01
1.13
1.12
3.00
f1 (ppm)

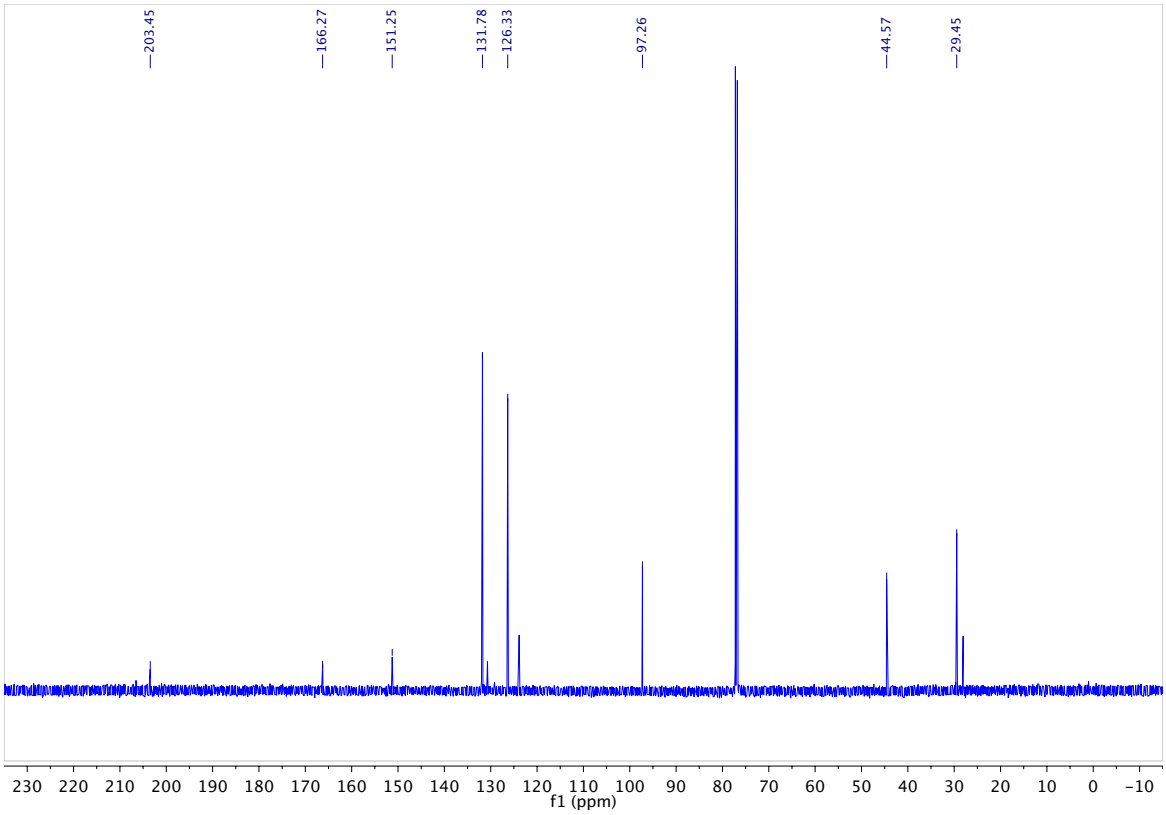
203.45
166.27
151.25
131.78
126.33
97.26
44.57
29.45
f1 (ppm)

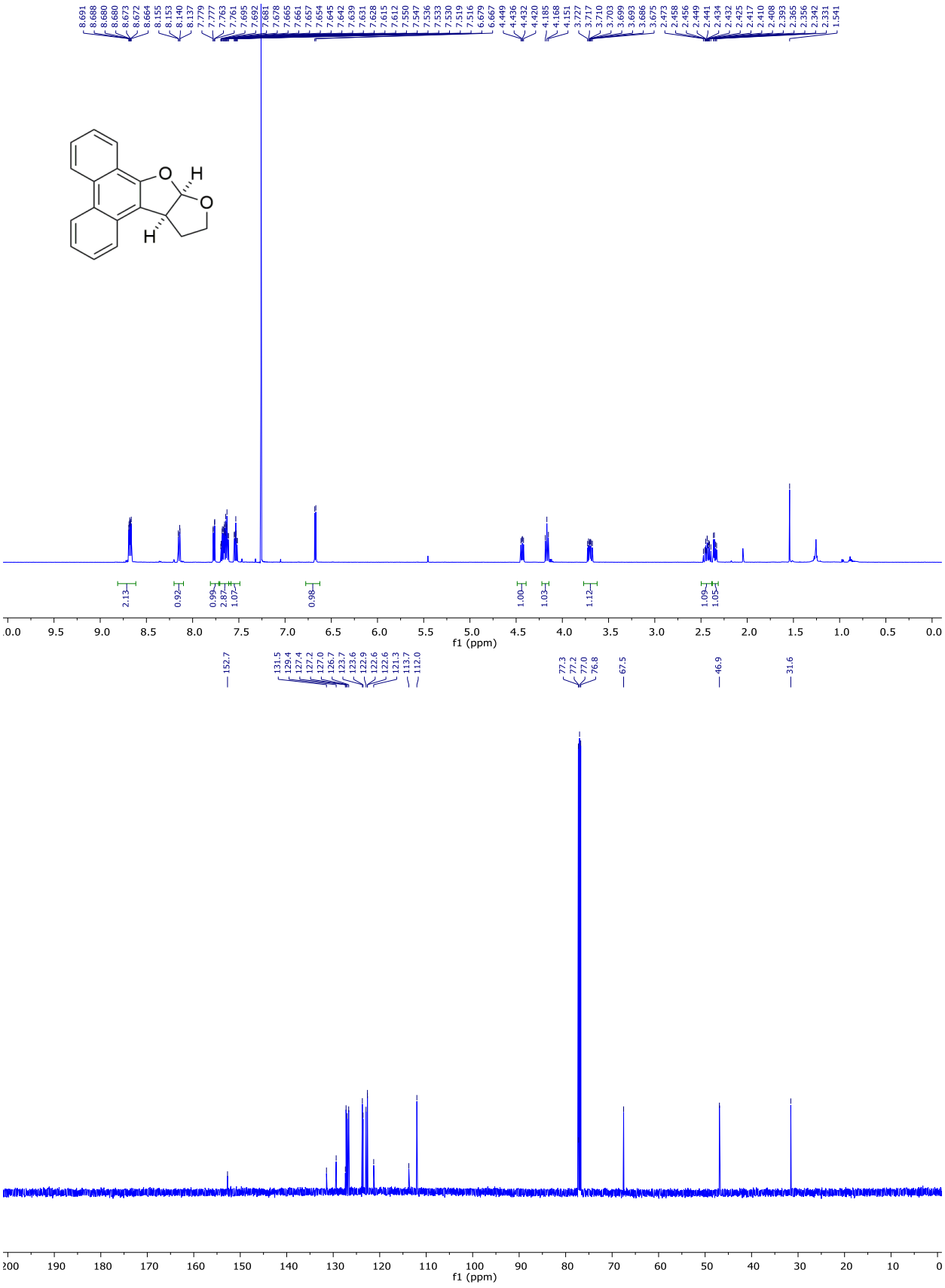
8.691
8.688
8.680
8.680
8.673
8.672
8.664
8.155
8.153
8.140
8.137
7.779
7.777
7.763
7.761
7.695
7.693
7.681
7.678
7.665
7.661
7.657
7.654
7.645
7.642
7.639
7.631
7.628
7.615
7.612
7.550
7.547
7.536
7.533
7.530
7.519
7.516
6.679
6.667
4.449
4.436
4.432
4.420
4.185
4.168
4.151
3.727
3.717
3.710
3.703
3.699
3.693
3.686
3.675
2.473
2.458
2.456
2.449
2.441
2.434
2.432
2.425
2.417
2.410
2.408
2.393
2.365
2.356
2.342
2.331
1.541
O
H
O
H
2.13
0.92
0.99
2.87
1.07
0.98
1.00
1.03
1.12
1.09
1.05
f1 (ppm)
152.7
131.5
129.4
127.4
127.2
127.0
126.7
123.7
123.6
122.9
122.6
122.6
121.3
113.7
112.0
77.3
77.2
77.0
76.8
67.5
46.9
31.6
f1 (ppm)

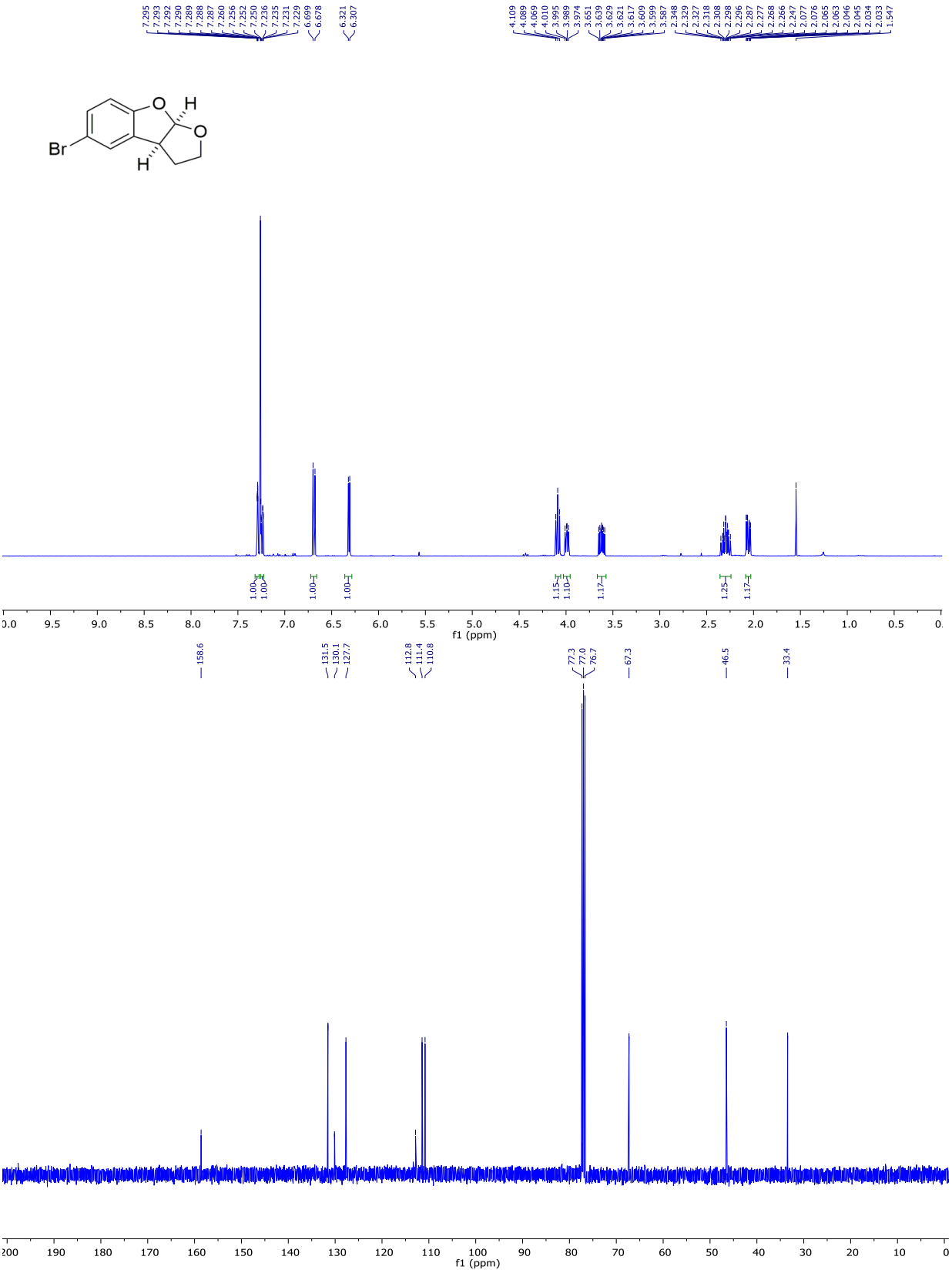
7.295
7.293
7.292
7.290
7.289
7.288
7.287
7.260
7.256
7.252
7.250
7.236
7.235
7.231
7.229
6.699
6.678
6.321
6.307
4.109
4.089
4.069
4.010
3.995
3.989
3.974
3.651
3.639
3.629
3.621
3.617
3.609
3.599
3.587
2.348
2.329
2.327
2.318
2.308
2.298
2.296
2.287
2.277
2.268
2.266
2.247
2.077
2.076
2.065
2.046
2.045
2.034
2.033
1.547
Br
O
H
O
H
1.00
1.00
1.00
1.00
1.15
1.10
1.17
1.25
1.17
f1 (ppm)
158.6
131.5
130.1
127.7
112.8
111.4
110.8
77.3
77.0
76.7
67.3
46.5
33.4
f1 (ppm)

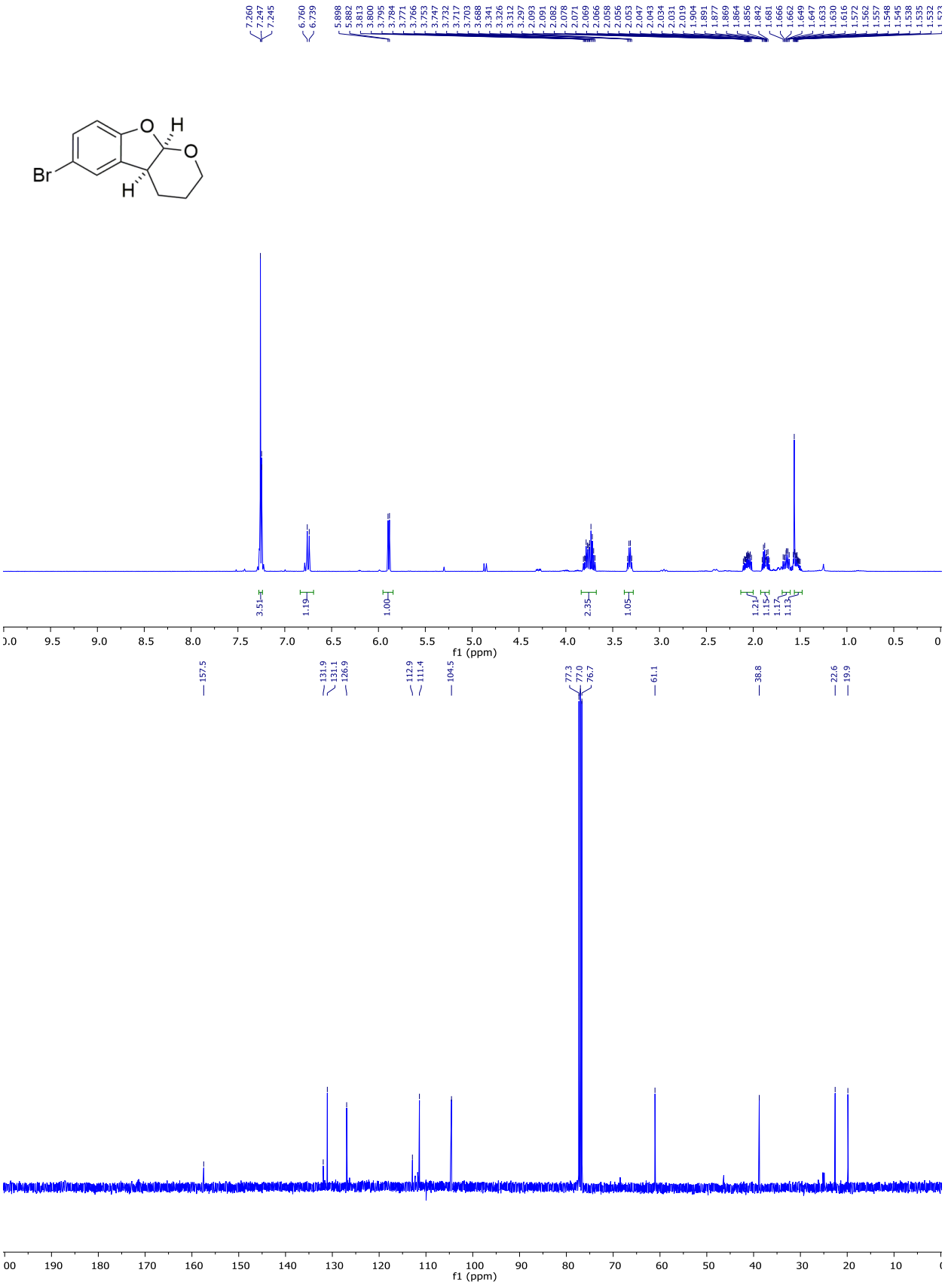
7.260
7.247
7.245
6.760
6.739
5.898
5.882
3.813
3.800
3.795
3.784
3.771
3.766
3.753
3.747
3.732
3.717
3.703
3.688
3.341
3.326
3.312
3.297
2.093
2.091
2.082
2.078
2.071
2.069
2.066
2.058
2.056
2.053
2.047
2.043
2.034
2.031
2.019
1.904
1.891
1.877
1.869
1.864
1.856
1.842
1.681
1.666
1.662
1.649
1.647
1.633
1.630
1.616
1.572
1.562
1.557
1.548
1.545
1.538
1.535
1.532
O
H
O
Br
H
3.51
1.19
1.00
2.35
1.05
1.21
1.15
1.17
1.13
f1 (ppm)
157.5
131.9
131.1
126.9
112.9
111.4
104.5
77.3
77.0
76.7
61.1
38.8
22.6
19.9
f1 (ppm)

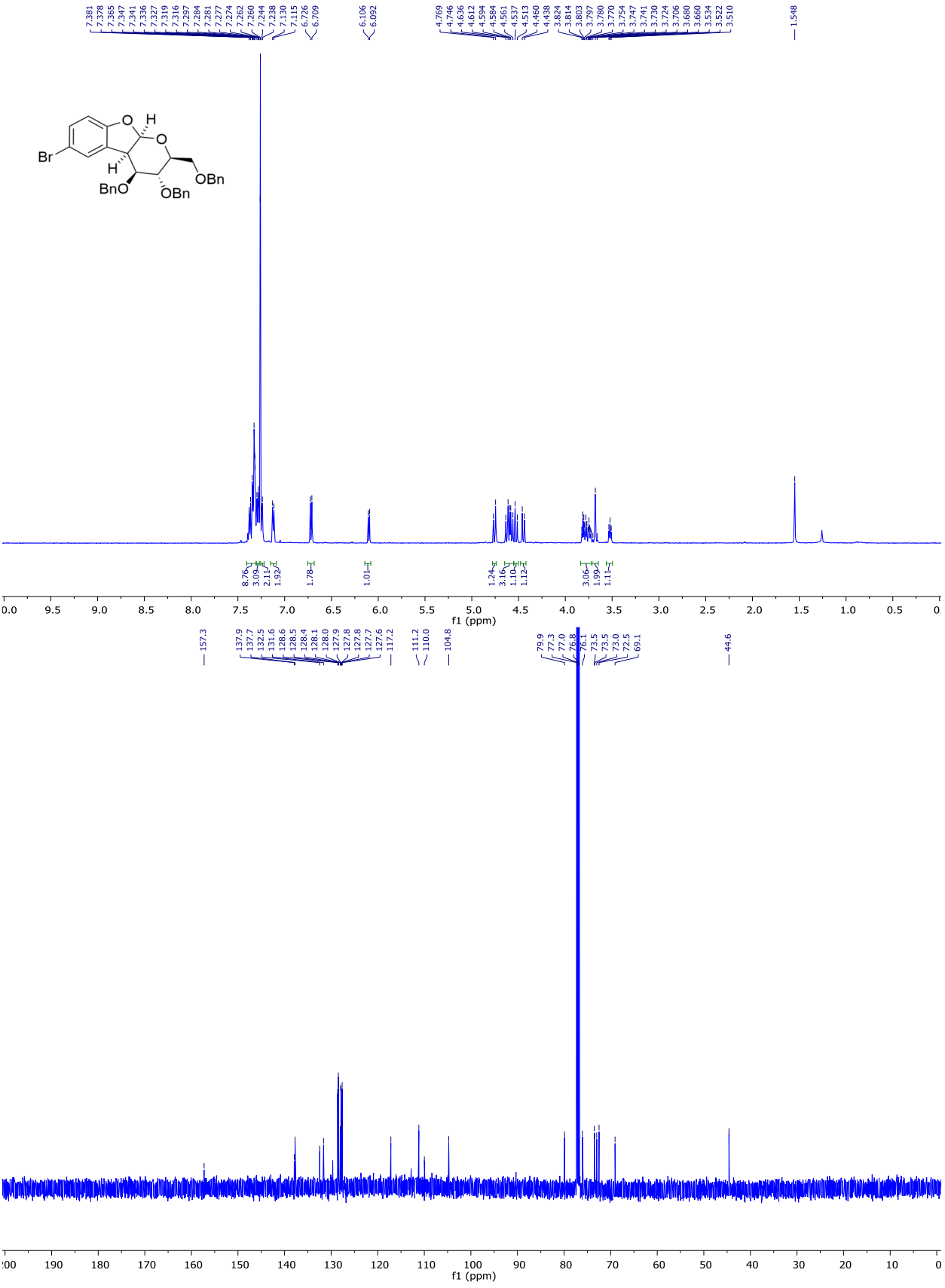
7.381
7.378
7.365
7.347
7.341
7.336
7.327
7.319
7.316
7.297
7.284
7.281
7.277
7.274
7.262
7.260
7.244
7.238
7.130
7.115
6.726
6.709
6.106
6.092
4.769
4.746
4.636
4.612
4.594
4.584
4.561
4.537
4.513
4.460
4.438
3.824
3.814
3.803
3.797
3.780
3.770
3.754
3.747
3.741
3.730
3.724
3.706
3.680
3.660
3.534
3.522
3.510
1.548
Br
O
H
O
H
BnO
OBn
OBn
8.76
3.09
2.11
1.92
1.78
1.01
1.24
3.16
1.10
1.12
3.06
1.99
1.11
f1 (ppm)
157.3
137.9
137.7
132.5
131.6
128.6
128.5
128.4
128.1
128.0
127.9
127.8
127.8
127.7
127.6
117.2
111.2
110.0
104.8
79.9
77.3
77.0
76.8
76.1
73.5
73.5
73.0
72.5
69.1
44.6
f1 (ppm)

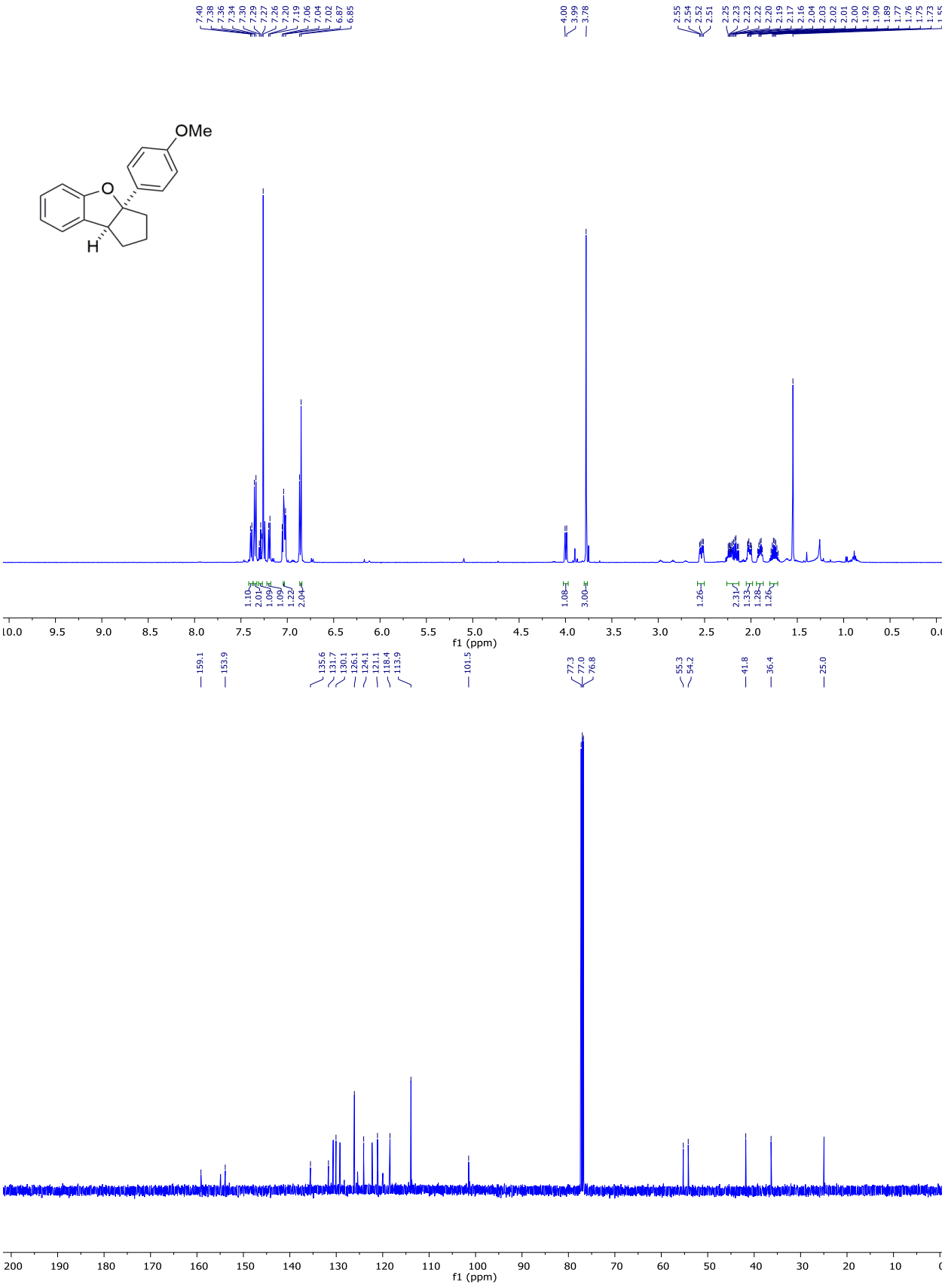
OMe
O
H
f1 (ppm)
f1 (ppm)

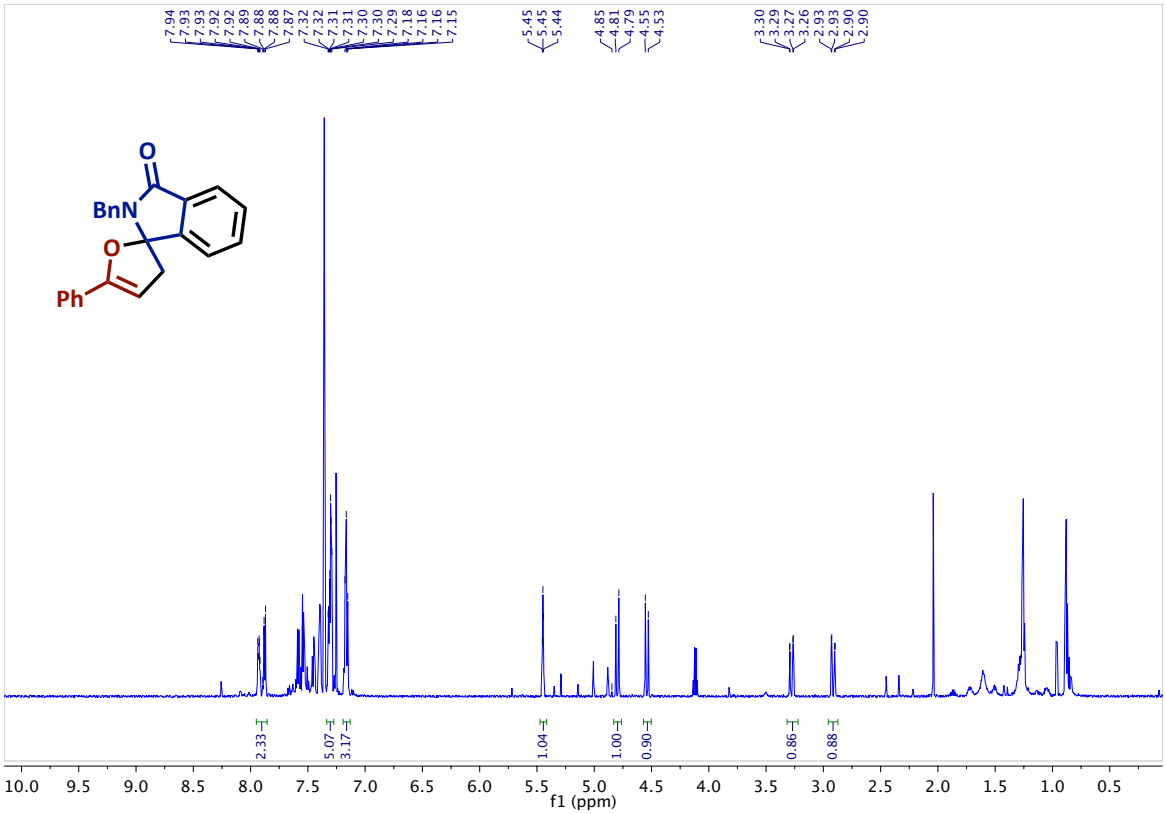
7.94
7.93
7.93
7.92
7.92
7.89
7.88
7.88
7.87
7.32
7.32
7.31
7.31
7.30
7.30
7.29
7.18
7.16
7.16
7.15
5.45
5.45
5.44
4.85
4.81
4.79
4.55
4.53
3.30
3.29
3.27
3.26
2.93
2.93
2.90
2.90
2.90
O
BnN
O
Ph
2.33
5.07
3.17
1.04
1.00
0.90
0.86
0.88
10.0 9.5 9.0 8.5 8.0 7.5 7.0 6.5 6.0 5.5 5.0 4.5 4.0 3.5 3.0 2.5 2.0 1.5 1.0 0.5
f1 (ppm)

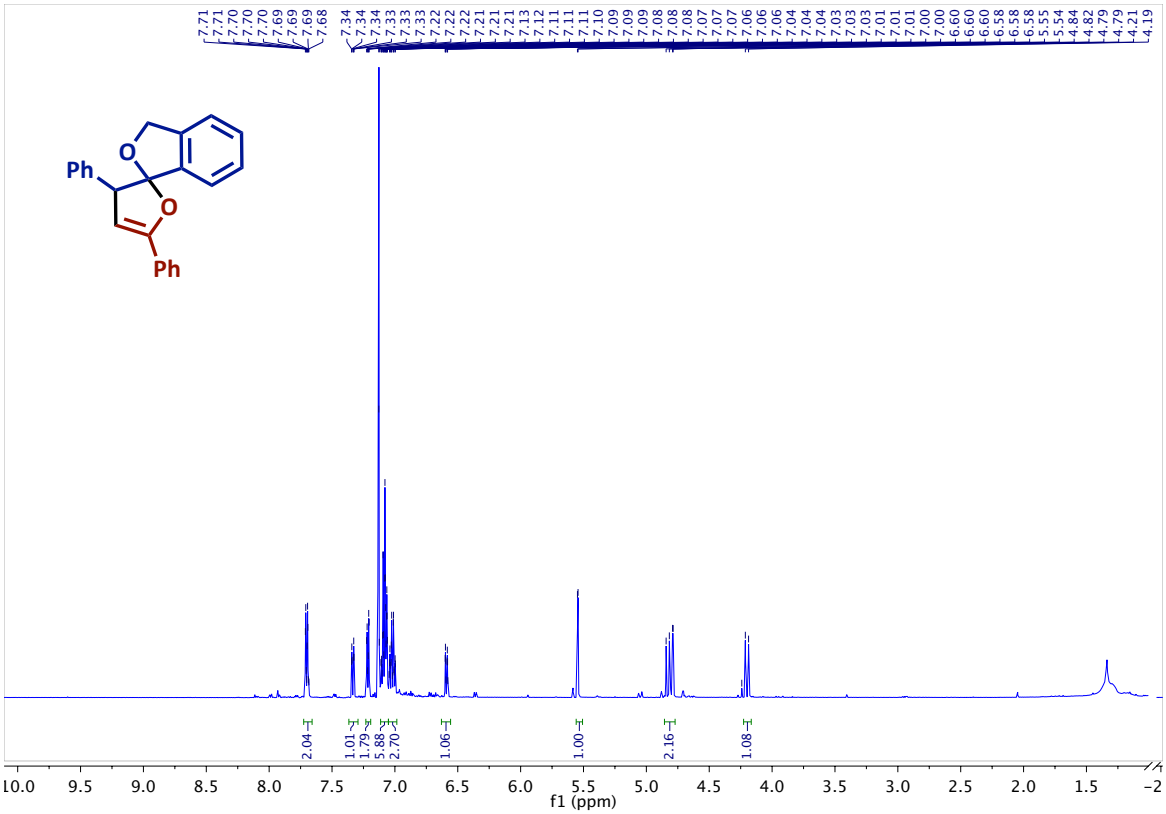
7.71
7.71
7.70
7.70
7.70
7.70
7.69
7.69
7.69
7.68
7.34
7.34
7.34
7.33
7.33
7.33
7.22
7.22
7.22
7.21
7.21
7.21
7.13
7.12
7.11
7.11
7.11
7.10
7.09
7.09
7.09
7.08
7.08
7.08
7.07
7.07
7.07
7.06
7.06
7.06
7.04
7.04
7.04
7.03
7.03
7.03
7.01
7.01
7.01
7.00
7.00
6.60
6.60
6.60
6.58
6.58
6.58
5.55
5.54
4.84
4.82
4.79
4.79
4.21
4.19
O
Ph
O
Ph
2.04
1.01
1.79
5.88
2.70
1.06
1.00
2.16
1.08
10.0 9.5 9.0 8.5 8.0 7.5 7.0 6.5 6.0 5.5 5.0 4.5 4.0 3.5 3.0 2.5 2.0 1.5 −2
f1 (ppm)

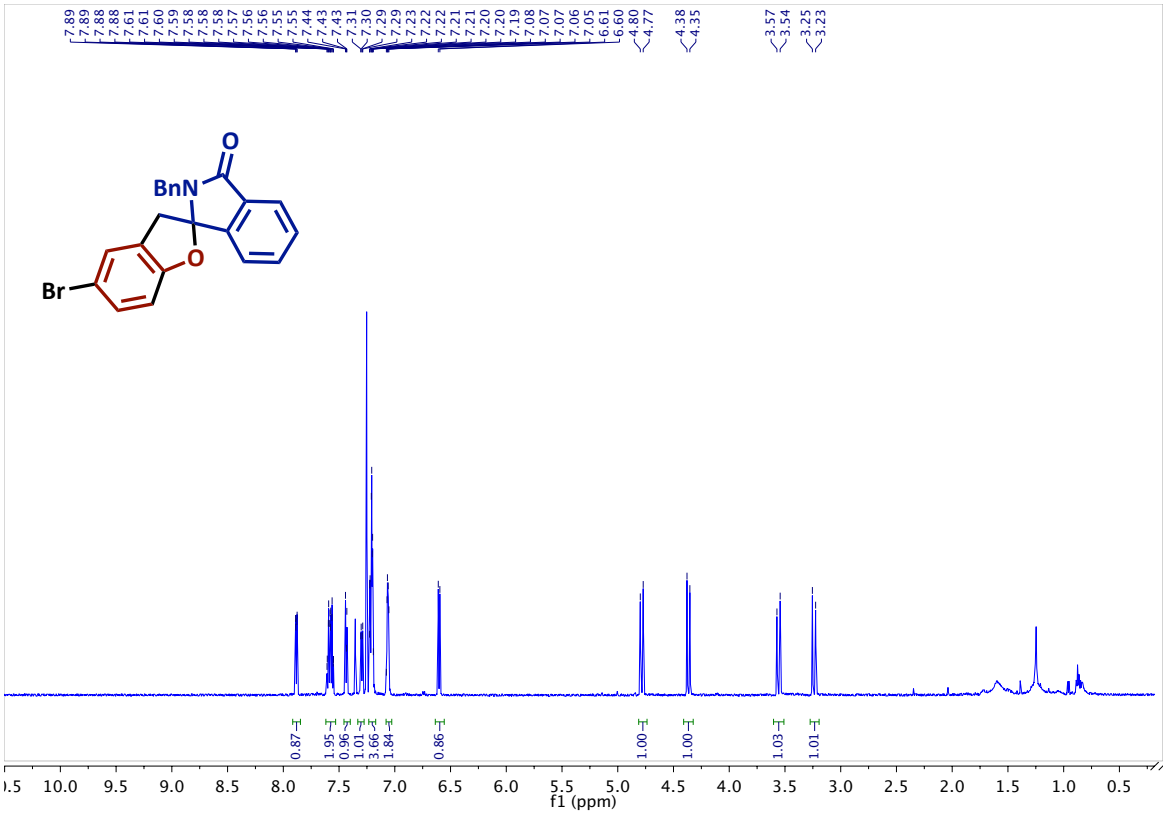
7.89
7.89
7.88
7.88
7.61
7.61
7.60
7.59
7.58
7.58
7.58
7.57
7.56
7.56
7.55
7.55
7.44
7.43
7.43
7.31
7.30
7.29
7.29
7.23
7.22
7.22
7.21
7.21
7.20
7.20
7.19
7.08
7.07
7.07
7.06
7.05
6.61
6.60
4.80
4.77
4.38
4.35
3.57
3.54
3.25
3.23
O
BnN
O
Br
0.87
1.95
0.96
1.01
3.66
1.84
0.86
1.00
1.00
1.03
1.01
10.0
9.5
9.0
8.5
8.0
7.5
7.0
6.5
6.0
5.5
5.0
4.5
4.0
3.5
3.0
2.5
2.0
1.5
1.0
0.5
f1 (ppm)

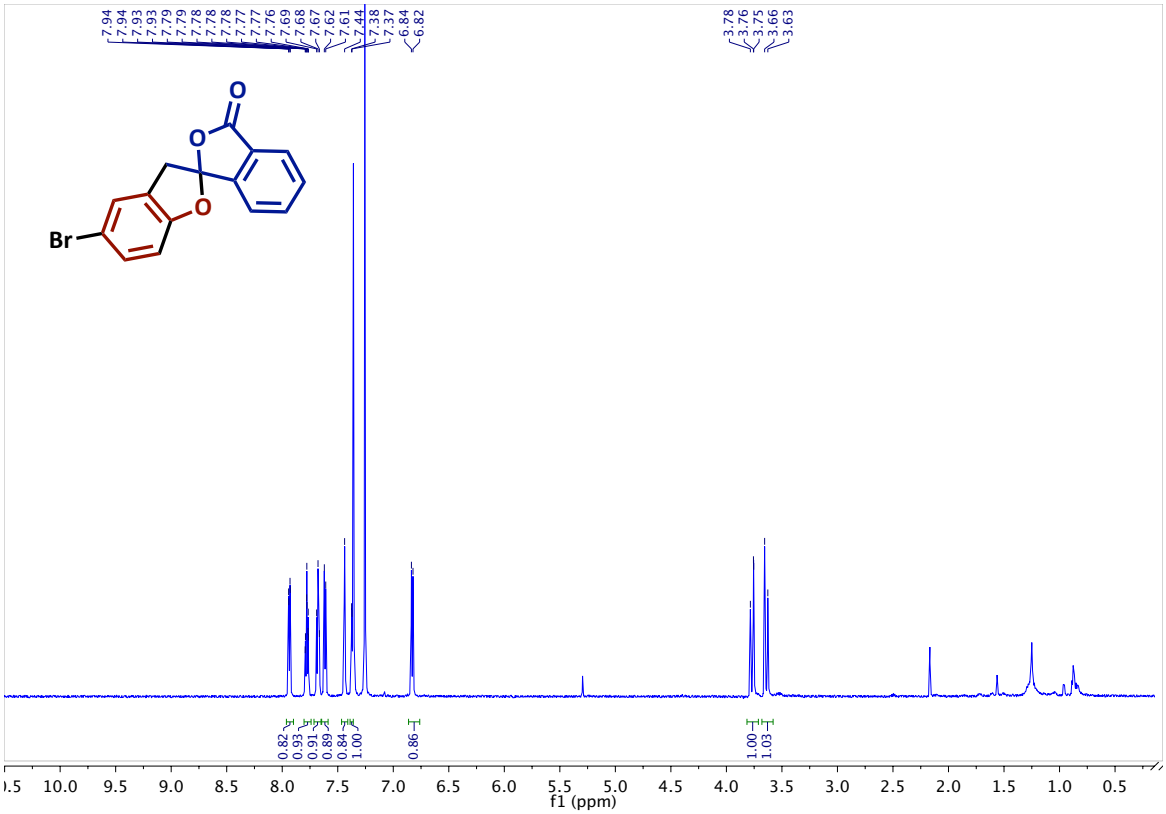
7.94
7.94
7.93
7.93
7.93
7.79
7.79
7.78
7.78
7.78
7.77
7.77
7.76
7.69
7.68
7.67
7.62
7.61
7.44
7.38
7.37
6.84
6.82
3.78
3.76
3.75
3.66
3.63
O
O
O
Br
0.82
0.93
0.91
0.89
0.84
1.00
0.86
1.00
1.03
10.0
9.5
9.0
8.5
8.0
7.5
7.0
6.5
6.0
5.5
5.0
4.5
4.0
3.5
3.0
2.5
2.0
1.5
1.0
0.5
f1 (ppm)

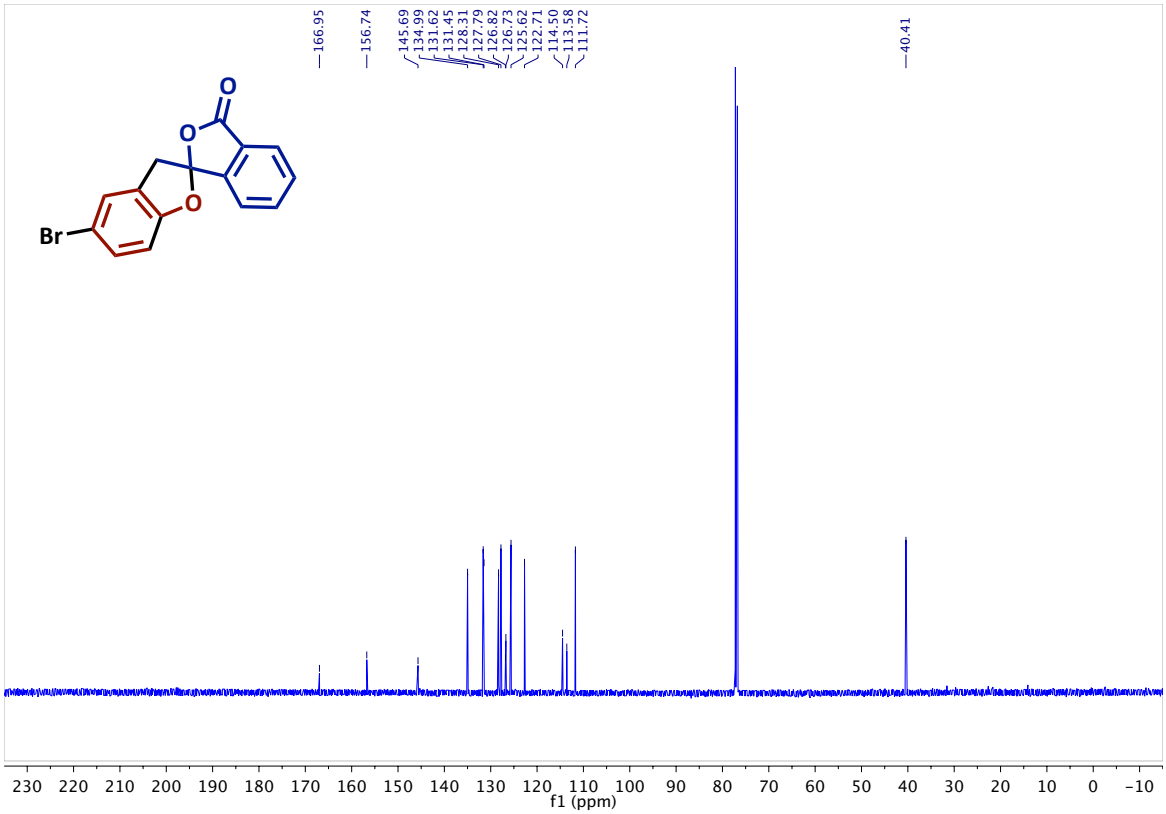
166.95
156.74
145.69
134.99
131.62
131.45
128.31
127.79
126.82
126.73
125.62
122.71
114.50
113.58
111.72
40.41
O
O
O
Br
230 220 210 200 190 180 170 160 150 140 130 120 110 100 90 80 70 60 50 40 30 20 10 0 −10
f1 (ppm)

CHAPTER 6

Conclusions

The goal of the research completed within this dissertation was to utilize metal carbene initiated cascade reactions to conduct the efficient synthesis of spirocyclic scaffolds. The value of this research was centralized around the importance of spirocycles and their under-exploitation in the field of drug discovery. Upon completion of this work a better understanding of the reactivity of metal carbenes and their use in cascade spirocyclizations was obtained. Metal carbenes, which are ambiphilic in nature, provided the possibility of conducting sequential reactions with a nucleophile and electrophile inbuilt in the same molecule. This cascade reactivity allowed us to stereoselectively install spirocenters in "single pot" reactions.

Within this dissertation a new strategy to prepare α-acyloxy carbonyl scaffolds, γ-butyrolactones, and tetrahydrofurans from readily available starting materials was developed (**Chapter 2**). During the development of this methodology we were able to identify two novel catalytic systems that were critical to the success of our chemistry: 1)

$Rh_2(esp)_2$ as a single catalyst for the efficient insertion of carboxylic acids into very stable A/A diazocarbonyls and 2) $Rh_2(esp)_2$/PPh_3AuOTf as a synergistic catalytic combination for the O–H insertion/Conia-ene cascade.

After completing the aforementioned work, we were able to take the insights learned during that methodology development to equip ourselves with knowledge necessary for the development of methodology to access highly valuable spiroethers and azaspiro-ring systems (**Chapter 3**). The synthesis of these spirocyclic ring scaffolds were not achieved without encountering challenges. The challenges we confronted during the synthesis of spiroethers and azaspiro-ring systems caused us to explore different catalytic conditions, temperatures, and reagent addition methods providing valuable insight into the reactivity of metal carbenes in cascade reactions with different nucleophilic sources.

With the successful application of our Rh(II)/Au(I) catalytic system to the synthesis of spiroethers and azaspiro-ring systems, we gained confidence in our ability to apply this system to the difficult synthesis of all-carbon spirocenters. After thorough optimization and a modification that required the substitution of AgOTf with $(CuOTf)_2$-tol as our Au(I) activator, we were able to extend our previously identified Rh(II)/Au(I) catalytic cocktail to a general approach for the synthesis of 5-, 6-, and 7-membered oxindole hybridized spirocarbocycles (**Chapter 4**).

Lastly, we decided to let our ambition navigate our research in an attempt to apply our Rh(II)/Au(I) catalytic system to the synthesis of spiroketals, however, an unsuccessful retrosynthetic disconnection limited our ability to complete this task. Nevertheless, a serendipitous discovery using α-diazoketones provided us with insight into a different

mode of reactivity that could be used in the synthesis of spiroketals using metal carbenes. With this insight, we identified a new retrosynthetic disconnection that exploited *exo*-alkenes and metal carbenes obtained from α-diazoketones and metal-quinoid carbenes (**Chapter 5**). Upon completion of this work we were able to access a variety of spiroketals and spiroaminals.

AUTOBIOGRAPHICAL STATEMENT

Education

08/2014-present **PhD Candidate in Organic Chemistry** University of Oklahoma (Advisor: Dr. Indrajeet Sharma)

Doctoral Dissertation: *"Metal Carbene Initiated Stereoselective Spirocyclizations"*

09/2010-06/2014 **B.A. in Chemistry** Dartmouth College in Hanover, NH (Advisor: Dr. Gordon Gribble)

Undergraduate Thesis: *"Synthetic Application of 3-nitroindole Derivatives in Natural Product Synthesis"*

Publications

1. **Hunter, A.C.;** Chinthapally, K.; Legg-Jack, I.; Sharma, I., "Synergistic Catalysis in Rhodium Carbene Chemistry" (*In Review)*

2. **Hunter, A.C.;** Chinthapally, K.; Bain, A.; Stevens, J.C.; Sharma, I., "Rh/Au Dual Catalysis in Carbene sp^2-CH Functionalization/Conia-ene Cascade for the Stereoselective Synthesis of Diverse Spirocarbocycles". *Adv. Synth. Catal.* **2019** DOI: 10.1002/adsc.201900079

3. **Hunter, A.C.;** Almutwalli, B.; Bain, A.; Sharma, I., "Trapping of Rh(II) Carbenoids with Amino-Alkynes for the Synthesis of Functionalized *N*-Heterocycles". *Tetrahedron.* **2018**, *74*, 5451–5457. *Invited Article in Honor of Sir Derek Barton*

4. **Hunter, A.C.;** Schlitzer, S.C.; Stevens, J.C.; Almutwalli, B.; Sharma, I., "A Convergent Approach to Diverse Spiroethers through Stereoselective Trapping of Rhodium Carbenoids with Gold-Activated Alkynols". *J. Org. Chem.* **2018**, *83*, 2744–2752. DOI: 10.1002/chem.201603934

5. **Hunter, A.C.,** Schlitzer, S.C., Sharma, I., "Synergistic Diazo –OH Insertion/Conia-Ene Cascade Catalysis for the Stereoselective Synthesis of γ-Butyrolactones and Tetrahydrofurans". *Chem. Eur. J.*, **2016**, *22*, 16062–16065. DOI: 10.1002/chem.201603934

6. **Hunter, A.C.,** Chinthapally, K., Sharma, I., "$Rh_2(esp)_2$: An Efficient Catalyst for O–H Insertion Reactions of Carboxylic Acids into Acceptor/Acceptor Diazo Compounds". Eur. J. Org. Chem., **2016,** 2260-2263. ***Cover Page Article***

Conference Presentations

1. **Hunter, A.C.,** Schlitzer, S., Sharma, I. "Metal Carbenoid Initiated Cascade Reactions for Assembling Molecular Complexity". Natural Products and Bioactive Compounds Gordon Research Conference (July 2018)

2. **Hunter, A.C.,** Schlitzer, S., Chinthapally, K., Sharma, I. "Building Molecular Complexity Utilizing Diazo-Synthons" Gordon Research Conference (July 17-22, 2016)

3. **Hunter, A.C.,** Sharma, I. "A Biomimetic Diversity-Oriented Approach to Azaspirene via Metal Carbenoid Chemisty" Poster Session, National Organization for the Professional Development of Black Chemists and Chemical Engineers. Orlando, Florida (September 21-25, 2015)

4. **Hunter et al.** "A Biomimetic Diversity-Oriented Approach to the Pseurotins" Poster Session, American Society of Pharmacognosy, Copper Mountain, Colorado (July 25–29, 2015)

Awards and Fellowships

01/2019 **Three Minute Thesis (3MT) Competition Runner-Up and People's Choice Awardee** Participated in the 3MT competition at The University of Oklahoma. Criteria for awards were based on presenting doctoral research in a compelling and engaging manner to a non-specialist audience in just three minutes.

10/2018 **NextGen Under 30 Oklahoma** Selected as a member of the 2018-2019 cohort of NextGen Under 30 awardees, an award honoring innovative, creative, and inspiring Oklahomans under 30.

04/2018 **Carl Storm Underrepresented Minority Fellowship** Funding granted on behalf of the Gordon Research Conferences as an initiative to increase diversity at their highly prestigious conferences.

04/2018 **Sherril D. Christian Scholarship from the University of Oklahoma** A premier graduate student award in the Department of Chemistry and Biochemistry. Selected on the basis of outstanding research contributions to one's field.

04/2018 **Nancy L. Mergler Dissertation Fellow** 1 of 7 Ph.D. Candidates selected at The University of Oklahoma for an award of $15,000 that recognizes meritorious dissertation projects and supports their completion.

05/2017 **Jerry J. Zuckerman Scholarship from the University of Oklahoma** Awarded to a student in the Chemistry/Biochemistry Department that has made exception advances and findings in the field of Organometallic Chemistry

05/2016 **Ronald E. Lehr Scholarship from the University of Oklahoma** Awarded to a student in the Chemistry/Biochemistry Department that has shown exceptional leadership and success in research and teaching.

04/2016 **SMART (Science, Mathematics, and Research for Transformation) Fellowship from the Department of Defense** Program aims to increase the number of civilian scientists and engineers working at Department of Defense laboratories

11/2015 **Robberson Research Grant at The University of Oklahoma** Financial assistance provided to graduate students whose research project is leading to significant advances in their field of interest or shows high levels or creativity.

04/2014 **Ernest Everett Just Fellow at Dartmouth College** Monetary award and travel grants to attend STEM and Biomedical Research conferences. Prompted greater awareness for STEM success amongst minority student at Dartmouth College